

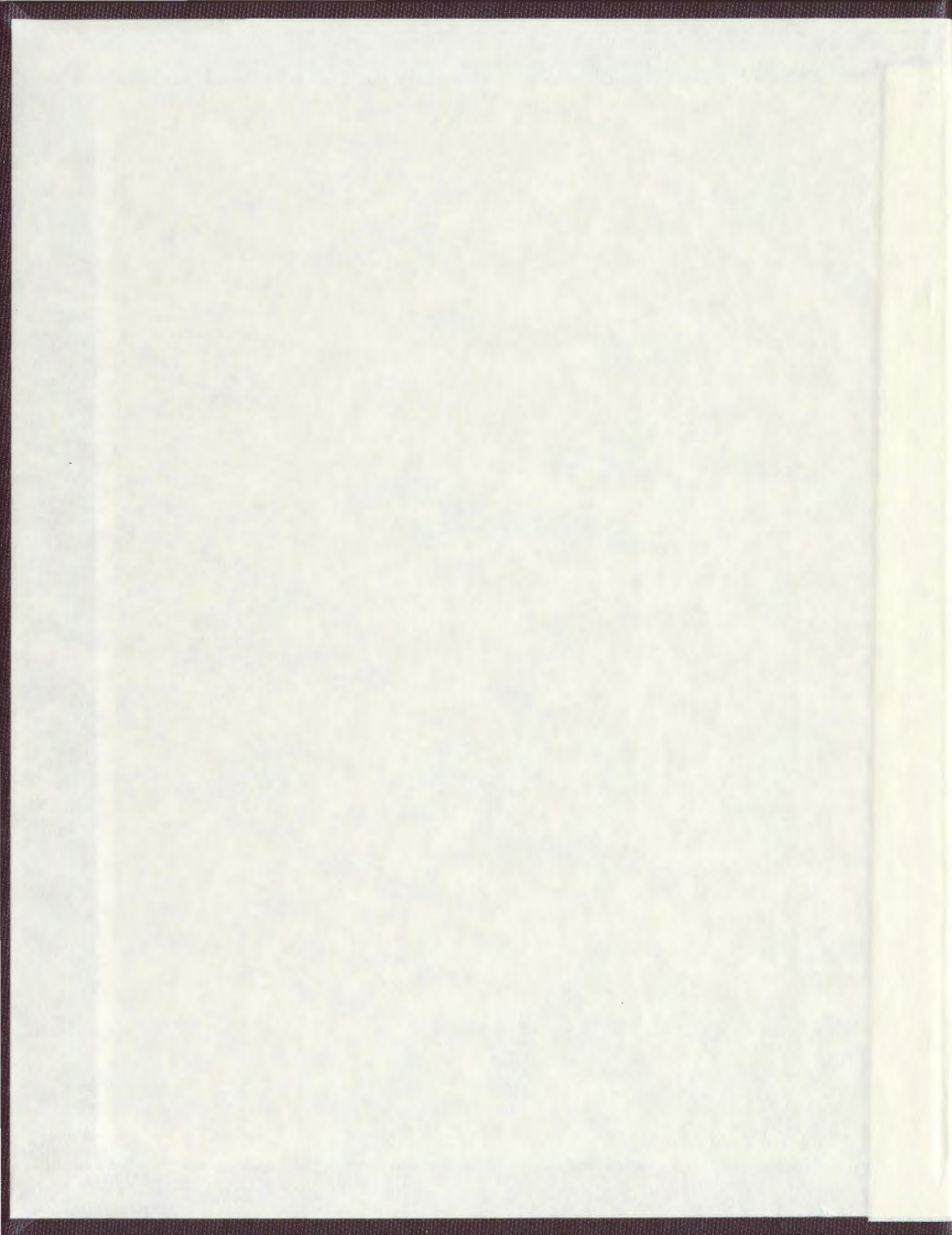
THE BASAL GABBRO SUBDIVISION AND
ASSOCIATED MAGMATIC NICKEL-COPPER
SULPHIDE MINERALIZATION OF THE PANTS LAKE
INTRUSION, LABRADOR, CANADA:
A COMBINED GEOLOGICAL, PETROLOGICAL,
GEOCHEMICAL, AND METALLOGENIC STUDY

CENTRE FOR NEWFOUNDLAND STUDIES

**TOTAL OF 10 PAGES ONLY
MAY BE XEROXED**

(Without Author's Permission)

RODERICK L. SMITH



The Basal Gabbro Subdivision and Associated Magmatic
Nickel-Copper Sulphide Mineralization of the
Pants Lake Intrusion, Labrador, Canada:

A Combined Geological, Petrological, Geochemical, and
Metallogenic Study

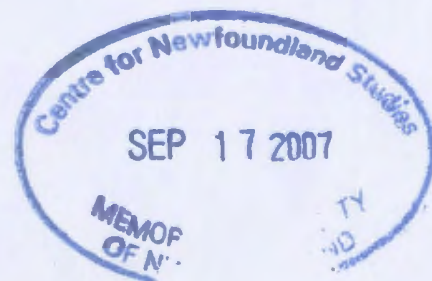
by

© Roderick L. Smith, B.Sc. (Hons.), P.Geo.

*A Thesis Submitted to the School of Graduate Studies in
Partial Fulfillment of the Requirements for the Degree
of Master of Science*

*Department of Earth Sciences
Memorial University of Newfoundland
St. John's, Newfoundland*

2006





Library and
Archives Canada

Bibliothèque et
Archives Canada

Published Heritage
Branch

Direction du
Patrimoine de l'édition

978-0-494-19398-3

395 Wellington Street
Ottawa ON K1A 0N4
Canada

395, rue Wellington
Ottawa ON K1A 0N4
Canada

Your file *Votre référence*

ISBN:

Our file *Notre référence*

ISBN:

NOTICE:

The author has granted a non-exclusive license allowing Library and Archives Canada to reproduce, publish, archive, preserve, conserve, communicate to the public by telecommunication or on the Internet, loan, distribute and sell theses worldwide, for commercial or non-commercial purposes, in microform, paper, electronic and/or any other formats.

The author retains copyright ownership and moral rights in this thesis. Neither the thesis nor substantial extracts from it may be printed or otherwise reproduced without the author's permission.

AVIS:

L'auteur a accordé une licence non exclusive permettant à la Bibliothèque et Archives Canada de reproduire, publier, archiver, sauvegarder, conserver, transmettre au public par télécommunication ou par l'Internet, prêter, distribuer et vendre des thèses partout dans le monde, à des fins commerciales ou autres, sur support microforme, papier, électronique et/ou autres formats.

L'auteur conserve la propriété du droit d'auteur et des droits moraux qui protègent cette thèse. Ni la thèse ni des extraits substantiels de celle-ci ne doivent être imprimés ou autrement reproduits sans son autorisation.

In compliance with the Canadian Privacy Act some supporting forms may have been removed from this thesis.

Conformément à la loi canadienne sur la protection de la vie privée, quelques formulaires secondaires ont été enlevés de cette thèse.

While these forms may be included in the document page count, their removal does not represent any loss of content from the thesis.

Bien que ces formulaires aient inclus dans la pagination, il n'y aura aucun contenu manquant.


Canada



Frontispiece: Exploration camp located on the southwestern shore of Pants Lake, Labrador. Picture, viewing east from a helicopter, photographed during late August 1998.

Abstract

The Pants Lake Intrusion (PLI), located in northern Labrador, represents an early phase of the 1.34 to 1.29 billion-year Nain Plutonic Suite that is located amongst the 1.45 to 1.46 billion-year old Harp Lake Intrusive Suite, the 1.85 billion-year Nain-Churchill Province suture zone, and the 2.78 to 1.74 billion-year Churchill Province which actually hosts the intrusion. The early evolution of the Pants Lake Intrusion is similar to that described for the Voisey's Bay Intrusion.

The PLI is composed of two separate intrusions termed the North and South Pants Lake Intrusion. A U/Pb zircon and baddeleyite igneous crystallization age of 1322.2 ± 2 million years was derived from the north intrusion, whereas a U/Pb baddeleyite igneous crystallization age of 1337 ± 2 million years was derived from the south intrusion. Apart from geographical proximity, and common origin and host, the north and south intrusions do not share many characteristics; in fact, the north intrusion intrudes the south intrusion.

The South Pants Lake Intrusion, located in the southern part of the study area, is a weakly layered mafic body that intrudes the Harp Lake Intrusive Suite. The south intrusion is characterized by olivine cumulate-textured peridotite and troctolite compositions, high MgO abundances (up to 21 wt %), elevated light rare earth elements, positive Eu anomalies ($\text{Eu}/\text{Eu}^* = 1.19$), and Ce/Yb ratios that resembles the range reported for the troctolites of the Voisey's Bay Intrusion ($\text{Ce}/\text{Yb} = 26-31$).

Disseminated, blotchy, net, and less abundant massive textured sulphides are widespread in the south intrusion and are dominated by pyrrhotite with lesser chalcopyrite and pentlandite. Nickel tenors of the sulphide minerals are slightly elevated compared to those in the north intrusion due to the greater percentage of nickel available to partition into the localized sulphide liquid (as indicated by the elevated modal olivine). Sulphur isotopic ratios of sulphide mineral separates from the south intrusion range from -5.25 to -1.99 ‰, indicating the influence of the local sedimentary sulphide source. Partially digested gneissic inclusions are widespread and closely resemble inclusions present in the north intrusion, as well as inclusions described from the Voisey's Bay Intrusion.

The North Pants Lake Intrusion is spatially much larger (up to 60 km^2) than the south intrusion (10 to 15 km^2). The north intrusion is a layered, horizontal to sub-horizontal, mafic sill-like body that is divided into the Upper and Basal Gabbro Subdivisions. These two subdivisions are present only in the north intrusion. Collectively the two subdivisions range from 100 to 400 meters thick, with the thickest parts present in the north part of the intrusion. The footwall contact of the intrusion is undulating and locally brecciated which aided the deposition of semi-massive to massive sulphide. Not much is known about the upper contact of the north intrusion, only that there was very little assimilation with the country rock gneiss.

Unlike the south intrusion, the north intrusion pooled in a secondary magma chamber located in the upper crust prior to its final ascension and lateral emplacement. While in the secondary magma chamber, the magma fractionated, producing a plagioclase and olivine cumulate silicate liquid. With increasing assimilation of the surrounding sulphide-bearing Tasiuyak paragneiss, as indicated by sulphur isotopic ratios of -3.33 to -1.99 ‰, sulphide saturation and subsequent production of an immiscible sulphide liquid was induced within the silicate liquid. This was followed by partitioning of nickel from the silicate magma into the available immiscible sulphide liquid ($< 650 \text{ ppm Ni}$ in olivines of the north intrusion). The first pulses of fractionated silicate liquid to enter the sill chamber formed the Upper Gabbro, followed by the denser olivine-rich liquid that formed the Basal Gabbro. The point

of entry for the silicate liquid feeding the Upper and Basal Gabbro as it entered the sill was near the northwest mapped boundary of the north intrusion. Magma injection into the northern part of the intrusion continued well after the main volume of Basal Gabbro had flowed into the sill.

As the name implies, the Upper Gabbro forms the uppermost part of the north intrusion and is the more voluminous of the two subdivisions. Variations in the mineralogy and texture of the Upper Gabbro allow for the designation of four primary subunits. These are the Altered Gabbro, Coarse- to Medium-Grained Gabbro, Pegmatitic Gabbro, and Olivine Gabbro. These subunits constitute variations in a medium- to coarse-grained gabbro, containing cumulate plagioclase with intercumulate olivine and clinopyroxene, which are typically void of visible foreign contaminants and sulphides. Chemically, the Upper Gabbro is less varied than its basal counterpart. The Upper Gabbro has slightly elevated SiO_2 , Na_2O , Al_2O_3 , CaO , Rb , and Sr contents, but much lower FeO , MgO , Ni , Cu , and S concentrations compared to the Basal Gabbro. Rare earth element patterns exhibit slightly decreasing light to heavy rare earth element patterns and an average Europium anomaly of 1.24 which is comparable to the Basal Gabbro.

The Basal Gabbro, present at the base of the North Pants Lake Intrusion, is approximately 27 meters thick and is distinguished primarily by the presence of partially digested gneissic inclusions coupled with the occurrence of magmatic-textured sulphides similar to the varied textured troctolites and basal breccia sequences described from the Voisey's Bay deposits. The Basal Gabbro is further subdivided into four primary subunits. These constitute the Transition Gabbro, Gabbro Hybrid, Olivine Gabbro, and Leopard Gabbro that collectively forms a recurring sequence present throughout the entire north intrusion. Overall, the major, trace, and rare earth element chemistry of the Basal Gabbro subunits mimics the chemistry of the Upper Gabbro, and where variations are present, they are most typically a direct consequence of gneissic and sulphide influences.

Magmatic sulphide textures observed in the Basal Gabbro vary from disseminated, blotchy, leopard, to semi-massive and massive. The leopard texture, not present in the northern part of the intrusion, indicates areas of less turbulent flow. The largest massive sulphide intersection discovered to date is 15.7 meters of 1.13 % Ni , 0.78 % Cu and 0.20 % Co . Typical massive sulphide intersections are much smaller (< 1 meter) but have similar to slightly higher grades. Pyrrhotite is the most common sulphide present in the intrusion followed by chalcopyrite and pentlandite. Pentlandite is present as small (< 1 cm) inclusions and exsolutions within the pyrrhotite. Sulphides observed in the footwall are of two types, that is, sulphides remobilized from the main sulphide mass in the Basal Gabbro and unrelated sedimentary sulphides. One remobilized footwall sulphide intersection assayed 11.75 % Ni , 9.70 % Cu and 0.43 % Co over 1.1 meters.

The North Pants Lake Intrusion is the closest analogue to intrusive rocks at the Voisey's Bay deposits recognized to date in Labrador. The present lack of identification of Voisey's Bay-like mineralization may be a function of observation level within the magmatic system. The northwestern margin of the intrusion offers the best exploration potential due to the recognition of new magma pulses, the potential feeder entry-point, and of course, spatial proximity to the most significant sulphide intersections encountered to date.

Acknowledgements

This thesis study was made possible through financial and technical support of Donner Minerals Limited. Kerry Sparkes of Donner is sincerely thanked for his personal support and interest in this study, not to mention his patience. Kerry is undoubtedly one of the world's leading mineral explorers and to work beside him was an honor.

Dr. Derek Wilton was my supervisor during the entire thesis project. Derek's support was continuously unwavering, and though at times writing was grounded to a halt, he was always able to inspire me to pick up the "pen" once more. Derek is a true mentor. He has definitely gained the privilege of assuming the title "Skipper".

During my field investigations in the summer of 1998, I obtained valuable technical and non-technical support from the geological personnel employed by Teck Exploration Ltd. (now Teck Cominco) namely Paul Moore, Guy MacGillvary, Steve House, Floyd House, Heather MacDonald, Trevor Rice, and from time to time, Dr. Tom Lane. Thanks guys!

I would also like to acknowledge the staff, faculty and students of the Earth Science Department of Memorial University who have provided great assistance towards the completion of this study. These people include Rick Soper (lapidary services), Pam King (XRF), Mike Tubrett (LAM-ICP-MS), Sean Bailey (preliminary sample preparation), Maggie Piranin (microprobe), Alison Pye (sulphur isotopes), Lakmali Hewa (ICP-MS), Dr. George Jenner, and Dr. Mark Wilson. Dan Mulrooney provided much needed and valued assistance near the very end. Dr. Steve Piercey, who is no longer a Memorial University resident, provided valuable technical support. Piercey's M.Sc. thesis was a guide for my own and will continue to be for thesis studies yet to come.

Altius Resources, in particular Roland Butler and Brian Dalton, is thanked for providing much needed time and space to allow me to finish prior to the impending deadline.

Lawrence Winter, a true and sincere friend of mine, provided constant 'heckling' to finish my thesis and during the early days, was a constant supporter of 'brown-bottle' activities, often accompanied by a good fry of moose.

My parents, Lloyd and Fran Smith, will never be thanked enough. They have provided knowledge and guidance not found in the pages of scientific literature.

I am also indebted to my wife Angie who encouraged me to finally get this thesis completed. Our paths crossed sometime during Chapter 3, and since that time our life has evolved together. I am very grateful that she is with me to share the experience of finally completing this project. We shall celebrate with a bottle of wine in due time.

This thesis study represents the most significant achievement of my academic career. However, my sons James Lloyd Smith, born on November 23, 2003 and Liam Roderick Carl Smith, born of April 18, 2004, are my greatest life achievements. To them I dedicate this thesis.

Table of Contents

| | |
|---|-------------|
| Title Page..... | I |
| Abstract..... | III |
| Acknowledgements..... | V |
| Table of Contents..... | VI |
| List of Figures..... | XI |
| List of Tables..... | XV |
| List of Plates..... | XVII |
| List of Selected Abbreviations..... | XXII |
| Map: Pants Lake Intrusion Geological Map, Vertical Longitudinal Sections, and Sulphide Occurrence Locations..... | Back Pocket |

Chapter 1: Introduction

| | | |
|-----|---|-----|
| 1.1 | Preamble..... | 1-1 |
| 1.2 | Location and Access..... | 1-4 |
| 1.3 | Physiography and Glaciation..... | 1-5 |
| 1.4 | Previous and Present Geological investigations..... | 1-6 |
| 1.5 | Field Work..... | 1-7 |
| 1.6 | Purpose and Scope of Present Study..... | 1-9 |

Chapter 2: Geological Overview of Labrador and Associated Magmatic Nickel-Copper Sulphide Mineralization

| | | |
|-----|---|------|
| 2.1 | Introduction..... | 2-1 |
| 2.2 | Geological Overview of Labrador..... | 2-2 |
| | 2.2.1 The Nain Province..... | 2-3 |
| | 2.2.2 The Superior Province..... | 2-4 |
| | 2.2.3 The Churchill Province..... | 2-4 |
| | 2.2.4 The Makkovik Province..... | 2-5 |
| | 2.2.5 The Grenville Province..... | 2-5 |
| | 2.2.6 The Nain Plutonic and Harp Lake Intrusive Suites..... | 2-6 |
| 2.3 | Magmatic Ni-Cu Sulphide Mineralization in Labrador..... | 2-7 |
| | 2.3.1 Introduction: The Voisey's Bay Ni-Cu-Co Deposit..... | 2-7 |
| | 2.3.1.1 Regional Setting of the Voisey's Bay Deposits..... | 2-8 |
| | 2.3.1.2 Geology and Mineralization of the Voisey's Bay Intrusion..... | 2-9 |
| | 2.3.2 The Cirque Prospect..... | 2-12 |
| | 2.3.3 The Krinor Prospect..... | 2-13 |
| | 2.3.4 The OKG Prospect..... | 2-14 |
| | 2.3.5 The Nain Hill Prospects..... | 2-15 |
| | 2.3.6 The Franco Prospect..... | 2-16 |
| | 2.3.7 Prospects within the Harp Lake Intrusive Suite..... | 2-17 |
| | 2.3.7.1 The A-1 Prospect..... | 2-18 |
| | 2.3.7.2 The Colette II Prospect..... | 2-18 |

| | | |
|---------|--------------------------|------|
| 2.3.7.3 | The Dart Prospect | 2-19 |
| 2.3.7.4 | The Ninety-Nine Prospect | 2-19 |
| 2.3.8 | The Baikie Prospect | 2-20 |

Chapter 3: Regional Setting, Morphology, Geology, Petrography, and Mineralization of the Pants Lake Intrusion

| | | |
|---------|--|------|
| 3.1 | Introduction | 3-1 |
| 3.2 | Regional Geological Setting of the Pants Lake Intrusion | 3-2 |
| 3.2.1 | Nain Province | 3-3 |
| 3.2.2 | Churchill Province | 3-3 |
| 3.2.3 | Nain / Churchill Province Boundary | 3-5 |
| 3.2.4 | Harp Lake Intrusive Suite | 3-5 |
| 3.2.5 | Nain Plutonic Suite | 3-6 |
| 3.2.6 | Mafic Dikes | 3-7 |
| 3.2.7 | Age of the Pants Lake Intrusion | 3-8 |
| 3.3 | Morphology of the Pants Lake Intrusion | 3-9 |
| 3.3.1 | Surface Distribution and Dimensions of the Pants Lake Intrusion | 3-9 |
| 3.3.2 | Subsurface Geometry of the Pants Lake Intrusion | 3-10 |
| 3.4 | Geology of the Pants Lake Intrusion: Previous Interpretation | 3-12 |
| 3.4.1 | Black Gabbro | 3-12 |
| 3.4.2 | Olivine Gabbro | 3-13 |
| 3.4.3 | Upper Olivine Gabbro/Gabbro | 3-14 |
| 3.5 | Geological Subdivisions and Petrography of the Pants Lake Intrusion | 3-14 |
| 3.5.1 | The Upper Gabbro Subdivision of the Pants Lake Intrusion | 3-16 |
| 3.5.1.1 | Coarse- to Medium-Grained Gabbro | 3-17 |
| 3.5.1.2 | Olivine Gabbro | 3-19 |
| 3.5.1.3 | Pegmatitic Gabbro | 3-20 |
| 3.5.1.4 | Altered Coarse-Grained Gabbro | 3-21 |
| 3.5.2 | The Basal Gabbro Subdivision of the Pants Lake Intrusion | 3-22 |
| 3.5.2.1 | Transition Gabbro | 3-24 |
| 3.5.2.2 | Gabbro Hybrid | 3-26 |
| 3.5.2.3 | Olivine Gabbro | 3-29 |
| 3.5.2.4 | Leopard-Textured Gabbro | 3-30 |
| 3.5.2.5 | Medium-Grained Gabbro | 3-32 |
| 3.5.2.6 | Contact Gneiss | 3-33 |
| 3.6 | Mineralogy, Textural Variations, Distribution and Petrography of Sulphide Minerals from the Pants Lake Intrusion and surrounding Country Rocks | 3-34 |
| 3.6.1 | Disseminated Sulphide | 3-35 |
| 3.6.2 | Blotchy Sulphide | 3-36 |
| 3.6.3 | Leopard-Textured Sulphide | 3-38 |
| 3.6.4 | Semi-Massive Sulphide | 3-39 |
| 3.6.5 | Massive Sulphide | 3-40 |
| 3.6.6 | Remobilized Sulphides | 3-41 |

| | | |
|-------|---|------|
| 3.7 | Surface Sulphide Occurrences associated with the Pants Lake Intrusion | 3-43 |
| 3.7.1 | NDT Sulphide Occurrences | 3-44 |
| 3.7.2 | Happy Face Lake Sulphide Occurrence | 3-46 |
| 3.7.3 | GG Sulphide Occurrence | 3-48 |
| 3.7.4 | Mineral Hill Sulphide Occurrence | 3-50 |

Chapter 4: Major, Trace, and Rare Earth Element Geochemistry

| | | |
|---------|--|------|
| 4.1 | Introduction | 4-1 |
| 4.2 | Major and Trace Element Geochemistry | 4-2 |
| 4.2.1 | Upper Gabbro Subdivision | 4-3 |
| 4.2.1.1 | Discrimination-Type Diagrams | 4-3 |
| 4.2.1.2 | MgO versus Major Element Plots | 4-4 |
| 4.2.1.3 | MgO versus Trace Element Plots | 4-5 |
| 4.2.2 | Basal Gabbro Subdivision | 4-6 |
| 4.2.2.1 | Discrimination-Type Diagrams | 4-6 |
| 4.2.2.2 | MgO versus Major Element Plots | 4-9 |
| 4.2.2.3 | MgO versus Trace Element Plots | 4-12 |
| 4.2.3 | Mafic Dikes | 4-15 |
| 4.2.3.1 | Discrimination-Type Diagrams | 4-15 |
| 4.2.3.2 | MgO versus Major Element Plots | 4-16 |
| 4.2.3.3 | MgO versus Trace Element Plots | 4-17 |
| 4.2.4 | Churchill Province Gneiss | 4-17 |
| 4.2.4.1 | Discrimination-Type Diagrams | 4-17 |
| 4.2.5 | Element Distribution and Contamination Effects | 4-19 |
| 4.2.5.1 | Internal Stratigraphic Variations in Elemental Abundances | 4-19 |
| 4.2.5.2 | Spatial Variations of Elemental Abundance | 4-21 |
| 4.3 | Rare Earth Element Geochemistry | 4-24 |
| 4.3.1 | REE Geochemistry in this Study | 4-25 |
| 4.3.1.1 | Primitive Mantle Normalized REE Diagrams | 4-26 |
| 4.3.1.2 | Multi-Element Normalized Diagram | 4-28 |
| 4.4 | Contamination Trends using Major, Trace and REE Geochemistry | 4-30 |
| 4.5 | Olivine Geochemistry of the Pants Lake Intrusion | 4-33 |
| 4.5.1 | Introduction to LAM-ICP-MS Technique | 4-33 |
| 4.5.2 | Olivine Geochemistry in this Study | 4-34 |
| 4.5.3 | Results of Olivine Geochemistry Study | 4-35 |
| 4.6 | Metal Tenor and Distribution within the Pants Lake Intrusion | 4-38 |
| 4.6.1 | Metal Tenor | 4-39 |
| 4.6.2 | Metal Distribution | 4-40 |

Chapter 5: Sulphur Isotope Geochemistry

| | | |
|-----|---|-----|
| 5.1 | Introduction | 5-1 |
| 5.2 | Notations and Theory | 5-1 |
| 5.3 | Sample Locations | 5-3 |
| 5.4 | Analytical Results | 5-4 |
| 5.5 | Comparison of Results to Regional Sulphur Isotope Studies | 5-5 |

Chapter 6: Discussion and Conclusions

| | | |
|-----|-----------------------|------|
| 6.1 | Discussion | 6-1 |
| 6.2 | Conclusions | 6-10 |
| 6.3 | Recommendations | 6-12 |

Appendix A: Diamond Drill Hole and Sample Data

| | | |
|------------|---|-----|
| Table A.1. | Diamond drill hole information for re-logged drill cores utilized in M.Sc study by the author. Drill hole information obtained from Fitzpatrick <i>et al.</i> (1999). Sample information located in Table A.2 | A-2 |
|------------|---|-----|

| | | |
|------------|--|-----|
| Table A.2. | Sample checklist pertaining to the analysis and preparation of samples collected from diamond drill core by the author | A-3 |
|------------|--|-----|

| | | |
|------------|--|-----|
| Table A.3. | Sample checklist pertaining to the analysis and preparation of samples collected from drill core by other sources and obtained by the author | A-7 |
|------------|--|-----|

Appendix B: Geochemical Results, Analytical Procedures, Precision, and Accuracy

| | | |
|------------|---|------|
| B.1.1 | XRF (pressed pellet) – Analytical Technique | B-2 |
| B.1.2 | XRF (pressed pellet) – Precision and Accuracy | B-21 |
| B.2.1 | ICP-MS – Analytical Technique | B-22 |
| B.2.2 | ICP-MS – Precision and Accuracy | B-26 |
| B.3.1 | LAM-ICP-MS – Analytical Technique | B-27 |
| B.3.2 | LAM-ICP-MS – Precision and Accuracy | B-30 |
| B.4.1 | Sulphur Isotope Analysis – Analytical Technique | B-31 |
| B.4.2 | Sulphur Isotope Analysis – Precision and Accuracy | B-33 |
| Table B.1. | MUN –XRF pressed pellet data. Major elements are reported in wt %, all other elements reported in ppm | B-3 |
| Table B.2. | MUN ICP-MS analytical data. All results reported in ppm | B-23 |

Table B.3 LAM-ICP-MS data of olivine grains from diamond drill holes SVB-97-91, SVB-96-04, SVB-98-102, and SVB-96-09. Major element data reported in wt%, trace element data reported in ppm. < indicates below detection limits..... B-28

Table B.4. Sulphur isotope character of magmatic sulphides from the Basal Gabbro Subdivision of the Pants Lake Intrusion, Churchill Province gneiss, and footwall anorthosite (unknown affinity). The mean and standard deviation of each sample population is reported in Section 5.4 (Analytical Results). (* Indicates duplicate sample taken)..... B-32

Appendix C: Logs of Diamond Drill Holes used in Study

| | |
|-----------------|------|
| SVB-96-02..... | C-2 |
| SVB-96-04..... | C-3 |
| SVB-96-07..... | C-4 |
| SVB-96-08..... | C-5 |
| SVB-96-09..... | C-6 |
| SVB-96-10..... | C-7 |
| SVB-96-15..... | C-8 |
| SVB-96-16..... | C-9 |
| SVB-96-17..... | C-11 |
| SVB-96-20..... | C-12 |
| SVB-96-27..... | C-13 |
| SVB-96-29..... | C-14 |
| SVB-96-34..... | C-16 |
| SVB-96-36..... | C-17 |
| SVB-96-44..... | C-18 |
| SVB-96-47..... | C-19 |
| SVB-96-48..... | C-20 |
| SVB-96-52..... | C-21 |
| SVB-96-53..... | C-23 |
| SVB-97-57..... | C-24 |
| SVB-97-58..... | C-25 |
| SVB-97-59..... | C-27 |
| SVB-97-60..... | C-29 |
| SVB-97-61..... | C-30 |
| SVB-97-68..... | C-31 |
| SVB-97-69..... | C-32 |
| SVB-97-73..... | C-33 |
| SVB-97-79..... | C-34 |
| SVB-97-81..... | C-36 |
| SVB-97-91..... | C-37 |
| SVB-97-92..... | C-38 |
| SVB-98-102..... | C-39 |
| SVB-98-113..... | C-41 |
| SVB-98-116..... | C-43 |

Appendix D: Geochronological Reports

| | |
|---|-----|
| Report on the U/Pb Zircon + Baddeleyite Age of Crystallization of sample SVB97-67, 150M from South Voisey's Bay | D-2 |
| Report on U/Pb Geochronology for Sample SVB-97-79 | D-6 |

List of Figures

| | |
|---|------|
| <p>Figure 1.1. Locations of the South Voisey's Bay Project and Voisey's Bay deposits compared to the Precambrian structural Provinces of Labrador (after Greene, 1972), Nain Plutonic Suite (NPS) and Harp Lake Intrusive Suite (HLIS). The inset box illustrates the outline of the South Voisey's Bay Project boundary (as of January 30, 1999). The area inside the dashed line of the inset box represents the coverage of the Pants Lake Intrusion geological map (see inside back cover).....</p> | 1-10 |
| <p>Figure 2.1. Structural Provinces of the North American-Greenland-Baltic Shields with associated ages (modified after Hoffman, 1988). Labrador consists of the North American Shield and the North Atlantic Craton.....</p> | 2-24 |
| <p>Figure 2.2. Principle tectonic elements of northern Labrador and adjacent north-eastern Quebec (James, 1997). Only portions of the Makkovik and Grenville Provinces are shown.....</p> | 2-24 |
| <p>Figure 2.3. Geology of northern Labrador (modified after Kerr and Smith, 1997). The Pants Lake Intrusion is situated between the southern mapped boundary of the NPS, the northern mapped boundary of the HLIS, and the western side of the proposed structural boundary of the Nain / Churchill provinces. The circled stars indicate the location of selected magmatic Ni-Cu sulphide prospects in northern Labrador. All of these prospects, including the Voisey's Bay deposits, are discussed in Section 2.3.....</p> | 2-25 |
| <p>Figure 2.4. Geological map of the area north of Voisey's Bay, Labrador (modified after Lightfoot, 1998). The Voisey's Bay deposits, hosted in the Voisey's Bay Intrusion, are projected to surface....</p> | 2-27 |
| <p>Figure 2.5. Surface projection of the troctolite-gabbroic rocks, sulphide zones, and major structural elements associated with the Voisey's Bay deposits (Evans-Lamswood, 2000). The location and surrounding geology of this figure is shown in Figure 2.4.....</p> | 2-28 |
| <p>Figure 2.6. Voisey's Bay sulphide mineralization projected to a vertical longitudinal section (Lightfoot and Naldrett, 1999). The conduit assemblage shown in this figure is equivalent to the Feeder Troctolite in Figure 2.5.....</p> | 2-28 |
| <p>Figure 3.1. Principle geographic components of the Pants Lake Intrusion (outlined by a black, dashed line). The mineralized regions (outlined by a black, dotted line) are the areas where diamond drilling has been concentrated, and where sulphide occurrences crop out at surface. These mineralized regions are the primary focus of this study. See geological map (inside, back cover) for an explanation of the geological units.....</p> | 3-51 |
| <p>Figure 3.2. Basal contact topography, relative to sea level, of the North and Central gabbros. All contours constructed using drill hole information from Fitzpatrick <i>et al.</i> (1999).....</p> | 3-52 |
| <p>Figure 3.3. Three-dimensional view of the Pants Lake Intrusion. See Pants Lake Intrusion geological map for section locations and unit explanations (inside, back cover).....</p> | 3-52 |
| <p>Figure 3.4. Idealized cross-section through the Upper gabbro subdivision of the Pants Lake intrusion. The subunits belonging to the Upper Gabbro are shown in their relative position as they would occur in drill core or outcrop. These subunits are not always present in all drill cores or outcrops.....</p> | 3-54 |
| <p>Figure 3.5. Idealized drill log through the Basal Gabbro subdivision of the Pants Lake Intrusion. The subunits are shown in their relative position, as they would normally appear in core or outcrop. The dashed lines represent the contacts between the subunits and also serve to illustrate the general thickness of each subunit layer.....</p> | 3-54 |

| | |
|--|------|
| Figure 3.6. Outline of the Pants Lake Intrusion with the locations of diamond drill holes (DDH) and re-logged drill holes used for this study. The * indicates the presence of each Basal Gabbro subunit in the re-logged diamond drill holes. Figure 3.6a indicates the location of the Transition gabbro subunit, Figure 3.6b indicates the location of the Gabbro Hybrid subunit, Figure 3.6c indicates the location of the Fine-Grained Olivine Gabbro / Troctolite subunit, Figure 3.6d indicates the location of the Leopard Textured Gabbro subunit, and 3.6e indicates the Medium-Grained Gabbro and Peridotite subunit..... | 3-55 |
| Figure 3.7. Sulphide textural variations observed in the Basal Gabbro subdivision of the Pants Lake Intrusion, Labrador. The numbered columns represent a select range of variations that exist throughout the intrusion. The most consistent sulphide textures, with respect to the relative position above the basement contact, are the leopard / net textured sulphide and the massive to semi-massive textured sulphide. The leopard / net textured sulphide is consistently situated near the center of the Basal Gabbro subdivision. The massive to semi-massive textured sulphide is consistently situated adjacent to, or just above, the basement contact. The subunits of the Basal Gabbro subdivision, depicted in Figure 3.5, are presented in this figure to illustrate the association between sulphide texture and host. The location of the different sulphide textures observed in the re-logged drill cores are noted in Figures 3.8 a, b, c, d, e, and f..... | 3-57 |
| Figure 3.8. Outline of the Pants Lake Intrusion with the locations of diamond drill holes (DDH) and re-logged DDH used for this study. The * indicates the presence of each sulphide textural variation in the re-logged DDH. Figure 3.8a indicates the presence of disseminated textured sulphide, Figure 3.8b indicates the presence of blotchy textured sulphide, Figure 3.8c indicates the presence of leopard / net textured sulphide, Figure 3.8d indicates the presence of semi-massive textured sulphide, Figure 3.8e indicates the presence of massive textured sulphide, and Figure 3.8e indicates the presence of remobilized sulphide..... | 3-58 |
| Figure 3.9. Local geology hosting the NDT sulphide occurrences. Refer to the enclosed geology map for location of figure..... | 3-74 |
| Figure 3.10. Local geology of the Happy Face Lake sulphide occurrence. Refer to the enclosed geology map for location of figure..... | 3-75 |
| Figure 3.11. Local geology of the GG sulphide occurrence. Refer to the enclosed geology map for location of figure..... | 3-76 |
| Figure 3.12. Local geology of the Mineral Hill sulphide occurrence. Refer to the enclosed geology map for location of figure..... | 3-78 |
| Figure 4.1. Total alkalis (Na ₂ O + K ₂ O) vs. SiO ₂ plot, with alkaline and subalkaline fields (Irvine and Baragar, 1971). This plot illustrates the difficulty in using SiO ₂ data obtained by the X-ray Fluorescence (XRF) method on pressed pellets. The Pants Lake Intrusion (PLI) samples (this study) clearly plot in the alkaline field as do PLI samples from Wilson (1998) (blue outline); both sets of samples were analyzed using pressed pellets. Using the same set of samples from Wilson (1998), samples analyzed using the XRF method on fused disks (red outline) clearly plotted in the subalkaline field. This suggest that SiO ₂ values are substantially lower using pressed pellets compared to fused disks, however Na ₂ O and K ₂ O concentrations remain relatively equal regardless of method. The plot in the lower right corner of the larger plot further illustrates the deviation of SiO ₂ using pressed pellet..... | 4-42 |
| Figure 4.2. Discrimination diagrams for rocks belonging to the Upper Gabbro (undifferentiated), (a) Winchester and Floyd (1977), (b) Irvine and Baragar (1971) and (c) Jensen (1976)..... | 4-43 |
| Figure 4.3. MgO versus major element plots of the Upper Gabbro subdivision including (a) SiO ₂ , (b) FeO*, (c) Na ₂ O, (d) TiO ₂ , (e) CaO, (f) Al ₂ O ₃ , (g) MnO, and (h) K ₂ O..... | 4-44 |

| | |
|--|------|
| Figure 4.4. MgO versus trace element plots of the Upper Gabbro including (a) Cr, (b) Ga, (c) Sr, (d) Rb, (e) V, (f) Cu, (g) Ni and, (h) S..... | 4-46 |
| Figure 4.5. Discrimination diagrams for rocks belonging to the subunits of the Basal Gabbro, Churchill Province gneiss, and footwall anorthosite, (a) Winchester and Floyd (1977), (b) Irvine and Baragar and, (c) Jensen (1976). The Upper Gabbro field is plotted on each diagram for reference. Individual samples are outlined with a small circle of the same field color (see Figure 4.5c for example)..... | 4-47 |
| Figure 4.6. MgO versus major element plots of rocks belonging to the subunits of the Basal Gabbro including (a) SiO ₂ , (b) FeO*, (c) Na ₂ O, (d) TiO ₂ , (e) CaO, (f) Al ₂ O ₃ , (g) MnO and, (h) K ₂ O. The Upper Gabbro field is included in each plot..... | 4-48 |
| Figure 4.7. MgO versus trace element plots of rocks belonging to the subunits of the Basal Gabbro including (a) Cr, (b) Ga, (c) Sr, (d) Rb, (e) V, (f) log Cu, (g) log Ni and, (h) log S. The Upper Gabbro field is included in each plot..... | 4-51 |
| Figure 4.8 Discrimination diagrams for footwall mafic diabase dikes including (a) Winchester and Floyd (1977), Irvine and Baragar (1971) and, (c) Jensen (1976)..... | 4-54 |
| Figure 4.9. MgO versus major element plots of mafic diabase dikes including (a) SiO ₂ , (b) FeO*, (c) Na ₂ O, (d) TiO ₂ , (e) CaO, (f) Al ₂ O ₃ , (g) MnO and, (h) K ₂ O..... | 4-55 |
| Figure 4.10. MgO versus trace element plots of mafic diabase dikes including (a) Cr, (b) Ga, (c) Sr, (d) Rb, (e) V, (f) Cu, (g) Ni and, (h) S..... | 4-57 |
| Figure 4.11. Calculated mean concentrations, presented as histograms, of major and trace element chemistry of Upper Gabbro (undifferentiated), Basal Gabbro (subunits defined), Churchill Province, and mafic dike samples. The placement of the sample categories is based on their relative location in the PLI stratigraphy defined in Chapter 3 (see Table 3.2 and Figure 3.5)..... | 4-58 |
| Figure 4.12. (A) Average major element abundances for the Upper Gabbro sample suite. (B) Average trace element abundances for the Upper Gabbro sample suite. (C) Average major element abundances for the Transition Gabbro sample suite. (D) Average trace element abundances for the Transition Gabbro sample suite. (E) Average major element abundances for the Gabbro Hybrid sample suite. (F) Average trace element abundances for the Gabbro Hybrid sample suite. (G) Average major element abundances for the Olivine Gabbro sample suite. (H) Average trace element abundances for the Olivine Gabbro sample suite. (I) Average major element abundances for the Leopard Gabbro sample suite. (J) Average trace element abundances for the Leopard Gabbro sample suite. (K) Average major element abundances for the Medium-grained Gabbro sample suite. (L) Average trace element abundances for the Medium-grained Gabbro sample suite. (M) Average major element abundances for the Churchill Province sample suite. (N) Average trace element abundances for the Churchill Province sample suite..... | 4-59 |
| Figure 4.13. Primitive mantle normalized REE diagrams for rocks belonging to the (a) Upper Gabbro subdivision, (b) Basal Gabbro subdivision, and (c) Churchill Province (CP) gneiss, Mafic dikes, and Semi-massive (SM) sulphide. The legend for the symbols utilized in each diagram is illustrated in Figure 4.14. Figure 4.13d illustrates the fields from each REE plot for comparative reasons. Normalizing values from Sun and McDonough (1989)..... | 4-73 |
| Figure 4.14. Primitive mantle normalized extended trace element plots after Sun and McDonough (1989) for rocks belonging to the (a) Upper Gabbro subdivision, PLI, (b) Basal Gabbro subdivision, PLI (c) Churchill Province (CP) gneiss, and (d) Voisey's Bay Intrusion and Mushuau Intrusion (after Lightfoot <i>et al.</i> , 2000)..... | 4-74 |

| | |
|--|------|
| Figure 4.15. Selected major and trace element plots for samples of the Churchill Province, PLI, and mafic dikes. These plots illustrate the effects of gneissic contamination. (a) [CaO wt% + (Sr x 10 ppm)] versus [Log K ₂ O wt% + (Rb x 10 ppm)], (b) [Log Zr ppm] versus [K ₂ O wt%], (c) [Log Cr ppm] versus [Log Rb ppm], and (d) [Log Rb ppm] versus [Log (Y + Nb ppm)]..... | 4-76 |
| Figure 4.16. Variations in Ce versus Yb illustrating compositional differences in magmas and the extent of crustal contamination. See text for explanation of abbreviations. The Ce and Yb data from Voisey's Bay is taken from Li et al. (2000)..... | 4-77 |
| Figure 4.17. Plot of Th / Nb versus La / Sm ratios for rocks of the Pants Lake Intrusion, country rocks, and footwall mafic dikes. The trend of troctolitic rocks of the Voisey's Bay intrusion are included in the diagram (after Li et al., 2000)..... | 4-77 |
| Figure 4.18. Outline of the Pants Lake Intrusion showing the collar location of the diamond drill holes (DDH) utilized for the olivine study..... | 4-78 |
| Figure 4.19. Diamond drill hole profiles with sample locations and names, and the number of olivine grains ablated for study..... | 4-78 |
| Figure 4.20. Depth profiles of diamond drill holes (DDH's) SVB-96-04, SVB-96-09, SVB-98-102, and SVB-97-91 plotted against average Forsterite (Fo) and Ni in olivines from the Pants Lake Intrusion. Refer to Figure 4.19 for sample names and Table 4.11 for average values..... | 4-80 |
| Figure 4.21. Mole percent Forsterite (Fo) and Ni contents of olivine grains from the Pants Lake Intrusion (this study; Naldrett, 1999) along with data for olivines collected within the Voisey's Bay and Mushuau Intrusions (after Li et al., 2000). See Table 4.11 for a summary of the average element and mole % Fo abundances of olivines used in this study. The fractionation curves were modeled by Naldrett (op cit) in his study of olivine grains in the South Voisey Bay area and are utilized in this diagram as a means of comparison with data from this study..... | 4-81 |
| Figure 4.22. Metal contents (Ni and Cu) of rocks belonging to the Pants Lake Intrusion. (A) Log plot of Ni (ppm) versus Cu (ppm) of Upper Gabbro (green circles) and Basal Gabbro (red squares). (B) Log plots of Ni (ppm) versus Cu (ppm) of Basal Gabbro samples from the mineralized regions throughout the PLI (refer to Figure 3.1). Both plots show a general trend of Ni:Cu = 1..... | 4-82 |
| Figure 4.23. Dot plot graphs depicting Ni and Cu distribution throughout the Upper and Basal Gabbro subdivisions within the Pants Lake Intrusion. (A) Dot plot of Ni in Upper Gabbro rocks. (B) Dot plot of Cu in Upper Gabbro rocks. (C) Dot plot of Ni in Basal Gabbro rocks. (D) Dot plot of Cu in Basal Gabbro. See text for explanation of population intervals..... | 4-84 |
| Figure 5.1. Sulphur isotopic variations in nature, expressed as $\delta^{34}\text{S}$ (Ohmoto and Rye, 1978)..... | 5-7 |
| Figure 5.2. Sulphur isotope ranges of sulphide separates from the Basal Gabbro Subdivision (BGS) of the Pants Lake Intrusion, potential sulphur contaminants, and magmatic Ni-Cu prospects located throughout the Nain Plutonic Suite and the Harp Lake Intrusive Suite. Isotope ranges are expressed as per mil. Refer to Table 5.1 and Table B.4 for isotope data and sources..... | 5-7 |
| Figure 5.3. Geology of northern Labrador (modified after Kerr and Smith, 1997) (see Figure 2.3) with locations of regional sulphur isotope data reported in this study. The majority of the prospects shown in this figure are detailed in Section 2.3. The NBK and Ed prospects, not included in Section 2.3, are detailed by Piercey (1988) and Kerr and Smith (2000), respectively..... | 5-9 |
| Figure 6.1. Proposed model developed by the author for the formation of the Basal Gabbro Subdivision of the Pants Lake Intrusion, Labrador. Many components of this model are adopted from studies by MacDonald (1999), Kerr (1998, 2003), and Barnes and Maier (1999)..... | 6-15 |

List of Tables

| | |
|---|------|
| Table 2.1. Summary table of selected magmatic Ni-Cu sulphide prospects/deposits located in Labrador. See Figure 2.3 for the location of each prospect. Refer to Section 2.3 for a condensed description of each prospect named below..... | 2-26 |
| Table 3.1. Summary table of ages reported for selected mafic intrusions of the Nain Plutonic Suite. Included with this table are ages reported in the section entitled 'Regional Geological Setting of the Pants Lake Intrusion' (Section 3.2) of the various geological elements surrounding the Pants Lake Intrusion..... | 3-50 |
| Table 3.2. Geographic components of the Pants Lake Intrusion. Different parts of the Pants Lake Intrusion were originally mapped by Hill (1982) and Thomas and Morrison (1991). The entire Pants Lake Intrusion was mapped by Donner Minerals Ltd and Teck Exploration Ltd. Descriptions and nomenclature of the various subunits of the Pants Lake Intrusion are reported by Fitzpatrick <i>et al.</i> (1999) and by MacDonald (1999). The nomenclature used by Smith (this study) is analogous to the nomenclature utilized by Fitzpatrick <i>et al.</i> (1999) and by MacDonald (1999). The flow chart at the bottom of this table summarizes the components, the subdivisions, and the subunits of the Pants Lake Intrusion utilized by Smith (this study)..... | 3-53 |
| Table 4.1. Major element ranges (reported in wt %) of Upper Gabbro samples..... | 4-45 |
| Table 4.2. Trace element ranges (reported in ppm) of Upper Gabbro samples..... | 4-45 |
| Table 4.3. Major element ranges (reported in wt %) of Basal Gabbro samples..... | 4-50 |
| Table 4.4. Trace element ranges (reported in ppm) of Basal Gabbro samples..... | 4-53 |
| Table 4.5. Major element ranges (reported in wt %) of Mafic Dike samples..... | 4-56 |
| Table 4.6. Trace element ranges (reported in ppm) of Mafic Dike samples..... | 4-56 |
| Table 4.7. Average major element (reported in wt %) and trace element (reported in ppm) compositions of rocks from the mineralized regions (see Figure 3.1) within the Upper Gabbro (Up Gabbro) of the Pants Lake Intrusion (subunits are undifferentiated). Average values calculated from the analytical results of samples reported in Appendix B..... | 4-66 |
| Table 4.8. Average major element (reported in wt %) and trace element (reported in ppm) compositions of rocks from the mineralized regions (see Figure 3.1) within the Basal Gabbro of the Pants Lake Intrusion. Tr Gabbro indicates the Transition Gabbro subunit. Average values calculated from the analytical results of samples reported in Appendix B. G Hybrid indicates the Gabbro Hybrid subunit. LT Gabbro indicates the Leopard Textured Gabbro subunit, and SM Sulphide indicates Semi-Massive Sulphide. Ol Gabbro indicates the Olivine Gabbro subunit. MG Gabbro indicates the Medium-Grained Gabbro subunit..... | 4-67 |
| Table 4.9. Average major element (reported in wt %) and trace element (reported in ppm) compositions of samples from footwall mafic dikes (FW dike) and Churchill Province gneisses (CP gneiss) within the mineralized regions of the Pants Lake Intrusion. Average values calculated from the analytical results of samples reported in Appendix B..... | 4-72 |
| Table 4.10. Rare earth element ratios for rock types of the Pants Lake Intrusion, Churchill Province gneiss, and footwall mafic dikes. Normalization values are from Sun and McDonough (1989). The Europium Anomaly (<i>ie.</i> Eu/Eu*) was calculated using the formula suggested by Taylor and McLennan (1985)..... | 4-75 |

Table 4.11. Summary data of average element and calculated average mole % forsterite (Fo) abundances for olivine grains from selected drill core samples throughout the Pants Lake Intrusion (see Figures 4.18 and 4.19 for sample locations and Table B.3 for the complete data set). The mole % forsterite abundances were calculated using an online calculator for this purpose following the calculations of Sack and Ghiorso (1989), and Hirschmann (1991). Sample names followed by an * indicate Upper Gabbro samples, all other samples are Basal Gabbro.....4-79

Table 4.12. Summary of average Ni and Cu concentrations determined by the XRF technique at Memorial University of Upper and Basal Gabbro drill core samples located throughout the Pants Lake Intrusion (refer to Figure 3.1 for locations). Ni and Cu in 100% sulphide are calculated following the formula suggested by Kerr (1999).....4-83

Table 5.1. Summary of the sulphur isotope ranges from selected Labrador Sulphide prospects within the Nain Plutonic Suite (NPS) and the Harp Lake Intrusive Suite (HLIS). Isotope values obtained from the Tasiuyak gneiss (Churchill Province), Nain Province gneiss, and Churchill Province gneiss are also given. Figure 5.2 illustrates and compares the isotope range of each prospect and geological entity.....5-8

List of Plates

- Frontispiece: Exploration camp located on the southwestern shore of Pants Lake, Labrador. Picture, viewing east from a helicopter, photographed during late August 1998..... II
- Plate 3.1. Outcrop exposure near the Major General sulphide occurrence. This plate shows the typical weathered surface of a coarse-grained, leucocratic gabbro subunit. A small patch of the pegmatitic gabbro subunit is located near the lower edge of the photo. Both subunits belong to the Upper Gabbro. The contact between the two subunits is subtle. The cumulate plagioclase grains are tan to buff white. The interstitial clinopyroxene (\pm olivine) grains are dark green to black. The scale bar is in centimeters.....3-60
- Plate 3.2. Drill core segments from drill hole, SVB-96-16. Core segment A, taken at 3.6m, is a typical example of the coarse-grained, cumulate textured leucocratic gabbro belonging to the Coarse to Medium-grained Gabbro Subunit. Core segment B, taken at 8.9m, is a typical example of a pegmatitic gabbro belonging to the Pegmatitic Gabbro subunit. Core segment C, taken at 35.2m, is a typical example of the medium-grained, cumulate textured gabbro belonging to the Coarse to Medium-grained Gabbro Subunit. Plagioclase grains are dull white and clinopyroxene grains are black. The scale bar is in centimeters.....3-60
- Plate 3.3. Petrographic section from drill hole SVB-97-27 at 1.3m (magnification = 1.5x, cross polarized light). Leucocratic, coarse to medium-grained gabbro belonging to the Coarse to Medium-grained subunit (Upper Gabbro subdivision). Euhedral, cumulate plagioclase grains with subophitic clinopyroxene grains. Intercumulate olivine grains are rimmed with iddingsite.....3-60
- Plate 3.4. Petrographic section from drill hole SVB-98-102 at 32.5m (magnification = 1.5x, cross polarized light). Melacratic, coarse to medium-grained gabbro belonging to the Coarse to Medium-grained subunit (Upper Gabbro subdivision). Euhedral, cumulate plagioclase grains with intercumulate clinopyroxene and lesser olivine grains.....3-60
- Plate 3.5. Drill core segments from drill hole, SVB-96-27. Core segment A, taken at 1.3 m, is a coarse-grained, cumulate textured gabbro belonging to the Coarse to Medium-grained Gabbro Subunit. Core segment B, taken at 4.7 m, is a medium to fine-grained, ophitic to cumulate textured olivine gabbro belonging to the Olivine Gabbro Subunit. Core segment C, taken at 8.9 m, is an ophitic textured olivine gabbro belonging to the Olivine Gabbro Subunit. Plagioclase grains are white, clinopyroxene grains are dark grey to black, and olivine grains are forest green. The scale bar is in centimeters.....3-61
- Plate 3.6. Petrographic section from drill hole SVB-96-04 at 4.15 m (magnification = 1.5x, cross polarized light). Medium-grained olivine gabbro belonging to the Olivine Gabbro subunit (Upper Gabbro). Cumulate, euhedral plagioclase with ophitic clinopyroxene containing granular olivine and lesser euhedral plagioclase grains.....3-61
- Plate 3.7. Drill core from drill hole SVB-96-36 centered at \sim 78.0 m. The darker core is unaltered, coarse-grained gabbro. The lighter core is altered gabbro belonging to the Altered Gabbro Subunit. The altered gabbro contains milky white, saussertized plagioclase grains with intercumulate green hornblende grains. The contact between altered and unaltered gabbro (at 79.2 m) is relatively sharp. The scale bar is in centimeters.....3-61
- Plate 3.8. Petrographic section from drill hole SVB-96-36 at 14.1 m (magnification = 1.5x, crossed polarized light). Altered, coarse-grained gabbro belonging to the Altered Gabbro subunit (Upper Gabbro). Large pyroxene grain altered to fine-grained hornblende engulfed by finer grained subhedral to anhedral plagioclase grains.....3-61

Plate 3.9. Outcrop exposure adjacent to the Mineral Hill sulphide occurrence. This plate shows the weathered contact between the Upper Gabbro and Basal Gabbro. The upper portion of the plate is a medium-grained cumulate textured leucocratic gabbro. The lower portion of the photo is a typical example of the Transition Gabbro subunit. The thin, lighter coloured bands are coarse to medium-grained plagioclase with lesser clinopyroxene. The finer-grained, brownish weathered material is cumulate olivine with lesser plagioclase and clinopyroxene. The scale bar is in centimeters.....3-62

Plate 3.10. Drill core segments from drill hole, SVB-97-77 at 412.3 m (top) and drill hole, SVB-98-116 at 107.4 m (bottom). Both drill core segments are examples of the Transition Gabbro subunit. The upper drill segment was derived from a leucocratic gabbro (plagioclase grains are white). The lower drill segment was derived from a melanocratic gabbro (plagioclase grains are purplish-grey). Both core segments illustrate the coarser-grained banding in the finer-grained olivine gabbro. Disseminated sulphides and sulphide blotches are closely associated with the coarser bands.....3-62

Plate 3.11. Petrographic section from drill hole SVB-98-111 at 107.5 m (magnification = 1.5x, cross polarized light). Transition Gabbro subunit (Basal Gabbro subdivision) with coarse-grained plagioclase and ophitic clinopyroxene band (center), in a fine-grained olivine gabbro matrix. A small sulphide blotch is in the center of the coarser band.....3-62

Plate 3.12. Petrographic section from drill hole SVB-98-111 at 107.5 m (magnification = 1.5x, plane polarized light). Refer to Plate 3.11 for caption description.....3-62

Plate 3.13. Outcrop exposure near the NDT sulphide occurrences. This plate shows the weathered surface of the Gabbro Hybrid / Olivine Gabbro subunit (Basal Gabbro). In the center of the plate is a partially digested melanocratic gneissic inclusion. Pocketknife (~ 8 cm) used for scale.....3-63

Plate 3.14. Drill core segments from drill hole, SVB-96-10 at 12.3 m. Drill core segments of the Gabbro Hybrid subunit (Basal Gabbro) with multiple, semi-rounded melanocratic inclusions in a fine-grained olivine gabbro matrix. Disseminated and blotchy sulphides (pyrrhotite ± chalcopyrite, pentlandite) are present within the matrix. The scale bar is in centimeters.....3-63

Plate 3.15. Drill core segment from drill hole, SVB-96-02 at 6.2 m. Drill core segment of the Gabbro Hybrid subunit (Basal Gabbro) with several partially digested, melanocratic, gneissic inclusions in a fine-grained olivine gabbro. Blotchy textured sulphide is also present. The scale bar is in centimeters.....3-63

Plate 3.16. Drill core segments from drill hole, SVB-98-102 at 173.5 m (top) and 194.0m (bottom). Drill core segments of the Gabbro Hybrid subunit (Basal Gabbro) with several partially digested, leucocratic, gneissic inclusions. Blotchy and disseminated textured sulphides are also present. The scale bar is in centimeters.....3-63

Plate 3.17. Petrographic section from drill hole SVB-96-09 at 54.45 m (magnification = 1.5x, cross polarized light). Leucocratic gneissic inclusion (only the edge is shown) in gabbro. The rim of the inclusion composed of spinel and fine-grained plagioclase. The center of the inclusion comprised of acicular corundum grains and plagioclase grains.....3-64

Plate 3.18. Petrographic section from drill hole SVB-96-09 at 54.45 m (magnification = 1.5x, plane polarized light). Refer to Plate 3.17 for caption description. Disseminated sulphide (black) is present.....3-64

Plate 3.19. Petrographic section from drill hole SVB-96-36 at 165.3 m (magnification = 2.5x, plane polarized light). Center of a leucocratic inclusion comprised of plagioclase, corundum and Fe-spinel.....3-64

- Plate 3.20. Petrographic section from drill hole **SVB-96-09** at 58.1 m (magnification = 1.5x, plane polarized light). Melanocratic inclusion comprised of Fe-spinel, biotite and plagioclase grains..... 3-64
- Plate 3.21. Drill core from drill hole **SVB-96-02** centered at ~ 71.8 m. Fine-grained, melanocratic olivine gabbro of the Olivine Gabbro subunit (Basal Gabbro). A group of pyrrhotite blotches are located in the center of the photograph. The scale bar is in centimeters.....3-65
- Plate 3.22. Drill core from drill hole **SVB-97-92** at 247.0 m. Fine-grained olivine gabbro of the Olivine Gabbro subunit (Basal Gabbro) with 4-5% fine-grained disseminated sulphide. The scale bar is in centimeters.....3-65
- Plate 3.23. Petrographic section from drill hole **SVB-96-02** at 71.8 m (magnification = 2.5x, cross polarized light). Fine-grained olivine gabbro with granular olivines, plagioclase and lesser ophitic clinopyroxene.....3-65
- Plate 3.24. Petrographic section from drill hole **SVB-97-79** at ~ 504 m (magnification = 1.5x, cross polarized light). Fine-grained olivine gabbro with granular olivines, plagioclase and lesser ophitic clinopyroxene. Plagioclase grains are aligned parallel to layering.....3-65
- Plate 3.25. Outcrop exposure within the Happy Face Lake sulphide occurrence. Photograph shows the typical weathered surface of the Leopard Textured Gabbro subunit (Basal Gabbro). Clinopyroxene oikocrysts are present within a recessive weathered olivine, plagioclase, sulphide matrix. The pencil is used for scale.....3-66
- Plate 3.26. Drill core segment from drill hole **SVB-96-02** at 20.1 m. Typical appearance of the Leopard Textured gabbro subunit (Basal Gabbro) with clinopyroxene oikocrysts (dark spots) set in a fine-grained olivine gabbro matrix with 10% fine-grained, disseminated sulphide. Scale bar is in centimeters.....3-66
- Plate 3.27. Petrographic section from drill hole **SVB-96-02** at 24.6 m (magnification = 1.5x, cross polarized light). Clinopyroxene oikocryst (center of plate) surrounded by plagioclase, olivine, disseminated sulphide (opaque), and lesser clinopyroxene.....3-66
- Plate 3.28. Petrographic section from drill hole **SVB-96-02** at 24.6 m (magnification = 1.5x, plane polarized light). Refer to Plate 3.27 for caption description.....3-66
- Plate 3.29. Drill core segment from drill hole **SVB-97-79** at 691.3 m. Medium-grained gabbro of the Medium-grained Gabbro subunit (Basal Gabbro). Interstitial plagioclase grains are white, olivine grains and clinopyroxene grains are dark coloured. The scale bar is in centimeters.....3-67
- Plate 3.30. Drill core segment from drill hole **SVB-97-79** at 738.1 m. Medium-grained gabbro of the Medium-grained Gabbro subunit (Basal Gabbro) with large sulphide blotches. The scale bar is in centimeters.....3-67
- Plate 3.31. Petrographic section from drill hole **SVB-97-79** at 691.3 m (magnification = 1.5x, cross polarized light). Cumulate olivine and lesser cumulate clinopyroxene with altered, intercumulate plagioclase and biotite.....3-67
- Plate 3.32. Petrographic section from drill hole **SVB-97-79** at 691.3 m (magnification = 1.5x, plane polarized light). Refer to Plate 3.31 for caption description.....3-67
- Plate 3.33. Petrographic section from drill hole **SVB-97-92** at 246.7 m (magnification = 1.5x, plane polarized light). Disseminated sulphide (opaque) grown between plagioclase and olivine grains.....3-68

- Plate 3.34. Petrographic section from drill hole **SVB-97-92** at 246.7m (magnification = 2.5x, reflecting light). Disseminated sulphide grains between silicate grains. Disseminated sulphide grains comprised of pyrrhotite (Po) with small chalcopyrite (Cpy), pentlandite (Pn), and magnetite (Mag) exsolutions.....3-68
- Plate 3.35. Outcrop exposure at the Major General sulphide occurrence. Oxidized sulphide blotches in fine-grained olivine gabbro. The geological hammer is for scale.....3-69
- Plate 3.36. Drill core segments from drill hole **SVB-96-10** at ~ 24.6 m. Dominantly pyrrhotite blotches with plagioclase intergrowths hosted in a fine-grained olivine gabbro. Segments also host several melanocratic gneissic inclusions. The scale bar is in centimeters.....3-69
- Plate 3.37. Drill core segment from drill hole **SVB-96-04** at 51.3 m. Large sulphide blotch hosted in a fine-grained olivine gabbro. Sulphide blotch has an upper portion of magnetite (Mag) and chalcopyrite (Cpy). The scale bar is in centimeters.....3-69
- Plate 3.38. Drill core segment from drill hole **SVB-96-04** at 58.6 m. Large pyrrhotite (Po) blotch in center of photo, hosted in a fine-grained olivine gabbro, has an upper chalcopyrite (cpy) rim. The scale bar is in centimeters.....3-69
- Plate 3.39. Petrographic section from drill hole **SVB-96-10** at 24.6 m (magnification = 2.5x, reflecting light). Pyrrhotite (Po) blotch with small chalcopyrite (Cpy) exsolutions present predominantly near the contact. Plagioclase grains are grown into the sulphide boundary.....3-70
- Plate 3.40. Petrographic section from drill hole **SVB-97-79** at 729.4 m (magnification = 2.5x, reflecting light). Edge of a pyrrhotite (Po) blotch with pentlandite (Pn) originating internally and grown outwards to the edge. Chalcopyrite (Cpy) and magnetite (Mag) are also adjacent to the sulphide boundary.....3-70
- Plate 3.41. Petrographic section from drill hole **SVB-97-57** at 165.3 m (magnification = 2.5x, reflecting light). Chalcopyrite (Cpy) and pentlandite (Pn) exsolutions formed on the pyrrhotite (Po) / silicate (dark grey) boundary. Magnetite (Mag) formed in the cracks of the pentlandite.....3-70
- Plate 3.42. Petrographic section from drill hole **SVB-96-02** at 69.15 m (magnification = 2.5x, reflecting light). Pentlandite (Pn) and chalcopyrite (Cpy) formed at the edge of pyrrhotite (Po). Magnetite (Mag) is present within cracks in the pentlandite and chalcopyrite.....3-70
- Plate 3.43. Drill core from drill hole **SVB-98-116** at 123.1 m. Semi-massive sulphide located above footwall contact. Sulphide comprised of mainly pyrrhotite with minor (< 2%) chalcopyrite. Sulphide is hosted in a fine-grained olivine gabbro with minor gneissic contamination. The scale bar is in centimeters.....3-71
- Plate 3.44. Drill core from drill hole **SVB-98-113** centered at 100 m. Massive sulphide intervals located just above the basement contact. Massive sulphide interval, comprised of pyrrhotite and lesser chalcopyrite and pentlandite, has several inclusions. The scale bar is in centimeters.....3-71
- Plate 3.45. Drill core segment from drill hole **SVB-98-113** at 100.4 m. Massive pyrrhotite (Po) with lesser chalcopyrite and pentlandite. The darker spots are gneissic inclusions. Note the sharp rounded contacts between the sulphide and the inclusions. The scale bar is in centimeters.....3-71
- Plate 3.46. Drill core segments from drill hole **SVB-97-75** at ~ 175 m. High grade, coarsely crystalline massive sulphide from a sulphide interval 13 meters below the footwall contact. Photo courtesy of Dr. Andrew Kerr.....3-71

- Plate 3.47. Petrographic section from drill hole **SVB-98-102** at 183 m (magnification = 10x, reflecting light). Massive pyrrhotite (Po) with exsolution lamellae of pentlandite flames.....3-72
- Plate 3.48. Petrographic section from drill hole **SVB-97-61** at 123.2 m (magnification = 2.5x, reflecting light). Massive pyrrhotite with small exsolution grains of pentlandite (Pn) and chalcopyrite (Cpy) located adjacent to silicate inclusions.....3-72
- Plate 3.49. Petrographic section from drill hole **SVB-97-75** at ~ 175 m (magnification = 2.5x, reflecting light). Massive sulphide with large crystalline pentlandite (Pn) grain located between pyrrhotite (Po) and chalcopyrite (Cpy). Magnetite (Mag) is present within cracks of the pentlandite.....3-72
- Plate 3.50. Petrographic section from drill hole **SVB-97-75** at ~ 175 m (magnification = 2.5x, reflecting light). Massive sulphide comprised of chalcopyrite (Cpy) and pentlandite (Pn). Pyrrhotite (Po) is present as rims around the pentlandite grains.....3-72
- Plate 3.51. Petrographic section from drill hole **SVB-97-75** at ~175 m (magnification = 10x, reflecting light). Massive sulphide comprised of pyrrhotite (Po), chalcopyrite (Cpy) and lesser pentlandite (Pn). Note the exsolution lamellae of cubanite in chalcopyrite.....3-73
- Plate 3.52. Petrographic section from drill hole **SVB-97-75** at ~ 175 m (magnification = 10x, reflecting light). Massive chalcopyrite (Cpy) with pyrrhotite (Po) formed at the chalcopyrite grain boundaries.....3-73
- Plate 3.53. Petrographic section from drill hole **SVB-97-58** at 163.5 m (magnification = 10x, reflecting light). Silicate grains in massive sulphide. Chalcopyrite (Cpy) located in the center of the plate is remobilized into the cracks developed into the silicate minerals.....3-73
- Plate 3.54. Petrographic section from drill hole **SVB-97-75** at ~ 175 m (magnification = 2.5x, reflecting light). Edge of massive sulphide with chalcopyrite (Cpy) remobilized between the silicate grain boundaries.....3-73
- Plate 3.55. Photograph looking east of the NDT sulphide occurrences/gossans (seen in the background). The North Gossan is separated from the South Gossan by a v-shaped wedge of Churchill Province gneiss (seen in the foreground).....3-74
- Plate 3.56. Photograph looking northeast at the Happy Face Lake sulphide occurrence (seen in the middle of the photograph). Three Basal Gabbro subunits are observed here. The lower Basal Gabbro contact was not observed here. The upper contact is shown in the inset plate.....3-75
- Plate 3.57. Photograph looking northeast at the GG sulphide occurrence (seen in Center of the photograph). The Leopard Textured Gabbro subunit is between the Fine-Grained Gabbro subunit. The lower Basal Gabbro subdivision contact is scree covered.....3-76
- Plate 3.58. Photograph looking northwest at the Mineral Hill sulphide occurrence. This location is an excellent example of igneous layering. The inset plate shows a close-up view of the contact between the Upper and Basal Gabbro subdivisions.....3-77

List of Selected Abbreviations

| | |
|------------|--|
| AMCG | Anorthosite-Monzonite-Charnockite-Granite |
| ASL | Above Sea Level |
| BBS | Basal Breccia sequence |
| BGS | Basal Gabbro Subdivision |
| CDT | Canon Diablo Triolite |
| Co | Cobalt |
| Cg | Coarse Grain |
| CP | Churchill Province |
| Cpx | Clinopyroxene |
| Cpy | Chalcopyrite |
| Cu | Copper |
| Diss | Disseminated |
| DDH | Diamond Drill Hole |
| Fg | Fine Grain |
| Fo | Forsterite |
| FW | Footwall |
| Ga | Billion Years |
| Hbl | Hornblende |
| HLIS | Harp Lake Intrusive Suite |
| HREE | Heavy Rare Earth Elements |
| ICP-MS | Inductively Coupled Plasma-Mass Spectrometry |
| IUGS | International Union of Geological Sciences |
| LAM-ICP-MS | Laser Ablation Microprobe-Inductively Coupled Plasma-Mass Spectrometry |
| LD | Limit of Detection |
| LREE | Light Rare Earth Elements |
| Ma | Million Years |
| Mag | Magnetite |
| Mg (MG) | Medium Grain |
| MI | Michikamau Intrusion |
| Ni | Nickel |
| NPS | Nain Plutonic Suite |
| NTS | National Topographic Sheet |
| NTT | Normal Textured Troctolites |
| OI | Olivine |
| OVB | Overburden |
| Plag | Plagioclase |
| PGE | Platinum Group Element |
| PLI | Pants Lake Intrusion |
| Pn | Pentlandite |
| Po | Pyrrhotite |
| ppb | Parts Per Billion |
| ppm | Parts Per Million |
| PR | Press Release |
| REE | Rare Earth Element |
| SM | Semi-Massive |
| Std Dev | Standard Deviation |
| SVB | South Voisey's Bay |
| Tr | Trace |
| UGS | Upper Gabbro subdivision |
| UTM | Universal Transverse Mercator |
| VTT | Variable Textured Troctolites |
| Wt% | Weight Percent |
| XRF | X-Ray Fluorescence |

Chapter 1: Introduction

1.1 Preamble

The discovery of the Voisey's Bay nickel-copper-cobalt deposits by Archean Resources Limited (with the financial support of Diamond Field Resources Incorporated) in November 1993 caused a staking frenzy unprecedented in the history of Newfoundland and Labrador. The intense geological exploration that soon followed this world-class mineral discovery had one common goal; that is, to find other deposits of the same grandeur as the deposits at Voisey's Bay.

Explorationists soon discovered that finding the next "Voisey's Bay" was not a simple endeavor. The initial hindrance to exploration (not considering that large tracts of ground had already been claimed by Archean Resources Ltd.) was the scarcity of information pertaining to the geological context of the deposit within the Labrador setting. Prior to this period, the federal and provincial geological surveys had only vaguely described parameters for potential magmatic nickel-copper sulphide ore bodies that might exist in Labrador (Swinden *et al.*, 1991). Consequently, most of the property acquisition that followed the announcement of the Voisey's discovery was governed more by geographic proximity to the deposit, rather than rational geological reasoning. Fewer properties were acquired by utilizing the limited regional geological and geochemical surveys that existed at the time (*eg.* Ryan and Lee, 1989; Ryan, 1990).

At the end of the staking frenzy, a large corridor containing several thousand mineral claims (one mineral claim equals a $\frac{1}{4}$ km², 500 m x 500m area) blanketed most of north and central Labrador. These mineral claims covered the majority of rocks belonging to the Nain Plutonic Suite (NPS), Harp Lake Intrusive Suite (HLIS), and a

small group of rocks belonging to the Nain and Churchill structural provinces. One sizeable cluster of claims, located to the south of the NPS (Figure 1.1), covered a relatively unknown, layered, mafic intrusion (later termed the Pants Lake Intrusion or PLI). Coincident with this intrusion is a cluster of high nickel values in lake-sediments (Davenport *et al.*, 1999) as well as previously noted pyrrhotite mineralization (Thomas and Morrison, 1991). All of these factors made the PLI a viable target.

Donner Minerals Ltd., a Vancouver-based junior exploration company, conducted initial field-based work in the area of the PLI during the 1995 and 1996 field seasons on several claim blocks. Furnished with published information that promptly followed the Voisey's Bay discovery (*eg.* Ryan *et al.*, 1995; Naldrett *et al.*, 1996), Donner Minerals Ltd. believed that the PLI had similar geological attributes as the host rocks of the Voisey's Bay deposits (Donner Minerals Ltd., company and property portfolio, 1997). In conjunction with the ongoing field-based work, Donner Minerals Ltd. established a consortium involving thirteen claim holders located in the PLI vicinity, eventually merging the divided claim blocks that covered the PLI. With this consortium in place, the South Voisey's Bay (SVB) project was conceived. In September 1996, Teck Exploration Ltd. obtained a vested interest in the project and acted as the consortium's general contractor during the 1997 and 1998 field seasons. Teck Exploration Ltd. opted out of the project in 1999. In 2001, the South Voisey's Bay Nickel Company was formed to simplify the consortium and shortly thereafter, Falconbridge Ltd. joined the project to earn a 50% interest. Falconbridge Ltd. explored the PLI during 2002 and 2003; however in 2004 Falconbridge too opted out of the project.

Presently, Donner Minerals Ltd. (and its affiliates) have achieved some of the more promising results of any exploration company working in Labrador (outside of the Voisey's Bay deposits) in exploring for "Voisey's Bay-type" magmatic nickel-copper sulphide mineralization. Kerr (1999) stated, "The PLI is the closest analogue to the Voisey's Bay [deposits] host rocks recognized to date in Labrador...". Apart from favorable geology, a number of significant, and potentially economic sulphide intersections were obtained during the SVB drilling programs. For example, drill hole 98-075 intersected a 1.1 m massive sulphide interval averaging 11.75 % nickel, 9.70 % copper, and 0.43 % cobalt, and drill hole 97-096 intersected a 15.7 m massive sulphide interval containing 1.13 % nickel, 0.78 % copper, and 0.20 % cobalt (Donner Minerals Ltd. web site). The results of the exploration conducted thus far by Donner Minerals Ltd. with previous support from Teck Exploration Ltd. and Falconbridge Ltd. strongly suggests the presence of economic grades of sulphide mineralization hosted by the PLI. The implications of these results are that potential economic accumulations of sulphides can be found elsewhere in Labrador and are not confined only to the area encompassing the Voisey's Bay deposits.

It is with that premise that this M.Sc study was initiated by Donner Minerals Ltd. and Memorial University of Newfoundland. The focus of this study is the magmatic sulphide mineralization and the Basal Gabbro subdivision of the Pants Lake Intrusion that is host to this mineralization. The purpose and scope of this study is elaborated at the end of this chapter (Section 1.6). The remainder of this chapter, as well as chapter two, contains information regarding the context of this study.

1.2 Location and Access

The SVB project is located geographically in the remote interior of north central Labrador, Canada (Figure 1.1). The nearest community is the isolated, coastal village of Natuashish located approximately 70 km to the northeast. The town of Happy Valley-Goose Bay lies approximately 260 km to the south-southeast of the project area, and the Voisey's Bay Ni-Cu-Co deposit is approximately 90 km due north of the SVB project area. The entire project area encompasses roughly 1200 km² and includes portions of NTS map sheets 13M/08, 13M/09, 13N/05 and 13N/12 (see inset, Figure 1.1). The approximate geographic center of the project is located at the UTM coordinate 573700 E, 6150600 N in UTM Zone 20, North America Datum 27 projection for Canada.

Personnel required for the exploration programs reside in the exploration camp situated on the southwestern shore of a large northwest-trending lake informally named Pants Lake (camp location; UTM coordinate 559250 E, 6145450 N) (see geological map, inside back cover). The drill core-logging facility and the core storage site are located adjacent to the exploration camp.

Access to the project area can be gained via helicopter and fixed wing aircraft stationed in the communities of Nain or Happy Valley-Goose Bay. During favorable weather conditions, fixed wing aircraft equipped with floats are able to land on Pants Lake. Alternatively, fixed wing aircraft can utilize a temporary gravel airstrip established 23 km to the southeast of the exploration camp. From this airstrip location, personnel and supplies can be transported to the camp by helicopter. The interior of the project area is best accessed by helicopter and/or by traverse on foot.

1.3 Physiography and Glaciation

The topographic features in this particular region, composed of rugged undulating hills and valleys, are typical of the Labrador plateau highland. Topographic relief within the entire project area ranges from 150 to 500 m above mean sea level. Hilltops are frequently smooth and rounded due to glaciation, notably during the Pleistocene (Thomas and Morrison, 1991). Numerous glacial striae, chattermarks, and roches moutonée have been noted on hilltops on the SVB property. In many cases, the slopes of hills are gentle and terminate at the base as broad, flat lying plains and valleys. In fewer cases, the slopes of hills are terminated by steep cliffs. Broad U-shaped valleys, common in this region, are often filled with deep accumulations of terraced alluvium and glacial erratics. These U-shaped valleys serve as pathways for small streams, ponds, and rivers. Although less common and much narrower, V-shaped valleys tend to be northwest orientated and are continuous over further distances than the more common U-shaped valleys. Larger lakes in the region, such as Pants Lake and Sarah Lake, are located in flat, low-lying depressions between hills of low to moderate elevation. Drainage entering and exiting these lakes typically flows through the valleys. The Adlatok River, located to the south of the PLI, flows from west to east and is connected to several tributaries along its route.

Vegetation is scarce in this region due to the severe climate and poor soil development. Most hilltops are devoid of vegetation with the exception of moss, lichen and low-lying shrubs. This lack of vegetation on hilltops provides excellent outcrop exposure. The lower slopes of hills and valley floors, where protected by the winds, have a significant increase in vegetation. The vegetation on the leeward side of hills consists of stunted black spruce, grasses and wind-deformed tamarack.

1.4 Previous and Present Geological Investigations

Prior to the discovery of the Voisey's Bay deposits, geological interest within the project area was minimal. Portions of the project area were previously included in 1:50 000 to 1:250 000 scale regional mapping and lake sediment sampling projects conducted by provincial and federal geological surveys. Emslie (1980) included a small southern section of the SVB project area in a major 1:250 000 scale regional study of the Harp Lake Intrusive Suite. Hill (1982) included the northern half of the SVB project area during a regional 1:100 000 scale mapping project of selected areas along the central part of the Ugjoktok River. Likewise, Thomas and Morrison (1991) included the southern half of the project area during a mapping project in the Flowers River area. Other studies focused on supracrustal rocks of the Ingrid Group in the southeastern corner of the project area (*eg.* Ermanovics and Korstgaard, 1981; Ermanovics, 1993). Government geochemical surveys, completed during the mid-1970's, were limited to reconnaissance-style lake sediment geochemistry which included a number of lakes within the interior of the SVB project (Davenport *et al.*, 1999).

Since the conception of the SVB project in 1995, numerous geological, geochemical and geophysical surveys have been conducted within the project area. The majority of work conducted thus far has focused on locating economic concentrations of nickel-copper-cobalt sulphide mineralization within the PLI. Donner Minerals with aid from both Teck and Falconbridge has by far completed the most work within the area. At the conclusion of the 2003 field season, there are over 140 diamond drill holes, the entire project area was mapped on both a reconnaissance and detailed scale (1:10 000), and numerous airborne, ground and down-hole geophysical surveys have been conducted.

Donner Minerals Ltd. has also contributed to several university and government studies. These studies include B.Sc thesis work by Hodder (1998), Twyne (1999), and Hearn (2001), M.Sc thesis work by MacDonald (1999), as well as work conducted by the author. Studies by Kerr and Smith (1997), Kerr (1998, 1999, 2003), Kerr and Ryan (2000), Kerr *et al.* (2001), and Li *et al.* (2001) have all benefited from the support extended by Donner Minerals Ltd. as well.

McConnell (1998 & 2000) completed a lake-sediment and stream-water survey over known areas of mineralization within the SVB project area as a follow-up from the lake sediment survey conducted during the 1970's. The results of McConnell's survey further illustrates that metal concentrations, including nickel, are elevated in lake sediments near known surface mineralization.

1.5 Field Work

The field component of this study was completed from early July to mid-September, 1998. During this period, the author resided at the exploration camp. Field-work pertaining to this study was divided into two components. The first component focused on the re-logging and sampling of representative diamond drill cores from the entire PLI that were obtained during the 1996, 1997 and 1998 drilling programs. Refer to the geological map of the PLI (inside back cover) for drill hole locations and Table A.1 for DDH information. The second component of this study involved mapping of several sulphide occurrences throughout the project area (refer to the geological map of the PLI, inside back cover, for locations of sulphide occurrences). In both components, the focus was to describe and sample lithologies that host the sulphide mineralization.

Thirty-four diamond drill cores were re-logged (Appendix C) and selectively sampled as part of this thesis study (refer to Table A.2 and A.3 for sample locations). Drill cores from other parts of the PLI were briefly observed, and as such their data have only a minor role in this study. Approximately 180 core samples, averaging 30 cm in length, were collected from these representative drill holes. Samples were cut in two equal lengthwise portions using a water-cooled diamond blade saw located on site. One portion of the sample was placed back into the core box for later reference whereas the opposite portion was described, photographed, properly labeled, bagged and shipped to the Department of Earth Sciences at Memorial University of Newfoundland.

The mapping component was completed in the later part of the field season after the core re-logging was completed. Seven sulphide surface showings were visited, photographed, and mapped at a scale of 1: 5000 for this study. During each visit, several reference samples were collected, however, due to the deeply weathered and sometimes gossanous state of the outcrops, no samples were selected for geochemistry or petrography. Lithological variations and sulphide textures noted in drill core were commonly observed at the sulphide showings. The relative position above the basement contact, the thickness, and the lateral continuity of the lithological variations and sulphide textures was especially noted. In a few cases, however, the basement contact was covered by scree. Rocks above and below the sulphide mineralization were observed and described, but in lesser detail.

1.6 Purpose and Scope of Present Study

Recent mineral exploration in the southern periphery of the NPS has revealed a relatively unknown gabbroic intrusion containing genetically associated magmatic sulphide mineralization. Previous studies have provided petrological and geochemical information on select portions of the intrusion, predominantly in its upper, unmineralized layers. Apart from the limited work conducted by MacDonald (200) and Kerr (1998, 1999, 2003), a complete, in depth study of the sulphide mineralization, host lithologies, and metallogenic history, has yet to be completed. Therefore, the objective of this study is three fold:

The first objective is to define the regional context and morphology of the Pants Lake Intrusion. A compilation of previous studies (*e.g.* MacDonald, 2000; Kerr, 1998, 1999, 2003; Fitzpatrick *et al.*, 1998, 1999; Thomas and Morrison, 1991; Hill, 1982), combined with current information and drill hole data, will achieve this objective.

The second objective is to document, locate and characterize the sulphide mineralization and the host lithologies within the Pants Lake Intrusion. This objective will be achieved by utilizing observations gathered during field work (*e.g.* drill core and outcrop observations) along with observations from petrographic sections.

The third objective is directly linked with the second objective. That is, to provide a comprehensive geochemical evaluation of the described sulphide mineralization as well as, gabbroic rocks in the Pants Lake Intrusion, in particular, the Basal Gabbro Subdivision that is host to the sulphide mineralization. This objective is accomplished using major, trace, and rare-earth element geochemistry, in combination with stable isotope geochemistry.

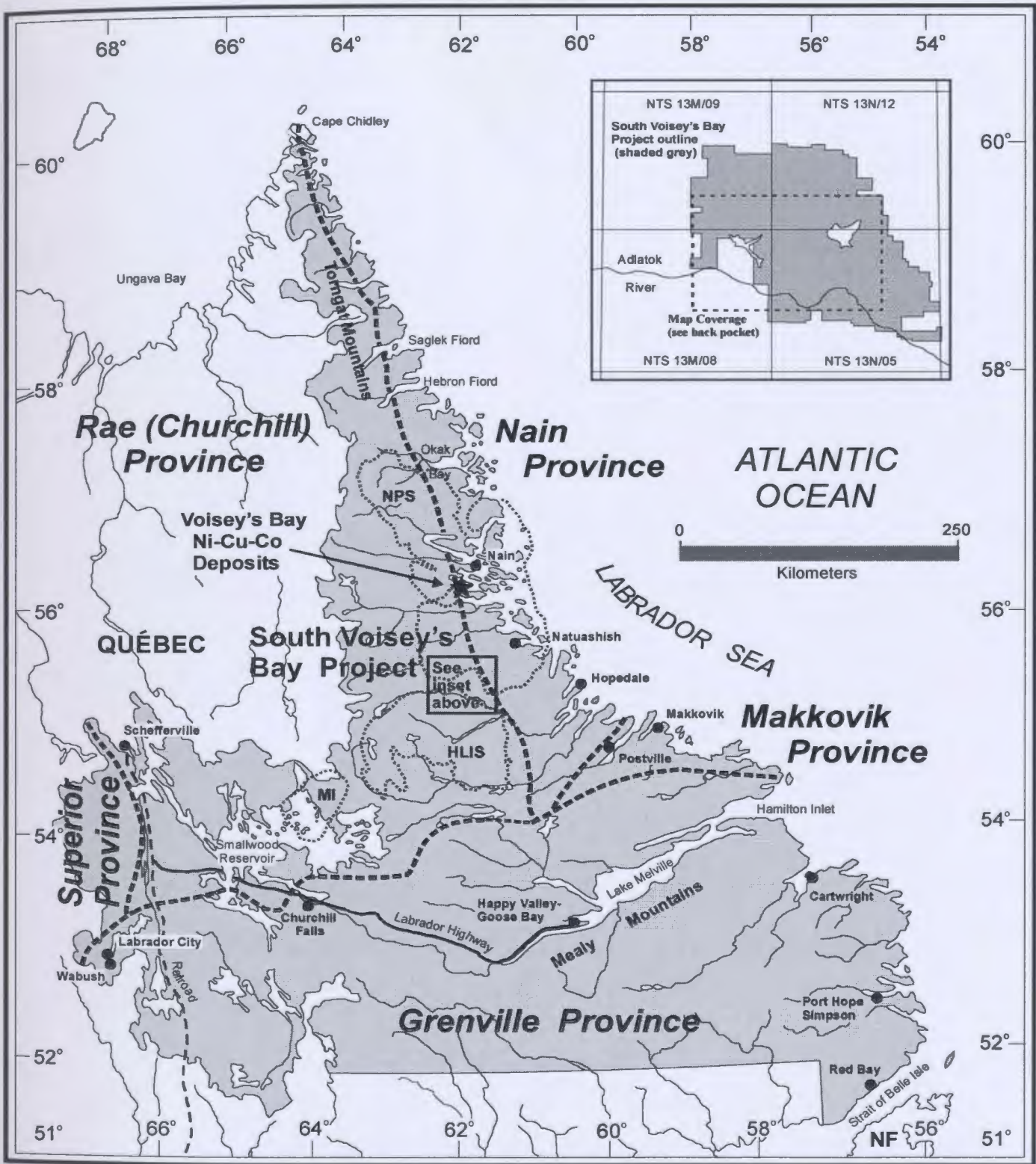


Figure 1.1. Locations of the South Voisey's Bay Project and Voisey's Bay deposits compared to the Precambrian structural provinces of Labrador (after Greene, 1972), the Nain Plutonic Suite (NPS), the Harp Lake Intrusive Suite (HLIS), and the Michikamau Intrusion (MI) (shown as dotted outlines). The inset box (upper right corner) illustrates the outline of the South Voisey's Bay Project boundary (as of January 30, 1999). The area inside the dashed line of the inset box represents the coverage of the Pants Lake Intrusion geological map (see inside back cover).

Chapter 2: Geological Overview of Labrador and Associated Magmatic Nickel-Copper Sulphide Mineralization

2.1 Introduction

The geology of Labrador represents a diverse collage of five structural provinces (Nain, Superior, Churchill, Makkovik, and Grenville), merged together during several episodes of orogenesis active over hundreds of millions of years. Anorogenic intrusions, emplaced into the structural provinces during the Mesoproterozoic Era, are another prominent component of Labrador's geological landscape. The Nain Plutonic Suite, Harp Lake Intrusive Suite, Mistastin Batholith, and Michikamau Intrusion are examples of anorogenic plutonism in Labrador. Labrador's geology has also generated numerous diverse metallogenic environments. One metal-bearing environment is magmatic nickel-copper sulphide. This environment is the focus of this study.

The first part of this chapter will briefly describe the five structural provinces and three plutonic suites (Nain Plutonic Suite, Harp Lake Intrusive Suite, and Michikamau Intrusion). The goal of the first part of this chapter is to introduce the broad geological setting of the Pants Lake Intrusion. Therefore, a few of the geological elements described in this chapter will be further elaborated upon in the section entitled 'Regional Geological Setting of the Pants Lake Intrusion' (Section 3.2).

The second part of this chapter will describe several examples of magmatic nickel-copper sulphide mineralization located in Labrador outside of the Pants Lake Intrusion (*e.g.* the Voisey's Bay deposits, the Cirque prospect, the Krinor prospect, *etc.*). The local geology, host lithologies, sulphide mineralogy, and sulphide textures of each example will be included in the descriptions. Descriptions of these other magmatic

nickel-copper occurrences provided in this chapter are compared and/or contrasted with descriptions of the same from the Pants Lake Intrusion in the final chapter of this thesis.

2.2 Geological Overview of Labrador

Labrador is composed mainly of five structural provinces, namely the Nain, the Superior, the Churchill, the Makkovik, and the Grenville Province, and four anorogenic Mid to Late Proterozoic plutonic intrusions, namely the Nain Plutonic Suite, Harp Lake Intrusive Suite, Mistastin Batholith, and Michikamau Intrusion. The combined surface area of each province covers only a minute fraction (250 000 km²) of the much larger Precambrian North American Shield (located on the eastern edge of the Canadian Shield) and North Atlantic Craton (Hoffman, 1988; Swinden *et al.*, 1991) (Figure 2.1).

The geological evolution of Labrador spans a period that began sometime during the Archean (>3.9 Ga) and ended during the Cretaceous (Wilton, 1996); through this period, Labrador experienced at least five separate orogenies. These orogenic events lead to the merger and structural deformation of different structural provinces. Two orogens, the Torngat and the New Quebec, are shown in Figure 2.2. The Nain Plutonic Suite, the Harp Lake Intrusive Suite, and the Churchill Province are the three main geological elements that encompass the known boundaries of the Pants Lake Intrusion (Figure 1.1 and Figure 2.3).

2.2.1 The Nain Province

The Archean Nain Province forms the western terminus of the North Atlantic Craton (Figure 1.1 and Figure 2.3), and is geographically located along the northeastern edge of Labrador (Bridgewater *et al.*, 1973; Hoffman, 1988). The Nain Province is divided into two distinct blocks, the northern Saglek block and the southern Hopedale block (Figure 1.1 and Figure 2.3). The Nain Plutonic Suite separates these two blocks. Geological mapping and chronological investigations suggest that the Hopedale and the Saglek blocks represent two distinct Archean terranes juxtaposed during circa 2.57 to 2.55 Ga continental accretion (Ryan, 1991; Connelly and Ryan, 1992, 1993). The Saglek block contains high-grade tonalitic gneiss, and narrow supracrustal belts metamorphosed to granulite facies (Wardle *et al.*, 1997). The oldest rocks in the Saglek block, also the oldest rocks known in Labrador, are the pre-3.9 Ga Nanok gneisses (Collerson, 1991). These rocks are overlain unconformably by Paleoproterozoic sedimentary-mafic volcanic sequences of the Ramah and Mugford groups (Wardle *et al.*, 1997). The Hopedale Block is dominated by 3100 Ma gneisses, linear volcanic greenstone belts (ca. 3000 Ma) (*e.g.* Florence Lake and Hunt River), and 2800 Ma tonalite-trondhjemite-granite intrusions (*op cit.*). The Florence Lake Greenstone Belt is also mentioned in the section entitled 'The Baikie Prospect' (Section 2.3.8).

2.2.2 The Superior Province

The Archean Superior Province is located in a small segment of western Labrador (Figure 1.1 and Figure 2.2). The Superior Province in Labrador is underlain by Neoproterozoic (ca. 2700 to 2650 Ma) granulite-facies gneisses and associated tonalite to granite plutons of the Ashuanipi Complex (Wardle *et al.*, 1997). Paleoproterozoic rocks of the Knob Lake Group overlie rocks in the eastern portion of the Superior Province.

2.2.3 The Churchill Province

The Churchill Province comprises a large area in northwestern Labrador (Figure 1.1) and was developed by oblique collision of the Nain and Superior Provinces between 1860 and 1740 Ma. The Churchill Province contains a central Archean core termed the 'Rae Craton'.. (Figure 2.1) (Hoffman, 1988; Wardle and Wilton, 1995; Wardle *et al.*, 1997). The Churchill Province is bounded on the western and eastern flanks by the New Quebec Orogen and the Torngat Orogen, respectively. The New Quebec Orogen forms the boundary between the Rae Craton and Superior Province, whereas the Torngat Orogen developed between the Nain and Rae Craton (Hoffman, 1988). Sedimentary margins of the Rae Craton were thrust upon the Nain and Superior Provinces during these orogenic events (ca. 1.86 Ga) (Ryan *et al.*, 1995). Metasedimentary Tasiuyak gneisses, derived from the Nain and Churchill provinces, and the Abloviak shear zone mark the collisional suture between the Nain and Churchill Provinces (*op cit.*). The Churchill and Nain Provinces were both intruded by Mesoproterozoic anorthosite-monzonite-charnockite-granite (AMCG) associations of the Nain Plutonic Suite and the Harp, Mistastin, and Michikamau intrusions.

2.2.4 The Makkovik Province

The Makkovik Province, located along the southern margin of the Nain Province (Figure 1.1 and Figure 2.2), is divided into three domains, namely the Kaipokok, Aillik and Cape Harrison domains (Wardle *et al.*, 1997). Archean gneisses, and Paleoproterozoic sedimentary and mafic volcanic rocks underlie the Kaipokok domain, located to the northwest of the Makkovik Province. The Aillik domain, located in the center of the Makkovik Province, consists of Paleoproterozoic sedimentary, mafic and felsic volcanic rocks. The Cape Harrison Domain contains (ca. 1840 to 1720 Ma) granitoid plutons, minor volcanic rocks, and older gneissic rocks. The Aillik and Cape Harrison Domains were accreted to the Nain Province margin (Gower *et al.*, 1982; Ryan, 1984; Ketchum *et al.*, 2002).

2.2.5 The Grenville Province

The Grenville Province, located in southern Labrador (Figure 1.1 and Figure 2.2), is subdivided into two components; a northern exterior thrust belt and a southern interior magmatic belt (Wardle *et al.*, 1997). The exterior thrust belt is composed of juvenile crust formed during the Labrador orogeny (ca. 1710 to 1620 Ma) and is further divided into a number of thrust-bounded terranes (*op cit.*). The interior magmatic belt contains an abundance of Grenvillian magmatic intrusions (ca. 1080 to 960 Ma) intruded into the Labradorian crust. There are also numerous post-tectonic granite plutons of ca. 970 to 900 Ma age (*op cit.*).

2.2.6 Anorogenic Plutonic Suites

The volumetrically significant 1350 to 1290 Ma Nain Plutonic Suite (NPS), 1450 Ma Harp Lake Intrusive Suite (HLIS), and 1460 Ma Michikamau Intrusion (MI) are classic examples of anorogenic plutonic suites. Both the NPS and HLIS were emplaced across the Nain / Churchill Province boundaries (Emslie, 1980; Emslie *et al.*, 1994; Ryan, 1997), whereas the MI was emplaced within the southeastern terminus of the Churchill Province where it meets the Grenville Front (Figure 1.1).

The Nain Plutonic Suite (NPS) covers some 20 000 km² between Okak Bay and Hunt Lake (Figure 1.1 and Figure 2.2). The NPS is a multicompositional igneous batholith containing aggregated, unsynchronous plutons of anorthositic, granitic, troctolitic and dioritic compositions (Ryan, 1997). On surface, anorthositic and granitoid rocks constitute over 80 % of the NPS (Kerr and Ryan, 2000). Additional descriptions of the NPS are given by Ryan (1990 & 1997), and the reader is encouraged to refer to these articles. One model explaining the formation of the NPS was proposed by Emslie *et al.* (1984) who suggested that the compositional ranges of the NPS could be accommodated by processes associated with mantle plumes or hot-spot activity at the base of the crust, and subsequent emplacements of large intrusions arising therefrom.

The Harp Lake Intrusive Suite (HLIS) is located in central Labrador, north of the Grenville Front (Figure 1.1 and Figure 2.2). This oval-shaped plutonic suite is surrounded by orthogneiss and paragneiss assigned to the Churchill Province, and Archean orthogneiss of the Nain Province. The HLIS is dominated by anorthosite and granitoid rocks with lesser amounts of mafic and Fe-rich intermediate plutonic rocks.

The HLIS consists of a core of anorthositic rocks surrounded by a rim of granitoid rocks. East-northeast-trending diabase dikes (ca. 1274 Ma) are common in the HLIS.

The Michikamau Intrusion (MI) straddles the Labrador-Québec border in west central Labrador (Figure 1.1 and Figure 2.2) and much of the intrusion currently lies beneath the Smallwood hydroelectric reservoir. The surrounding country rocks to the intrusion include Archean orthogneiss of the Sail Lake Intrusive Suite, Paleoproterozoic supracrustal rocks of the Petscapiskau Group, and low-grade Paleoproterozoic volcanic and sedimentary rocks of the Mackenzie Lake Group (Nunn, 1993). The MI was originally lopolithic in shape and is presently dissected by numerous fault-bounded blocks. The MI is unmetamorphosed and undeformed, and comprises five discrete layered mafic units namely (from youngest to oldest) the Marginal Zone, the Layered Series, the Anorthosite Zone, the Upper Border Zone, and the Transgressive Group (Emslie, 1970).

2.3 Magmatic Nickel-Copper Sulphide Mineralization in Labrador

There are numerous examples of magmatic nickel-copper sulphide mineralization in Labrador. Descriptions of each sulphide example mentioned in this section will be utilized in the discussion in the final chapter of this thesis. Magmatic nickel-copper sulphide mineralization was known to exist in Labrador prior to the discovery of the Voisey's Bay deposits (Swinden *et al.*, 1991). Of the pre-Voisey's Bay era, the most widely known nickel-copper occurrences were hosted by the Harp Lake Intrusive Suite (*e.g.* the Dart prospect, the Collette II prospect, *etc.*), occurrences in the Florence Lake Greenstone Belt (*e.g.* the Baikie prospect), and the lesser known occurrences associated

with the Marginal Zone of the Michikamau Intrusion (*e.g.* the Fraser Lake prospect). The potential of Nain Plutonic Suite to host magmatic sulphide mineralization was not fully appreciated until the discovery of the Voisey's Bay deposits in 1993. Many of the examples of magmatic nickel-copper sulphide mineralization discussed in this section resulted from exploratory work carried out after the Voisey's Bay discovery. The locations of the magmatic sulphide examples are shown in Figure 2.3. Table 2.1 summarizes the main points of each prospect/deposit.

2.3.1 Introduction: The Voisey's Bay Nickel-Copper-Cobalt Deposits

The Voisey's Bay deposits are located in northeastern Labrador, approximately 20 km southwest of the coastal community of Nain (Figure 1.1 and Figure 2.3). The original indications of sulphide mineralization in the Voisey's Bay area (ultimately leading to the Voisey's Bay discovery) were found during a grass-roots exploration program in 1993. Following the success of the initial exploration program, a second exploration program was undertaken in 1994, consisting of a horizontal loop electromagnetic survey and a four-hole drilling program (Evans-Lamswood *et al.*, 2000). The results of the original drilling were so impressive that a second phase of drilling was begun in January 1995 and by July of the same year; the Ovoid deposit had been delineated. Later that same year the Eastern Deeps deposit was discovered and in early 1997, the Reid Brook zone was discovered. The current estimate of cumulative reserves and resources of all deposits in the Voisey's Bay area stands at 141×10^6 tonnes, grading 1.63 wt. % Ni, 0.85 wt. % Cu and 0.09 wt. % Co (Inco Ltd. web site, 2003). To date, the

Voisey's Bay deposits remain the most significant accumulation of magma associated nickel-copper-cobalt sulphide mineralization discovered in Labrador.

2.3.1.1 Regional Setting of the Voisey's Bay Deposits

The Voisey's Bay deposits are hosted by the Voisey's Bay Intrusion (Figure 2.4). The Voisey's Bay Intrusion, formally part of the Reid Brook Igneous Complex (Ryan and Lee, 1989), is one of several distinct troctolitic-gabbroic intrusions in the Voisey's Bay area. A second intrusion, the Mushuau Intrusion, is located to the north of the Voisey's Bay Intrusion. The Voisey's Bay Intrusion and the Mushuau Intrusion are both assigned to the Mesoproterozoic Nain Plutonic Suite. Troctolitic rocks from the Voisey's Bay Intrusion have yielded maximum U-Pb zircon ages of 1330 Ma (Amelin *et al.*, 1999) and 1338 Ma (Ryan *et al.*, 1995), whereas the Mushuau Intrusion has yielded an age of 1314 Ma (Evans-Lamswood *et al.*, 2000).

Troctolitic and gabbroic rocks assigned to the Voisey's Bay Intrusion and the Mushuau Intrusion (between Annakhtalak Bay and Voisey's Bay) intrude quartzofeldspathic to mafic gneisses of the Nain Province, as well as garnet-bearing paragneisses and enderbitic orthogneisses of the Churchill Province (Figure 2.4). The boundary between the Nain and Churchill petro-tectonic province is adjacent to these troctolitic and gabbroic intrusions.

The relationship between anorthosites and the Voisey's Bay Intrusion is unclear. The relationship of the granites with the Voisey's Bay Intrusion is such that the Voisey's Bay Intrusion is cut by sub-horizontal granitic sheets that may be temporally and compositionally related to the granitoid complexes in the area.

The Mushuau Intrusion is located within quartzofeldspathic to mafic gneisses belonging to the Nain Province (Figure 2.4). The Mushuau Intrusion has a steep contact and basinal shape, and contains metatroctolites, leucotroctolites and olivine gabbros. At the base of the Mushuau Intrusion are small accumulations of magmatic textured chalcopyrite, pyrite, pyrrhotite and pentlandite associated with a basal unit of variable textured troctolite containing paragneiss fragments.

2.3.1.2 Geology and Mineralization of the Voisey's Bay Intrusion

The largest portion of the Voisey's Bay Intrusion, referred to as the Eastern Deeps Chamber, consists of troctolite-gabbro and extends to the west as a subvertical conduit (feeder dike) of ferrodiorite, ferrogabbro, olivine gabbro and troctolitic rocks (Figure 2.5 and Figure 2.6). Further to the west, troctolitic and gabbroic rocks are dissected by the Makhavinekh Pluton.

The Eastern Deeps chamber has a sub-vertical wall and near the base of the wall, it is connected to a gabbroic-troctolite sheet. The Eastern Deeps mineralization is located where the thin sheet intersects the large chamber and is associated with a breccia sequence. The Eastern Deeps sheet contains basal accumulations of magmatic sulphides at the entry point of an east-west, sub-horizontal sheet (Lightfoot and Naldrett, 1999). The Eastern Deep segment is hosted by the Nain Gneiss and cut by 1306-1307 Ma felsic sheets. The Eastern Deeps stratigraphy consists of a lower sequence of fine-grained gabbro and breccia with igneous-texture matrix (BBS) containing disseminated to semi-massive sulphide mineralization cross-cut by massive sulphide mineralization. On top of this unit is inclusion-bearing and inclusion-free leopard textured troctolite with

interstitial sulphides. This unit is in turn overlain by variable textured troctolite (VTT) containing coarse-grained patches of silicate and sulphide in finer-grained, less mineralized troctolite. Above this is a normal textured troctolite (NTT). The uppermost rocks are leucotroctolite and olivine gabbro. The roof rocks are generally Nain orthogneiss.

The Ovoid Deposit, located west of the Eastern Deeps (Figure 2.5), is a 500 meter wide and 150 meter deep, bowl-shaped depression surrounded by enderbitic orthogneiss. The Ovoid is linked at the northern margin to a north-dipping sheet of troctolite, that appears to rollover and dip towards the south. There is speculation that the Ovoid may be a bulge located within a conduit or feeder dike, possibly close to the entry point of a large chamber (Evans-Lamswood *et al.*, 2000). The Ovoid deposit narrows to the west into a dike-like conduit to form the Mini-Ovoid. It is apparent that mineralization is commonly associated with thicker domains of the conduit. The Ovoid deposit is a thick lens of massive sulphide overlying inclusion-rich gabbroic and troctolitic rocks (termed the Basal Breccia Sequence-BBS). Troctolitic rocks below the Ovoid are approximately 50 m thick and contain only disseminated sulphides. The massive sulphides of the deposit are coarse-grained and contain resorbed magnetite in pyrrhotite and chalcopyrite. Pentlandite occurs as large eyes within the chalcopyrite at the margins of pyrrhotite grains, and within the pyrrhotite as exsolution lamellae. Pyrrhotite is hexagonal and contains exsolved triolite. Other minerals present include cubanite, argentopentlandite and galena.

Towards the west, the conduit links at depth into a large troctolite-olivine subchamber termed the Western Subchamber. Mineralization, although not exclusively,

is associated with the Reid Brook Zone, located 200 meters up-dip of point of entry of the conduit into the Western Subchamber. The Western Extension sheet, or dike, has been traced west from the Ovoid for 2.5 km to a depth of approximately 4 km. The sheet is constantly changing in its orientation. The dike has a fine-grained chilled margin whereas the core is typically medium-grained troctolite containing leopard-textured sulphides and a distinctive breccia sequence. In addition to the typical BBS, another breccia sequence hosts troctolitic and melatroctolitic fragments. This other breccia sequence is spatially associated with massive sulphides that commonly cross-cut the BBS. To the east, the sheet widens into a lens of massive sulphide termed the mini-ovoid.

2.3.2 The Cirque Prospect

The Cirque prospect, discovered in 1995, was explored by Cartaway Resources. This prospect is located approximately 40 km south of Okak Bay in northern Labrador (Figure 2.3). The surrounding area is underlain by anorthosite-norite-gabbro-leucotroctolite rocks of the Nain Plutonic Suite (Dwyer, 1999 and 2001). The Cirque prospect is an extensive, yet discontinuous, gossan zone exposed in the cliff walls of a glacial cirque. The main host rock to the sulphides is a varied textured leucoanorthosite with well-preserved grey material having net-like adcumulate growth, to fine-grained, pale-green material that seems entirely recrystallized (Kerr and Smith, 1997). Sulphide mineralization is clearly magmatic, consisting of massive, net, and disseminated textured pyrrhotite, with lesser chalcopyrite. Mineralization is typically irregular to chaotic. Local sulphide zones range in thickness of a few centimeters to thickness greater than 1m (*op*

cit.). Massive sulphides are in places pod-like with an associated halo of disseminated sulphides (Dwyer, 1999 and 2001). The highest assay derived from surface grab samples yielded 0.36 % Ni, 0.61 % copper and 0.12 % Co (Cartaway Resources, PR, August 31, 1995). The best assay results obtained during drilling included a 5 m interval containing 0.44 % Ni and 0.27 % Cu (Cartaway Resources, PR, May 17, 1996). When present, the massive sulphide contains silicate inclusions and aggregates of plagioclase. Dwyer (2001) provided evidence for remobilization of the sulphides, especially with chalcopyrite. Finer-grained pyrrhotite is present in crosscutting fracture systems. The sulphides typically consist of coarsely crystalline pyrrhotite, with minor chalcopyrite concentrations at the margins of sulphide zones. Pseudo-network-textured zones developed within the anorthosites marginal to the massive sulphide zones indicate thermal erosion and disaggregation of the anorthosite by the sulphide liquid (*op cit.*). The contacts from sulphide to anorthosite are generally sharp to gradual while plagioclase grains typically show signs of thermal erosion and alteration.

2.3.3 The Krinor Prospect

The Krinor prospect, discovered in 1995, is located in the Alliger Lake map area immediately south of the Puttuaalu Brook valley (Figure 2.3) and was formally owned by Castle Rock Exploration (now called Castle Metals Exploration). The Krinor prospect is actually a cluster of prospects and is underlain by a series of layered norite and leuconorite of the Nain Plutonic Suite (Kerr and Smith, 1997). The main prospect, named the Krinor prospect, is an extensively rusty zone situated through a steep gully at the edge of a 300 m high shear cliff. Assays from the prospect yielded on average 0.56 to

0.82 % Ni, 0.16 to 0.6 % Cu and 0.1 to 0.13 % Co (*op cit.*). The most significant result of the exploration program was a grab sample containing 1.31 % Ni, 0.52 % Cu and 0.21 % Co (Castle Rock Exploration Corp., PR, October 4, 1995). One drill hole intersected sulphide mineralization up to 14 m thick, predominantly of disseminated pyrrhotite. Massive sulphide is rare and where present, is typically coarse-grained, crystalline pyrrhotite with lesser amounts of chalcopyrite (Kerr and Smith, 1997). Disseminated sulphides were found on the fringes of the massive sulphide. The contact between noritic host rock and massive sulphide varies from sharp to gradational (*op cit.*).

2.3.4 The OKG Prospect

The OKG prospect is located in the Umiakoviarusek Lake region, approximately 90 km to the northeast of the community of Nain, and less than 10 km south of Okak Bay (Figure 2.3). Castle Rock Exploration initially discovered the OKG prospect during a routine exploration program conducted in 1995. The majority of the information presented in this section is the work of Piercey (1998) and Piercy and Wilton (1999). The OKG prospect is geologically situated in the northern extreme of the NPS and contains pyroxenite-hosted magmatic Ni-Cu-Co sulphide mineralization. Mineralized pyroxenites are post Torngat deformation, which defines the age of mineralization as being Mesoproterozoic. Ryan *et al.* (1998), however, suggested that the anorthosites are Paleoproterozoic. Anorthositic wall rocks exhibit ductile shearing, intense recrystallization, and secondary replacement of the original igneous minerals. The exposed mineralization at the OKG prospect is restricted to a 450 x 40 m wide region containing two zones; the Main Zone and the North Zone. Both zones contain podiform

massive sulphides located proximal to both pyroxenitic-leucotroctolitic intrusive rocks and mylonitic shear zones. Normal grading process was observed, with approximately 5 % sulphide at the top, grading to massive sulphide near the base. Sulphide mineral assemblages are dominated by pyrrhotite which host the other sulphide/oxide phases including magnetite, pyrite, chalcopyrite, and pentlandite. Massive sulphides collected from surface showings assayed up to 1.78 % Ni, 1.41 % Cu, and 0.21 % Co (Wilton and Baker, 1996). At the Main Zone, the sulphide mineralogy is dominated by pyrrhotite and chalcopyrite, whereby pyrrhotite forms large grains and chalcopyrite is present as thin stringers along pyrrhotite boundaries or is associated with fragments of anorthositic wall rock. Disseminated sulphide is also present within the pyroxenite. The North Zone mineralization is spatially associated with a ductile shear zone and is dominantly disseminated sulphide with lesser massive sulphide. Blebs and stringers of chalcopyrite are also present. Within the massive sulphide, chalcopyrite and pentlandite are proportional, though pyrrhotite remains the dominant sulphide mineral.

2.3.5 The Nain Hill Prospects

The Nain Hill prospects are located approximately 3 km outside of the community of Nain, and are part of the former NDT/Takla Star Resources Joint Venture, Project 44 (Figure 2.3). The prospects are magmatic Ni-Cu-Co sulphide-oxide occurrences hosted by variably foliated anorthosite of the Nain Plutonic Suite (Hinchey, 1999). Nain Hill is dominated by anorthosite and gabbro-norite of the NPS. The sulphide and oxide mineralization is commonly spatially associated with a finer grained, mafic, gabbro-norite to proxenite that intrudes the anorthosite that contains the disseminated sulphides and

magnetite (Kerr, 1998). Sulphide mineralization contains less than 0.6 % Ni, and 0.4 % Cu, but grades locally range up to 1.6 % Ni (Hinchey *et al.*, 1999). There are three main sulphide zones present, namely the Valley, Unity East, and Unity West. The Valley Zone had a drill interval of 6.94 m assaying 0.51 % Ni, 0.37 % Cu, and 0.04 % Co (NDT, PR, July 30, 1996). In the Valley Zone, mineralization is exposed as extensive, deeply weathered gossans that are rich in magnetite, and contain fewer sulphides than the other zones. The mineralization is associated with a finer grained melanocratic rock type, possibly gabbronorite (Kerr and Smith, 1997). The host rock for the Unity Zone (Unity East and Unity West) consists of variably recrystallized white-grey anorthosite. Mineralization comprises minor disseminated sulphide in the anorthosite, massive to semi-massive veins (also associated with magnetite), disseminated sulphides and magnetite hosted by a fine- to medium-grained gabbronorite to pyroxenite. Unity East Zone had a drill interval of 6.28 m assaying 0.4 % Ni, 0.35 % Cu, and 0.15 % Co with smaller intervals containing 1.33 % Ni. The gabbronorite apparently has intruded the anorthosite. Sulphides are dominantly pyrrhotite with lesser chalcopyrite. Magnetite often forms beads in massive sulphide. Pentlandite occurs as small exsolutions in pyrrhotite generally around grain boundaries. The massive oxide and sulphide mineralization in both zones is gradational with the gabbronorite to pyroxenite intervals, and semi-massive to massive mineralization is gradational with the gabbronorite and pyroxenite.

2.3.6 The Franco Prospect

Archean Resources Ltd. discovered the Franco prospect in 1995 using standard airborne geophysical techniques in an attempt to uncover additional Ni-Cu-Co mineralization outside of the Voisey's Bay deposit. The prospect is located near the coast of northern Labrador, approximately 35 km north of the community of Nain (Figure 2.3). The information presented in this section is based on the work of Wells (1997) on two drill holes and limited geological mapping. Sulphide mineralization within this prospect is hosted by a Fe-rich variety of leucotroctolite belonging to the Hettasch Intrusion. The Hettasch Intrusion is a layered intrusion containing troctolite, anorthosite, and olivine leucogabbro. This intrusion is structurally exposed as an asymmetrical syncline (Berg, 1973) that is intruded by the Kiglipait Intrusion. Both the Hettasch and Kiglipait intrusions are part of the NPS. Leucotroctolitic rocks of the Hettasch Intrusion consist of cumulate plagioclase, intercumulus olivine/orthopyroxene, and varying amounts of oxides and sulphide. Sulphide textures observed in drill holes range between disseminated and massive. Typically, the drill holes display disseminated sulphide textures near the top, coarse, blotchy sulphides in the middle and narrow, semi-massive to massive intervals near the bottom. Sulphides are typically pyrrhotite with minor exsolutions of chalcopyrite and lesser pentlandite. Pyroxenite inclusions are abundant near the base of the main host rock (leucotroctolite). One reported assay from drill core included a small interval of massive sulphide containing 0.37 % Ni, 0.21 % Cu, and 0.062 % Co. Disseminated sulphide typically has more pentlandite than does the massive sulphide in this prospect.

2.3.7 Prospects within the Harp Lake Intrusive Suite

Kerr and Smith (2000) summarized the magmatic Ni-Cu sulphide mineralization in the Harp Lake Intrusive Suite and much of the information presented in this section was derived from that report. Although Kerr and Smith provided an overview of over ten sulphide prospects, only four will be discussed in this section. The four prospects were selected because of their spatial distribution in the Harp Lake Intrusive Suite and the varying lithologies that host the sulphides. The Harp Lake Intrusive Suite is largely an anorthositic, anorthosite to granitic pluton. Mineral exploration in the Harp Lake Intrusive Suite occurred as early as the 1970's (*e.g.* Kennco Exploration Ltd.) and continued throughout the Voisey's Bay exploration era. Most sulphide mineralization in the Harp Lake Intrusive Suite consists of disseminated, interstitial sulphides in leucotroctolite and anorthosite, which form concordant, stratiform, zones of syngenetic character (Kerr and Smith, 2000). There are more than 100 mineralized gossan zones reported within the Harp Lake Intrusive Suite.

2.3.7.1 The A-1 Prospect

A-1 prospect (also known as Gossan 37) is located near the southern boundary of the Harp Lake Intrusive Suite, north of Shipiskan Lake (Figure 2.3). Sulphides are hosted in a medium- to coarse-grained olivine-norite to leucotroctolite with well-defined igneous textures; the sulphides have patchy appearances in outcrop. Trench samples exhibit interstitial patches of pyrrhotite and lesser chalcopyrite. Sulphide proportions are typically small (<5%) and minor disseminated sulphide was observed in a nearby pyroxenite. Kennco's rock samples assayed an average 0.12 % Cu and 0.13 % Ni

(McAuslan, 1973b). The best drill hole assay results were from a 1.3 interval with 0.17 % Ni and 0.14 % Cu.

2.3.7.2 The Colette II Prospect

Colette II prospect (also known as gossan 44) is located southeast of Harp Lake (Figure 2.3). It is the single largest sulphide-bearing gossan known in the Harp Lake Intrusive Suite with a strike length of 1.4 km. The showing is hosted by massive anorthositic rocks between noritic anorthosite in the south and olivine-bearing anorthosite to leucotroctolite to the north. The mineralization is contained within dark-grey pyroxene-bearing anorthosite. Sulphides are part of a large stratiform zone containing interstitial pyrrhotite and chalcopyrite with low total sulphides (<5%). Assays from grab samples range from 0.1 to 0.28 % Ni, 0.09 to 0.13 % Cu (Kerr and Smith, 2000).

2.3.7.3 The Dart Prospect

The Dart prospect (also known as gossans 17 and 18), which was discovered (Figure 2.3) and worked by Kennco (McAuslan, 1973a, b), contains massive and disseminated sulphide. The main Dart showing is a thin massive sulphide layer developed at the base of a thicker unit containing disseminated sulphide mineralization (*op cit*). The host rocks were described as gabbroic, leucogabbro, and troctolitic. The contacts between the sulphides and the mafic rocks are sharp but irregular. The sulphide layers are approximately 2 m thick. Ni and Cu contents range from 0.32 % Ni and 0.8 % Cu with elevated Cu at 1.2 %. Pyrrhotite is the dominate sulphide. A grab sample of semi-massive sulphide assayed 0.53 % Ni and 0.2 % Cu. Disseminated sulphides are apparently enriched in cobalt.

2.3.7.4 The Ninety-Nine Prospect

Ninety-Nine prospect (gossan 99), discovered in 1973, is located northwest of Cleaver Lake, on the edge of the mappable exposure for the HLIS (Figure 2.3). No relationship is apparent between the mineralization and the margin of the Harp Lake Intrusive Suite. The sulphide gossan covers an area greater than 150 x 150 m, and typically consists of massive pyrrhotite and chalcopyrite mineralization. The country rock surrounding the mineralization is fresh, leucocratic, monomineralic anorthosite that is somewhat recrystallized. Sharp contacts exist between mineralized and unmineralized anorthosite. Anorthosite is commonly cut by thin sulphide veins and minor disseminated mineralization. Massive sulphides are dominated by pyrrhotite containing irregular chalcopyrite segregations. A number of sulphide zones that cut through the anorthosite assayed 0.44 % Ni and 0.62 % Cu (McAuslan, 1973b) and 0.51 % Ni and 1.27 % Cu (Osmand, 1992; Olshefsky, 1996). Disseminated sulphide have a tendency to contain more chalcopyrite. Cobalt assayed up to 0.18 % in massive sulphide.

2.3.8 The Fraser Lake Prospects

The Fraser Lake prospects collectively refer to a series of gossanous Ni-Cu bearing occurrences (*i.e.* Loon Lake, Main, and Hook Lake) located north of the Smallwood hydroelectric reservoir near Fraser Lake (Figure 2.3). Emslie (1970) originally described the gossans as occurring along the eastern margin of the Michikamau Intrusion hosted in what he termed the Marginal Zone. The Marginal Zone occurs on the outer edge of the intrusion and includes a contact chill zone that is about 30 cm in thickness. Inwards from this chilled margin is a fine to medium-grained, thickly banded

olivine gabbro that is approximately 250 m thick which grades into a medium and coarse-grained gabbro and troctolite (Dyke *et al.*, 2004). Sulphide mineralization occurs in troctolite, melatroctolite, and norite of the Marginal Zone and is typically disseminated to blotchy, with lesser “vein-like” or massive occurrences (*op cit*). The partially digested gneissic inclusions occurring within the Marginal Zone are akin to inclusions observed at Voisey’s Bay and Pants Lake (Kerr, 1999, 2003). Noranda Exploration Company Ltd. and Kennecott Canada Inc. explored the gossans for base and precious metals in 1991-1993 (prior to the discovery of the Voisey’s Bay deposits), and consequently drilled seven shallow holes to test AEM conductors and surface mineralization. Drilling intersected some minor disseminated and massive sulphide mineralization, but assays indicated that the mineralization was sub-economic (*e.g.* DDH FL93-02 contained 5 m averaging 0.31% Ni and 0.18% Cu, DDH FL93-04 contained 3 m averaging 0.34% Ni and 0.20 % Cu) (Kerr, 1999). Drilling did not intersect the basal contact to the intrusion. A surface channel measuring 3 m of gossanous rock assayed 0.30 % Cu, 0.90 % Ni, and 0.15 % Co.

2.3.9 The Baikie Prospect

The Baikie prospect, located approximately 80 km to the southwest of the coastal community of Hopedale (Figure 2.3), represents one of the few known examples of Archean, komatiite-related sulphide mineralization in Labrador. The showing, discovered in 1960 by BRINEX personnel, is hosted by one of two mappable greenstone belts within the 3.3 to 2.8 Ga Hopedale Block (Ermanovics, 1993), namely the Florence Lake greenstone belt. The Florence Lake greenstone belt consists of mafic and ultramafic flows, pillow lavas, mafic subvolcanic intrusive rocks, and minor felsic metasedimentary rocks, all of which were metamorphosed to greenschist to amphibolite facies (Swinden *et al.*, 1991). The Florence Lake greenstone belt is further divided into sub-belts defined by structural and intrusive contacts (Miller, 1996). The Baikie prospect is part of the Baikie sub-belt. There are a number of Ni-Cu occurrences known within the Baikie sub-belt (*e.g.* Boomerang Showing and DCP showing; *op cit*), the most economically significant being the Baikie prospect.

The Baikie prospect comprises locally massive and disseminated pentlandite, pyrrhotite, pyrite, and minor chalcopyrite and magnetite. Typical assay values from grab samples were 0.84 to 2.65 % Ni and 0.01 to 0.07 % Cu (Sutton, 1970; Brace and Wilton, 1990). Diamond drill core assayed 2.19 % Ni, 0.22 % Cu, and 0.16 % Co over 11.32 m (McLean *et al.*, 1992). Sulphides are enriched in PGE's and when chondrite normalized, the PGE profiles are similar to those for Archean, komatiite-related mineralization (Brace and Wilton, 1990). The sulphide mineralization, confined to xenoliths, is hosted by meta-ultramafic and actinolite schist enclaves in the Kanairiktok Intrusive Suite. Ultramafic rocks have been replaced by an alteration mineral assemblage consisting of

talc + carbonate + chlorite (*op cit.*). Ultramafic units mapped in the Baikie sub-belt are relatively thin, distal, sheet flow units with associated thin sulphidic sediment units (Miller, 1996). Ni-Cu mineralization is syngenetic to the intrusion of ultramafic bodies. The ultramafic volcanic rocks and associated Ni-Cu mineralization in the Florence Lake Belt exhibit many of the characteristics of the Kambalda-type or peridotite-hosted model (Leshner, 1989; Leshner and Arndt, 1995).

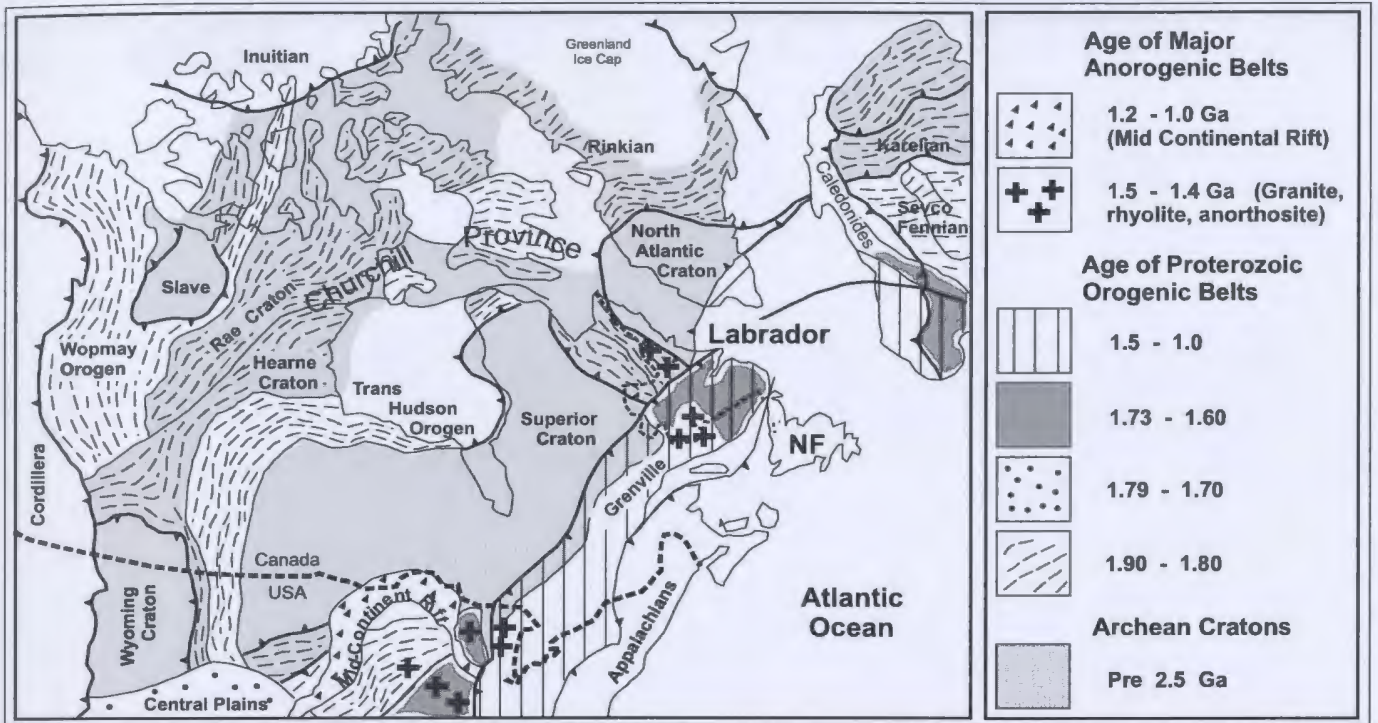


Figure 2.1. Structural Provinces of the North American-Greenland-Baltic shields with associated ages (modified after Hoffman, 1988).

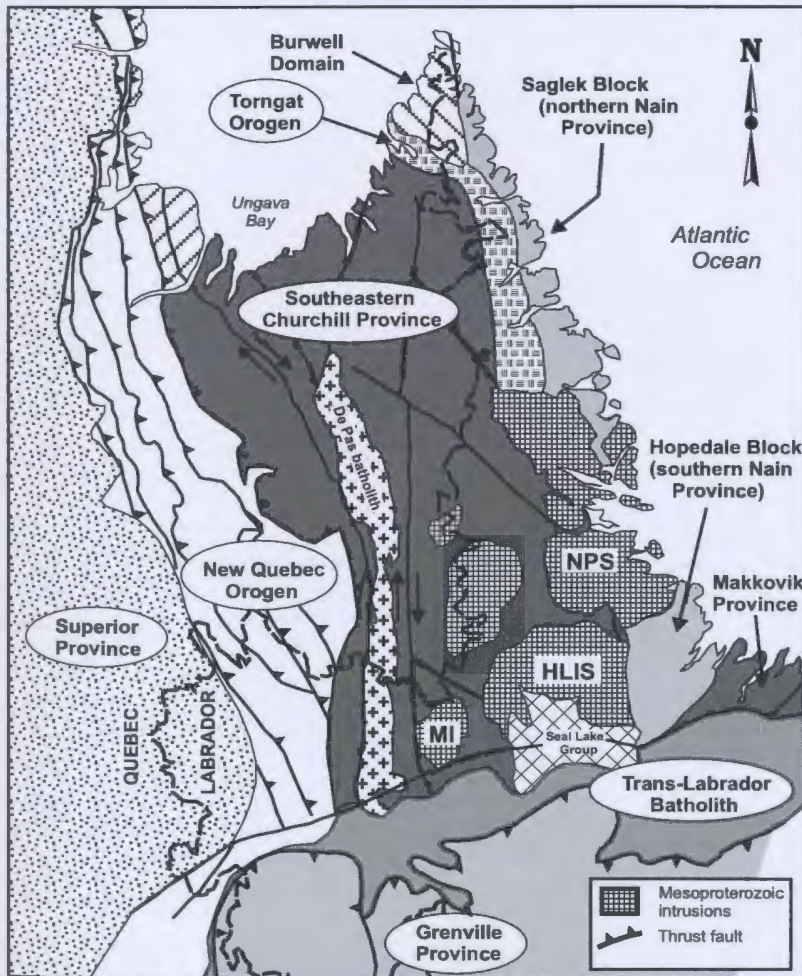


Figure 2.2. (Left) Principle tectonic elements of northern Labrador and adjacent northeastern Quebec (James, 1997). Only portions of the Makkovik and Grenville Provinces are shown.

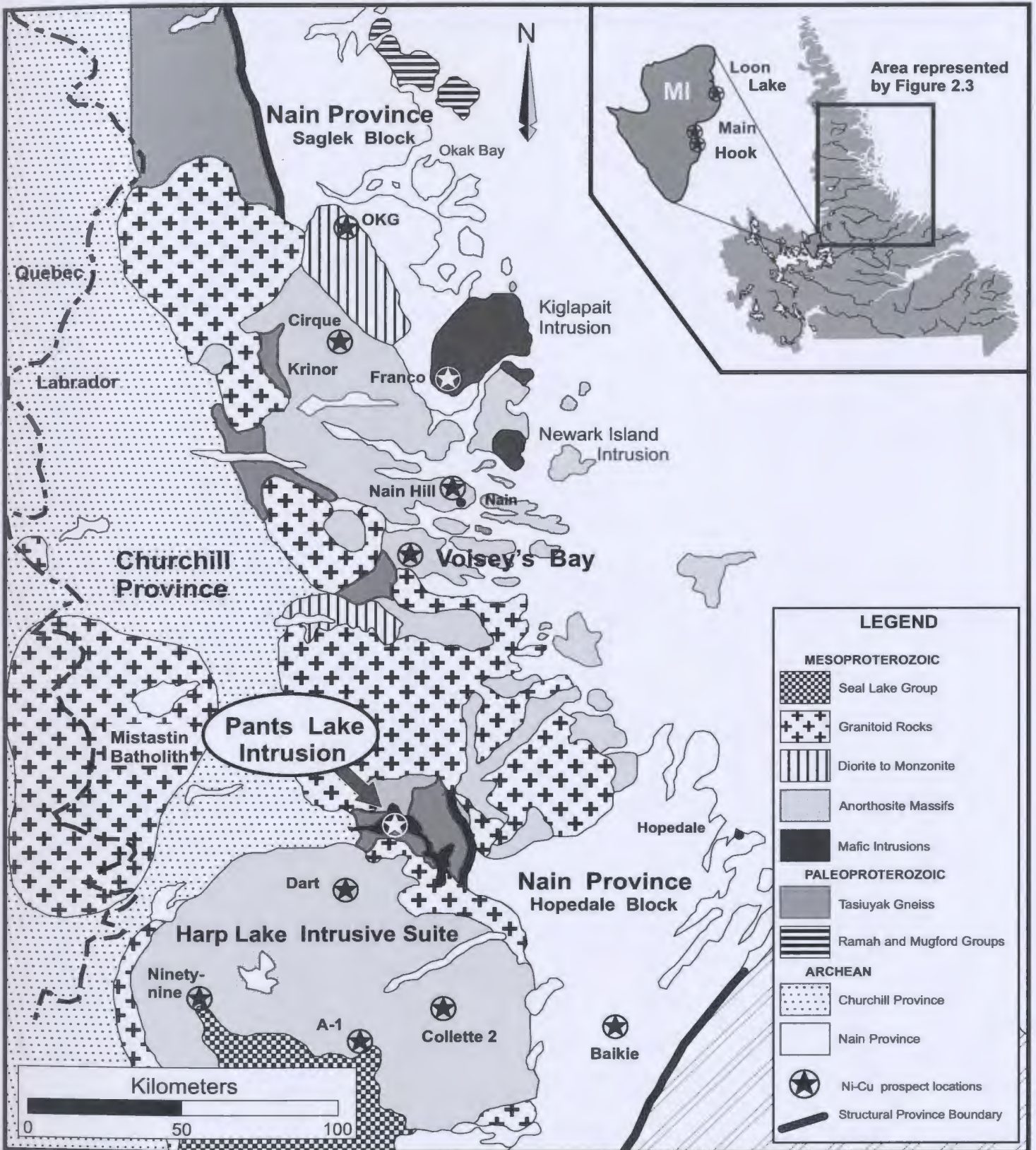


Figure 2.3. Geology of northern Labrador (modified after Kerr and Smith, 1997). The Pants Lake Intrusion is situated between the southern mapped boundary of the NPS, the northern boundary of the HLIS, and the western side of the proposed structural boundary of the Nain and Churchill provinces. The circled stars indicate the location of selected magmatic Ni-Cu sulphide prospects in northern Labrador. All of these prospects, including the Voisey's Bay deposits, are discussed in Section 2.3. The Michikamau Intrusion (MI) occurrences are located to the west of this area (see inset map above).

Table 2.1. Summary table of selected magmatic Ni-Cu sulphide prospects/deposits located in Labrador. See Figure 2.3 for the location of each prospect. Refer to Section 2.3 for a condensed description of each prospect named below.

| Prospect name | Geological setting / sulphide host rock | Inferred age of mineralization (Ma) | Major sulphide minerals | Sulphide textures | Best reported assay results | Selected references |
|---|---|-------------------------------------|--|---|---|---|
| Voiseys Bay | Voiseys Bay Intrusion (Nain Plutonic Suite) / troctolite and olivine gabbro | ca. 1330 | Pyrrhotite, chalcopyrite and pentlandite | Massive, semi-massive, clots/blotches, disseminated, remobilized, net. | Cumulative reserves and resources of all deposits: 124.4 x 10 ⁶ tonnes @ 1.66 wt % Ni, 0.88 wt % Cu, 0.09 wt % Co. | Li and Naldrett (1999) Evans-Lamswood <i>et al.</i> (2000) Lightfoot and Naldrett (1999) Naldrett <i>et al.</i> (1996) |
| Cirque | Nain Plutonic Suite / leucoanorthosite | ca. 1350-1290 | Pyrrhotite, lesser chalcopyrite & pentlandite | Massive pods, net, disseminations, remobilized | 0.44 % Ni, 0.27 % Cu | Dwyer (1999) Kerr and Smith (1997) Cartaway, PR (08/31/95) Kerr, 1998 |
| Krlnor | Nain Plutonic Suite / norite and leuconorite | ca. 1350-1290 | Pyrrhotite and chalcopyrite | Disseminations, lesser massive | 1.31 % Ni, 0.52 % Cu, 0.21 % Co | Castle rock, PR (04/10/95) Kerr and Smith (1997) Kerr (1998) |
| OKG | Nain Plutonic Suite / pyroxenite, leucotroctolite and anorthosite | ca. 1350-1290 | Pyrrhotite, chalcopyrite, pentlandite and pyrite | Massive pods, blebs, disseminations and remobilized | 1.78 % Ni, 1.42 % Cu, 0.21 % Co | Piercey (1998) Piercey and Wilton (1999) Kerr and Smith (1997) Wilton and Baker (1996) |
| Nain Hill: Three sulphide zones; Valley, Unity East and Unity West | Nain Plutonic Suite / Gabbronorite, pyroxenite and anorthosite | ca. 1350-1290 | Pyrrhotite, chalcopyrite and pentlandite | Disseminated, massive to semi-massive veins | 0.51 % Ni, 0.37 % Cu, 0.04 % Co | Hinchey (1999) Hinchey <i>et al.</i> (1999) NDT, PR (07/30/96) Kerr (1998) Kerr and Smith (1997) |
| Franco | Hettash Intrusion (Nain Plutonic Suite) / Fe-rich leucotroctolite | Older than 1306 | Pyrrhotite, lesser chalcopyrite and pentlandite | Disseminations, massive and blotchy | 0.37 % Ni, 0.21 % Cu, 0.062 Co | Wells (1997) |
| A-1 Dart Ninety-nine Colette II | Harp Lake Intrusive Suite / norite to leucotroctolite, anorthosite; gabbro and troctolite; anorthosite respectively | ca. 1450-1460 | Pyrrhotite and chalcopyrite | Disseminations; disseminations; massive (pod-like), disseminations; massive and disseminations respectively | 0.17 % Ni, 0.14 % Cu; 0.28 % Ni, 0.13 % Cu; 0.53 % Ni, 0.2 % Cu; 0.44 % Ni, 0.62 % Cu respectively | Kerr and Smith (2000) McAuglan (1973, a, b) Osmand (1992) Olshensky (1996) |
| Baikie | Florence Lake Greenstone Belt (Hopedale block, Nain Province) / meta-volcanics | ca. 3.3-2.8 Ga | Pentlandite, pyrrhotite, pyrite and chalcopyrite | Massive and disseminations | 2.19 % Ni, 0.22 % Cu, 0.16 % Co, enriched in PGEs | Miller (1996) James <i>et al.</i> (1996) Brace and Wilton (1990) McLean <i>et al.</i> (1992) |
| Fraser Lake: Loon, Main, Hook | Michikamau Intrusion / Marginal Zone gabbros, troctolites and norites | ca. 1460 | Pyrrhotite, chalcopyrite, pentlandite | Semi-massive to massive, disseminated, and blotchy | 0.90 % Ni, 0.30 % Cu, 0.15% Co | Dyke <i>et al.</i> (2004) Nunn (1993) Emslie (1970) Kerr (1999a) |
| South Voiseys Bay | Pants Lake Intrusion (Nain Plutonic Suite) / olivine gabbro and gabbro | ca. 1322 | Pyrrhotite, chalcopyrite and pentlandite | Massive, semi-massive, clots/blotches, disseminated, remobilized, net. | 11.75 % Ni, 9.70 % Cu, 0.43 % Co | Smith <i>et al.</i> (1999) Smith (this study) Kerr (1999) |

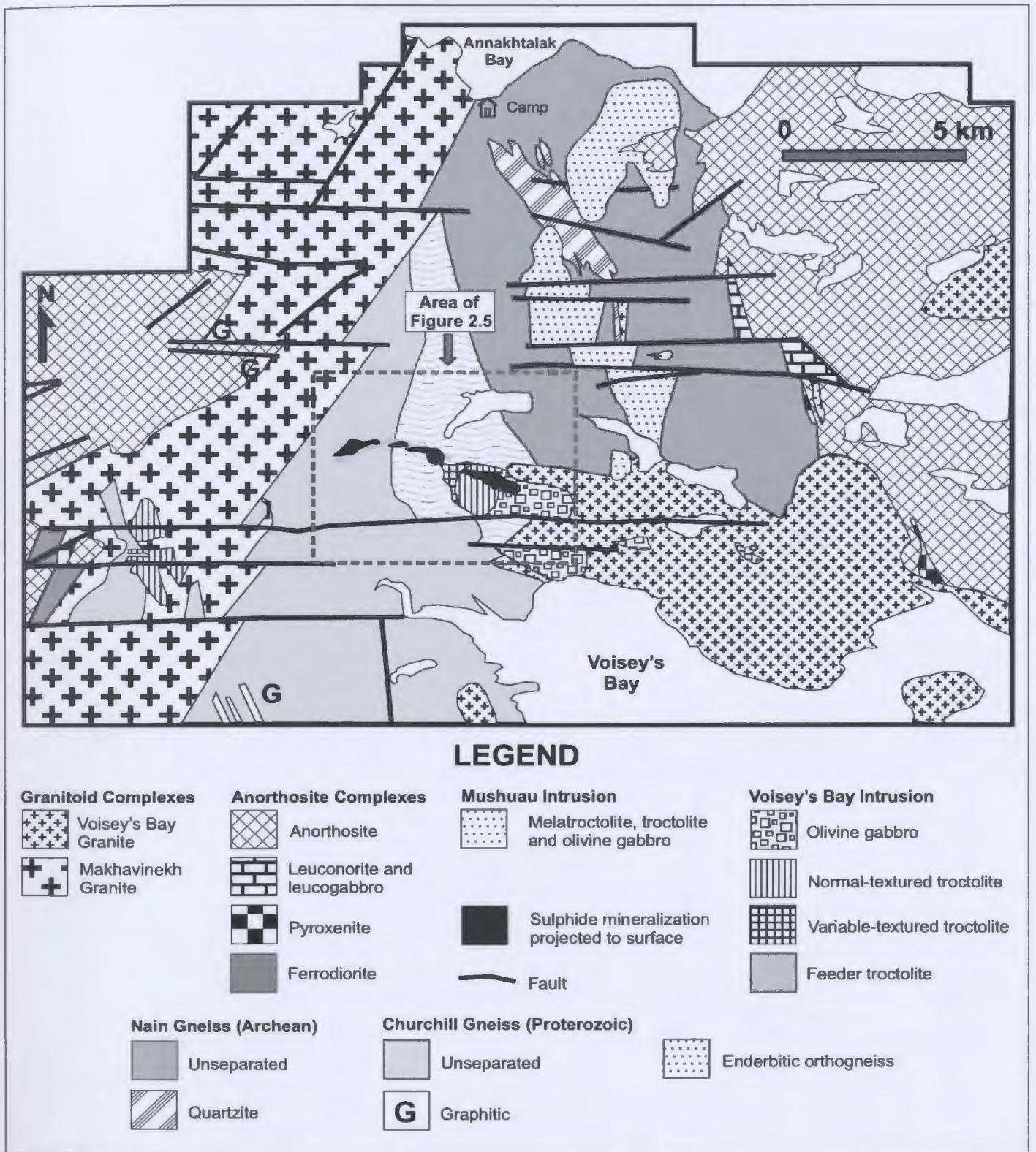


Figure 2.4. Geological map of the area north of Voisey's Bay, Labrador (modified after Lightfoot, 1998). The Voisey's Bay deposits, hosted in the Voisey's Bay Intrusion, are projected to surface.

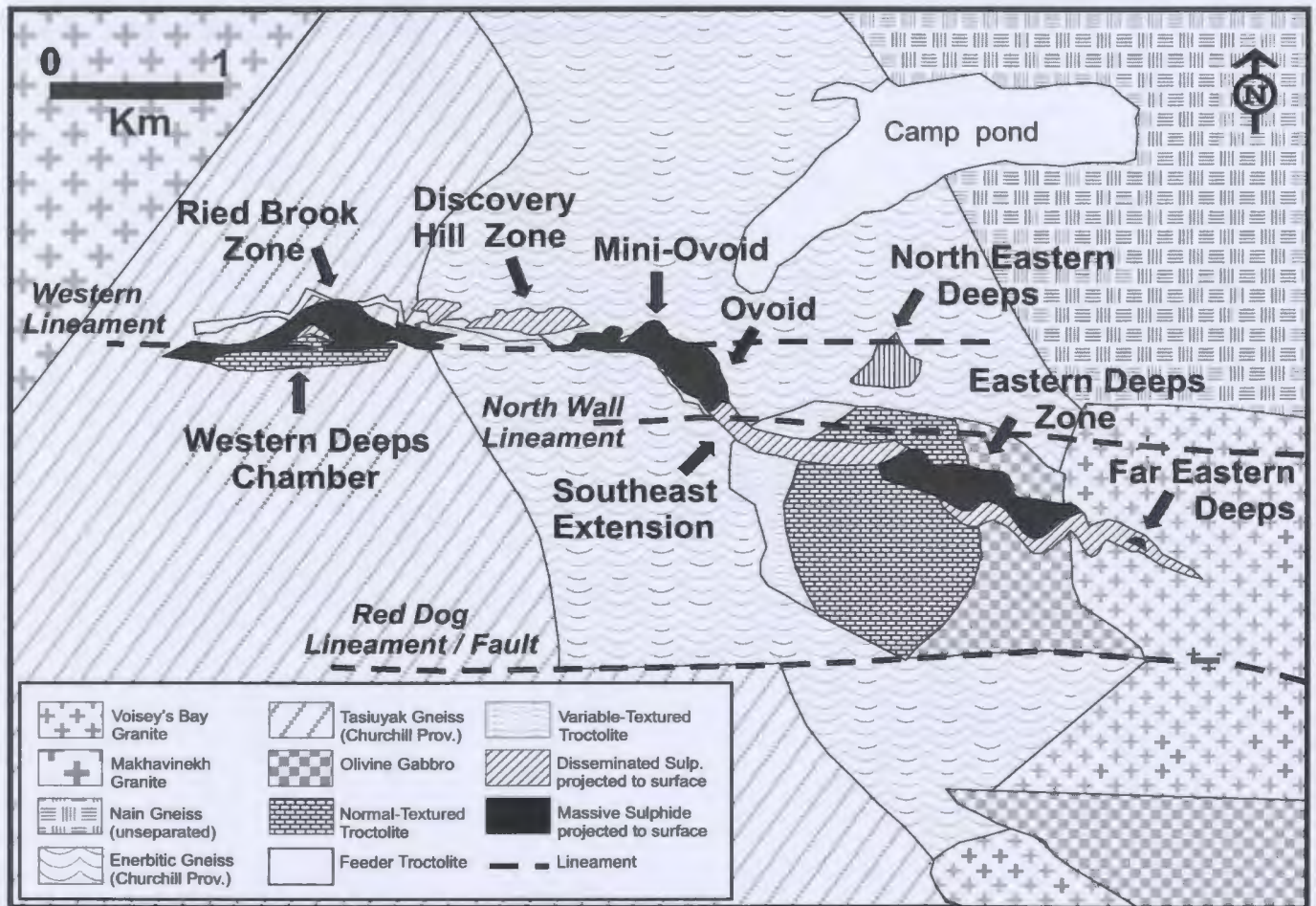


Figure 2.5. Surface projection of the troctolitic-gabbroic rocks, sulphide zones, and major structural elements associated with the Voisey's Bay deposits (Evans-Lamswood *et al.*, 2000). The location and surrounding geology of this figure is shown in Figure 2.4.

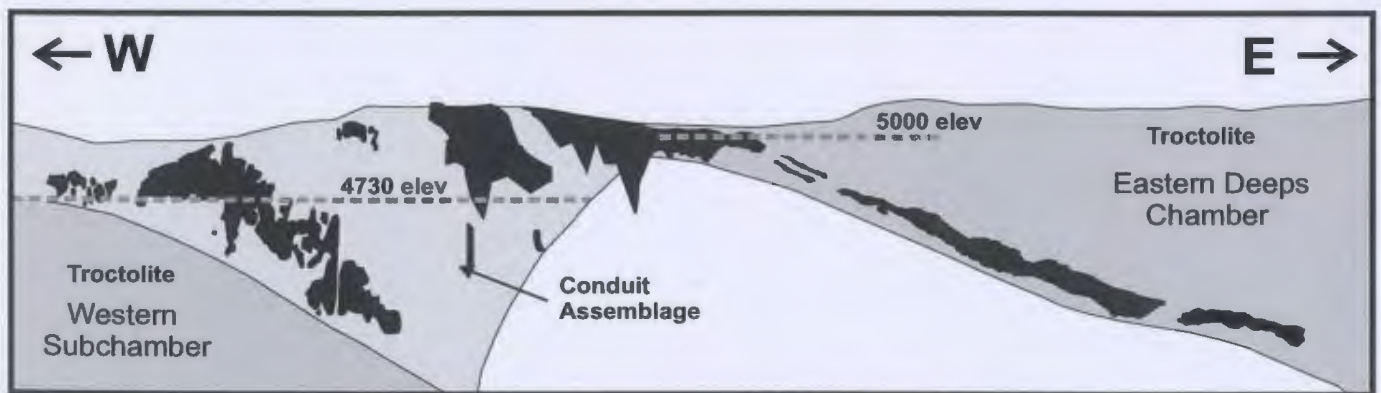


Figure 2.6. Voisey's Bay sulphide mineralization projected to a vertical longitudinal section (Lightfoot and Naldrett, 1999). The conduit assemblage shown in this figure is equivalent to the Feeder Troctolite shown in Figure 2.5.

Chapter 3: Regional Setting, Morphology, Geology, Petrography and Mineralization of the Pants Lake Intrusion

3.1 Introduction

The Pants Lake Intrusion (PLI) is one of several layered, mafic intrusions exposed in north-central Labrador (*e.g.* Kiglapait Intrusion, Mushua Intrusion, Hettash Intrusion, Barth Island Intrusion, *etc.*). The geological attributes common to these Labrador intrusions also appear in layered, mafic intrusions worldwide (*e.g.* Skaergaard Intrusion, Greenland; Stillwater Intrusion, Montana; Duluth Complex, Minnesota; Bushveld Intrusion, South Africa, *etc.*).

The primary purpose of chapter three is to document the geological characteristics of the PLI, emphasizing the unique sulphide-bearing and contaminated basal subdivision of the intrusion referred to by the author as the 'Basal Gabbro subdivision'. The secondary purpose of this chapter is to provide a foundation from which data in subsequent chapters concerning trace, major, rare earth element, and stable isotope geochemistry can be interpreted.

This chapter will include a compilation of the regional geological setting as reported by Hill (1982), Thomas and Morrison (1991), and Fitzpatrick *et al.* (1998, 1999). The morphology and broad-scale geology of the PLI is summarized from the author's own observations, combined with drill hole information and observations of Fitzpatrick *et al.* (1998, 1999), MacDonald (1999), and Kerr (1999). The centerpiece of chapter three are the descriptions and petrography of the subunits, sulphides, and xenoliths recognized within the Basal Gabbro subdivision, and to a lesser extent, the Upper Gabbro subdivision. All of the subunits are named according to the IUGS classification of mafic

rocks (Streckeisen, 1975). The final section of this chapter describes four surface occurrences located within the interior and flanks of the PLI.

3.2 Regional Geological Setting of the Pants Lake Intrusion

The regional geology encompassing the Pants Lake Intrusion (PLI) is illustrated on the geological map located in the inside, back pocket. This geology map, derived from the work of Donner Minerals Ltd and Teck Exploration Ltd personnel, represents a surface area of 25 x 35 km (the enclosed map location and map coverage is illustrated in Figure 1.1 and on the enclosed map).

The PLI is one among five prominent geological elements within the study area. These five geological elements include: 1) metamorphic rocks of the Archean Nain Province; 2) metamorphic rocks of the lower Proterozoic Churchill Province; 3) the north-south trending suture zone between the Nain and Churchill Provinces; 4) anorogenic plutonic rocks of the mid-Proterozoic Harp Lake Intrusive Suite; and 5) anorogenic plutonic rocks of the mid-Proterozoic Nain Plutonic Suite (Fitzpatrick *et al.*, 1998, 1999). Diabase and pegmatite dikes (not shown on the enclosed map) are also present in the map area. Ages for most of these geological elements are summarized in Table 3.1.

3.2.1 Nain Province

Gneissic rocks belonging to the ca. 3002-2500 Ma Hopedale Block (Ryan, 1991) of the Nain Province are located adjacent to the eastern border of the enclosed map. These rocks are the oldest lithologies mapped on the property, but do not appear to have any relationship with the PLI (Fitzpatrick *et al.*, 1998, 1999). There are two units present in the map area that belong to the Nain Province; an orthogneiss unit and a paragneiss unit.

The orthogneiss unit is typically white-weathered, fine- to coarse-grained, and granoblastic. Compositional banding is common with 1 to 50 cm wide, alternating bands of biotite (\pm hornblende) granodiorite to tonalite (Fitzpatrick *et al.*, 1998, 1999). The paragneiss unit is typically rusty-brown weathered, fine- to medium-grained, and composed of biotite-rich, tonalitic gneiss (*op cit.*). There is no apparent relationship between the paragneiss unit of the Nain Province and the paragneiss unit belonging to the Churchill Province (*op cit.*).

3.2.2 Churchill Province

Supracrustal gneisses of the 2780 to 1740 Ma (Swinden *et al.*, 1991) Churchill Province are intruded by the PLI. The Churchill Province gneisses in the area comprise: 1) pelitic and psammitic paragneiss, 2) leucocratic granitic orthogneiss, and 3) lesser amounts of mafic and granitoid gneiss. The paragneiss and orthogneiss units underlie approximately 50 % of the total surface area shown on the PLI geology map.

The paragneiss unit in the map area is typically white weathered with local linear rusty zones that contain between 5 to 10 % disseminated pyrrhotite (\pm pyrite), with a

similar amount of disseminated to foliated graphite. Alternating regular and contorted leucocratic and melanocratic mineralogical banding, ranging from 2 cm wide, upwards to 2 m, is typically observed in the unit. Paragneiss contains a range of minerals including garnet, quartz, feldspar, cordierite, biotite, muscovite, with subordinate hypersthene, magnetite, ilmenite, \pm sillimanite (Thomas and Morrison, 1991; Fitzpatrick *et al.*, 1998, 1999). The paragneiss unit described above is analogous to the Churchill Province Tasiuyak Gneiss that crops out along the length of the Nain-Churchill Province boundary (Thomas and Morrison, 1991; Kerr, 1999). The orthogneiss unit in this area intrudes the paragneiss unit and is a typically medium to coarse-grained, white to pink weathered, well foliated to augen gneiss. Coarse-grained garnet (\pm pyroxene) porphyroblasts are common, as well as large (up to 5 cm), elongated potassium feldspar grains. The matrix around these porphyroblasts contains quartz, plagioclase, orthopyroxene, and amphibole.

All gneissic units of the Churchill Province exhibit signs of polydeformation with a north-trending and east to west steeply dipping gneissic banding. Mylonitic zones developed in the paragneiss have a northwest-southeast trend (Fitzpatrick *et al.*, 1998, 1999). Inclusions observed in the Basal Gabbro subdivision of the PLI appear to have been derived from these Churchill Province gneisses. This topic will be elaborated in Section 3.5.2.

3.2.3 Nain-Churchill Province Boundary

The ca. 1850 Ma (Ryan *et al.*, 1995) Nain-Churchill boundary, shown as a dashed line on the enclosed geological map, represents a major Paleoproterozoic strike-slip crustal suture between two cratons (Ryan, 1996). This north-south trending, eastward

dipping mylonitic suture zone is located approximately 7 km east from the easternmost surface expression of the PLI. Although not shown on the enclosed map, the northern and southern continuations of this suture are obscured by the Nain Plutonic Suite and Harp Lake Intrusive Suite, respectively. The location of the Nain-Churchill Province suture within the map area was defined by the eastern termination of the paragneiss unit (described above) belonging to the Churchill Province. This correlation is also noted elsewhere in Labrador (Ryan, 1996).

3.2.4 Harp Lake Intrusive Suite

Located to the south and covering approximately 20 % of the map area is the 1460 to 1450 Ma (Emslie, 1980) Harp Lake Intrusive Suite. This anorogenic plutonic suite, superimposed over the Nain/Churchill province boundary, intrudes gneisses from both the Churchill and Nain Provinces within the map area. Rocks belonging to the PLI intrude phases of the Harp Lake Intrusive Suite (Fitzpatrick *et al.*, 1999).

This relatively undeformed and unmetamorphosed suite comprises a broad range of rock types, including anorthosite, leucogabbro, leuconorite, and granitoid. Outcrops of anorthosite, leucogabbro, and leuconorites have beige to rusty weathered surfaces, and are typically medium- to coarse-grained with cumulate texture. Rocks are comprised of plagioclase with intercumulate pyroxene, hornblende, and Fe-Ti oxides (*op cit.*). Granitoid rocks, the most abundant lithologies in the Harp Lake Intrusive Suite, are white to rusty-weathered, and include monzonite, granite, and syenite. These rocks are megacrystic with a distinctive rapikivi texture, containing potassium feldspar, plagioclase, hornblende, quartz, and lesser pyroxene (*op cit.*).

3.2.5 Nain Plutonic Suite

Rocks of the 1350 to 1290 Ma (Ryan, 1998) Nain Plutonic Suite, located on the northern corners of the enclosed map, represent less than 10 % of the surface area. The main rock types include: 1) anorthosite, 2) a variety of diorite, and 3) granitoid.

The anorthositic association is typically rusty-white weathered and composed of anorthosite, norite, and gabbro. Overall, this unit has cumulate and subophitic to porphyritic texture, defined by the minerals of plagioclase, olivine, orthopyroxene, clinopyroxene, magnetite and minor hornblende. Xenoliths of very coarse-grained anorthosite and Churchill Province rocks are present locally in the anorthosite (Fitzpatrick *et al.*, 1999). Dioritic rocks are rusty-white weathered consisting mainly of diorite, and quartz monzonite to quartz diorite. These units contain hornblende, clinopyroxene, and quartz, interstitial to plagioclase phenocrysts, and rare xenoliths of anorthosite - leuconorite and Churchill Province gneiss (*op cit.*). Granitoid rocks, composed of syenite, quartz syenite, and minor granite, are typically rusty-pink weathered. Their composition is variable, containing potassium feldspar as phenocrysts with interstitial hornblende, Fe-Ti oxides, clinopyroxene, quartz, and feldspar (*op cit.*).

3.2.6 Mafic Dikes

Mafic dikes intrude rocks of the Nain Plutonic Suite and Harp Lake Intrusive Suite, as well as Churchill Province gneiss. Mafic dikes, however, have not been observed to intrude the PLI, or *vice versa*. The mafic dikes present in the Nain Plutonic Suite and Harp Lake Intrusive Suite have ages of 1280 (Ryan *et al.*, 1995) and 1274 ± 2 Ma (Cadman *et al.*, 1993), respectively. The age of the diabase dikes that intrude

Churchill Province gneisses, as seen from drill core within the map area, are at present time unknown. An estimate of somewhere between 1280 and 1274 Ma, however, is probable. These northeast-trending dikes are typically dark green to dark grey, fine- to medium-grained, and comprised of olivine gabbro with a distinctive diabasic texture. Dikes observed in drill core range from 0.5 to 5.0 m, have aphanitic chill margins, and locally contain small (0.5 to 2 cm), partially digested, gabbroic/anorthositic xenoliths. Selected dikes have been sampled and will be discussed in a future section with respect to their geochemistry and relationship to the PLI.

3.2.7 Age of the Pants Lake Intrusion

It is imperative to state at this point that the PLI is in all likelihood a member of the Nain Plutonic Suite. This conclusion is based on three pieces of evidence. Firstly, the PLI is mineralogically similar and proximal to the NPS. Secondly, the PLI intrudes rocks belonging to the northern margin of the Harp Lake Intrusive Suite (see enclosed map). The final evidence is U-Pb baddeleyite and zircon crystallization ages from an olivine gabbro located in the Northern Gabbro (Hole SVB-97-67) of 1322.2 ± 2 Ma (Dunning, 1998; Appendix D). A second U-Pb baddeleyite crystallization age was determined from an olivine gabbro located in the Southern Gabbro (Hole SVB-97-79) of $1337 \pm 4/-2$ Ma (Connelly, 2001; Appendix D). These ages place the PLI within the age range established for the Nain Plutonic Suite (stated at the beginning of this section) and outside of the range for the HLIS (ca. 1460-1450 Ma). Refer to Table 3.1. The second crystallization age, $1337 \pm 4/-2$ Ma, is similar to the age reported from the Voisey's Bay Intrusion (1338 Ma; Ryan *et al.*, 1995).

3.3 Morphology of the Pants Lake Intrusion

3.3.1 Surface Distribution and Dimensions of the Pants Lake Intrusion

Intrusive rocks belonging to the PLI were initially investigated by Hill (1982) and Thomas and Morrison (1991) during large-scale regional mapping surveys (refer to Previous and Present Geological Surveys, Section 1.4). These initial surveys roughly outlined the geographic distribution of the PLI, but it was not until recent geological mapping and diamond drilling was completed that the surface and subsurface extent of the PLI was first documented. The enclosed geological map (inside pocket) shows the present-day surface exposure of the PLI. To aid in describing the distribution of the PLI, the PLI is subdivided into three geographic components: 1) the North Gabbro, 2) the Central Gabbro (or Worm Gabbro), and 3) the South Gabbro. These geographic components are shown in Figure 3.1.

The largest exposed component of the PLI is the North Gabbro, which is composed of one large body with several smaller, satellite bodies. The North Gabbro has a crude, triangular shape, measuring 16 km along the southern base, and 8 km from the southern base to the northern apex. The Central Gabbro forms a linear link between the North and South Gabbro, measuring approximately 7 km from north to south, and less than 1 km wide. The South Gabbro comprises a package of large and small, isolated, north-trending bodies. The length of the South Gabbro package is approximately 12 km and the width ranges from 2 to 5 km. A few isolated, small ($< 0.5 \text{ km}^2$), gabbroic outcrops were reported outside of the aforementioned components. These isolated outcrops are present to the east of the South Gabbro, approximately 1 km west of the projected Nain/Churchill Province boundary (see enclosed map). Overall, the PLI is

orientated northeast and southwest. The distance from the northern mapped boundary to the southern mapped boundary of the PLI exceeds 20 km. An estimate of the exposed surface area covered by the PLI is 70 km².

3.3.2 Subsurface Geometry of the Pants Lake Intrusion

The full subsurface extent of the PLI is presently unknown. Diamond drilling collared on, and adjacent to the intrusion, (see enclosed map for drill collar locations) has roughly defined the subsurface morphology of the intrusion, but not the subsurface limits. The PLI is a horizontal to sub-horizontal, sheet-like body. The thickness of this body is quite variable in places. For example, in the North Gabbro, the maximum vertical thickness intersected by drilling is approximately 400 m, whereas in the Worm Gabbro, the maximum vertical thickness is approximately 150 m. Diamond drilling conducted approximately 5 km to the east of the eastern margin of the PLI has intersected a thin, shallow dipping, layer of gabbroic rocks of probable PLI affinity beneath gneisses of the Chuchill Province. These observations suggest that the intrusion is much more extensive to the east than is exposed on surface. Only one or two drill holes have been collared to the west of the intrusion and these holes indicate that the PLI may have pinched out below the gneisses. Until further drilling is conducted outside of the mapped boundary of the PLI, the true extent of the PLI will remain unknown.

The footwall contact of the PLI with the surrounding country rocks appears to be broadly undulating with localized depressions. This pattern probably reflects magma emplacement and lateral propagation of the PLI into the surrounding country rock. The geometry of the PLI, although complex, can be simplified by utilizing drill hole data

projected to vertical longitudinal sections, or drill hole data used to create isopach maps of different features (*e.g.* the basal contact, Figure 3.2). The vertical longitudinal sections (see enclosed map) of the PLI illustrate a number of interesting features.

The North Gabbro plunges beneath Churchill Province gneisses to the north-northwest and east-northeast from a centralized, elevated core (refer to sections A-A¹, B-B¹, C-C¹, D-D¹ and F-F¹). This characteristic is further portrayed in Figure 3.2 of the contoured basal contact topography of the North and Central Gabbro (relative to sea level) map. In addition to the above observations, a trough-like structure, plunging to the north-northwest and localized to the center of the North Gabbro is apparent. The Central Gabbro plunges slightly beneath Churchill Province gneiss to the east and northeast.

The South Gabbro is distinct from its northern correlatives. The South Gabbro exhibits evidence of multiple layers in the country rock that may, or may not, thicken at depth (refer to sections F-F¹ and E-E¹). Due to the lack of sufficient drilling over the entire South Gabbro, it is difficult to ascertain its true geometry and plunging directions, that is, if plunging exists.

Figure 3.3 illustrates a combined three-dimensional perspective of the three components showing the complex geometry of the PLI (the sections in this Figure 3.3 are taken from the sections plotted on the bottom of the enclosed map). Figure 3.3 also shows the variable thickness of the PLI. The South Gabbro and the western portion of the North Gabbro are the thickest, ranging somewhere between a maximum of 750 to 400 m, while the minimum thickness of the PLI is approximately 30 to 40 meters. It is difficult to predict the true thickness of the PLI because the amount of material that was removed during erosion and glaciation is uncertain.

3.4 Geology of the Pants Lake Intrusion: Previous Interpretation

The geology of the PLI as shown on the enclosed map represents the interpretation of the geology as mapped by Donner Minerals Ltd. and Teck Exploration Ltd. personnel who subdivided the PLI into three primary subunits. These primary subunits, separated largely on grain size and composition, are; 1) black gabbro, 2) olivine gabbro, and 3) upper olivine gabbro to gabbro. Two secondary subunits, including a contact breccia subunit and a contaminated olivine gabbro subunit, were also delineated. Brief lithological descriptions and comments on the spatial distribution of the primary subunits, simplified from information provided by Fitzpatrick *et al.* (1998, 1999) and MacDonald (1999), are presented in this section. The nomenclature applied to the primary subunits is largely derived by Fitzpatrick *et al.* (1998, 1999), and MacDonald (1999). Although these names are appropriate, it is more convenient to incorporate the primary and secondary subunits to conform to the author's descriptions and interpretations of the PLI subsurface geology. Therefore, descriptions of the primary and secondary subunits presented in the following text will be elaborated on in a later section. Table 3.2 summarizes the nomenclature used to describe the geology of the PLI.

3.4.1 Black Gabbro

Black gabbro is located primarily at the northern apex of the North Gabbro. This subunit is so named because of the distinctive dark-grey to violet-grey weathered and fresh surfaces. The dark color was determined optically to be due to an abundance of fine-grained, opaque, oxide inclusions, likely ilmenite and hematite, in the plagioclase and pyroxene grains (Fitzpatrick *et al.*, 1999; MacDonald, 1999). The black gabbro

includes medium- to coarse-grained gabbro to olivine gabbro, and a finer-grained olivine gabbro variety. The essential minerals and modal abundances of the coarser black gabbro include 60 to 65 % cumulate plagioclase, with 25 to 30 % and 10 to 20 % intercumulate olivine and clinopyroxene, respectively. Biotite, phlogopite, and magnetite are the chief accessory minerals. The finer grained, black gabbro has increased olivine and pyroxene contents, and lesser plagioclase than the coarser grained black gabbro. The coarser grained black gabbro usually overlies the much thinner, finer grained black gabbro. The contact between the Black Gabbro subunit and other subunits of the PLI was reported as being very gradational (*op cit.*). MacDonald (1999) suggested, however, that the black gabbro is intrusive into the olivine gabbro.

3.4.2 Olivine Gabbro

Olivine gabbro has a distinctive reddish-brown weathered surface. This subunit was mapped mainly on the flanks of the North and Central Gabbro, generally in topographic lows, corresponding to the lower layers of the intrusion. The South Gabbro on the other hand is dominated by this subunit. Olivine gabbro is mainly medium- to fine-grained, with local coarse-grained intervals. This subunit also well developed, 10 to 30 cm wide. The main minerals and modal abundances in this subunit are 20 to 40 % cumulus olivine, with 60 to 75 % intercumulus plagioclase, and 1 to 5 % clinopyroxene. Secondary minerals include biotite, magnetite, ilmenite, and apatite (MacDonald, 1999).

3.4.3 Upper Olivine Gabbro/Gabbro

Upper olivine gabbro to gabbro overlies most other subunits predominantly in the North and Central Gabbro, and to a lesser extent, in the South Gabbro. This subunit typically weathers grey to beige-brown with a mainly coarse to medium-grain size with widespread, isolated, thin pegmatitic intervals. The upper gabbro is typically massive and layering is not common. The main minerals and modal abundances of this subunit are 70 to 80 % cumulus plagioclase, with 10 to 20 % intercumulus clinopyroxene and olivine. Secondary minerals, magnetite and ilmenite are also present (MacDonald, 1999). Hornblende occurs in altered examples of this unit, predominantly in the situation where the unit is capped by gneiss.

3.5 Geological Subdivisions and Petrography of the Pants Lake Intrusion

The geology of the PLI is more complex than what the enclosed geological map can portray. This geological complexity is best observed in drill core and in cases where deep valleys penetrate to the base of the intrusion. Beneath the surface of the PLI, the previously mentioned primary subunits, among others, are recognized as an integral part of an internal, layered stratigraphy, representing not just one intrusion, but rather multiple intrusions. Each subunit layer typically resides in a fixed stratigraphic elevation, relative to the footwall contact. Therefore, in order to satisfy the purpose of this study, the author has divided the PLI into two major subdivisions. These subdivisions, based largely on drill core observations, are presented such that the reader may have a clearer understanding of both the lateral and vertical extents of the various lithologies. It is then necessary that the primary subunits presented in an earlier section (Section 3.4) be

incorporated into these subdivisions. The first major subdivision includes rocks in the upper layers of the PLI, henceforth referred to as the Upper Gabbro subdivision. The second major subdivision, and focus of this study, includes rocks from the basal layer of the intrusion, henceforth referred to as the Basal Gabbro subdivision.

The most simplistic perception of these two subdivisions is that the Basal Gabbro contains greater than trace amounts of magmatic sulphide and/or, partially digested, xenoliths, whereas the Upper Gabbro is relatively barren of sulphides and xenoliths. The relationship between the two subdivisions, and surrounding country rocks, is illustrated in the vertical longitudinal sections located on the enclosed map. The Upper Gabbro everywhere, without exception, stratigraphically overlies the Basal Gabbro, and in turn, the Basal Gabbro everywhere overlies the country rock. Outcrop and drill core evidence indicates that the Basal Gabbro intruded into the country rock prior to the emplacement of the Upper Gabbro (Fitzpatrick *et al.*, 1999). On the periphery of the intrusion, the Upper Gabbro sometimes pinches into or underplates the country rock. The contacts between the two subdivisions are normally gradational, although examples of sharp contacts do exist. The contact between the Basal Gabbro and the country rock is extremely variable. The Upper Gabbro is the volumetrically dominant phase of the two major PLI subdivisions with ratios of Upper Gabbro to Basal Gabbro of approximately 5:1 in places where the PLI is thickest and 4:1 where the PLI is thinnest. Both subdivisions are spatially distributed throughout the entire PLI, whereas in some rare localities, the Basal Gabbro may be absent. The Upper Gabbro is easily recognized on surface, predominantly on hilltops. Observations of the Basal Gabbro, outside of those from drill core, are

confined to outcrops located on the flanks of the intrusion, or in places where erosion has provided a penetrative valley downwards to the base of the intrusion.

The author's complete descriptions of the two subdivisions are presented in the following sections. It should be emphasized that rock descriptions are based mainly on observations derived from a spatial distribution of thirty-four drill cores concentrated on the mineralized regions throughout the PLI (Figure 3.1 and Appendix A). Outcrop observations are also used in the many rock descriptions. The location and source of all observations will be clearly stated and referenced in the text.

3.5.1 The Upper Gabbro Subdivision of the Pants Lake Intrusion

The Upper Gabbro subdivision of the PLI does not represent a single rock unit, but rather comprises multiple subunits. The differences between the various subunits are based largely on grain size, texture, and mineralogy. Petrographic descriptions of the subunits in the Upper Gabbro succeed each subunit description. In most cases, the textural and mineralogical variations distinguish the subunits. However, variations in grain size and colour are generally the most pronounced feature of a particular subunit when observed in outcrop or in drill core.

The Upper Gabbro is broadly subdivided into: 1) coarse- to medium-grained gabbro, 2) fine to medium-grained olivine gabbro, 3) pegmatic gabbro, and 4) altered gabbro. The third and fourth subunits are likely a derivative from the coarse- to medium-grained gabbro. The previously defined Black Gabbro and Upper Olivine Gabbro (Sections 3.4.1 and 3.4.2 respectively) are analogous to the first subunit presented in this section (Table 3.2). The olivine gabbro subunit described below is correlative with the

primary subunit with the same name (Table 3.2). During the course of core re-logging, the author utilized the subunit names listed above. Figure 3.4 shows the relevant vertical location of the subunits within the Upper Gabbro. Figure 3.4 however, is an idealized section constructed primarily on drill core observations and should be used only as a cursory guide to accompany the following subunit descriptions.

3.5.1.1 Coarse- to Medium-Grained Gabbro

Coarse- to medium-grained gabbro is found throughout the entire PLI, and is commonly observed on hilltops (Plate 3.1) and from the upper intervals of drill core intersections where drill holes collared in the Upper Gabbro (Plate 3.2). Coarse-grained gabbro dominates the upper layers of the Upper Gabbro, whereas medium-grained gabbro is dominant in the middle to lower layers (refer to Figure 3.4). However, several examples were observed in drill cores whereby drill core intervals alternated between coarse- and medium-grained gabbros (*e.g.* SVB-96-52, SVB-97-57, SVB-97-59, *etc.*). Fine-grained gabbro is locally present, although subordinate to the coarser grained gabbros. Grain size fluctuations are normally gradational between coarse- and medium-grained gabbro. Two distinct colour varieties of the coarse- and medium-grained subunit are leucogabbro and melagabbro.

The primary Black Gabbro, described previously in Section 3.4.1, is amalgamated under the melagabbro variety for two main reasons. Firstly, there is no defined chemical or textural trait that can distinguish the Black Gabbro from other gabbros in the PLI (Fitzpatrick *et al.*, 1999), and secondly, the Black Gabbro has the dark appearance

prevalent in a melagabbro. Apart from colour, the leucogabbro and melagabbro are relatively the same rock type, and will be referred to as gabbro unless otherwise stated.

Both the medium-grained gabbro and coarse-grained gabbro are composed of cumulate plagioclase, with lesser interstitial clinopyroxene and olivine. Magnetite and ilmenite (\pm pyrrhotite) are the main secondary minerals. Seriated, euhedral plagioclase grains range from 0.5 to 2 cm in length. Plagioclase grains from the leucogabbro are dominantly white in drill core and beige in outcrop. In drill core and outcrop examples of the melagabbro, plagioclase grains have a deep grey to greyish-purple colour. The smaller pyroxene and olivine grains generally have dark grey to dark green colour as seen in drill core and outcrops from both the leuco and melagabbros. Sulphide minerals are rare in this subunit, and if present, they are normally comprised of fine-grained, disseminated pyrrhotite typically associated with interstitial magnetite.

Petrographic observations of leuco and melagabbro from this subunit show that they are similar in texture and composition (Plate 3.3 and Plate 3.4). All rocks belonging to this subunit are cumulate. The main silicate minerals are plagioclase (70-80%) and clinopyroxene (10-15%), with minor olivine (3-5%). Secondary minerals include biotite, rutile, actinolite, sericite, and serpentine (< 5% total), and trace pyrrhotite and magnetite (\pm ilmenite). The orthocumulate plagioclase grains are bladed, euhedral, and range in size between 1-8 mm, typically 4-5 mm in length. Some plagioclase grains are weakly to moderately sericitized, whereas a few plagioclase grains are zoned. Clinopyroxene is typically intercumulate and locally subophitic. Clinopyroxene grains range in size, between 0.5 to 6 mm, and in places encloses several smaller plagioclase and olivine grains. Reaction rims of actinolite or amphibole are common on clinopyroxene grains.

Olivine grains are typically intercumulate, euhedral, small (< 2 mm), and commonly have iddingsite alteration rims or are weakly altered to serpentine (Plate 3.3). Trace, disseminated, intercumulate sulphides and oxides are rare, and where present are typically fine grained. Biotite and rutile typically partially surround sulphide and oxide grains.

3.5.1.2 Olivine Gabbro

The Olivine Gabbro subunit of the Upper Gabbro is not as common as the gabbro subunit described above, but is present in several drill cores examined for this study (*e.g.* SVB-96-04, SVB-96-17, SVB-96-29, *etc.*). Olivine gabbro is found predominantly in the lower layers of the Upper Gabbro, normally just above the upper Basal Gabbro contact (refer to Figure 3.4). Thin, diffuse layers of olivine gabbro also occur between layers of medium- to coarse-grained gabbro. Olivine gabbro is typically fine- to medium-grained.

Outcrops of this subunit typically have a reddish-brown weathered surfaces, but grey or beige weathered surfaces of this subunit were also observed. In drill core, this subunit has a greenish-grey appearance (Plate 3.5). Textures in this subunit are quite variable (ophitic to cumulate), but normally contain cumulate, fine-grained, greenish-grey plagioclase with interstitial olivine and pyroxene. In other examples of this subunit, granular olivine is the main cumulate phase, giving the core a patchy appearance (Plate 3.5). Interstitial, trace, disseminated pyrrhotite is present, but uncommon. In rare examples, lone, partially digested, leucocratic inclusions were observed.

Petrographic observations of this illustrate that the texture is ophitic to subophitic (Plate 3.6). This texture is defined by 60 to 65% seriated, 0.4 to 3.0 mm, euhedral to subhedral plagioclase grains partially enclosing small (0.2 to 0.5 mm), granular olivine

grains that normally comprise 20 to 25% of this subunit. Large (0.5 to 5.0 mm) clinopyroxene grains contain several plagioclase and olivine grains. It is probable that the early-formed olivine grains were followed by the crystallization of olivine and plagioclase and then succeeded by clinopyroxene. Sulphide and oxide minerals are rare in this subunit; however, magnetite appears to be the most abundant. Both sulphides and oxides are fine-grained, disseminated, and appear interstitial to the olivine and plagioclase minerals. In most cases, magnetite grains are isolated; however, pyrrhotite is closely associated with magnetite.

3.5.1.3 Pegmatitic Gabbro

Pegmatitic gabbro occurs dominantly within the leucogabbro (and melagabbro) subunit described above, but was also observed in the olivine gabbro (refer to Figure 3.4). This subunit is the least voluminous of the lithological subunits in the Upper Gabbro subdivision, but is commonly observed throughout the entire PLI where coarse- to medium-grained gabbro exists. Due to the very large grain size, petrographic information is difficult to obtain.

Pegmatitic gabbro normally forms thin (10 to 30 cm), horizontal to subhorizontal, discontinuous layers in the host rock. It is common to observe multiple layers of pegmatic gabbro, separated by coarse-grained gabbro, within outcrops or drill core. In lesser examples, patches of pegmatitic gabbro, rather than layers are observed on outcrop surfaces (Plate 3.1). Cumulate plagioclase and interstitial clinopyroxene minerals comprise the major mineralogy at 65 % and 30 % respectively, with minor interstitial magnetite (\pm ilmenite). In rare examples, trace amounts of interstitial, fine-grained

pyrrhotite are present. Plagioclase grains are cloudy white to beige in outcrop (white in drill core), very coarse-grained, ranging from 1 to 4 cm, and are randomly orientated (Plate 3.2). Clinopyroxene grains are very dark green in outcrop (black in drill core), and have smaller grain sizes (0.5 to 3 cm) than the larger plagioclase grains. The upper and lower contacts are quite visible, and are noted for the extreme change in grain size. In a few examples, pegmatitic gabbro appear to blend gradationally into the host rock.

3.5.1.4 Altered Coarse-Grained Gabbro

The altered coarse-grained gabbro was initially recognized by MacDonald (1999) and Fitzpatrick *et al.* (1999), who referred to this subunit as “Upper Sequence Gabbro”. However, so as not to confuse this name with terminology used by the author, the subunit heading will be used in this and subsequent sections. The author did not observe this subunit in the field; however, MacDonald (1999) reported that outcrops of this subunit have a distinctive bright-green colour. Drill core examples of this subunit are typically coarse-grained, composed mainly of altered, cloudy white plagioclase and forest green hornblende (Plate 3.7). Hornblende grains usually have thin (< 2 mm), dark green rims. Plagioclase grains are cumulate, whereas hornblende grains are normally interstitial to the plagioclase grains. The grain sizes of the seriated, subhedral plagioclase grains range from 0.5 to 2 cm. Subhedral to anhedral hornblende grains are somewhat smaller than the plagioclase grains, typically 0.25 to 1 cm. The author did not observe sulphides in this subunit.

The intensity of alteration varies in core intersections. Altered gabbro normally occurs predominantly within the upper level of the Upper Gabbro (although, not observed

in all drill holes) and is closely associated with unaltered coarse-grained gabbros whereby contacts are gradational to relatively sharp (Figure 3.7). This subunit was also found adjacent to, or in contact with, overlying gneiss. Kerr (1999) also noted this relationship in drill core. The normal thickness of this subunit, based on the average intersection in drill core, is approximately 10 to 15 m.

Petrographic observations of this subunit indicate silicate textures similar to those observed in the Coarse- to Medium-grained Gabbro subunit. This subunit was originally a cumulate gabbro but was altered to amphibole, and less abundant serpentine, chlorite and sericite. Plate 3.8 illustrates the degree of alteration in this subunit. The large grain to the left on this plate contains very fine-grained hornblende grains rimmed by coarser grained amphibole. The finer-grained cumulate groundmass is comprised of fine to medium-grained (lesser coarse-grained), subhedral to anhedral plagioclase grains, and minor fine-grained hornblende, chlorite, and serpentine.

3.5.2 The Basal Gabbro Subdivision of the Pants Lake Intrusion

The Basal Gabbro subdivision of the PLI refers to the diverse assemblage of layered, gabbroic rocks, located exclusively beneath Upper Gabbro rocks of the PLI, and Churchill Province gneissic rocks. Outcrop exposure of the Basal Gabbro is infrequent, and as stated in section 3.5 entitled 'Subdivisions within the Pants Lake Intrusion', crops out where the base of the intrusion is exposed. Similar to the Upper Gabbro, the Basal Gabbro comprises multiple subunits. These subunits represent a repetitive sequence of layers, residing above the basement contact in a semi-fixed position. The main visual criteria for recognizing the Basal Gabbro are the presence of partially digested xenoliths

and/or sulphides. Fine-grained (lesser medium-grained) olivine gabbro and/or troctolite are the typical host rocks for both the sulphides and xenoliths. Unlike rocks in the Upper Gabbro, olivine is in many cases a cumulate phase in the Basal Gabbro. These criteria, among others, will be discussed in the context of the subunit variations described below, and in subsequent sections.

The Basal Gabbro appears to parallel the basement contact (refer to the vertical longitudinal sections on the enclosed map), and varies moderately in thickness from drill hole location to the next. Thickness variations may be the result of the local basal topography whereby thicker Basal Gabbro intersections are apparently associated with localized footwall depressions. The maximum thickness of the Basal Gabbro intersected in drill core exceeded 100 m (drill hole SVB-97-79, South Gabbro), whereas the smallest intersection was approximately 6 m (drill hole SVB-97-81, North Gabbro). The average true thickness of the Basal Gabbro, based on the visual observation of 32 drill holes, is 27 m. The upper and lower contacts of the Basal Gabbro have a broad range from sharp to gradational to diffuse. The footwall contact is commonly engulfed by graphite and sulphide minerals, which ultimately make determination of the precise contact difficult. Aphanitic chill margins, although less common, have also been observed throughout the PLI. Internal contacts between subunits are normally diffuse. The contact between the Upper Gabbro and Basal Gabbro subdivisions is not as difficult to determine and is relatively sharp, or is marked by the Transition Gabbro subunit.

As was mentioned previously, the Basal Gabbro comprises several subunits. Subunit descriptions are derived from detailed drill core observations, and to a lesser extent, outcrop observations. The main subunits of the Basal Gabbro are: 1) Transition

Gabbro, 2) Gabbro Hybrid, 3) Olivine Gabbro, 4) Leopard Textured Gabbro, and 5) Medium-Grained Gabbro. A sixth subunit, although not directly related to the PLI, is the Contact Gneiss subunit. The relative position of each subunit is shown in Figure 3.5. Other subunits have been recognized in the BGS (*e.g.* Peridotite), but are not as common as those listed above. The petrography of these subunits will be described in Section 3.5 following the subunit descriptions. Sulphide textures and sulphide mineralogy will be briefly introduced in the context of the Basal Gabbro subunit descriptions. A full account of the sulphide textural variations, distribution, and petrography is given in Section 3.7. Descriptions, distribution, and petrography of foreign xenoliths is included in Section 3.5.2.2 (Gabbro Hybrid).

3.5.2.1 Transition Gabbro

The Transition Gabbro subunit is one of the most recurrent and widespread subunits observed within the Basal Gabbro (refer to Figure 3.6a). This subunit occurs between the upper contact of the Basal Gabbro and the lower contact of the Upper Gabbro (Figure 3.5). In one drill hole (SVB-96-29), however, this subunit was present 5 to 10 m above the Basal Gabbro contact. The thickness of this subunit ranges between 0.5 to 15 meters (refer to Figure 3.5). The weathered surface is typically tan to orange-brown, depending on the sulphide content (Plate 3.9). Originally, this subunit was termed “gabbroic pseudo-breccia” (Smith *et al.*, 1998) but this terminology was discontinued.

This subunit has a unique brecciated appearance defined by thin, medium- to coarse-grained, leucocratic bands (melacratic bands in the Black Gabbro) intergrown within fine-grained, forest green to greyish-green olivine gabbro (Plate 3.9 and Plate

3.10). Banding constitutes 5 to 15 % (up to 40 % locally) of this subunit. These leucocratic bands are typically perpendicular to the core axis, and in outcrop exposures, these coarser grained bands often parallel the contact (Plate 3.9). In local examples, the bands are randomly orientated yielding a core interval with a weak pseudo-breccia appearance. The thickness of these bands range from 0.3 to 2 cm (up to 5 cm locally). The composition of the bands includes cloudy white plagioclase (purplish-grey in the Black Gabbro) and black clinopyroxene (\pm olivine). Plagioclase grains are weakly orientated perpendicular to the bands and appear to grow inwards from the rim of these bands. The dark pyroxene grains are normally ophitic and form in the center of the band. In a few examples, the inner pyroxene core is not as noticeable, and plagioclase appears as the dominant phase. The finer grained olivine gabbro constituent of this subunit is compositionally and texturally homogeneous, and is akin to the Olivine Gabbro subunit.

The sulphide content in this unit is consistent, usually $<1\%$ but can reach as high as 5% locally. Locally, some intervals are barren of visible sulphides. Pyrrhotite is the dominant sulphide mineral with minor chalcopyrite and lesser pentlandite. Sulphides are commonly fine grained and disseminated within the fine-grained olivine gabbro and coarser bands. Sulphide clots are common as well, and appear to be closely associated with the coarser bands (Plate 3.10).

Petrographic observations of rocks from this subunit indicate two distinct textures. The majority of samples display subophitic texture defined by fine-grained (0.2 to 0.5mm), subhedral, granular, isolated to connected olivine grains within a plagioclase and clinopyroxene matrix (Plate 3.11 and Plate 3.12). The coarser bands are ophitic defined by coarse-grained (2.0 to 5.0 mm) clinopyroxene grains and less abundant medium- to

coarse-grained plagioclase grains. Sulphides and oxides are typically disseminated and fine-grained (<1 mm). Some disseminated sulphide grains are much larger (0.5 mm). Larger sulphide grains or blotches are closely associated with the coarser grained bands (Plate 3.11 and Plate 3.12).

3.5.2.2 Gabbro Hybrid

The Gabbro Hybrid subunit is typically a combination of two subunits, namely the Transition Gabbro and the fine-grained Olivine Gabbro subunits (although not exclusively) and is widely distributed throughout the entire Pants Lake Intrusion (refer to Figure 3.6b). The position of the Gabbro Hybrid subunit within the Basal Gabbro is variable and is not confined to a single position (Figure 3.5). Contacts between this and the surrounding subunits of the Basal Gabbro are frequently quite diffuse, ranging from 20 to 50 cm, and are often difficult to determine accurately. Based on xenolith content, the Gabbro Hybrid subunit is clearly the most contaminated subunit of the Basal Gabbro.

Outcrop exposures of this subunit are typically greyish-brown to orange-brown (Plate 3.13). In drill core, the color variation of this subunit ranges from various shades and tints of green to deep purple or a combination of the two colours (Plates 3.14, 3.15, and 3.16). This subunit is typically fine-grained and composed of variable amounts of olivine, pyroxene, and plagioclase with minor to moderate chlorite and serpentine alteration. In a few examples of this subunit, the core has a fragmental appearance defined by dark green, fine-grained “clasts” within a lighter, fine-grained matrix (possibly a relict of the Transition Gabbro texture).

This subunit contains a higher percentage of xenoliths than the other subunits (approximately 5-15 % but as high as 25 % of the rock locally). Depending on the degree of digestion, xenoliths can be clearly recognized with distinct boundaries. Locally, some xenoliths are not as well defined, and they appear to melt or fade into the surrounding matrix. All xenoliths appear to be derived from gneisses. The size of the gneissic xenoliths ranges from 2 to 4 cm (measured on the long axis). Some xenoliths have dark-grey inner cores with a fine-grained (2-3 mm) white rim, whereas other inclusions have a light inner core and dark rim (Plates 3.14, 3.15, and 3.16). Xenoliths with light or dark cores are localized, however, in some examples of drill cores, the different xenolith types exist in the same drill hole (Plate 3.16).

The sulphide content of this subunit ranges between 1 to 5 %, but on average is 2%. Sulphides consist of fine- to medium-grained disseminations, as well as blotches of pyrrhotite. Generally, the blotches of pyrrhotite are 0.5 to 2.5 cm (measured on the long axis) with an irregular boundary defined by inward growths of plagioclase and other mafic minerals (*e.g.* olivine and pyroxene). The occurrence of chalcopyrite is minor to trace, and is commonly observed near the rim of the pyrrhotite blotches or contained internally as thin wisps. It is also common to find short intervals (<10 cm) of semi-massive sulphide near the lower contact of this subunit.

Petrographic observations of samples from this subunit indicate that fine-grained, subophitic to ophitic olivine gabbro to gabbro, akin to the fine-grained phase of the Transition Gabbro subunit, hosts the majority of gneissic xenoliths observed in this subunit. It is apparent that the xenoliths originated from the same source (quartz-feldspar-garnet-sillimanite paragneiss) and the colour variations noted above are the

result of a reaction continuum. The original sillimanite and garnet mineralogy of the gneissic inclusions have been totally replaced with spinel and corundum. The xenoliths with the leucocratic cores are the least reacted, whereas the xenoliths with the melanocratic inner cores are the most reacted. The leucocratic xenoliths are comprised of medium- to fine-grained, acicular corundum and strained plagioclase enclosed by a thin (<2 mm) rim of brownish, granular spinel and/or plagioclase (Plate 3.17 and Plate 3.18). The core also contains minor amounts of quartz in a few examples of these xenolithic types. In Plate 3.19, corundum is beginning to be replaced by a dark green, fine-grained spinel. The melanocratic xenoliths are comprised of 60 to 70 %, dark green spinel, with lesser plagioclase and biotite (Plate 3.20). Minor amounts of magnetite are present in some local samples. The thin leucocratic rims commonly associated with these melanocratic xenoliths is comprised of fine to medium-grained plagioclase formed subperpendicular to the xenolith boundary.

3.5.2.3 Olivine Gabbro

The Olivine Gabbro subunit is widespread in the Basal Gabbro subdivision (Figure 3.6c). This subunit is commonly located adjacent to the lower Basal Gabbro contact, but is not exclusive to this location. The textural and mineralogical traits of this subunit are shared among other subunits (*e.g.* Transition Gabbro and Gabbro Hybrid) therefore; the contacts between subunits adjacent to this subunit are notably diffuse. In several drill holes (*e.g.* SVB-96-04, SVB-97-27, SVB-97-27, *etc.*), a sharp chilled contact was observed adjacent to the basement contact. The weathered surface is typically tan or slightly orange-brown, similar to the Gabbro Hybrid depicted in Plate 3.13.

The Olivine Gabbro subunit is typically dark grey in colour (melanocratic), whereas in some locations, the colour is masked by a slight greenish hue. This subunit is everywhere fine-grained (Plate 3.21 and Plate 3.22). The main silicate constituents of this subunit include plagioclase, olivine, and lesser pyroxene. Modal abundances are difficult to determine in drill core because of the dark colour and the fine-grained composition, however, olivine does appear to be the dominant mineral phase. In some local examples, the olivine gabbro is actually troctolite where olivine content is elevated (15 to 20%), and clinopyroxene content decreases (<5%).

Partially digested gneissic inclusions (described in Section 3.5.2.2) are frequently present but, unlike the Gabbro Hybrid subunit, gneissic inclusions are typically isolated and in lower concentrations. Gneissic inclusions within this subunit are often highly digested and widely spaced, and constitute < 5% of the subunit over 0.5 to 1.0 m intervals. The sulphide content is generally between 2 to 4 %, containing disseminated sulphides and lesser sulphide blotches (Plate 3.21 and Plate 3.22). Sulphide blotches are

normally comprised of pyrrhotite with trace amounts of chalcopyrite (\pm pentlandite) partially surrounding the sulphide periphery. Disseminated sulphides may reach as high as 5-10 % in short intervals of 10 to 20 cm

The Olivine Gabbro subunit is texturally and mineralogically homogeneous. Rocks belonging to this subunit are ophitic to subophitic. It is characterized by 20 to 25% cumulate, fine-grained (0.2 to 0.5 mm), granular, subhedral olivine grains and 65 to 70% fine-grained (0.2 to 4.0 mm), euhedral plagioclase laths (Plate 3.23 and Plate 3.24). Subophitic, medium-grained (0.5 to 3.0 mm) clinopyroxene grains are localized and constitute 5-10% of the modal mineralogy. Biotite, chlorite, serpentine, and sericite are the normal secondary and accessory minerals. Biotite is often associated with sulphide grains. Chlorite and serpentine are the alteration products of olivine. Plagioclase grains are weakly sericitized.

3.5.2.4 Leopard-Textured Gabbro

The Leopard-Textured Gabbro subunit is one of the least abundant subunits in the Basal Gabbro subdivision (refer to Figure 3.6d). This subunit is typically located within the center of the Basal Gabbro subdivision (Figure 3.7), and contacts between adjacent subunits are typically diffuse. The weathered surface of this subunit is easily recognizable in the field, defined by small (<1 cm), purple spheres surrounded by a recessively weathered, orange-brown, fine-grained, sulphide-bearing matrix (Plate 3.25). Leopard- Textured Gabbros normally do not form in laterally continuous layers, but in several small pods confined to a stratigraphic layer.

The Leopard-Textured Gabbro subunit comprises 30 to 40 % isolated, rounded, coarse grained (<1 cm) oikocrysts of deep purple to black clinopyroxene surrounded by a dark grey to green, fine-grained matrix of granular olivine and minor plagioclase (Plate 3.26). Disseminated and/or net textured sulphides encompass the poikilitic clinopyroxenes. Sulphide composition is dominantly pyrrhotite (10 – 20 %) with trace chalcopyrite. Minor, small (0.5 cm) blotches of pyrrhotite also occur in this unit but are quite rare (Plate 3.26). In a number of drill holes (*e.g.* SVB-96-09, SVB-96-15, SVB-96-36, *etc.*) there is a faint texture that resembles the leopard texture described above. However in these examples, the poikilitic clinopyroxenes are not as well defined and the sulphide content is much lower. The texture of the sulphides common in this subunit is elaborated in Section 3.6.3.

The poikilocrysts of the Leopard-Textured Gabbro subunit comprises 25 to 30%, seriated, fine-grained (0.2 to 0.5 mm), euhedral to subhedral plagioclase laths enclosed by large (up to 1 cm) clinopyroxene grains (Plate 3.27 and Plate 3.28). Fine-grained, granular olivine grains are subordinate (<5%) and are normally absent. Surrounding the clinopyroxene dominant poikilocrysts is a fine-grained, ophitic to subophitic textured olivine gabbro. Olivine grains constitute 25 to 30% of the matrix, plagioclase constitutes 40 to 50%, clinopyroxene constitutes 10%, and disseminated or weakly formed net-texture sulphide minerals constitute the remaining mineralogy.

3.5.2.5 Medium-Grained Gabbro

This subunit is the least common of the subunits recognized in the Basal Gabbro subdivision (refer to Figure 3.6e) and was observed in only one re-logged drill hole (SVB-97-79). Drill hole SVB-97-86, located 850 m to the south-southwest of SVB-97-79 did contain this subunit, but was not re-logged or sampled for this study. This subunit has not been observed on surface, and therefore field relationships and weathering properties are not reported here. Peridotite is commonly associated with this subunit.

The Medium-Grained Gabbro subunit is typically medium-grained, dark-grey to black, and commonly has a distinctive salt-and-pepper appearance (Plate 3.29). Subhedral to anhedral, intercumulate, cloudy-white plagioclase grains constitute 20 to 30% of this subunit. Dark green to dark grey, granular olivine grains are the dominant phase of this subunit (40 to 50%), whereas intercumulate clinopyroxene is subordinate (trace to < 5% of the rock). Disseminated to blotchy sulphides comprised of pyrrhotite, with lesser chalcopyrite and pentlandite, are common (Plate 3.29 and Plate 3.30). Locally, sulphides constitute 5 to 10% of this subunit over 10 to 15 m intervals. Isolated, well-digested, 2-3 cm, melanocratic xenoliths (described in Section 3.5.2.2) are present locally, commonly associated with intervals bearing 5 to 10 % sulphide.

Petrographic observations of this subunit are limited to samples from this drill hole (SVB-97-79). All samples of this subunit are comprised of 40 to 50%, medium-grained, subhedral, cumulate olivine grains (Plate 3.31 and Plate 3.32). Peridotite samples have a higher percentage of olivine (50 to 65%). Rims and cracks of olivine grains are weakly altered to serpentine. The intercumulate mineralogy is typically fine-

grained comprised of sericitized plagioclase (20 to 30%) with lesser clinopyroxene (<5%).

Accessory biotite and chlorite is also intercumulate.

3.5.2.6 Contact gneiss

This subunit does not appear to be a magmatic product but rather the result of the interaction between the magma and the basement gneiss, and is commonly found at the base of the Pants Lake Intrusion. This subunit is notable because of the relatively high sulphide content and diffuse contacts with the overlying intrusive rocks of the Basal Gabbro. This subunit is normally melanocratic with an associated graphite content that ranges from 20 to 40 %, and a sulphide content that ranges from 10 to 20 % comprised of pyrrhotite with minor chalcopyrite (<1%). Typically, this subunit is extremely foliated and/or crenulated with pyrrhotite stringers and elongated pyrrhotite clots parallel to the foliation. The gneissic host is difficult to distinguish within this zone due to the graphite and sulphide contents. This unit appears to have been extensively melted and has a very diffuse upper and lower contact which makes it difficult to determine the exact position of the gabbro / gneiss contact.

3.6 Mineralogy, Textural Variations, Distribution and Petrography of Sulphide Minerals from the Pants Lake Intrusion and Surrounding Country Rocks

Sulphide mineralization within the map area was originally reported by Hill (1982) who briefly described the presence of disseminated pyrrhotite and pyrite associated with coarse-grained, cumulate anorthosite and leucogabbro. The sulphide minerals, chiefly pyrrhotite, chalcopyrite, and pentlandite (\pm cubanite), are associated with the Basal Gabbro of the Pant Lake Intrusion, and to a lesser extent, paragneiss and orthogneiss of the Churchill Province (Smith *et al.*, 1998 and 1999; Fitzpatrick *et al.*, 1999; Kerr, 1999). Only minor to trace amounts (<1%) of sulphide have as yet been observed in the Upper Gabbro.

Six predominant sulphide textures occur in the Basal Gabbro. The nomenclature of the various sulphide textures presented in this section has been commonly utilized in other studies describing magmatic sulphide deposits (*e.g.* Voisey's Bay, Sudbury, Jinchuan, Noril'sk-Talnakh, Duluth, *etc.*). The various sulphide textures recognized in the Pants Lake Intrusion include: 1) disseminated sulphide, 2) blotchy (or clot) sulphide, 3) leopard or net-textured sulphide, 4) semi-massive sulphide, 5) massive sulphide, and 6) remobilized sulphide. Apart from petrographic examinations, all descriptions of sulphides within the map area are based on observations from a representative suite of 34 re-logged drill holes (see Appendix C) spatially distributed throughout the entire Pants Lake Intrusion. Figure 3.7 illustrates the relative vertical position of each sulphide textural variation recognized in the Basal Gabbro. Figure 3.8 depicts the spatial distribution of each sulphide texture observed in the 34 re-logged drill holes.

3.6.1 Disseminated Sulphide

Disseminated sulphide is the most common and widely distributed textural form of sulphide in the Basal Gabbro (Figure 3.8a). It is common to observe gabbro and olivine gabbro containing disseminated sulphides in the field where the Basal Gabbro crops out at surface. Rocks exposed at surface with >10 % disseminated sulphides are highly weathered and are normally oxidized with a reddish-orange stain. The re-logged drill cores that intersected the Basal Gabbro all contain disseminated sulphides. Churchill Province paragneiss and orthogneiss also contain examples of this sulphide texture. Locally, disseminated sulphides occur in the Upper Gabbro subdivision. The descriptions provided in this section are based on observations of the re-logged drill cores and petrographic sections. Figure 3.7 illustrates the idealized vertical distribution of the disseminated sulphide through the Basal Gabbro.

Disseminated sulphides in the Basal Gabbro are normally interstitial, fine to medium (1 to 5 mm) polygonal grains, consisting mainly of pyrrhotite (Plate 3.22). In rare examples, chalcopyrite is the main disseminated sulphide mineral. Disseminated pyrrhotite grains frequently include small grains or rims of chalcopyrite and/or pentlandite. Disseminated sulphide grains are usually interstitial to the cumulate silicate minerals (*e.g.* plagioclase, clinopyroxene, olivine), therefore the shape and size of the sulphide grain is dictated by the orientation and shape of the silicate mineralogy (Plate 3.33). Because disseminated sulphide grains are interstitial, they are isolated from similar grains, but generally occur in 'clouds or clusters' of grains dispersed throughout a core interval. Disseminated sulphide grains comprise only a minor constituent (<1 %) of the rock over a core interval. However, in some drill cores, the disseminated sulphide

content can reach as high as 20 % over a core interval of 4 to 5 m (*e.g.* drill hole SVB-96-09). In a few drill cores (*e.g.* drill hole SVB-97-92), the disseminated sulphide content increased down-hole (< 1% to 20 %).

It appears that the disseminated sulphides have no particular preference for either subunit of the Basal Gabbro (Figure 3.7). However, there does appear to be a correlation between rocks containing blotchy, leopard or net-textured sulphides. Disseminated sulphides also occur in the Churchill Province basement gneisses where the sulphide content can reach as much as 10 to 15 % over 1 to 2 meter intervals. Sulphide textures of any type are rare in the Upper Gabbro. However, disseminated sulphides have been observed just above the lower contact of the Upper Gabbro and are generally associated with medium to fine-grained gabbro containing small concentrations (<1 %) of interstitial magnetite and/or ilmenite.

Reflecting light microscopy reveals that the sulphide (and oxide) compositions of the disseminated sulphide grains can be quite variable between drill holes, or for that matter, between individual grains. Typically, disseminated sulphide grains are comprised of 70 to 80% (up to 95%) pyrrhotite with lesser chalcopyrite and pentlandite (\pm magnetite) (Plate 3.34). The chalcopyrite content of the disseminated sulphide grains typically exceeds the pentlandite content. Small (< 0.5 mm) inclusions of chalcopyrite and pentlandite are commonly adjacent to the sulphide/silicate boundary, and in lesser cases, internally. Magnetite grains are subordinate and are less common than the chalcopyrite and pentlandite grains.

3.6.2 Blotchy Sulphide

Blotchy sulphide is the second most common and widely distributed textural form of sulphide in the Basal Gabbro (Figure 3.8b). Basal Gabbro outcrops containing blotchy sulphides are widespread, and usually contain isolated, semi-circular, 1 to 3 cm, rust coloured patches (Plate 3.35). All of the re-logged drill holes that intersected the Basal Gabbro contain blotchy textured sulphides (see Appendix C). It is also common to observe sulphide blotches in the Churchill Province gneisses that are dominantly chalcopyrite rich. Figure 3.7 illustrates the idealized vertical distribution of the blotchy textured sulphide throughout the Basal Gabbro.

Blotchy sulphides, as the name suggests, appear as blotches of sulphide. Some authors also refer to this texture as clot or bleb sulphides (*e.g.* Lightfoot and Naldrett, 1999). Sulphide blotches are typically discrete, isolated, semi-rounded to irregular shaped, and range in size from 0.5 to 3.0 cm (measured on the longest axis) (Plates 3.36, 3.37, and 3.38). The boundary of a sulphide blotch is normally irregular, marked by projections of plagioclase grains (lesser clinopyroxene and olivine grains) into the sulphide (Plate 3.36). A sulphide blotch is normally comprised of pyrrhotite, chalcopyrite, and pentlandite. The ratio of each sulphide mineral is variable from blotch to blotch; however, pyrrhotite generally constitutes over 85 % of the sulphide composition. Chalcopyrite and pentlandite commonly form partial rims or inclusions in the pyrrhotite blotch. In several examples, chalcopyrite forms the upper rim of the pyrrhotite blotch (Plate 3.38).

Similar to the disseminated textured sulphide, sulphide blotches typically occur in close proximity to each other; however, it is also common to find single blotches

separated by meters of barren or weakly mineralized gabbros. Sulphide blotches often reside near the upper contact of the Basal Gabbro with the Transition Gabbro subunit; however, they are not confined to that position (Figure 3.7). There also appears to be a moderate correlation between sulphide blotches and gneissic inclusions.

Reflected light microscopy of sulphide blotches illustrates that the composition of individual sulphide blotches can be quite variable. Smaller, discrete chalcopyrite and pentlandite grains are commonly formed on blotch boundaries (Plate 3.39, 3.40, 3.41 and 3.42). In lesser examples of sulphide blotches, chalcopyrite and pentlandite grains are present internally, or penetrate inwards within the sulphide blotch from the sulphide/silicate boundary (Plate 3.40). Magnetite is commonly observed in cracks of pentlandite grains (Plate 3.41 and Plate 3.42).

3.6.3 Leopard-Textured Sulphide

Leopard-textured sulphide, or net-textured as it is sometimes referred to, is directly related to the Leopard-Textured Gabbro subunit discussed in Section 3.5.2.4, and is less common than the disseminated and blotchy textured sulphide (Figure 3.8c). Outcrops with leopard textured sulphides are normally well oxidized to a deep red-orange/purple colour and have unique recessive-weathering pattern (Plate 3.25). Leopard-textured sulphides are present in several re-logged drill holes that have intersected the Basal Gabbro (*e.g.* drill holes SVB-96-09, SVB-96-15, SVB-96-48). This sulphide texture has not been observed in rocks belonging to the Upper Gabbro or Churchill Province gneisses. Leopard-textured sulphide is always present in the center of the Basal Gabbro, normally with olivine gabbro layers above and below that is relatively

barren of sulphide mineralization apart for the occasional sulphide blotch or trace amounts of disseminated sulphide. Figure 3.7 illustrates the idealized vertical distribution of the leopard- and net-textured sulphide throughout the Basal Gabbro.

Rock samples containing leopard-textured sulphides are easily recognizable due to the unique spotted appearance, defined by a matrix of disseminated to heavily disseminated sulphide surrounding semi-rounded (<1 cm), violet to black, oikocrysts of clinopyroxene (\pm olivine and plagioclase) (Plate 3.26). Sulphide grains are normally interstitial in the silicate minerals where sulphide content is relatively low (<15 % sulphide) (Plate 3.27). As the sulphide content increases (>15 % sulphide), sulphide grain boundaries overlap, giving the rock a 'net-like' appearance (Plate 3.28). Pyrrhotite is the main sulphide mineral and both chalcopyrite and pentlandite are the secondary sulphide minerals. The relationship of the differing sulphide minerals is similar to the disseminated sulphide textures whereby chalcopyrite and pentlandite grains form as inclusions or partial rims on the larger pyrrhotite grain. The normal ratio of pyrrhotite to pentlandite to chalcopyrite is 8:1:1, whereas in some local examples, the ratio is 7:1.5:1.5 where the pentlandite and chalcopyrite concentration increases.

3.6.4 Semi-Massive Sulphide

Semi-massive sulphide is uncommon within the Basal Gabbro (Figure 3.8d). Outcrop exposures containing this sulphide texture, although rare, are deeply weathered and oxidized to a bright reddish-orange or reddish-purple colour, and are often accompanied by yellow sulphur staining. Semi-massive sulphide is more easily recognized in the re-logged drill cores and is exclusive to the Basal Gabbro and Churchill

Province gneisses. Semi-massive sulphide normally occurs adjacent to the footwall contact, often preceding massive textured sulphide (Figure 3.7).

Semi-massive textured sulphide represents a sulphide texture whereby the sulphide content of a rock is between 40 to 60 %. Typical drill core intervals bearing semi-massive textured sulphide are short (5 to 20 cm), but can be as thick as 1 m (Plate 3.43). Smaller intervals of semi-massive sulphide are present locally throughout Basal Gabbro as thin 2 to 4 cm wide bands, frequently accompanied by graphite. These small intervals have a melted appearance, with discrete, well-defined, rounded, silicate inclusions. Similar to the previously described sulphide textures, semi-massive sulphides is comprised of pyrrhotite with minor chalcopyrite, and lesser pentlandite (< 5%).

3.6.5 Massive Sulphide

Massive sulphide is one of the least commonly observed sulphide textures within the map area (Figure 3.8e) and is not commonly observed in outcrops because of the intense oxidation and weathering of the sulphide. Massive sulphides are located predominantly, although not exclusively, in the North Gabbro. Figure 3.7 illustrates the vertical location of the massive sulphide in the Basal Gabbro.

Massive sulphides are similar to the semi-massive sulphide texture, although the sulphide content exceeds 60% of the rock, and both typically occur proximal to each other (Plate 3.44, 3.45, and 3.46). Massive sulphide, where present, occurs adjacent to or masks the footwall contact, and occurs as isolated lens, possible lying in footwall depressions (Figure 3.7). Drill core intersections are quite variable in thickness. In the

re-logged drill holes SVB-98-102 and SVB-98-113 (Plate 3.44), the thickness of the massive sulphide interval was < 1 m thick. In the drill hole, SVB-97-67, a 15.7 m massive sulphide interval was intersected.

In all examples of this sulphide texture, pyrrhotite is the main sulphide mineral with lesser chalcopyrite and pentlandite. Typically, sulphide engulfs gabbro or gneiss inclusions (Plate 3.45). Most frequently, the upper and lower contacts of the massive sulphide interval are quite variable and it is possible to begin with semi-massive sulphide, which becomes upgraded to massive sulphide down hole. In many examples, the lower contacts are sharp.

Reflected light microscopy of samples containing massive textured sulphide further illustrate that the sulphide comprises 70 to 80% pyrrhotite with lesser chalcopyrite and pentlandite (\pm magnetite and cubanite) (Plate 3.47 and Plate 3.48). It is common to find exsolution lamellae of pentlandite flames within pyrrhotite (Plate 3.47) or small inclusions of both chalcopyrite and pentlandite grains adjacent to silicate inclusions (Plate 3.48). Magnetite, although not common, is present within cracks developed within the pentlandite grains (Plate 3.49) or as discrete grains within the host rock.

3.6.6 Remobilized Sulphides

Remobilized sulphides are not common and are frequently difficult to distinguish from the blotchy, the semi-massive or the massive textured sulphides. Remobilized sulphides are normally hosted in the Churchill Province basement gneisses but likely originated from the main sulphide mass of Basal Gabbro. Remobilized sulphides are common in magmatic systems and often form high-grade footwall deposits (*e.g.* the

footwall deposits at Sudbury; Morrison *et al.*, 1996). Remobilized sulphides typically have higher than average nickel and copper tenors. The best example of this textural type is from drill hole SVB-97-75, where a 1.1 m interval of massive sulphide was intersected 13 m below the base of the intrusion in Churchill Province gneisses (Plate 3.46). In this example, chalcopyrite is the main sulphide constituent and the pentlandite concentration is increased significantly. In other examples, chalcopyrite-rich blotches are often located in the footwall gneisses approximately 1 to 2 m below the basal contact with the intrusion.

Reflected light microscopy of samples with this textural type is chalcopyrite-rich with lesser pentlandite and pyrrhotite. The presence of cubanite is local and mainly associated with chalcopyrite as exsolution lamellae (Plate 3.51). Chalcopyrite grains are significantly larger (3-5 mm) and pyrrhotite locally rims the chalcopyrite and pentlandite grains (Plate 3.50, 3.51 and 3.52). In small-scale examples of this texture, chalcopyrite grains that formed from the larger pyrrhotite grains were remobilized into small cracks developed with the silicate host rock (Plate 3.53 and Plate 3.54).

3.7 Surface Sulphide Occurrences Associated with the Pants Lake Intrusion

Sulphide mineralization is present in many locations throughout the South Voisey's Bay Project area in two chief associations: sulphide in Churchill Province paragneisses, and sulphide in the Basal Gabbro of the Pants Lake Intrusion. The latter association is the more significant because of the economic mineral assemblage (pyrrhotite, chalcopyrite, and pentlandite) whereas the former association contains only minor disseminated pyrrhotite and pyrite mineralization.

Ninety percent of the sulphide occurrences observed in the South Voisey's Bay Project area are located on the boundary between the Pants Lake Intrusion and gneiss (typically paragneiss) of the Churchill Province. Sulphide mineralization is confined, although not exclusively, to the subunits of the Basal Gabbro.

Seven main sulphide occurrences are known on the property (refer to the enclosed geology map), four of which are described below (NDT, Happy Face Lake, GG, and Mineral Hill). These occurrences exhibit similar characteristics and where possible, the host subunits, the sulphide textures and mineralogy, and the internal and external contacts between subunits and subdivisions are described. Only brief descriptions of the outlying rocks are included in each section.

3.7.1 NDT Sulphide Occurrences

The NDT sulphide occurrences are located approximately 1 km north of Pants Lake on the southwestern mapped boundary of the North Gabbro (UTM coordinate for the center of the NDT sulphide occurrences is 558500mE, 6149300mN; approximate elevation 490 to 495m ASL) (see enclosed geology map and Figure 3.9). Outcrop exposure in the area is greater than 70 percent. A valley plunging to the southeast crosscuts the map area exposing a cross-section through the PLI and Churchill Province gneisses (Figure 3.9) which accounts for the numerous exposed sulphide occurrences (gossans) located on the slopes of the valley.

Two principal gossanous zones are in the NDT area, namely the North Gossan and the South Gossan (Plate 3.55). Each gossan comprises several large, isolated mineralized outcrops akin to the Basal Gabbro subdivision (BGS). Mineralized outcrops

containing 3-5% sulphide are extremely oxidized and weathered, and are heavily Fe-stained locally. The top of the North Gossan appears to be stratigraphically higher than the top of the South Gossan by about 6 to 8 m, although there appears to be some minor overlap in between. Mapping indicates that the upper subunits of the BGS are prevalent in the North Gossan, whereas the lower subunits of the BGS are prevalent in the South Gossan. The gossans exhibit similar silicate and sulphide textures and mineralogy; however, there are some differences. The average thickness of each gossan ranges between 4 to 6 m.

The upper contact between the BGS and Upper Gabbro subdivision (UGS) was not observed in this area; however, rocks akin to the Transition Gabbro subunit were observed on top of the North Gossan in some localities (Figure 3.9). This subunit weathers tan to beige, and is composed of fine-grained, olivine gabbro with minor (<10%) randomly orientated, medium-grained, thinly (< 1.0 cm) banded cloudy white plagioclase and black pyroxene grains. Disseminated to blotchy sulphides are scarce (<1%). Below the Transition Gabbro is a tan to beige weathered, locally heavily Fe-stained, fine-grained olivine gabbro with 2-5 %, blotchy and disseminated pyrrhotite (\pm chalcopyrite); this rock is akin to the Olivine Gabbro subunit. Sulphide blotches are isolated and range in size from 1 to 2 cm.

The South Gossan extends along a ridge orientated northwest-southeast. It is quite gossanous, with a rusty brown-purple color and minor, local pale yellow sulphur staining. The South Gossan appears to be zoned with respect to sulphide concentration and mineralogical textures. The Olivine Gabbro subunit described above resides in the west to central portion of the South Gossan. Olivine gabbro outcrops in the western part

of the South Gossan contain several small (2-4 cm) irregular to rounded partially digested inclusions, with dark-grey centers and thin white rims (refer to Plate 3.13). In the eastern portion of the South Gabbro is a 2 to 3 m thick Leopard Textured Gabbro (Figure 3.9). The Leopard Textured Gabbro is extremely oxidized and weathered, with the unique knobby weathering associated with this subunit. This subunit contains 10 to 20% disseminated pyrrhotite and trace chalcopyrite. Below the Leopard Textured Gabbro, and in contact with the paragneiss locally, is fine-grained Olivine Gabbro containing < 5% sulphide.

Rocks belonging to the Upper Gabbro are stratigraphically above the two gossans and sulphides were not observed in these rocks. In elevated areas, especially towards the west where the paragneiss becomes pinched, there is a large sequence of massive, fine-grained, grey weathered olivine gabbro (Olivine Gabbro subunit). In the east and north of the North Gossan, coarse- to medium-grained gabbroic rocks (Coarse- to Medium-grained Gabbro subunit), weathered to a brownish-grey colour, are present. In several outcrops, parallel layering is evident comprised of medium- and coarse-grained gabbro intruded by small (10-15 cm) intervals of brownish weathered pegmatite (Pegmatitic Gabbro subunit). No mapping was conducted beyond the property boundary.

3.7.2 Happy Face Lake Sulphide Occurrence

The Happy Face Lake (HFL) sulphide occurrence is located near the northwest shoreline of a small lake (informally named Happy Face Lake) in the center of the North Gabbro (UTM coordinate for the HFL sulphide occurrence is 561900mE, 6152600mN; approximate elevation is 410m ASL) (see enclosed geology map and Figure 3.10).

Outcrop exposure in the area is moderate (60-70%). The topography in the area is somewhat hilly.

The Happy Face Lake sulphide occurrence (gossan) is a maximum of 4.5 m thick in the center of the gossan (from the top of the gossan to the water level), and pinches into the lake on both sides (Plate 3.56). The gossan appears to dip approximately 5° towards the north-northeast, and is locally moderately fractured. The gossan is highly weathered and oxidized with a brown-reddish colour near the shoreline, which dissipates slightly towards the upper contact of the gossan. The lower contact of the gossan was not observed owing to the location of the lake. Mapping in this area indicates that the subunits of the Basal Gabbro host the sulphide mineralization that is approximately 5% to 10% locally.

The contact between rocks belonging to the Upper and Basal Gabbro subdivisions is quite sharp, less than 2 cm thick and is denoted by a thin (4 cm), medium- to coarse-grained plagioclase and pyroxene (\pm magnetite) layer parallel to horizontal (see inset photo, Plate 3.56). Rocks akin to the Transition Gabbro immediately follow this. The Transition Gabbro is approximately 1 to 1.5 m thick, tan to beige-orange weathered, with < 10% thin (< 1 cm) randomly orientated bands (weakly parallel to the upper contact) of medium-grained plagioclase and pyroxene grains in fine-grained olivine gabbro. Small (1-2 cm) rusty pyrrhotite blotches are commonly observed near the upper contact.

Below the Transition Gabbro is the Olivine Gabbro, which dominates the center of the gossan, and is present near the water line (Plate 3.56). The Olivine Gabbro weathers to orange-beige where sulphide content is low (< 2%). Fresh surfaces are greyish to greyish-green. Sulphide mineralization comprises 4 to 5% disseminated

pyrrhotite that appears evenly dispersed throughout the Olivine Gabbro, and minor (< 1%) blotches of pyrrhotite (\pm chalcopyrite) occurs locally.

The Leopard-Textured Gabbro occurs in a number of small (1 x 2 m) discrete zones near the water line. This subunit produces a distinctive knobby weathering with 25 to 30% dark rounded, small (0.5 to 1.0 cm) pyroxene (\pm plagioclase, olivine) oikocrysts separated by a recessive weathered, fine-grained matrix composed of plagioclase, pyroxene and 10% disseminated sulphide (Plate 3.25).

Rocks stratigraphically above and on the northern outlier of the Happy Face Lake sulphide occurrence belong to the Upper Gabbro (Figure 3.10 and Plate 3.56). Massive to weakly layered, coarse-grained, lesser medium-grained, gabbro (Coarse- to Medium-grained Gabbro subunit) are typically weathered beige-brown, and composed of seriated, cumulate cloudy white to beige plagioclase grains with intercumulate black pyroxene \pm olivine grains. Rocks in the southern outlier of the Happy Face Lake occurrence are typically leucocratic, medium- to coarse-grained, well foliated, quartzo-feldspathic paragneisses with 40 to 50 % quartz, feldspar and small (>1 cm) retrogressed garnets.

3.7.3 GG Sulphide Occurrence

The GG sulphide occurrence is located on the southeastern boundary of the North Gabbro (UTM coordinate for the GG sulphide occurrence is 564200mE, 6150500mN; approximate elevation 470m ASL) (see enclosed geology map and Figure 3.11). Outcrop exposure in the area is greater than 70 percent. The topography in the area is slightly hilly.

The GG sulphide occurrence (gossan) is exposed on the western, northern and southern slopes of a small, isolated hill (Plate 3.57). The approximate thickness of the gossan is 25 m, and it dips slightly (5°) to the east-northeast. The upper contact of the gossan is eroded away, and the lower contact is scree covered. The gossan is highly weathered and oxidized with an orange-brown, locally purplish colour. Mapping in this area indicates that rocks belonging to the Basal Gabbro host the gossan. The GG gossan comprises three distinct subunit layers. Layering appears to parallel the contours of the hill. Internal contacts are diffuse and are locally undulating.

The upper 2-3 m of the gossan comprises fine-grained Olivine Gabbro with local areas of the Transition Gabbro (Plate 3.57). Both subunits are weathered beige to tan, locally orange-brown, containing local minor ($> 2\%$) disseminated and blotchy pyrrhotite (\pm chalcopyrite). At the top of the hill, several, small (3-4 cm), leucocratic, fine to medium-grained, partially digested inclusions were observed in the Olivine Gabbro.

The middle layer is dominated by the Leopard-Textured Gabbro (Plate 3.57), and is the most oxidized and weathered of the three layers with a reddish-purple colour and local pale yellow sulphur staining. This subunit is approximately 7-8 m thick and is defined by distinctive rubbly weathering of dark rounded pyroxene oikocrysts enclosed by a matrix of recessively weathered, fine-grained plagioclase and olivine grains with 10-15 % disseminated pyrrhotite. In this interval, the Olivine Gabbro is present in several small localities suggesting that the leopard-textured gabbro is not a continuous layer.

The lower layer is similar to the Olivine Gabbro described above containing local disseminated and blotchy sulphides. Few partially digested inclusions (gneissic?) are also present in this layer.

East of the GG sulphide occurrence are several outcrops of well-foliated, leucocratic, medium-grained, rust coloured paragneiss (Plate 3.57). Approximately 2-4% disseminated pyrrhotite (\pm pyrite) is commonly observed in these paragneiss. Mapping was not conducted west of the GG gossan.

3.7.4 Mineral Hill Sulphide Occurrence

The Mineral Hill sulphide occurrence is located on the northwest side of the South Gabbro (UTM coordinate for the Mineral Hill sulphide occurrence is 569300mE, 6143700mN; approximate elevation is 450m ASL) (see enclosed geology map and Figure 3.12). Outcrop exposure in the area is moderate, approximately 60%. The topography in the area is moderately hilly.

The Mineral Hill sulphide occurrence (gossan) is 4 to 5 m, locally 7 m, thick and dips slightly ($5-6^\circ$) towards the north-northeast. The gossan is distinctly layered and continues on the northern slope of the hill upon which it is located (Plate 3.58). Several smaller gossans are present in the immediate area (northeast) that exhibit similar characteristics to the gossan on Mineral Hill (Figure 3.12). The Mineral Hill gossan is highly weathered and oxidized with an orange-brown, locally reddish-purple, colour, and the contact between the Upper and Basal Gabbro is well defined. The lower contact was not observed in this area. Mapping indicates that the subunits of the Basal Gabbro host the sulphide mineralization.

The upper contact of the Basal Gabbro is locally defined by a 30 to 40 cm, recessively weathered, unmineralized, medium-grained gabbro (olivine gabbro) layer (see inset photo, Plate 3.58). Immediately above the contact is a coarse-grained, grey to beige

weathered cumulate gabbro belonging to the Upper Gabbro. Locally, this medium-grained layer is not present, and is replaced by the Transition Gabbro. Above the Transition Gabbro is a small (2 cm) pegmatitic gabbro interval of pale-white plagioclase and black pyroxene grains (similar as the upper contact of the Happy Face Lake sulphide occurrence). The Transition Gabbro, if present, is normally > 1m thick and has a tan to slightly orange-brown weathered surface. The Transition Gabbro is defined by an erratic (brick-like) medium-grained banding in a finer-grained, olivine gabbro matrix. Sulphide content is variable, between 1-3%, normally disseminated to blotchy. Below the Transition Gabbro is a 3-4 m layer of orange-brown weathered (fresh surface is grey), fine-grained, olivine gabbro containing 3 to 5% disseminated pyrrhotite and 1-2%, small (2 cm) pyrrhotite (\pm chalcopyrite) blotches.

A gneissic outlier surrounds the Mineral Hill gossan and is typically coarse to medium-grained, with local rusty staining. These gneisses contain numerous rounded garnet grains, between 0.2 to 1.5 cm, within a matrix of medium-grained quartz and feldspar. Minor (<2%) disseminated pyrrhotite and pyrite is present locally with the gneiss.

Table 3.1. Summary table of ages reported for selected mafic intrusions of the Nain Plutonic Suite. Included with this table are ages reported in the section entitled 'Regional Geological Setting of the Pants Lake Intrusion' (Section 3.2) for the various geological elements surrounding the Pants Lake Intrusion.

| Mafic Intrusions of the Nain Plutonic Suite | Age (Ma) | References |
|--|-----------------|-------------------------------|
| Pants Lake Intrusion - North Gabbro | 1322 | Dunning (1998) |
| Pants Lake Intrusion - South Gabbro | 1337 | Connelly (2001) |
| Voisey's Bay Intrusion | 1333 | Amelin <i>et al.</i> (1999) |
| | 1338 | Ryan <i>et al.</i> (1995) |
| Mushuau Intrusion | 1313 | Li <i>et al.</i> (2000) |
| Jonathon Intrusion | 1312 | Hamilton <i>et al.</i> (1994) |
| Kiglapait Intrusion | 1306 | Morse (1996) |
| Newark Island Intrusion | 1305 | Simmons <i>et al.</i> (1986) |
| Barth Island Intrusion | 1322 | Hamilton <i>et al.</i> (1994) |

| Geological elements surrounding the Pants Lake Intrusion | Age (Ma) | References |
|---|-----------------|------------------------------|
| Nain Plutonic Suite | 1350 - 1290 | Ryan (1996) |
| Harp Lake Intrusive Suite | 1460 - 1450 | Emslie (1980) |
| Churchill Province | 2780 - 1740 | Swinden <i>et al.</i> (1991) |
| Nain-Churchill suture | 1850 | Ryan <i>et al.</i> (1995) |
| Diabase dikes (Harp) | 1280 | Ryan <i>et al.</i> (1995) |
| Diabase dikes (Nain) | 1274 | Cadman <i>et al.</i> (1993) |

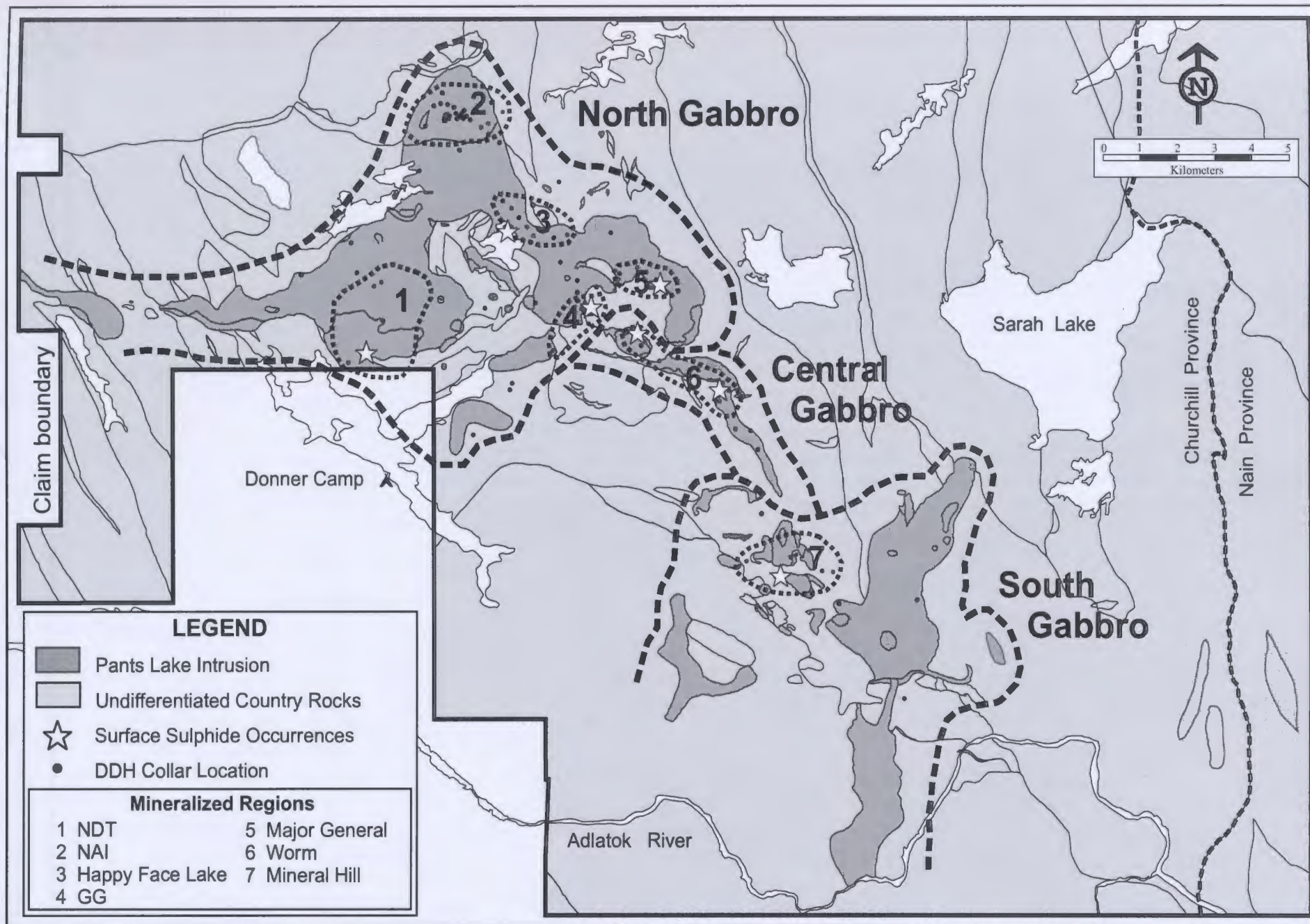


Figure 3.1. Principle geographic components of the Pants Lake Intrusion (outlined by a black, dashed line). The mineralized regions (outlined by a black, dotted line) are areas where diamond drilling has been concentrated and where sulphide occurrences crop out at surface. These mineralized regions are the primary focus of this study. See geological map (inside, back cover) for an explanation of the geological units.

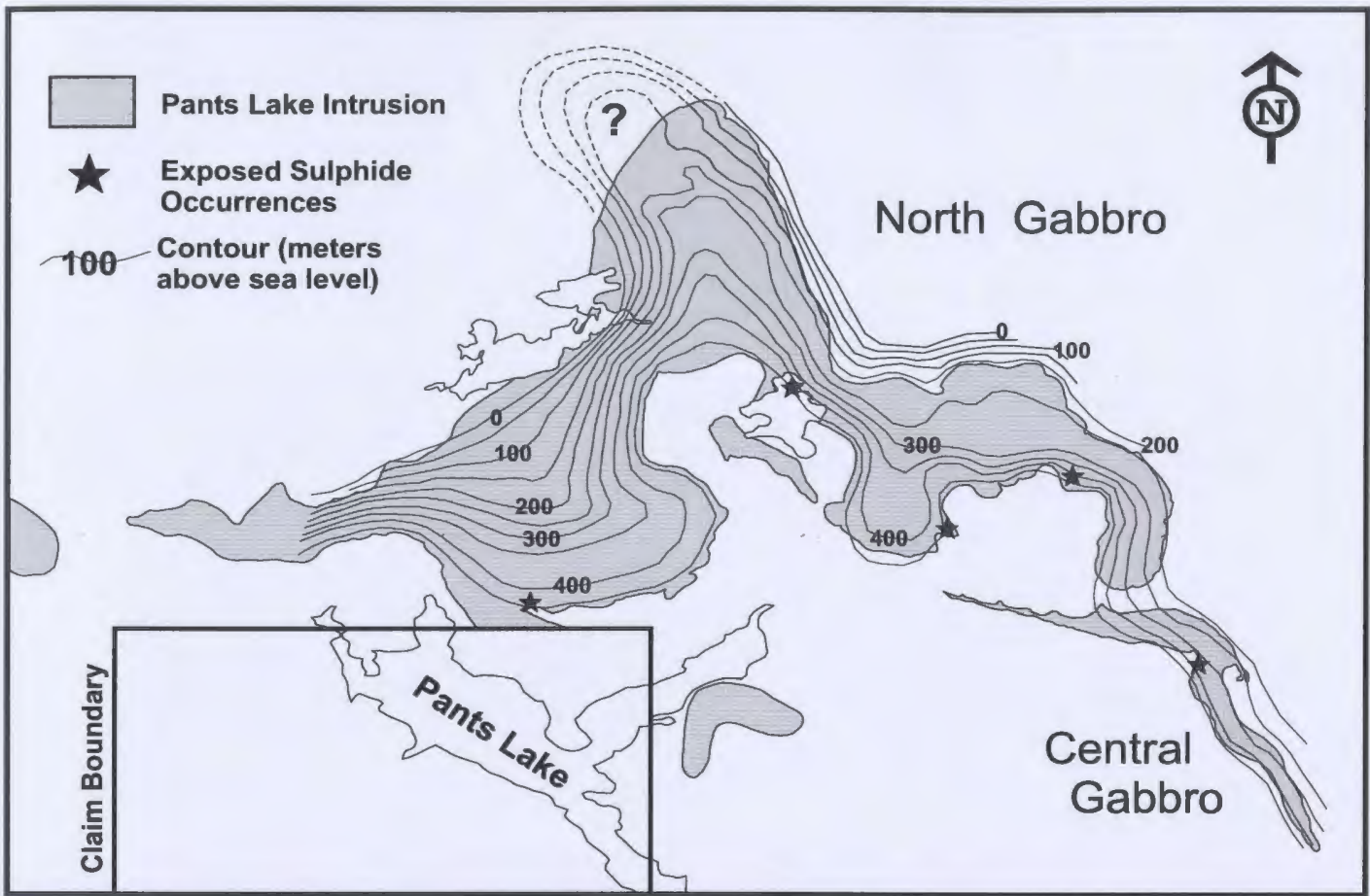


Figure 3.2. Basal contact topography, relative to sea level, of the North and Central gabbros. All contours constructed using drill hole information from Fitzpatrick *et al.* (1999).

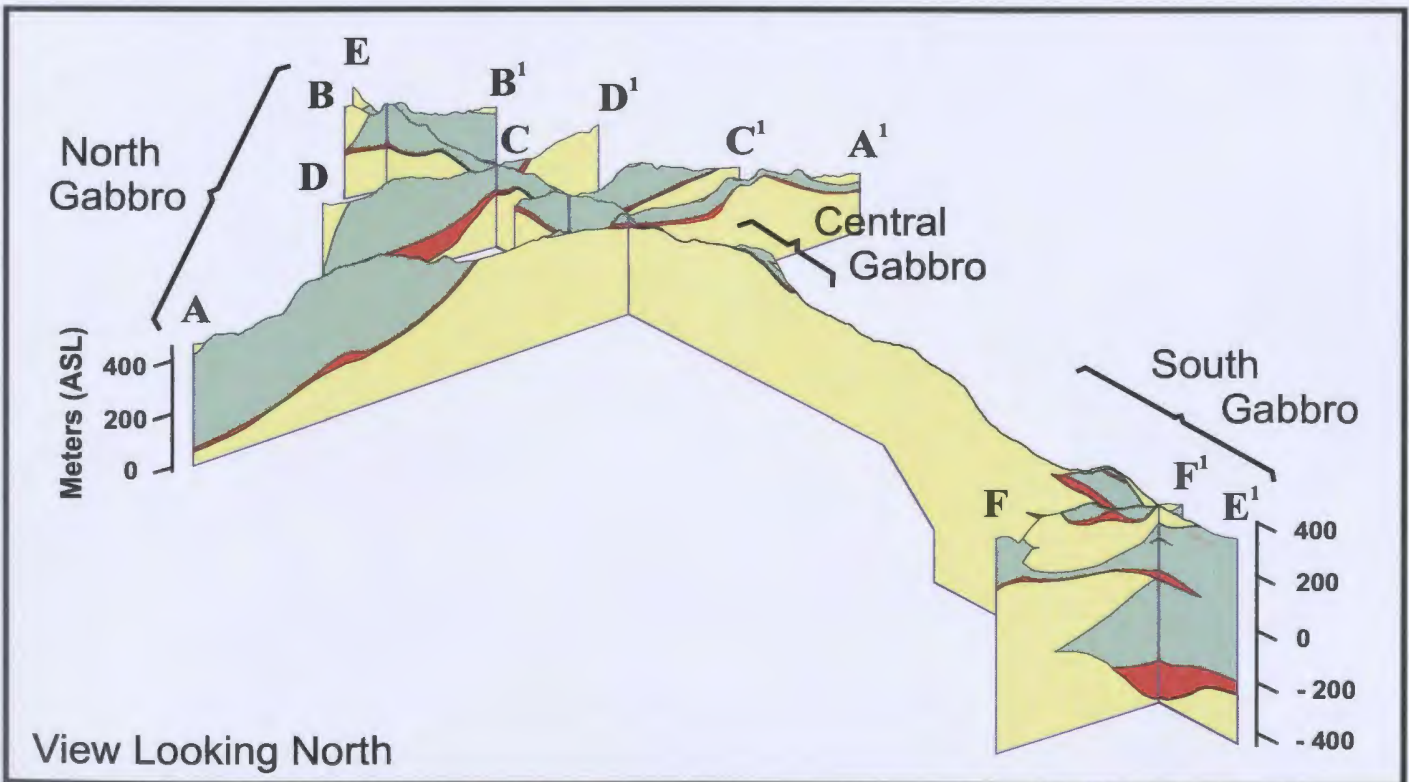
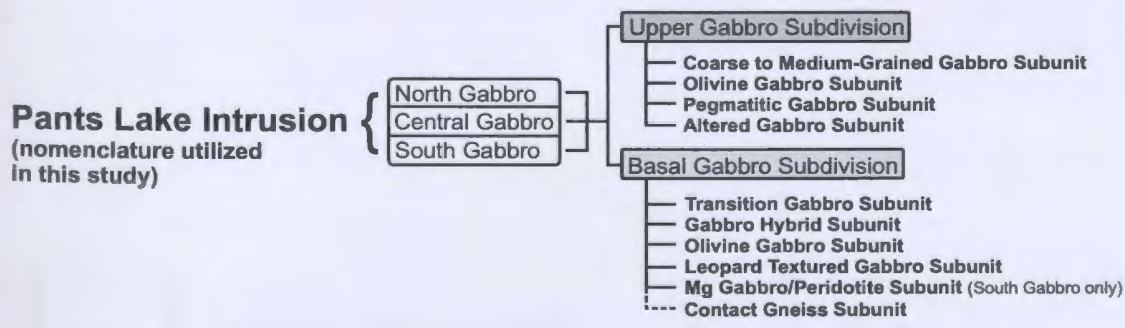
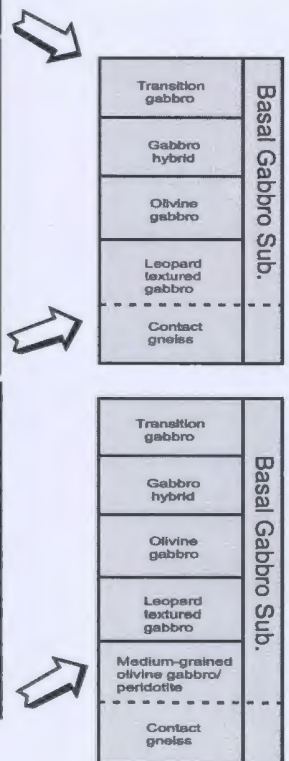


Figure 3.3. Three dimensional view of the Pants Lake Intrusion. See Pants Lake Intrusion geological map for section locations and unit explanations (inside, back cover).

Table 3.2. Geographic components of the Pants Lake Intrusion. Different parts of the Pants Lake Intrusion were originally mapped by Hill (1982) and Thomas and Morrison (1991). The entire Pants Lake Intrusion was mapped by Donner Minerals Ltd. and Teck Exploration Ltd. Descriptions and nomenclature of the various subunits of the Pants Lake Intrusion are reported by Fitzpatrick *et al.* (1999) and MacDonald (1999). The nomenclature used by Smith (this study) is analogous to the nomenclature utilized by Fitzpatrick *et al.* (1999) and Macdonald (1999). The flow chart at the bottom of this table summarizes the components, the subdivisions, and the subunits of the Pants Lake Intrusion utilized by Smith (this study).

| Geographic Components of the PLI | Pants Lake Intrusion mapped in parts, no definite affinity known | | Surface mapping and relationships established, mapped as a member of the Nain Plutonic Suite | | |
|----------------------------------|--|---|--|--|-------------------|
| | Hill (1982) | Thomas & Morrison (1991) | Fitzpatrick <i>et al.</i> (1999) MacDonald (1999) | Smith (this study) | |
| North Gabbro | Included as part of the Nain Plutonic Suite | Not covered during regional mapping | Upper sequence gabbro | Altered gabbro | Upper Gabbro Sub. |
| | | | Black Gabbro | C to mg gabbro | |
| | | | Upper Olivine Gabbro | Pegmatitic gabbro | |
| | | | Olivine gabbro | Olivine gabbro | |
| | | | Olivine Gabbro | Olivine gabbro | |
| Fg contaminated gabbro | Basal Gabbro | | | | |
| Central Gabbro | Not covered during regional mapping | Included as part of the Harp Lake Intrusive Suite | Upper Olivine gabbro | Same as the North Gabbro (no black gabbro present) | Basal Gabbro Sub. |
| | | | Olivine gabbro | | |
| | | | Fg contaminated gabbro | Basal Gabbro | |
| South Gabbro | Not covered during regional mapping | Included as part of the Harp Lake Intrusive Suite | Same as central Gabbro | Same as the North Gabbro (no black gabbro present) | Basal Gabbro Sub. |
| | | | Fg contaminated gabbro | | |



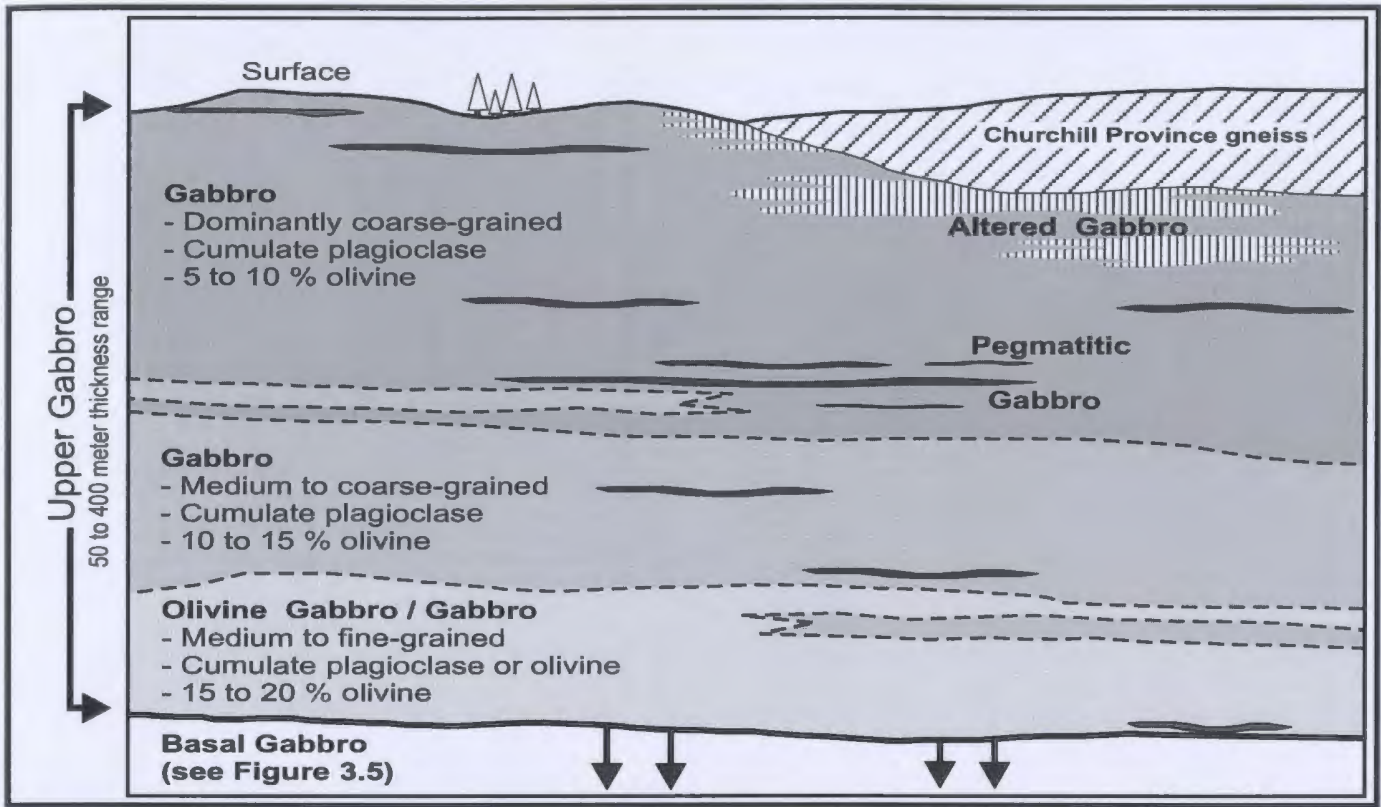


Figure 3.4. Idealized cross-section through the Upper Gabbro subdivision of the Pants Lake Intrusion. The subunits belonging to the Upper Gabbro are shown in their relative positions as they would occur in drill core or outcrop. These subunits are not present in all drill cores or in outcrops.

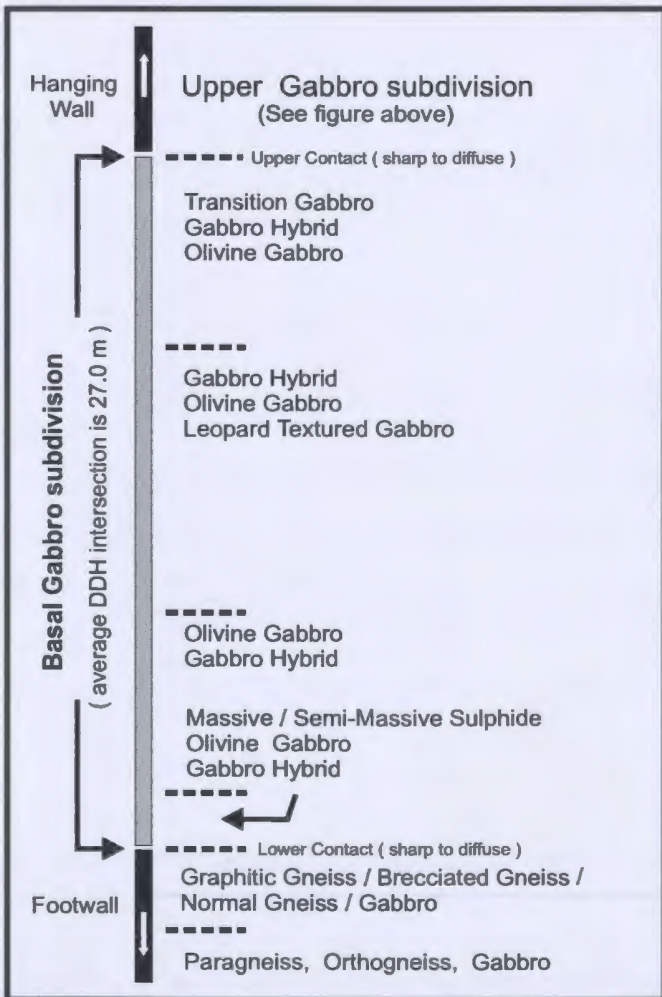


Figure 3.5. Idealized drill log through the Basal Gabbro subdivision of the Pants Lake Intrusion. The subunits are shown in their relative position as they would normally appear in core or outcrop. The dashed lines represent the contacts between the subunits and also serve to illustrate the general thickness of each subunit layer. Note the repetitive nature of the subunits although they are not always present in drill cores or outcrops. The massive / semi-massive sulphide texture is added to this figure because it is normally located adjacent to the footwall contact. Other sulphide textural variations do not have the same consistency. The average DDH intersection of 27.0 m is based on the average of 32 drill holes.

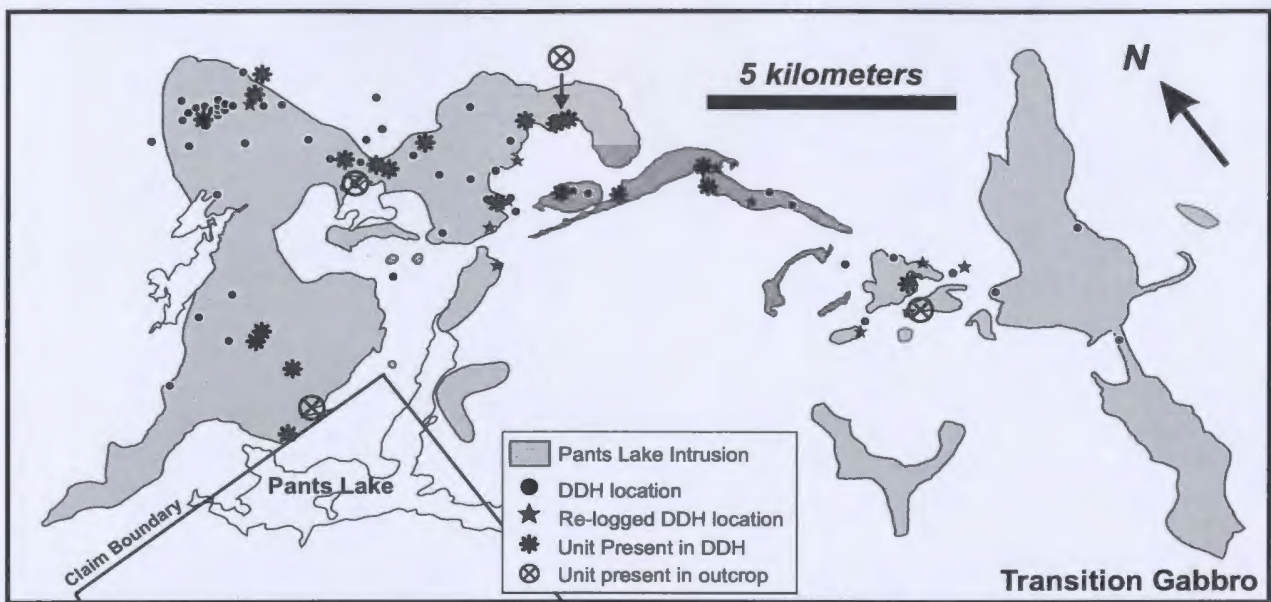


Figure 3.6a

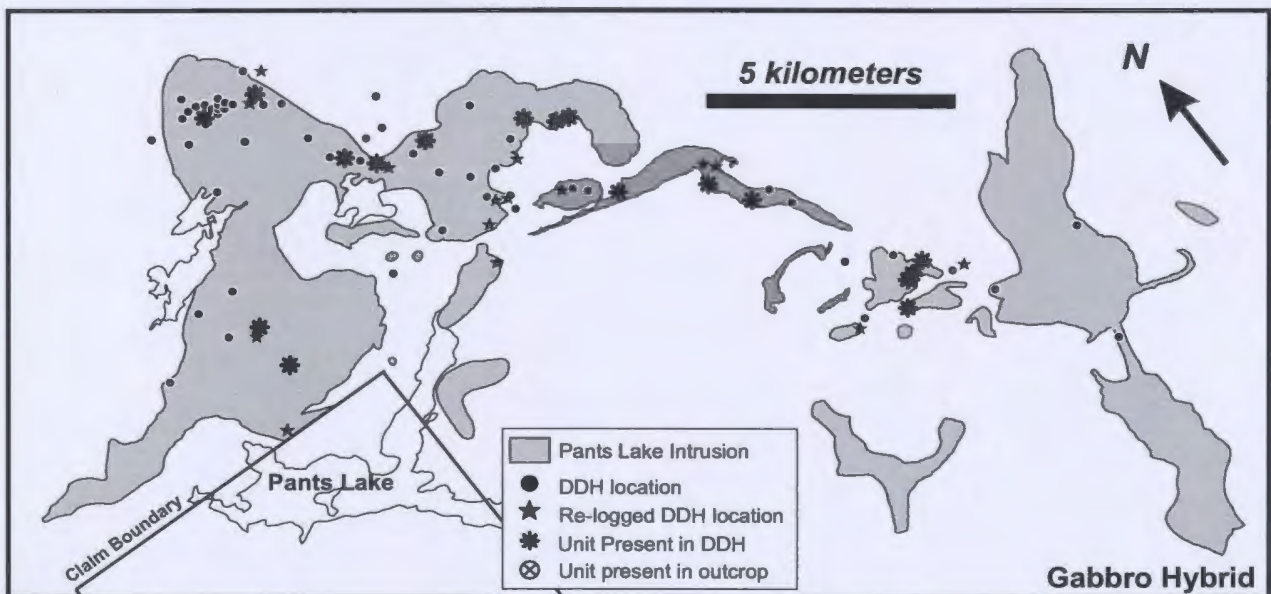


Figure 3.6b

Figure 3.6. Outline of the Pants Lake Intrusion with the locations of diamond drill holes (DDH) and re-logged diamond drill hole used for this study. The * indicates the presence of each Basal Gabbro subunit in the re-logged diamond drill holes. Figure 3.6a indicates the location of the Transition Gabbro subunit, Figure 3.6b indicates the location of the Gabbro Hybrid subunit, Figure 3.6c indicates the location of the Fine-Grained Olivine / Troctolite subunit, Figure 3.6d indicates the location of the Leopard Textured Gabbro subunit, and Figure 3.6e indicates the location of the Medium-Grained Gabbro & Peridotite subunit.

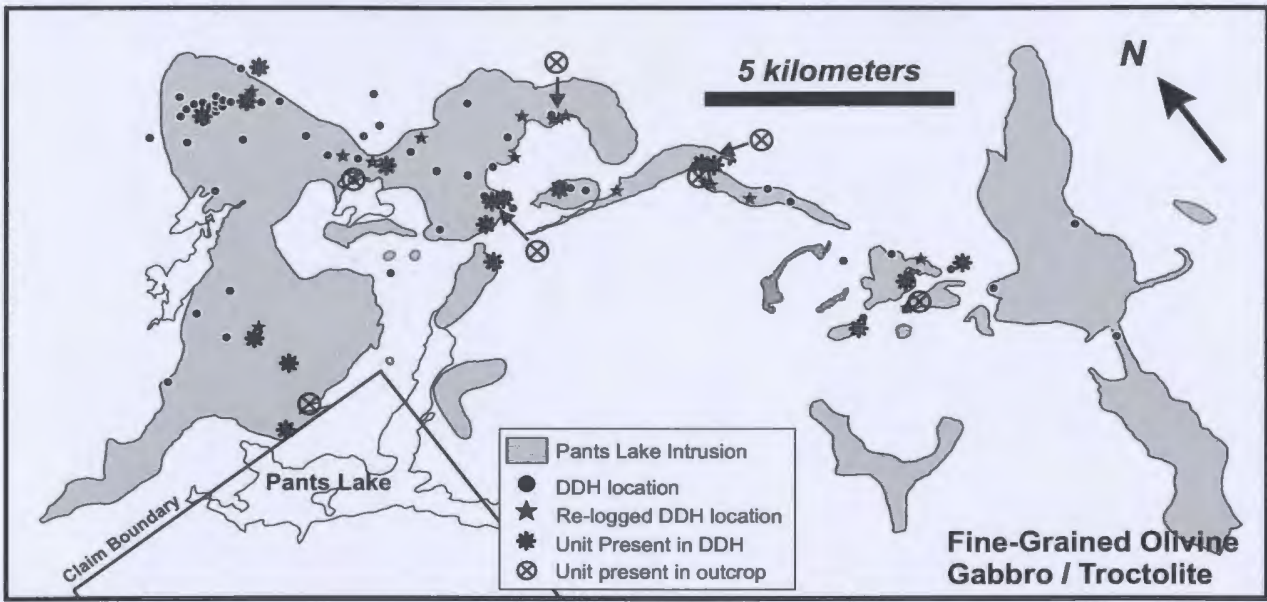


Figure 3.6c

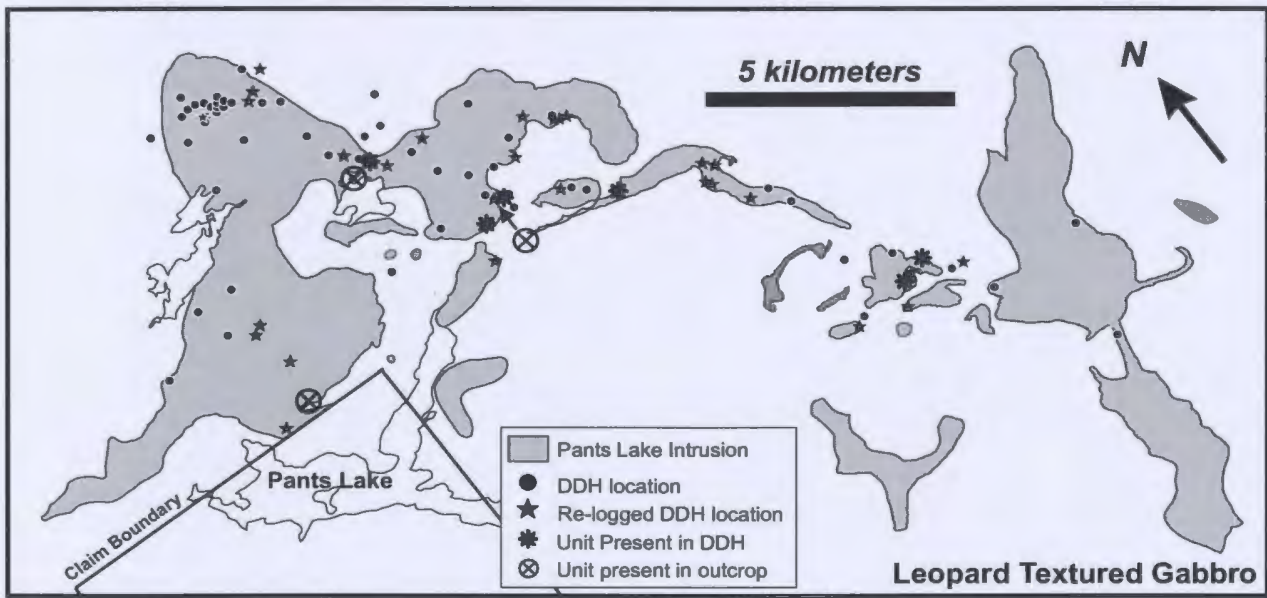


Figure 3.6d

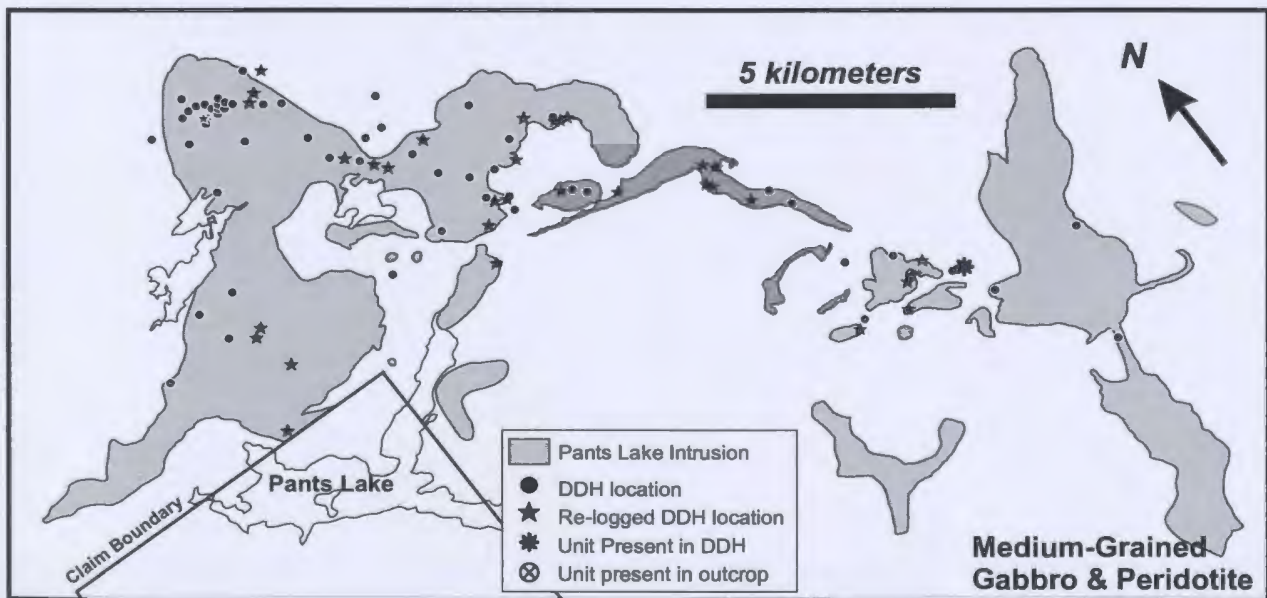


Figure 3.6e

Figure 3.6 (continued)

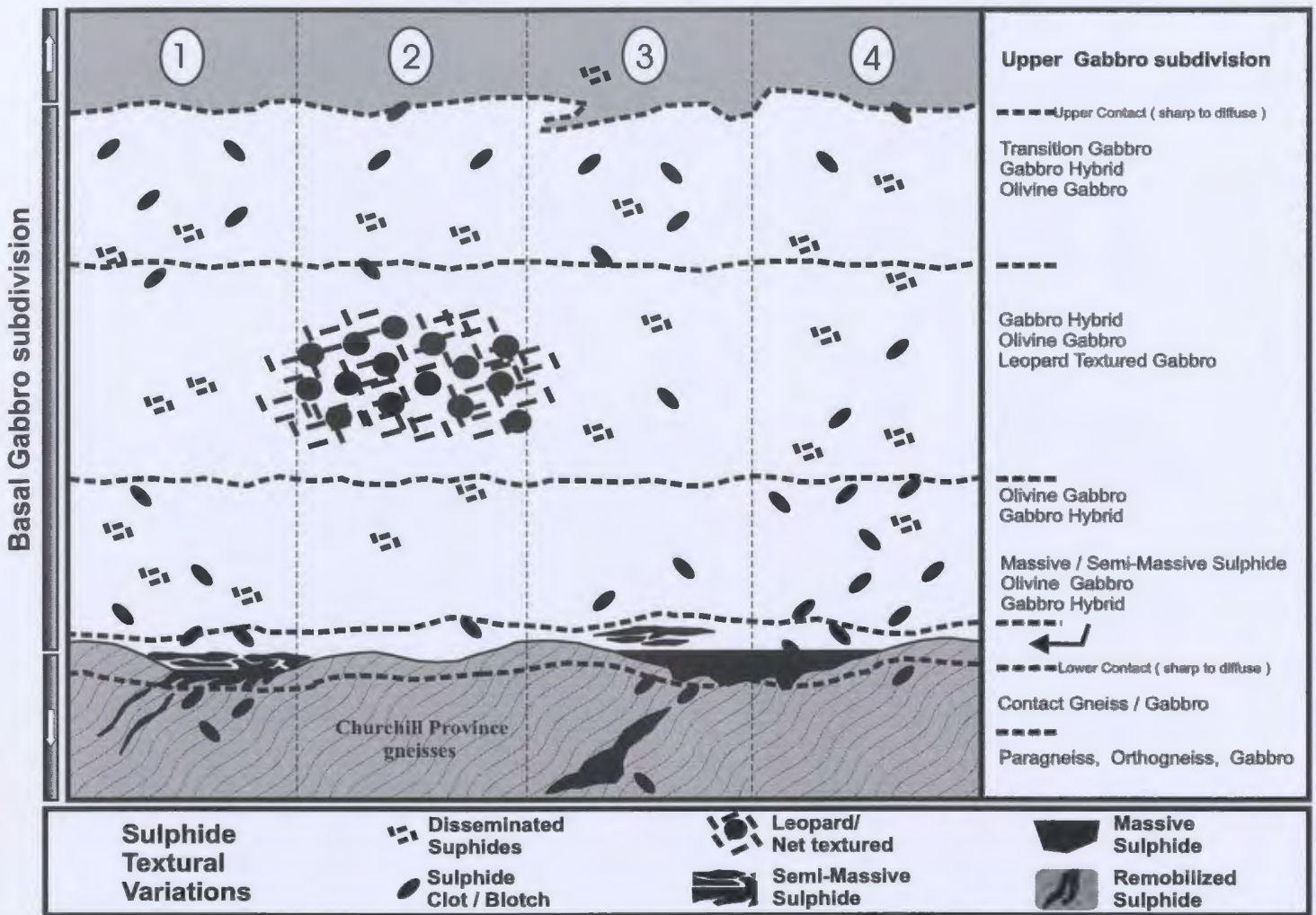


Figure 3.7. Sulphide textural variations observed in the Basal Gabbro subdivision of the Pants Lake Intrusion, Labrador. The numbered columns represent a select range of variations that exist throughout the intrusion. The most consistent sulphide textures, with respect to relative position above the basement contact, are the leopard / net-textured sulphide and the massive to semi-massive textured sulphide. The leopard / net-textured sulphide is consistently situated near the center of the Basal Gabbro subdivision. The massive to semi-massive textured sulphide is consistently situated adjacent to, or just above, the basement contact. The subunits of the Basal Gabbro subdivision, depicted in Figure 3.5, are presented in this figure to illustrate the association between sulphide texture and host. The locations of the different sulphide textures observed in the re-logged drill holes are noted in figures 3.8 a, b, c, d, e and f.

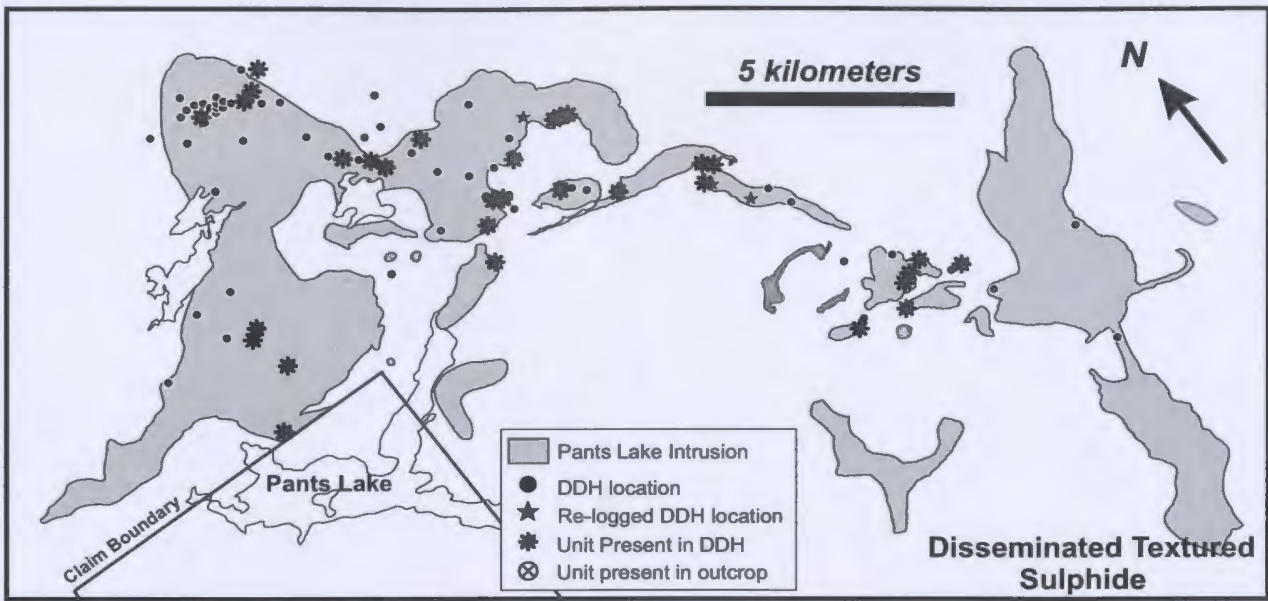


Figure 3.8a

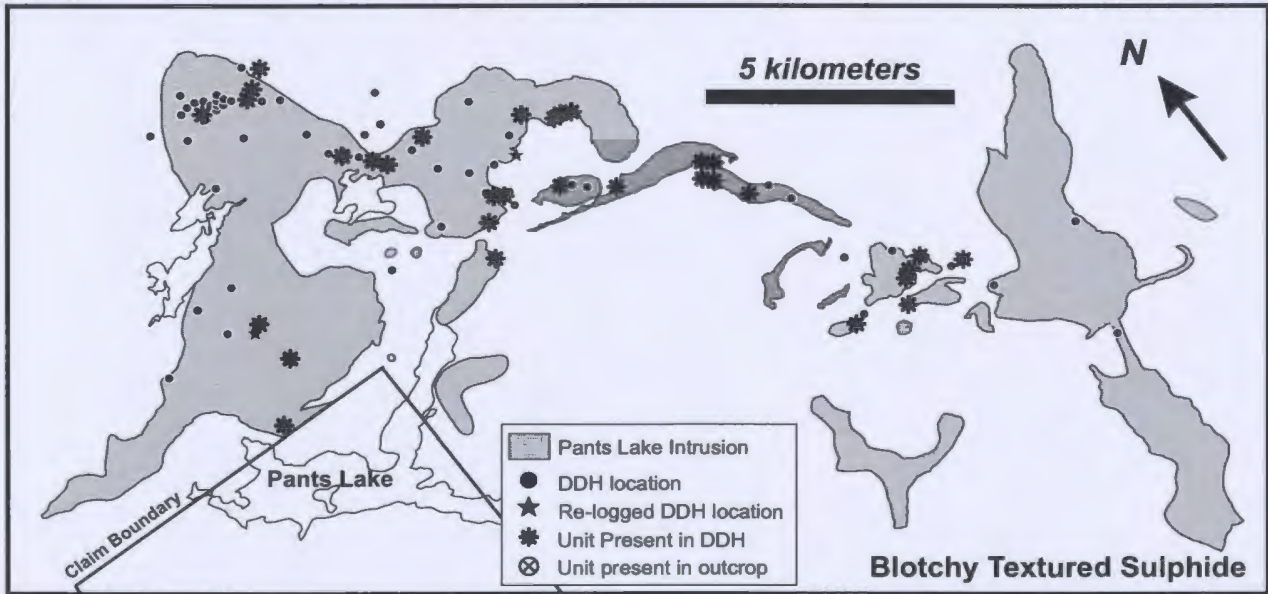


Figure 3.8b

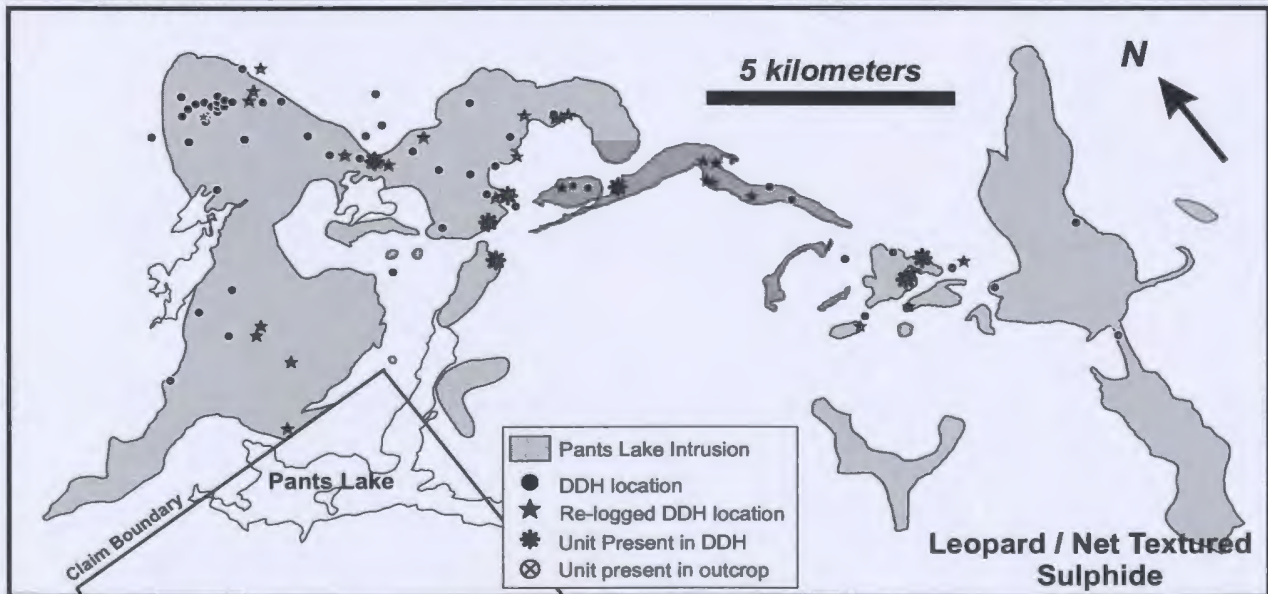


Figure 3.8c

Figure 3.8. Outline of the Pants Lake Intrusion with the locations of diamond drill holes (DDH) and re-logged DDH used for this study. The * indicates the presence of each sulphide textural variation in the re-logged DDH. Figure 3.8a indicates the presence of disseminated textured sulphide, Figure 3.8b indicates the presence of blotchy textured sulphide, Figure 3.8c indicates the presence of leopard / net textured sulphide...(see next page).

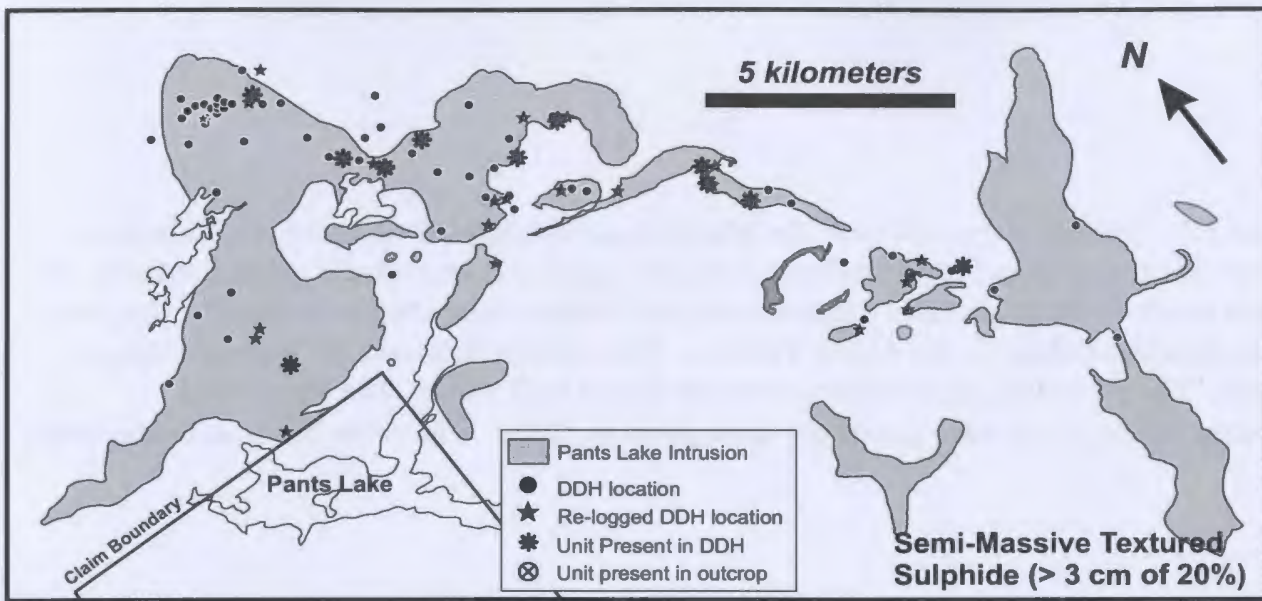


Figure 3.8d

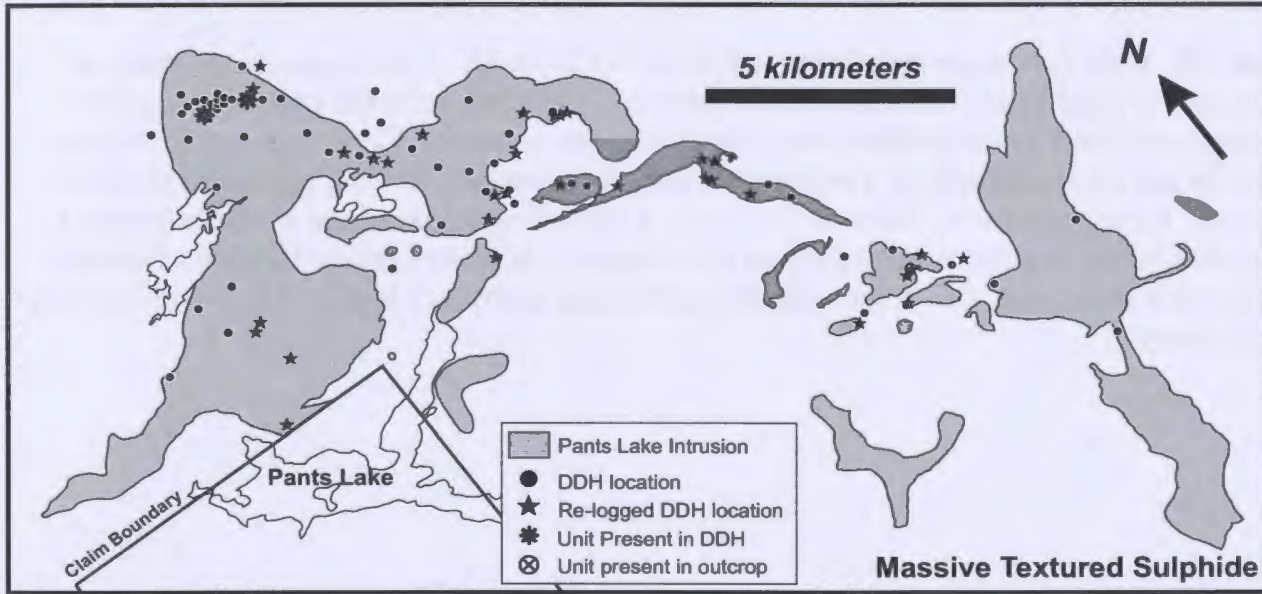


Figure 3.8e

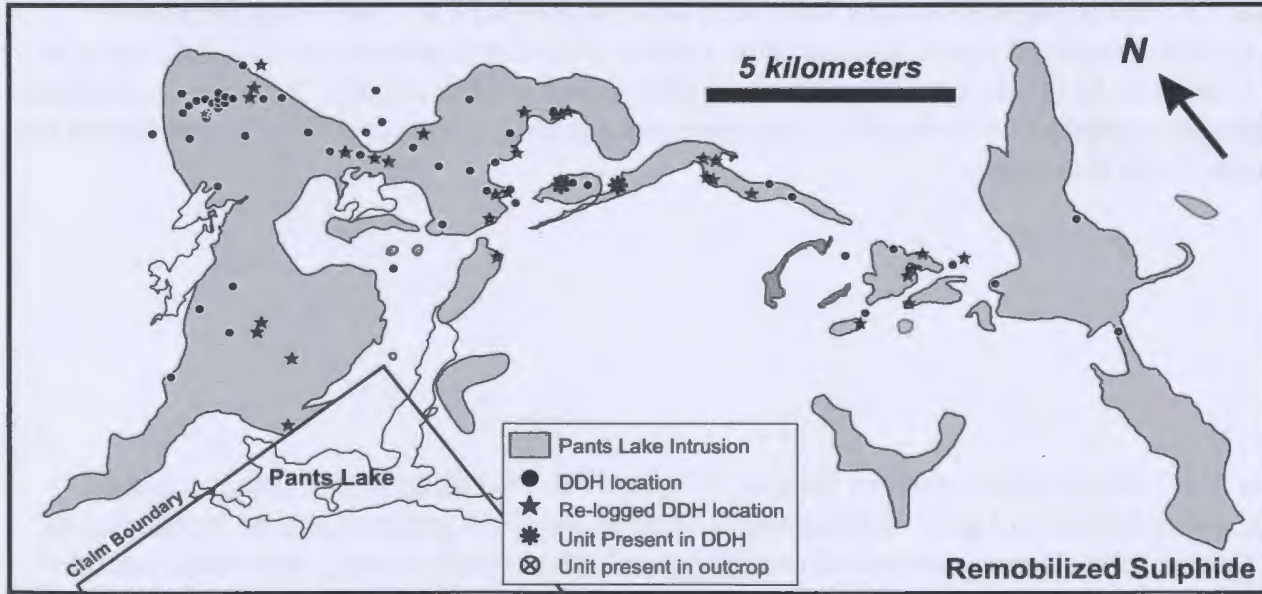


Figure 3.8f

Figure 3.8 (continued) Figure 3.8d indicates the presence of semi-massive textured sulphide, Figure 3.8e indicates the presence of massive textured sulphide, and Figure 3.8e indicates the presence of remobilized sulphide.

Plate 3.1. Outcrop exposure near the Major General sulphide occurrence. This plate shows the typical weathered surface of a coarse-grained, leucocratic gabbro subunit. A small patch of the pegmatitic gabbro subunit is located near the lower edge of the photo. Both subunits belong to the Upper Gabbro. The contact between the two subunits is subtle. The cumulate plagioclase grains are tan to buff white. The interstitial clinopyroxene (\pm olivine) grains are dark green to black. The scale bar is in centimeters.

Plate 3.2. Drill core segments from drill hole, SVB-96-16. Core segment A, taken at 3.6m, is a typical example of the coarse-grained, cumulate textured leucocratic gabbro belonging to the Coarse to Medium-grained Gabbro Subunit. Core segment B, taken at 8.9m, is a typical example of a pegmatitic gabbro belonging to the Pegmatitic Gabbro subunit. Core segment C, taken at 35.2m, is a typical example of the medium-grained, cumulate textured gabbro belonging to the Coarse to Medium-grained Gabbro Subunit. Plagioclase grains are dull white and clinopyroxene grains are black. The scale bar is in centimeters.

Plate 3.3. Petrographic section from drill hole SVB-97-27 at 1.3m (magnification = 1.5x, cross polarized light). Leucocratic, coarse to medium-grained gabbro belonging to the Coarse to Medium-grained subunit (Upper Gabbro subdivision). Euhedral, cumulate plagioclase grains with subophitic clinopyroxene grains. Intercumulate olivine grains are rimmed with iddingsite.

Plate 3.4. Petrographic section from drill hole SVB-98-102 at 32.5m (magnification = 1.5x, cross polarized light). Melacritic, coarse to medium-grained gabbro belonging to the Coarse to Medium-grained subunit (Upper Gabbro subdivision). Euhedral, cumulate plagioclase grains with intercumulate clinopyroxene and lesser olivine grains.

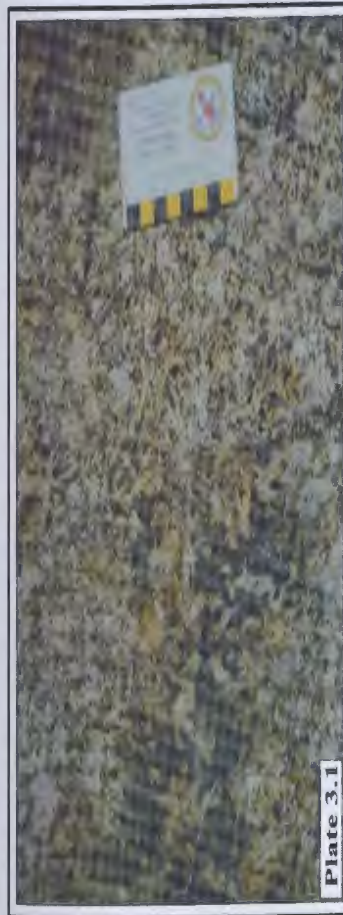


Plate 3.5. Drill core segments from drill hole, SVB-96-27. Core segment A, taken at 1.3 m, is a coarse-grained, cumulate textured gabbro belonging to the Coarse to Medium-grained Gabbro Subunit. Core segment B, taken at 4.7 m, is a medium to fine-grained, ophitic to cumulate textured olivine gabbro belonging to the Olivine Gabbro Subunit. Core segment C, taken at 8.9 m, is an ophitic textured olivine gabbro belonging to the Olivine Gabbro Subunit. Plagioclase grains are white, clinopyroxene grains are dark grey to black, and olivine grains are forest green. The scale bar is in centimeters.

Plate 3.6. Petrographic section from drill hole SVB-96-04 at 4.15 m (magnification = 1.5x, cross polarized light). Medium-grained olivine gabbro belonging to the Olivine Gabbro subunit (Upper Gabbro). Cumulate, euhedral plagioclase with ophitic clinopyroxene containing granular olivine and lesser euhedral plagioclase grains.

Plate 3.7. Drill core from drill hole SVB-96-36 centered at ~ 78.0 m. The darker core is unaltered, coarse-grained gabbro. The lighter core is altered gabbro belonging to the Altered Gabbro Subunit. The altered gabbro contains milky white, saussuritized plagioclase grains with intercumulate green hornblende grains. The contact between altered and unaltered gabbro (at 79.2 m) is relatively sharp. The scale bar is in centimeters.

Plate 3.8. Petrographic section from drill hole SVB-96-36 at 14.1 m (magnification = 1.5x, crossed polarized light). Altered, coarse-grained gabbro belonging to the Altered Gabbro subunit (Upper Gabbro). Large pyroxene grain altered to fine-grained hornblende engulfed by finer grained subhedral to anhedral plagioclase grains.

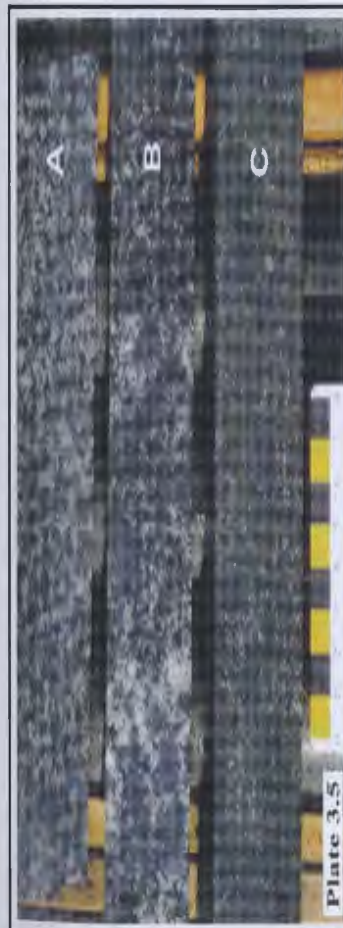


Plate 3.9. Outcrop exposure adjacent to the Mineral Hill sulphide occurrence. This plate shows the weathered contact between the Upper Gabbro and Basal Gabbro. The upper portion of the plate is a medium-grained cumulate textured leucocratic gabbro. The lower portion of the photo is a typical example of the Transition Gabbro subunit. The thin, lighter coloured bands are coarse to medium-grained plagioclase with lesser clinopyroxene. The finer-grained, brownish weathered material is cumulate olivine with lesser plagioclase and clinopyroxene. The scale bar is in centimeters.

Plate 3.10. Drill core segments from drill hole, SVB-97-77 at 412.3 m (top) and drill hole, SVB-98-116 at 107.4 m (bottom). Both drill core segments are examples of the Transition Gabbro subunit. The upper drill segment was derived from a leucocratic gabbro (plagioclase grains are white). The lower drill segment was derived from a melanocratic gabbro (plagioclase grains are purplish-grey). Both core segments illustrate the coarser-grained banding in the finer-grained olivine gabbro. Disseminated sulphides and sulphide blotches are closely associated with the coarser bands.

Plate 3.11. Petrographic section from drill hole SVB-98-111 at 107.5 m (magnification = 1.5x, cross polarized light). Transition Gabbro subunit (Basal Gabbro subdivision) with coarse-grained plagioclase and ophitic clinopyroxene band (center), in a fine-grained olivine gabbro matrix. A small sulphide blotch is in the center of the coarser band.

Plate 3.12. Petrographic section from drill hole SVB-98-111 at 107.5 m (magnification = 1.5x, plane polarized light). Refer to Plate 3.11 for caption description.

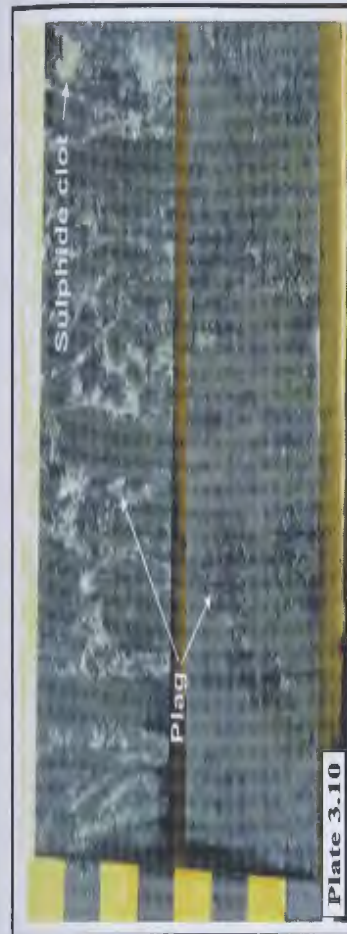


Plate 3.13. Outcrop exposure near the NDT sulphide occurrences. This plate shows the weathered surface of the Gabbro Hybrid / Olivine Gabbro subunit (Basal Gabbro). In the center of the plate is a partially digested melanocratic gneissic inclusion. Pocketknife (~ 8 cm) used for scale.

Plate 3.14. Drill core segments from drill hole, SVB-96-10 at 12.3 m. Drill core segments of the Gabbro Hybrid subunit (Basal Gabbro) with multiple, semi-rounded melanocratic inclusions in a fine-grained olivine gabbro matrix. Disseminated and blotchy sulphides (pyrrhotite ± chalcopyrite, pentlandite) are present within the matrix. The scale bar is in centimeters.

Plate 3.15. Drill core segment from drill hole, SVB-96-02 at 6.2 m. Drill core segment of the Gabbro Hybrid subunit (Basal Gabbro) with several partially digested, melanocratic, gneissic inclusions in a fine-grained olivine gabbro. Blotchy textured sulphide is also present. The scale bar is in centimeters.

Plate 3.16. Drill core segments from drill hole, SVB-98-102 at 173.5 m (top) and 194.0m (bottom). Drill core segments of the Gabbro Hybrid subunit (Basal Gabbro) with several partially digested, leucocratic, gneissic inclusions. Blotchy and disseminated textured sulphides are also present. The scale bar is in centimeters.



Plate 3.17. Petrographic section from drill hole SVB-96-09 at 54.45 m (magnification = 1.5x, cross polarized light). Leucocratic gneissic inclusion (only the edge is shown) in gabbro. The rim of the inclusion composed of spinel and fine-grained plagioclase. The center of the inclusion comprised of acicular corundum grains and plagioclase grains.

Plate 3.18. Petrographic section from drill hole SVB-96-09 at 54.45 m (magnification = 1.5x, plane polarized light). Refer to Plate 3.17 for caption description. Disseminated sulphide (black) is present.

Plate 3.19. Petrographic section from drill hole SVB-96-36 at 165.3 m (magnification = 2.5x, plane polarized light). Center of a leucocratic inclusion comprised of plagioclase, corundum and Fe-spinel.

Plate 3.20. Petrographic section from drill hole SVB-96-09 at 58.1 m (magnification = 1.5x, plane polarized light). Melanocratic inclusion comprised of Fe-spinel, biotite and plagioclase grains.

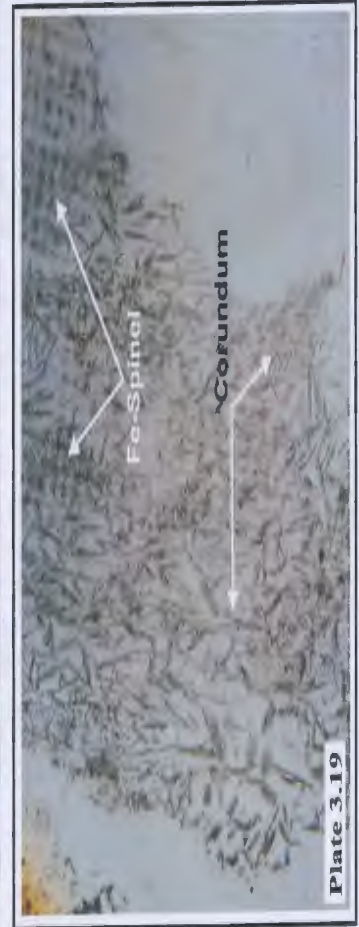
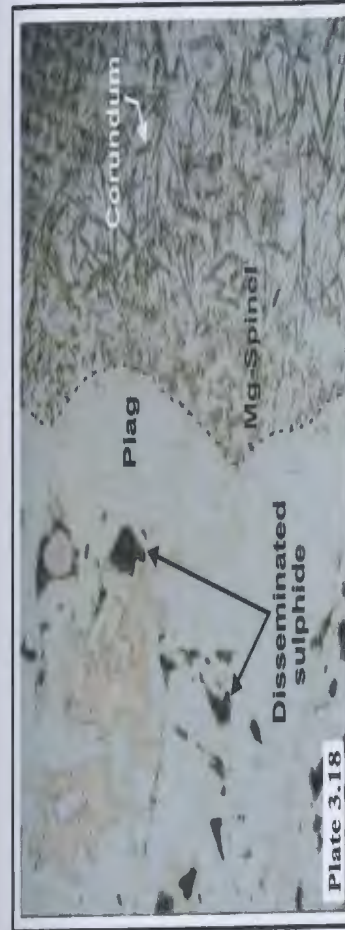


Plate 3.21. Drill core from drill hole SVB-96-02 centered at ~71.8 m. Fine-grained, melanocratic olivine gabbro of the Olivine Gabbro subunit (Basal Gabbro). A group of pyrrhotite blotches are located in the center of the photograph. The scale bar is in centimeters.

Plate 3.22. Drill core from drill hole SVB-97-92 at 247.0 m. Fine-grained olivine gabbro of the Olivine Gabbro subunit (Basal Gabbro) with 4-5% fine-grained disseminated sulphide. The scale bar is in centimeters.

Plate 3.23. Petrographic section from drill hole SVB-96-02 at 71.8 m (magnification = 2.5x, cross polarized light). Fine-grained olivine gabbro with granular olivines, plagioclase and lesser ophitic clinopyroxene.

Plate 3.24. Petrographic section from drill hole SVB-97-79 at ~504 m (magnification = 1.5x, cross polarized light). Fine-grained olivine gabbro with granular olivines, plagioclase and lesser ophitic clinopyroxene. Plagioclase grains are aligned parallel to layering.

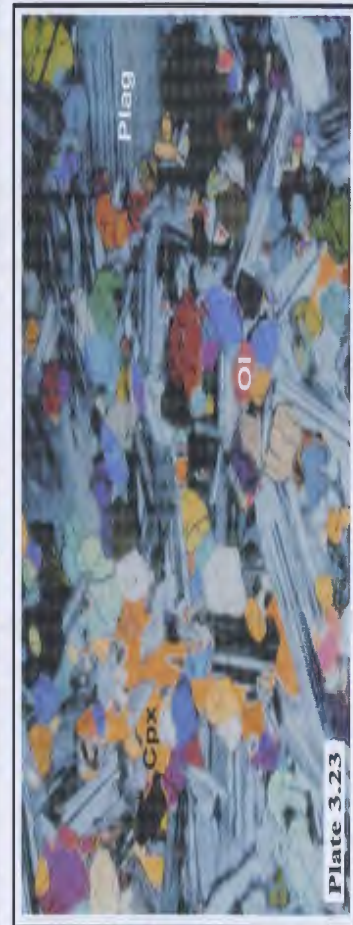
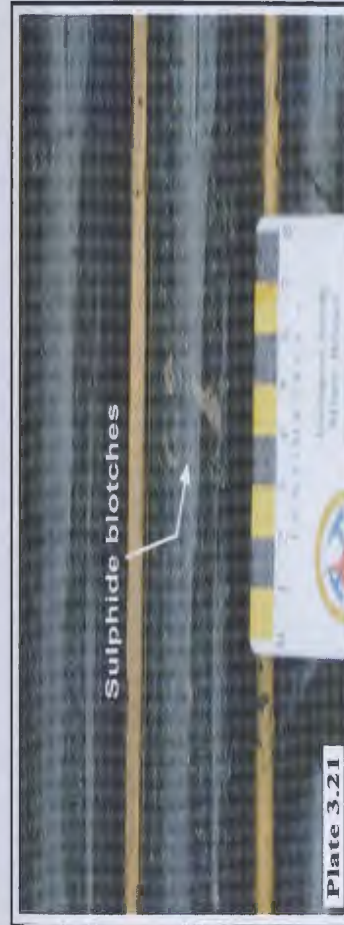


Plate 3.25. Outcrop exposure within the Happy Face Lake sulphide occurrence. Photograph shows the typical weathered surface of the Leopard Textured Gabbro subunit (Basal Gabbro). Clinopyroxene oikioocrysts are present within a recessive weathered olivine, plagioclase, sulphide matrix. The pencil is used for scale.

Plate 3.26. Drill core segment from drill hole SVB-96-02 at 20.1 m. Typical appearance of the Leopard Textured gabbro subunit (Basal Gabbro) with clinopyroxene oikioocrysts (dark spots) set in a fine-grained olivine gabbro matrix with 10% fine-grained, disseminated sulphide. Scale bar is in centimeters.

Plate 3.27. Petrographic section from drill hole SVB-96-02 at 24.6 m (magnification = 1.5x, cross polarized light). Clinopyroxene oikioocryst (center of plate) surrounded by plagioclase, olivine, disseminated sulphide (opaque), and lesser clinopyroxene.

Plate 3.28. Petrographic section from drill hole SVB-96-02 at 24.6 m (magnification = 1.5x, plane polarized light). Refer to Plate 3.27 for caption description.



Plate 3.29. Drill core segment from drill hole SVB-97-79 at 691.3 m. Medium-grained gabbro of the Medium-grained Gabbro subunit (Basal Gabbro). Interstitial plagioclase grains are white, olivine grains and clinopyroxene grains are dark coloured. The scale bar is in centimeters.

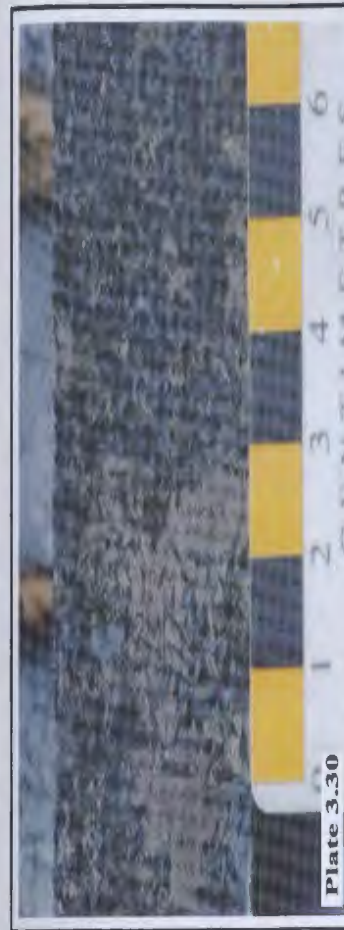


Plate 3.30. Drill core segment from drill hole SVB-97-79 at 738.1 m. Medium-grained gabbro of the Medium-grained Gabbro subunit (Basal Gabbro) with large sulphide blotches. The scale bar is in centimeters.

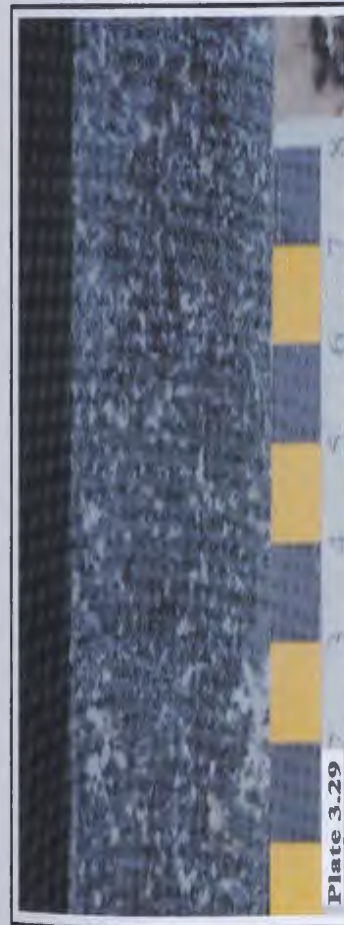


Plate 3.31. Petrographic section from drill hole SVB-97-79 at 691.3 m (magnification = 1.5x, cross polarized light). Cumulate olivine and lesser cumulate clinopyroxene with altered, intercumulate plagioclase and biotite.

Plate 3.32. Petrographic section from drill hole SVB-97-79 at 691.3 m (magnification = 1.5x, plane polarized light). Refer to Plate 3.31 for caption description.

Plate 3.33. Petrographic section from drill hole SVB-97-92 at 246.7 m (magnification = 1.5x, plane polarized light). Disseminated sulphide (opaque) grown between plagioclase and olivine grains.



Plate 3.34. Petrographic section from drill hole SVB-97-92 at 246.7m (magnification = 2.5x, reflecting light). Disseminated sulphide grains between silicate grains. Disseminated sulphide grains comprised of pyrrhotite (Po) with small chalcopyrite (Cpy), pentlandite (Pn), and magnetite (Mag) exsolutions.

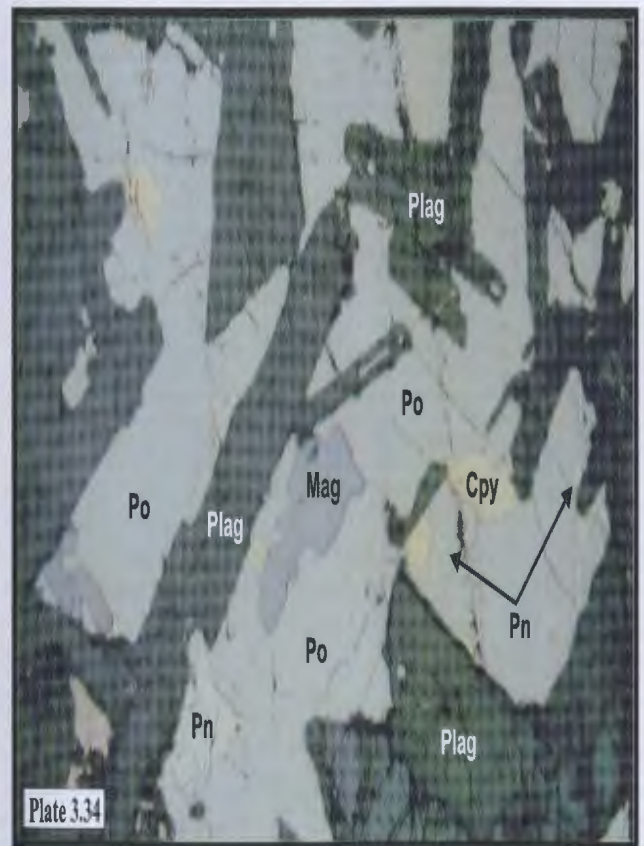


Plate 3.35. Outcrop exposure at the Major General sulphide occurrence. Oxidized sulphide blotches in fine-grained olivine gabbro. The geological hammer is for scale.

Plate 3.36. Drill core segments from drill hole SVB-96-10 at ~24.6 m. Dominantly pyrrhotite blotches with plagioclase intergrowths hosted in a fine-grained olivine gabbro. Segments also host several melanocratic gneissic inclusions. The scale bar is in centimeters.

Plate 3.37. Drill core segment from drill hole SVB-96-04 at 51.3 m. Large sulphide blotch hosted in a fine-grained olivine gabbro. Sulphide blotch has an upper portion of magnetite (Mag) and chalcopyrite (Cpy). The scale bar is in centimeters.

Plate 3.38. Drill core segment from drill hole SVB-96-04 at 58.6 m. Large pyrrhotite (Po) blotch in center of photo, hosted in a fine-grained olivine gabbro, has an upper chalcopyrite (cpy) rim. The scale bar is in centimeters.



Plate 3.39. Petrographic section from drill hole SVB-96-10 at 24.6 m (magnification = 2.5x, reflecting light). Pyrrhotite (Po) blotch with small chalcopyrite (Cpy) exsolutions present predominantly near the contact. Plagioclase grains are grown into the sulphide boundary.

Plate 3.40. Petrographic section from drill hole SVB-97-79 at 729.4 m (magnification = 2.5x, reflecting light). Edge of a pyrrhotite (Po) blotch with pentlandite (Pn) originating internally and grown outwards to the edge. Chalcopyrite (Cpy) and magnetite (Mag) are also adjacent to the sulphide boundary.

Plate 3.41. Petrographic section from drill hole SVB-97-57 at 165.3 m (magnification = 2.5x, reflecting light). Chalcopyrite (Cpy) and pentlandite (Pn) exsolutions formed on the pyrrhotite (Po) / silicate (dark grey) boundary. Magnetite (Mag) formed in the cracks of the pentlandite.

Plate 3.42. Petrographic section from drill hole SVB-96-02 at 69.15 m (magnification = 2.5x, reflecting light). Pentlandite (Pn) and chalcopyrite (Cpy) formed at the edge of pyrrhotite (Po). Magnetite (Mag) is present within cracks in the pentlandite and chalcopyrite.

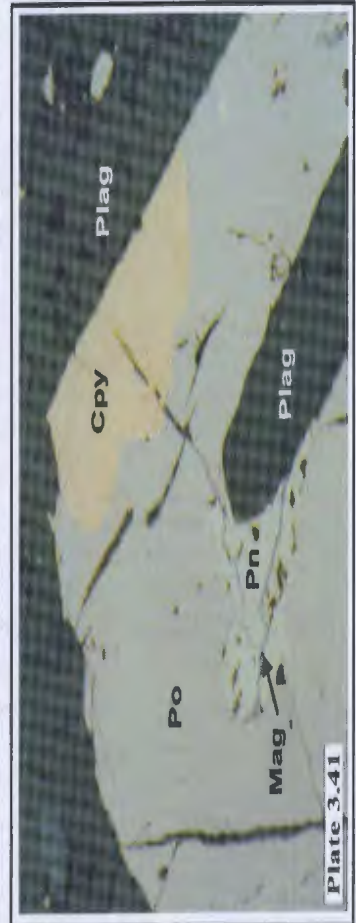
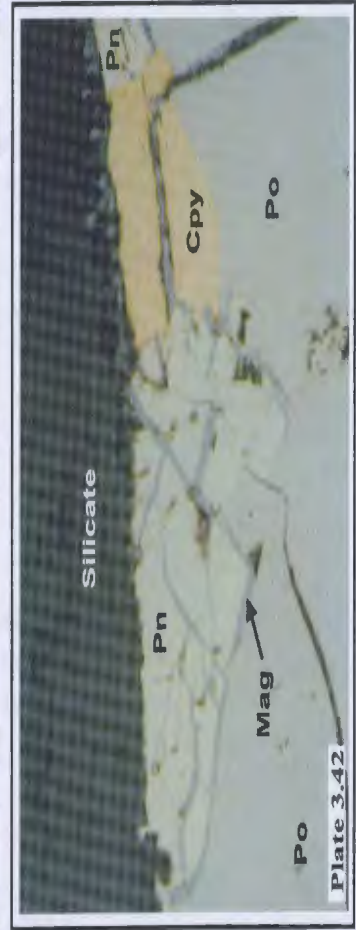
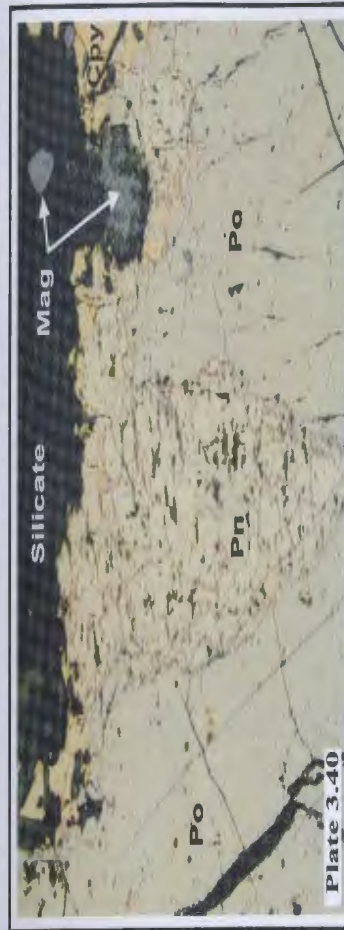


Plate 3.43. Drill core from drill hole SVB-98-116 at 123.1 m. Semi-massive sulphide located above footwall contact. Sulphide comprised of mainly pyrrhotite with minor (> 2%) chalcopyrite. Sulphide is hosted in a fine-grained olivine gabbro with minor gneissic contamination. The scale bar is in centimeters.

Plate 3.44. Drill core from drill hole SVB-98-113 centered at 100 m. Massive sulphide intervals located just above the basement contact. Massive sulphide interval, comprised of pyrrhotite and lesser chalcopyrite and pentlandite, has several inclusions. The scale bar is in centimeters.

Plate 3.45. Drill core segment from drill hole SVB-98-113 at 100.4 m. Massive pyrrhotite (Po) with lesser chalcopyrite and pentlandite. The darker spots are gneissic inclusions. Note the sharp rounded contacts between the sulphide and the inclusions. The scale bar is in centimeters.

Plate 3.46. Drill core segments from drill hole SVB-97-75 at ~ 175 m. High grade, coarsely crystalline massive sulphide from a sulphide interval 13 meters below the footwall contact. Photo courtesy of Dr. Andrew Kerr, Department of Natural Resources.

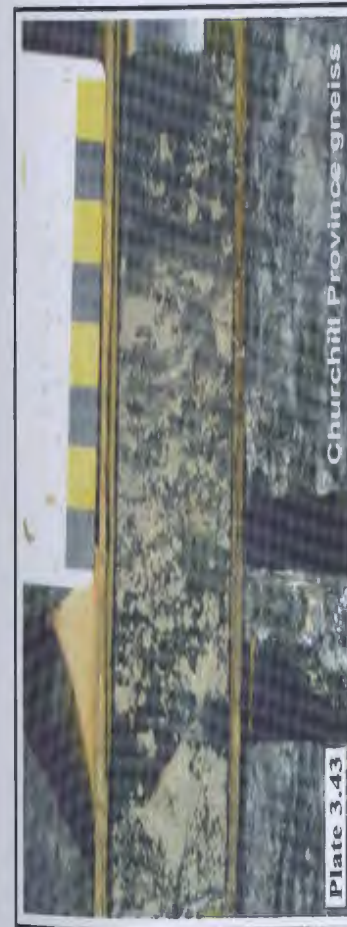
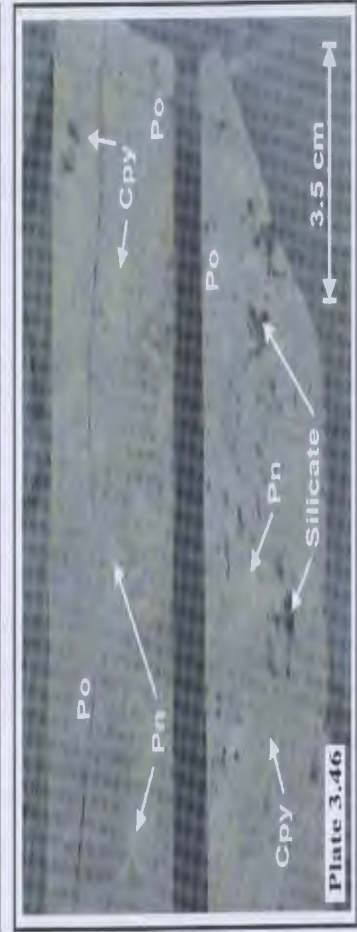
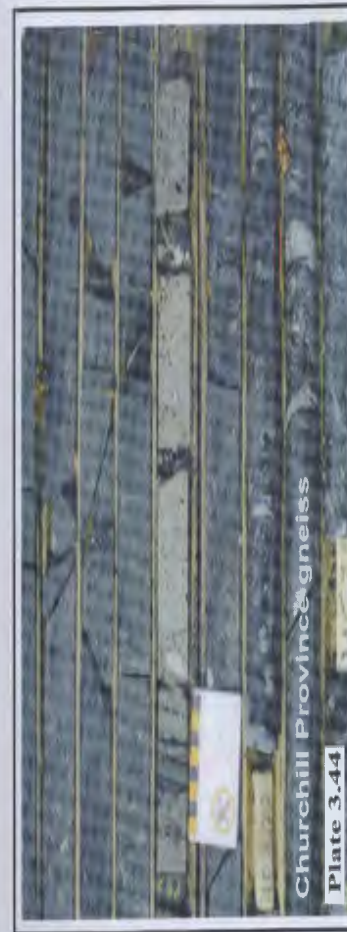


Plate 3.47. Petrographic section from drill hole SVB-98-102 at 183 m (magnification = 10x, reflecting light). Massive pyrrhotite (Po) with exsolution lamellae of pentlandite flames (Pn).

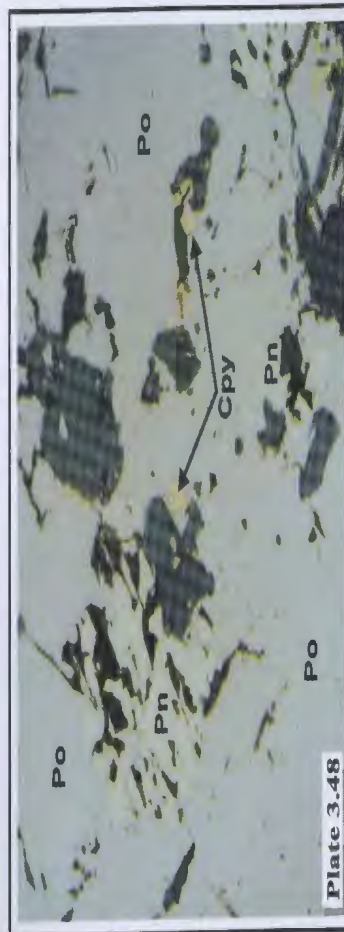


Plate 3.48. Petrographic section from drill hole SVB-97-61 at 123.2 m (magnification = 2.5x, reflecting light). Massive pyrrhotite with small exsolution grains of pentlandite (Pn) and chalcopyrite (Cpy) located adjacent to silicate inclusions.

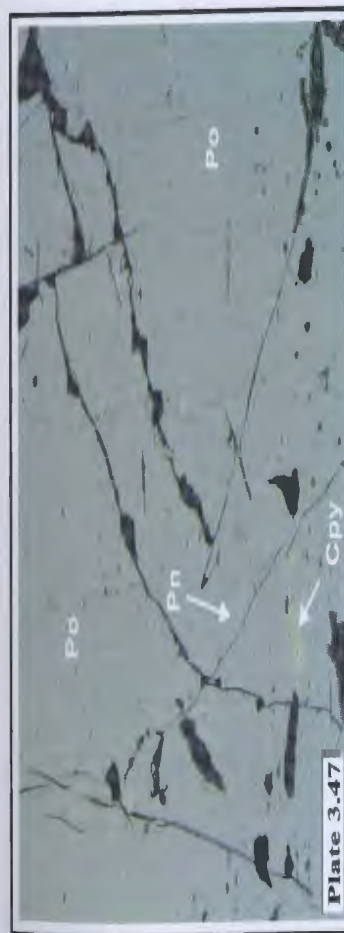


Plate 3.49. Petrographic section from drill hole SVB-97-75 at ~175 m (magnification = 2.5x, reflecting light). Massive sulphide with large crystalline pentlandite (Pn) grain located between pyrrhotite (Po) and chalcopyrite (Cpy). Magnetite (Mag) is present within cracks of the pentlandite.

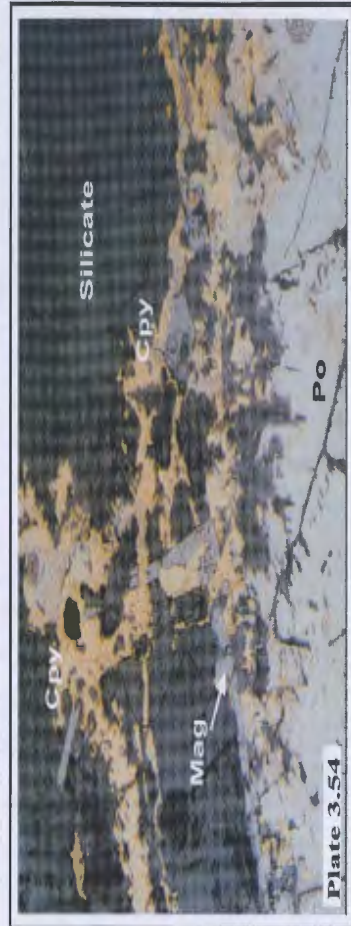
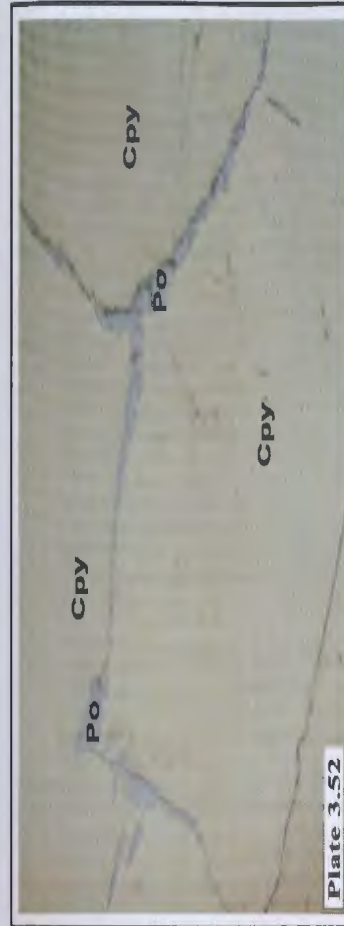
Plate 3.50. Petrographic section from drill hole SVB-97-75 at ~175 m (magnification = 2.5x, reflecting light). Massive sulphide comprised of chalcopyrite (Cpy) and pentlandite (Pn). Pyrrhotite (Po) is present as rims around the pentlandite grains.

Plate 3.51. Petrographic section from drill hole SVB-97-75 at ~175 m (magnification = 10x, reflecting light). Massive sulphide comprised of pyrrhotite (Po), chalcopyrite (Cpy) and lesser pentlandite (Pn). Note the exsolution lamellae of cubanite in chalcopyrite.

Plate 3.52. Petrographic section from drill hole SVB-97-75 at ~175 m (magnification = 10x, reflecting light). Massive chalcopyrite (Cpy) with pyrrhotite (Po) formed at the chalcopyrite grain boundaries.

Plate 3.53. Petrographic section from drill hole SVB-97-58 at 163.5 m (magnification = 10x, reflecting light). Silicate grains in massive sulphide. Chalcopyrite (Cpy) located in the center of the plate is remobilized into the cracks developed into the silicate minerals.

Plate 3.54. Petrographic section from drill hole SVB-97-75 at ~175 m (magnification = 2.5x, reflecting light). Edge of massive sulphide with chalcopyrite (Cpy) remobilized between the silicate grain boundaries.



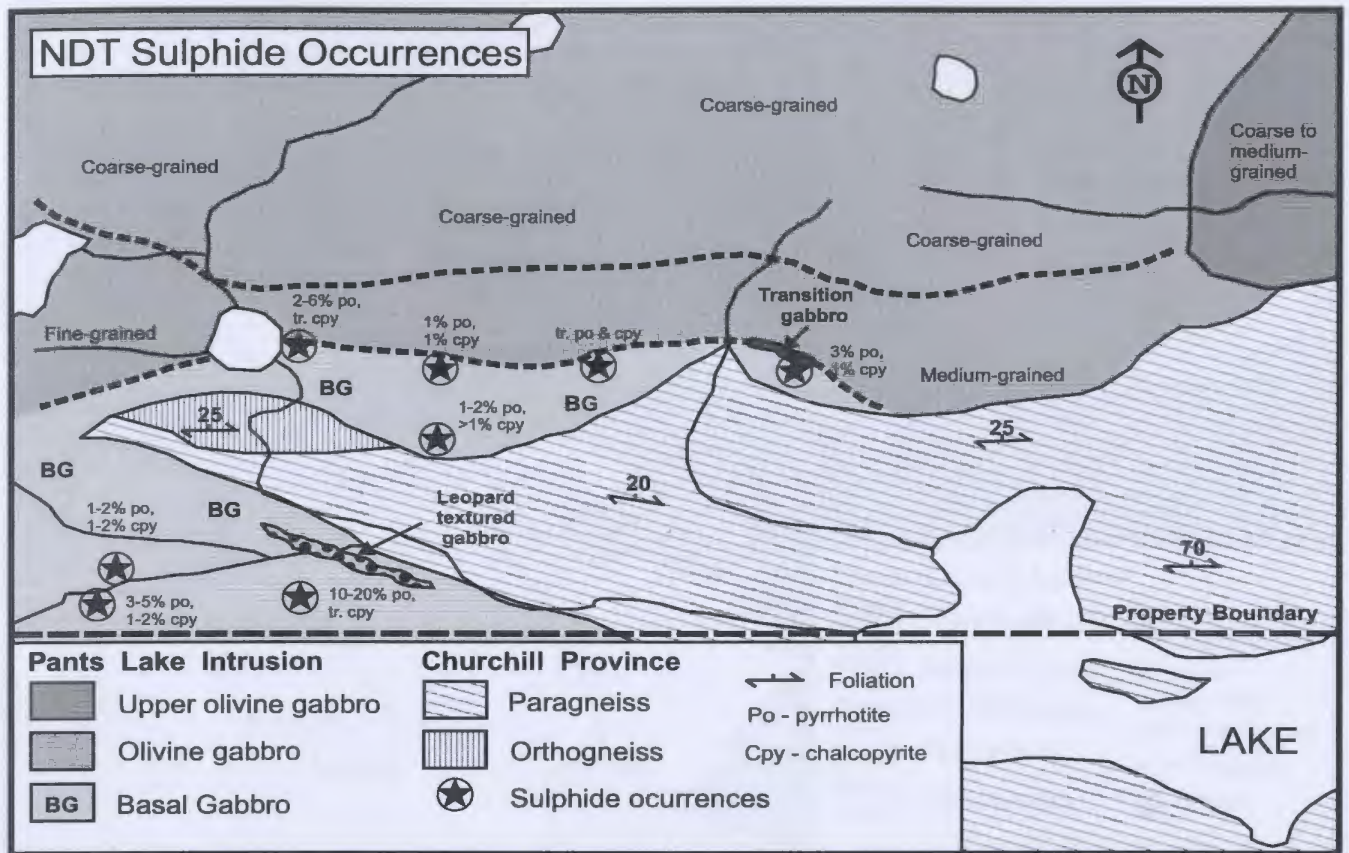


Figure 3.9. Local geology of the NDT sulphide occurrences. Refer to the enclosed geology map for location of figure.

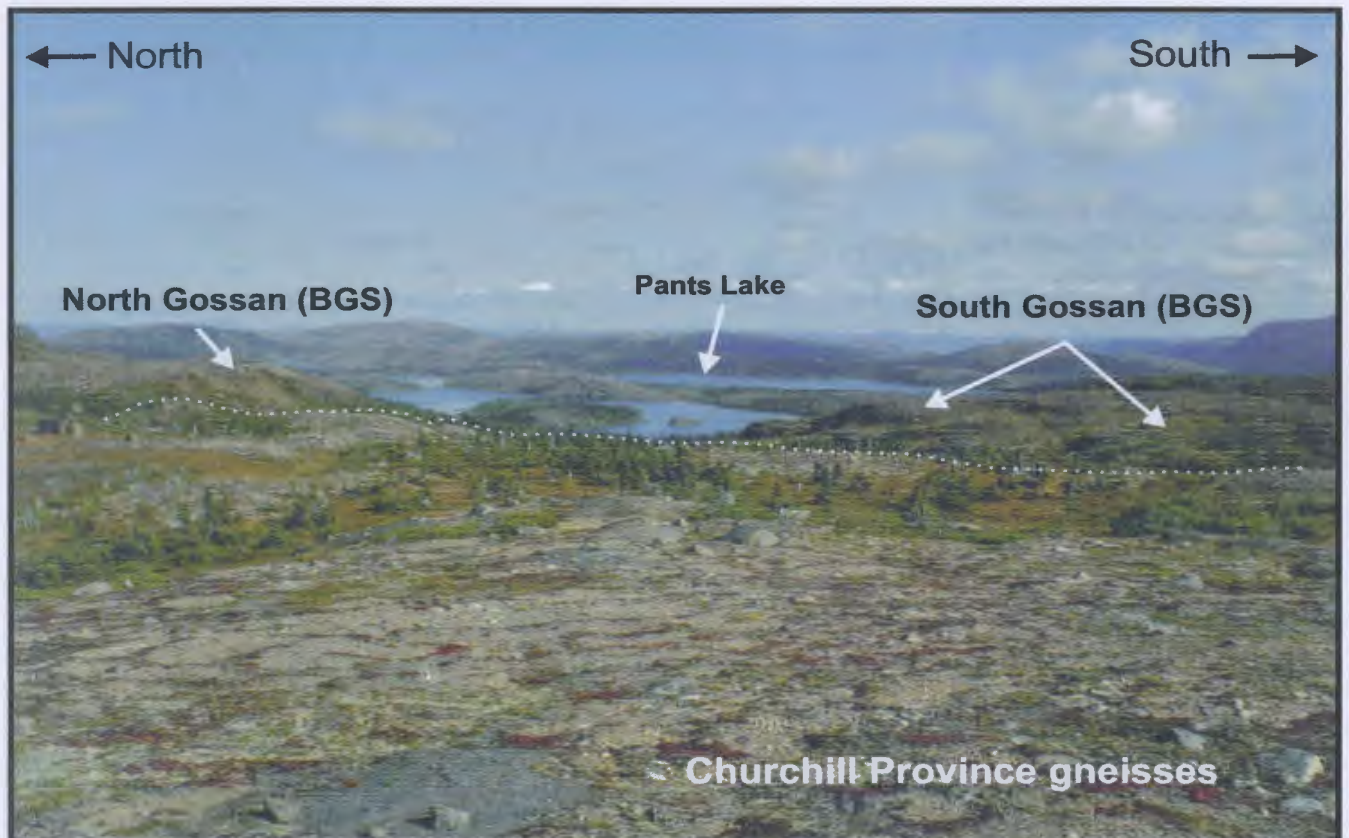


Plate 3.55. Photograph looking east along the NDT sulphide occurrences/gossans (seen in the background). The North Gossan is separated from the South Gossan by a v-shaped wedge of Churchill Province gneiss (seen in the foreground).

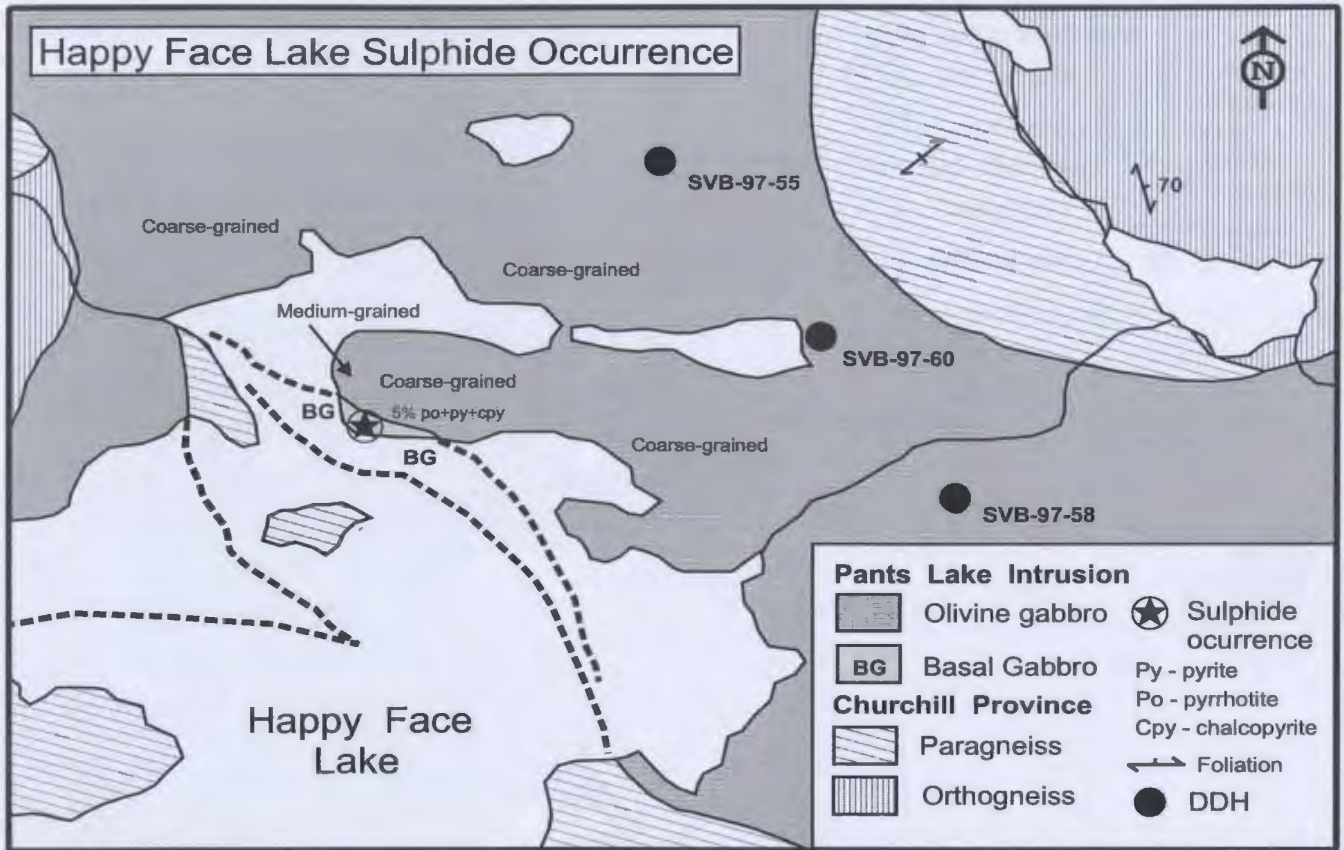


Figure 3.10. Local geology of the Happy Face Lake sulphide occurrence. Refer to the enclosed geology map for location of figure.

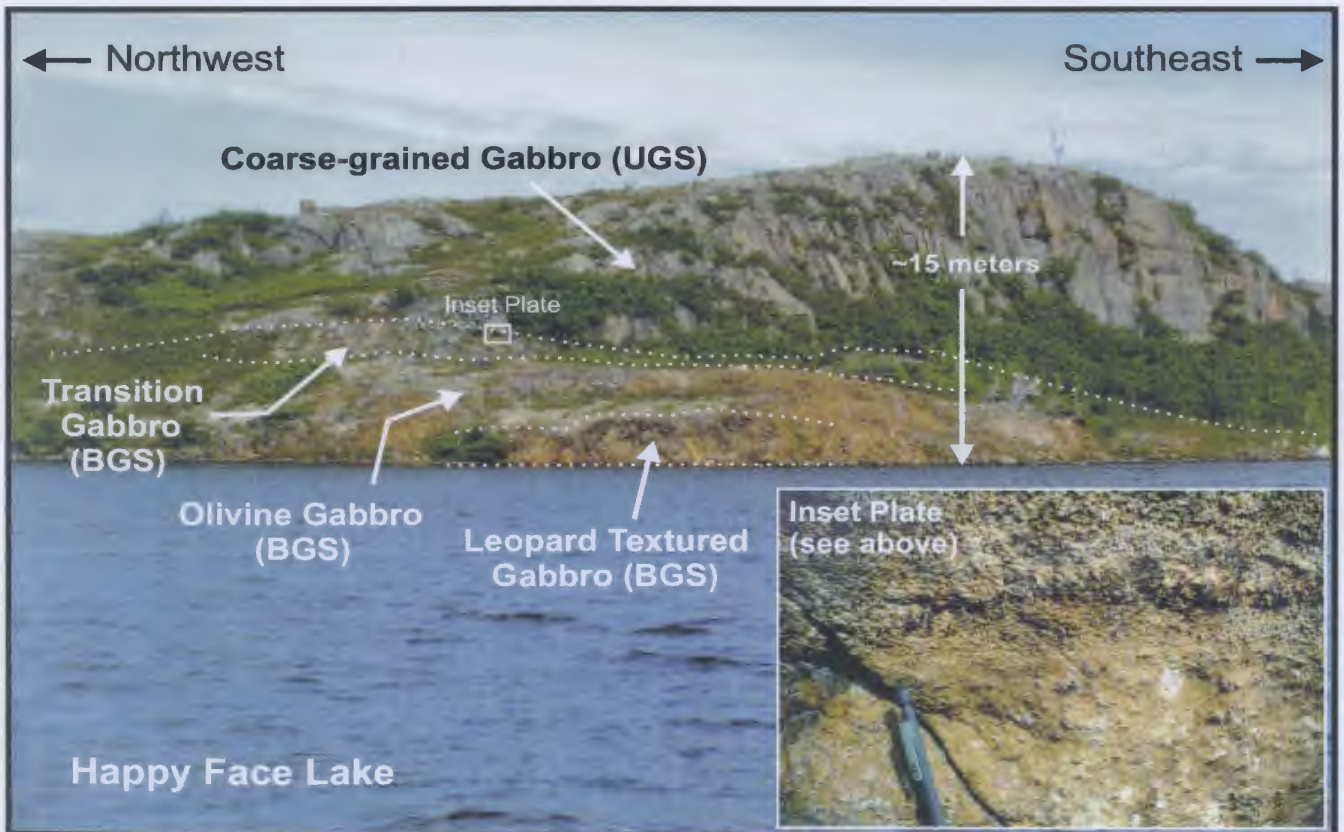


Plate 3.56. Photograph looking northeast at the Happy Face Lake sulphide occurrence (seen in the middle of photograph). Three Basal Gabbro subunits are observed here. The lower Basal Gabbro contact was not observed. The upper contact is shown in the inset plate.

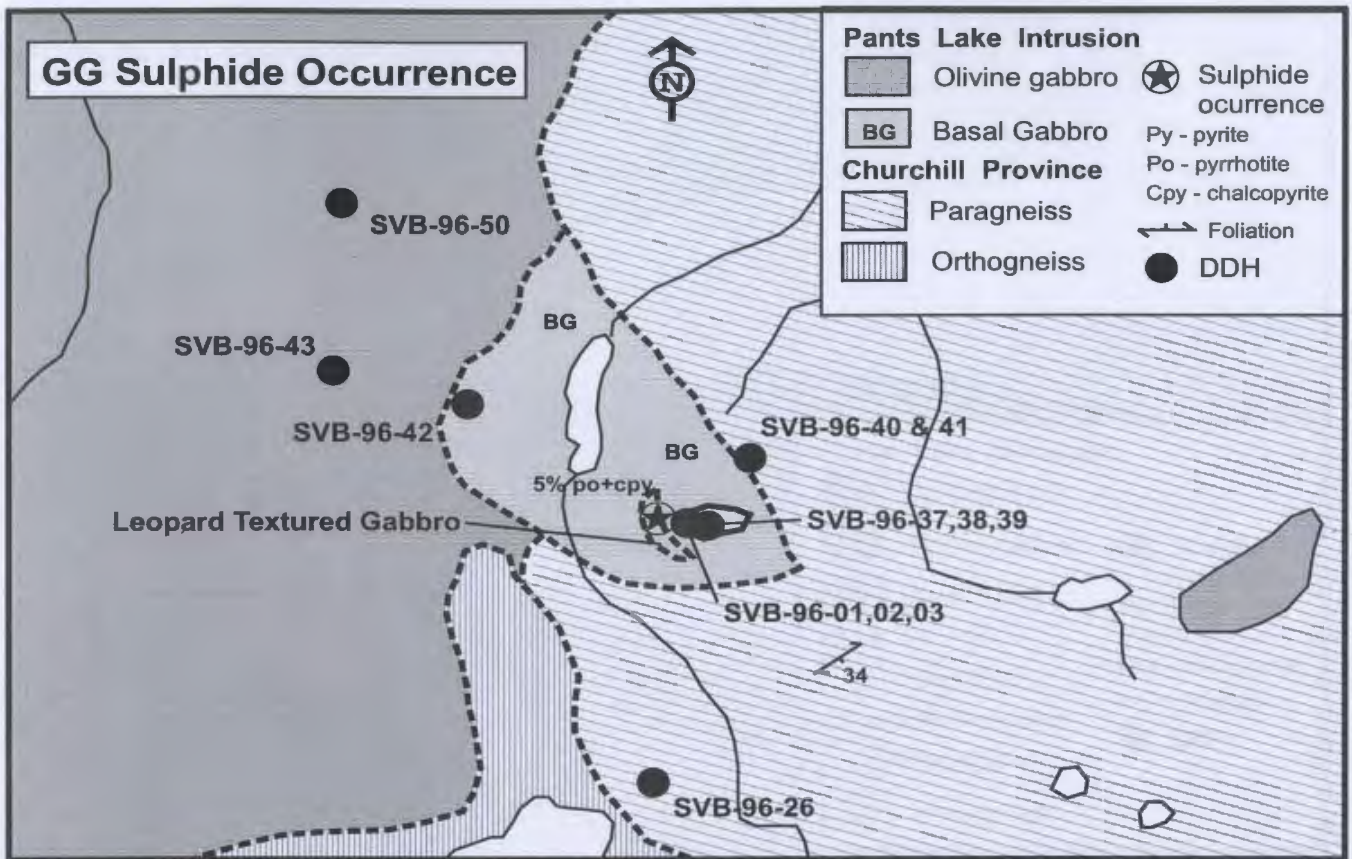


Figure 3.11. Local geology of the GG sulphide occurrence. Refer to the enclosed geology map for location of figure.

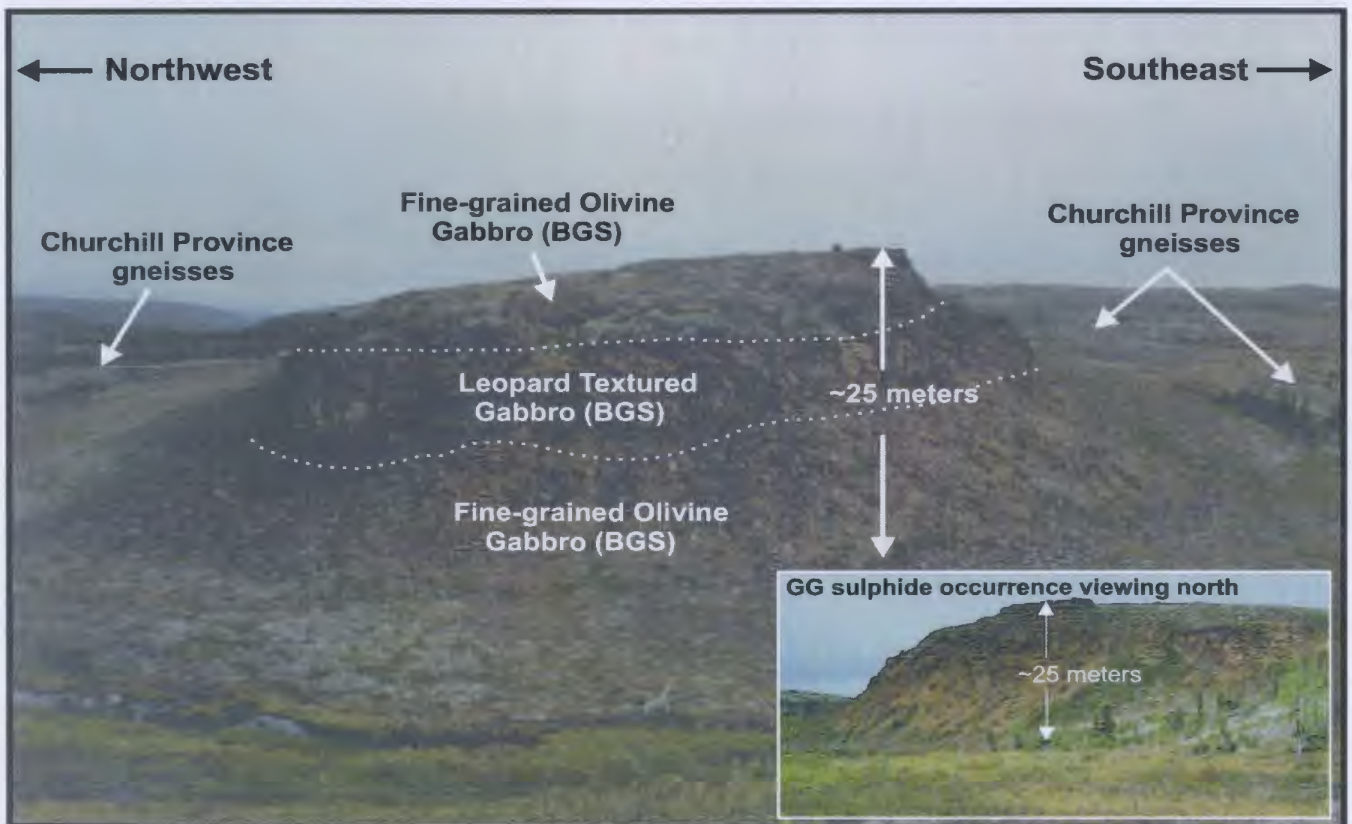


Plate 3.57. Photograph looking northeast at the GG sulphide occurrence (seen in center of photograph). The Leopard Textured gabbro subunit is between the Fine-grained Olivine Gabbro subunit. The lower Basal Gabbro subdivision contact is scree covered.

Chapter 4: Major, Trace, and Rare Earth Element Geochemistry

4.1 Introduction

In this chapter, the subunits of the Pants Lake Intrusion, gneiss of the Churchill Province, and mafic dikes are examined on the basis of their major, trace, and rare earth element (REE) geochemistry. The role of the geochemical data in this chapter is as follows: 1) to define the chemical composition of the subunits, gneiss, and mafic dikes within the map area, 2) to assess the role of cumulate and accessory mineralogy in the subunits, 3) to determine if chemical trends exist laterally or vertically within, or between, subunits, 4) to assess the degree of crustal contamination in the subunits, and 5) to decipher the petrogenetic and metallogenetic controls on the formation of the various subunits.

This chapter is organized into four sections. The list of elements, analytical results, analytical procedures, precision, and accuracy are presented in Appendix B. The first section describes and evaluates major and trace element geochemical data for samples from the Upper Gabbro, the Basal Gabbro, the Churchill Province, and the mafic dikes (refer to Appendix B.1). Data for this component were derived via the X-Ray Fluorescence (XRF) analytical method on 123 pressed pellets following the procedures outlined by Longerich (1995).

The second section of this chapter describes and evaluates REE data for the same geological units (refer to Appendix B.2). This component utilizes data derived by Na_2O_2 sinter inductively coupled plasma-mass spectrometry (ICP-MS) techniques (after Jenner *et al.*, 1990) and is based on 18 samples.

The third section of this chapter describes and evaluates the major and trace element geochemistry of multiple olivine grains present in lithologies from four diamond drill holes (SVB-96-04, SVB-96-09, SVB-98-102, and SVB-97-91) (Refer to Appendix B.3). Olivine grains are analyzed by the laser ablation microprobe-inductively coupled plasma-mass spectrometry (LAM-ICP-MS) method at Memorial University of Newfoundland following the similar procedure outlined by Longerich *et al.* (1991).

The final section of this chapter describes the metal tenor and metal distribution within the Pants Lake Intrusion. This component utilizes data from XRF pressed pellet analyses.

4.2 Major and Trace Element Geochemistry

Major and trace element geochemistry is widely accepted as a useful approach to understanding the chemistry and petrogenesis of igneous rocks. The major and trace element geochemistry presented in the following sections is interpreted to reflect the cumulate compositions (*e.g.* plagioclase, olivine, clinopyroxene, biotite, sulphide, *etc.*) of the rocks belonging to the PLI, and therefore, does not likely represent liquid compositions.

In the following sections, the Upper Gabbro, Basal Gabbro, and mafic dikes will be evaluated using major and trace element geochemical data. In the case of the Churchill gneiss samples, only a reconnaissance examination of the major and trace elements is reported in this section. All major element data are reported in oxide wt %, normalized to 100%, and volatile free. Trace element data, constituting < 0.1% of the sample, are reported in parts per million (ppm). Discrimination-type diagrams, although

used primarily for volcanic rocks (*e.g.* basalts, rhyolites, andesites, komatiites, *etc.*), are used in this section as a cursory means of visualizing chemical affinities and associations within the PLI. Considering that the mineral assemblage of the PLI is dominantly mafic (*i.e.* olivine, pyroxene, plagioclase, *etc.*), MgO is used as an index to measure fractionation and the effects of cumulus and accessory mineralogical trends. For that purpose, MgO is plotted against several major elements (SiO_2 , FeO^* , Na_2O , TiO_2 , CaO , Al_2O_3 , MnO , K_2O) and several trace elements (Cr, Ga, Sr, Rb, V, Cu, Ni, S).

4.2.1 Upper Gabbro Subdivision

4.2.1.1 Discrimination-Type Diagrams for Upper Gabbro Samples

Samples of the Upper Gabbro are plotted on four discrimination-type diagrams; 1) Irvine and Baragar's (1971) TAS diagram (Figure 4.1), 2) the Winchester and Floyd (1977) diagram (Figure 4.2a), 3) Irvine and Baragar's AFM diagram (1971) (Figure 4.2b), and 4) Jensen's (1976) tholeiitic versus komatiitic diagram (Figure 4.2c).

On the TAS (total alkalis versus silica) diagram (Figure 4.1), Upper Gabbro samples (denoted by red dots) plot in the alkaline field, as do the majority of Pants Lake Intrusion samples. However, it is certain that the SiO_2 concentrations determined by the XRF method on pressed pellets are approximately 4 to 6 % lower than the actual SiO_2 concentrations of the sample; therefore Upper Gabbro samples would plot in the subalkaline field if the SiO_2 concentrations were corrected (see Figure 4.1 for elaboration of the SiO_2 problem).

On the Winchester and Floyd (1977) ratio diagram of immobile elements (Zr/TiO_2 versus Nb/Y), the Upper Gabbro samples plot in the andesite/basalt field, above the field

for subalkaline basalts. The Winchester and Floyd diagram correlates well with the assumption that Upper Gabbro rocks are subalkaline rather than alkaline. In this diagram, there are two noticeable sample clusters reflecting variations in the Nb/Y ratios. Sample clustering is prominent in several major and trace element plots depicted in sections 4.2.1.2 and 4.2.1.3.

On the AFM ($\text{Na}_2\text{O} + \text{K}_2\text{O}$ - FeO^* - MgO) diagram (Figure 4.2b), the Upper Gabbro samples cluster between the total Fe (FeO^*) and MgO apex, with a slight calc-alkaline affinity or shift towards the $\text{Na}_2\text{O} + \text{K}_2\text{O}$ apex. This trend correlates with the crystallization of intercumulate olivine and clinopyroxene (higher MgO) and plagioclase crystallization (higher Na_2O). Samples with elevated total Fe (FeO^*) contain trace amounts of sulphide or oxides (*e.g.* elevated magnetite \pm ilmenite contents).

The Upper Gabbro samples plot in a broad cluster within the komatiitic field on the Jensen (1976) diagram, between the MgO and Al_2O_3 apexes, with a slight shift towards the Al_2O_3 apex (Figure 4.2c). This pattern of samples corresponds to the crystallization of olivine (high MgO) and plagioclase (high Al_2O_3). The two samples that plot outside of this field are samples of medium-grained olivine gabbro containing trace amount of sulphides and oxides (*e.g.* magnetite \pm ilmenite).

4.2.1.2 MgO versus Major Element Plots for Upper Gabbro Samples

The major elements SiO_2 , FeO^* , Na_2O , TiO_2 , CaO , Al_2O_3 , MnO and K_2O of Upper Gabbro rocks are plotted against MgO on Figures 4.3a, b, c, d, e, f, g, and h, respectively. On all element versus element plots, arbitrary lines denoting sample trends are added, as well as mineral references to justify the likely increasing or decreasing

chemical behavior of the rocks (refer to Table 4.1 for the range, mean, and standard deviation of the selected major elements).

The MgO values for samples of the Upper Gabbro range between 2.88 wt % for the least mafic samples and 12.50 wt % for the most mafic samples. Samples do not plot evenly over this range, but are weakly divided into two clusters. This feature is also recognized in the MgO versus major and trace element plots of Figures 4.3, 4.4, 4.6, and 4.7. The Mg #'s (*i.e.* $\text{MgO} / [\text{MgO} + \text{FeO}^*] \times 100$) of Upper Gabbro rocks range between 39.97 and 65.50.

It is apparent that the elements SiO_2 , Na_2O , CaO , and Al_2O_3 are negatively correlated with MgO. This signifies enrichment of these elements in plagioclase (\pm pyroxene), and their negative correlation to MgO reflects the crystallization of olivine (higher MgO) at the expense of plagioclase. The elements FeO^* and TiO_2 positively correlate with MgO reflecting the enrichment of these elements in either sulphide or oxide phases with elevated olivine abundances. The elements MnO and K_2O are also positively correlated to increasing MgO; however, this may not be a result of primary igneous fractionation.

4.2.1.3 MgO versus Trace Element Plots for Upper Gabbro Samples

The elements Cr, Ga, Sr, Rb, V, Cu, Ni, and S of the Upper Gabbro rocks are plotted against MgO on Figures 4.4a, b, c, d, e, f, g, and h, respectively, to show the effects of mineral phases on trace element geochemistry. The existence of plagioclase and pyroxene at the expense of olivine (or *vice versa*) is undoubtedly the greatest factor in

explaining the chemical trends observed in these plots (refer to Table 4.2 for the range, mean, and standard deviation of the selected trace elements).

The elements Cr, V, and Ni are positively correlated with MgO. Cr and Ni are likely elevated due to the presence of oxide and sulphide phases; in addition, Ni is also likely affected by the presence of olivine. The presence of pyroxene could likely be responsible for increased concentrations of V. The elements Ga and Sr show a negative correlation with MgO. Ga is good a monitor for the behavior of Al_2O_3 , and Sr is likewise for the behavior of CaO. The elements Cu, S and Rb are relatively unchanged with increasing or decreasing MgO. It is likely that the increasing Cu and S result from the changing sulphide content. Rb is akin to the behavior of K_2O and is likely a response to the presence of alkali feldspars introduced to the magma by country rock assimilation.

4.2.2 Basal Gabbro Subdivision

4.2.2.1 Discrimination-Type Diagrams for Basal Gabbro Samples

Rock samples of the Basal Gabbro subunits are plotted on four discrimination-type diagrams: 1) Irvine and Baragar's (1971) TAS diagram (Figure 4.1), 2) the Winchester and Floyd (1977) diagram (Figure 4.5a), 3) Irvine and Baragar's AFM diagram (1971) (Figure 4.5b), and 4) Jensen's (1976) tholeiitic versus komatiitic diagram (Figure 4.5c). Unlike the diagrams for the Upper Gabbro rocks where individual samples have been plotted, the following diagrams in Figure 4.5 show the fields for the Basal Gabbro subunits. Peridotite and semi-massive sulphide samples are plotted as individual samples. The Upper Gabbro field is included with each diagram for reference and comparison to the Basal Gabbro fields.

On the TAS (total alkalis versus silica) diagram (Figure 4.1), the majority of Basal Gabbro samples (refer to legend, Figure 4.1) are clustered in the alkaline field and overlap with the Upper Gabbro field. One sample of the Gabbro Hybrid does plot outside of the alkaline field into the subalkaline field. Three Gabbro Hybrid samples and two footwall anorthosite samples show elevated concentrations of $\text{Na}_2\text{O} + \text{K}_2\text{O}$ and SiO_2 and are similar, but slightly lower than the three samples of Churchill Province gneiss. As stated in Section 4.2.1.1, it is certain that the SiO_2 concentrations determined by the XRF method on pressed pellets are 4 to 6 % lower than actual concentrations and should plot in the subalkaline field with Upper Gabbro samples if the SiO_2 concentrations are corrected (see Figure 4.1 for further explanation of problem).

On the Winchester and Floyd (1977) diagram of immobile elements (Zr/TiO_2 versus Nb/Y) (Figure 4.5a) the majority of Basal Gabbro samples are concentrated across the andesite/basalt field (similar to the Upper Gabbro), with a moderate shift into the andesite and subalkaline Basalt fields. The Transition Gabbro field is tightly clustered and overlaps well with the Upper Gabbro field suggesting that the two rock types are chemically similar. The Gabbro Hybrid field shows the greatest deviation from the andesite/basalt field, reflecting the probable assimilation of Churchill Province gneiss (The effect of gneissic assimilation will be elaborated upon in Section 4.3). The Olivine Gabbro is divided into two fields, both similar to the Upper Gabbro. Unlike the Upper Gabbro, however, the Olivine Gabbro shifts into the andesite and subalkaline basalt fields. The Leopard-Textured Gabbro is also divided into two fields, overlapping well with the Olivine Gabbro and Upper Gabbro fields. The Medium-grained Gabbro field is spread between the andesite/basalt field and the subalkaline Basalt field. Samples of

semi-massive sulphide plot in the rhyodacite/dacite field, as does one sample of the Gabbro Hybrid. Peridotite samples are clustered in the center of the andesite/basalt field and overlap with each of the Basal Gabbro subunit fields and Upper Gabbro field.

The Basal Gabbro subunits fields are spread between the total Fe (FeO*) and MgO apex on the AFM (Na₂O + K₂O-FeO*-MgO) diagram (Figure 4.5b), and are only slightly shifted toward the alkali (Na₂O + K₂O) apex. Samples which trend towards the FeO* apex are affected by the presence of sulphides or oxides. Alternatively, samples trending towards the MgO apex are affected by increasing modal percentages of olivine. The Transition Gabbro is the most tightly clustered of all the subunit fields and overlaps well with the Upper Gabbro field. The Gabbro Hybrid field is dispersed between the FeO* and MgO apexes, with a bias towards the FeO* apex and a slight shift towards the Alkali apex. The Olivine Gabbro field shows the greatest spread, and there is a noticeable shift towards all three apexes, with a modest bias towards the FeO* apex. The Leopard-Textured Gabbro field is roughly linear between the FeO* and MgO apexes, with a bias towards the FeO* apex, probably reflecting the variable sulphide content. The Medium-grained Gabbro is divided into two fields; one field overlaps with all subunit fields, whereas the second field, closer to the MgO apex, overlaps only with the Olivine Gabbro field. This isolated Medium-grained Gabbro field contains samples with the highest MgO contents of all rock types, corresponding to the elevated modal abundance of olivine described in Section 3.5.2.5. Apart from one sample, all semi-massive sulphide samples plot towards the FeO* apex because of their high sulphide contents. Two peridotite samples overlap with the majority of rock associations;

however, one peridotite sample is adjacent to the MgO-rich Medium-Grained Gabbro field.

On the Jensen (1976) discrimination diagram, the Basal Gabbro subunit samples plot in the tholeiitic and komatiitic fields with trends towards all three apexes (Figure 4.5c). The Transition Gabbro field is tightly clustered in the center of the diagram (komatiitic field), overlapping with the Upper Gabbro, Olivine Gabbro and Gabbro Hybrid fields. However, one sample of the Transition Gabbro plots within the tholeiitic field and is strongly biased towards the $\text{FeO} + \text{Fe}_2\text{O}_3 + \text{TiO}_2$ apex. The Gabbro Hybrid is divided into two fields. The first field is strongly komatiitic the second field is tholeiitic. The Olivine Gabbro field shows the greatest dispersion of any rock association. The Leopard-Textured Gabbro is also divided into two fields. One field is clearly within the tholeiitic field, whereas the other field straddles the boundary between the two fields. As on the AFM diagram, the Medium-Grained Gabbro is divided into two fields; one field overlaps with the majority of rock fields, while the second field is highly anomalous in MgO.

4.2.2.2 MgO versus Major Element Plots for Basal Gabbro Samples

The major elements SiO_2 , FeO^* , Na_2O , TiO_2 , CaO , Al_2O_3 , MnO and K_2O of rocks belonging to subunits of the Basal Gabbro are plotted against MgO. These plots are illustrated in Figures 4.6a, b, c, d, e, f, g, and h respectively. Similar to the discrimination plots illustrated in Figures 4.5a, b and c, the Basal Gabbro subunits are shown as fields in the following major element plots in order to avoid congestion on the

diagrams. The Upper Gabbro field is included in each plot for reference and comparison to the Basal Gabbro subunits.

The MgO values for samples of the Basal Gabbro (excluding the semi-massive and peridotite samples) range between 1.60 wt % for the least mafic samples (*e.g.* Gabbro Hybrid) to 21.92 wt % for the most mafic samples (*e.g.* Medium-Grained Gabbro). The Mg #'s (*i.e.* $\text{MgO} / [\text{MgO} + \text{FeO}^*] \times 100$) of Basal Gabbro subunits range from 21.81 to 98.50. Table 4.3 presents the range, sample mean, and standard deviation of the major element values for each Basal Gabbro subunit, as well as the semi-massive and peridotite samples.

On the SiO₂ versus MgO diagram (Figure 4.6a), the majority of Basal Gabbro samples are chemically similar to samples of Upper Gabbro and are negatively correlated with MgO. The greatest overlap of the Basal Gabbro fields occurs at approximately 5 to 6 wt % MgO, and 37 to 42 wt % SiO₂. Although clustering around the Upper Gabbro is prominent, several samples of semi-massive sulphide are depleted in SiO₂ and MgO, and therefore plot outside of this cluster. Two samples of the Gabbro Hybrid have the highest SiO₂ concentrations (up to 49.78 wt %) but are depleted in MgO. Two samples of the Medium-Grained Gabbro and one sample of the Olivine Gabbro have the highest MgO values in conjunction with average SiO₂ concentrations of approximately 33 wt %.

On the FeO* versus MgO diagram (Figure 4.6b), all of the Basal Gabbro fields overlap with the Upper Gabbro field and a positive trend of increasing FeO* with increasing MgO is evident. This feature coincides with the crystallization of cumulate olivine. At approximately 6 wt % MgO, a second trend is defined by increased FeO* concentrations. This FeO* enrichment reflects the sulphide content within the samples.

Semi-massive sulphide samples are the most enriched in FeO* but are depleted in MgO. The Upper Gabbro field has the lowest FeO* values, apart from one sample of Transition Gabbro.

On the Na₂O versus MgO diagram (Figure 4.6c), all of the Basal Gabbro fields overlap with the Upper Gabbro field and a negative trend of decreasing Na₂O with increasing MgO is evident. This feature is correlative to the crystallization of cumulate plagioclase (high Na₂O) versus the crystallization of olivines (high MgO). Although most Basal Gabbro samples cluster around the Upper Gabbro field, there is a significant scatter array for samples with > 7 wt % MgO. Notably, individual Olivine Gabbro, Gabbro Hybrid and Medium-Grained Gabbro samples are depleted in Na₂O, but are enriched in MgO. The sulphide samples are depleted in both Na₂O and MgO.

On the TiO₂ versus MgO diagram (Figure 4.6d), the Basal Gabbro fields are closely associated to the Upper Gabbro field with only slight deviations. The most obvious deviation (enrichment or depletion) of this trend is individual samples of semi-massive sulphide, Medium-grained Gabbro and Gabbro Hybrid subunits. There are also several Olivine Gabbro samples that also plot outside of this trend. A plausible reason for this deviation is the varying concentration of Ti-bearing ilmenite and/or biotite within the samples.

On the CaO versus MgO diagram (Figure 4.6e), the Basal Gabbro samples are closely associated with the Upper Gabbro field and a negative correlation of CaO to MgO is evident. This trend may reflect the crystallization of pyroxene or plagioclase (high CaO) versus the crystallization of olivine (high MgO). Semi-massive sulphide samples

are clearly depleted in CaO. Upper Gabbro samples have the highest concentration of CaO (up to 10.67 wt %).

On the Al₂O₃ versus MgO diagram (Figure 4.6f), the Basal Gabbro samples are closely associated to the Upper Gabbro samples and a negative correlation of Al₂O₃ with MgO is displayed. At approximately 6 wt % MgO, the Basal Gabbro samples deviate from this trend, notably with a depletion of Al₂O₃. Semi-massive sulphides are depleted in Al₂O₃ with respect to the other sample fields.

On the MnO versus MgO diagram (Figure 4.6g), the Basal Gabbro samples are closely associated with the Upper Gabbro samples and a positive trend is defined. Semi-massive sulphides are the most depleted in MnO compared to the other samples. Atypical of the overall sample population is one sample of the Transition Gabbro which contains 30.83 wt % MnO; however, the reason for this is yet to be determined.

On the K₂O versus MgO diagram (Figure 4.6h), the Basal Gabbro samples are similar to the Upper Gabbro samples and have relatively constant K₂O values with increasing MgO. However, for samples between 5 to 7 wt % MgO, the K₂O concentration significantly increases. Semi-massive sulphides normally have the highest K₂O, apart from several individual samples of Gabbro Hybrid and Olivine Gabbro.

4.2.2.3 MgO versus Trace Element Plots for Basal Gabbro Samples

The trace elements Cr, Ga, Sr, Rb, V, Cu, Ni, and S of the Basal Gabbro rocks are plotted against MgO on Figures 4.7a, b, c, d, e, f, g, and h, respectively. Similar to the discrimination plots illustrated in Figures 4.5a, b, c, and the previous major element plots, the Basal Gabbro subunits are shown as fields in the following trace element plots. The

Upper Gabbro field is included in each plot for reference and comparison to the Basal Gabbro subunits. Table 4.4 presents the range, sample mean and standard deviation of the trace element values for each Basal Gabbro subunit, as well as the semi-massive and peridotite samples.

On the Cr versus MgO diagram (Figure 4.7a), many of Basal Gabbro samples show a positive correlation with Cr to MgO, similar to the Upper Gabbro field. All of the Basal Gabbro fields overlap between 5 to 6 wt % MgO and Cr values averaging approximately 55 ppm. Semi-massive sulphide samples have high Cr values (up to 285 ppm), and stable MgO values (>0.5 to 5 wt %). Two samples of Medium-Grained Gabbro have Cr values between 150-160 ppm with high MgO values. One sample from each of the Olivine Gabbro and Gabbro Hybrid subunits shows the highest Cr concentrations (> 290 ppm).

On the Ga versus MgO diagram (Figure 4.7b), the Ga concentrations of the Basal Gabbro samples show a negative correlation with MgO. Overall, the Basal Gabbro samples overlap well with Upper Gabbro samples. Semi-massive sulphide samples are the most depleted in Ga (< 5 ppm) compared to the other samples. Several outlier samples associated with high MgO values are also depleted in Ga. At approximately 5-6 wt % MgO, there is a noticeable increase or decrease of Ga in the Basal Gabbro samples. Gabbro Hybrid samples appears to have the highest concentration of Ga (up to 48 ppm).

On the Sr versus MgO diagram (Figure 4.7c) the Sr values of the Basal Gabbro samples show negative correlation with MgO. The majority of Basal Gabbro samples cluster between 2 to 8 wt% MgO and between 250 to 410 ppm Sr. Semi-massive

sulphide samples are depleted in Sr (<160 ppm). Samples of Medium-Grained gabbro and Gabbro Hybrid have the highest Sr values (> 500 ppm).

On the Rb versus MgO diagram (Figure 4.7d), the Rb concentrations of the Basal Gabbro samples remain relatively constant with increasing MgO. Rb values of the Gabbro Hybrid and semi-massive sulphide samples however, show positive correlations with MgO. The Gabbro Hybrid, semi-massive sulphide and Olivine Gabbro samples have the highest concentration of Rb. The Medium-Grained Gabbro samples do not show any significant increase in Rb.

On the V versus MgO diagram (Figure 4.7e), the Basal Gabbro samples overlap with the Upper Gabbro field. Most of the Basal Gabbro samples cluster at the 2 to 4 wt % MgO range and between the 100 to 200 ppm V range. The two samples of peridotite are slightly higher than the average sample group. Samples of Olivine Gabbro and Gabbro Hybrid have the highest concentration of V.

On the Log Cu versus MgO diagram (Figure 4.7f), the Basal Gabbro samples show significant increases in Cu at the 5 to 6 wt% MgO range. The semi-massive sulphide samples have the highest concentration of Cu. There are two sample clusters, a clustering of samples at 800 ppm Cu, and a clustering of samples at 30 ppm Cu (constant Cu with increasing MgO). Medium-grained samples and Olivine Gabbro samples show the greatest deviation, that is, low MgO with low Cu, low MgO with high Cu, and high MgO with high Cu values.

On the Log Ni versus MgO diagram (Figure 4.7g), the Basal Gabbro samples show positive correlation of Ni with MgO. This feature is similar to the pattern depicted

in the Log Cu versus MgO plot and reflects the concentration of Ni in both olivine and sulphide phases.

On the Log S versus MgO diagram (Figure 4.7h), the Basal Gabbro samples overlap and are significantly higher than the Upper Gabbro field and there is an apparent clustering around the 4 to 6 wt% MgO range. This plot is akin to the Log Cu plot. There is also a large spread of Cu values for samples with > 4 wt % MgO.

4.2.3 Mafic Dikes

4.2.3.1 Discrimination-Type Diagrams for Mafic Dike Samples

Five samples collected from mafic dikes are plotted on four discrimination-type diagrams: 1) Irvine and Baragar's (1971) TAS diagram (Figure 4.1), 2) the Winchester and Floyd (1977) diagram (Figure 4.8a), 3) Irvine and Baragar's (1971) AFM diagram (Figure 4.8b), and 4) the Jensen (1976) tholeiitic versus komatiitic diagram (Figure 4.8c).

On the TAS (total alkalis versus silica) diagram (Figure 4.1), the mafic dike samples, symbolized by red triangles, plot in the alkaline field with the majority of the Pants Lake Intrusion samples. However, if the actual SiO₂ content is corrected, the mafic dike samples will plot in the sub-alkaline field, as does the Pants Lake Intrusion samples (see Figure 4.1 for elaboration of the SiO₂ problem).

On the Winchester and Floyd (1977) immobile element diagram (Zr/TiO₂ versus Nb/Y) (Figure 4.8a), two mafic dike samples straddle the boundary between the andesite and the andesite/basalt fields, and the remaining three samples plot in the andesite field. This is similar to the plot of the Basal Gabbro samples; in particular, the Olivine Gabbro and Gabbro Hybrid samples, in that, samples in the andesite field correlate with a higher Nb/Y ratio.

On the AFM ($\text{Na}_2\text{O} + \text{K}_2\text{O} - \text{FeO}^* - \text{MgO}$) diagram (Figure 4.8b), all of the mafic dike samples plot in the Tholeiitic field, between the total Fe (FeO^*) and MgO apex, with a slight shift towards the FeO^* apex. This is consistent with samples of the Upper and Basal Gabbro subdivisions.

On the Jensen (1976) diagram (Figure 4.8c), three mafic dike samples plot in the komatiitic field and two mafic dike samples plot in the tholeiitic field. This is consistent with samples of the Upper and Basal Gabbro subdivisions. In the same diagram, Upper Gabbro samples dominate the komatiitic field whereas Basal Gabbro samples plot in both fields. Basal Gabbro samples that plot in the tholeiitic field have higher abundances of Fe-sulphides, oxides (ilmenite and magnetite) and probable country-rock contamination.

4.2.3.2 MgO versus Major Element Plots for Mafic Dike Samples

The major elements SiO_2 , FeO^* , Na_2O , TiO_2 , CaO , Al_2O_3 , MnO , and K_2O of mafic dike samples are plotted against MgO on Figures 4.9a, b, c, d, e, f, g, and h, respectively. The MgO values for mafic dike samples range between 5.19 wt % for the least mafic sample, and 9.33 wt % for the most mafic sample. The Mg #'s (*ie.* $\text{MgO} / [\text{MgO} + \text{FeO}^*] \times 100$) of mafic dike samples range between 45.01 and 63.36. Refer to Table 4.5 for the range, mean, and standard deviation of the selected major elements.

It is difficult to predict trends in the major element plots of the mafic dikes due to the paucity of samples. Compared to similar plots of the Upper and Basal Gabbro rocks, however, the mafic dike samples are more closely related to samples of the Basal Gabbro. In particular, there is a close affinity of mafic dike samples with the Basal Gabbro samples when the Na_2O , TiO_2 , Al_2O_3 and K_2O versus MgO plots are compared.

4.2.3.3 MgO versus Trace Element Plots for Mafic Dike Samples

The trace elements Cr, Ga, Sr, Rb, V, Cu, Ni, and S of the mafic dike samples are plotted against MgO on Figures 4.10a, b, c, d, e, f, g, and h, respectively. Refer to Table 4.6 for the range, mean, and standard deviation of the selected trace elements.

Similar to the major element plots for the mafic dike samples, it is difficult to predict trends in the trace element plots for the mafic dikes due to the insufficient number of samples. When compared to similar plots of the Upper and Basal Gabbro samples, the mafic dike rocks are more closely related to samples of the Basal Gabbro. This is particularly true for the Cr, Rb, V, and S versus MgO plots.

4.2.4 Churchill Province Gneiss

4.2.4.1 Discrimination-Type Diagrams for Churchill Province Gneiss Samples

The four samples of Churchill Province gneiss are plotted on four discrimination-type diagrams; 1) Irvine and Baragar's (1971) TAS diagram (Figure 4.1), 2) Winchester and Floyd (1977) diagram (Figure 4.5a), 3) Irvine and Baragar's AFM diagram (1971) (Figure 4.5b), and 4) Jensen (1976) tholeiitic versus komatiitic diagram (Figure 4.5c). Although the later three diagrams are more applicable for mafic rocks akin to the PLI, the gneissic samples are plotted in these diagrams as a means of comparison with mafic samples from the Pants Lake Intrusion. Sample 97-61-46 contains a significant concentration of sulphur (130 524 ppm) that effectively masks the concentrations of the major and traces.

On the TAS (total alkalies versus silica) diagram (Figure 4.1), three gneissic samples plot in the subalkaline field (high $\text{Na}_2\text{O} + \text{K}_2\text{O}$ and high SiO_2) located outside of

the field for the Pants Lake Intrusive samples. However, if the actual SiO_2 concentrations of the samples were corrected, then the majority of PLI samples would plot in the subalkaline field (see Figure 4.1 for elaboration of the SiO_2 problem). Three samples of the Gabbro Hybrid subunit plot between the gneissic end-member and the PLI end-member. This was expected however, because the Gabbro Hybrid samples do contain gneissic inclusions.

On the Winchester and Floyd (1977) diagram of immobile elements (Zr/TiO_2 versus Nb/Y) (Figure 4.5a), three gneissic samples plot in the rhyodacite/dacite field and one sample plots in the trachy-andesite field. This is similar with the semi-massive sulphide samples and one sample from the Gabbro Hybrid subdivision.

On the AFM ($\text{Na}_2\text{O} + \text{K}_2\text{O} - \text{FeO}^* - \text{MgO}$) diagram (Figure 4.5b), the gneissic samples are widely spaced with two samples plotting in the tholeiitic field and two samples plotting in the calc-alkaline field. Sample 97-61-46 plots near the FeO^* apex due to the high sulphide content. A second sample plots mid-way between the FeO^* and $\text{Na}_2\text{O} + \text{K}_2\text{O}$ apex. The remaining two gneiss samples plot in the middle of the diagram.

On the Jensen (1976) diagram (Figure 4.5c), the four gneiss samples do not have any particular affinity for either field. Two samples plot in the komatiitic field with the main cluster of PLI samples, whereas the remaining two samples are divided; one sample plots close to the $\text{FeO} + \text{Fe}_2\text{O}_3 + \text{TiO}_2$ apex suggesting sulphide and/or oxide influence, the other sample plots mid-way between the Al_2O_3 and $\text{FeO} + \text{Fe}_2\text{O}_3 + \text{TiO}_2$ apex.

4.2.5 Element Distribution and Contamination Effects

In the previous sections of this chapter, geochemical plots using major and trace element data provided insight into the chemical and mineral behavior of the units described in Chapter 3. In this section, the same geochemical data will be utilized for slightly different purposes, that is: 1) to chemically characterize the internal Pants Lake Intrusion sequence as defined in Chapter 3, 2) to document the major and trace element abundances in each of the mineralized zones (*i.e.* NDT, NAI, HFL, *etc.*), and 3) to determine if country rock assimilation had any effect on the major and trace element geochemistry of the PLI.

4.2.5.1 Internal Stratigraphic Variations in Element Abundances

On the histograms of Figure 4.11, rocks of the entire PLI sequence (refer to Figures 3.4 and 3.5) are quantified using the calculated mean concentrations of major element and trace element geochemical data as illustrated on Tables 4.1 to 4.6. These histograms are similar to the plots used by Lightfoot and Naldrett (1999), Lesher (1989), MacDonald (1999) *etc.*, to effectively illustrate chemical trends versus depth within an intrusion. The histograms representing the internal stratigraphic sequence of the PLI illustrate a number of important general features. These features are discussed in the following paragraphs.

It is apparent from the histograms of Figure 4.11 that the Basal Gabbro is slightly more mafic than the Upper Gabbro, and the distinction between the two subdivisions is gradational rather than definitive. This is inferred by the decreasing modal abundance of plagioclase and pyroxene (as indicated by the histograms for SiO_2 , Na_2O , Al_2O_3 , CaO ,

and Sr showing an abundance decrease), and is countered by the increasing modal abundance of olivine (as indicated by the histograms for MgO, FeO*, and Ni showing an abundance increase). MgO is probably the best indicator of mafic affinity, and as the histogram for MgO indicates, the Medium-Grained gabbro subunit is by far the most mafic. These features are consistent with petrographic observations discussed in Section 3.5 (Geological Subdivisions and Petrography of the Pants Lake Intrusion).

As indicated by the histograms, the sulphur and metal contents (illustrated by the elements S, Ni, Cu \pm FeO) of the Basal Gabbro are significantly greater than the Upper Gabbro by at least 50%, and the Ni, Cu, and S ratios are similar among each rock type. The highest metal and sulphur tenors are exhibited by the Leopard Gabbro, whereas the second highest is contributed to the Medium-grained subunit. Massive and semi-massive sulphide samples, not shown on these diagrams, have the highest metal tenors. The Churchill Province Gneiss shows slight enrichment in these elements, whereby the mafic dikes are similar to Upper Gabbro abundances.

The chemical effects of country rock assimilation on the PLI are also noted in the histograms of Figure 4.11. Relative to the PLI, the Churchill Province gneiss is elevated in K₂O, SiO₂, Rb, and Cr. As expected, the Gabbro Hybrid, Medium-grained Gabbro, and Mafic dike (\pm Olivine Gabbro) rock types are also elevated in this element suite due to the assimilation from the Churchill Province in these elements. Cr and K₂O appear to be the best indicators of contamination. Surprisingly, the Upper Gabbro is elevated in Rb, comparable to the abundance in the Gabbro Hybrid subunit.

4.2.5.2 Spatial Variations of Element Abundance

This section is based on a series of fourteen histograms (Figures 4.12a to 4.12n) portraying the average element (MgO, Fe₂O₃, TiO₂, K₂O, Na₂O, Zr, Rb, and Ga) abundances in the units (namely Upper Gabbro, Basal Gabbro, Churchill Province) sampled within the seven mineralized regions of the PLI (*i.e.* NDT, NAI, HFL, GG, MG, WG, and MH; see Figure 3.1). Each histogram includes a vertical reference line that represents the average major and trace element value for the entire geochemical data set (excluding the data from Churchill Province gneiss). The purpose of these histograms is to gauge the average element compositions for each of the mineralized regions described in Chapter 3, and to determine if the PLI is chemically homogeneous or diverse. Table 4.7, 4.8, and 4.9 lists the average major element and trace element abundances for rocks from the mineralized regions for the Upper Gabbro, Basal Gabbro, mafic dikes, and Churchill Province gneiss. The following text summarizes the main points provided by each histogram depicted in Figures 4.12a to 4.12n.

The MgO abundance of each region within the PLI is fairly constant, and in all but a few cases, is close to the average wt% recorded for the PLI (*i.e.* 6.68%). The MgO content of the Upper Gabbro, Transition Gabbro, and Gabbro Hybrid rocks for each region is slightly below the average with few exceptions. The MgO contents of the Olivine Gabbro, Leopard Gabbro, and Medium-Grained Gabbro show a slight to significant increase compared to other rocks in the regions. Rocks of the Olivine Gabbro in the NDT and Major General regions (Figure 4.12g), as well as rocks of the Mineral Hill region (Figure 4.12k), are significantly higher than their counterparts.

The Fe_2O_3 abundance of each region within the PLI is fairly homogeneous and in many cases is close to the average wt% recorded for the PLI (*i.e.* 13.74 %). As expected, the Fe_2O_3 contents of the Upper Gabbro rocks for most regions are below average whereas the Fe_2O_3 content of most rocks belonging to the Basal Gabbro subdivision are close to, or exceed the average wt %. The regions containing the Leopard Gabbro subdivision (excluding Mineral Hill; Figure 4.12i) have the highest average Fe_2O_3 , as does the Churchill Province gneiss sample from the Happy Face Lake region (Figure 4.12m). This is likely an effect of high sulphide content.

The TiO_2 abundance of each region within the PLI is fairly consistent and there is not much deviation from the average wt% recorded for the PLI (*i.e.* 1.61 %). In the majority of cases (PLI and Churchill Province rocks), the average wt% per region is below the average wt% recorded for the PLI. However, the TiO_2 abundance of Gabbro Hybrid rocks of the GG region (Figure 4.12e) is well above the other rock-types for each region resulting in a higher recorded average.

The K_2O abundance of each region within the PLI is stable and in most cases, deviates little from the recorded average wt% for the PLI (*i.e.* 2.38%). The K_2O abundances for Gabbro Hybrid rocks of the NAI and GG regions (Figure 4.12e), as well as Olivine Gabbro rocks of the NAI region (Figure 4.12g) exceed the average PLI composition. This is also the case for the Churchill Province rocks (Figure 4.12m).

The Na_2O abundance of each region in the PLI is very stable and there is not much variation from the average wt % recorded for the PLI (*i.e.* 2.38 %). However, rocks of the Churchill Province gneiss have a much broader range (Figure 4.12m) than rocks of the PLI.

The Zr abundance of each region shows a broad range as compared to the average wt % recorded for the PLI (*i.e.* 75.73 ppm). The Upper Gabbro rocks for all regions are below average (Figure 4.12b), as is the case for the Leopard-Textured Gabbro rocks (Figure 4.12j). The Transition Gabbro, Gabbro Hybrid, and Olivine Gabbro rocks types show much greater range of Zr abundances for each region (Figure 4.12d, 4.12f, 4.12h respectively). The Gabbro Hybrid and Olivine Gabbro rock-types for the NAI region are well above the other rock types for each region. The Churchill Province gneiss samples far exceed the Zr abundances in the mafic rocks of the PLI (Figure 4.12n).

The Rb abundance of each region is comparable to the Zr abundance such that both elements have a broad range compared to the average wt % recorded for the PLI (*i.e.* 12.74 ppm). The Upper Gabbro samples from each region are below average, with exception of Upper Gabbro rocks of the Mineral Hill region that exceed the average (Figure 4.12a). The Transition Gabbro, Leopard Gabbro, and Medium-grained Gabbro rock-types for each region are consistently below average (Figure 4.12d, 4.12j, 4.12l respectively). Typically, the Gabbro Hybrid and Olivine Gabbro rock types are close to the average (Figure 4.12f and 4.12h), however the NAI region is well above average for these two rock types and the HFL region is above average for the Gabbro Hybrid rock-type. The Churchill Province gneiss rocks far exceed the Rb abundances for the mafic rocks of the PLI (Figure 4.12n).

The Ga abundance of each region within the PLI is very stable and there is not much variation from the average wt % recorded for the PLI (*i.e.* 22.23 ppm). This feature is similar to the Na₂O abundance of the PLI and Churchill Province samples.

4.3 Rare Earth Element Geochemistry

The rare earth elements (REE) comprise a series of isovalent (3+) high field strength elements (HFSE) with atomic numbers 57 to 71 (Lanthanum to Lutetium) (Rollinson, 1993). Elements with low atomic numbers (*i.e.* 57 to 60; La, Ce, Pr, Nd) are referred to as the light rare earth elements (LREE), whereas elements with higher atomic numbers (*i.e.* 68 to 71; Er, Tm, Yb, Lu) are referred to as the heavy rare earth elements (HREE) (*op cit*). Rare earth elements have similar chemical and physical properties arising from the common 3+ ions; however, it is the slight differences of the REE that enable them to be used as good petrological indicators (Cerium and Europium exists in oxidation states other than 3+, that is Ce^{4+} and Eu^{2+}) (*op cit*).

Rare earth element abundances in rocks are normalized to a common reference standard (*e.g.* chondritic meteorites, primitive mantle) and are presented on concentration (logarithm to the base 10) versus increasing atomic number (Lanthanum to Lutetium) diagrams. Trends on a REE diagram are referred to as REE patterns and the shape of the REE pattern often reflects petrological processes (*op cit*). Another way of presenting REE data is on a multi-element diagram based upon a grouping of elements incompatible with respect to typical mantle mineralogy (*op cit*).

In many cases, Europium is outside of the general trend defined by the other REE. This feature is referred to as a Europium anomaly. Europium anomalies may be quantified by comparing the measured concentration (referred to as Eu) with an expected concentration obtained by interpolating between the normalized values of Samarium (Sm) and Gadolinium (Gd) (referred to as Eu^*). The ratio of Eu/Eu^* is a measure of the Europium anomaly; a value greater than 1.0 indicates a positive anomaly, and a value less

than 1.0 is a negative anomaly. Rollinson (1993) suggested using the geometric mean and calculated the Europium anomaly by the following equation:

$$\text{Eu/Eu}^* = \text{Eu}_N / \sqrt{[(\text{Sm}_N)(\text{Gd}_N)]}$$

The degree of fractionation as detailed by Rollinson (1993) of a REE pattern can be expressed by the ratio of the normalized LREE (*eg.* La or Ce) to the HREE (*eg.* Yb or Y). The ratio $(\text{La/Yb})_N$ is often plotted against either Ce_N or Yb_N on a bivariate graph and is a measure of the degree of REE fractionation with changing REE content. Similar diagrams may be constructed to measure LREE fractionation $[(\text{La/Sm})_N$ versus Sm_N], HREE fractionation $[(\text{Gd/Yb})_N$ versus Yb_N], and Eu anomaly $[(\text{La/Sm})_N$ versus $(\text{Eu/Eu}^*)]$ in individual REE patterns (*op cit*).

4.3.1 REE Geochemistry in this Study

REE geochemistry, like major and trace element geochemistry, is widely accepted as a useful approach to understanding the chemistry and petrogenesis of igneous rocks. As a reminder, in this study the REE geochemistry reflects the cumulate and lesser intercumulate compositions of the rocks and therefore, does not represent parental magma compositions.

In the following sections, the Upper Gabbro, Basal Gabbro, mafic dikes and Churchill Province gneiss are evaluated using REE geochemical data. The REE data are presented on REE diagrams (Figures 4.13a to 4.13c) and multi-element diagrams (Figures 4.14a to 4.14d) normalized to the primitive mantle values of Sun and McDonough (1989). The complete REE data set is provided in Appendix B.2. Normalized REE ratios and Europium anomalies are presented in Table 4.10.

4.3.1.1 Primitive Mantle Normalized REE Diagrams

On the primitive mantle-normalized REE diagram of Figure 4.13a, the four samples of the Upper Gabbro subdivision define a coherent geochemical suite that exhibit REE patterns that decrease slightly from the LREE to the HREE. The LREE are 8.87-7.03 times primitive mantle values [$(La/Yb)_N = 2.23-2.73$; $(Ce/Yb)_N = 2.09-2.51$; $(La/Sm)_N = 1.42-1.61$] and the HREE are 4.10-3.55 times primitive mantle values [$(Gd/Yb)_N = 1.42-1.47$]. These samples have slightly positive Eu anomalies ($Eu/Eu^* = 1.15-1.36$).

On the primitive mantle normalized REE diagram of Figure 4.13b, the eight samples of the Basal Gabbro subunits (Transition Gabbro, Gabbro Hybrid, Leopard Gabbro, Olivine Gabbro, Medium-Grained Gabbro) have similar REE patterns as exhibited by the Upper Gabbro subdivision samples on Figure 4.13a. For the Transition Gabbro samples, the LREE are 10.36-8.31 times primitive mantle values [$(La/Yb)_N = 2.27-2.46$; $(Ce/Yb)_N = 2.11-2.26$; $(La/Sm)_N = 1.44-1.52$], the HREE are 4.93-4.26 times primitive mantle values [$(Gd/Yb)_N = 1.42-1.44$], and the Eu anomalies ($Eu/Eu^* = 1.12-1.17$) are just slightly positive. For the Gabbro Hybrid samples, the LREE are 7.31-5.36 times primitive mantle values [$(La/Yb)_N = 2.59-2.74$; $(Ce/Yb)_N = 2.32-2.45$; $(La/Sm)_N = 1.69-1.71$], the HREE are 2.94-2.70 times primitive mantle values [$(Gd/Yb)_N = 1.33-1.38$], and the Eu anomalies ($Eu/Eu^* = 1.20-1.53$) are slightly positive. For the Leopard Gabbro samples, the LREE are 7.80-5.61 times primitive mantle values [$(La/Yb)_N = 2.27$; $(Ce/Yb)_N = 2.43$; $(La/Sm)_N = 1.77$], the HREE are 3.13-2.84 times primitive mantle values [$(Gd/Yb)_N = 1.37$], and the Eu anomaly ($Eu/Eu^* = 1.35$) is slightly positive. For the Olivine Gabbro samples, the LREE are 14.23-8.98 times primitive mantle values

$[(La/Yb)_N = 3.81-3.83; (Ce/Yb)_N = 3.23-3.35; (La/Sm)_N = 2.02-2.32]$, the HREE are 4.10-3.72 times primitive mantle values $[(Gd/Yb)_N = 1.32-1.54]$, and the Eu anomalies ($Eu/Eu^* = 1.11-1.25$) are slightly positive. For the Medium-Grained Gabbro samples, the LREE are 19.96-14.70 times primitive mantle values $[(La/Yb)_N = 7.13; (Ce/Yb)_N = 6.66; (La/Sm)_N = 2.08]$, the HREE are 3.42-2.70 times primitive mantle values $[(Gd/Yb)_N = 2.37]$, and the Eu anomaly ($Eu/Eu^* = 1.19$) is slightly positive.

On the primitive mantle normalized REE diagram of Figure 4.13c, three samples of Churchill Province gneiss, two samples of mafic dikes, and one sample of semi-massive sulphide are plotted together. For the single massive sulphide sample, the LREE are 4.38-1.51 times primitive mantle values $[(La/Yb)_N = 11.37; (Ce/Yb)_N = 8.22; (La/Sm)_N = 6.48]$, the HREE are 0.33-0.41 times primitive mantle values $[(Gd/Yb)_N = 1.13]$, and the Eu anomaly ($Eu/Eu^* = 1.12$) is slightly positive. For the Churchill Province samples, the LREE are 59.56-23.84 times primitive mantle values $[(La/Yb)_N = 21.02-38.57; (Ce/Yb)_N = 16.26-28.85; (La/Sm)_N = 4.44-5.26]$, the HREE are 2.49-2.43 times primitive mantle values $[(Gd/Yb)_N = 0.67-0.97]$, and the Eu anomalies ($Eu/Eu^* = 0.67-0.97$) are slightly negative. For the mafic dike samples, the LREE are 20.58-12.06 times primitive mantle values $[(La/Yb)_N = 6.09-7.15; (Ce/Yb)_N = 5.18-5.97; (La/Sm)_N = 2.38-2.80]$, the HREE are 3.42-3.11 times primitive mantle values $[(Gd/Yb)_N = 1.78-1.81]$, and the Eu anomalies ($Eu/Eu^* = 1.01-1.03$) are slightly positive.

It is apparent that the REE abundances, REE patterns, and magnitude of the Eu anomalies of the samples utilized in this study are controlled by their modal mineralogy. The Upper Gabbro, Basal Gabbro, and mafic dike samples exhibit slight to moderate LREE enrichment, positive Eu anomalies, and overall low total REE enrichment with

respect to primitive mantle (Figure 4.13d) indicative of a common source region. The Churchill Province samples are unlike the other samples within this suite, exhibiting significant total REE enrichment with respect to primitive mantle and corresponding negative Eu anomalies. In general, there appears to be a REE transition developed within this suite of samples from low total REE with positive Eu anomalies to a high total REE with negative Eu anomalies, more precisely; Upper PLI ↔ Transition Gabbro, Gabbro Hybrid, Leopard Gabbro ↔ Olivine Gabbro, Medium-Grained Gabbro ↔ mafic dikes ↔ Churchill Province gneiss.

4.3.1.2 Multi-Element Normalized Diagrams

On the primitive mantle-normalized extended trace element diagram of Figure 4.14a, the four samples of the Upper Gabbro subdivision define a uniquely similar geochemical suite with low total element abundances and a generally flat to slightly negative slope from the least compatible to the more compatible elements (left to right). The Upper Gabbro samples also have strong to weak positive Ba, Pb, Sr and Eu anomalies, and pronounced negative Cs, U, Th, Nb, and Zr anomalies with respect to primitive mantle.

The nine samples of the Basal Gabbro subunits (Transition Gabbro, Gabbro Hybrid, Leopard Gabbro, Olivine Gabbro, Medium-Grained Gabbro, Semi-Massive Sphide) are plotted on the primitive mantle normalized extended trace element diagram of Figure 4.14b. The Transition Gabbro, Gabbro Hybrid and Leopard Gabbro have similar low to moderate total elemental abundances and a slightly negative slope from the least compatible to the more compatible elements. These samples have positive Rb, Pb,

Sr and Eu anomalies, negative U, Nb, and Zr anomalies, and variable Cs content with respect to primitive mantle. The two Olivine Gabbro samples are similar to the patterns of three previously discussed Basal Gabbro subunits but with a higher total elemental abundance. For one of the Olivine Gabbro samples (sample 98-102-155) the incompatible elements Cs, Rb, and Th are elevated compared to the other samples in this plot (Note: sample 98-102-155 contains up to 5% digested gneissic fragments). The single Medium-Grained Gabbro sample also has a similar pattern of the other Basal Gabbro samples but with some minor differences. The Medium-Grained Gabbro has the highest total element abundance from the entire Basal Gabbro sample suite; in addition, it does not have such a pronounced negative Nb and Zr anomaly as pronounced as the other samples. The single semi-massive sulphide sample has the lowest total element abundance but shares a similar pattern to the other Basal Gabbro samples. The main differences between the semi-massive sulphide samples and other samples from the Basal Gabbro are the negative Ba and Sr, and flat Zr anomaly.

On the primitive mantle normalized REE diagram of Figure 4.14c, three samples of Churchill Province gneiss and two samples of mafic dikes are plotted together. The two samples of mafic dikes define a uniquely similar geochemical suite with high total element abundances and a large negative slope from the least compatible to the more compatible elements (left to right). The mafic dike samples also have strong to weak positive Rb and Pb anomalies, and pronounced negative Nb and Zr anomalies with respect to primitive mantle. The three samples of Churchill Province gneiss also define a uniquely similar geochemical suite with high total element abundances and a large negative slope from the least compatible to the more compatible elements. The

Churchill Province samples also have weak to strong positive Th and Pb anomalies, and negative Ba, Nb and Sr anomalies.

The remaining primitive mantle normalized REE diagram, Figure 4.14d, plots the average Voisey's Bay Intrusion and Mushuau Intrusion data from Li *et al.* (2000) for comparative purposes in the final chapter of this study. In general, the total elemental abundances and patterns exhibited by the Voisey's Bay and Mushuau data are comparable to the subunits of the Basal Gabbro.

4.4 Contamination Trends using Major, Trace and REE Geochemistry

The elements CaO, K₂O, Sr, Rb, Zr, Cr, Y, and Nb are utilized to illustrate the effects of gneissic contamination on the geochemistry of rocks of the Pants Lake Intrusion. The aforementioned elements were selected because of the contrast in abundances reflecting the differing mineral compositions between PLI samples and Churchill Province samples.

To illustrate contamination trends, all of the available XRF geochemical data are plotted on bivariate plots, namely: 1) [CaO + (Sr x 10)] versus [K₂O + (Rb x 10)] (Figure 4.15a), 2) Zr versus K₂O (Figure 4.15b), 3) Cr versus Rb (Figure 4.15c), and 4) Rb versus (Y + Nb) (Figure 4.15d). It is assumed that the chemistry of samples bearing gneissic inclusions (*e.g.* Gabbro Hybrid) and samples in direct contact with the Churchill Province (*e.g.* Semi-massive sulphide, mafic dike) should differ significantly from samples not exhibiting country-rock contamination (*e.g.* Upper Gabbro).

On each of the four plots (Figures 4.15a to 4.15d), a general trend defining two end members is observed; Churchill Province gneiss and Upper Gabbro (for clarity, the

Churchill Province rocks are outlined and termed “CP Gneiss field”). In most instances, the gap between the end members is bridged by samples of Basal Gabbro. A second generalization pertaining to these diagrams is the Gabbro Hybrid, Semi-massive sulphide, mafic dike, and a few Olivine Gabbro samples trend toward and commonly plot within the “CP Gneiss field”. These two generalizations concur with the assumption stated in the previous paragraphs regarding contamination. However, there are a small number of Upper Gabbro samples that plot near the “CP Gneiss field”, and though this does not conform to the general assumption, this variance may result from the same processes experienced by the Basal Gabbro, but on a lesser scale. It is plausible that contamination may occur at the uppermost interface between the magma and country-rock, but is not as evident as in the Basal Subdivision due to the present-day erosion level.

The effects of contamination are further illustrated in Figure 4.16 (Yb versus Ce plot) and Figure 4.17 (La/Sm versus Th/Nb plot). For comparison, the Voisey’s Bay Intrusion data (Li *et al.*, 2000) are included on both figures. Figure 4.16 utilizes the ratio of Ce (light rare earth element) and Yb (heavy rare earth element) to distinguish magma types and trends. On Figure 4.16, PLI data from previous studies (MacDonald, 1999; Wilson, 1998) are included to establish the ranges of the North Gabbro (Ce/Yb = 5 to 7.8) and the South Gabbro (Ce/Yb = 20 to 28). Overlapping with the North Gabbro trend are nine samples denoted as Upper Gabbro and Basal Gabbro (this study). However, not all PLI rocks follow the North Gabbro path. Two Olivine Gabbro (BGS, North Gabbro) samples plot outside of the North Gabbro, and two mafic dike samples and one Medium-grained Gabbro (drill hole SVB-97-79) sample plot within the range of the South Gabbro.

The South Gabbro also overlaps with the range of the Varied Textured Troctolites (VTT) ($Ce/Yb = 22$ to 27) and Normal Textured Troctolites (NTT) ($Ce/Yb = 26$ to 31) of the Voisey's Bay Intrusion. The single Churchill Province sample is outside of all ranges ($Ce/Yb \sim 65$) described above. Based on the Ce to Yb ratios, samples of the Medium-Grained Gabbro (South Gabbro) and mafic dikes show a closer affinity to the Churchill Province sample, suggesting that there was significant interaction between these units.

On Figure 4.17, the North Gabbro samples cluster near the apex, equivalent to low La/Sm and Th/Nb ratios. The Churchill Province samples however, have high La/Sm and Th/Nb ratios, similar to the results reported by Li *et al.* (2000) for Tasiuyak paragneiss samples collected within the perimeter of the Voisey's Bay Intrusion. Two mafic dike samples and one Olivine Gabbro sample plot between the North Gabbro and Churchill Province field. This is similar to the trend observed in the Yb versus Ce diagram (Figure 4.16). The main difference between the trends of the two diagrams is the affiliation of the South Gabbro sample with the trend of the Voisey's Bay troctolitic rocks (low Th/Nb ratios). The South Gabbro sample does not show closeness to the contamination trend indicated on Figure 4.17.

4.5 Olivine Geochemistry of the Pants Lake Intrusion

4.5.1 Introduction to LAM-ICP-MS Technique

Laser Ablation Microprobe - Inductively Coupled Plasma - Mass Spectrometry (LAM-ICP-MS) has become more frequently utilized over the last decade to accurately and precisely measure trace-element mineral concentrations *in situ* at very low limits of detection when compared to other analytical techniques (*e.g.* electron microprobe, solution ICP-MS, pressed pellet and fused disk XRF), LAM-ICP-MS has several distinct advantages (Longerich *et al.*, 1995).

In general, the LAM-ICP-MS technique uses a focused, pulsed laser beam directed onto the surface of a solid whereby plasma is produced and the ablated material is carried via an airtight, continuous gas flow chamber to the ICP-MS (the LAM-ICP-MS technique will be elaborated on in Appendix B.3). Various minerals (silicates, carbonates, phosphates, oxides, sulphides), silicate glasses, and materials ranging from otoliths to metals have been studied using this method (web site: <http://www.esd.mun.ca/~mpoujol/AGG/test/laser.htm>; Longerich *et al.*, 1995). The LAM-ICP-MS technique has become the preferred method of choice for studies of partition coefficients between minerals, and elemental concentrations and zoning within mineral grains (*e.g.* Canil and Fedortchouk, 2001; Blundy *et al.*, 2000; Brenan *et al.*, 2003; Eggins *et al.*, 1998; Sylvester and Eggins, 1997).

For trace element determinations in olivine grains, the electron microprobe has routinely been utilized (*e.g.* MacDonald, 1999; Naldrett, 1999; Li *et al.*, 2000). However, the LAM-ICP-MS method is equally effective and can also routinely achieve a wider array of trace and REE elements at much lower detection limits.

4.5.2 Olivine Geochemistry in this Study

In this study, the LAM-ICP-MS method was utilized to measure major (MgO, FeO, SiO₂) and trace (Ni, Cu, Co) element concentrations in olivine grains selected from drill core samples of the PLI. The primary purpose is to determine the relationships of Ni and forsterite (MgO and FeO) abundances in olivine grains collected from the PLI and to make some inferences regarding magma processes.

The locations of the drill holes (SVB-96-04, SVB-96-09, SVB-97-91, SVB-98-102) utilized for this study are shown in Figure 4.18, and the actual sample locations within the drill holes where the grains were sampled are shown on Figure 4.19. Drill holes were selected on the basis of spatial distribution throughout the PLI, whereas samples were selected to obtain a representative sample suite within the Upper and Basal Gabbro subdivisions.

In total, 124 euhedral olivine grains from 20 samples were ablated and analyzed using the LAM-ICP-MS method (Table 4.11 provides the number of olivine's ablated per sample). Olivine grain compositions were found to be fairly homogeneous; however, studies by MacDonald (1999) and Naldrett (1999) indicated that some olivine grains are actually chemically zoned. Their interpretative approach was to derive average element concentrations for olivine grains from a particular sample; this approach will also be used by the author. The major and trace element LAM-ICP-MS data for this study are shown in Table B.3. Data of average element and average forsterite values are presented in Table 4.11.

4.5.3 Results of Olivine Geochemistry Study

The maximum and minimum average ranges for the entire Pants Lake Intrusion olivine sample suite determined in this study are 20.63-13.33 wt% MgO, 55.63-34.81 wt% FeO, 644.6-63.86 ppm Ni, 12.54 ppm to < detection limits for Cu, 296.6-166.7 ppm Co, and 58.40-31.70 mole % forsterite (refer to Table 4.11). Due to their low values in olivine, Cu data will not be discussed further. In addition, only the Ni and forsterite contents will be described for the various subdivisions and accompanying diagrams.

The maximum and minimum average values for olivine samples classified as Upper Gabbro are 644.6-63.86 ppm Ni and 58.40-31.70 mole % forsterite. For the Basal Gabbro samples, the ranges are 560.1-76.70 ppm Ni and 56.70-33.20 mole % forsterite. The maximum and minimum average values for olivine samples from each drill hole are as follows; SVB-96-04: 644.7-188.8 ppm Ni and 58.40-42.20 mole % forsterite, SVB-96-09: 545.6-95.57 ppm Ni and 56.70-37.20 mole % forsterite, SVB-98-102: 244.5-105.4 ppm Ni and 48.60-36.30 mole % forsterite, and SVB-97-91: 255.3-63.86 ppm Ni and 54.60-31.70 mole % forsterite. The Spearman ranked correlation coefficient (r') between Ni and forsterite for each drill hole is as follows; SVB-96-04 (r') = -0.54, SVB-96-09 (r') = +0.53, SVB-98-102 (r') = +0.40, and SVB-97-91 (r') = +0.90.

The drill profiles of Figure 4.20 plot depth versus average mole % forsterite and Ni. In the profile of SVB-96-04, the upper interval shows a reverse of the normal differentiation trend, that is, decreasing Fo with increasing depth from Upper Gabbro to the center of the Basal Gabbro. Naldrett (1999) suggested that such features result from fluxes of hotter, new magma entering the sill. The fractionation trend observed in the upper interval of SVB-96-04 is unlike what is observed in the other drill holes (SVB-96-

09, SVB-98-102, SVB-97-91) in which normal fractionation trends of increasing Fo with increasing depth are present, starting from the Upper Gabbro downwards to the center or near center of the Basal Gabbro. For normal fractionation, as the mafic magmas crystallize Mg-rich olivine, the remaining melt becomes enriched in Fe consequently the later-forming olivine will contain more Fe relative to Mg and therefore will have lower Fo values (MacDonald, 1999). In all of the drill holes studied, the reverse of the normal fractionation trend is apparent from the center to the bottom of the Basal Gabbro. These features are also consistent with drill holes studied by Naldrett (1999) and MacDonald (1999).

The Ni versus depth patterns for SVB-96-09, SVB-98-102, and SVB-97-91 are weakly to strongly analogous to Fo versus depth patterns for the same holes; however, at the bottom of the drill holes the reverse of this trend is true. This feature is most reasonably explained as normal fractionation processes that were interrupted by the presence of trapped sulphide liquid, notably within the Basal Gabbro. In the case of SVB-96-04, there does not appear to be any sort of correlation between Ni and Fo with increasing depth. This feature may be explained by a number of processes. One, if orthopyroxene or clinopyroxene crystallize along with olivine and plagioclase, the Ni is not depleted so rapidly with forsterite, since these minerals remove almost as much Mg but much less Ni than olivine (Naldrett, 1999), and two, local Fe-Ni exchange between olivine and trapped sulphide liquids in the rocks where olivine in areas with much sulphide may become reequilibrated with the sulphide, thus affecting the Ni content in olivine (Li *et al.*, 2000). The author agrees with the second process.

Figure 2.21 illustrates the variations of average Ni contents and mole percent forsterite in the Pants Lake, Voisey's Bay and Mushuau intrusions. Added to this diagram are three fractionation curves modeled by Naldrett (1999) to show: 1) olivine and plagioclase fractionation, 2) olivine fractionation, and 3) olivine, plagioclase, and sulphide fractionation. The Voisey's Bay and Mushuau data used in this figure were reported by Li *et al.* (2000).

Olivines from this study define a slightly scattered trend with a subtle positive slope. Samples collected from drill holes SVB-98-102 and SVB-97-91 have the lowest Ni values (<250 ppm) and the highest Ni value was reported from a sample collected in drill hole SVB-96-04. Forsterite values range between 58.40-31.70 mole %; however, most samples are above 40 mole % with only five samples below this value.

The majority of samples in this study overlap with the field established by Naldrett (1999) for SVB olivine samples, as well as two fields belonging to the Voisey's Bay Intrusion (*i.e.* Olivine Gabbro, Feeder Olivine Gabbro) and the field defined by the Mushuau Intrusion. When compared to the fractionation curves calculated by Naldrett, a number of intrinsic features are revealed. SVB-98-102 and SVB-97-91 correlate well with the olivine + plagioclase + sulphide fractionation curve which further explains the patterns developed in the Fo and Ni versus depth diagrams (Figure 4.20). Olivine apparently fractionated with plagioclase and sulphide hence the Ni was transferred to the sulphide thus explaining the lower than average Ni values in these two drill holes. SVB-96-04 has the highest degree of scatter for any of the four drill holes which may be a reflection of differing fractionation phases linked to influxes of new magma pulses as also suggested by the Fo versus depth profile for this hole.

4.6 Metal Tenor and Distribution within the Pants Lake Intrusion

The purpose of this section is to provide some insight on the metal tenors and metal distributions within the Pants Lake Intrusion as defined by the XRF data (Appendix B – Table B.1). Nickel (Ni) and copper (Cu), typically present as pentlandite $[(\text{Fe},\text{Ni})_9\text{S}_8]$ and chalcopyrite (CuFeS_2) respectively, are the principal metals discussed in this section. Cobalt (Co) is closely associated with the two aforementioned metals; however, Co was not routinely analyzed during this study and therefore will not be mentioned further in this section unless quoted from other sources. Platinum (Pt) and Palladium (Pd), commonly referred to as Platinum Group Elements, were not measured during this study due to low, typically < 20 ppb, abundances as determined during earlier exploration phases (unpublished data, Donner Mineral Ltd.).

At present, the highest metal tenors have been determined from drill intersections encountered over the last decade, including: 1) 1.13% Ni, 0.78% Cu, and 0.20% Co over a 15.70 meter interval in DDH 97-096, 2) 11.60% Ni, 10.20% Cu, and 0.41% Co over a 1.10 meter interval in DDH 98-075, 3) 4.49% Ni, 2.60% Cu, and 0.28% Co over a 0.20 meter interval in DDH 98-113, 4) 3.44% Ni, 0.50% Cu, and 0.46% Co over a 0.30 meter interval in DDH 98-113, and 5) 1.97% Ni, 1.03% Cu, and 0.26% Co over a 0.60 meter interval in DDH 98-067 (<http://www.donner-minerals.com/svbproject>). All of these drill holes listed above are within the northernmost apex (NAI mineralized region) of the North Gabbro.

4.6.1 Metal Tenor

The maximum Ni and Cu contents determined in this study for the Upper and Basal Gabbro samples are as follows: Upper Gabbro ($\text{Ni}_{\text{max}} = 1597$ ppm, $\text{Cu}_{\text{max}} = 1480$ ppm), and Basal Gabbro ($\text{Ni}_{\text{max}} = 11980$ ppm, $\text{Cu}_{\text{max}} = 11239$ ppm) (Appendix B – Table B.1). The ratio of Ni to Cu for rocks of the PLI is generally 1:1, especially for Basal Gabbro rocks (Figure 4.22a) with a few exceptions, notably for samples belonging to the NDT and Mineral Hill regions (Figure 4.22b). This 1:1 ratio is not particularly true for the Upper Gabbro rocks where Ni to Cu ratios range from 0.4 to 3 (Figure 4.22a).

Table 4.12 provides a summary of the average Ni and Cu concentrations of the Upper and Basal Gabbro within each mineralized region (Figure 3.1) located throughout the Pants Lake Intrusion. It is quite apparent from this table, that the Basal Gabbro subdivision is enriched in Ni and Cu, whereas the Upper Gabbro is relatively depleted, regardless of geographic location. This feature is further illustrated in Figure 4.22a where the Ni and Cu contents for the majority of Upper Gabbro samples are much lower than the Ni and Cu contents of the Basal Gabbro samples.

A similar story is illustrated for Ni and Cu calculated to 100% sulphide for the Upper and Basal Gabbro samples (Table 4.12) following the calculation outlined by Kerr (1999). The rationale behind calculating to 100% sulphide is based on the premise the Ni and Cu are essentially contained in the sulphide phases, and if the sulphide content is known, the “potential grade” of massive sulphide accumulations can be calculated (*op cit*). The highest potential grades determined by this method were 3.74% Ni (NDT region) and 1.65% Cu (Worm Gabbro region).

4.6.2 Metal Distribution

The Ni and Cu contents of sulphides are not evenly distributed throughout the PLI. In section 4.6.1, it was well established that the Basal Gabbro subdivision contains significantly more Ni and Cu than the Upper Gabbro. In Table 4.12, the Basal Gabbro of the NAI has the highest average Ni (2425 ppm) and Cu (1844 ppm) values of any other mineralized regions within the PLI. This is substantiated by drilling results to date.

Within Figure 4.23, there are four diagrams (A to D) depicting the outline of the PLI and the location of the drill holes used for this study. For each diagram, the intent is to show the geographical distribution of Ni and Cu concentrations for Upper and Basal Gabbro rocks throughout the PLI. In this case, sample intervals represented by dots and stars were utilized. The sample intervals on the diagrams were determined as follows: The highest interval (red dot) denotes the samples above the top 10% when arranged from high to low, the mid-interval (green dot) denotes the samples between the top 10% and 50%, and the lowest interval (star) indicates all other samples. The reader is encouraged to review Figure 3.1 (Chapter 3) prior to reading the following text.

On Figure 4.23a and Figure 4.23b, it is apparent that the highest Ni and Cu values within the Upper Gabbro are reported for the South and Central Gabbro components, in particular, the Mineral Hill, Worm Gabbro, and GG regions. In the case of Ni (Figure 4.23a) the mid-interval values envelope the high values for all parts of the PLI, whereas for Cu (Figure 4.23b), there is a strong association of the mid-interval values with the South and Central Gabbro components.

On Figure 4.23c and Figure 4.23d, it is overwhelmingly obvious that the highest Ni and Cu values are associated with the NAI and HFL regions of the North Gabbro

component (also see Figure 4.22b). As well, for the mid-interval samples of Ni and Cu, there are also closely linked to the North Gabbro component, illustrating that the Basal Gabbro of the South and Central Gabbro components are relatively depleted compared to the northern counterpart.

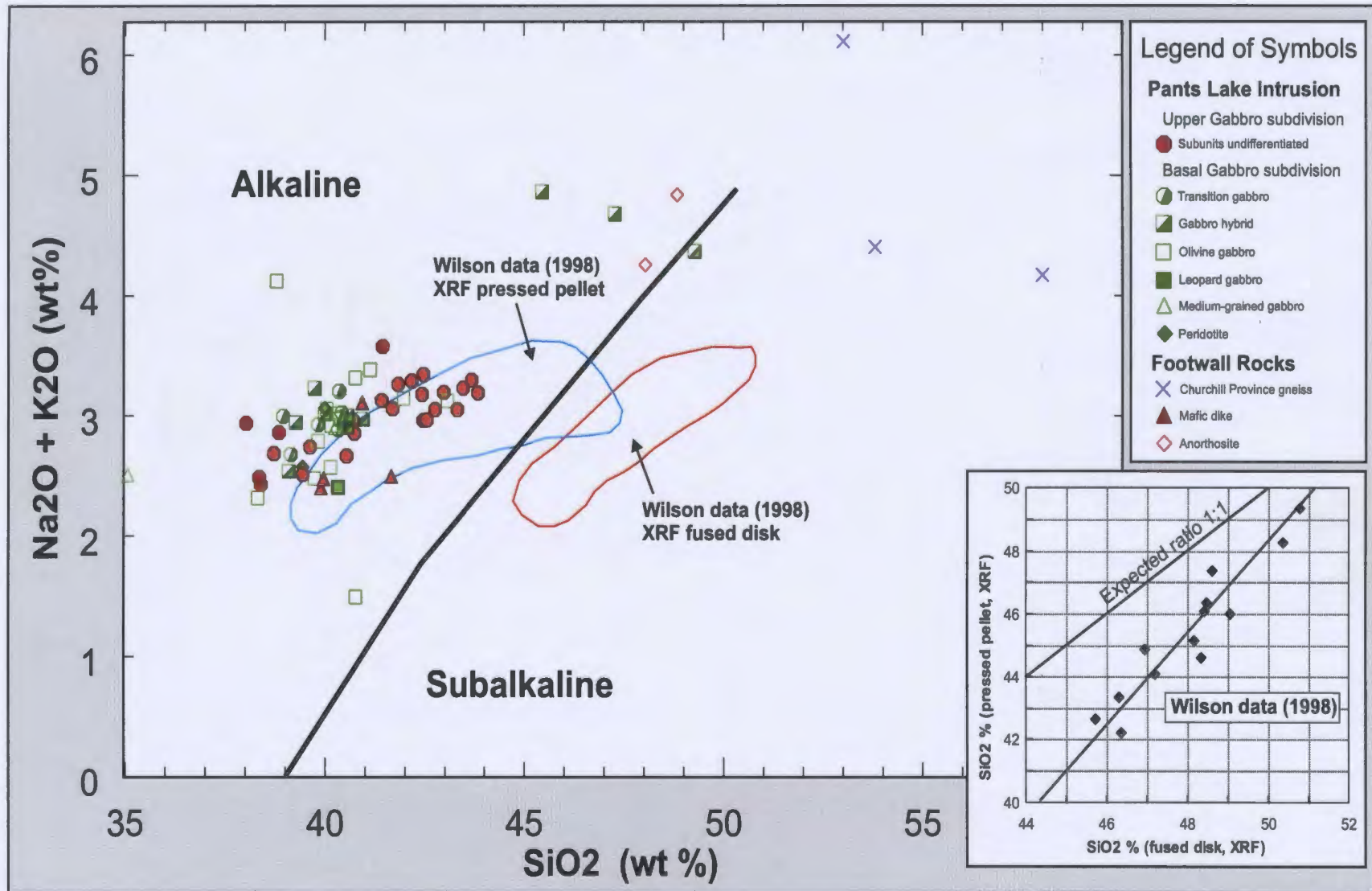


Figure 4.1. Total alkalis ($\text{Na}_2\text{O} + \text{K}_2\text{O}$) vs. SiO_2 plot, with alkaline and subalkaline fields (Irvine and Baragar, 1971). This plot illustrates the difficulty in using SiO_2 data obtained by the X-ray Fluorescence (XRF) method on pressed powder pellets. The Pants Lake Intrusion (PLI) samples (this study) clearly plot in the alkaline field as do PLI samples from Wilson (1998) (blue outline); both sets of samples were analyzed using pressed pellets. Using the same set of samples from Wilson (1998), samples analyzed using the XRF method on fused disks (red outline) clearly plotted in the subalkaline field. This suggests that SiO_2 values are substantially lower using pressed pellets compared to fused disks, however Na_2O and K_2O concentrations are equivalent regardless of method. The plot in the lower right corner of the larger plot further illustrates the deviation of SiO_2 using pressed pellet.

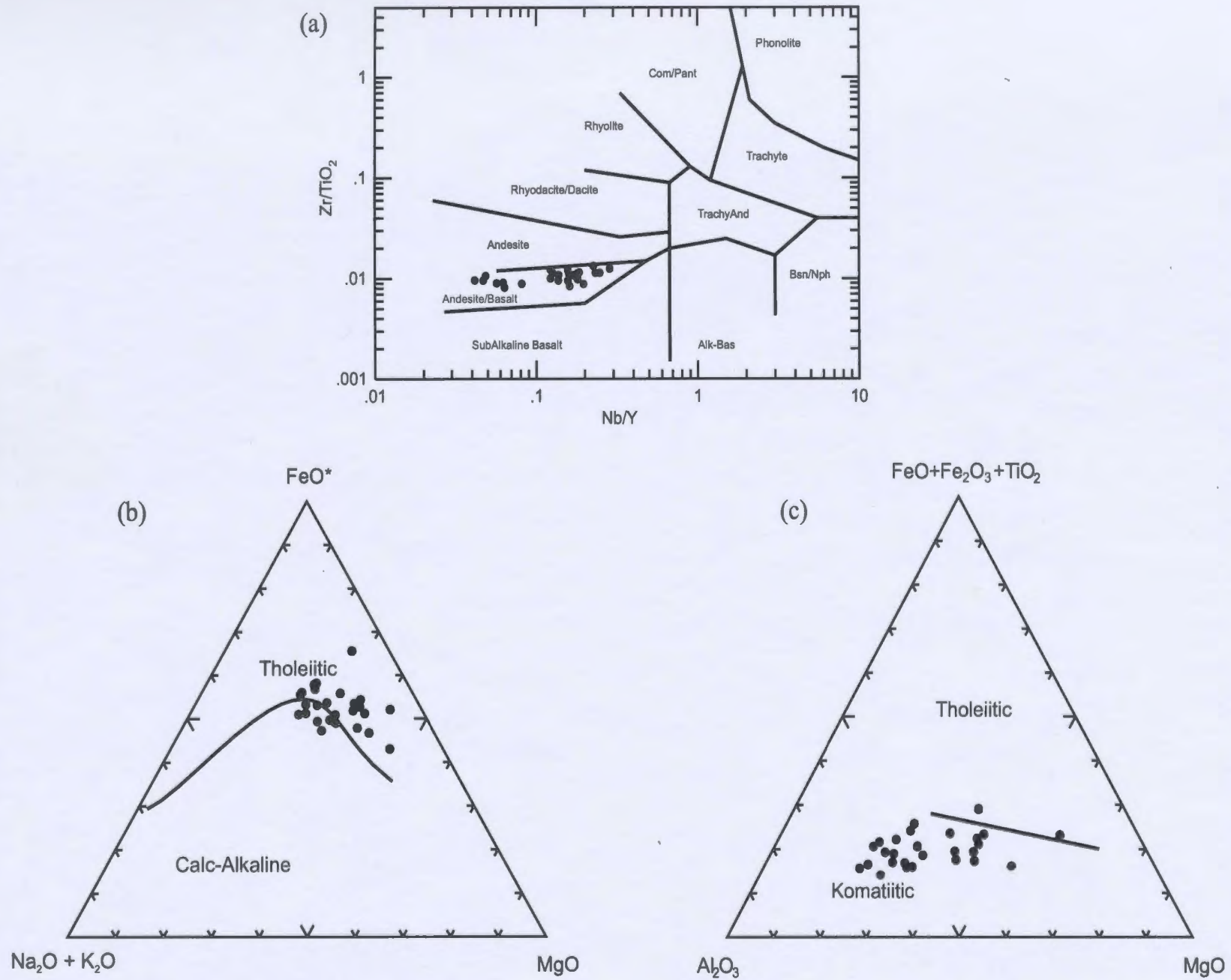


Figure 4.2. Discrimination diagrams for rocks belonging to the Upper Gabbro (undifferentiated), (a) Winchester and Floyd (1977), (b) Irvine and Baragar (1971), and (c) Jensen (1976).

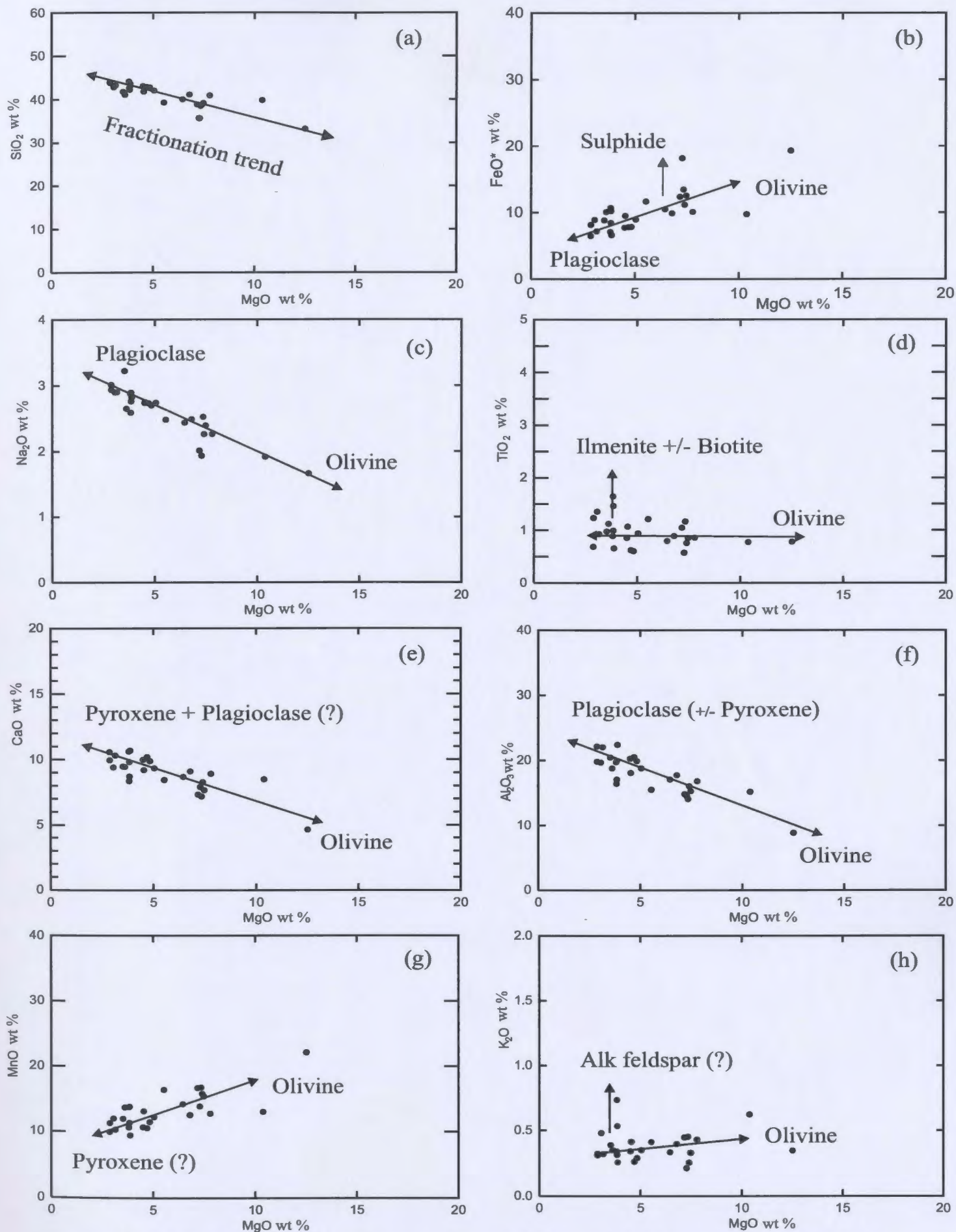


Figure 4.3. MgO versus major element plots of the Upper Gabbro subdivision including (a) SiO₂, (b) FeO*, (c) Na₂O, (d) TiO₂, (e) CaO, (f) Al₂O₃, (g) MnO, and (h) K₂O.

Table 4.1 Major element ranges (reported in wt %) of Upper Gabbro samples

| | No. of samples | MgO wt % (mean, std. dev) | SiO ₂ wt % (mean, std. dev) | FeO* wt % (mean, std. dev) | Na ₂ O wt % (mean, std. dev) | TiO ₂ wt % (mean, std. dev) | CaO wt % (mean, std. dev) | Al ₂ O ₃ wt % (mean, std. dev) | MnO wt % (mean, std. dev) | K ₂ O wt % (mean, std. dev) | Mg # % (mean, std. dev) |
|-------------------|----------------|------------------------------|---|-------------------------------|--|---|------------------------------|---|------------------------------|---|------------------------------|
| Upper Gabbro, PLI | 27 | 2.88-12.50 (5.48, 2.38) | 33.31-44.15 (41.10, 2.60) | 6.48-19.27 (10.12, 3.08) | 1.92-3.22 (2.58, 0.37) | 0.57-1.46 (0.95, 0.26) | 4.64-10.67 (8.97, 1.31) | 8.84-22.39 (17.83, 3.04) | 9.43-27.0 (13.18, 2.75) | 0.21-0.73 (0.37, 0.12) | 39.97-65.50 (49.80, 6.75) |

Table 4.2 Trace element ranges (reported in ppm) of Upper Gabbro samples

| | No. of samples | Cr (ppm) (mean, std. dev) | Ga (ppm) (mean, std. dev) | Sr (ppm) (mean, std. dev) | Rb (ppm) (mean, std. dev) | V (ppm) (mean, std. dev) | Cu (ppm) (mean, std. dev) | Ni (ppm) (mean, std. dev) | S (ppm) (mean, std. dev) |
|-------------------|----------------|-------------------------------|------------------------------|-------------------------------|------------------------------|-------------------------------|-------------------------------|------------------------------|-----------------------------|
| Upper Gabbro, PLI | 27 | 20.00-106.0 (45.63, 19.69) | 15.80-26.20 (21.52, 4.27) | 200.4-426.4 (347.4, 82.25) | 2.77-384.8 (20.68, 72.86) | 73.00-163.0 (109.3, 22.96) | 15.70-746.0 (52.77, 138.7) | 7.80-667.0 (59.85, 126.7) | 704.0-47064 (2860, 8841) |

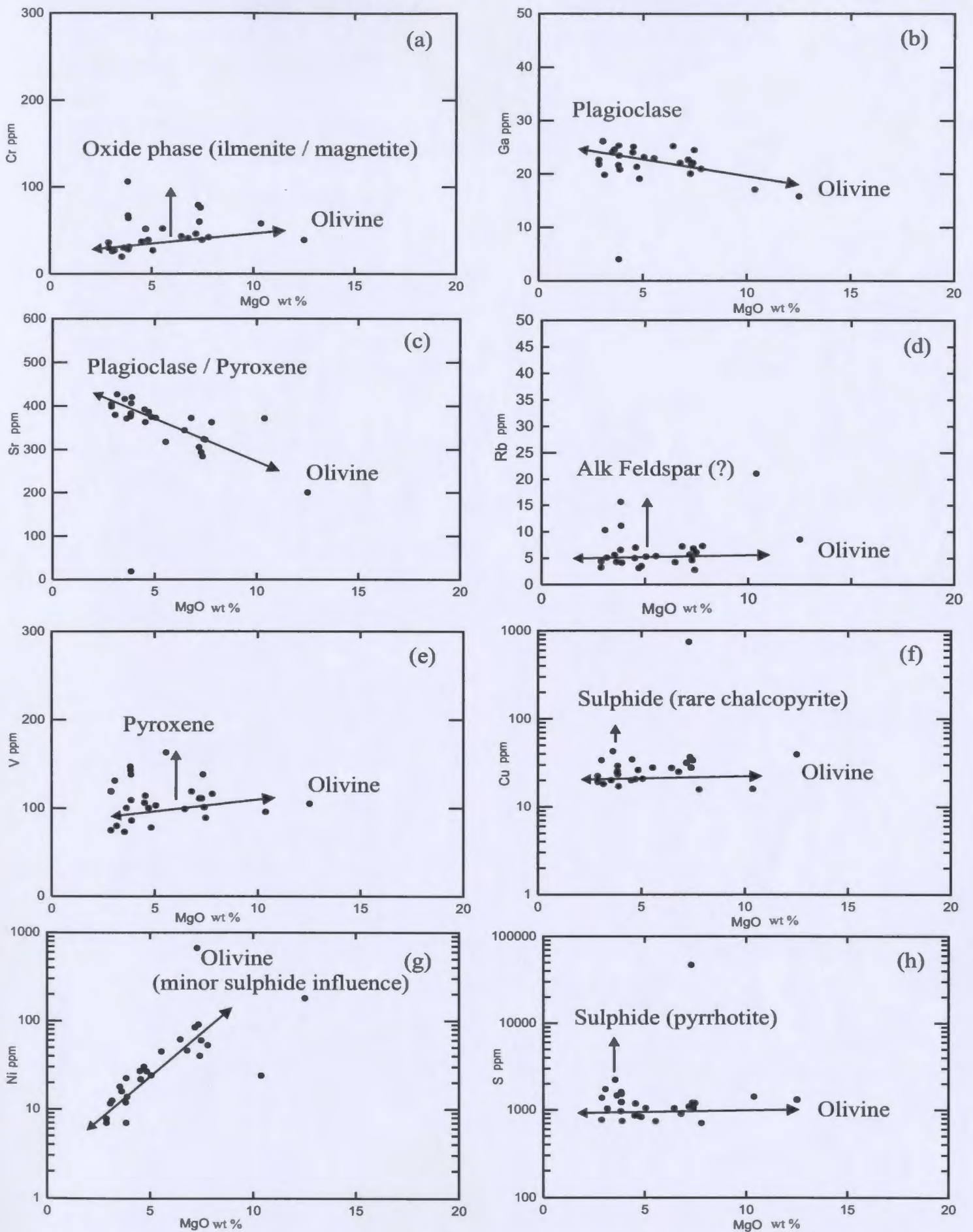


Figure 4.4. MgO versus trace element plots of the Upper Gabbro including (a) Cr, (b) Ga, (c) Sr, (d) Rb, (e) V, (f) Cu, (g) Ni, and (h) S.

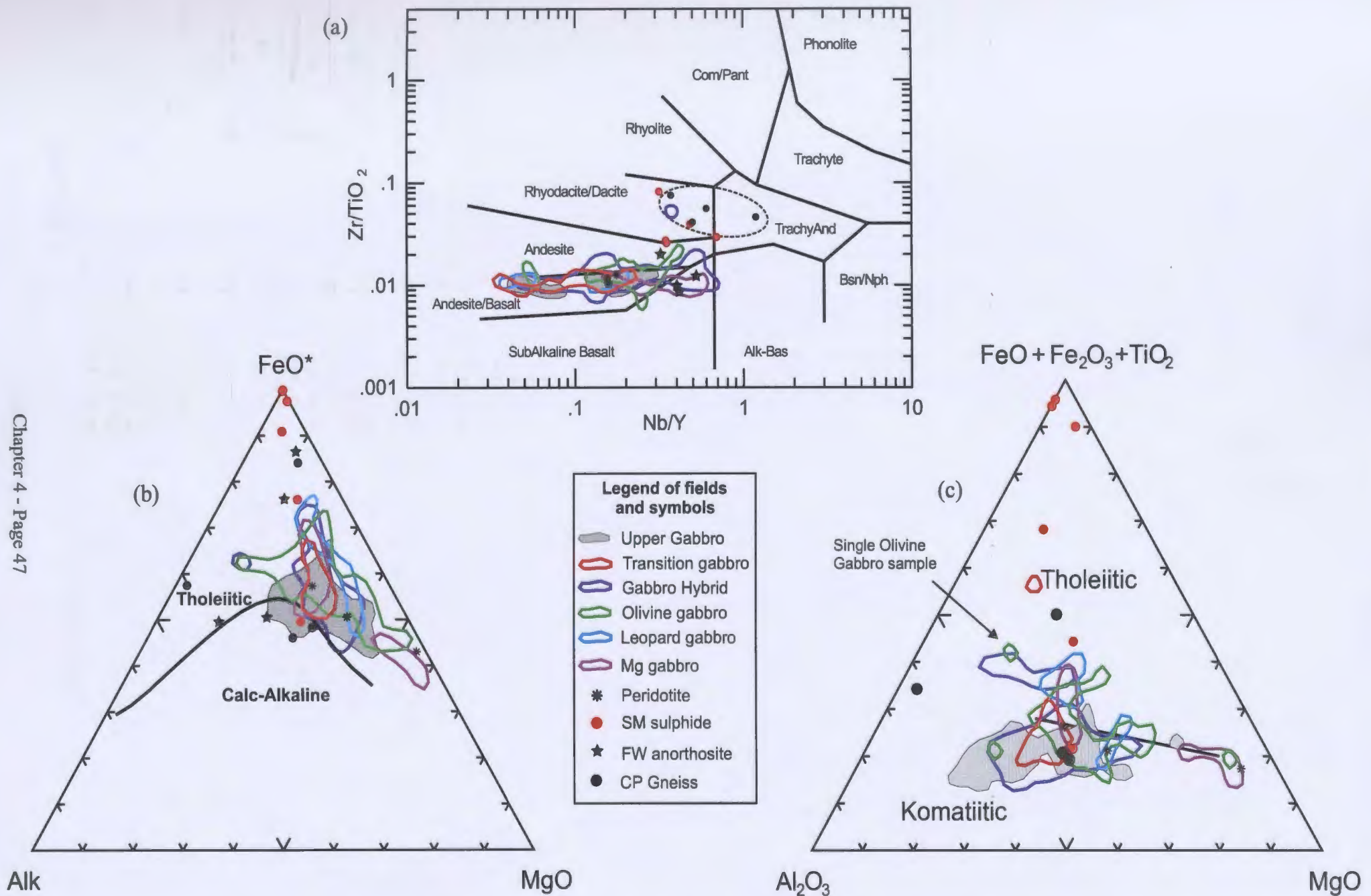


Figure 4.5. Discrimination diagrams for rocks belonging to the subunits of the Basal Gabbro, Churchill Province gneiss, and footwall anorthosite, (a) Winchester and Floyd (1977), (b) Irvine and Baragar, and (c) Jensen (1976). The Upper Gabbro field is plotted on each diagram for reference. Individual samples are outlined with a small circle of the same field color (see Figure 4.5c for example).

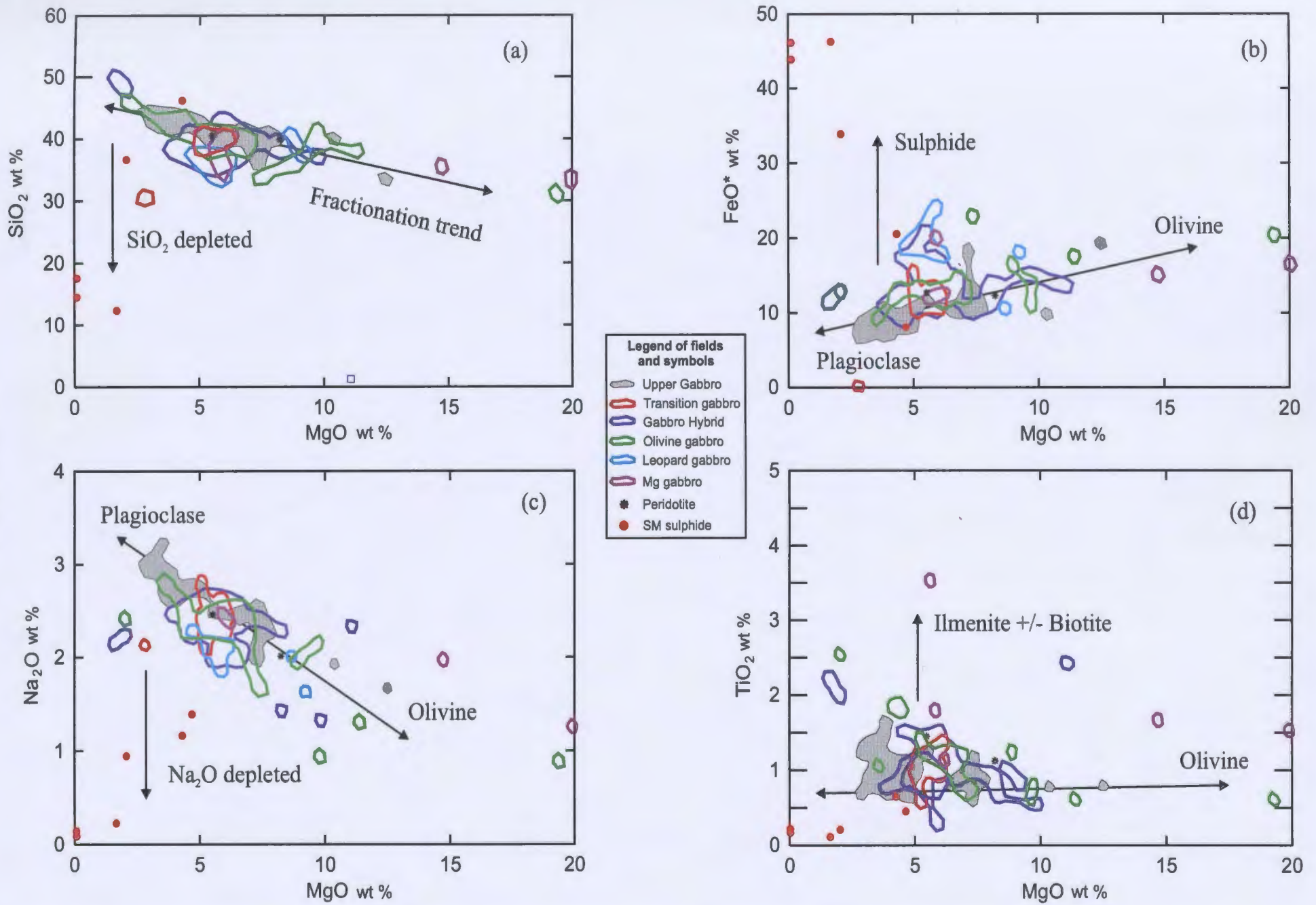


Figure 4.6. MgO versus major element plots of rocks belonging to the subunits of the Basal Gabbro including (a) SiO₂, (b) FeO*, (c) Na₂O, (d) TiO₂, (e) CaO, (f) Al₂O₃, (g) MnO, and (h) K₂O. The Upper Gabbro field is included in each plot.

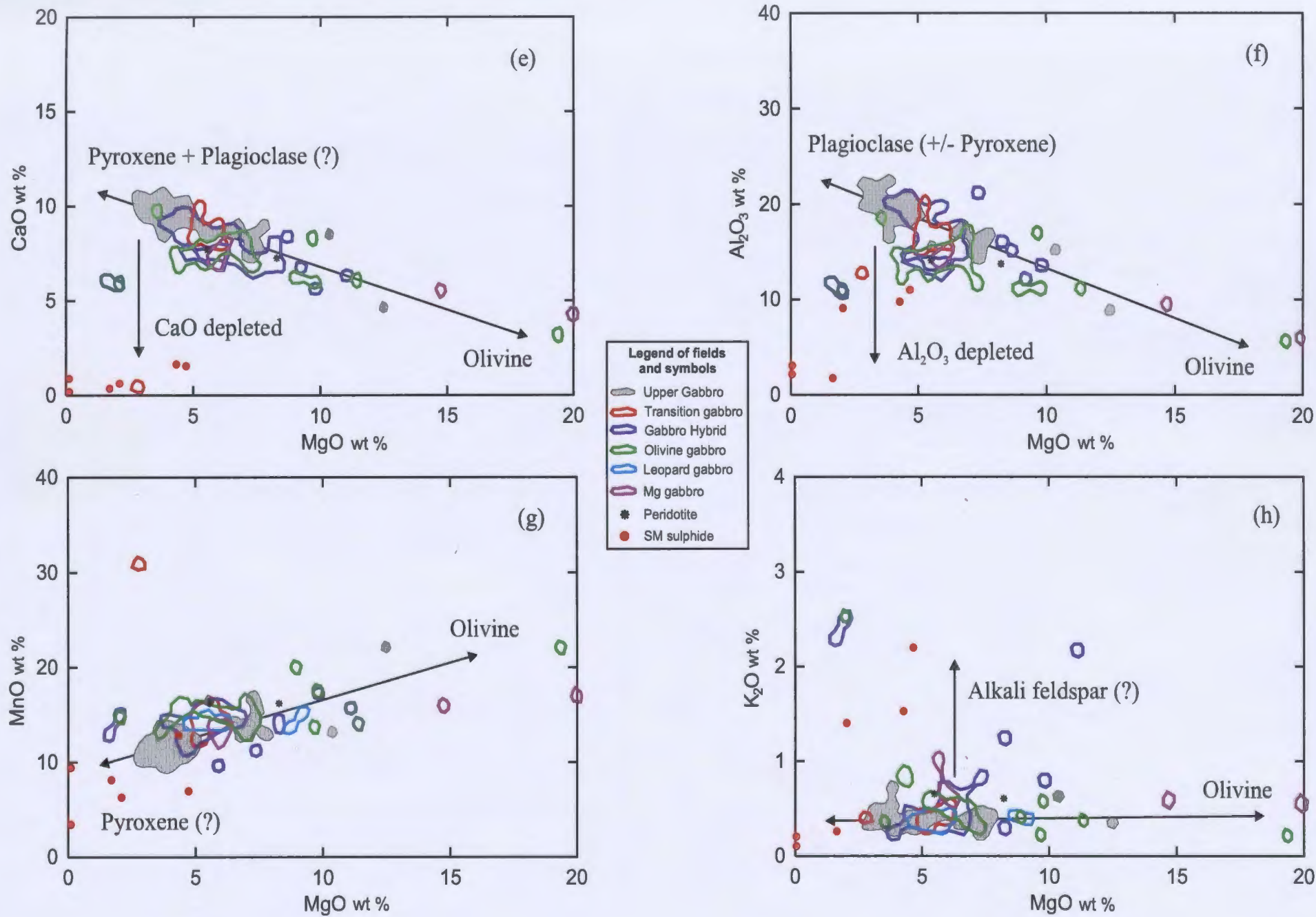


Figure 4.6. Continued

Table 4.3. Major element ranges (reported in wt %) of Basal Gabbro samples.

| Basal Gabbro subunit | No. of samples | MgO wt % (mean, std. dev) | SiO ₂ wt % (mean, std. dev) | FeO* wt % (mean, std. dev) | Na ₂ O wt % (mean, std. dev) | TiO ₂ wt % (mean, std. dev) | CaO wt % (mean, std. dev) | Al ₂ O ₃ wt % (mean, std. dev) | MnO wt % (mean, std. dev) | K ₂ O wt % (mean, std. dev) | Mg # % (mean, std. dev) |
|-----------------------|----------------|------------------------------|---|-------------------------------|--|---|------------------------------|---|------------------------------|---|-------------------------------|
| Transition Gabbro | 12 | 2.80-6.13 (5.83, 0.90) | 30.44-40.80 (39.09, 2.84) | 0.11-15.35 (10.69, 3.64) | 2.07-2.81 (2.43, 0.22) | 0.58-20.07 (2.63, 5.50) | 0.39-9.98 (8.01, 2.47) | 12.73-20.08 (16.54, 1.78) | 12.36-30.83 (15.49, 4.93) | 0.29-0.54 (0.41, 0.07) | 38.24-98.50 (52.12, 15.12) |
| Gabbro Hybrid | 27 | 1.60-9.83 (5.88, 2.00) | 1.25-49.78 (38.62, 8.07) | 8.77-20.83 (12.78, 2.61) | 1.32-2.67 (2.26, 0.33) | 0.27-2.43 (1.12, 0.48) | 5.61-9.61 (7.85, 1.10) | 10.66-21.13 (17.36, 6.14) | 9.58-17.23 (13.83, 1.62) | 0.24-2.50 (0.69, 0.63) | 21.81-61.46 (45.54, 9.68) |
| Leopard Gabbro | 7 | 4.68-9.18 (6.44, 1.75) | 33.74-40.74 (36.94, 2.09) | 10.48-23.92 (18.25, 4.10) | 1.63-2.28 (2.01, 0.21) | 0.69-1.15 (0.89, 0.16) | 6.74-8.38 (7.42, 0.54) | 12.06-15.12 (13.58, 1.01) | 13.49-15.10 (14.20, 0.54) | 0.29-0.44 (0.38, 0.01) | 30.22-60.36 (39.22, 11.45) |
| Olivine Gabbro | 22 | 3.54-19.31 (6.99-3.50) | 30.97-45.99 (39.54, 3.21) | 9.02-22.91 (13.90-3.26) | 0.88-2.82 (2.13, 0.52) | 0.59-2.55 (1.17, 0.50) | 3.13-9.65 (7.25, 1.28) | 5.55-18.56 (13.79, 2.84) | 12.77-22.05 (15.47, 2.18) | 0.20-2.51 (0.58, 0.47) | 23.44-63.55 (47.59, 9.71) |
| Medium-Grained Gabbro | 6 | 5.64-21.92 (12.36, 7.48) | 33.48-39.23 (36.39, 2.90) | 11.93-20.08 (15.31-2.96) | 1.16-3.16 (2.06, 0.76) | 0.92-3.53 (1.76, 0.93) | 4.21-7.24 (6.05-1.63) | 5.78-14.21 (10.92, 4.07) | 12.21-17.01 (14.68, 1.79) | 0.30-1.01 (0.61, 0.23) | 33.76-73.21 (56.12, 15.39) |
| Semi-Massive Sulphide | 6 | 0.03-4.65 (2.10, 1.99) | 12.33-63.72 (31.84, 20.64) | 8.06-46.25 (33.12-15.77) | 0.09-1.39 (0.66, 0.57) | 0.11-0.65 (0.30, 0.20) | 0.21-1.65 (0.89-0.60) | 1.79-11.01 (6.14, 4.23) | 3.43-12.81 (7.84, 3.16) | 0.10-2.20 (0.95, 0.88) | 0.08-50.87 (14.71, 20.13) |
| Peridotite | 3 | 5.48-21.81 (11.83, 8.75) | 31.18-40.45 (37.17, 5.19) | 12.20-19.98 (14.94-4.37) | 0.66-2.45 (1.70, 0.93) | 0.47-1.45 (1.02, 0.50) | 3.38-7.66 (6.09-2.36) | 5.17-14.05 (10.97, 5.02) | 16.17-20.28 (17.56, 2.36) | 0.10-0.65 (0.45, 0.30) | 46.17-69.74 (57.69, 11.79) |

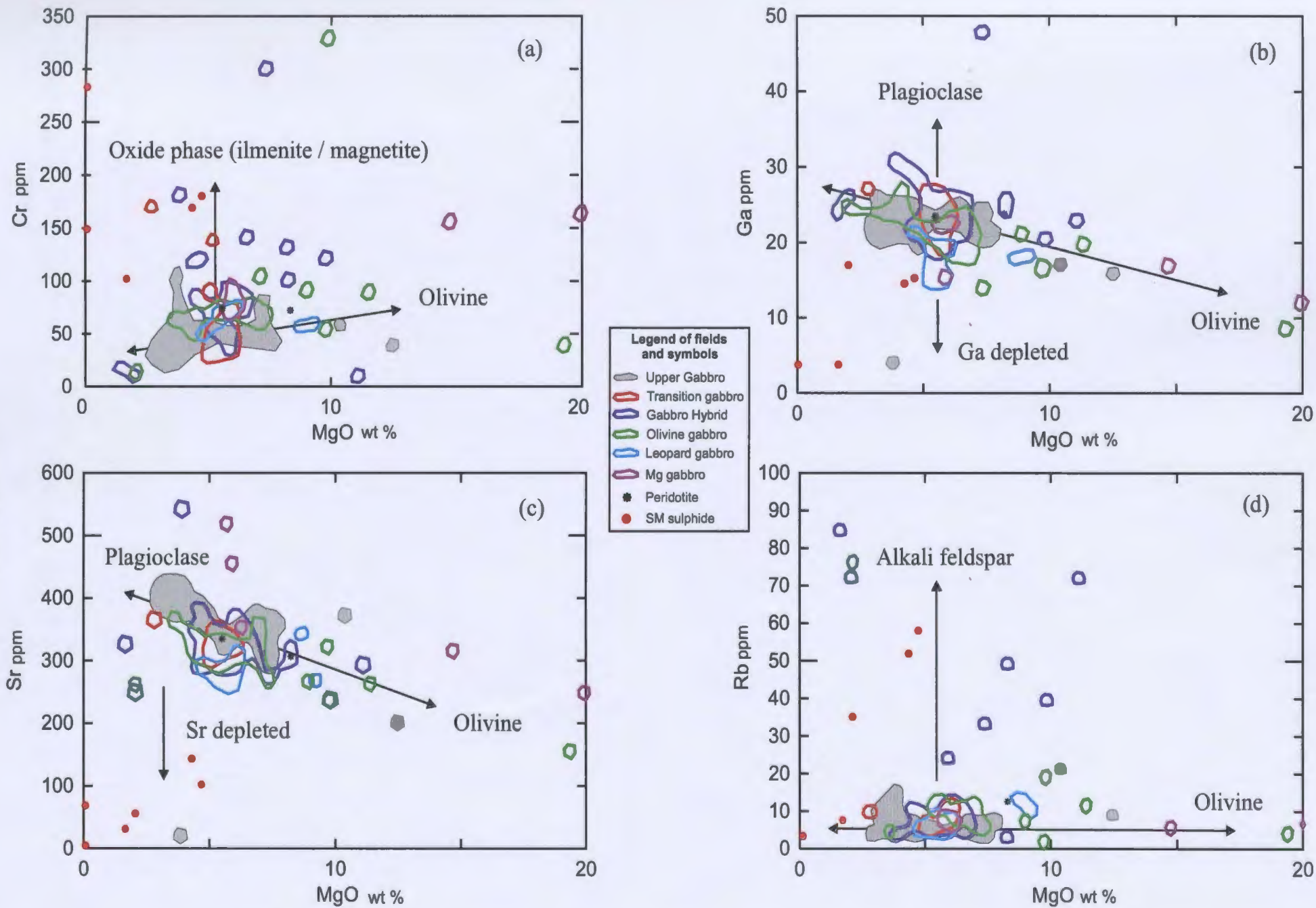


Figure 4.7. MgO versus trace element plots of rocks belonging to the subunits of the Basal Gabbro including (a) Cr, (b) Ga, (c) Sr, (d) Rb, (e) V, (f) log Cu, (g) log Ni, and (h) log S. The Upper Gabbro field is included in each plot.

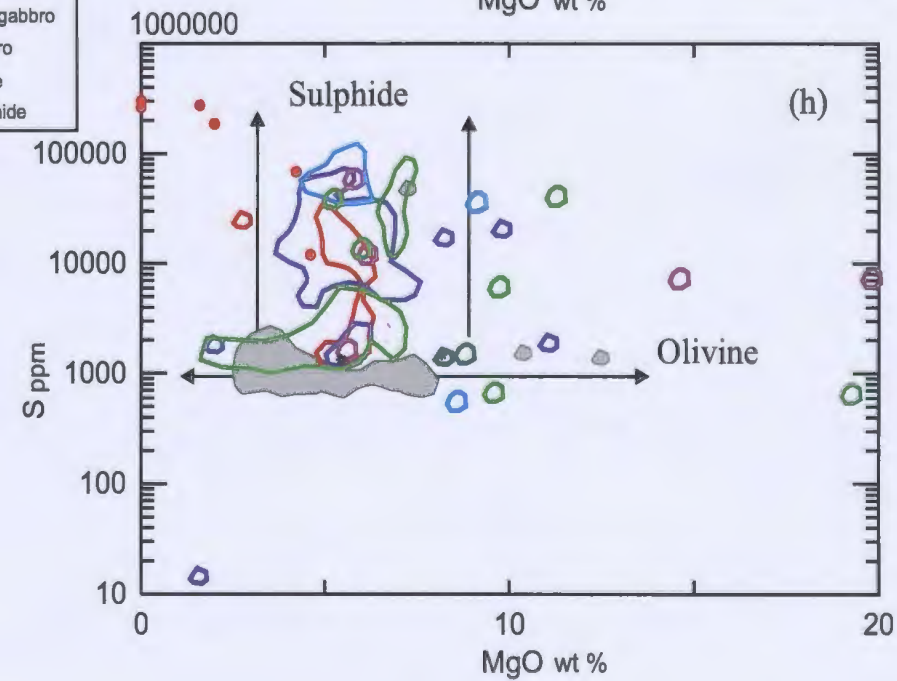
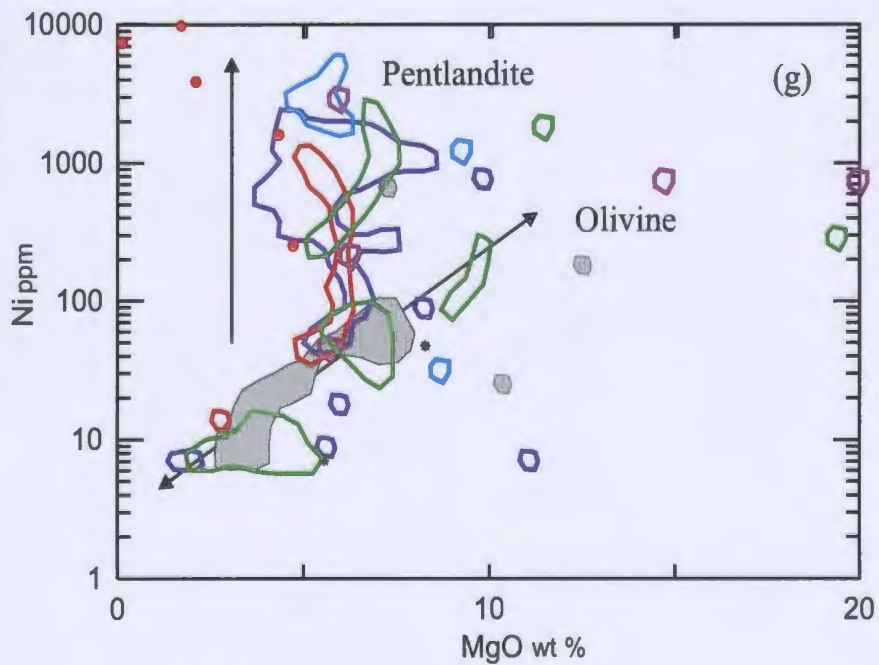
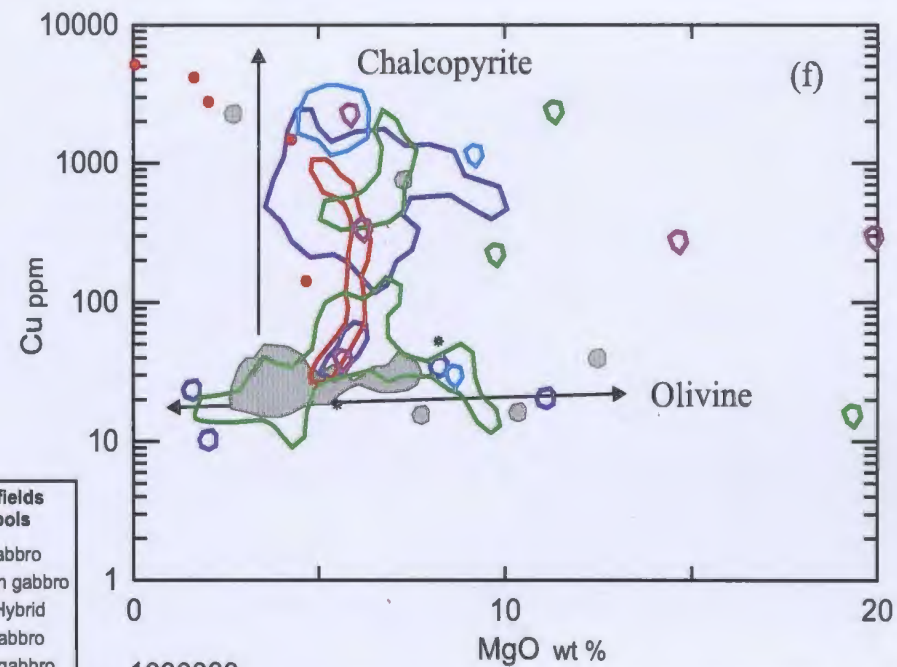
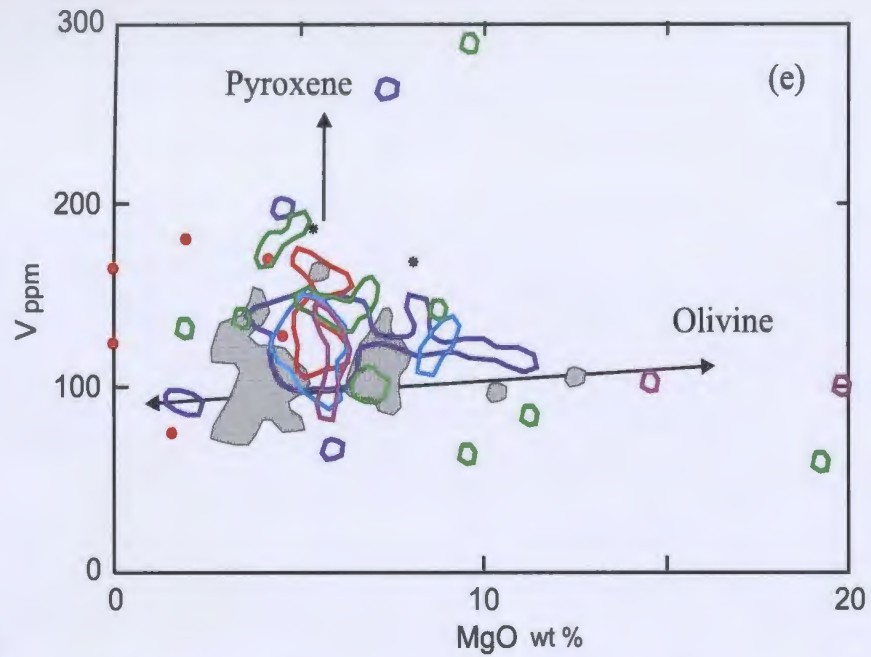


Figure 4.7. Continued.

Table 4.4. Trace element ranges (reported in ppm) of Basal Gabbro samples.

| Basal Gabbro subunit | No. of samples | Cr (ppm) (mean, std. dev) | Ga (ppm) (mean, std. dev) | Sr (ppm) (mean, std. dev) | Rb (ppm) (mean, std. dev) | V (ppm) (mean, std. dev) | Cu (ppm) (mean, std. dev) | Ni (ppm) (mean, std. dev) | S (ppm) (mean, std. dev) |
|-----------------------|----------------|-------------------------------|------------------------------|-------------------------------|------------------------------|-------------------------------|-------------------------------|--------------------------------|----------------------------------|
| Transition Gabbro | 12 | 27.00-170.0 (72.08, 43.92) | 18.90-27.50 (23.86, 2.21) | 295.4-365.0 (331.1, 18.40) | 4.50-11.70 (7.47, 2.17) | 110.0-170.0 (122.0, 42.23) | 30.00-2162 (508.9, 620.9) | 14.10-1126.7 (399.5, 420.3) | 1228-27187 (10002, 9744) |
| Gabbro Hybrid | 27 | 10.00-301.0 (90.59, 58.36) | 18.20-47.80 (24.94, 5.37) | 236.3-543.7 (325.9, 55.45) | 2.90-84.90 (19.43, 23.57) | 66.00-263.0 (124.5, 43.92) | 10.00-1987 (550.3, 508.8) | 7.00-1991 (571.0, 579.6) | 1300-60618 (14749, 14384) |
| Leopard Gabbro | 7 | 49.00-76.00 (62.71, 9.52) | 14.90-21.60 (17.86, 2.38) | 259.7-341.2 (288.0, 29.50) | 4.30-13.60 (7.66, 3.41) | 94.00-146.0 (120.9, 17.51) | 30.00-2949 (1743, 1027) | 31.00-5118 (2363, 1647) | 547.0-95907 (49124, 29861) |
| Olivine Gabbro | 22 | 13.00-329.0 (78.14, 58.94) | 8.80-27.30 (20.80, 4.06) | 153.9-365.3 (300.6, 45.99) | 2.10-76.30 (13.28, 14.87) | 61.00-291.0 (139.6, 49.19) | 11.00-2378 (374.3, 634.3) | 7.00-2398 (424.1, 674.9) | 655.0-73161 (12314, 18702) |
| Medium-Grained Gabbro | 6 | 69.00-164.0 (118.8, 42.84) | 9.50-22.80 (16.55, 5.30) | 241.3-458.0 (355.7, 112.7) | 2.50-6.80 (6.38, 2.21) | 54.00-142.0 (102.0, 29.95) | 37.40-2158 (559.7, 790.1) | 44.80-2869 (1026, 1044) | 1630-59451 (15705, 21696) |
| Semi-Massive Sulphide | 6 | 102.0-485.0 (228.0-139.3) | 4.00-17.20 (9.92, 6.53) | 3.90-143.2 (67.22, 49.91) | 3.60-58.40 (26.89, 25.10) | 77.00-183.0 (142.5, 39.57) | 142.3-11239 (4159, 3907) | 252.4-11980 (5799, 4658) | 12292-306862 (188279, 121749) |
| Peridotite | 3 | 72.00-101.0 (82.33, 16.20) | 9.00-24.00 (18.90, 8.57) | 115.9-333.5 (251.8, 118.5) | 2.80-20.00 (8.22, 5.09) | 100.0-188.0 (152.7, 46.49) | 52.00-295.0 (121.8, 151.0) | 7.00-460.0 (171.3, 250.8) | 1345-11847 (4896, 6020) |

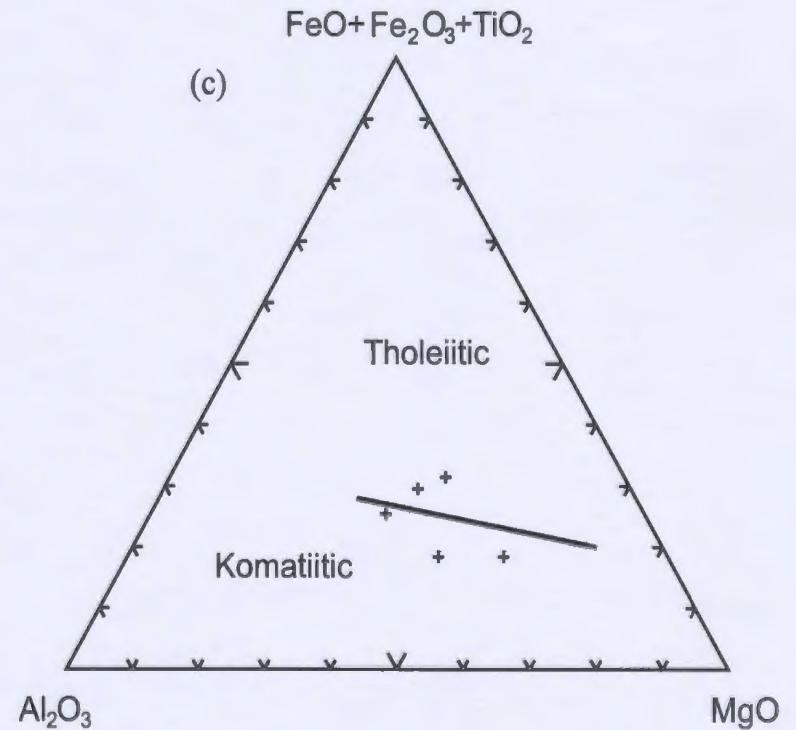
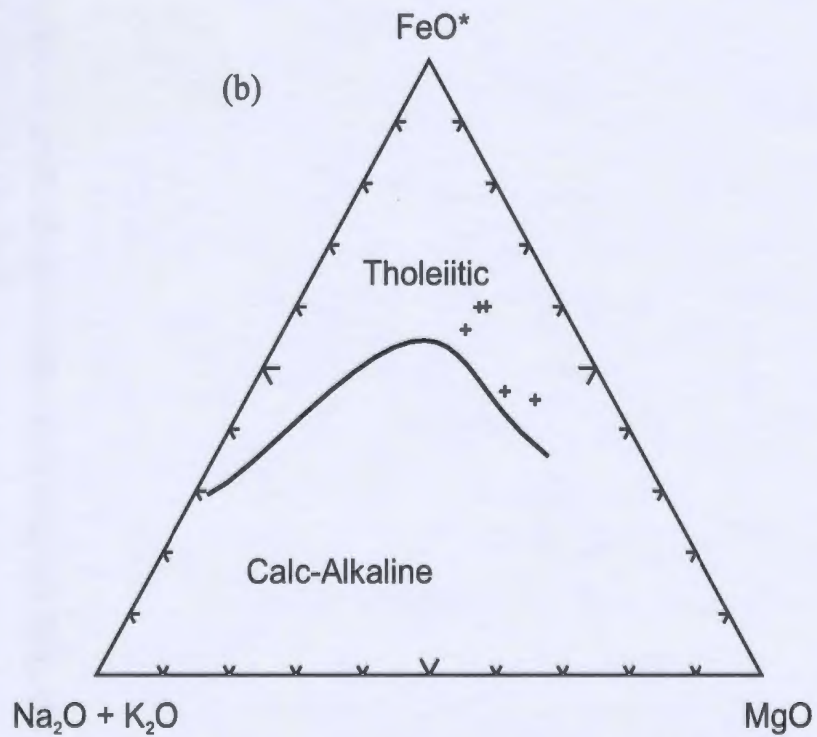
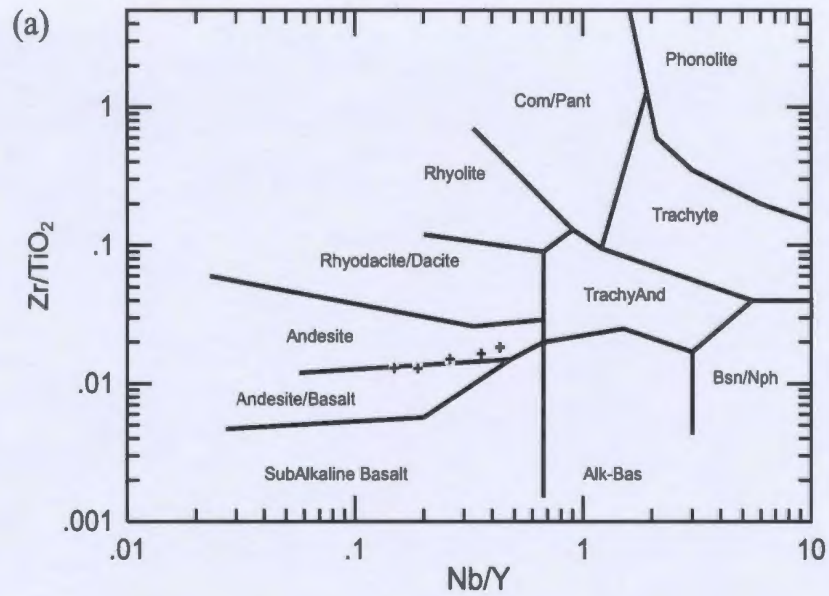


Figure 4.8 Discrimination diagrams for footwall mafic diabase dikes including (a) Winchester and Floyd (1977), Irvine and Baragar (1971), and (c) Jensen (1976).

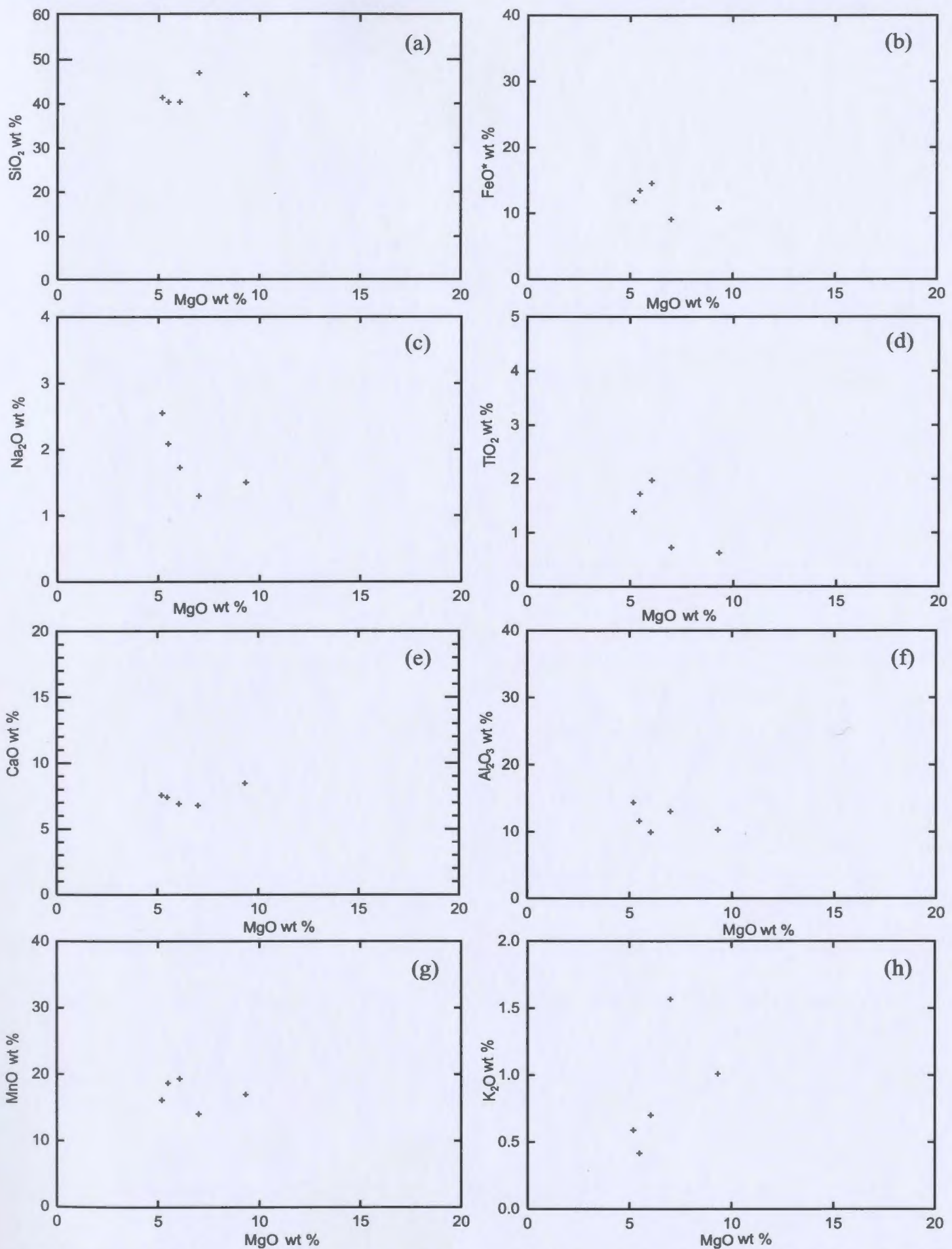


Figure 4.9. MgO versus major element plots of mafic diabase dikes including (a) SiO₂, (b) FeO*, (c) Na₂O, (d) TiO₂, (e) CaO, (f) Al₂O₃, (g) MnO, and (h) K₂O.

Table 4.5 Major element ranges (reported in wt %) of Mafic Dike samples

| | No. of samples | MgO wt % (mean, std. dev) | SiO ₂ wt % (mean, std. dev) | FeO* wt % (mean, std. dev) | Na ₂ O wt % (mean, std. dev) | TiO ₂ wt % (mean, std. dev) | CaO wt % (mean, std. dev) | Al ₂ O ₃ wt % (mean, std. dev) | MnO wt % (mean, std. dev) | K ₂ O wt % (mean, std. dev) | Mg # % (mean, std. dev) |
|----------------------|----------------|------------------------------|---|---------------------------------|--|---|------------------------------|---|----------------------------------|---|---------------------------------|
| Footwall mafic dikes | 5 | 5.19 9.33 (6.61, 1.67) | 40.41- 46.96 (42.25, 2.72) | 9.08- 14.53 (11.96, 2.15) | 1.30-2.55 (1.83, 0.50) | 0.63-1.97 (1.29, 0.60) | 6.79-8.46 (7.42, 0.66) | 9.91- 14.36 (11.83, 1.87) | 13.99- 19.31 (17.01, 2.12) | 0.42-1.57 (0.86-0.45) | 45.01- 63.36 (52.04-8.73) |

Table 4.6 Trace element ranges (reported in ppm) of Mafic Dike samples

| | No. of samples | Cr (ppm) (mean, std. dev) | Ga (ppm) (mean, std. dev) | Sr (ppm) (mean, std. dev) | Rb (ppm) (mean, std. dev) | V (ppm) (mean, std. dev) | Cu (ppm) (mean, std. dev) | Ni (ppm) (mean, std. dev) | S (ppm) (mean, std. dev) |
|----------------------|----------------|----------------------------------|----------------------------------|-----------------------------------|---------------------------------------|-----------------------------------|----------------------------------|---------------------------------|--------------------------------|
| Footwall mafic dikes | 5 | 61.00- 496.0 (175.6-184.0) | 14.70- 25.00 (20.90, 4.30) | 283.7- 375.2 (323.1, 36.40) | 8.70-55.70 (23.50, not calculated) | 164.0- 260.0 (218.0, 36.60) | 17.80- 40.90 (29.80, 8.30) | 7.00 46.00 (14.80, 17.44) | 1370- 10585 (4036, 3901) |

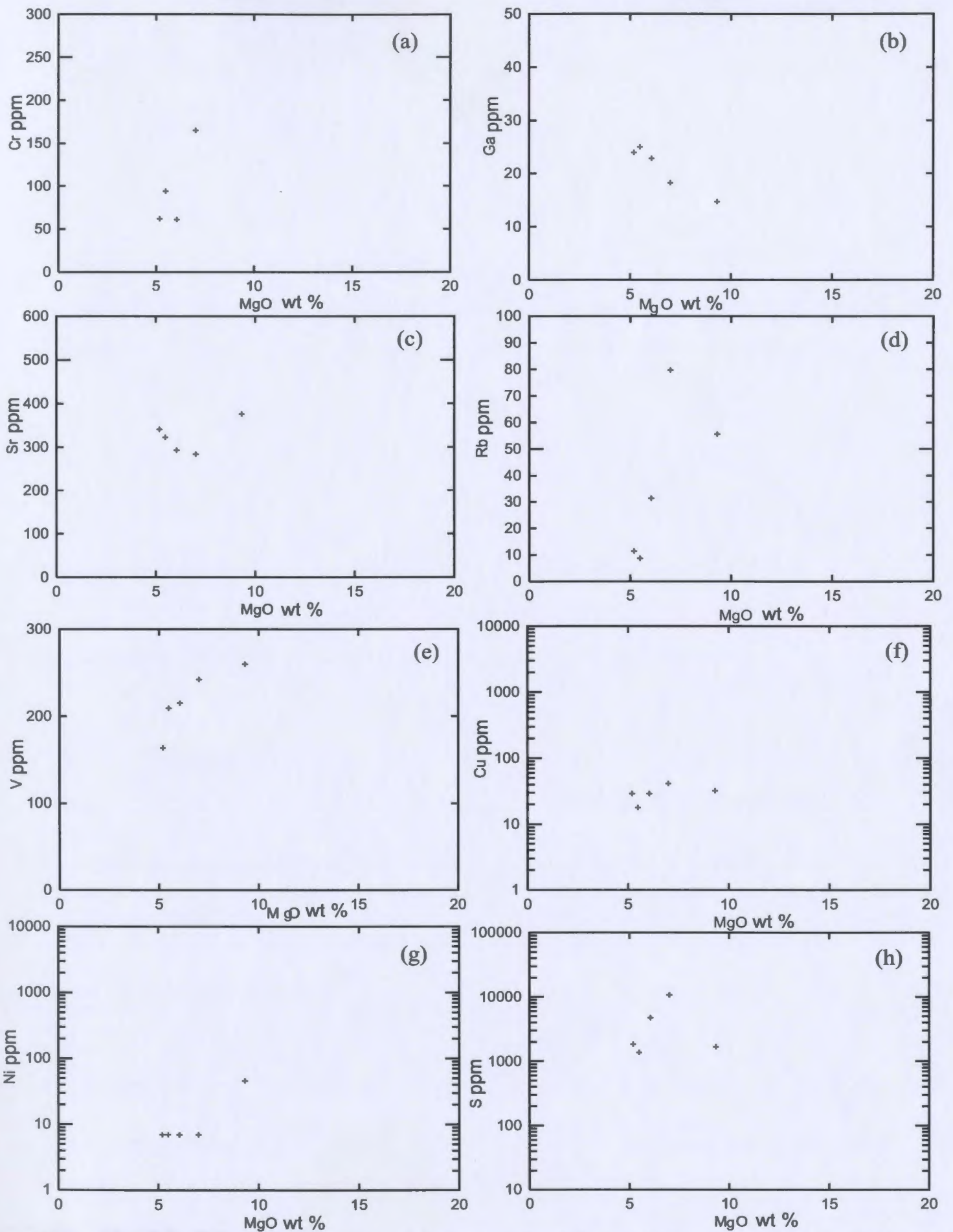


Figure 4.10. MgO versus trace element plots of mafic diabase dikes including (a) Cr, (b) Ga, (c) Sr, (d) Rb, (e) V, (f) Cu, (g) Ni, and (h) S.

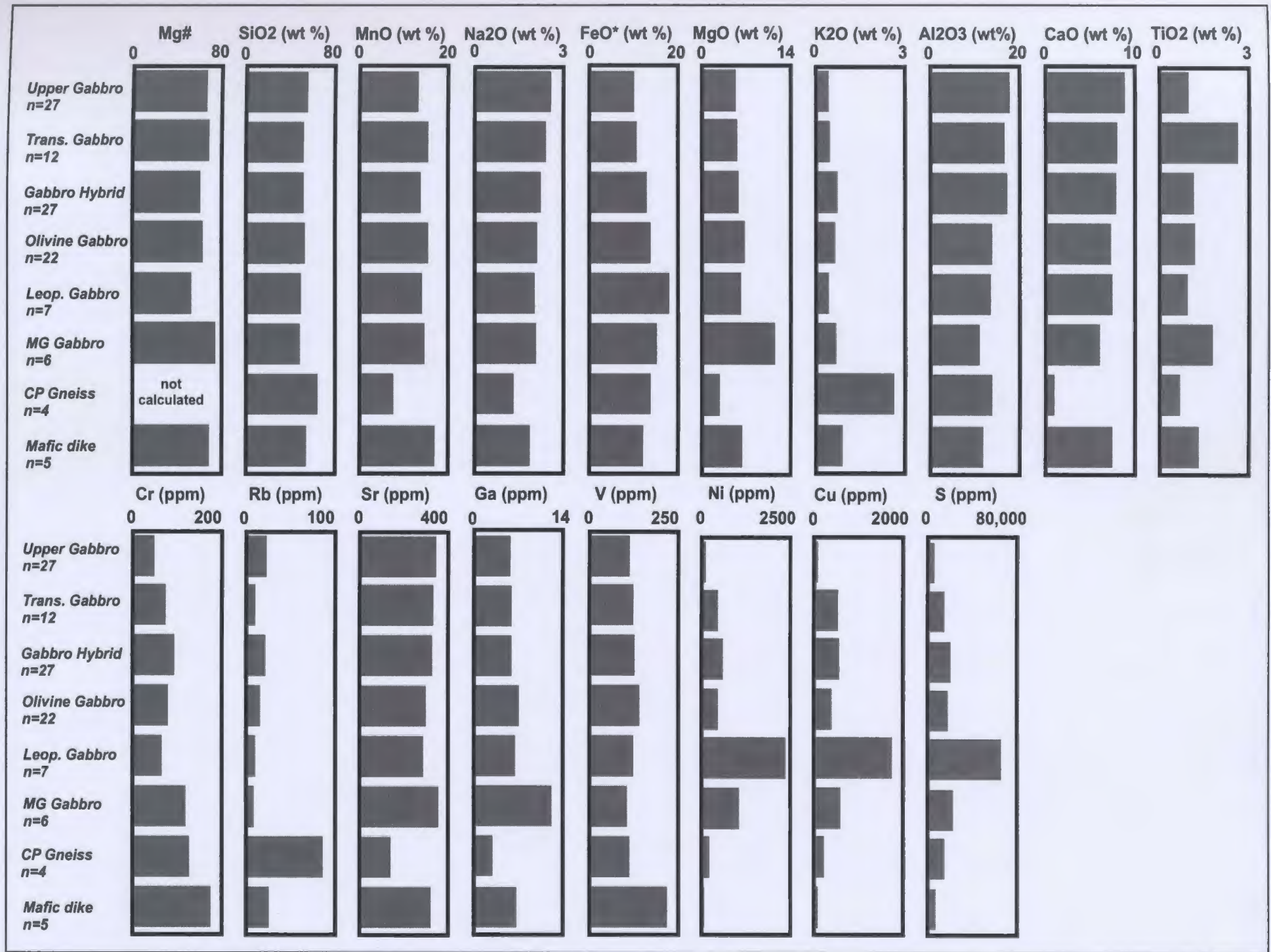


Figure 4.11. Calculated mean concentrations, presented as histograms, of major and trace element chemistry of Upper Gabbro (undifferentiated), Basal Gabbro (subunits defined), Churchill Province, and mafic dike samples. The placement of the sample categories is based on their relative location in the PLI stratigraphy defined in Chapter 3 (see Table 3.2 and Figure 3.5).

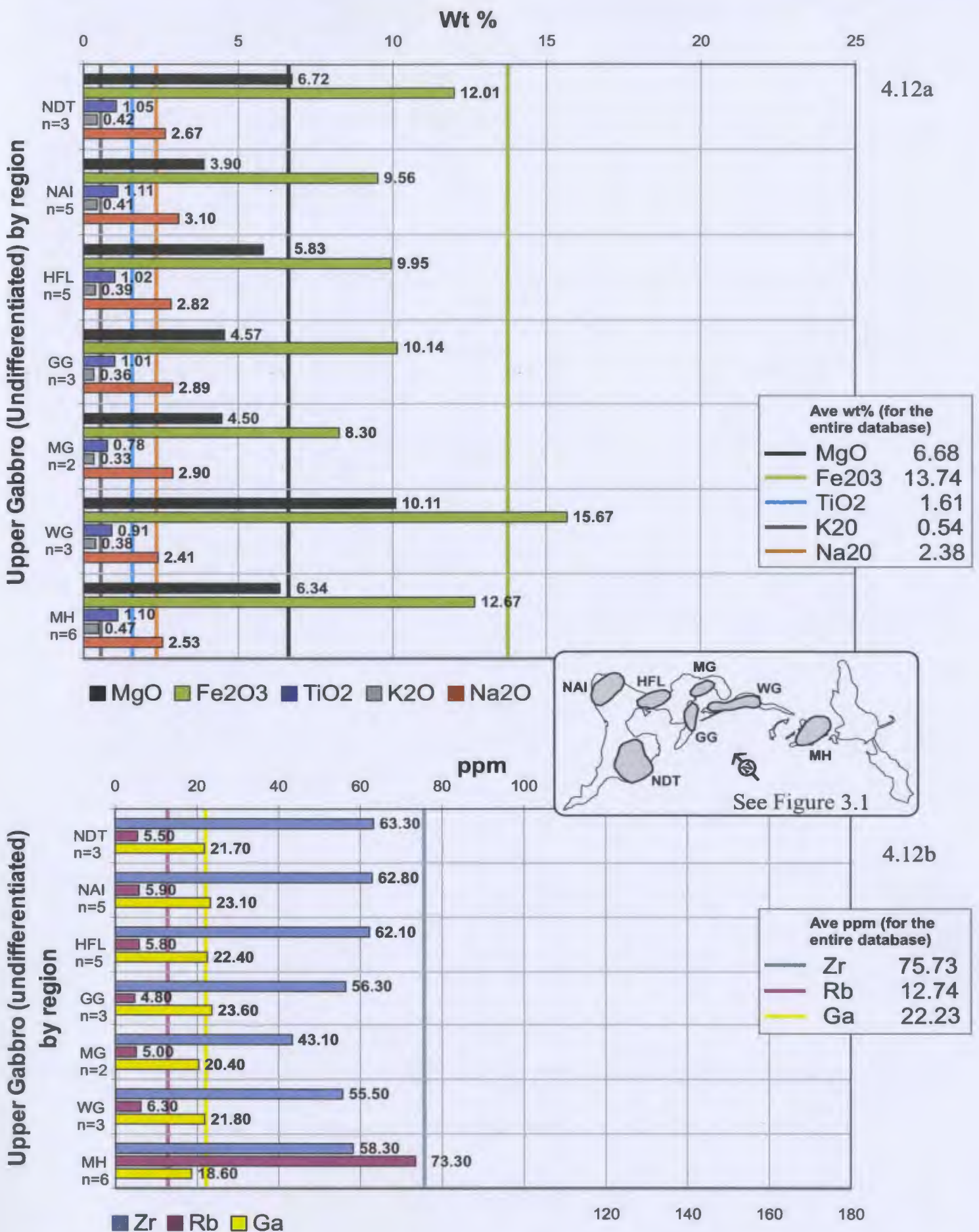


Figure 4.12: (A) Average major element abundances for the Upper Gabbro sample suite. (B) Average trace element abundances for the Upper Gabbro sample suite.

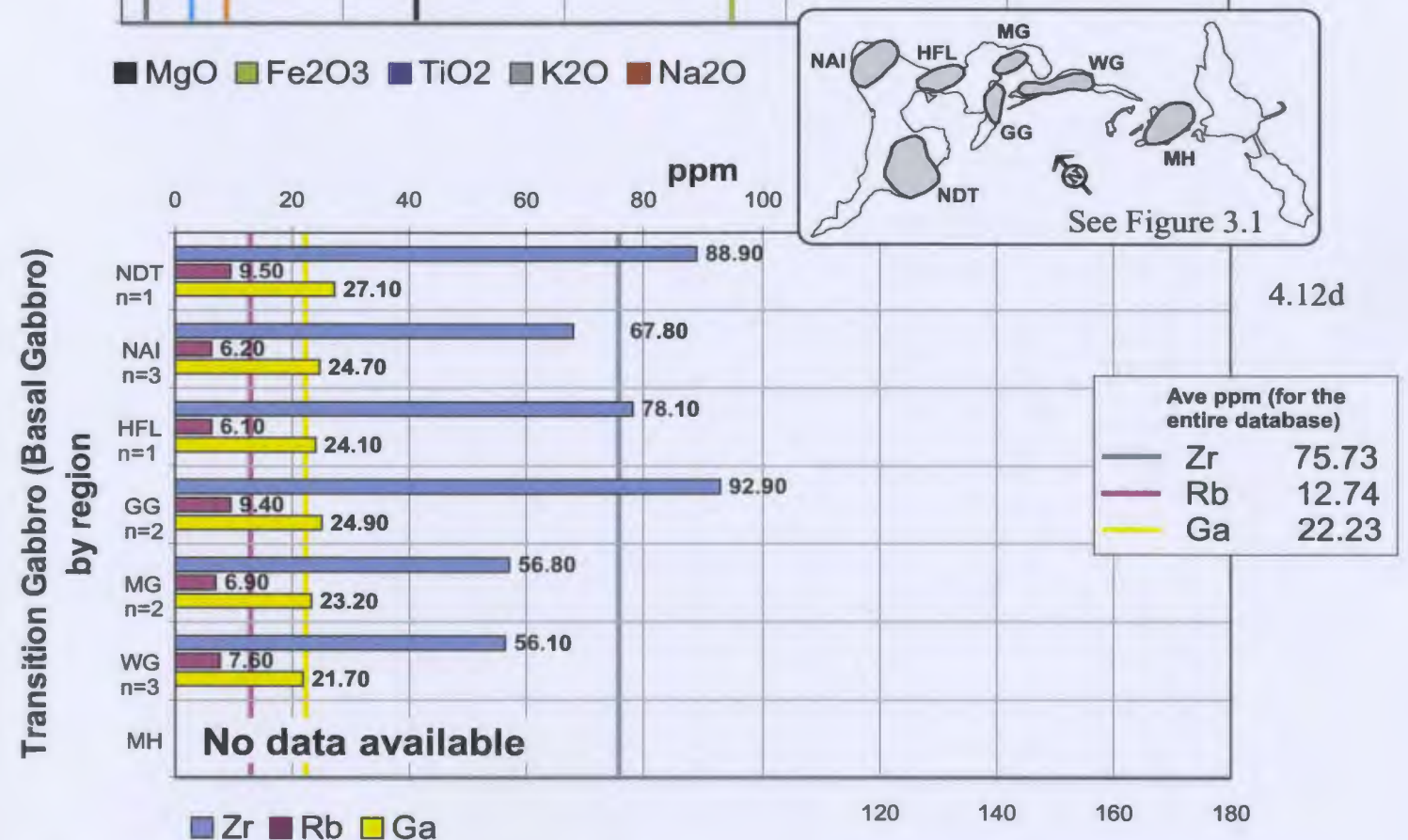
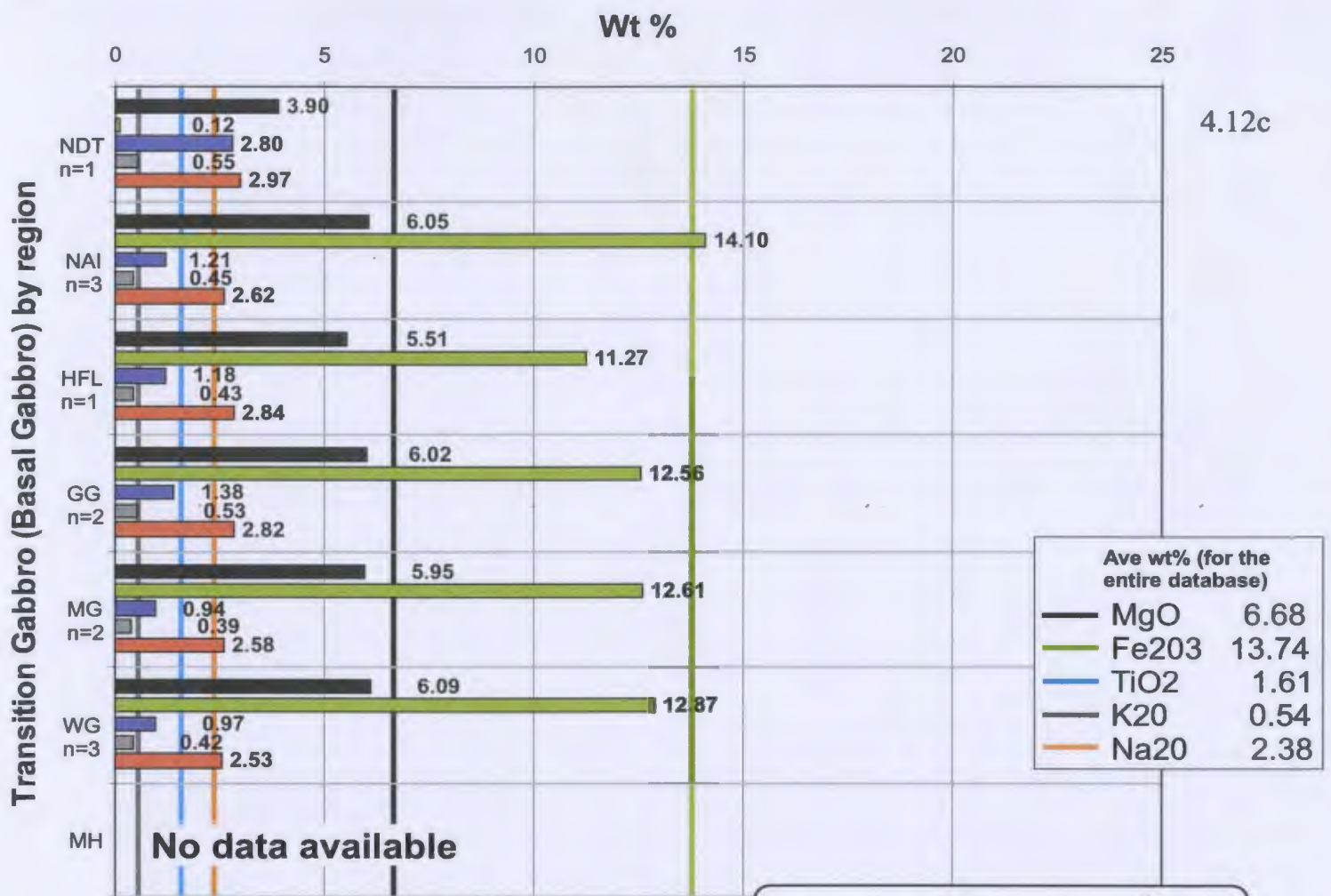


Figure 4.12: (C) Average major element abundances for the Transition Gabbro sample suite. (D) Average trace element abundances for the Transition Gabbro sample suite.

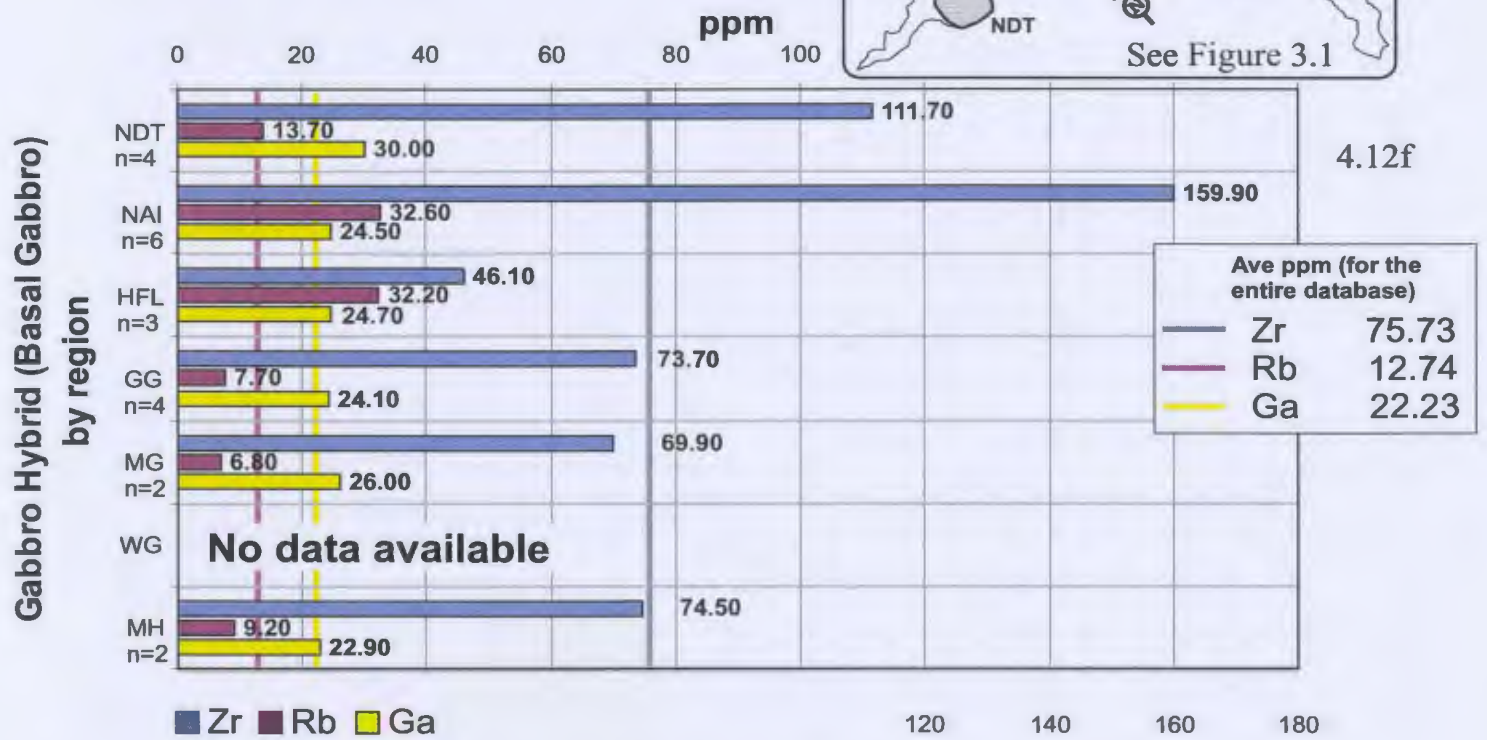
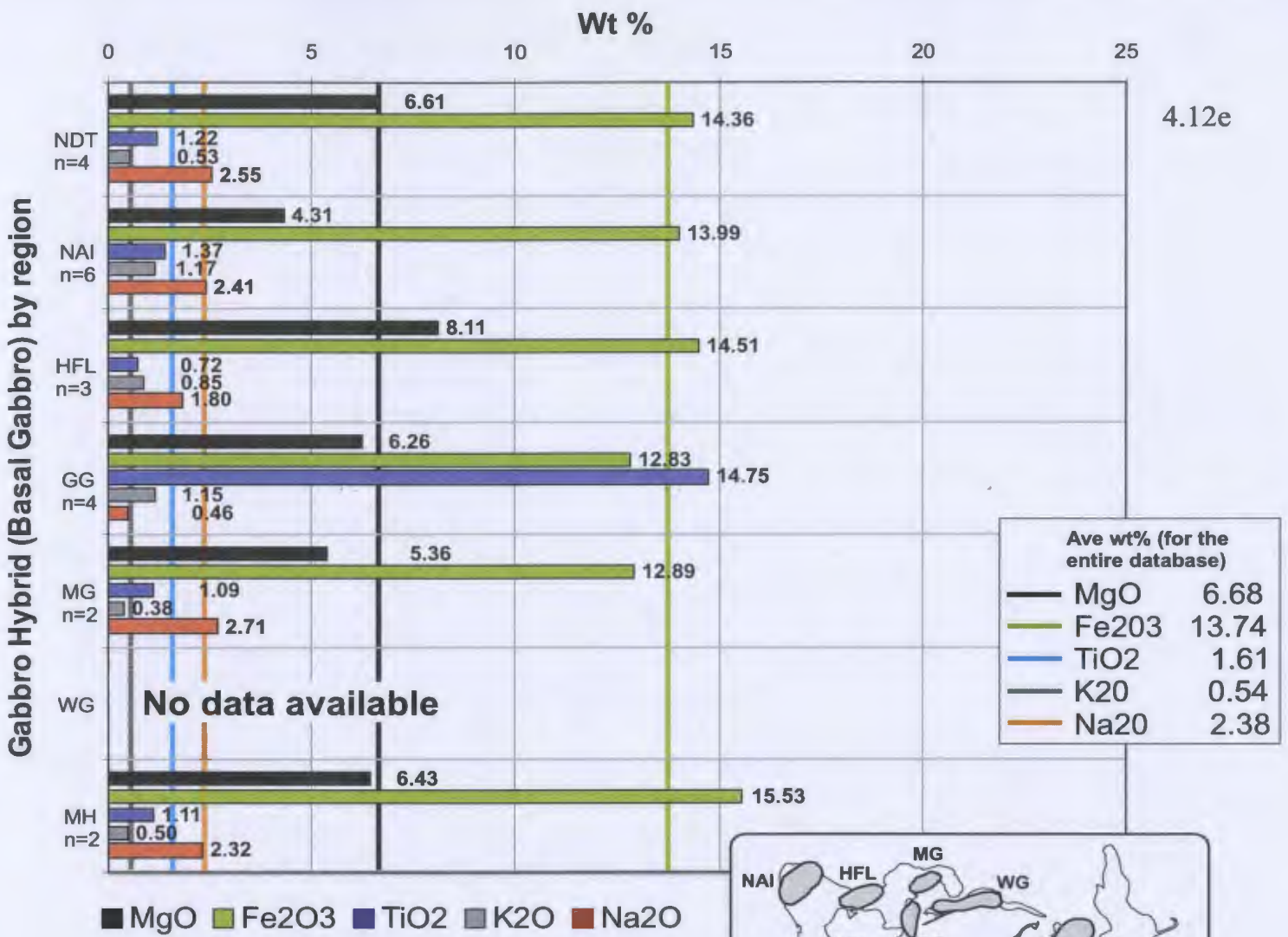


Figure 4.12: (E) Average major element abundances for the Gabbro Hybrid sample suite. (F) Average trace element abundances for the Gabbro Hybrid sample suite.

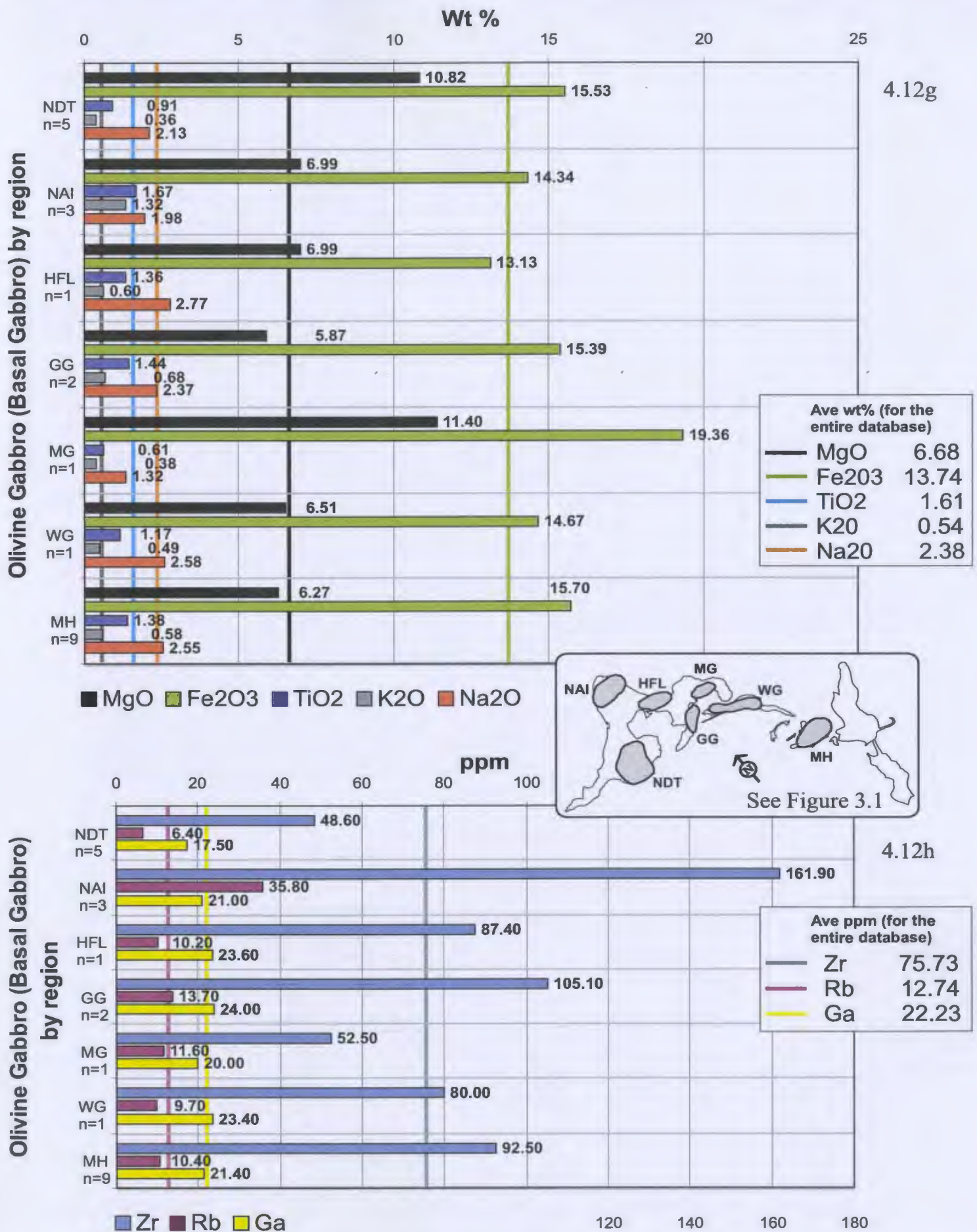


Figure 4.12: (G) Average major element abundances for the Olivine Gabbro sample suite. (H) Average trace element abundances for the Olivine Gabbro sample suite.

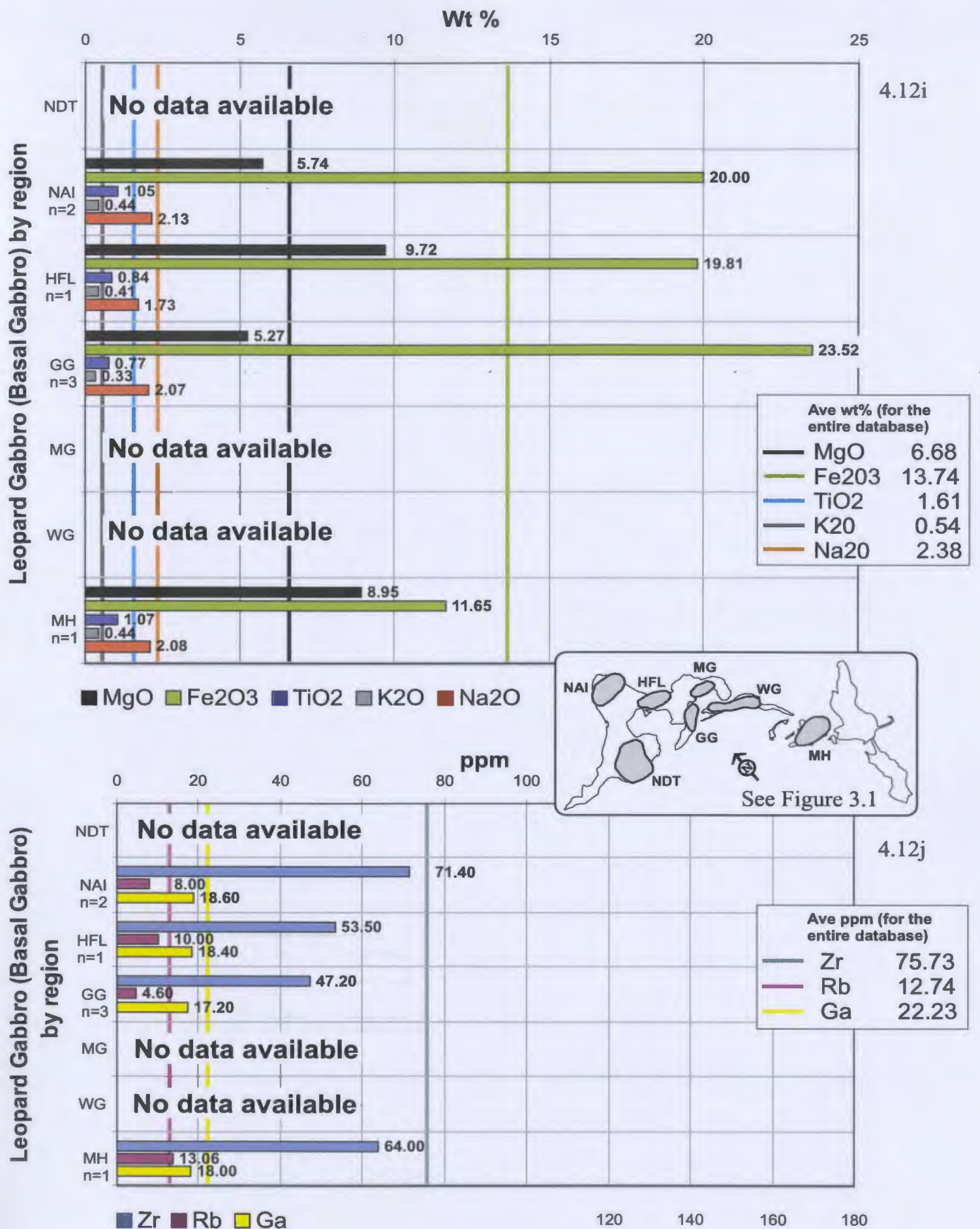


Figure 4.12: (I) Average major element abundances for the Leopard Gabbro sample suite. (J) Average trace element abundances for the Leopard Gabbro sample suite.

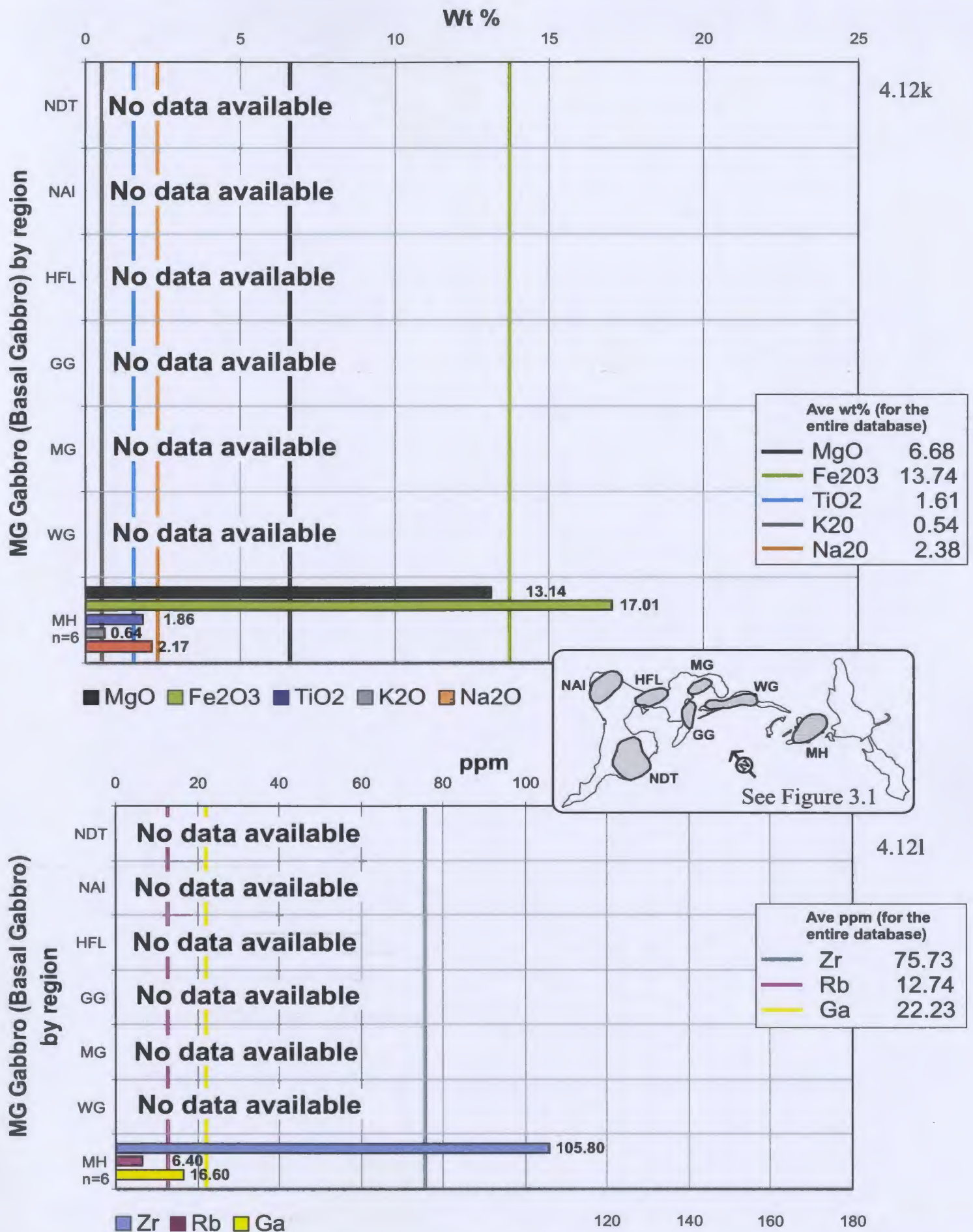


Figure 4.12: (K) Average major element abundances for the Medium-grained Gabbro sample suite. (L) Average trace element abundances for the Medium-grained Gabbro sample suite.

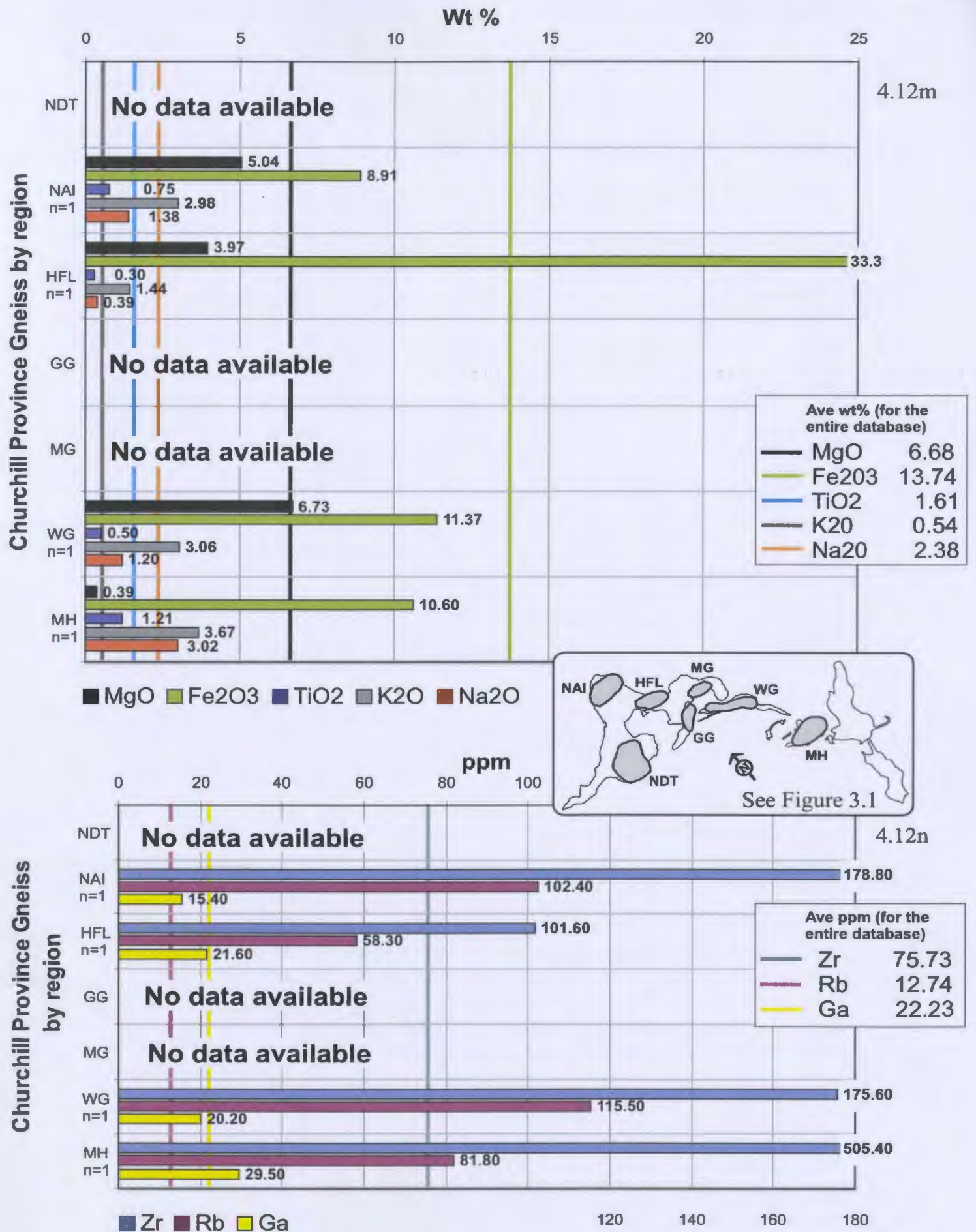


Figure 4.12: (M) Average major element abundances for the Churchill Province sample suite. (N) Average trace element abundances for the Churchill Province sample suite.

Table 4.7 Average major element (reported in wt %) and trace element (reported in ppm) compositions of rocks from the mineralized regions (see Figure 3.1) within the Upper Gabbro (**Up Gabbro**) of the Pants Lake Intrusion (subunits are undifferentiated). Average values calculated from the analytical results of samples reported in Appendix B.

| Region: rock association | NAI: Up Gabbro | NDT: Up Gabbro | HFL: Up Gabbro | MG: Up Gabbro | GG: Up Gabbro | WG: Up Gabbro | MH: Up Gabbro |
|--------------------------------|----------------|----------------|----------------|---------------|---------------|---------------|---------------|
| Average of n samples | (n=5) | (n=3) | (n=5) | (n=2) | (n=3) | (n=3) | (n=6) |
| SiO ₂ | 45.08 | 43.91 | 45.25 | 45.19 | 44.79 | 42.00 | 42.49 |
| Al ₂ O ₃ | 21.27 | 18.55 | 20.00 | 20.59 | 20.43 | 15.21 | 17.41 |
| Fe ₂ O ₃ | 9.56 | 12.01 | 9.95 | 8.30 | 10.14 | 15.67 | 12.67 |
| MgO | 3.90 | 6.72 | 5.83 | 4.50 | 4.57 | 10.11 | 6.34 |
| CaO | 10.28 | 9.11 | 10.13 | 10.64 | 10.26 | 7.75 | 9.04 |
| Na ₂ O | 3.10 | 2.67 | 2.82 | 2.90 | 2.89 | 2.41 | 2.53 |
| K ₂ O | 0.41 | 0.42 | 0.39 | 0.33 | 0.36 | 0.38 | 0.47 |
| TiO ₂ | 1.11 | 1.05 | 1.02 | 0.78 | 1.01 | 0.91 | 1.10 |
| MnO | 13.00 | 15.67 | 12.80 | 11.50 | 13.33 | 19.67 | 14.33 |
| P ₂ O ₅ | 0.14 | 0.18 | 0.13 | 0.10 | 0.13 | 0.14 | 0.16 |
| S | 1,301 | 1,013 | 980 | 897 | 1,166 | 1,188 | 8,986 |
| Ni | 19.00 | 62.90 | 31.40 | 19.40 | 22.60 | 100.4 | 127.9 |
| Cu | 24.50 | 28.50 | 20.1 | 25.30 | 32.60 | 33.60 | 144.6 |
| Cr | 32.20 | 45.70 | 35.40 | 72.50 | 39.70 | 40.30 | 62.00 |
| Zn | 36.10 | 41.80 | 36.70 | 20.20 | 32.60 | 57.50 | 44.20 |
| Pb | 6.00 | 5.70 | 6.20 | 6.00 | 6.00 | 5.80 | 7.00 |
| Ba | 188.9 | 203.5 | 147.6 | 143.0 | 183.2 | 159.9 | 192.7 |
| Sc | 19.60 | 19.70 | 21.40 | 22.50 | 18.30 | 19.70 | 21.70 |
| Ga | 23.10 | 21.70 | 22.40 | 20.40 | 23.60 | 21.80 | 18.60 |
| Rb | 5.90 | 5.50 | 5.80 | 5.00 | 4.80 | 6.30 | 73.30 |
| Sr | 388.5 | 336.3 | 379.3 | 375.1 | 373.2 | 288.9 | 299.2 |
| Y | 17.60 | 19.00 | 17.10 | 14.60 | 16.50 | 16.50 | 24.10 |
| Zr | 62.80 | 63.30 | 62.10 | 43.10 | 56.30 | 55.50 | 58.30 |
| Nb | 2.70 | 2.40 | 3.00 | 1.20 | 2.50 | 2.60 | 35.60 |
| V | 104.4 | 111.7 | 112.6 | 112.5 | 104.7 | 97.70 | 116.3 |
| Cl | 160.4 | 88.70 | 307.6 | 203.5 | 87.30 | 123.0 | 156.5 |

Table 4.8 Average major element (reported in wt %) and trace element (reported in ppm) compositions of rocks from the mineralized regions (see Figure 3.1) within the Basal Gabbro of the Pants Lake Intrusion. **Tr Gabbro** indicates the Transition Gabbro subunit. Average values calculated from the analytical results of samples reported in Appendix B.

| Region: rock association | NAI: Tr Gabbro | NDT: Tr Gabbro | HFL: Tr Gabbro | MJ: Tr Gabbro | GG: Tr Gabbro | WG: Tr Gabbro |
|--------------------------------|----------------|----------------|----------------|---------------|---------------|---------------|
| Average of n samples | (n=3) | (n=1) | (n=1) | (n=2) | (n=2) | (n=3) |
| SiO ₂ | 42.35 | 42.46 | 43.60 | 43.00 | 43.66 | 42.66 |
| Al ₂ O ₃ | 17.44 | 17.75 | 18.30 | 18.69 | 17.52 | 18.90 |
| Fe ₂ O ₃ | 14.10 | 0.12 | 11.27 | 12.61 | 12.56 | 12.87 |
| MgO | 6.05 | 3.90 | 5.51 | 5.95 | 6.02 | 6.09 |
| CaO | 9.11 | 0.55 | 9.68 | 9.71 | 8.83 | 9.60 |
| Na ₂ O | 2.62 | 2.97 | 2.84 | 2.58 | 2.82 | 2.53 |
| K ₂ O | 0.45 | 0.55 | 0.43 | 0.39 | 0.53 | 0.42 |
| TiO ₂ | 1.21 | 28.00 | 1.18 | 0.94 | 1.38 | 0.97 |
| MnO | 16.33 | 43.00 | 15.00 | 14.00 | 15.50 | 14.67 |
| P ₂ O ₅ | 0.16 | 0.19 | 0.18 | 0.14 | 0.20 | 0.12 |
| S | 10,698 | 24,710 | 1,228 | 11,057 | 5,357 | 9,720 |
| Ni | 491.9 | 14.10 | 41.10 | 588.2 | 242.3 | 533.9 |
| Cu | 390.6 | 2162 | 31.30 | 486.0 | 165.4 | 479.6 |
| Cr | 55.70 | 170.0 | 49.00 | 70.50 | 50.00 | 79.30 |
| Zn | 57.3 | 48.10 | 38.50 | 42.30 | 52.20 | 46.30 |
| Pb | 9.20 | 7.40 | 6.00 | 7.50 | 6.00 | 7.30 |
| Ba | 212.4 | 216.6 | 204.2 | 163.6 | 273.5 | 179.9 |
| Sc | 27.00 | 9.10 | 25.00 | 15.50 | 17.50 | 19.00 |
| Ga | 24.70 | 27.10 | 24.10 | 23.20 | 24.90 | 21.70 |
| Rb | 6.20 | 9.50 | 6.10 | 6.90 | 9.40 | 7.60 |
| Sr | 312.8 | 365.0 | 347.3 | 333.2 | 326.5 | 334.6 |
| Y | 18.90 | 24.70 | 21.70 | 16.80 | 24.00 | 15.80 |
| Zr | 67.80 | 88.90 | 78.10 | 56.80 | 92.90 | 56.10 |
| Nb | 1.60 | 3.80 | 3.10 | 2.20 | 3.80 | 0.70 |
| V | 148.7 | 1.60 | 134.0 | 115.5 | 146.0 | 119.7 |
| Cl | 252.3 | 0.20 | 82.00 | 73.00 | 68.00 | 91.70 |

Table 4.8 Continued. **G Hybrid** indicates the Gabbro Hybrid subunit

| Region: rock association | MH: G Hybrid | NAI: G Hybrid | NDT: G Hybrid | HFL: G Hybrid | MJ: G Hybrid | GG: G Hybrid |
|------------------------------------|---------------------|----------------------|----------------------|----------------------|---------------------|---------------------|
| Average of n samples | (n=6) | (n=6) | (n=4) | (n=3) | (n=2) | (n=4) |
| SiO₂ | 40.89 | 45.05 | 42.04 | 40.68 | 43.03 | 43.56 |
| Al₂O₃ | 16.22 | 16.66 | 18.08 | 17.41 | 19.00 | 18.28 |
| Fe₂O₃ | 15.53 | 13.99 | 14.36 | 14.51 | 12.89 | 12.83 |
| MgO | 6.43 | 4.31 | 6.61 | 8.11 | 5.36 | 6.26 |
| CaO | 8.26 | 8.11 | 8.22 | 7.73 | 9.49 | 9.09 |
| Na₂O | 2.32 | 2.41 | 2.55 | 1.80 | 2.71 | 2.67 |
| K₂O | 0.50 | 1.17 | 0.53 | 0.85 | 0.38 | 0.46 |
| TiO₂ | 1.11 | 1.37 | 1.22 | 0.72 | 1.09 | 1.15 |
| MnO | 14.67 | 14.17 | 15.25 | 15.00 | 14.00 | 14.75 |
| P₂O₅ | 0.18 | 0.44 | 0.20 | 0.09 | 0.15 | 0.18 |
| S | 18,917 | 16,464 | 13,739 | 15,983 | 11,384 | 9,817 |
| Ni | 386.7 | 702.3 | 738.9 | 810.0 | 685.0 | 527.6 |
| Cu | 414.3 | 655.6 | 630.7 | 687.7 | 543.3 | 459.5 |
| Cr | 88.70 | 88.70 | 110.8 | 125.0 | 99.00 | 71.80 |
| Zn | 67.40 | 71.70 | 69.80 | 77.00 | 50.50 | 53.10 |
| Pb | 6.80 | 13.30 | 7.20 | 14.30 | 6.10 | 7.30 |
| Ba | 258.4 | 405.1 | 186.0 | 255.4 | 177.8 | 217.7 |
| Sc | 15.70 | 25.30 | 22.00 | 14.70 | 15.00 | 14.80 |
| Ga | 22.90 | 24.50 | 30.00 | 24.70 | 26.00 | 24.10 |
| Rb | 9.20 | 32.60 | 13.70 | 32.20 | 6.80 | 7.70 |
| Sr | 335.9 | 340.6 | 304.0 | 306.4 | 328.5 | 337.9 |
| Y | 17.90 | 22.20 | 25.00 | 11.50 | 18.80 | 20.20 |
| Zr | 74.50 | 159.9 | 111.7 | 46.10 | 69.90 | 73.70 |
| Nb | 4.10 | 7.60 | 5.10 | 1.30 | 2.70 | 4.20 |
| V | 123.8 | 120.3 | 159.8 | 116.7 | 139.5 | 128.5 |
| Cl | 157.7 | 211.8 | 95.00 | 892.0 | 87.50 | 92.30 |

Table 4.8 Continued. **LT Gabbro** indicates the Leopard Textured Gabbro subunit, and **SM Sulphide** indicates Semi-Massive Sulphide.

| Region: rock association | NAI: LT Gabbro | HFL: LT Gabbro | GG: LT Gabbro | MH: LT Gabbro | NAI: SM Sulphide | HFL: SM Sulphide | MJ: SM Sulphide |
|--------------------------------|----------------|----------------|---------------|---------------|------------------|------------------|-----------------|
| Average of n samples | (n=2) | (n=1) | (n=3) | (n=1) | (n=2) | (n=2) | (n=2) |
| SiO ₂ | 36.99 | 39.39 | 35.70 | 42.29 | 8.42 | 19.68 | 53.71 |
| Al ₂ O ₃ | 13.75 | 12.78 | 13.51 | 15.69 | 1.24 | 4.50 | 10.11 |
| Fe ₂ O ₃ | 20.00 | 19.81 | 23.52 | 11.65 | 51.34 | 43.20 | 15.89 |
| MgO | 5.74 | 9.72 | 5.27 | 8.95 | 0.51 | 0.82 | 4.34 |
| CaO | 7.51 | 7.14 | 7.31 | 8.66 | 0.40 | 0.32 | 1.56 |
| Na ₂ O | 2.13 | 1.73 | 2.07 | 2.08 | 0.12 | 0.40 | 1.25 |
| K ₂ O | 0.44 | 0.41 | 0.33 | 0.44 | 0.15 | 0.59 | 1.82 |
| TiO ₂ | 1.05 | 0.84 | 0.77 | 1.07 | 0.11 | 0.14 | 0.54 |
| MnO | 14.50 | 16.00 | 14.00 | 14.00 | 5.50 | 3.50 | 9.50 |
| P ₂ O ₅ | 0.15 | 0.10 | 0.10 | 0.13 | 0.01 | 0.02 | 0.06 |
| S | 42,245 | 36,424 | 74,136 | 547.0 | 274,804 | 248,956 | 41,081 |
| Ni | 1,926 | 1,197 | 3,821 | 31.00 | 10,871 | 5,601 | 925.2 |
| Cu | 1577 | 1118 | 2634 | 30.00 | 7704 | 3963 | 811.1 |
| Cr | 73.00 | 59.00 | 59.30 | 56.00 | 192.5 | 317.0 | 174.5 |
| Zn | 70.50 | 91.10 | 68.90 | 65.00 | 336.5 | 144.9 | 109.0 |
| Pb | 30.00 | 21.30 | 9.30 | 6.00 | 14.90 | 28.20 | 27.90 |
| Ba | 179.8 | 115.1 | 132.4 | 176.0 | 30.00 | 81.50 | 348.4 |
| Sc | 20.00 | 27.00 | 17.70 | 25.00 | 11.00 | 11.00 | 12.00 |
| Ga | 18.60 | 18.40 | 17.20 | 18.00 | 4.00 | 10.60 | 15.20 |
| Rb | 8.00 | 10.00 | 4.60 | 13.60 | 5.80 | 19.50 | 55.30 |
| Sr | 289.1 | 266.7 | 275.7 | 341.2 | 49.40 | 29.80 | 122.6 |
| Y | 19.70 | 13.30 | 13.40 | 18.10 | 2.00 | 8.20 | 15.50 |
| Zr | 71.40 | 53.50 | 47.20 | 64.00 | 15.40 | 67.00 | 106.7 |
| Nb | 3.60 | 0.70 | 1.60 | 0.70 | 37.90 | 3.30 | 6.60 |
| V | 136.5 | 132.0 | 108.7 | 115.0 | 101.5 | 175.0 | 151.0 |
| Cl | 164.5 | 259.0 | 125.0 | 278.0 | 106.5 | 254.5 | 752.0 |

Table 4.8 Continued. **OI Gabbro** indicates the Olivine Gabbro subunit.

| Region: rock association | NAI: OI Gabbro | NDT: OI Gabbro | HFL: OI Gabbro | MG: OI Gabbro | GG: OI Gabbro | WG: OI Gabbro | MH: OI Gabbro |
|------------------------------------|-----------------------|-----------------------|-----------------------|----------------------|----------------------|----------------------|----------------------|
| Average of n samples | (n=3) | (n=5) | (n=1) | (n=1) | (n=2) | (n=1) | (n=9) |
| SiO₂ | 47.32 | 41.78 | 44.13 | 38.11 | 43.71 | 41.92 | 42.49 |
| Al₂O₃ | 13.50 | 15.48 | 16.60 | 11.14 | 14.86 | 16.20 | 15.22 |
| Fe₂O₃ | 14.34 | 15.53 | 13.13 | 19.36 | 15.39 | 14.67 | 15.70 |
| MgO | 6.99 | 10.82 | 6.99 | 11.40 | 5.87 | 6.51 | 6.27 |
| CaO | 7.24 | 7.83 | 8.55 | 6.07 | 7.87 | 8.40 | 8.12 |
| Na₂O | 1.98 | 2.13 | 2.77 | 1.32 | 2.37 | 2.58 | 2.55 |
| K₂O | 1.32 | 0.36 | 0.60 | 0.38 | 0.68 | 0.49 | 0.58 |
| TiO₂ | 1.67 | 0.91 | 1.36 | 0.60 | 1.44 | 1.17 | 1.38 |
| MnO | 18.00 | 17.20 | 16.00 | 14.00 | 16.00 | 16.00 | 17.00 |
| P₂O₅ | 0.56 | 0.12 | 0.20 | 0.09 | 0.22 | 0.17 | 0.23 |
| S | 3,600 | 7,530 | 3,842 | 42,370 | 16,779 | 13,510 | 14,352 |
| Ni | 108.8 | 495.4 | 81.40 | 1,855 | 1,202 | 411.7 | 197.1 |
| Cu | 118.8 | 251.3 | 75.10 | 2378 | 939.7 | 451.2 | 204.2 |
| Cr | 134.7 | 66.00 | 66.00 | 89.00 | 63.50 | 69.00 | 70.40 |
| Zn | 75.00 | 59.70 | 58.30 | 103.8 | 65.50 | 54.00 | 66.40 |
| Pb | 10.40 | 7.20 | 8.50 | 25.20 | 6.40 | 11.50 | 8.40 |
| Ba | 567.6 | 172.4 | 263.8 | 138.8 | 377.2 | 236.0 | 304.4 |
| Sc | 37.00 | 18.20 | 23.00 | 15.00 | 22.00 | 22.00 | 22.30 |
| Ga | 21.00 | 17.50 | 23.60 | 20.00 | 24.00 | 23.40 | 21.40 |
| Rb | 35.80 | 6.40 | 10.20 | 11.60 | 13.70 | 9.70 | 10.40 |
| Sr | 267.7 | 295.8 | 320.3 | 263.0 | 314.6 | 314.4 | 311.7 |
| Y | 29.40 | 13.20 | 21.50 | 13.50 | 21.30 | 21.60 | 22.90 |
| Zr | 161.9 | 48.60 | 87.40 | 52.50 | 105.1 | 80.00 | 92.50 |
| Nb | 9.60 | 3.50 | 4.60 | 0.70 | 6.60 | 2.70 | 4.50 |
| V | 193.0 | 104.6 | 138.0 | 86.00 | 141.0 | 145.0 | 146.6 |
| Cl | 195.0 | 242.4 | 92.00 | 666.0 | 124.0 | 102.0 | 112.9 |

Table 4.8 Continued. **MG Gabbro** indicates the Medium-Grained Gabbro subunit.

| Region: rock Association | MH: MG Gabbro | NAI: Peridotite | MH: Peridotite |
|------------------------------------|----------------------|------------------------|-----------------------|
| Average of n samples | (n=6) | (n=1) | (n=2) |
| SiO₂ | 38.33 | 44.39 | 40.90 |
| Al₂O₃ | 11.44 | 15.22 | 10.86 |
| Fe₂O₃ | 17.01 | 13.56 | 18.13 |
| MgO | 13.14 | 9.13 | 15.94 |
| CaO | 6.34 | 8.05 | 6.25 |
| Na₂O | 2.17 | 2.23 | 1.75 |
| K₂O | 0.64 | 0.67 | 0.42 |
| TiO₂ | 1.86 | 1.25 | 1.09 |
| MnO | 15.50 | 18.00 | 21.00 |
| P₂O₅ | 0.58 | 0.18 | 0.15 |
| S | 15,705 | 1,497 | 6,596 |
| Ni | 1,026 | 47.00 | 233.5 |
| Cu | 559.7 | 52.00 | 156.7 |
| Cr | 118.8 | 72.00 | 87.50 |
| Zn | 82.50 | 60.00 | 76.60 |
| Pb | 12.30 | 9.00 | 6.50 |
| Ba | 322.2 | 310.0 | 219.7 |
| Sc | 11.70 | 23.00 | 23.00 |
| Ga | 16.60 | 24.00 | 16.40 |
| Rb | 6.40 | 12.90 | 5.90 |
| Sr | 355.7 | 305.9 | 224.7 |
| Y | 18.60 | 20.30 | 16.90 |
| Zr | 105.80 | 85.50 | 62.20 |
| Nb | 7.20 | 3.60 | 2.70 |
| V | 102.0 | 170.0 | 144.0 |
| Cl | 821.8 | 315.0 | 888.0 |

Table 4.9 Average major element (reported in wt %) and trace element (reported in ppm) compositions of samples from footwall mafic dikes (FW dike) and Churchill Province gneisses (CP gneiss) within the mineralized regions of the Pants Lake Intrusion. Average values calculated from the analytical results of samples reported in Appendix B.

| Region: rock association | NDT: FW dike | MG: FW dike | WG: FW dike | MH: FW dike | NAI: CP gneiss | HFL: CP gneiss | WG: CP gneiss | MH: CP gneiss |
|--------------------------------|--------------|-------------|-------------|-------------|----------------|----------------|---------------|---------------|
| Average of n samples | (n=1) | (n=2) | (n=1) | (n=1) | (n=1) | (n=1) | (n=1) | (n=1) |
| SiO ₂ | 47.08 | 48.20 | 46.23 | 45.48 | 60.58 | 29.23 | 52.02 | 57.98 |
| Al ₂ O ₃ | 11.50 | 12.63 | 16.05 | 13.03 | 13.06 | 11.49 | 16.50 | 15.02 |
| Fe ₂ O ₃ | 11.97 | 13.12 | 13.29 | 14.94 | 8.91 | 33.30 | 11.37 | 10.60 |
| MgO | 10.44 | 7.21 | 5.80 | 6.17 | 5.04 | 3.97 | 6.73 | 0.39 |
| CaO | 9.47 | 7.58 | 8.43 | 8.33 | 1.79 | 0.15 | 0.40 | 5.15 |
| Na ₂ O | 1.69 | 1.68 | 2.85 | 2.35 | 1.38 | 0.39 | 1.20 | 3.02 |
| K ₂ O | 1.13 | 1.24 | 0.66 | 0.47 | 2.98 | 1.44 | 3.06 | 3.67 |
| TiO ₂ | 0.70 | 1.52 | 1.55 | 1.94 | 0.75 | 0.30 | 0.50 | 1.21 |
| MnO | 19.00 | 18.50 | 18.00 | 21.00 | 10.00 | 5.00 | 5.00 | 12.00 |
| P ₂ O ₅ | 0.17 | 0.23 | 0.23 | 0.25 | 0.04 | 0.01 | 0.03 | 0.44 |
| S | 1,664 | 7,651 | 1,846 | 1,370 | 4,958 | 130,524 | 17,341 | 944 |
| Ni | 46.0 | 7.00 | 7.00 | 7.00 | 178.8 | 3,485 | 214.5 | 7.00 |
| Cu | 32.30 | 34.90 | 29.20 | 17.80 | 213.3 | 2210 | 202.6 | 10.00 |
| Cr | 496.0 | 113.0 | 62.00 | 94.00 | 314.0 | 329.0 | 232.0 | 11.00 |
| Zn | 381.3 | 342.7 | 63.90 | 58.60 | 123.9 | 256.9 | 164.7 | 126.1 |
| Pb | 67.10 | 17.90 | 6.00 | 6.00 | 24.30 | 14.70 | 28.10 | 20.30 |
| Ba | 321.4 | 366.7 | 384.1 | 319.2 | 778.3 | 175.7 | 657.4 | 1862.2 |
| Sc | 42.00 | 30.50 | 34.00 | 36.00 | 35.00 | 11.00 | 17.00 | 25.00 |
| Ga | 14.70 | 20.50 | 23.90 | 25.00 | 15.40 | 21.60 | 20.20 | 29.50 |
| Rb | 55.70 | 55.50 | 11.40 | 8.70 | 102.4 | 58.30 | 115.5 | 81.80 |
| Sr | 375.2 | 288.5 | 340.4 | 322.7 | 245.8 | 55.50 | 92.70 | 294.5 |
| Y | 14.30 | 23.10 | 26.30 | 31.50 | 20.00 | 6.20 | 17.90 | 64.20 |
| Zr | 61.90 | 116.6 | 108.0 | 156.1 | 178.8 | 101.6 | 175.6 | 505.4 |
| Nb | 5.10 | 6.20 | 3.90 | 8.20 | 10.10 | 7.40 | 10.90 | 24.20 |
| V | 260.0 | 228.5 | 164.0 | 209.0 | 186.0 | 174.0 | 161.0 | 28.00 |
| Cl | 300.0 | 1031 | 127.0 | 859.0 | 329.0 | 165.0 | 125.0 | 367.0 |

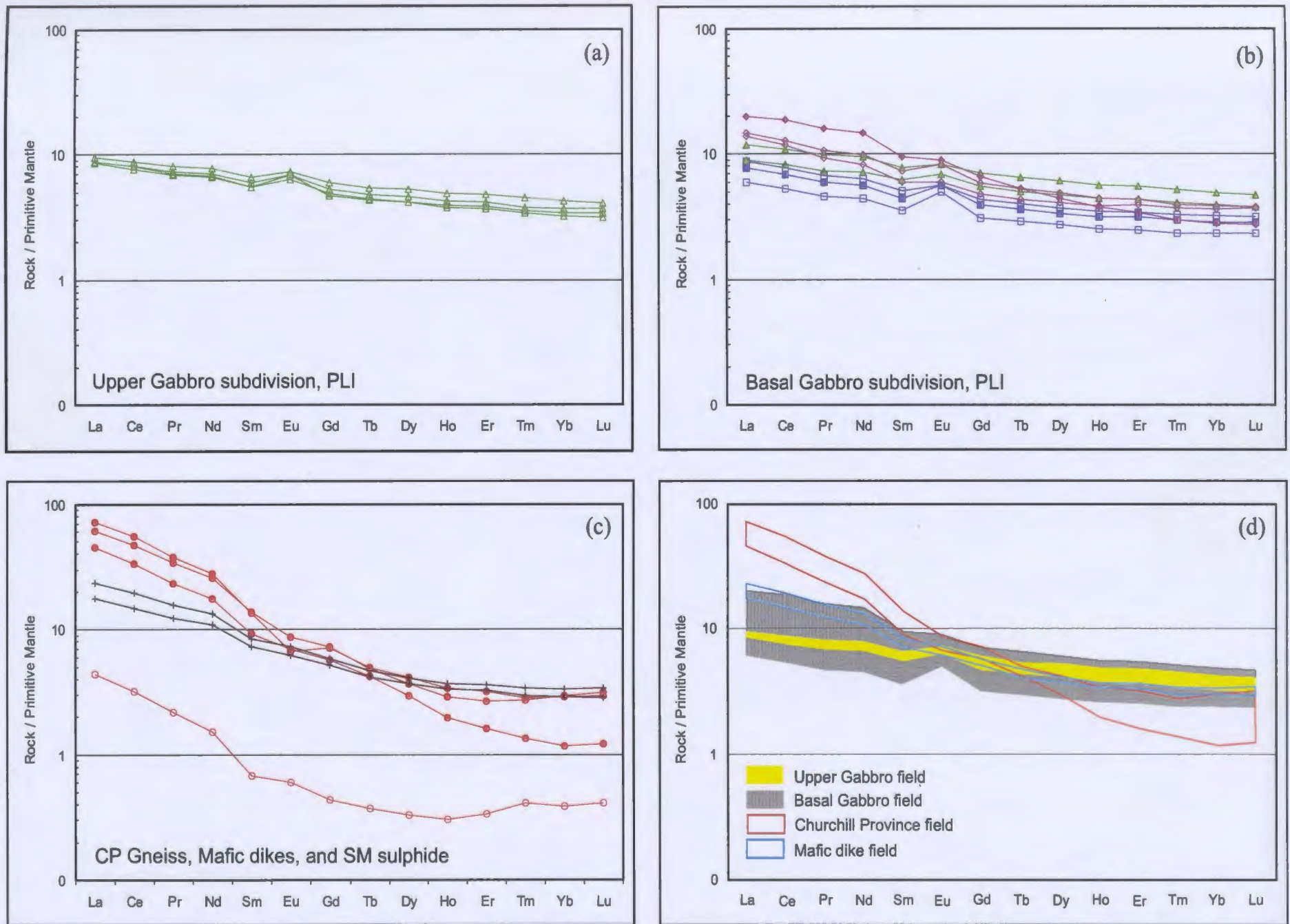


Figure 4.13. Primitive mantle normalized REE diagrams for rocks belonging to the (a) Upper Gabbro subdivision, (b) Basal Gabbro subdivision, and (c) Churchill Province (CP) gneiss, Mafic dikes, and Semi-massive (SM) sulphide. The legend for the symbols utilized in each diagram is illustrated in Figure 4.14. Figure 4.13d illustrates the fields from each REE plot for comparative reasons. Normalizing values are from Sun and McDonough (1989).

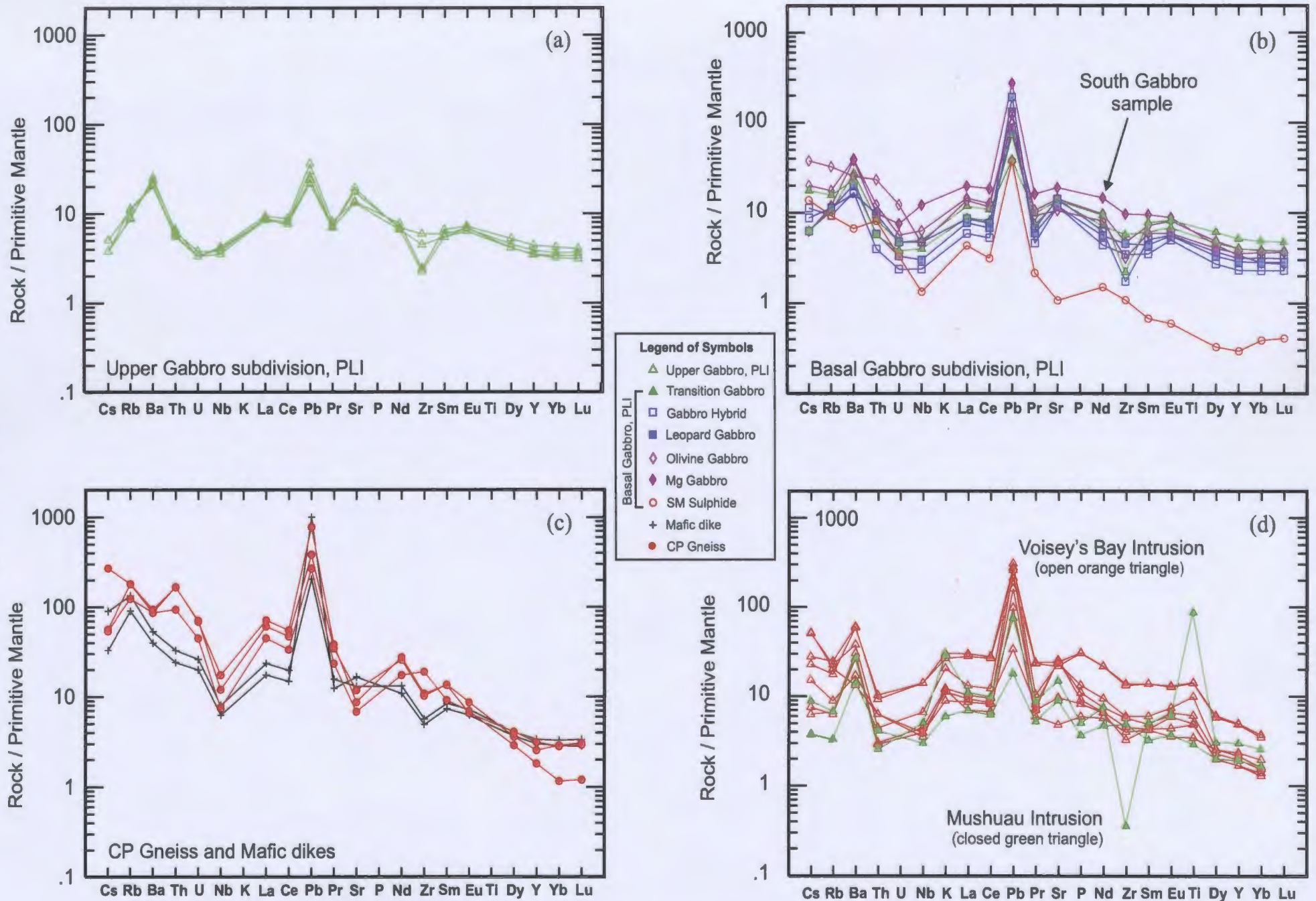


Figure 4.14. Primitive mantle normalized extended trace element plots after Sun and McDonough (1989) for rocks belonging to the (a) Upper Gabbro subdivision, PLI, (b) Basal Gabbro subdivision, PLI (c) Churchill Province (CP) gneiss, and (d) Voisey's Bay Intrusion and Mushuau Intrusion (after Li *et al.*, 2000).

Table 4.10 Rare earth element ratios for rock types of the Pants Lake Intrusion, Churchill Province gneiss, and footwall mafic dikes. Normalization values are from Sun and McDonough (1989). The Europium Anomaly (*ie.* Eu/Eu*) was calculated using the formula suggested by Taylor and McLennan (1985).

| Rock Type | (La/Yb) _N | (Ce/Yb) _N | (La/Sm) _N | (Gd/Yb) _N | Eu* | Eu/Eu* |
|---|----------------------------------|----------------------------------|-------------------------------|-------------------------------|--------------------------------|-------------------------------|
| Upper Gabbro (n = 4) | 2.23-2.73 (Average = 2.46) | 2.09-2.51 (Average = 2.25) | 1.42-1.61 (Average = 1.51) | 1.42-1.47 (Average = 1.45) | 5.07-6.30 (Average = 5.53) | 1.15-1.36 (Average = 1.24) |
| Transition Gabbro (n = 2) | 2.27-2.46 (Average = 2.38) | 2.11-2.26 (Average = 2.19) | 1.44-1.52 (Average = 1.48) | 1.42-1.44 (Average = 1.43) | 5.83-7.38 (Average = 6.61) | 1.12-1.17 Average = 1.14) |
| Gabbro Hybrid (n = 2) | 2.59-2.74 (Average = 2.68) | 2.32-2.45 (Average = 2.40) | 1.69-1.71 (Average = 1.70) | 1.33-1.38 (Average = 1.36) | 3.28-4.70 (Average = 3.99) | 1.20-1.53 (Average = 1.34) |
| Leopard Gabbro (n = 1) | 2.27 | 2.43 | 1.77 | 1.37 | 4.14 | 1.35 |
| Olivine Gabbro (n = 2) | 3.81-3.83 (Average = 3.82) | 3.23-3.35 (Average = 3.29) | 2.02-2.32 (Average = 2.15) | 1.32-1.54 (Average = 1.43) | 5.34-6.53 (Average = 5.93) | 1.11-1.25 (Average = 1.19) |
| Medium-Grained Gabbro (n = 1) | 7.13 | 6.66 | 2.08 | 2.37 | 7.97 | 1.19 |
| Semi-massive Sulphide (n = 1) | 11.37 | 8.22 | 6.48 | 1.13 | 0.54 | 1.12 |
| Churchill Province Gneiss (n = 3) | 21.02-38.57 (Average = 25.68) | 16.26-28.85 (Average = 19.69) | 4.44-5.26 (Average = 4.86) | 2.50-4.85 (Average = 2.91) | 7.28-10.09 (Average = 9.09) | 0.67-0.97 (Average = 0.83) |
| Mafic Dike (n = 2) | 6.09-7.15 (Average = 6.65) | 5.18-5.97 (Average = 5.60) | 2.38-2.80 (Average = 2.60) | 1.78-1.81 (Average = 1.79) | 6.20-7.04 (Average = 6.62) | 1.01-1.03 (Average = 1.02) |

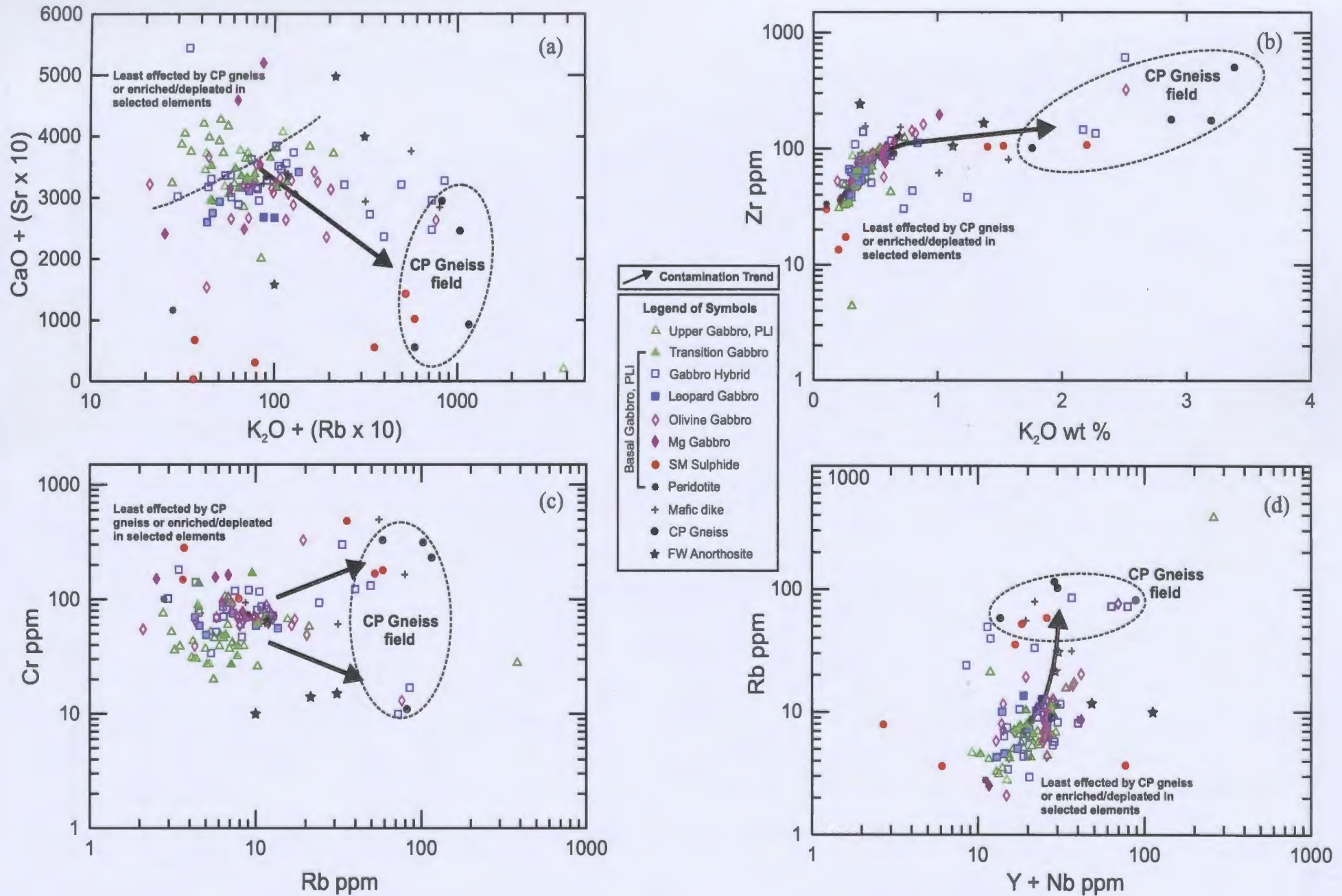


Figure 4.15. Selected major and trace element plots for samples of the Churchill Province, PLI, and mafic dikes. These plots illustrate the effects of gneissic contamination. (a) [CaO wt% + (Sr x 10 ppm)] versus [Log K₂O wt% + (Rb x 10 ppm)], (b) [Log Zr ppm] versus [K₂O wt%], (c) [Log Cr ppm] versus [Log Rb ppm], and (d) [Log Rb ppm] versus [Log (Y + Nb ppm)].

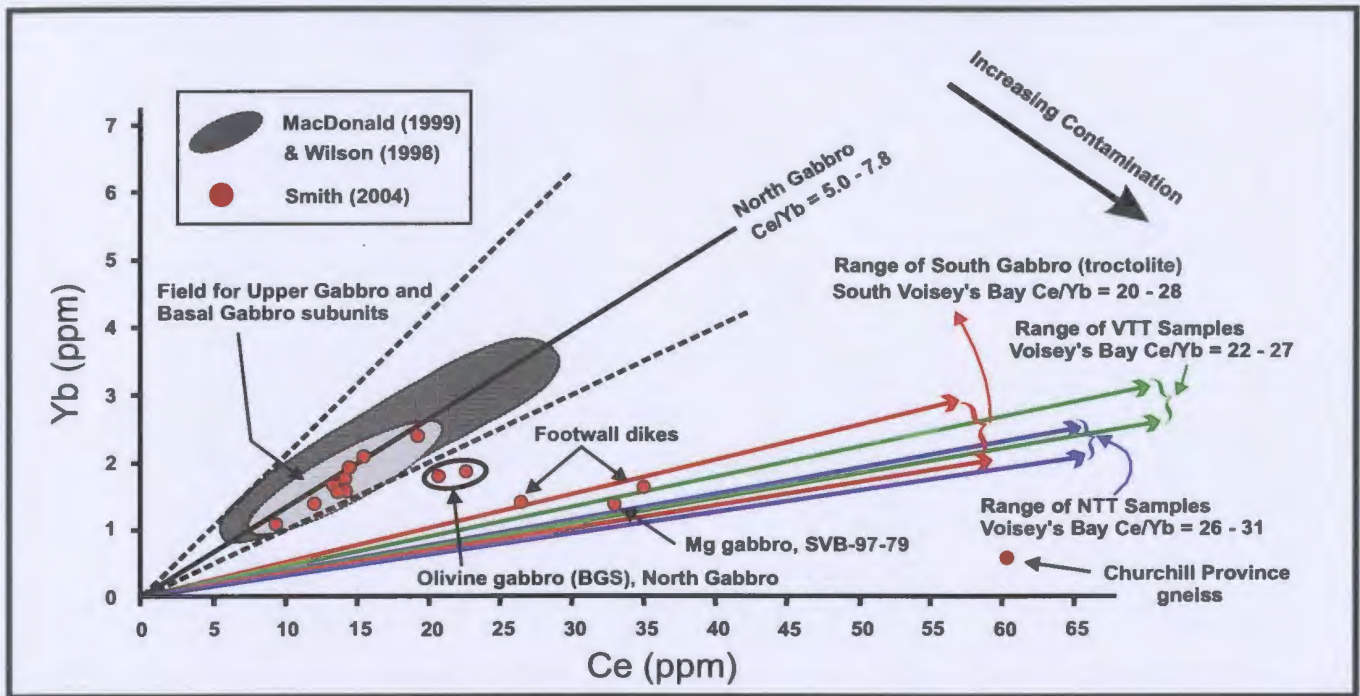


Figure 4.16. Variations in Ce versus Yb illustrating compositional differences in magmas and the extent of crustal contamination. See text for explanation of abbreviations. The Ce and Yb data from Voisey's Bay are from Li *et al.* (2000).

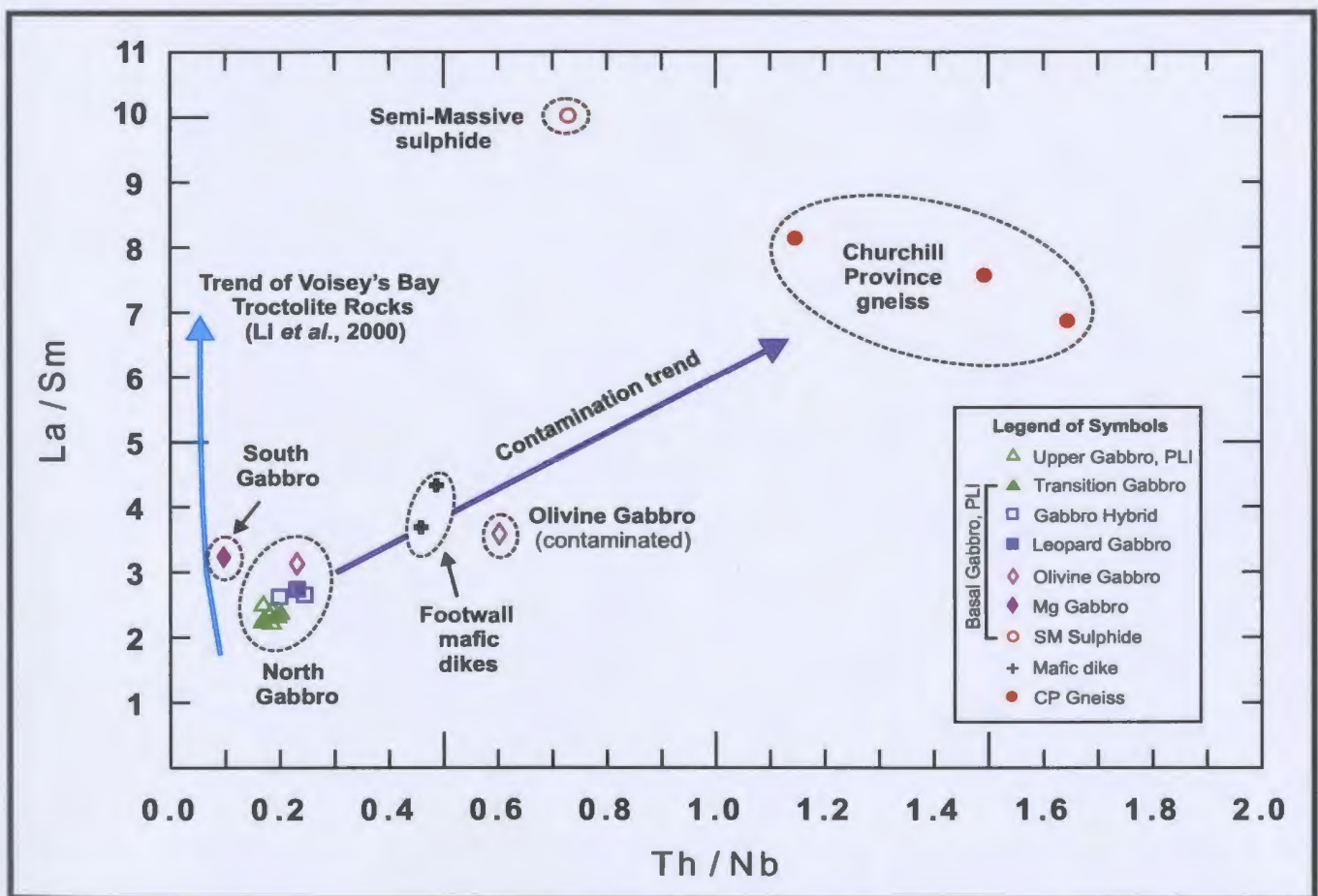


Figure 4.17. Plot of Th / Nb versus La / Sm ratios for rocks of the Pants Lake Intrusion, country rocks, and footwall mafic dikes. The trend of troctolitic rocks of the Voisey's Bay intrusion are included in the diagram (after Li *et al.*, 2000).

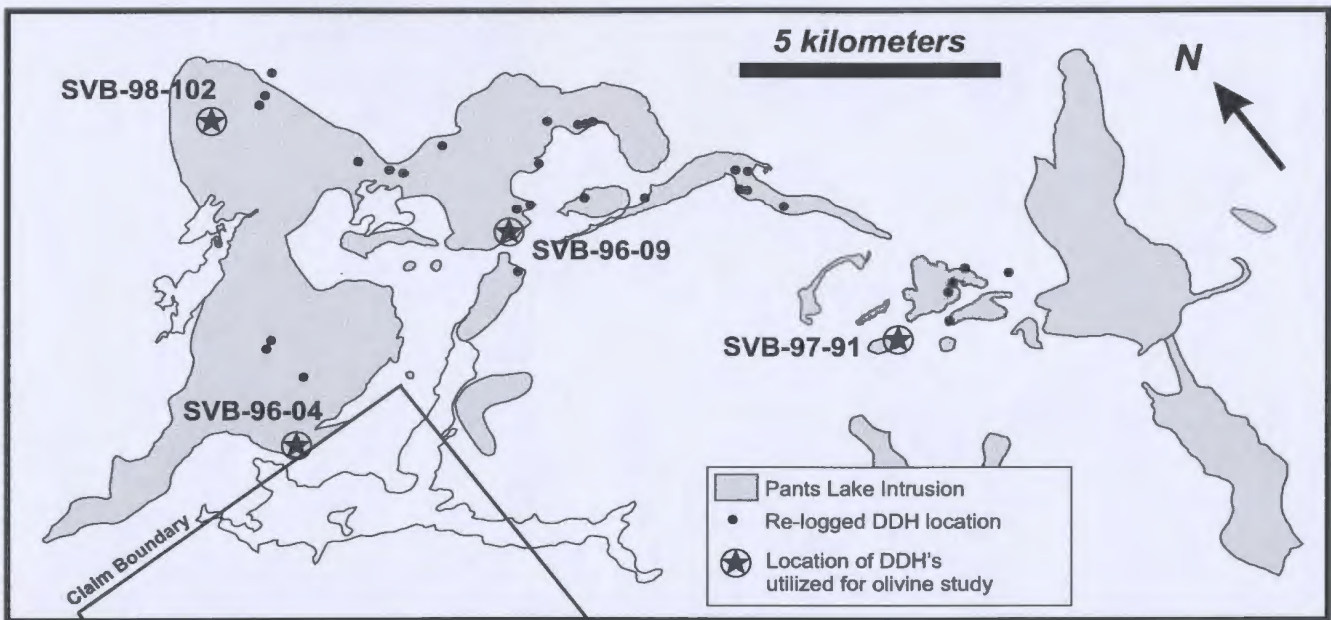


Figure 4.18. Outline of the Pants Lake Intrusion showing the collar location of the diamond drill holes (DDH) utilized for the olivine study.

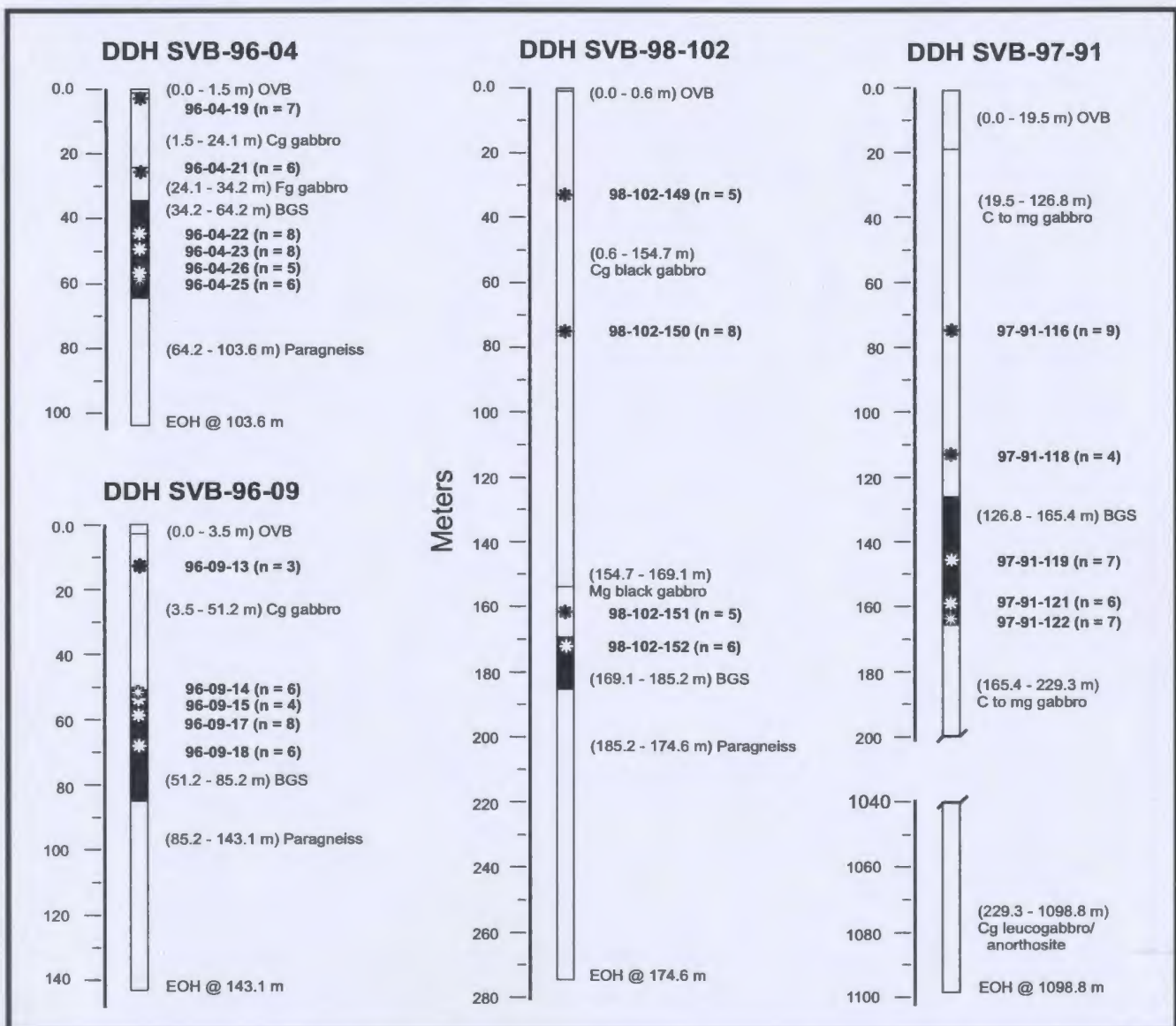


Figure 4.19. Diamond drill hole profiles with sample locations and names, and the number of olivine grains ablated for study.

Table 4.11 Summary data of average element and calculated average mole % forsterite (Fo) abundances for olivine grains from selected drill core samples throughout the Pants Lake Intrusion (see Figures 4.18 and 4.19 for sample locations and Table B.3 for the complete data set). The mole % forsterite abundances were calculated using an online calculator for this purpose following the calculations of Sack and Ghiorso (1989), and Hirschmann (1991). See <http://ctserver.uchicago.edu/MeltsCALC/olivine.html>. Sample names followed by an * indicate Upper Gabbro samples, all other samples are Basal Gabbro.

| Sample | Drill Hole | Region | Sample Depth (m) | Olivine s Ablated | MgO wt % | FeO wt % | SiO2 wt % | Ni ppm | Cu ppm | Co ppm | Mole % Fo |
|-------------|------------|--------------|------------------|-------------------|----------|----------|-----------|--------|--------|--------|-----------|
| 96-04-19* | SVB-96-04 | NDT | 4.15 | 7 | 27.55 | 34.92 | 40.13 | 325.0 | <LD | 203.8 | 58.40 |
| 96-04-21* | SVB-96-04 | NDT | 25.90 | 6 | 21.18 | 34.81 | 37.77 | 644.7 | 12.29 | 167.3 | 52.00 |
| 96-04-22 | SVB-96-04 | NDT | 44.30 | 8 | 22.77 | 44.26 | 34.78 | 416.2 | 9.09 | 268.5 | 47.80 |
| 96-04-23 | SVB-96-04 | NDT | 49.50 | 8 | 20.81 | 50.79 | 34.43 | 560.1 | 7.54 | 245.5 | 42.20 |
| 96-04-26 | SVB-96-04 | NDT | 58.15 | 6 | 27.10 | 37.08 | 35.54 | 188.8 | 11.23 | 220.8 | 56.50 |
| 96-04-25 | SVB-96-04 | NDT | 58.63 | 5 | 24.56 | 47.40 | 35.33 | 453.9 | 14.52 | 296.6 | 48.00 |
| 96-09-13* | SVB-96-09 | GG | 13.75 | 3 | 16.38 | 49.29 | 32.54 | 95.57 | 5.99 | 175.5 | 37.20 |
| 96-09-14 | SVB-96-09 | GG | 51.10 | 6 | 19.46 | 46.75 | 33.98 | 161.0 | 7.04 | 191.0 | 42.50 |
| 96-09-15 | SVB-96-09 | GG | 53.40 | 4 | 22.20 | 47.59 | 36.18 | 215.6 | 8.26 | 212.4 | 45.40 |
| 96-09-17 | SVB-96-09 | GG | 58.10 | 8 | 28.05 | 38.12 | 37.52 | 435.8 | 11.16 | 279.3 | 56.70 |
| 96-09-18 | SVB-96-09 | GG | 68.50 | 6 | 20.63 | 49.20 | 34.95 | 545.5 | 8.00 | 267.7 | 42.70 |
| 98-102-149* | SVB-98-102 | NAI | 32.50 | 5 | 17.88 | 55.63 | 33.70 | 105.4 | 8.09 | 193.9 | 36.30 |
| 98-102-150* | SVB-98-102 | NAI | 75.95 | 8 | 24.94 | 47.01 | 34.73 | 158.5 | 12.54 | 206.8 | 48.60 |
| 98-102-151* | SVB-98-102 | NAI | 161.85 | 5 | 20.36 | 42.17 | 34.22 | 131.4 | <LD | 191.4 | 46.20 |
| 98-102-152 | SVB-98-102 | NAI | 170.50 | 6 | 19.08 | 44.86 | 33.98 | 244.5 | <LD | 216.9 | 43.10 |
| 97-91-116* | SVB-97-91 | Mineral Hill | 76.75 | 9 | 13.33 | 50.18 | 32.92 | 63.86 | 3.68 | 174.8 | 31.70 |
| 97-91-118* | SVB-97-91 | Mineral Hill | 113.80 | 4 | 16.38 | 48.76 | 33.21 | 116.5 | 6.41 | 166.8 | 36.80 |
| 97-91-119 | SVB-97-91 | Mineral Hill | 146.90 | 7 | 25.95 | 38.37 | 35.49 | 255.3 | 11.10 | 178.7 | 54.60 |
| 97-91-121 | SVB-97-91 | Mineral Hill | 159.80 | 6 | 22.73 | 37.74 | 35.25 | 79.40 | 5.23 | 170.9 | 51.70 |
| 97-91-122 | SVB-97-91 | Mineral Hill | 164.15 | 7 | 16.06 | 51.11 | 33.15 | 76.70 | 3.88 | 169.3 | 33.20 |

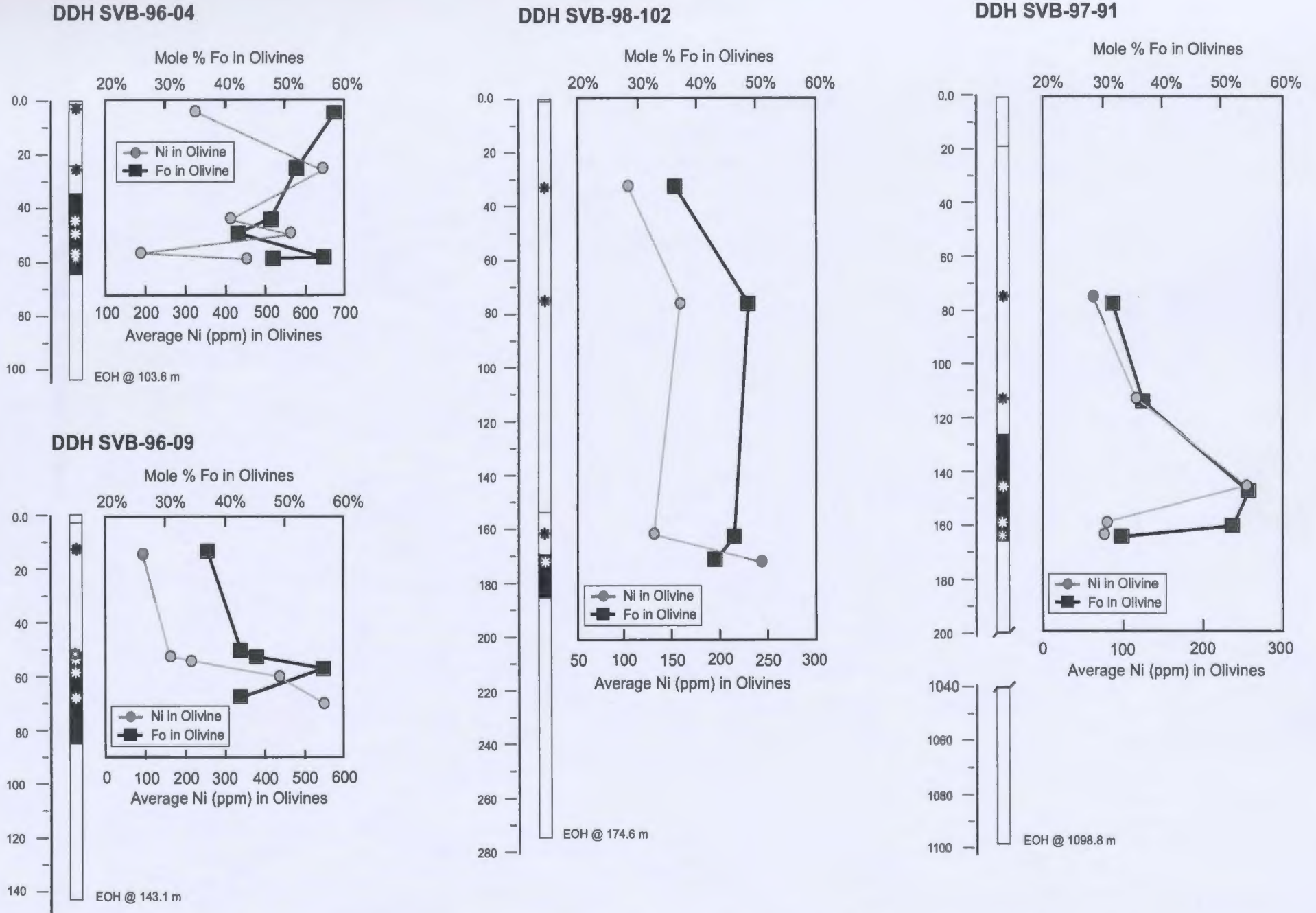


Figure 4.20. Depth profiles of diamond drill holes (DDH's) SVB-96-04, SVB-96-09, SVB-98-102, and SVB-97-91 plotted against average Forsterite (Fo) and Ni in olivines from the Pants Lake Intrusion. Refer to Figure 4.19. for sample names and Table 4.11 for average values.

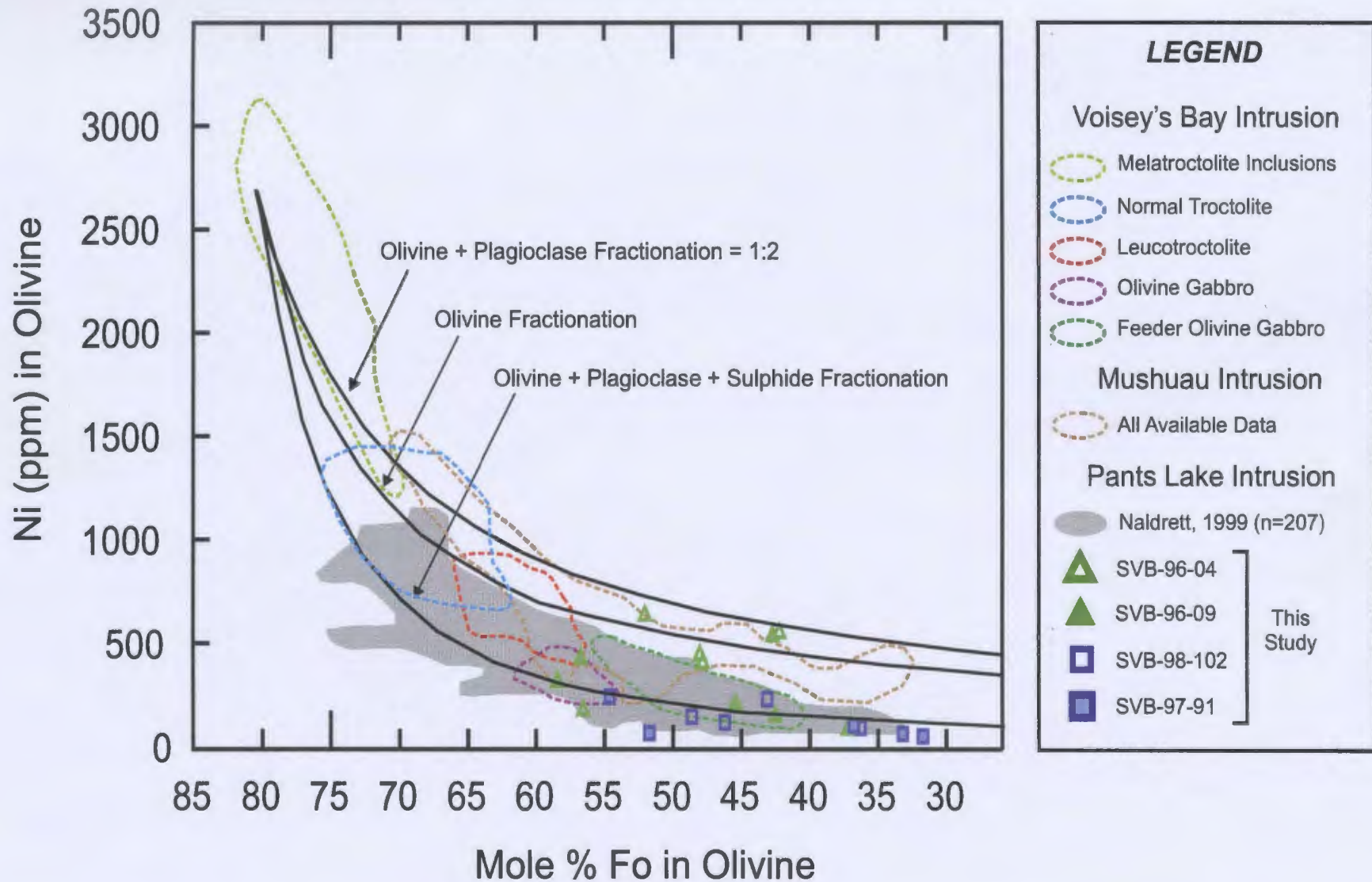


Figure 4.21. Mole percent Forsterite (Fo) and Ni contents in olivine grains from the Pants Lake Intrusion (this study; Naldrett, 1999) along with data for olivines within the Voisey's Bay and Mushuau Intrusions (after Li *et al.*, 2000). See Table 4.11 for a summary of the average element and mole % Fo abundances of olivines used in this study. The fractionation curves were modeled by Naldrett (*op cit*) in his study of olivine grains in the South Voisey Bay area and are utilized on this diagram as a means of comparison with data from this study.

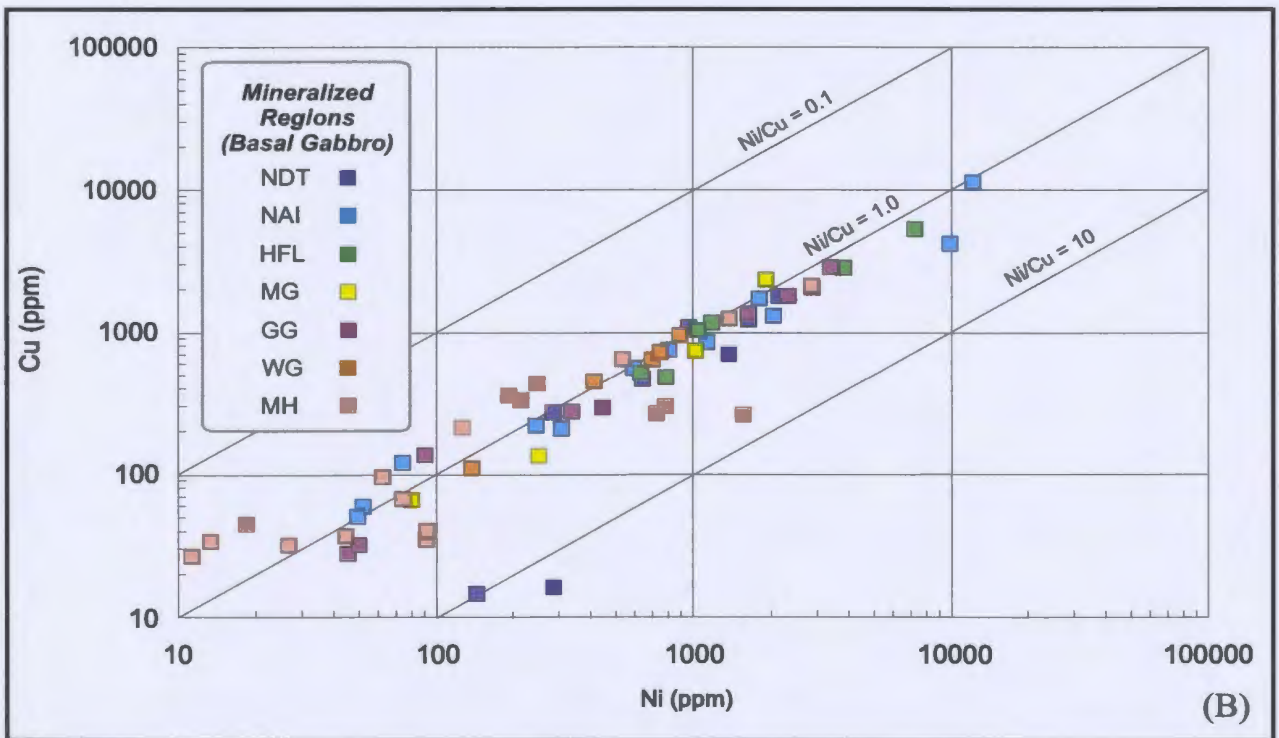
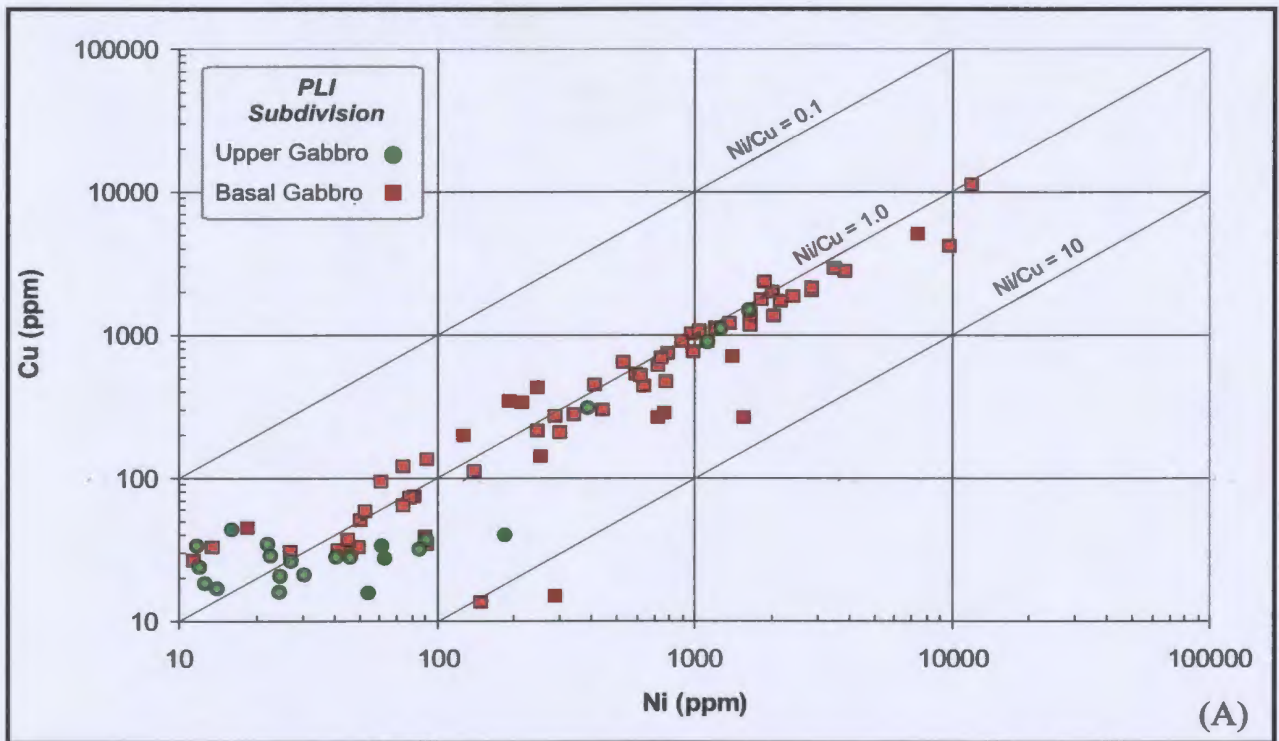


Figure 4.22. Metal contents (Ni and Cu) of rocks belonging to the Pants Lake Intrusion. (A) Log plot of Ni (ppm) versus Cu (ppm) of Upper Gabbro (green circles) and Basal Gabbro (red squares). (B) Log plots of Ni (ppm) versus Cu (ppm) of Basal Gabbro samples from the mineralized regions throughout the PLI (refer to Figure 3.1). Both plots show a general trend of Ni:Cu = 1.

Table 4.12 Summary of average Ni and Cu concentrations determined by the XRF technique at Memorial University of Upper and Basal Gabbro drill core samples located throughout the Pants Lake Intrusion (refer to Figure 3.1 for locations). Ni and Cu in 100% sulphide are calculated following the formula suggested by Kerr (1999).

| <i>Location</i> | <i>No. of Samples</i> | <i>S (ppm) W Rock</i> | <i>S (wt %) W Rock</i> | <i>Ni (ppm) W Rock</i> | <i>Ni (wt %) W Rock</i> | <i>Cu (ppm) W Rock</i> | <i>Cu (wt %) W Rock</i> | <i>Ni 100% Sulphide</i> | <i>Cu 100% Sulphide</i> | <i>Ni : Cu 100% Sulphide</i> |
|-----------------|-----------------------|-----------------------|------------------------|------------------------|-------------------------|------------------------|-------------------------|-------------------------|-------------------------|------------------------------|
| NAI (Upper PLI) | n=4 | 1067 | 0.11 | 19.21 | 0.00 | 25.55 | 0.00 | 0.79 | 0.91 | 0.75 |
| NAI (Basal PLI) | n=13 | 59409 | 5.94 | 2430 | 0.24 | 1844 | 0.18 | 1.55 | 1.34 | 1.21 |
| NDT (Upper PLI) | n=3 | 1013 | 0.10 | 62.93 | 0.01 | 28.44 | 0.00 | 2.00 | 0.96 | 1.98 |
| NDT (Basal PLI) | n=10 | 11731 | 1.17 | 758.7 | 0.08 | 552.4 | 0.06 | 3.74 | 1.44 | 3.89 |
| HFL (Upper PLI) | n=3 | 1047 | 0.10 | 25.69 | 0.00 | 18.54 | 0.00 | 1.14 | 0.65 | 1.51 |
| HFL (Basal PLI) | n=8 | 73419 | 7.34 | 1869 | 0.19 | 1402 | 0.14 | 1.27 | 1.06 | 1.26 |
| MG (Upper PLI) | n=2 | 896.5 | 0.09 | 19.34 | 0.00 | 25.24 | 0.00 | 0.78 | 0.99 | 0.76 |
| MG (Basal PLI) | n=7 | 24202 | 2.42 | 893.1 | 0.09 | 865.5 | 0.09 | 1.50 | 1.33 | 1.20 |
| GG (Upper PLI) | n=3 | 1166 | 0.12 | 22.61 | 0.00 | 32.60 | 0.00 | 0.76 | 0.96 | 0.82 |
| GG (Basal PLI) | n=9 | 23167 | 2.32 | 1260 | 0.13 | 1006 | 0.10 | 1.70 | 1.36 | 1.27 |
| WG (Upper PLI) | n=3 | 1188 | 0.12 | 100.4 | 0.01 | 33.81 | 0.00 | 2.86 | 0.99 | 2.83 |
| WG (Basal PLI) | n=5 | 12362 | 1.24 | 581.7 | 0.06 | 559.8 | 0.06 | 1.79 | 1.65 | 1.07 |
| MH (Upper PLI) | n=6 | 13335 | 1.33 | 222.1 | 0.02 | 202.7 | 0.02 | 0.52 | 0.62 | 0.81 |
| MH (Basal PLI) | n=19 | 13799 | 1.38 | 473.6 | 0.05 | 345.4 | 0.03 | 1.56 | 0.90 | 1.41 |

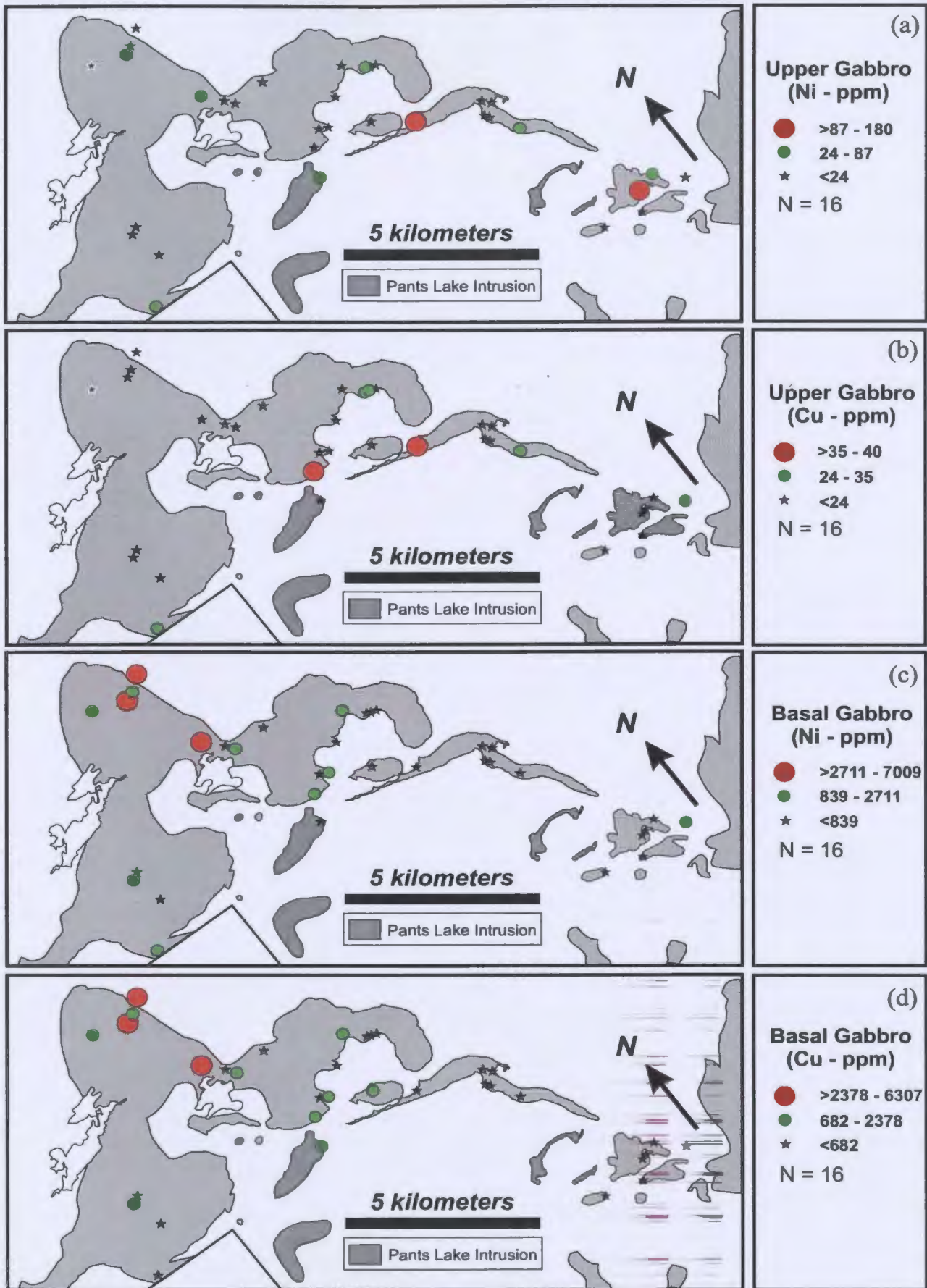


Figure 4.23. Dot plot graphs depicting Ni and Cu distribution throughout the Upper and Basal Gabbro subdivisions within the Pants Lake Intrusion. (A) Dot plot of Ni in Upper Gabbro rocks. (B) Dot plot of Cu in Upper Gabbro rocks. (C) Dot plot of Ni in Basal Gabbro rocks. (D) Dot plot of Cu in Basal Gabbro. See text for explanation of population intervals.

Chapter 5: Sulphur Isotope Geochemistry

5.1 Introduction

Sulphur isotope ratio determinations are an integral and widely accepted method in the study of magmatic systems (cf. Ripley, 1981, 1997; Saskaki, 1969; Mainwaring and Naldrett, 1977; Godlevskii and Grinenko, 1963; Liebenberg, 1970). The application of sulphur isotope ratios in this study is two fold: 1) to determine the isotope range and character of sulphide minerals hosted by the Basal Gabbro of the Pants Lake Intrusion, and 2) to compare the results of this study with regional sulphur isotope data such that trends and possible geological affinities might be determined.

5.2 Notations and Theory

Sulphur is a stable isotope, similar to the isotopes of O, H, C and N. The chief rationale for the study of stable isotope systems relies on the separation of the isotopes by their mass rather than their chemistry (Rollinson, 1993). There are four stable sulphur isotopes including ^{32}S , ^{33}S , ^{34}S and ^{36}S with natural abundances of 95.02 %, 0.75 %, 4.21 %, and 0.02 %, respectively. The majority of sulphur isotope studies ratio the two most common sulphur isotopes (*i.e.* $^{34}\text{S} / ^{32}\text{S}$) that are expressed as $\delta^{34}\text{S}$ values. The $\delta^{34}\text{S}$ value is determined using the reference standard Triolite (FeS) from the Canon Diablo iron meteorite (CDT) and is calculated by the following equation:

$$\delta^{34}\text{S} \text{ ‰} = \left[\frac{{}^{34}\text{S} / {}^{32}\text{S}}{({}^{34}\text{S} / {}^{32}\text{S})_{\text{(sample)}}} - \frac{{}^{34}\text{S} / {}^{32}\text{S}}{({}^{34}\text{S} / {}^{32}\text{S})_{\text{(standard, CDT)}}} \right] \times 1000$$

If the $\delta^{34}\text{S}$ value is positive then the sulphur sample is regarded as being isotopically heavier than the standard CDT. Alternatively, if the $\delta^{34}\text{S}$ value of the sample is negative, then it is isotopically lighter than the standard CDT. If the $\delta^{34}\text{S}$ values within sulphide minerals of a deposit have a narrow range, then these sulphides may be in equilibrium with each other and represent a single, homogeneous source. If the $\delta^{34}\text{S}$ values have a broad range, then this may indicate a heterogeneous sulphur composition or contamination from an external sulphur source.

Sulphur isotope ratios are dependent on which form the sulphur in an ore-forming system represents. This can include native sulphur, sulphate and sulphide minerals, gaseous H_2S and SO_2 , as well as oxidized and reduced sulphur ions in solution (Ohmoto and Rye, 1978). The reservoirs of sulphur with their ranges of $\delta^{34}\text{S}$ include, mantle-derived sulphur ($0 \pm 3 \text{‰}$), seawater sulphate ($+20 \text{‰}$), and strongly reduced sedimentary sulphide (typically large negative values, *i.e.* -20‰) (Rollinson, 1993).

Figure 5.1 (Ohmoto and Rye, 1978) illustrates the sulphur isotopic variation in nature. The $\delta^{34}\text{S}$ ratios of sulphur in both felsic and mafic igneous sulphides are widely variable, typically between $\pm 10 \text{‰}$. The $\delta^{34}\text{S}$ ratio of sulphur in meteorites, however is thought to represent mantle values, has a narrow $\delta^{34}\text{S}$ similar to the CDT (*i.e.* 0‰). Sediment-hosted sulphides have the largest $\delta^{34}\text{S}$ range of values, between $\pm 40 \text{‰}$. Figure 5.1 also illustrates the $\delta^{34}\text{S}$ ratio variation for sulphur in oceans and evaporites through time.

Variations in the isotopic composition of sulphur are caused by two processes: 1) reduction of sulphate ions to sulphide by anaerobic bacteria which results in the enrichment of the product sulphide in ^{32}S , and 2) various isotopic exchange reactions

between sulphur-bearing ions, molecules and solids by which ^{34}S is generally concentrated in compounds having the highest oxidation state of sulphur, or greatest bond strength (Bachinski, 1969).

When sulphide minerals are precipitated from aqueous solutions or crystallize from sulphide liquids, small differences may occur in the $\delta^{34}\text{S}$ of cogenetic minerals due to equilibrium fractionation between the solids and solids or liquid (Faure, 1986). The fractionation of sulphur isotopes between coexisting mineral pairs is a function of temperature. Reflecting this statement, the $\delta^{34}\text{S}$ ratios in some common sulphide minerals decrease on the order of pyrite > sphalerite > chalcopyrite > galena (Bachinski, 1969). The $f\text{O}_2$ and the pH, can also affect sulphur isotope fractionation.

5.3 Sample Locations

The $\delta^{34}\text{S}$ ratios of sulphide separates utilized in this study are listed in Table B.4 (Appendix B) with reference to the geographic components of the PLI (refer to Figure 3.1) and the diamond drill hole (DDH) from which a particular sample was obtained (see enclosed geology map). Table A.2 (Appendix A) gives the actual sample interval where the sulphide separates were retrieved.

A total of thirty-five sulphide separates were collected from the PLI and surrounding country rocks for this study. Twenty-five sulphide separates were taken from the Basal Gabbro. The twenty-five Basal Gabbro sulphide separates represent the various sulphide minerals (pyrrhotite, chalcopyrite, *etc.*) and textures (disseminated, massive, *etc.*) observed in the Basal Gabbro and were collected at various heights above the basal contact. Five sulphide separates of disseminated pyrrhotite were derived from

the Churchill Province gneiss. The remaining five sulphide separates were taken from the footwall gabbro/anorthosite of disseminated pyrrhotite. There are four duplicate samples. All samples were analyzed at Memorial University of Newfoundland following the procedure of Pye (1998) (see Appendix B.4).

5.4 Analytical Results

The $\delta^{34}\text{S}$ ratios obtained from the 25 Basal Gabbro sulphide separates range between -5.25 to -1.93 ‰ (average, -2.76 ‰; mean, -2.68 ‰; standard deviation, 0.73 ‰) (Table B.4, Appendix B) (Figure 5.2). Within these 25 samples, the ratios for 18 sulphide separates from the North Gabbro range between -3.33 to -1.93 ‰ (average, -2.61 ‰, mean, -2.58 ‰; standard deviation, 0.42 ‰). The North Gabbro ratios were slightly less negative compared to the range of -5.25 to -1.99 ‰ obtained from the seven sulphide separates of the South Gabbro (average, -3.13 ‰; mean, -2.96 ‰; standard deviation, 1.18 ‰). If the large negative $\delta^{34}\text{S}$ ratio of -5.25 ‰ is removed from the average $\delta^{34}\text{S}$ calculation for the South Gabbro, however, the recalculated average of -2.77 ‰ would be similar to the average $\delta^{34}\text{S}$ value of the North Gabbro (*i.e.* -2.61 ‰).

The differences in the $\delta^{34}\text{S}$ ratios between distinct sulphide minerals (*i.e.* pyrrhotite, chalcopyrite) and sulphide textures (refer to Section 3.6) were negligible. Sulphide separates from different heights above the basement contact in the Basal Gabbro did not yield any observable trends with respect to increasing or decreasing $\delta^{34}\text{S}$ ratios.

The $\delta^{34}\text{S}$ ratios of five representative sulphide separates from the Churchill Province gneiss range between -4.91 to -1.32 ‰ (average, -3.04 ‰; mean, -2.59 ‰; standard deviation, 1.76 ‰). The $\delta^{34}\text{S}$ ratios of -6.43 to -0.99 ‰ (average, -4.03 ‰;

mean, -3.33 ‰; standard deviation, 2.29 ‰) were obtained from five sulphide separates of the footwall gabbro/anorthosite.

5.5 Comparison of Results to Regional Sulphur Isotope Studies

The $\delta^{34}\text{S}$ ratios of sulphide mineral separates from the Basal Gabbro of the PLI are consistently low, negative values with a range of -5.25 to -1.93 ‰. The range of $\delta^{34}\text{S}$ ratios stated above is comparable to, and overlaps with the reported igneous sulphide range of ± 3.0 ‰ and the range for sedimentary sulphides as depicted in Figure 5.1.

Sulphide separates from the anorthosite and Churchill Province gneiss in the footwall to the Pants Lake Intrusion had $\delta^{34}\text{S}$ ratio ranges of -6.43 to -0.99 ‰ and -4.91 to -1.32 ‰, respectively. Regional $\delta^{34}\text{S}$ values of sulphide separates reported for the Churchill Province gneisses (unseparated) were broad, ranging between -9.4 to +10.7 ‰ (refer to Figure 5.2 and Table 5.1). The regional $\delta^{34}\text{S}$ ratio of sulphide separates from the Tasiuyak gneiss (Churchill Province) were also broad, but significantly negative (*i.e.* -17.0 to -0.9 ‰). Regional $\delta^{34}\text{S}$ ratios of sulphide separates for the Nain Province gneiss are narrow and positive (*i.e.* +0.20 to +3.30 ‰). Apart from the Nain Province gneiss, all other $\delta^{34}\text{S}$ ratio ranges overlap with Basal Gabbro $\delta^{34}\text{S}$ ratios.

The sulphur isotope ratios of several magmatic sulphide occurrences located in the Nain Plutonic Suite (NPS) and the Harp Lake Intrusive Suite (HLIS) are reported in Table 5.1. The location of these sulphide occurrences is shown in Figure 5.3. Sulphide occurrences in the NPS, excluding the Voisey's Bay deposits, show a distinct trend. That is, all $\delta^{34}\text{S}$ ratios are consistently positive with narrow ranges (*i.e.* +1.00 to +3.00

‰). $\delta^{34}\text{S}$ ratios reported for the Voisey's Bay deposits have a broad range, between –4.10 to +2.70 ‰. However, individual deposits (Western Extension, Ovoid, *etc*) have narrower ranges (refer to Table 5.1). The $\delta^{34}\text{S}$ ratios for prospects of the Harp Lake Intrusive Suite are dominantly narrow (*i.e.* -0.04 to +0.27 ‰) and reflect igneous sulphide ratios. The Basal Gabbro $\delta^{34}\text{S}$ ratios overlap with the negative spectrum of the Voisey Bay deposit ratios.

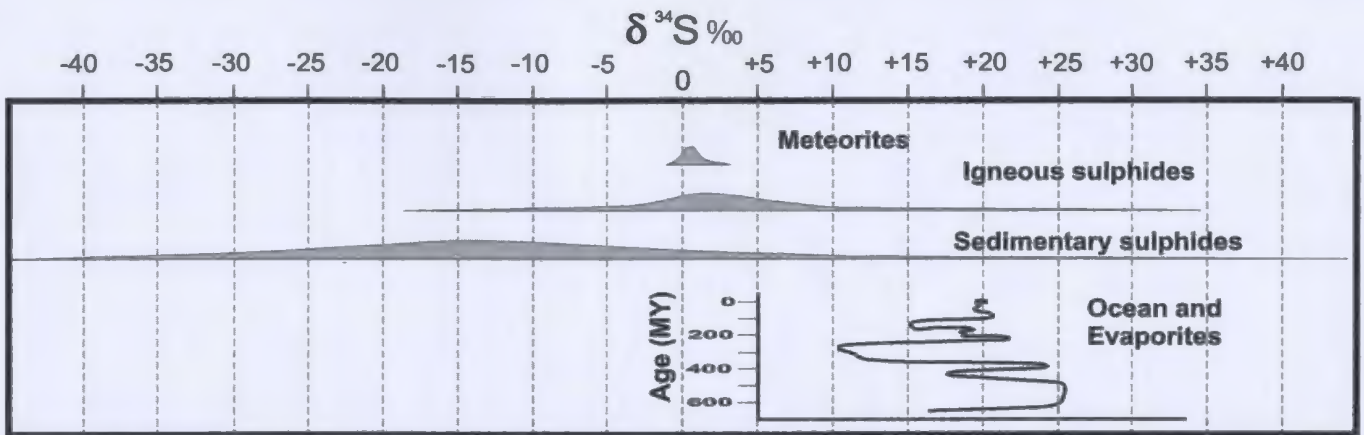


Figure 5.1. Sulphur isotopic variations in nature, expressed as $\delta^{34}\text{S}\text{‰}$ (Ohmoto and Rye, 1978)

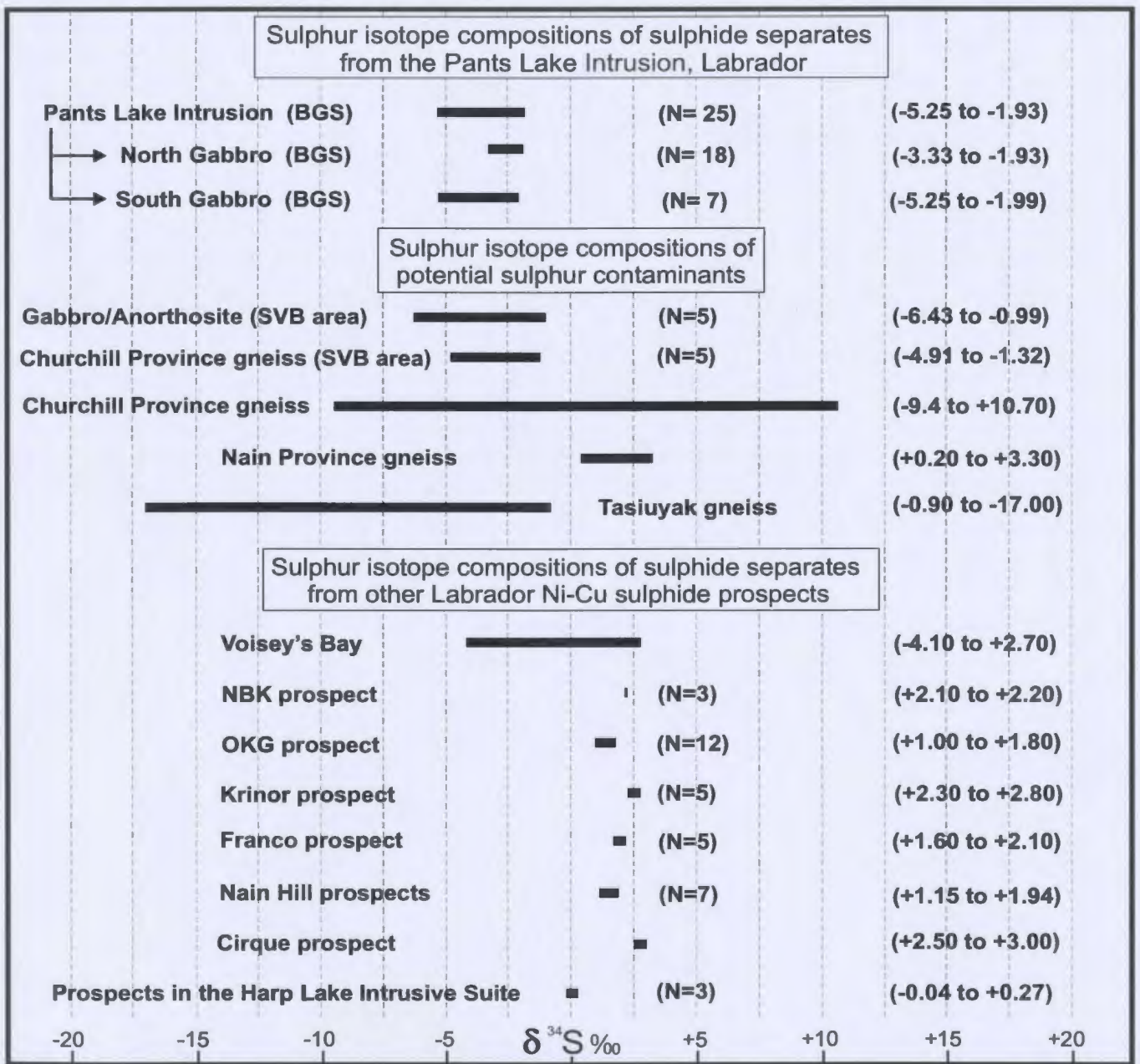


Figure 5.2. Sulphur isotope ranges of sulphide separates from the Basal Gabbro Subdivision (BGS) of the Pants Lake Intrusion, potential sulphur contaminants, and magmatic Ni-Cu prospects located throughout the Nain Plutonic Suite and the Harp Lake Intrusive Suite. Isotope ranges are expressed as per mil. Refer to Table 5.1 and Table B.4 for isotope data and sources.

Table 5.1. Summary of the sulphur isotope ranges from selected Labrador Sulphide prospects within the Nain Plutonic Suite (NPS) and the Harp Lake Intrusive Suite (HLIS). Isotope values obtained from the Tasiuyak gneiss (Churchill Province), Nain Province gneiss, and Churchill Province gneiss are also given. Figure 5.2 illustrates and compares the isotope range of each prospect and geological entity.

| Sample Location | Mineral Separate | $\delta^{34}\text{S}$ ‰ | Source of Data |
|-----------------------------|----------------------------------|-------------------------|-----------------------------|
| Pants Lake Intrusion (NPS) | Pyrrhotite, chalcopyrite | -5.25 to -1.93 | This Study |
| Voisey's Bay deposits (NPS) | Not quoted | -4.10 to +2.70 | Ripley <i>et al.</i> (1997) |
| Western Extension | Not quoted | -4.10 to +1.40 | Ripley <i>et al.</i> (1997) |
| Ovoid & Mini-Ovoid | Not quoted | -2.10 to 0.00 | Ripley <i>et al.</i> (1997) |
| Eastern Deeps | Not quoted | -2.00 to +2.70 | Ripley <i>et al.</i> (1997) |
| OKG prospect (NPS) | Pyrite, pyrrhotite, chalcopyrite | +1.00 to +1.80 | Piercey (1998) |
| NBK prospect (NPS) | Pyrite, pyrrhotite, chalcopyrite | +2.10 to +2.20 | Piercey (1998) |
| Krinor prospect (NPS) | Pyrrhotite, chalcopyrite | +2.30 to +2.80 | Piercey (1998) |
| Cirque prospect (NPS) | Pyrrhotite, chalcopyrite | +2.50 to +3.00 | Dwyer (2001) |
| Nain Hill prospects (NPS) | Pyrrhotite, pyrite | +1.15 to +1.94 | Hinchey (1999) |
| Franco prospect (NPS) | Pyrrhotite | +1.60 to +2.10 | Piercey (1998) |
| Collette II prospect (HLIS) | Pyrrhotite | +0.02 | This Study |
| Ed prospect (HLIS) | Pyrrhotite | +0.04 | This Study |
| Dart prospect (HLIS) | Pyrrhotite | +0.27 | This Study |
| Tasiuyak gneiss (CP) | Pyrrhotite | -0.90 to -17.00 | Ripley <i>et al.</i> (1997) |
| Nain Province gneiss | Not quoted | +0.20 to +3.30 | Ripley <i>et al.</i> (1997) |
| Churchill Province gneiss | Pyrite | -9.40 to +10.70 | Piercey (1998) |

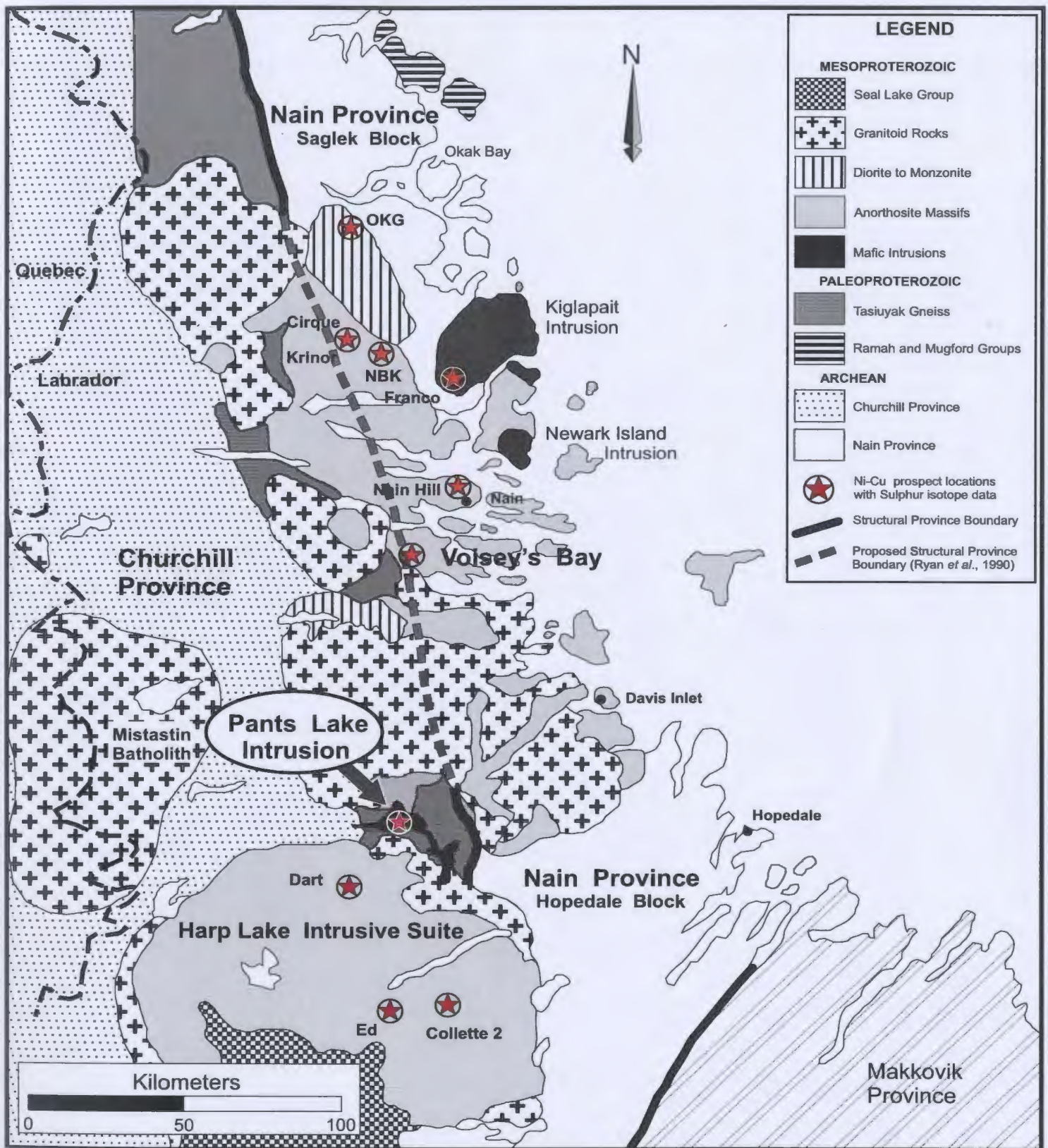


Figure 5.3. Geology of northern Labrador (modified after Kerr and Smith, 1997) (see Figure 2.3) with locations of regional sulphur isotope data reported in this study. The majority of the prospects shown in this figure are detailed in Section 2.3. The NBK and Ed prospects, not included in Section 2.3, are detailed by Piercy (1988) and Kerr and Smith (2000), respectively.

Chapter 6: Discussion and Conclusions

6.1 Discussion

Prior to the initiation of exploratory work directed by Donner Minerals Ltd. in the mid 1990's, the layered mafic intrusive rocks in the study area were relatively unknown. As exploration advanced and academic studies ensued, the Pants Lake Intrusion (PLI) was defined and the incipient seed of geological interpretation blossomed. Through the course of geological research, the PLI was recognized as being composed of two separate intrusions (*e.g.* North and South PLI; MacDonald, 1999) rather than a single intrusive unit. In addition, the economic importance of the contaminated and sulphide-bearing basal gabbroic layer of the North PLI (termed by this author the Basal Gabbro Subdivision) was recognized and became the focus for this study.

In order to facilitate a complete and thorough discussion, the Basal Gabbro Subdivision will be discussed in the context of an eight-stage “working” model (refer to Figure 6.1) that will also attempt to satisfy the objectives of this study as indicated in Chapter 1. The proposed model is complimented with information concerning the fundamental stages of magmatic sulphide systems (*e.g.* Naldrett *et al.*, 1984; Barnes and Maier, 1999; *etc.*), as well as the results of previous studies from the PLI and regional Labrador geology (*e.g.* MacDonald, 1999; Kerr, 1998 and 2003; Ryan *et al.*, 1999; *etc.*).

The first stage of the model occurred in the mantle where large enough volumes of primitive silicate partial melt (12 to 50 %) (Barnes and Maier, 1999), with ferropicritic composition (MacDonald, 1999) were generated to contain sufficient metal concentrations (*e.g.* Fe, Co, Ni, Cu, *etc.*) (Figure 6.1, Diagram A). In order to concentrate the metals in the melt phase during partial melting, the metals must be

incompatible with respect to the residual phases typically silicates, spinels, sulphides, and possible metal alloys (Barnes and Maier, 1999). Likewise, if all of the available sulphide is not consumed in the melt, a residual sulphide phase could potentially withhold the metals and the silicate melt would be depleted in the metals necessary to form a deposit (*op cit*; Barnes *et al.*, 1987). In the case of nickel and cobalt, however, these metals can readily partition into olivine under conditions where sulphide is not available (Barnes and Maier, 1999).

During the second stage, an upwelling mantle plume of metal-laden ferropicritic partial melt collected at the base of the crust adjacent to the regional, deep-seated, *ca.* 1850 Ma crustal penetrating suture zone (Ryan *et al.*, 1995) that separates the Nain and the Churchill provinces (Figure 6.1, Diagram B). Non-fractionated magma from the mantle plume source was rapidly uplifted through the lower crust to the upper crust via this Nain-Churchill suture zone-leading to the eventual emplacement of the Harp Lake Intrusive Suite (HLIS) (*ca.* 1460-1450 Ma; Emslie, 1980) followed by the emplacement of the Nain Plutonic Suite (NPS) (*ca.* 1350-1290 Ma; Ryan, 1996). The Nain-Churchill suture is also an important component for the Voisey's Bay genetic model (Ryan *et al.* 1995; Naldrett, 1997; Evans-Lamswood, 2000).

The third stage is closely linked to the second and occurred when two primitive magma batches ascended from the lower crust to the upper crust during the early evolution and emplacement of the NPS (Figure 6.1, Diagram C). The timing of ascension must have been relatively rapid because if the magma batches rose slowly or temporarily pooled *en route* to the upper crust, a sulphide phase could segregate from the magma, partitioning the metals, and leaving the ascending melt depleted in the necessary

metals to form a deposit (Barnes and Maier, 1999). The two magma batches, although likely from the same parental mantle source, did not share the same final crystallization at their respective intrusive locations.

The first magma batch, represented by the South PLI (including the Medium-Grained Gabbro Subunit), traveled directly to its final crystallization location (*ca.* 1337 Ma; Smith, this study) without significant resting or pooling periods *en route*, especially in the upper crustal levels (Figure 6.1, Diagram C). As an aside, it is now evident that the Medium-Grained Gabbro Subunit described in Chapter 3 is a close relative of the South PLI rather than a component of the Basal Gabbro Subdivision. The relatively elevated MgO abundances, coupled with the predominantly olivine cumulate-textures within the resultant peridotite and olivine gabbro to troctolite rock types, imply that the South PLI did not fractionate from an earlier magma chamber. The variety of rock types that comprise the South PLI is likely an artifact of *in situ* fractionation and differentiation within the final magma chamber. This assumption concurs with the results of MacDonald (1999). Apart from the differing fractionation history, it is also likely that the South PLI partook of an alternative intrusive route or assimilated both Nain and Churchill Province rock types as evidenced by higher LREE abundances (*i.e.* La/Yb_N; Ce/Yb_N) and differing trace element ratios (*i.e.* Ce vs Yb; La/Sm vs Th/Nb). It can be argued that the South PLI, in some respects, resembles the chemistry reported for the Voisey's Bay Intrusion (Li *et al.*, 2000) more so than does the North PLI. Of course, further work is needed to substantiate this argument.

MacDonald (1999) speculated that the South PLI may be a late stage component of the HLIS; however, the fact that the crystallization age of the South PLI (1337 Ma)

does not fall within the crystallization age range reported for the HLIS (1460-1450 Ma) seemingly rules out this suggested relation. In addition, the South PLI intruded anorthosite and granitoids belonging to the HLIS (Fitzpatrick *et al.*, 1998; see enclosed map).

The second magma batch (*i.e.* the precursor to the North PLI) also spawned during the early evolution of the NPS and ascended to the upper crust. Within the upper crust the magma collected in a chamber situated within the sulphide-bearing Tasiuyak paragneiss of the Churchill Province prior to its final emplacement and crystallization *ca.* 1322 Ma (Figure 6.1, Diagram C). As the silicate melt collected and pooled within this chamber, significant volumes of the enveloping Tasiuyak paragneiss were assimilated, thus contributing to sulphide saturation of the magma and the generation of two immiscible liquids; a sulphide liquid and a silicate liquid (Stage 4) (Figure 6.1, Diagram D). It is here that stage four of the model is invoked. A similar process may also be implied for the South PLI, but this is not within the scope of this present study. Refer to MacDonald (1999) and Kerr (2003) for further information relating to this topic.

Assimilation of the Tasiuyak paragneiss is favored as the principal factor that led to the sulphide saturation of the silicate melt (precursor to the North PLI) more so than any other known factor (*e.g.* assimilation of Nain gneiss, felsification, oxygen fugacity, pressure and temperature, *etc.*). The importance of this factor is clearly demonstrated by the major and trace element geochemical and sulphur isotope data, coupled with macro and microscopic observations within this study.

Assimilation of the Tasiuyak paragneiss led to a substantial increase in major and trace element concentrations within the silicate melt that define the Tasiuyak gneiss (*e.g.*

CaO, Rb, Ba, Zr, *etc.*). This is illustrated by the major and trace element plots depicted on Figures 4.5a, 4.15a, 4.15b, 4.15c, 4.16d, and 4.17. Rock samples with the most obvious contamination (*e.g.* Gabbro Hybrid \pm Olivine Gabbro) generally mimic or overlap with geochemical fields defined by the Tasiuyak paragneiss.

The sulphur isotope ratios of sulphides from the North and South PLI also indicate assimilation of an external sulphur source. The measured sulphur isotope ratios of the Tasiuyak paragneiss sulphides are negative, locally $\delta^{34}\text{S} = -4.91$ to -1.32 ‰, regionally $\delta^{34}\text{S} = -17.00$ to -0.90 (this study, Ripley *et al.*, 1997) which overlaps with the determined $\delta^{34}\text{S}$ isotopic ratios of the North PLI ($\delta^{34}\text{S} = -3.33$ to -1.93), as well as the South PLI. The measured Nain Province sulphur isotopic ratios are $\delta^{34}\text{S} = +0.2$ to $+3.3$ ‰ (Ripley *et al.*, 1997) which rules out the Nain gneisses as a significant sulphide source.

Fragments and partially dissolved inclusions of the Tasiuyak paragneiss are commonly observed in outcrops and drill core of the Basal Gabbro Subdivision, notably within the Gabbro Hybrid. This was also confirmed by Hearn (2001). In many examples, inclusions are nearly completely absorbed by the silicate melt and the relict inclusions can only be observed using petrographic techniques.

The fifth stage of this model started when sufficient sulphide liquid became available into which the available metals were able to partition at the expense of olivine (\pm pyroxene) (Figure 6.1, Diagram E). Metals will normally begin to separate from the silicate melt because of their chalcophile tendency and the preference of an element for the sulphides as compared to the silicate melt, otherwise expressed as the partition coefficient (Naldrett, 1996). The olivine grains analyzed in this study exhibit Ni depletion suggesting near complete transfer of the Ni into sulphide. The concentration of

Ni after separation of the sulphide liquid is termed the “R-value”. If the R-value is large (>2000) the deposit may have elevated metal values but the size of the deposit may be relatively small. Alternatively, if the R-value is small (100 to 2000) then the deposit may be relatively large but have low metal values. According to Kerr (2003) and MacDonald (1999), the R-values of the North and South PLI are relatively small (< 300) which concurs with the measured Ni and Cu contents of the Pants Lake Intrusion sulphide as determined in this study. It is noteworthy to mention here that the R-value for the Voisey’s Bay deposits is also considered small (600 to > 1000; Kerr, 2003).

Nearing the conclusion of stage five and the commencement of stage six, the Tasiuyak contaminated silicate melt began to fractionate and the immiscible sulphide liquid continued to acquire metals due to the interaction with the silicate melt. With changing pressures and temperatures in the magma chamber, the silicate melt and sulphide liquid were forced higher into the crust utilizing multiple upper crustal scale structures as conduits of least resistance (Figure 6.1, plan view of the PLI). These crustal scale features, represented mostly as east-west lineaments in the study area, are also present at Voisey’s Bay. After pressure and temperature conditions eased within the chamber, the ascending magma began to migrate laterally as a large sill complex, intruding the South PLI that had crystallized earlier (Figure 6.1, Diagram F and G). The point of entry of the magma entering the sill is assumed to have been either just below, or on the periphery of, the existing northwest mapped boundary of the North Intrusion (Figure 6.1, plan view of the PLI). This is assumed due to the relative thickness of the intrusion in this area, the presence of massive sulphide accumulations, lack of

leopard textures in the NAI area, and the influx of new and hotter magma batches in the NDT area, all of which indicate proximity to a feeder source.

The North PLI formed from multiple magma pulses that traveled via two routes (Figure 6.1, Diagram G) producing two unique, but chemically and petrographically similar mafic bodies; the melanocratic or Black Gabbro in the north (within the NAI area) and the leucogabbro in the south (within the NDT, HFL, WG, and MH areas). The only known difference between the two gabbroic bodies is the presence of microscopic oxide inclusions within the plagioclase grains (MacDonald, 1999) of the Black Gabbro. These inclusions suggest that the Black Gabbro was contaminated by an oxide-rich source during its ascension from the magma chamber. At present, the contact relationships of the two magmas, and the spatial extent of the Black Gabbro are unknown. Nevertheless, both gabbroic bodies formed from a series of pulsating magma injections akin to a heart pumping blood through arteries of the body. The first series of magma pulses produced the more buoyant plagioclase cumulate, sulphide-depleted rocks designated as the Upper Gabbro Subdivision. The second series of pulses produced the denser olivine cumulate, inclusion and sulphide abundant rocks designated as the Basal Gabbro Subdivision that squeezed beneath and underplated the Upper Gabbro. Both pulses carried the silicate melt to every region of the sill as determined by the laterally continuous and repetitive nature of the subunits. During the emplacement of the Basal Gabbro, the footwall gneiss underwent considerable thermal erosion, metamorphism, and alteration. Local footwall brecciation and assimilation of the adjacent silicate melt is frequently observed.

During the emplacement of the Basal Gabbro subdivision, the immiscible sulphide liquid was carried in suspension throughout the entire North Intrusion sill. The

undulating nature of the basal topography combined with narrowing and swelling of the intrusion invokes similar physical controls to those noted at Voisey's Bay within the conduit system that hosts the deposits (Evans-Lamswood *et al.*, 2000). As such, the dense sulphide liquid within the sill accumulated within footwall basal depressions or sites of depressed energy (*e.g.* NAI area), and the suspended sulphides were carried further from the feeder source and formed disseminations, leopard or net-textured sulphide textures (Figure 6.1, Diagram H and plan view of the PLI). Massive and semi-massive sulphide liquids pooled and melted within the footwall gneiss, oftentimes percolating into the gneiss for some distances where, according to Naldrett's (1989) work, the liquidus temperatures of the sulphide liquid would be in excess of 1200 °C and are quite capable of assimilating the footwall gneiss. The differences in metal tenors of the massive sulphide, as noted in the NAI area and elsewhere, are attributed to the continuous volume of magma flowing and interacting through the residing or settled sulphide, thus upgrading the metal contents of the effected sulphide.

Suspended country rock gneissic inclusions within the silicate melt are also transported along the entire span of the North Intrusion. Due to the enhanced feldspar and quartz contents, the inclusions migrate upwards within the denser mafic magma of the Basal Gabbro. The gneissic inclusions are partially or completely absorbed within the mafic magma contributing to local variations of the mafic rock chemistry and mineralogy.

The remaining stages of the proposed model occur during the final cooling and crystallization of the silicate-melt and contained sulphide liquid. As the silicate melt began to cool and the temperature of the sulphide decreases, the sulphide liquid is

fractionated. The first sulphide to crystallize from the sulphide liquid is pyrrhotite, a Fe-rich monosulphide solid solution that also contains Ni and Cu in solution. Continued fractionation of the Fe-rich sulphide liquid will cause pentlandite and chalcopyrite to separate from the sulphide liquid (*e.g.* exsolution laminae). These processes are frequently observed within large scale (*e.g.* massive sulphide) and small scale (*e.g.* sulphide blotch, disseminated sulphide) examples. Partitioning of metals from the adjacent olivine grains into the adjacent sulphide occurs on a local scale (Figure 6.1, Diagram I) within small pockets of uncrystallized silicate and sulphide liquid. The final process to note is the remobilization of high-grade fractionated chalcopyrite (\pm pentlandite and cubanite) into micro fractures surrounding individual sulphide grains and blotches. Remobilization of high-grade sulphides within the footwall gneiss also occurred on larger scales (*e.g.* NAI area) and is remarkably similar to the reported footwall deposits of the Sudbury region.

6.2 Conclusions

The Basal Gabbro Subdivision (BGS) and the Upper Gabbro Subdivision (UGS) collectively forms the North Pants Lake Intrusion (PLI) that crystallized circa 1322 Ma as part of the much larger Nain Plutonic Suite. The North PLI was emplaced as a relatively flat-lying sill complex into the Tasiuyak Paragneiss. The proximal and genetically similar South PLI crystallized at 1337 Ma, but does not have the distinctive BGS and UGS which make up the North PLI; in fact, the BGS of the North PLI intrudes the South PLI.

The BGS is defined by a recognizable stratigraphy of subunits that are repeated throughout the entire North PLI which in all likelihood result from a single-point of entry of the pulsating silicate melt into the north sill. The minor variations noted in the whole rock chemistry and mineralogy of the subunits are the direct result of gneissic contamination, either locally or from a distal source (chamber contamination?), and from the presence of Fe, Ni, Cu, and lesser Co-bearing magmatic sulphides. Overall, there is no substantial difference in the chemistry of the BGS subunits, nor between the BGS and the UGS.

The sulphides present in the BGS are typical of magmatic systems worldwide and in most cases they appear to have undergone the same processes implied for Voisey's Bay, Sudbury, *etc.*. Sulphide immiscibility and metal partitioning certainly occurred prior to entry into the sill, however, it is unlikely that this sulphide liquid was distributed evenly throughout the chamber which helps to explain why some subunits are relatively barren of sulphides. Sulphide settling occurred on a local scale, however, it was the changes in

the sill dynamics (*i.e.* basement depressions, swelling, and closing) that played the largest role in sulphide deposition.

Generally, sulphides of the BGS have low metal tenors compared to the metal tenors of the Voisey's Bay deposits. However, it has been demonstrated that there is potential for higher grade metal tenors in sulphides, especially in the northern apex of the North PLI (*e.g.* NAI area). Reports relating to the metal tenors of the Voisey's Bay deposits suggest upgrading by new silicate magma batches with the Ni-enriched olivines. New magma batches have been recognized on the northwest periphery of the North PLI in the NDT area.

The North PLI does have similar local features as the Voisey's Bay Intrusion (*e.g.* sulphide and silicate textures, gneissic contamination, *etc.*), however, the host rocks at Voisey's Bay represent a feeder or conduit of a much larger magmatic system, whereas the North PLI represents the endmember of the magmatic system connected to a conduit. In terms of the other regional Ni-Cu occurrences noted in Chapter 3, the PLI is quite unique most notably in the host rocks (layered olivine bearing gabbros), magmatic sulphide textures, primitive chemistry, and S isotopic values.

6.3 Recommendations

As with the completion of most geological studies of this scope, recommendations are often made to compliment the results of the present study, guide future studies, or to focus mineral exploration to areas with identified potential. The following points summarize the recommendations of this author.

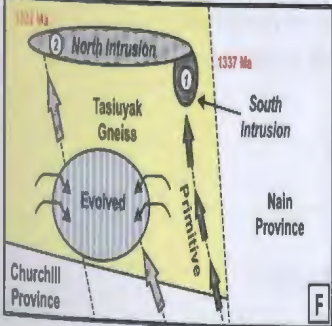
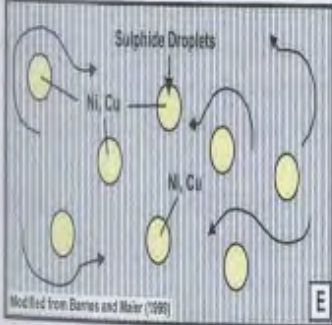
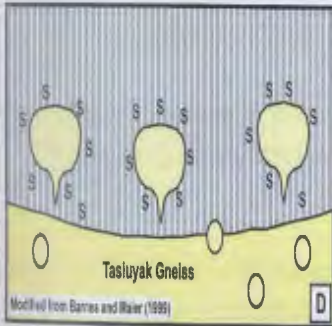
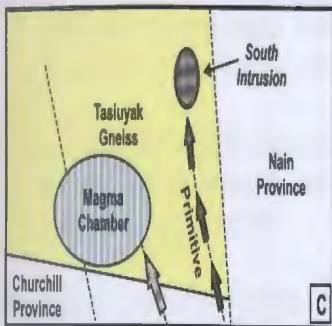
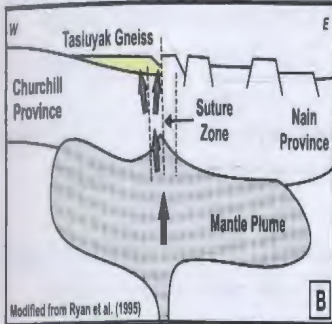
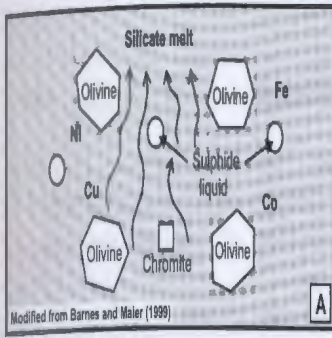
- The first recommendation regards utilizing the terms *Pants Lake Intrusive Suite* to collectively define the multiple intrusions in this area and *North Pants Lake Intrusion* or *South Pants Lake Intrusion* to define the respective individual intrusions. The current *Pants Lake Intrusion* nomenclature, although utilized in this study, should be discontinued in the future.
- The second recommendation is to initiate a study utilizing the Rb-Sm and Sm-Nd radiogenic isotope systems on the rocks of the North and South Pants Lake Intrusions, as well as rocks of the Churchill Province and adjacent Nain Province. The results from this study could provide a valuable tool to further access the petrogenesis and relationship between crust-mantle processes, as well as the level of crustal contamination and basement influence on the genesis of the two intrusions. Similar studies of these systems are reported for the Voisey's Bay deposits, OKG prospects, *etc.* and can be compared or contrasted with the results obtained from this study area.
- The third recommendation requires that olivine from drill cores dispersed throughout the North PLI, especially from drill holes located near the mapped northern boundary, be systematically analyzed. To increase speed and efficiency, the microprobe technique rather than the LAM-ICP-MS technique should be utilized considering that only the results for Ni, Cu, MgO, and FeO are required. The new data, compiled with

existing olivine databases (*e.g.* Naldrett, 1998; MacDonald, 1999; Smith, 2005), could potentially identify the point of entry for new magma injections within the chambers or sill, which may ultimately lead to the location of feeder conduits akin to the Voisey's Bay deposit system.

- The fourth recommendation involves further exploration for similar mineralization encountered in drill hole 97-75 (1.1 m of 11.9% Ni, 9.6% Cu, 0.43% Co, and 54 g/t Ag) considering that the attributes of this massive sulphide intersection are remarkably similar to the well-endowed footwall deposits described from the Sudbury mining camps (*e.g.* McCreedy East and West, Victor, Levack, *etc.*) and are worth approximately \$2,600 per tonne in today's markets. As a first start, a down hole UTEM survey of drill hole 97-75 should be implemented to determine if additional mineralization is located elsewhere. A detailed structural analysis of the immediate area, in the context of drill hole 97-75 and surrounding drill holes, may provide insight into basement structures that could potentially harbor high-grade footwall mineralization, especially in areas with massive sulphide adjacent to the footwall contact.

- The final recommendation involves contracting an airborne MEGATEM electromagnetic and magnetic survey, similar to the survey currently offered by Fugro Airborne Surveys. The airborne survey should cover a 10 km wide corridor centered above the North PLI and continued east and west over the surrounding Churchill Province (total area $\approx 10 \times 30$ km). Flight lines should be orientated north-south with a maximum of 200 meters spacing. Current 3-D inversion techniques are capable of modeling known anomalies (sulphide mineralization) as well as potential new anomalies up to 600 meters below surface. This survey is recommended due to the recognition of

the east-west trend of the gabbroic bodies located on the western side of the North Intrusion which coincidentally line-up with the jog or displacement of the Churchill and Nain Province boundary as indicated above Sarah Lake (see Geology Map, back pocket; Figure 6.1). This east-west trend may serve as a subsidiary structural corridor for magma similar to the conduit geometry implied at Voisey's Bay. It is plausible that magma entry into the North PLI may have originated from the west rather than the east and results from the MEGATEM survey may inspire renewed interest for this area.



Stage 1: The Pants Lake Intrusion (PLI) originated in the mantle where silicate melt was generated (12 to 50%) to absorb and collect sufficient metal concentrations including all of the available mantle sulphide (refer to diagram A). MacDonald (1999), suggested that the original melt composition was ferropicroitic.

Stage 2: A mantle plume of ferropicroite composition collected at the base of the crust (refer to diagram B). The 1850 Ma Nain-Churchill suture zone provided the necessary route for rapid magma ascension into the upper crust. During this stage, the Harp Lake Intrusive Suite (HLIS) was emplaced into the upper crust (ca. 1460-1450 Ma) followed by the Nain Plutonic Suite (NPS) (ca. 1350-1290) (HLIS & NPS not included in diagram). This is a similar model proposed for the Voisey's Bay Intrusion (after Ryan *et al.*, 1995).

Stage 3: During the formation of the NPS, two early magma batches traveled from the mantle plume to the upper crust (refer to diagram C). The first magma batch, represented by the South PLI, traveled directly to the final crystallization location without significant periods of "resting" enroute. The second batch pooled into a magma chamber within the sulphide bearing Tasuyak paragneiss of the Churchill Province prior to its intrusion to the final crystallization location (i.e. North PLI).

Stage 4: Within the magma chamber, significant assimilation of the country rock (paragneiss) occurred contributing to sulphide saturation and eventual sulphide immiscibility (refer to diagram D). When sufficient sulphide liquid became available, metals began to partition into the sulphide phase at the expense of olivine (lesser pyroxene) (refer to diagram E). It is likely that a similar process may have occurred for the South PLI.

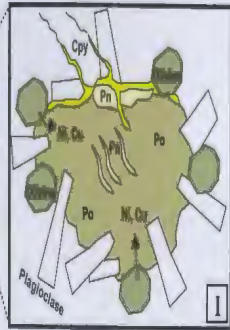
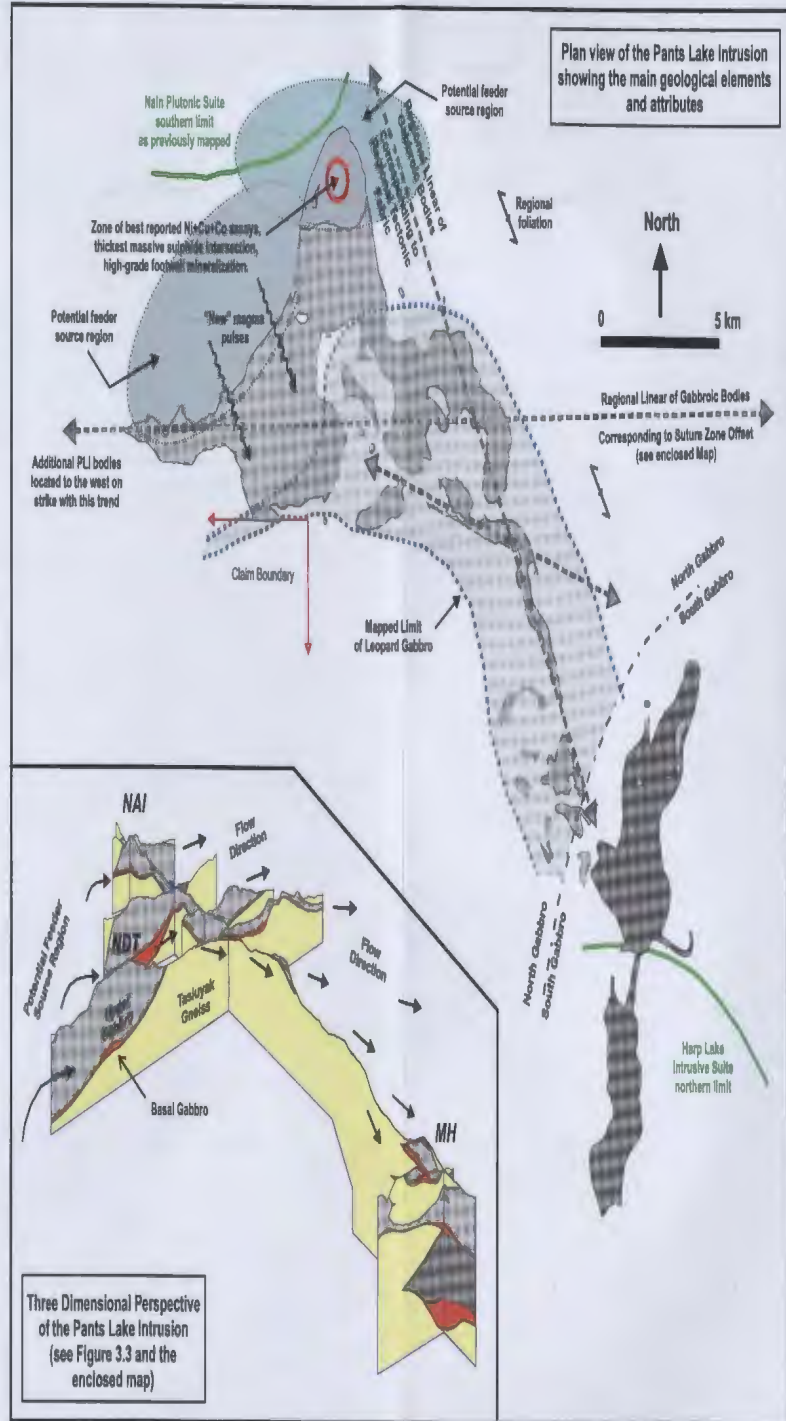
Stage 5: As the contaminated silicate melt in the magma chamber evolved through fractionation, the sulphide liquid continued to acquire metals. Due to chamber "dynamics", the North PLI magma began to ascend higher into the crust utilizing multiple crustal scale structures as conduits of least resistance (refer to plan view). When the magma reached a preferred horizon in the crust, the magma migrated laterally as sills, cutting the existing South PLI that crystallized circa 1337 Ma (refer to diagram F).

Stage 6: The North PLI formed from a series of magma pulses that traveled via two separate routes (refer to diagram G) producing two unique, but chemically and petrographically similar rock types (ca. 1322 Ma). The first pulse produced the plagioclase cumulate Upper Gabbro subdivision, whereas the second pulse produced the olivine cumulate Basal Gabbro.

Stage 7: During successive pulses, the denser sulphide liquid accumulated as massive sulphide within basal depressions or low energy sites and the suspended sulphides were carried further from the feeder source and formed as leopard or net-textured sulphide textures (refer to diagram H). The differences in metal tenors of the sulphide, as noted in the NAI area, are attributed to the continuous volume of magma flowing through the residing sulphide, thus upgrading of the metals into the sulphide.

Stage 8: The cooling sulphide (pyrrhotite) liquid exsolved pentlandite and chalcocypite. Partitioning of metals from olivine into the adjacent sulphide occurred on a local scale. (Refer to diagram I). High-grade chalcocypite (+/- pentlandite) re-mobilized into fractures and footwall structures.

Figure 6.1. Proposed model developed by the author for the formation of the Basal Gabbro Subdivision of the Pants Lake Intrusion, Labrador. Many components of this model are adopted from studies by MacDonald (1999), Ryan *et al.* (1995), and Barnes and Maier (1999).



References

- Amelin, Y., Li, C. and Naldrett, A.J., 1997. Multistage evolution of the Voisey's Bay complex, Labrador, Canada, revealed by U-Pb systematics of zircon, baddeleyite, and apatite. Abstracts, AGU 1997 Fall Meeting.
- Amelin, Y., Li, C. and Naldrett, A.J., 1999. Geochronology of the Voisey's Bay intrusion, Labrador, Canada, by precise U-Pb dating of coexisting baddeleyite, zircon, and apatite. *Lithos*, **47**: 33-51.
- Bachinski, D.J., 1969. Bond strength and sulphur isotopic fractionation in coexisting sulphides. *Economic Geology*, **64**: 56-65.
- Barnes, S-J. and Maier, W.D., 1999. The fractionation of Ni, Cu and the noble metals in silicate and sulphide liquids. *Edited by* Keays, R.R., Leshner, C.M., Lightfoot, P.C., and Farrow, C.E.G. Dynamic processes in magmatic ore deposits and their application to mineral exploration. Mineral Deposits Division, Geological Association of Canada, Short Course Notes, **13**: 69-106.
- Barnes, S-J. and Naldrett, A.J., 1987. Fractionation of the platinum-group elements and gold in some komatiites of the Abitibi Greenstone Belt, Northern Ontario, *Economic Geology*, **82**: 165-183.
- Berg, J.H., 1973. Geology of the Hettasch Lake area. The Nain Anorthosite Project, Labrador. *Edited by* S.A. Morse, Geology Department, University of Massachusetts; Field Report 1972, pp. 111-119.
- Blundy, J., Dalpe, C., and Higgins, M., 2000. The composition and distribution of trapped melt in the Kiglapait layered intrusion. *Journal of Conference Abstracts*, **5(2)**: p. 218.
- Brace, T.D. and Wilton, D.H.C., 1990. Platinum-group elements in the Archean Florence Lake Group, Central Labrador. *Canadian Mineralogist*, **28**: 419-429.
- Brenan, J.M., McDonough, W.F., and Dalpé, C., 2003. Experimental constraints on the partitioning of rhenium and some platinum-group elements between olivine and silicate melt. *Earth and Planetary Science Letters*, **212**: 135-150.
- Bridgwater, D., Watson, J., and Windley, B.F., 1973. The Archean craton of the North Atlantic Tranactions, Royal Society of London, **A273**: 427-437.
- Buchanan, D.L., Nolan, J., Wilkinson, N and de Villiers, J.P.R., 1983. An experimental investigation of sulphur solubility as a function of temperatures in synthetic silicate melts. *Geological Society of Africa, Special Publication 7*, pp. 383-391.

- Cadman, A.C., Heaman, L., Tarney, J., Wardle, R.J., and Krough, T.E., 1993. U-Pb geochronology and geochemical variation within two Proterozoic mafic dyke swarms, Labrador. *Canadian Journal of Earth Sciences*, **30**: 1490-1504.
- Canil, D., and Fedortchouk, Y., 2001. Olivine-liquid partitioning of vanadium and other trace elements, with applications to modern ancient picrites. *The Canadian Mineralogist* **39(2)**: 319-330.
- Collerson, K.D., 1991. New field and isotopic constraints on the evolution of early Archean gneisses in northern Labrador. ECSOOT Transect Meeting, Lithoprobe Report 32, pp. 96-101.
- Connelly, J.N., 2001. Interim report of the age date for the South Gabbro, Pants Lake Intrusion: Unpublished report prepared for Donner Minerals Ltd.
- Connelly, J.N., and Ryan, B., 1992. U-Pb constraints on the thermotectonic history of the Nain area. ECSOOT Transect Meeting, Lithoprobe Report 32, pp.137-144.
- Connelly, J.N., and Ryan, B., 1993. Late Archean and Proterozoic events in the Central Nain craton. ECSOOT Transect Meeting, Lithoprobe Report 36, pp. 53-61.
- Davenport, P.H., Nolan, L.W., Wardle, R.W., Stapleton, G.J., and Kilfoil, G.J., 1999. *Geoscience Atlas of Labrador*, Government of Newfoundland and Labrador, Department of Mines and Energy, Geological Survey, Open File LAB/1305.
- Donner Minerals Limited web site access, 1997 to 1998: <http://www.donnerminerals.com/svbproject/index.html>.
- Dunning, G., 1998. Unpublished Interim report of the U/Pb crystallization age of the North Gabbro, Pants Lake Intrusion, South Voisey's Bay project: Unpublished report prepared for Donner Minerals Ltd.
- Dwyer, L.B., 1999. Metallogeny of the Cirque Property, northern Nain Plutonic Suite, Labrador. GAC-MAC Joint Annual Meeting, Sudbury; Abstract vol. 24, pp. 34-35.
- Dwyer, L.B., 2001. A compiled geological, geochemical, and metallurgical study of the magmatic nickel-copper sulphide occurrence at the cirque property, Nain Plutonic Suite, Northern Labrador. Unpublished M.Sc thesis. Memorial University of Newfoundland, St. John's, Newfoundland.
- Dyke, B., Kerr, A., and Sylvester, P.J., 2004. Magmatic sulphide mineralization at the Fraser Lake Prospect (NTS 13L/5), Michikamau Intrusion, Labrador. Newfoundland Department of Mines & Energy, Geological Survey, Report 04-1.

- Eggins, S.M., Rudnick, R.L., and McDonough, W.F., 1998. The composition of peridotites and their minerals: a laser ablation ICP-MS study. *Earth and Planetary Science Letters*, **154**: 53-71.
- Emslie, R.F., 1970. The Geology of the Michikamau Intrusion, Labrador (13L, 23I). Geological Survey of Canada, Department of Mines, Energy and Resources. Paper 68-57.
- Emslie, R.F., 1980. Geology and petrology of the Harp Lake Complex, central Labrador: An example of Elsonian magmatism. Geological Survey of Canada, Bulletin 293.
- Emslie, R.F., Hamilton, M.A., and Theriault, R., 1994. Petrogenesis of a mid-Proterozoic anorthosite-mangerite-charnockite-granite (AMCG) complex: isotopic and chemical evidence from the Nain Plutonic Suite. *Journal of Geology*, **102**: 539-558.
- Ermanovics, I., and Korstgaard, J., 1981. Geology of the Hopedale Block and adjacent areas, Labrador, Report 3. Current Research, Part A, Geological Survey of Canada Paper 91-1A, pp.69-76.
- Ermanovics, I., 1993. Geology of the Hopedale Block, southern Nain Province, and the adjacent Proterozoic terranes, Labrador, Newfoundland. Geological Survey of Canada, Memoir 431.
- Evans-Lamswood, D.M., Butt, D.P., Jackson, R.S., Lee, D.V., Muggridge, M.G., Wheeler, R.I., and Wilton, D.H.C., 2000. Physical controls associated with the distribution of sulphides in the Voisey's Bay Ni-Cu-Co deposit, Labrador. *Edited by M.T. Einaudi. Economic Geology*, **95**: 749-769.
- Ewers, W.E. and Hudson, D.R., 1972. An interpretative study of a nickel iron sulphide ore intersection, Lunnon Shoot, Kambalda, Western Australia. *Economic Geology*, **67**: 1075-1092.
- Faure, G., 1986. Sulphur. *Principles of Isotope Geochemistry*, pp. 523-552.
- Fincham, C.J.B. and Richardson, F.D., 1954. The behavior of sulphur in silicate and aluminum melts. *Proc. Royal Society of London*, **223A**.
- Fitzpatrick, D., Moore, P., MacGillivray, G., House, S., and Emon, K., 1998. Report of work, South Voisey's Bay project, Central Labrador: Core Program. Teck Exploration Ltd. Unpublished assessment report submitted to the Department of Mines and Energy.

- Fitzpatrick, D., Moore, P., MacGillivray, G., House, S., and Emon, K., 1999. Report of work, South Voisey's Bay Project, Central Labrador: Teck Exploration Ltd. Unpublished assessment report submitted to the Department of Mines and Energy.
- Glesemann, A., Jager, H. J., Norman, A.L., Krouse, H.R., and Brand, W.A., 1994. On-line sulphur-isotope determination using an elemental analyzer coupled to a mass spectrometer. *Analytical Chemistry*, **66**: 2816-2819.
- Govindaraju, K., 1989. Compilation of working values and sample description for 272 geostandards. *Geostandards Newsletter-The Journal of Geostandards and Geoanalysis* **13**: 113.
- Godlevskii, M.N., and Grinenko, L.N., 1963. Some data on the isotopic composition of sulphur in the sulphides of the Noril'sk deposit. *Geochemistry*, **1**: 35-41.
- Gower, C.F., Flanagan, M.J., Kerr, A., and Bailey, D.G., 1982. Geology of the Kaipokok Bay-Big River area, Central Mineral Belt, Labrador. Newfoundland Department of Mines and Energy, Report 82-7.
- Green, B.A., 1972. Geological Map of Labrador. Newfoundland Department of Mines, Agriculture and Resources, Mineral Resources Division.
- Hamilton, M.A., Emslie, R.F., and Roddick, J.C., 1994. Detailed emplacement chronology of the Mid-Proterozoic Nain Plutonic Suite, Labrador: Insights from U-Pb systematics in zircon and badelleyite. Eighth International Conference on Cosmochronology and Isotope Geology. United States Geological Survey Circular 1107.
- Haughton, D.R., Roeder, P.L. and Skinner, B.J., 1974. Solubility of sulphur in mafic magmas. *Economic Geology*, **69**: 451-467.
- Hearn, J.G., 2001. Metamorphic petrology of the "country rock" gneisses adjacent to the Pants Lake Intrusion. B.Sc honours thesis dissertation, Department of Earth Sciences, Memorial University of Newfoundland.
- Hill, J.D., 1982, Geology of the Flowers River-Notakwanon River area, Labrador. Mineral Development Division, Department of Mines and Energy, Report 82-6.
- Hinchev, J.G., 1999. Magmatic sulphide-oxide mineralization in the Nain area, northern Labrador: A petrological and geochemical study. Unpublished B.Sc. (Hons), Memorial University of Newfoundland, St. John's.
- Hinchev, J. Kerr, A., and Wilton, D.H.C., 1999. Magmatic sulphide-oxide mineralization in the Nain Hill area (NTS 14C/12), northern Labrador. *Current Research*, Newfoundland Department of Mines and Energy, Report 99-1, pp. 183-194.

- Hirschmann, M.M., 1991. Thermodynamics of multicomponent olivines and the solution properties of $(\text{Ni,Fe,Mg})_2\text{SiO}_4$ and $(\text{Ca,Mg,Fe})_2\text{SiO}_4$ olivines. *American Mineralogist*, **76**: 1232-1248.
- Hodder, S.H., 1997. A drill core analysis and petrographic study of Ni-Cu bearing gabbros, South Voisey's Bay area, Labrador. B.Sc thesis dissertation, Department of Earth Sciences, Memorial University of Newfoundland.
- Hoffman, P.F., 1988. United Plates of America, the birth of a craton: Early Proterozoic assembly and growth of Laurentia. *Annual Reviews in Earth and Planetary Science*, **16**: 543-603.
- Inco Limited web site access, 2003. <http://www.inco.com/investorinfo/annualreports/2003>.
- Irving, T.N., and Baragar, W.R.A., 1971. A guide to the chemical classification of the common volcanic rocks. *Canadian Journal of Earth Sciences*, **8**: 523-548.
- James, D.T., 1997. The Archean Hunt River greenstone belt, Hopedale Block, eastern Labrador (NTS 13N/7 and 13N/10): Geology and exploration potential. Current Research. Newfoundland Department of Mines and Energy, Geological Survey Branch, Report 93-1, pp. 371-385.
- Jenner, G.A., Longerich, H.P., Jackson, S.E., and Fryer, B.J., 1990. ICP-MS- A powerful tool for high precision trace-element analysis in Earth Sciences: Evidence from analysis of selected U.S.G.S. reference samples. *Geochemical Geology*, **83**: 133-148.
- Jensen, L.S., 1976. A new cation plot for classifying subalkalic volcanic rocks. Ontario Division of Mines, Miscellaneous Paper 66.
- Keays, R.R., 1995. The role of komatitic and picritic magmatism and S-saturation in the formation of ore deposits. *Lithos*, **34**: 1-18.
- Kerr, A., MacDonald, H.E., and Naldrett, A.J., 2001. Geochemistry of the Pants Lake Intrusion, Labrador: Implications for Future Mineral Exploration. Current Research. Newfoundland Department of Mines, Geological Survey Branch.
- Kerr, A., and Ryan, B., 2000. Threading the eye of the needle: lessons from the search for another Voisey's Bay in Labrador, Canada. *Economic Geology*, **95**: 725-748.
- Kerr, A. and Smith, J.L., 2000. Magmatic Ni-Cu sulphide mineralization in the Harp Lake Intrusive Suite, Central Labrador. Current Research, Newfoundland Department of Mines and Energy, Geological Survey, Report 2000-1, pp. 1-24

- Kerr, A. and Smith, J.L., 1997. The search for magmatic Ni-Cu-Co mineralization in Northern Labrador: a summary of active exploration programs. Current Research, Newfoundland Department of Mines and Energy, Geological Survey, Mineral Deposits Section, Report 97-1, pp. 73-91.
- Kerr, A., 1998. Petrology of magmatic sulphide mineralization in Northern Labrador: preliminary results. Current Research, Newfoundland Department of Mines and Energy, Geological Survey, Mineral Deposits Section, Report 98-1, pp. 53-75.
- Kerr, A., 1999. Mafic rocks of the Pants Lake Intrusive Suite and related Ni-Cu-Co mineralization in North-Central Labrador. Current Research, Newfoundland Department of Mines and Energy, Geological Survey, Mineral Deposits Section, Report 99-1.
- Kerr, A., 2003. Nickeliferous gabbroic intrusions of the Pants Lake area, Labrador, Canada: implications for the development of magmatic sulphides in mafic systems. *American Journal of Science*, **303**: 221-258.
- Leshner, C.M., 1989. Komatiite-associated nickel sulphide deposits. Ore Deposition Associated with Magmas. *Edited by J.A. Whitney and A.J. Naldrett*; Reviews in Economic Geology, **4**: 45-101.
- Leshner, C. M. and Campbell, I.H., 1993. Geochemical and fluid dynamic modeling of compositional variations in Archean komatiite-hosted nickel sulfide ores in Western Australia *Economic Geology*, **88**: 804-816.
- Leshner, C.M. and Arndt, N.T., 1995. REE and Nd isotope geochemistry, petrogenesis and volcanic evolution of contaminated Komatiites at Kambalda, Western Australia. *Lithos*, **34**: 127-157.
- Li, C., Lightfoot, P. C., Amelin, Y., and Naldrett, A.J., 2000. Contrasting petrological and geochemical relationships in the Voisey's Bay and Mushuau intrusions, Labrador: Implications for ore genesis. *Economic Geology*, **95**: 771-800.
- Li, C. and Naldrett, A.J., 1999. Geology and petrology of the Voisey's Bay intrusion: reaction of olivine with sulphide and silicate liquids. *Lithos*, **47**: 1-31.
- Li, C., Naldrett, A.J., and Ripley, E.M., 2001. Critical factors for the formation of a Ni-Cu deposit: lessons from a comparison of the Pants Lake and Voisey's Bay deposits, Labrador. *Mineralium Deposita*, **36**: 85-92.
- Liebenberg, L., 1970. The sulphides in the layered sequence of the Bushveld Complex. Geological Society of South Africa, special publication 1, pp 108-207.

- Lightfoot, P.C. and Naldrett, A.J., 1999. Geological and geochemical relationships in the Voisey's Bay Intrusion, Nain Plutonic Suite, Labrador, Canada. *Edited by Keays, R.R., Lesher, C.M., Lightfoot, P.C., and Farrow, C.E.G. Dynamic processes in magmatic ore deposits and their application in mineral exploration, Geological Association of Canada, short course notes, 13: 1-30.*
- Lightfoot, P.C., 1998. Geological and geochemical relationships in the Ried Brook Intrusive Complex, Labrador: exploration strategies for magmatic Ni-Cu ores at Voisey's Bay. *Edited by Walton, G., and Jambor, J. Pathway's 1998 Extended Abstracts Volume, pp. 26-29.*
- Longerich, H.P., 1995. Analysis of pressed pellets of geological samples using wavelength-dispersion X-ray fluorescence spectrometer. *X-Ray Spectrometry, 24: 123-136.*
- Longerich, H.P., Jenner, G.A., Fryer, B.J., and Jackson, S.E., 1990. Inductively coupled plasma-mass spectrometric analysis of geological samples: a critical evaluation based on case studies. *Chemical Geology, 83: 105-118.*
- Longerich, H.P., Jackson, S.E., Fryer, B.J., and Strong, D.F., 1991. The laser ablation microprobe - inductively coupled plasma-mass spectrometer, *Geoscience Canada, 20.*
- MacDonald, H., 1999. The geology, petrography and geochemistry of gabbroic rocks of the Pants Lake Intrusive Suite on the Donner / Teck South Voisey's Bay property, North-Central Labrador, Canada. M.Sc thesis dissertation, Geology Department, University of Toronto.
- MacLean, W.H., 1969. Liquidus phase relations in the FeS-FeO-Fe₃O₄-SiO₂ system, and their application to geology. *Economic Geology, 64: 865-884.*
- Mainwaring, P.R. and Naldrett, A.J., 1977. Country rock assimilation and the genesis of Cu-Ni sulphides in the Waterhen Intrusion, Duluth Complex, Minnesota. *Economic Geology, 72: 1269-1284.*
- McAuslan, D.A., 1973a. Report on reconnaissance program-1972. Kennco Explorations Canada Ltd. Assessment report submitted to Newfoundland Department of Mines and Energy.
- McAuslan, D.A., 1973b. Report on reconnaissance program-1973. Kennco Explorations Canada Ltd. Assessment report submitted to Newfoundland Department of Mines and Energy.
- McConnell, J., 1998. The use of till and stream geochemistry to define lake-sediment / water anomalies in central Labrador. Report 1999. Department of Mines and Energy. Geochemistry, Geophysics and terrain Sciences Section.

- McConnell, J., 2000. Recent high-density lake-sediment and water surveys in central Labrador. In *Current Research, Newfoundland Department of Mines and Energy, Geological Survey, Report 2000-1*, pp. 75-99.
- McLean, S., Butler, D., and Osmand, R., 1992. Report on geological surveys, geophysical surveys and diamond drilling on mapped staked licences 377M, 403M, 456M and 457M, held by Falconbridge Limited, unpublished assessment report.
- Miller, R.R., 1996. Ultramafic rocks and Ni-Cu mineralization in the Florence Lake - Uqjoktok Bay area, Labrador. *Current Research, Newfoundland Department of Mines and Energy, Geological Survey, Report 96-1*, pp. 163-173.
- Morrison, G.G., Jago, B.C., and White, T.L., 1994. Footwall mineralization of the Sudbury Igneous Complex. *Proceedings of the Sudbury-Noril'sk Symposium. Edited by Lightfoot, P.C. and Naldrett, A.J. Ontario Geological Survey Special 5: 57-64.*
- Morse, S.A., 1969. The Kiglaipait Layered Intrusion, Labrador. *Geological Society of America Memoir 112.*
- Naldrett, A.J., 1989. Introduction: Magmatic Deposits Associated with Mafic Rocks. *In Ore Deposition Associated with Magmas, (ed.) J.A. Whitney and A.J. Naldrett. Reviews in Economic Geology, 4: 1-3.*
- Naldrett, A.J., 1996. Chapter 1, Introduction. *Magmatic Sulphide Deposits: Theory, Reality and Exploration. Ore Deposits Workshop '96. University of Toronto, p. 1-9.*
- Naldrett, A.J., 1996. Chapter 5, Therotical Considerations. *Magmatic Sulphide Deposits: Theory, Reality and Exploration. Ore Deposits Workshop '96. University of Toronto.*
- Naldrett, A.J., 1997. Key factors in the genesis of Noril'sk, Sudbury, Jinchuan, Voisey's Bay and other worlds-class Ni-Cu-PGE deposits: implications for exploration. *Australian Journal of Earth Sciences, 44: 283-315*
- Naldrett, A.J., 1999. Summary of work on olivine compositions, Pants Lake Project. Unpublished report submitted to Donner Minerals Ltd.
- Naldrett, A.J., Keats, H., Sparkes, K., and Moore, R., 1996. Geology of the Voisey's Bay Ni-Cu-Co deposit, Labrador, Canada. *Exploration Mining Geology, 5(2): 169-179.*
- Naldrett, A.J., Duke, J.M., Lightfoot, P.C., and Thompson, J.F.H., 1984. Quantitative Modelling of Segregation of Magmatic Sulfides: an Exploration Guide. *Canadian Institute Mining and Metalurgy Bulletin, 77: 46-57.*

- Nunn, G.A.G., 1993. Geology of the Northeastern Smallwood Reservoir (NTS map 13L/SW), Labrador. Department of Mines and Energy, Geological Survey Branch, Report 93-3.
- Ohmoto, H. and Rye, R.O., 1978. Isotopes of sulphur and carbon. Geochemistry of Hydrothermal Ore Deposits, second edition. *Edited by* Barnes, H.L.
- Olshefsky, K., 1996. Report on rock geochemistry sampling and petrographic study on licences 411M, 413M, 414M, 415M, 458M and 459M, Harp Lake property, Labrador. Falcobridge Canada Ltd. Unpublished assessment report submitted to Newfoundland Department of Mines and Energy.
- Osmand, R., 1992. Report on prospecting and lithogeochemical surveys, Harp Lake properties, Labrador. Falcobridge Canada Ltd. Unpublished assessment report submitted to Newfoundland Department of Mines and Energy.
- Piercey, S.J., 1998. An integrated study of magmatism, magmatic Ni-Cu sulphide mineralization, and metallogeny in the Umiakoviarusek Lake region, Labrador, Canada. Unpublished M.Sc. thesis, Memorial University of Newfoundland. St. John's, Newfoundland.
- Piercey, S.J. and Wilton, D.H.C., 1999. Sulphide petrology and mineralization of the OKG Ni-Cu-Co sulphide prospect, Umiakoviarusek Lake region, Labrador. in Current research, Newfoundland Department of Mines and Energy, Geological Survey Report 99-1, pp. 297-310.
- Pye, A., 1998. EA-Continuous flow SO₂ analysis – minerals: preparation requirements. Internal unpublished Memorial University document, Earth Science Department.
- Ripley, E.M., 1981. Sulphur isotopic studies of the Dunka Road Cu-Ni Deposit, Duluth Complex, Minnesota. *Economic Geology*, **78**: 610-620.
- Ripley, E.M., Young-Rok, P., Li, C., and Naldret, A.J., 1997. Sulphur and oxygen isotope studies of the Voisey's Bay Ni-Cu-Co Deposit, Labrador, Canada. American Geophysical Union, Fall Meeting, San Francisco. Programs with abstracts.
- Rollinson, H., 1993. Using sulphur isotopes. Using geochemical data: evaluation, presentation, interpretation, pp. 303-315.
- Ryan, A.B., 1984. Regional geology of the central part of the Central Mineral Belt, Labrador. Newfoundland Department of Mines and Energy, Memoir 3.
- Ryan, A.B., 1991. New perspectives on the Nain Plutonic Suite and its country rocks. Newfoundland Department of Mines and Energy, Report 91-1, pp. 231-255.

- Ryan, B., 1990. Preliminary geological map of the Nain Plutonic Suite and Surrounding Rocks (Nain-Nutak, NTS 14SW). Newfoundland Department of Mines and Energy, Map 90-44.
- Ryan, B., 1997. The Mesoproterozoic Nain Plutonic Suite in eastern Canada, and the setting of the Voisey's Bay Ni-Cu-Co sulphide deposit. *Geoscience Canada*, **24** (4): 173-188.
- Ryan, B., Wardle, R.J., Gower, C.F., and Nunn, G.A.G., 1995. Nickel-copper-sulphide mineralization in Labrador: The Voisey Bay discovery and its exploration implications. *Current Research, Newfoundland Department of Natural Resources, Geological Survey, Labrador Mapping Section, Report 95-1*, pp. 177-204.
- Ryan, B., Phillips, E., Shwetz, J., and Machado, G., 1998. A tale of more than ten plutons, geology of the region between Okak Bay and Staghorn Lake, Labrador. *Current Research, Newfoundland Department of Mines and Energy, Geological Survey Branch, Report 98-1*, pp. 143-171.
- Ryan, B., 1996. Commentary on the Location of the Nain-Churchill Boundary in the Nain Area. *Current Research, Newfoundland Department of Natural Resources, Geological Survey, Labrador mapping section, Report 96-1*, pp. 109-129.
- Ryan, B. and Lee, D., 1989. Geological map of the Reid Brook area (14D/8), 1:5000. Newfoundland Department of Mines and Energy, Geological Survey Branch, Open file 89-18.
- Sack, R.O. and Ghiorso, M.S., 1989. Importance of considerations of mixing properties in establishing an internally consistent thermodynamic database: thermochemistry of minerals in the system Mg_2SiO_4 - Fe_2SiO_4 - SiO_2 . *Contributions to Mineralogy and Petrology*, **102**: 41-68.
- Sasaki, A., 1969. Sulphur isotope study of the Muskox Intrusion, district of Mackenzie. Geological Survey of Canada, Paper 68.
- Simmons, K.R., Wiebe, R.A., Snyder, G.A., and Simmons, E.C., 1986. U-Pb zircon ages of the Newark Island Intrusion, Nain Anorthosite Complex, Labrador. *Geological Society of America, Abstracts with Program*, **18**: 751.
- Smith, R. and Wilton, D.H.C., 1998. Preliminary investigation of the mineralized and contaminated sequence of the Pants Lake Intrusion, South Voisey's Bay project, Labrador. Canadian Institute of Mining, Metallurgy and Petroleum, Newfoundland Section. Programs with abstracts.

- Smith, R., Wilton, D.H.C., and Sparks, K., 1999. Magmatic Ni-Cu-Co sulphide mineralization in the Pants Lake Intrusion, South Voisey's Bay project, Labrador. Geological Association of Canada-Mineralogical Association of Canada, Joint Annual Meeting, Sudbury. Programs with abstracts.
- Streckeisen, A.L., 1975. To each plutonic rocks its proper name. *Earth Science Reviews*, **12**: 1-33.
- Sun, S and McDonough, W.F., 1989. Chemical and isotopic systematics of oceanic basalts: implications for mantle compositions and processes. *Edited by Saunders, A.D. and Norry, M.J. Magmatism in the Ocean Basins*, Geological Society Special Publication No. 42, pp. 313-345.
- Sutton, J.S., 1970. Geological report. Area northwest of Florence Lake, Ugjoktok area, Labrador. BRINEX, unpublished assessment report.
- Swinden, H.S., Wardle, R.J., Davenport, P.H., Gower, C.F., Kerr, A., Meyer, J.R., Miller, R.R., Nolan, L., Ryan, A.B., and Wilton, D.H.C., 1991. Mineral exploration opportunities in Labrador: A perspective for the 1990's. *Current Research. Newfoundland Department of Mines and Energy, Geological Survey Branch, Report 91-1*, pp. 349-390.
- Sylvester, P.J., and Eggins, S.M., 1997. Analysis of Re, Au, Pd, Pt and Rh in NIST Glass Certified Reference Materials and Natural Basalt Glasses by Laser Ablatio ICP-MS. *Journal of Geostandards and Geoanalysis*, **21**: 215-229.
- Sylvester, P., Tubrett, M., King, P. and Poujol, M., 2003. Analytical Geochemistry group. MUN activities and financial report. April 2002-September 2003.
- Taylor, R.P., Jackson, S.E., Longrich, H.P., and Webster, J.D., 1997. In-situ trace element analysis of individual silicate melt inclusions by laser ablation microprobe-inuctively coupled plasma-mass spectrometry (LAM-ICP-MS). *Geochim. Cosmochim. Acta*, **61**: 2559-2567.
- Taylor, S.R., and McLennan, S.M., 1985. *The continental crust: its composition and evolution*. Blackwell, Oxford.
- Thomas, A. and Morrison, R. S., 1991. Geological map of the central part of the Ugjoktok River (NTS 13N/5 and parts of 13M/8, and 13N/6), Labrador (with accompanying notes). Geological Survey Branch, Department of Mines and Energy, Map 91-160.
- Twyne, S.A., 1999. The petrology of the mineralized gabbro from the South Voisey's Bay area, Pants Lake Intrusion, Labrador. B.Sc (Hons) thesis dissertation, Department of Earth Sciences, Memorial University of Newfoundland.

- Wardle, R.J., Gower, C.F., Ryan, B., Nunn, G.A.G., James, D.T., and Kerr, A., 1997. Geological map of Labrador; 1:1 million scale. Government of Newfoundland and Labrador, Department of Mines and Energy, Geological Survey, Map 97-07.
- Wardle, R.J. and Wilton, D.H.C., 1995. The geology and mineral deposits of Labrador: A guide for the exploration geologist. CERR/NDNR Report.
- Wendlandt, R.F., 1982. Sulfide saturation of basalt and andesite melts at high pressures and temperatures. *American Mineralogist*, **67**: 877-885.
- Wells, C.S., 1997. A documentation and study of sulphide mineralization in the Hettasch Intrusion, Labrador. Unpublished B.Sc (Hons.) thesis, Memorial University of Newfoundland, St. John's.
- Wilson, M.R., 1998. Unpublished XRF (trace and major) geochemical data: report provided to the Teck-Donner South Voisey's Bay project.
- Wilton, D.H.C., 1996. Metallogenic overview of the Nain Province, northern Labrador. *CIM Bulletin*, **89**: 43-52.
- Wilton, D.H.C. and Baker, N.W., 1996. The OKG Ni-Cu-Co showing: A new discovery in the Nain Plutonic Suite of northern Labrador. Geological Association of Canada-Mineralogical Association of Canada, Annual Meeting 1996, Winnipeg, Program with abstracts, **21**: 102.
- Winchester, J.A., and Floyd, P.A., 1977. Geochemical discrimination of different magma series and their differentiation products using immobile elements. *Chemical Geology*, **20**: 325-343.

Appendix A: Diamond Drill Hole and Sample Data

Table A.1. Diamond drill hole information for re-logged drill cores used in this study. Drill hole information obtained from Fitzpatrick *et al.* (1999). The diamond drill hole logs are in Appendix C. Sample information is located in Table A.2.

| Re-logged DDH Name | UTM Coordinates of Collar Location (easting / northing) | Collar Azimuth | Collar Dip (below horizontal) | Collar Elevation (AMSL) | DDH Length (meters) | No. of samples from DDH |
|--------------------|---|----------------|-------------------------------|-------------------------|---------------------|-------------------------|
| SVB-96-02 | 564219 / 6150429 | 250 ° | 60 ° | 480.0 | 94.5 | 7 |
| SVB-96-04 | 557708 / 6149175 | 210 ° | 45 ° | 523.9 | 103.6 | 9 |
| SVB-96-07 | 566211 / 6151063 | 265 ° | 88 ° | 476.9 | 70.6 | 2 |
| SVB-96-08 | 566108 / 6151105 | 210 ° | 88 ° | 485.1 | 44 | 6 |
| SVB-96-09 | 563514 / 6150172 | 210 ° | 70 ° | 510.0 | 143.1 | 6 |
| SVB-96-10 | 565190 / 6149921 | 20 ° | 50 ° | 527.8 | 51.2 | 4 |
| SVB-96-15 | 566130 / 6149220 | 220 ° | 45 ° | 480.0 | 118.9 | 5 |
| SVB-96-16 | 567705 / 6148185 | 270 ° | 88 ° | 426.5 | 73.2 | 2 |
| SVB-97-17 | 567657 / 6148227 | 270 ° | 50 ° | 427.2 | 63.1 | 5 |
| SVB-96-20 | 565989 / 6151170 | 210 ° | 88 ° | 485.6 | 46.3 | 5 |
| SVB-96-27 | 563193 / 6149484 | 360 ° | 88 ° | 478.6 | 82.3 | 5 |
| SVB-96-29 | 568136 / 6147426 | 225 ° | 45 ° | 445.4 | 76.2 | 4 |
| SVB-96-34 | 569268 / 6143695 | 225 ° | 88 ° | 455.7 | 48.8 | 6 |
| SVB-96-36 | 570097 / 6144369 | 10 ° | 60 ° | 395.5 | 149.2 | 8 |
| SVB-96-44 | 563880 / 6150580 | 180 ° | 88 ° | 475.0 | 47.5 | 2 |
| SVB-96-47 | 569761 / 6144243 | 140 ° | 60 ° | 363.9 | 67.1 | 5 |
| SVB-96-48 | 569610 / 6144174 | 225 ° | 88 ° | 370.5 | 76.2 | 3 |
| SVB-96-52 | 567870 / 6148923 | 40 ° | 67 ° | 407.7 | 131.4 | Nil |
| SVB-96-53 | 567968 / 6148688 | 40 ° | 87 ° | 397.7 | 85.0 | 1 |
| SVB-97-57 | 558605 / 6150247 | 360 ° | 90 ° | 556.4 | 190.5 | 6 |
| SVB-97-58 | 562690 / 6152430 | 360 ° | 90 ° | 439.1 | 210.3 | 4 |
| SVB-97-59 | 558606 / 6151246 | 360 ° | 90 ° | 579.1 | 407.5 | 5 |
| SVB-97-60 | 562520 / 6152644 | 360 ° | 90 ° | 410.0 | 198.1 | 3 |
| SVB-97-61 | 562115 / 6153118 | 360 ° | 90 ° | 417.1 | 134.4 | 4 |
| SVB-97-68 | 564899 / 6151000 | 360 ° | 45 ° | 437.1 | 89.0 | 1 |
| SVB-97-69 | 565497 / 6151600 | 180 ° | 45 ° | 404.5 | 107.0 | 5 |
| SVB-97-73 | 558396 / 6151126 | 180 ° | 90 ° | 597.5 | 712.6 | 3 |
| SVB-97-79 | 570690 / 6143804 | 360-111 ° | 90 ° | 327.2 | 999.7 | 8 |
| SVB-97-81 | 563622 / 6152449 | 360 ° | 90 ° | 410.0 | 198.1 | 3 |
| SVB-97-91 | 568219 / 6143804 | 180-360 ° | 90 ° | 330.0 | 1098.8 | 21 |
| SVB-97-92 | 561873 / 6155590 | 180-324 ° | 90-84 ° | 289.5 | 1097.3 | 5 |
| SVB-98-102 | 560328 / 6155501 | 180-89 ° | 90 ° | 376.2 | 274.6 | 10 |
| SVB-98-113 | 561295 / 6155201 | 180-98 ° | 90 ° | 334.9 | 213.1 | 9 |
| SVB-98-116 | 561498 / 6155301 | 180-59 ° | 90 ° | 313.6 | 208.2 | 4 |

Table A.2. Sample checklist pertaining to the analysis and preparation of samples collected from diamond drill core by the author. The sample name uses three series of numbers separated by hyphens; the first series of numbers indicates the year the hole was drilled, the second series indicates the drill hole identification, and the third series indicates the sample number. Note: Some samples are reference samples only, and have not been prepared or analyzed according to the table headings. Also, some samples (indicated by an asterisk) were used for this study, but the DDH from where they were obtained was not re-logged.

| Sample Name | Sample Interval (from-to) in meters, measured below surface | Thin Section | XRF, pressed pellet | LAM-ICP-MS (olivine) | Micro-probe (olivine) | Stable Isotope (sulphur) | ICP-MS (REE's), Solution |
|-------------|---|--------------|---------------------|----------------------|-----------------------|--------------------------|--------------------------|
| 96-02-01 | 3.25 - 3.45 | | | | | | |
| 96-02-02 | 8.1 - 8.4 | X | X | | | | |
| 96-02-03 | 22.35 - 22.45 | X | | | | | |
| 96-02-04 | 24.4 - 24.8 | X | X | | | | X |
| 96-02-05 | 69.0 - 69.3 | X | | | | | |
| 96-02-06 | 84.0 - 84.3 | | | | | | X |
| 96-02-07 | 93.7 - 93.95 | X | X | | | | |
| 96-27-08 | 1.2 - 1.35 | X | X | | | | |
| 96-27-09 | 4.55 - 4.8 | X | | | | | |
| 96-27-10 | 8.9 - 9.0 | X | X | | | | |
| 96-27-11 | 17.0 - 17.2 | X | | | | | |
| 96-27-12 | 22.8 - 22.95 | | X | | | | |
| 96-09-13 | 13.6 - 13.9 | X | X | X | X | | |
| 96-09-14 | 51.0 - 51.2 | X | X | X | X | | |
| 96-09-15 | 53.3 - 53.5 | X | X | X | X | | |
| 96-09-16 | 54.4 - 53.5 | X | X | | | | |
| 96-09-17 | 58.0 - 58.2 | X | X | X | X | | |
| 96-09-18 | 68.4 - 68.6 | X | X | X | X | | |
| 96-04-19 | 4.0 - 4.3 | X | X | X | X | | |
| 96-04-20 | 9.25 - 9.55 | X | | | | | |
| 96-04-21 | 25.8 - 26.0 | X | X | X | X | | |
| 96-04-22 | 44.2 - 44.4 | X | X | X | X | | |
| 96-04-23 | 49.4 - 49.6 | X | X | X | X | | |
| 96-04-24 | 53.9 - 54.2 | X | X | | | X | |
| 96-04-25 | 58.57 - 58.7 | X | X | | | | |
| 96-04-26 | 58.1 - 58.2 | X | X | X | X | | |
| 96-04-27 | 76.1 - 76.4 | | | | | | |
| 97-59-28 | 7.6 - 7.85 | X | X | | | | |
| 97-59-29 | 51.7 - 51.9 | X | | | | | |
| 97-59-30 | 244.0 - 244.2 | X | X | | | | |
| 97-59-31 | 287.25 - 287.5 | X | X | | | | |
| 97-59-32 | 346.3 - 346.2 | X | | | | | |
| 97-57-33 | 22.5 - 22.7 | | | | | | |
| 97-57-34 | 150.8 - 151.1 | X | | | | | |
| 97-57-35 | 157.6 - 157.75 | X | | | | | |
| 97-57-36 | 165.2 - 165.35 | X | X | | | | |
| 97-57-37 | 168.0 - 168.2 | | X | | | | X |
| 97-57-38 | 173.2 - 173.35 | | | | | | |
| 97-73-39 | 333.8 - 333.95 | X | X | | | | |
| 97-73-40 | 359.9 - 360.0 | X | | | | X | |
| 97-73-40 | 359.9 - 360.0 | X | | | | X | |

Table A.2. Continued

| Sample Name | Sample Interval (from-to) in meters, measured below surface | Thin Section | XRF, pressed pellet | LAM- ICP-MS (olivine) | Micro- probe (olivine) | Stable Isotope (sulphur) | ICP-MS (REE's), Solution |
|-------------|---|-----------------|---------------------------|-----------------------------|------------------------------|--------------------------------|--------------------------------|
| 97-73-40 | 359.9 - 360.0 | X | | | | X | |
| 97-73-41 | 443.7 - 443.9 | X | X | | | | X |
| 96-44-42 | 26.0 - 26.2 | X | | | | | |
| 96-44-43 | 33.75 - 33.9 | | X | | | | |
| 97-61-44 | 115.7 - 115.85 | | X | | | | |
| 97-61-45 | 117.8 - 117.95 | | X | | | | |
| 97-61-46 | 121.4 - 121.6 | X | X | | | | |
| 97-61-47 | 123.1 - 124.3 | X | X | | | | |
| 97-60-48 | 151.2 - 151.4 | | X | | | | |
| 97-60-49 | 163.7 - 163.9 | X | X | | | | |
| 97-60-50 | 171.5 - 171.7 | X | X | | | | |
| 97-60-51 | 177.0 - 177.2 | X | X | | | | |
| 97-58-52 | 176.4 - 176.55 | X | X | | | | |
| 97-58-53 | 203.7 - 203.9 | X | X | | | | |
| 97-58-54 | 205.0 - 205.1 | | X | | | X | |
| 97-58-55 | 207.35 - 207.5 | X | | | | | |
| 97-81-56 | 27.0 - 27.4 | | X | | | | |
| 97-81-57 | 145.7 - 145.9 | X | | | | | |
| 97-81-58 | 182.3 - 182.5 | | | | | | |
| 96-08-59 | 2.65 - 2.9 | X | X | | | | |
| 96-08-60 | 14.9 - 15.4 | | | | | | |
| 96-08-61 | 22.1 - 22.4 | | | | | | |
| 96-08-62 | 28.7 - 29.0 | X | | | | | |
| 96-08-63 | 32.0 - 32.4 | | X | | | | |
| 96-08-64 | 43.2 - 43.5 | X | | | | | |
| 96-07-65 | 35.8 - 35.95 | X | X | | | | |
| 96-07-66 | 31.3 - 31.6 | X | X | | | | |
| 96-20-67 | 6.1 - 6.3 | | X | | | | |
| 96-20-68 | 30.6 - 30.8 | X | X | | | | |
| 96-20-69 | 36.4 - 36.7 | X | X | | | X | |
| 96-20-70 | 38.0 - 38.5 | X | X | | | | |
| 96-20-71 | 38.0 - 38.95 | X | | | | | |
| 97-68-72 | 71.0 - 71.3 | X | X | | | | |
| 96-29-73 | 3.0 - 3.2 | X | X | | | | X |
| 96-29-74 | 29.5 - 29.8 | X | X | | | | |
| 96-29-75 | 34.0 - 34.3 | X | X | | | | |
| 96-29-76 | 42.35 - 42.45 | X | | | | | |
| 96-16-77 | 3.5 - 3.8 | X | | | | | |
| 96-16-78 | 45.1 - 45.4 | X | | | | | |
| 96-17-79 | 24.65 - 24.95 | X | | | | | |
| 96-17-80 | 27.2 - 27.5 | X | | | | | |
| 96-17-81 | 31.8 - 32.1 | X | | | | | |
| 96-17-82 | 34.1 - 34.3 | X | | | | | |
| 96-17-83 | 58.6 - 58.9 | X | | | | | |
| 96-15-84 | 11.3 - 11.5 | X | X | | | | |
| 96-15-85 | 75.6 - 75.8 | X | X | | | | X |
| 96-15-86 | 78.6 - 79.0 | X | | | | | |
| 96-15-87 | 83.0 - 83.3 | X | | | | | |

Table A.2. Continued

| Sample Name | Sample Interval (from-to) in meters, measured below surface | Thin Section | XRF, pressed pellet | LAM- ICP-MS (olivine) | Micro- probe (olivine) | Stable Isotope (sulphur) | ICP-MS (REE's), Solution |
|-------------|---|-----------------|---------------------------|-----------------------------|------------------------------|--------------------------------|--------------------------------|
| 96-15-88 | 86.4 - 87.4 | | | | | | |
| 96-10-89 | 11.5 - 11.9 | X | X | | | | |
| 96-10-90 | 20.8 - 21.0 | X | X | | | | |
| 96-10-91 | 29.7 - 30.3 | X | X | | | | |
| 96-10-92 | 36.2 - 36.5 | X | X | | | | |
| 96-48-93 | 21.5 - 21.7 | | X | | | | X |
| 96-48-94 | 40.7 - 41.0 | X | X | | | | |
| 96-48-95 | 59.2 - 59.5 | X | X | | | | |
| 96-34-96 | 2.9 - 3.1 | | | | | | |
| 96-34-97 | 16.7 - 16.9 | X | X | | | | |
| 96-34-98 | 27.0 - 27.3 | X | X | | | | |
| 96-34-99 | 31.7 - 32.1 | X | X | | | | |
| 96-34-100 | 40.1 - 40.3 | | X | | | X | |
| 96-34-101 | 43.3 - 43.5 | | | | | | X |
| 96-47-102 | 9.2 - 9.5 | | | | | | |
| 96-47-103 | 16.8 - 17.0 | X | | | | | |
| 96-47-104 | 48.8 - 49.1 | | | | | | |
| 96-47-105 | 56.3 - 56.6 | X | | | | X | |
| 96-47-106 | 66.6 - 67.0 | X | | | | | |
| 96-36-107 | 13.9 - 14.2 | X | | | | | |
| 96-36-108 | 70.8 - 71.0 | X | | | | | |
| 96-36-109 | 91.1 - 81.3 | | X | | | | |
| 96-36-110 | 88.0 - 88.3 | X | X | | | | |
| 96-36-111 | 107.1 - 107.4 | X | X | | | | |
| 96-36-112 | 119.0 - 119.4 | X | X | | | | |
| 96-36-113 | 137.1 - 137.3 | X | | | | | |
| 96-36-114 | 103.1 - 103.3 | X | | | | | |
| 97-91-115 | 64.0 - 64.3 | | | | | | |
| 97-91-116 | 76.6 - 76.9 | X | X | X | X | | |
| 97-91-117 | 86.5 - 86.95 | | | | | | |
| 97-91-118 | 113.7 - 113.9 | X | X | X | X | | |
| 97-91-119 | 146.5 - 146.8 | X | X | X | X | | |
| 97-91-120 | 156.0 - 159.4 | X | X | | | | |
| 97-91-121 | 159.6 - 160.0 | X | X | X | X | | |
| 97-91-122 | 164.0 - 164.3 | X | X | X | X | | |
| 97-91-123 | 189.8 - 190.1 | X | X | X | X | | |
| 97-91-124 | 212.1 - 212.3 | | | | | | |
| 97-91-125 | 219.0 - 219.4 | | | | | | |
| 97-91-126 | 299.9 - 300.2 | | | | | | |
| 97-91-127 | 316.9 - 317.3 | | | | | | |
| 97-91-128 | 356.4 - 356.7 | X | X | | | | |
| 97-91-129 | 434.6 - 434.9 | | | | | | |
| 97-91-130 | 566.1 - 566.4 | | | | | | |
| 97-91-131 | 732.3 - 732.5 | | | | | | |
| 97-91-132 | 770.3 - 770.6 | | | | | | |
| 97-91-133 | 817.4 - 817.7 | | | | | | |
| 97-91-134 | 931.1 - 931.4 | | | | | | |
| 97-91-135 | 1077.5-1077.9 | | | | | | |

Table A.2. Continued

| Sample Name | Sample Interval (from-to) in meters, measured below surface | Thin Section | XRF, pressed pellet | LAM- ICP-MS (olivine) | Micro- probe (olivine) | Stable Isotope (sulphur) | ICP-MS (REE's), Solution |
|-------------|---|-----------------|---------------------------|-----------------------------|------------------------------|--------------------------------|--------------------------------|
| 97-69-136 | 7.6 - 8.0 | X | | | | | |
| 97-69-137 | 18.0 - 18.3 | X | X | | | | |
| 97-69-138 | 36.1 - 36.3 | X | X | | | | X |
| 97-69-139 | 79.6 - 79.9 | | | | | | |
| 97-69-140 | 103.2 - 103.5 | | | | | | |
| 97-79-141 | 140.4 - 140.6 | X | X | | | X | |
| 97-79-142 | 254.8 - 255.0 | X | X | | | | |
| 97-79-143 | 260.5 - 260.7 | X | X | | | | |
| 97-79-144 | 632.6 - 632.8 | X | X | | | | |
| 97-79-145 | 691.2 - 691.4 | X | X | | | | |
| 97-79-146 | 705.8 - 706.0 | X | X | | | X | |
| 97-79-147 | 729.3 - 729.5 | X | X | | | X | X |
| 97-79-148 | 757.0 - 757.2 | X | X | | | | |
| 98-102-149 | 32.4 - 32.6 | X | X | X | X | | X |
| 98-102-150 | 75.8 - 76.1 | X | X | X | X | | |
| 98-102-151 | 161.7 - 162.0 | X | X | X | X | | X |
| 98-102-152 | 170.4 - 170.6 | X | X | X | X | | X |
| 98-102-153 | 173.4 - 173.6 | X | X | | | | X |
| 98-102-154 | 173.9 - 174.1 | X | | | | | X |
| 98-102-155 | 176.3 - 174.45 | X | X | X | X | | |
| 98-102-156 | 182.9 - 183.2 | X | X | | | | X |
| 98-102-157 | 185.5 - 185.8 | | X | | | | X |
| 98-102-158 | 177.8 - 178.0 | X | | | | | |
| 97-92-159 | 242.7 - 243.0 | X | X | | | | |
| 97-92-160 | 243.3 - 244.5 | | X | | | | |
| 97-92-161 | 246.6 - 246.9 | X | X | | | | |
| 97-92-162 | 253.4 - 253.7 | | | | | | |
| 97-92-163 | 261.6 - 261.9 | X | X | | | | |
| 98-113-164 | 56.3 - 56.8 | X | X | | | | |
| 98-113-165 | 85.7 - 86.9 | X | | | | | |
| 98-113-166 | 89.5 - 89.6 | X | | | | | |
| 98-113-167 | 89.9 - 90.1 | | X | | | | |
| 98-113-168 | 98.9 - 99.1 | X | X | | | | |
| 98-113-169 | 99.7 - 99.9 | X | X | | | X | |
| 98-113-170 | 102.3 - 102.7 | | | | | | |
| 98-113-171 | 105.4 - 105.6 | | | | | | |
| 98-113-172 | 107.8 - 108.0 | X | | | | | |
| 98-116-173 | 107.3 - 107.7 | X | | | | | |
| 98-116-174 | 115.2 - 115.4 | X | X | | | | |
| 98-116-175 | 121.1 - 121.3 | | X | | | | |
| 98-116-176 | 124.9 - 125.2 | | | | | | |
| 96-53-177 | 74.4 - 74.8 | X | X | | | | |
| NAI-1* | 170.0-170.3 | | | | | X | |
| NAI-2* | 170.8-171.0 | | | | | X | |
| 97-75-C1* | 176.5 - 176.6 | | | | | X | |
| 97-75-C2* | 176.5 - 176.6 | | | | | X | |
| 97-96-A* | 198.6 - 198.7 | | | | | X | |
| 97-96-B* | 191.9 - 192.0 | | | | | X | |

Table A.3. Sample checklist pertaining to the analysis and preparation of samples collected from drill core by other sources and used by the author. Note: other core samples have been collected, but were not used utilized in study.

| Sample Name | Sample Interval (from-to) in meters, measured below surface | Thin Section | XRF, pressed pellet | LAM-ICP-MS (olivine) | Micro-probe (olivine) | Stable Isotope (sulphur) | ICP-MS (REE's), Solution |
|-------------|---|--------------|---------------------|----------------------|-----------------------|--------------------------|--------------------------|
| sv97-92-03 | 186.8 – 187.2 | X | X | | | | |
| sv97-92-04 | 255.1 – 255.4 | X | X | | | | |
| sv97-92-05 | 410.8 – 411.2 | X | X | | | | |
| sv97-92-06 | 504.0 – 504.3 | X | X | | | | |
| sv97-92-07 | 557.7 – 558.0 | X | X | | | | |
| sv97-92-09 | 622.8 – 622.9 | X | X | | | | |
| sv97-92-10 | 705.3 – 705.6 | X | X | | | | |
| sv97-92-13 | 1060.8 – 1061.3 | X | X | | | | |
| sv97-61-01 | 80.8 – 81.5 | X | X | | | | |
| sv97-61-02 | 115.8 – 116.3 | X | X | | | | |
| Sv96-02-01 | 15.0 – 15.4 | X | X | | | | |
| w98-022 | 850.2 – 850.6 | X | X | | | | |
| sv97-91-04 | 720.8 – 721.3 | X | X | | | | |
| sv96-47-03 | 30.0 – 30.4 | X | X | | | | |
| sv97-92-12 | 833.0 – 833.4 | X | | | | X | |
| sv97-92-08 | 612.8 – 613.3 | X | | | | X | |
| sv97-92-11 | 781.5 – 781.9 | X | | | | X | |
| 98-136 | 288.3 – 288.4 | | | | | X | |
| 97-96 | 273.8 – 273.9 | | | | | X | |

**Appendix B: Geochemical Results, Analytical Procedures,
Precision and Accuracy**

B.1.1 XRF (pressed pellet) - Analytical Technique

All samples selected for X-Ray Fluorescence (XRF) analysis (see Table A.2), were initially reduced to small chips ($<1 \text{ cm}^2$) using a jaw-crusher and then further reduced to powders ($<0.5 \text{ mm}^2$) using a tungsten-carbide puck mill. The jaw crusher and puck mill were repeatedly cleaned between samples. The XRF analytical technique described by Longerich (1994) was followed for this study and is summarized below.

Five grams (± 0.05) of each powdered sample was mixed with 0.70 grams of a BRP-5933 Bakelite phenolic resin binder and placed on a roller mixer for approximately 10 minutes to provide thorough mixing of the powdered sample and resin. A *Herzog* pellet press was then utilized to compress the combined powders at a pressure of 20 tonnes into circular, flat pellets (3-4 mm thickness, 29 mm diameter) and each pellet was placed into an oven and baked at a temperature of 200 °C for 15 minutes.

Elemental abundances from the pressed pellets were determined using the Fisons/ARL 8420+ sequential wavelength –dispersion x-ray spectrometer at the Department of Earth Sciences, Memorial University. Quantitative determinations by this method include the following elements; P_2O_5 , K_2O , CaO , TiO_2 , MnO , Fe_2O_3 , Na_2O , MgO , Al_2O_3 , S, Cl, Sc, V, Cr, Ni, Cu, Zn, Ga, As, Rb, Sr, Y, Zr, Nb, Ba, Ce, Pb, Th, and U, whereas semi-quantitative determinations were for SiO_2 . Detection limits for these elements and oxides are quoted by Longerich (1995).

Collection of data was done by an automated computer system attached to the XRF, and raw data was reduced into a readable format using in-house software and spreadsheets. The XRF analytical data is compiled in Table B.1 whereas the precision and accuracy of the results is reported in Section B.1.2.

Table B.1. MUN-XRF pressed pellet data. Major elements are reported in wt %. Trace elements are reported in ppm. (<LD, value below limit of detection)

| Sample Name | 98-102-149 | 98-102-150 | 98-102-151 | 98-102-152 | 98-102-153 | 98-102-155 | 98-102-156 |
|----------------------------------|--------------|--------------|--------------|-------------------|---------------|----------------|--------------------|
| Subdivision, Subunit, etc. | Upper Gabbro | Upper Gabbro | Upper Gabbro | Transition Gabbro | Gabbro Hybrid | Olivine gabbro | Semi-mass Sulphide |
| SiO ₂ | 46.27 | 44.23 | 43.08 | 44.20 | 39.09 | 47.09 | 7.59 |
| Al ₂ O ₃ | 23.55 | 22.27 | 16.97 | 17.63 | 18.53 | 12.77 | 1.10 |
| Fe ₂ O ₃ T | 7.96 | 7.20 | 12.96 | 13.28 | 14.73 | 15.16 | 51.40 |
| MgO | 3.37 | 2.89 | 6.07 | 6.38 | 6.99 | 11.11 | 1.00 |
| CaO | 11.02 | 10.63 | 9.26 | 9.07 | 9.24 | 6.80 | 0.23 |
| Na ₂ O | 3.10 | 3.03 | 2.72 | 2.88 | 2.05 | 1.07 | 0.14 |
| K ₂ O | 0.34 | 0.31 | 0.45 | 0.52 | 0.32 | 0.66 | 0.16 |
| TiO ₂ | 0.99 | 0.69 | 1.33 | 1.44 | 0.92 | 0.91 | 0.07 |
| MnO | 0.11 | 0.10 | 0.18 | 0.18 | 0.15 | 0.20 | 0.05 |
| P ₂ O ₅ | 0.14 | 0.09 | 0.16 | 0.21 | 0.12 | 0.10 | 0.01 |
| S | 1033 | 766.0 | 739.0 | 1550 | 16025 | 6216 | 281117 |
| Ni | 12.50 | 7.80 | 45.00 | 50.60 | 786.2 | 245.6 | 9760 |
| Cu | 18.20 | 22.30 | 27.80 | 51.10 | 754.3 | 217.8 | 4168 |
| Cr | 27.00 | 36.00 | 52.00 | 46.00 | 142.0 | 329.0 | 102.0 |
| Zn | 30.80 | 19.20 | 51.90 | 54.70 | 60.10 | 72.00 | 465.8 |
| Pb | <LD | <LD | 5.80 | <LD | 5.70 | 10.60 | 23.80 |
| Ba | 165.5 | 155.8 | 235.8 | 216.2 | 133.9 | 205.0 | <LD |
| Sc | 13.00 | 13.00 | 35.00 | 23.00 | 22.00 | 44.00 | <LD |
| Ga | 19.80 | 22.60 | 22.90 | 26.30 | 21.80 | 16.90 | <LD |
| As | <LD | <LD | <LD | <LD | <LD | <LD | 20.60 |
| Rb | 5.10 | 3.25 | 5.37 | 6.40 | 4.36 | 19.30 | 7.89 |
| Sr | 426.4 | 403.9 | 317.2 | 314.2 | 316.8 | 234.8 | 30.70 |
| Y | 16.30 | 12.30 | 20.40 | 24.80 | 15.70 | 16.30 | <LD |
| Zr | 61.40 | 37.20 | 69.60 | 88.90 | 63.00 | 75.90 | 17.30 |
| Nb | 2.60 | <LD | 3.20 | 3.40 | 3.10 | 3.10 | <LD |
| V | 80.00 | 75.00 | 163.0 | 154.0 | 137.0 | 291.0 | 77.00 |
| Ce | <LD | <LD | <LD | <LD | <LD | <LD | <LD |
| Cl | 125.0 | 50.00 | 224.0 | 78.00 | 108.0 | 93.00 | 43.00 |
| Th | <LD | <LD | <LD | <LD | <LD | <LD | <LD |
| U | <LD | <LD | <LD | <LD | <LD | <LD | <LD |
| Total | 97.23% | 91.73% | 93.51% | 96.33% | 96.47% | 98.32% | 132.6% |

Table B.1. Continued

| Sample Name Subdivision, Subunit, etc. | 98-102-157 Churchill Gneiss | 97-092-159 Transition Gabbro | 97-092-160 Gabbro Hybrid | 97-092-161 Leopard Gabbro | 97-092-163 Olivine Gabbro | sv97-92-03 Upper Gabbro | sv97-92-04 Peridotite |
|--|-----------------------------------|------------------------------------|--------------------------------|---------------------------------|---------------------------------|-------------------------------|--------------------------|
| SiO ₂ | 60.58 | 42.23 | 40.16 | 36.48 | 44.51 | 45.39 | 44.39 |
| Al ₂ O ₃ | 13.06 | 18.64 | 21.03 | 13.58 | 15.69 | 22.21 | 15.22 |
| Fe ₂ O ₃ T | 8.91 | 11.95 | 12.04 | 19.31 | 13.62 | 9.81 | 13.56 |
| MgO | 5.04 | 6.44 | 4.06 | 6.00 | 7.66 | 3.83 | 9.13 |
| CaO | 1.79 | 9.56 | 9.52 | 7.48 | 8.42 | 10.28 | 8.05 |
| Na ₂ O | 1.38 | 2.40 | 2.57 | 2.08 | 2.22 | 3.50 | 2.23 |
| K ₂ O | 2.98 | 0.49 | 0.25 | 0.42 | 0.56 | 0.42 | 0.67 |
| TiO ₂ | 0.75 | 1.14 | 0.80 | 0.92 | 1.31 | 1.06 | 1.25 |
| MnO | 0.10 | 0.15 | 0.15 | 0.14 | 0.18 | 0.13 | 0.18 |
| P ₂ O ₅ | 0.04 | 0.15 | 0.11 | 0.14 | 0.17 | 0.14 | 0.18 |
| S | 4958 | 3356 | 14226 | 41786 | 2944 | 2226 | 1497 |
| Ni | 178.8 | 298.4 | 590.6 | 1813 | 73.80 | 18.00 | 47.00 |
| Cu | 213.3 | 211.2 | 541.1 | 1777 | 121.7 | 20.00 | 52.00 |
| Cr | 314.0 | 32.00 | 182.0 | 76.00 | 62.00 | 20.00 | 72.00 |
| Zn | 123.9 | 52.70 | 126.1 | 63.80 | 64.00 | 33.00 | 60.00 |
| Pb | 24.30 | 6.70 | 19.80 | 21.10 | 6.70 | <LD | 9.00 |
| Ba | 778.3 | 240.0 | 157.4 | 195.4 | 340.7 | 192.0 | 310.0 |
| Sc | 35.00 | 31.00 | 26.00 | 21.00 | 32.00 | 17.00 | 23.00 |
| Ga | 15.40 | 23.90 | 30.70 | 19.50 | 21.10 | 24.00 | 24.00 |
| As | <LD | <LD | <LD | <LD | <LD | <LD | <LD |
| Rb | 102.4 | 7.77 | 3.43 | 7.28 | 11.92 | 5.60 | 12.90 |
| Sr | 245.8 | 328.8 | 543.7 | 310.5 | 305.7 | 415.8 | 305.9 |
| Y | 20.00 | 17.30 | 14.50 | 17.10 | 22.80 | 15.50 | 20.30 |
| Zr | 178.8 | 63.40 | 50.10 | 66.80 | 89.30 | 57.70 | 85.50 |
| Nb | 10.10 | <LD | <LD | 3.30 | 5.30 | 2.80 | 3.60 |
| V | 186.0 | 122.0 | 139.0 | 127.0 | 155.0 | 73.00 | 170.0 |
| Ce | <LD | <LD | <LD | <LD | <LD | <LD | <LD |
| Cl | 329.0 | 377.0 | 183.0 | 143.0 | 210.0 | 159.0 | 315.0 |
| Th | 11.30 | <LD | <LD | <LD | <LD | <LD | <LD |
| U | <LD | <LD | <LD | <LD | <LD | <LD | <LD |
| Total | 96.22% | 94.20% | 94.57% | 97.58% | 95.28% | 96.99% | 95.41% |

Table B.1. Continued

| Sample Name Subdivision, Subunit, etc. | sv97-92-05 Gabbro Hybrid | sv97-92-06 Olivine Gabbro | sv97-92-07 Gabbro Hybrid | sv97-92-09 Gabbro Hybrid | sv97-92-10 Anorthosite | sv97-92-13 Anorthosite | 98-113-164 Upper Gabbro |
|--|--------------------------------|---------------------------------|--------------------------------|--------------------------------|---------------------------|---------------------------|-------------------------------|
| SiO ₂ | 54.43 | 50.36 | 1.36 | 54.25 | 49.87 | 50.36 | 46.44 |
| Al ₂ O ₃ | 12.14 | 12.05 | 48.82 | 12.79 | 15.99 | 21.06 | 21.33 |
| Fe ₂ O ₃ T | 14.08 | 14.24 | 14.94 | 12.36 | 8.87 | 7.24 | 9.88 |
| MgO | 2.32 | 2.20 | 12.02 | 1.74 | 3.42 | 1.66 | 3.32 |
| CaO | 6.61 | 6.50 | 6.90 | 6.61 | 7.59 | 8.16 | 10.19 |
| Na ₂ O | 2.54 | 2.64 | 2.52 | 2.34 | 3.01 | 3.84 | 3.14 |
| K ₂ O | 2.85 | 2.75 | 2.35 | 2.47 | 1.41 | 1.15 | 0.52 |
| TiO ₂ | 2.25 | 2.79 | 2.63 | 2.43 | 1.43 | 1.47 | 1.47 |
| MnO | 0.17 | 0.16 | 0.17 | 0.14 | 0.12 | 0.08 | 0.13 |
| P ₂ O ₅ | 1.04 | 1.41 | 1.36 | 1.22 | 0.30 | 0.23 | 0.17 |
| S | 1800 | 1641 | 1843 | 14.59 | 568.0 | 1024 | 1741 |
| Ni | <LD | <LD | <LD | <LD | <LD | <LD | 11.60 |
| Cu | 10.00 | 17.00 | 20.00 | 23.00 | 5.00 | 8.00 | 34.00 |
| Cr | <LD | 13.00 | 10.00 | 17.00 | 15.00 | 14.00 | 26.00 |
| Zn | 97.00 | 89.00 | 94.00 | 63.00 | 39.00 | 32.00 | 45.50 |
| Pb | 18.00 | 14.00 | 13.00 | 17.00 | 9.00 | <LD | <LD |
| Ba | 1075 | 1157 | 960.0 | 697.0 | 713.0 | 590.0 | 195.2 |
| Sc | 36.00 | 35.00 | 29.00 | 27.00 | 23.00 | 11.00 | 20.00 |
| Ga | 26.00 | 25.00 | 23.00 | 24.00 | 24.00 | 24.00 | 26.20 |
| As | <LD | <LD | <LD | <LD | <LD | <LD | <LD |
| Rb | 72.40 | 76.30 | 72.40 | 84.90 | 31.00 | 21.50 | 10.28 |
| Sr | 247.5 | 262.6 | 295.0 | 327.2 | 399.2 | 496.9 | 379.4 |
| Y | 57.50 | 49.10 | 43.80 | 21.80 | 22.90 | 19.00 | 23.50 |
| Zr | 611.9 | 320.4 | 145.2 | 135.3 | 166.7 | 105.3 | 88.10 |
| Nb | 21.60 | 20.30 | 19.40 | 14.70 | 7.50 | 10.10 | 4.00 |
| V | 89.00 | 133.0 | 114.0 | 93.00 | 130.0 | 71.00 | 131.0 |
| Ce | 155.0 | 156.0 | 143.0 | 57.00 | 61.00 | <LD | <LD |
| Cl | 362.0 | 282.0 | 197.0 | 288.0 | 372.0 | 182.0 | 244.0 |
| Th | 8.00 | 7.00 | 6.00 | 9.00 | <LD | <LD | <LD |
| U | <LD | <LD | <LD | <LD | <LD | <LD | <LD |
| Total | 99.24% | 95.81% | 94.67% | 96.92% | 92.39% | 95.69% | 97.19% |

Table B.1. Continued

| Sample Name Subdivision, Subunit, etc. | 98-113-167 Gabbro Hybrid | 98-113-168 Leopard Gabbro | 98-113-169 Semi-mass Sulphide | 98-116-174 Gabbro Hybrid | 98-116-175 Transition Gabbro | 96-004-019 Upper Gabbro | 96-004-021 Upper Gabbro |
|--|--------------------------------|---------------------------------|-------------------------------------|--------------------------------|------------------------------------|-------------------------------|-------------------------------|
| SiO ₂ | 45.25 | 37.49 | 9.24 | 37.12 | 40.63 | 41.89 | 43.61 |
| Al ₂ O ₃ | 20.69 | 13.91 | 1.38 | 14.79 | 16.06 | 15.98 | 15.91 |
| Fe ₂ O ₃ T | 11.27 | 20.69 | 51.27 | 19.47 | 17.06 | 13.74 | 14.95 |
| MgO | 6.16 | 5.47 | <LD | 4.61 | 5.33 | 7.73 | 8.32 |
| CaO | 8.34 | 7.54 | 0.57 | 8.35 | 8.71 | 7.89 | 8.13 |
| Na ₂ O | 2.74 | 2.18 | 0.09 | 2.24 | 2.57 | 2.17 | 2.86 |
| K ₂ O | 0.76 | 0.45 | 0.13 | 0.39 | 0.34 | 0.48 | 0.51 |
| TiO ₂ | 0.28 | 1.17 | 0.14 | 1.54 | 1.04 | 1.13 | 1.32 |
| MnO | 0.10 | 0.15 | 0.06 | 0.14 | 0.16 | 0.18 | 0.19 |
| P ₂ O ₅ | 0.03 | 0.15 | 0.01 | 0.14 | 0.11 | 0.23 | 0.21 |
| S | 18331.0 | 42704 | 268490 | 48389 | 27187 | 1091 | 1204 |
| Ni | 832.6 | 2038 | 11980 | 1990 | 1126 | 84.30 | 90.60 |
| Cu | 618.1 | 1376 | 11239 | 1987 | 909.6 | 31.60 | 36.70 |
| Cr | 94.00 | 70.00 | 283.0 | 87.00 | 89.00 | 46.00 | 60.00 |
| Zn | 34.00 | 77.20 | 207.2 | 49.90 | 64.60 | 51.00 | 57.40 |
| Pb | 9.50 | 38.80 | <LD | 9.70 | 15.00 | 5.10 | <LD |
| Ba | 207.8 | 164.1 | <LD | 159.5 | 181.1 | 257.1 | 212.0 |
| Sc | 18.00 | 19.00 | <LD | 23.00 | 27.00 | 14.00 | 26.00 |
| Ga | 23.60 | 17.60 | <LD | 21.00 | 23.90 | 22.60 | 21.70 |
| As | <LD | 20.30 | <LD | <LD | <LD | <LD | <LD |
| Rb | 24.12 | 8.75 | 3.69 | 6.35 | 4.50 | 5.66 | 6.81 |
| Sr | 320.7 | 267.6 | 68.00 | 287.7 | 295.4 | 305.2 | 283.9 |
| Y | 5.60 | 22.30 | <LD | 18.00 | 14.60 | 20.60 | 25.50 |
| Zr | 30.40 | 75.90 | 13.50 | 68.90 | 51.00 | 72.00 | 85.40 |
| Nb | 2.90 | 3.80 | 75.00 | 2.40 | | 2.60 | 4.00 |
| V | 66.00 | 146.0 | 126.0 | 198.0 | 170.0 | 111.0 | 138.0 |
| Ce | <LD | <LD | 31.60 | <LD | <LD | <LD | <LD |
| Cl | 104.0 | 186.0 | 170.0 | 226.0 | 302.0 | 132.0 | 44.00 |
| Th | <LD | <LD | <LD | <LD | <LD | <LD | <LD |
| U | <LD | <LD | 10.00 | <LD | <LD | <LD | <LD |
| Total | 100.5% | 100.5% | 132.4% | 101.5% | 99.20% | 92.38% | 96.45% |

Table B.1. Continued

| Sample Name | 96-004-022 | 96-004-023 | 96-004-024 | 96-004-025 | 96-004-026 | 97-059-028 | 97-059-030 |
|----------------------------------|------------------|------------------|------------------|-------------------|-------------------|-----------------|-------------------|
| Subdivision, Subunit, etc. | Gabbro Hybrid | Gabbro Hybrid | Gabbro Hybrid | Olivine gabbro | Olivine gabbro | Upper Gabbro | Olivine Gabbro |
| SiO ₂ | 44.74 | 41.78 | 39.07 | 40.96 | 44.27 | 46.22 | 42.79 |
| Al ₂ O ₃ | 17.89 | 16.10 | 15.91 | 17.61 | 18.81 | 23.75 | 18.70 |
| Fe ₂ O ₃ T | 12.34 | 15.37 | 18.81 | 15.01 | 13.31 | 7.34 | 12.12 |
| MgO | 6.47 | 5.67 | 6.48 | 7.37 | 7.61 | 4.11 | 10.66 |
| CaO | 9.20 | 8.71 | 8.09 | 8.65 | 9.04 | 11.32 | 9.17 |
| Na ₂ O | 2.83 | 2.58 | 2.20 | 2.36 | 2.68 | 2.99 | 2.35 |
| K ₂ O | 0.42 | 0.43 | 0.36 | 0.35 | 0.38 | 0.27 | 0.24 |
| TiO ₂ | 1.17 | 1.55 | 1.09 | 0.84 | 0.77 | 0.70 | 0.67 |
| MnO | 0.15 | 0.17 | 0.17 | 0.14 | 0.14 | 0.10 | 0.15 |
| P ₂ O ₅ | 0.19 | 0.27 | 0.22 | 0.10 | 0.10 | 0.09 | 0.09 |
| S | 1616 | 17562 | 29716 | 20369 | 14633 | 743.0 | 655.0 |
| Ni | 52.30 | 970.6 | 1645 | 1396 | 636.8 | 13.80 | 148.5 |
| Cu | 59.10 | 1017 | 1175 | 712.2 | 446.0 | 17.10 | 13.70 |
| Cr | 34.00 | 61.00 | 47.00 | 104.0 | 59.00 | 31.00 | 55.00 |
| Zn | 50.50 | 62.30 | 71.70 | 61.20 | 43.90 | 16.90 | 31.40 |
| Pb | <LD | 6.60 | 8.00 | 8.70 | 7.50 | <LD | <LD |
| Ba | 195.1 | 176.3 | 115.40 | 139.0 | 168.4 | 141.3 | 95.90 |
| Sc | 21.00 | 25.00 | 24.00 | 27.00 | 19.00 | 19.00 | <LD |
| Ga | 23.70 | 24.30 | 24.00 | 21.60 | 17.90 | 20.80 | 17.00 |
| As | <LD | <LD | <LD | <LD | <LD | <LD | <LD |
| Rb | 5.38 | 8.12 | 8.26 | 6.82 | 8.00 | 4.13 | 2.09 |
| Sr | 335.6 | 313.6 | 294.5 | 320.2 | 353.0 | 419.8 | 321.0 |
| Y | 24.50 | 35.30 | 26.00 | 13.10 | 10.60 | 11.00 | 11.80 |
| Zr | 86.00 | 140.0 | 108.7 | 48.20 | 48.90 | 32.40 | 36.30 |
| Nb | 3.70 | 4.70 | 4.20 | 3.60 | 3.30 | <LD | 3.10 |
| V | 130.0 | 142.0 | 104.0 | 108.0 | 99.00 | 86.00 | 64.00 |
| Ce | <LD | <LD | <LD | <LD | <LD | <LD | <LD |
| Cl | 57.00 | 98.00 | 95.00 | 116.0 | 104.0 | 90.00 | 58.00 |
| Th | <LD | <LD | <LD | <LD | <LD | <LD | <LD |
| U | <LD | <LD | <LD | <LD | <LD | <LD | <LD |
| Total | 95.96% | 97.42% | 100.3% | 98.88% | 101.0% | 97.17% | 97.20% |

Table B.1. Continued

| Sample Name Subdivision, Subunit, etc. | 97-059-031 Olivine Gabbro | 97-057-036 Gabbro Hybrid | 97-057-037 Olivine Gabbro | 97-073-039 Transition Gabbro | 97-073-041 Mafic Dike | 97-061-044 Upper Gabbro | 97-061-045 Gabbro Hybrid |
|--|---------------------------------|--------------------------------|---------------------------------|------------------------------------|--------------------------|-------------------------------|--------------------------------|
| SiO ₂ | 36.53 | 42.58 | 44.34 | 42.46 | 47.08 | 44.87 | 39.17 |
| Al ₂ O ₃ | 6.55 | 22.43 | 15.72 | 17.75 | 11.50 | 18.41 | 16.40 |
| Fe ₂ O ₃ T | 22.55 | 10.92 | 14.66 | 0.12 | 11.97 | 11.21 | 15.42 |
| MgO | 22.78 | 7.82 | 5.69 | 3.90 | 10.44 | 8.54 | 8.50 |
| CaO | 3.69 | 6.89 | 8.61 | 0.55 | 9.47 | 9.76 | 7.16 |
| Na ₂ O | 1.04 | 2.57 | 2.22 | 2.97 | 1.69 | 2.48 | 1.46 |
| K ₂ O | 0.23 | 0.89 | 0.62 | 178.0 | 1.13 | 0.47 | 1.27 |
| TiO ₂ | 0.70 | 1.05 | 1.55 | 28.00 | 0.70 | 0.94 | 0.68 |
| MnO | 0.26 | 0.12 | 0.17 | 43.00 | 0.19 | 0.14 | 0.14 |
| P ₂ O ₅ | 0.13 | 0.10 | 0.19 | 0.19 | 0.17 | 0.11 | 0.08 |
| S | 639.0 | 6060 | 1354 | 24710 | 1664 | 704.0 | 17499 |
| Ni | 289.2 | 287.5 | <LD | 14.09 | 46.00 | 52.90 | 1039 |
| Cu | 15.10 | 271.5 | 69.50 | 2162 | 32.30 | 15.70 | 1067 |
| Cr | 39.00 | 301.0 | 73.00 | 170.0 | 496.0 | 42.00 | 133.00 |
| Zn | 87.80 | 94.50 | 74.40 | 48.10 | 381.3 | 47.90 | 70.70 |
| Pb | <LD | 8.00 | 7.70 | 7.40 | 67.10 | <LD | 19.60 |
| Ba | 138.3 | 257.0 | 320.4 | 216.6 | 321.4 | 130.5 | 312.0 |
| Sc | <LD | 18.00 | 23.00 | 9.14 | 42.00 | 24.00 | 9.00 |
| Ga | 8.80 | 47.80 | 22.10 | 27.10 | 14.70 | 20.90 | 25.60 |
| As | <LD | <LD | <LD | 20.70 | <LD | <LD | <LD |
| Rb | 4.29 | 33.17 | 10.73 | 9.53 | 55.69 | 7.27 | 49.34 |
| Sr | 153.9 | 272.40 | 330.8 | 365.0 | 375.2 | 362.6 | 320.9 |
| Y | 12.60 | 14.10 | 18.10 | 24.70 | 14.30 | 16.70 | 10.70 |
| Zr | 52.60 | 112.10 | 56.80 | 88.90 | 61.90 | 56.00 | 38.30 |
| Nb | 2.80 | 7.80 | 4.50 | 3.80 | 5.10 | 2.30 | <LD |
| V | 61.00 | 263.0 | 191.0 | 1.58 | 260.0 | 116.0 | 122.0 |
| Ce | <LD | 77.80 | <LD | <LD | <LD | <LD | <LD |
| Cl | 804.0 | 130.0 | 130.0 | 0.19 | 300.0 | 703.0 | 1478 |
| Th | <LD | 7.90 | <LD | <LD | 6.00 | <LD | <LD |
| U | <LD | <LD | <LD | <LD | <LD | <LD | <LD |
| Total | 94.81% | 97.19% | 94.25% | 99.58% | 95.08% | 97.21% | 95.18% |

Table B.1. Continued

| Sample Name Subdivision, Subunit, etc. | 97-061-046 Churchill Gneiss | 97-061-047 Semi-mass Sulphide | sv97-61-01 Upper Gabbro | sv97-61-02 Upper Gabbro | 97-060-048 Upper Gabbro | 97-060-049 Gabbro Hybrid | 97-060-050 Leopard Gabbro |
|--|-----------------------------------|-------------------------------------|-------------------------------|-------------------------------|-------------------------------|--------------------------------|---------------------------------|
| SiO ₂ | 29.23 | 10.24 | 44.40 | 45.77 | 44.68 | 41.79 | 39.39 |
| Al ₂ O ₃ | 11.49 | 1.79 | 20.87 | 19.73 | 19.95 | 20.80 | 12.78 |
| Fe ₂ O ₃ T | 33.30 | 48.76 | 8.58 | 10.97 | 9.95 | 11.32 | 19.81 |
| MgO | 3.97 | <LD | 4.64 | 7.56 | 5.36 | 5.00 | 9.72 |
| CaO | 0.15 | 0.12 | 10.28 | 10.11 | 9.91 | 9.85 | 7.14 |
| Na ₂ O | 0.39 | 0.05 | 2.82 | 2.77 | 2.91 | 2.48 | 1.73 |
| K ₂ O | 1.44 | 0.06 | 0.35 | 0.44 | 0.37 | 0.39 | 0.41 |
| TiO ₂ | 0.30 | 0.10 | 0.88 | 0.99 | 1.00 | 0.89 | 0.84 |
| MnO | 0.05 | 0.02 | 0.11 | 0.14 | 0.13 | 0.12 | 0.16 |
| P ₂ O ₅ | 0.01 | 0.01 | 0.11 | 0.12 | 0.13 | 0.13 | 0.10 |
| S | 130524 | 306862 | 860.0 | 900.0 | 1052 | 10116 | 36424 |
| Ni | 3485 | 7348 | 27.00 | 46.00 | 24.10 | 616.2 | 1197 |
| Cu | 2210 | 5151 | 20.00 | 25.00 | 20.80 | 519.1 | 1118 |
| Cr | 329.0 | 149.0 | 37.00 | 41.00 | 27.00 | 119.0 | 59.00 |
| Zn | 256.9 | 12.60 | 24.00 | 37.00 | 32.40 | 48.50 | 91.10 |
| Pb | 14.70 | 24.20 | <LD | 7.00 | <LD | <LD | 21.30 |
| Ba | 175.7 | <LD | 166.0 | 152.0 | 167.4 | 200.4 | 115.1 |
| Sc | <LD | <LD | 19.00 | 23.00 | 17.00 | 20.00 | 27.00 |
| Ga | 21.60 | <LD | 24.00 | 22.00 | 23.10 | 28.10 | 18.40 |
| As | <LD | 32.00 | <LD | <LD | <LD | <LD | <LD |
| Rb | 58.25 | 3.64 | 5.00 | 7.20 | 5.27 | 7.50 | 10.04 |
| Sr | 55.50 | 3.90 | 391.8 | 371.8 | 372.5 | 361.9 | 266.7 |
| Y | 6.20 | 3.60 | 13.90 | 15.50 | 17.20 | 14.30 | 13.30 |
| Zr | 101.6 | 30.00 | 51.10 | 53.60 | 64.50 | 56.40 | 53.50 |
| Nb | 7.40 | 2.50 | 2.50 | 1.90 | 4.00 | <LD | <LD |
| V | 174.0 | 167.0 | 106.0 | 119.0 | 103.0 | 108.0 | 132.0 |
| Ce | <LD | <LD | <LD | <LD | <LD | <LD | <LD |
| Cl | 165.0 | 43.00 | 107.0 | 312.0 | 254.0 | 102.0 | 259.0 |
| Th | 11.20 | <LD | <LD | <LD | <LD | <LD | <LD |
| U | <LD | <LD | <LD | <LD | <LD | <LD | <LD |
| Total | 113.8% | 139.4% | 93.38% | 98.97% | 94.78% | 95.57% | 101.6% |

Table B.1. Continued

| Sample Name Subdivision, Subunit, etc. | 97-060-051 Olivine Gabbro | 97-058-052 Transition Gabbro | 97-058-053 Gabbro Hybrid | 97-058-054 Semi-mass Sulphide | 97-081-056 Upper Gabbro | 96-008-059 Upper Gabbro | 96-008-063 Semi-mass Sulphide |
|--|---------------------------------|------------------------------------|--------------------------------|-------------------------------------|-------------------------------|-------------------------------|-------------------------------------|
| SiO ₂ | 44.13 | 43.60 | 41.09 | 29.11 | 46.55 | 45.63 | 43.27 |
| Al ₂ O ₃ | 16.60 | 18.30 | 15.04 | 7.20 | 21.04 | 20.39 | 9.14 |
| Fe ₂ O ₃ T | 13.13 | 11.27 | 16.79 | 37.63 | 9.05 | 7.87 | 22.82 |
| MgO | 6.99 | 5.51 | 10.84 | 1.61 | 3.06 | 3.94 | 3.99 |
| CaO | 8.55 | 9.68 | 6.19 | 0.51 | 10.57 | 10.96 | 1.55 |
| Na ₂ O | 2.77 | 2.84 | 1.46 | 0.75 | 3.12 | 2.97 | 1.09 |
| K ₂ O | 0.60 | 0.43 | 0.88 | 1.11 | 0.34 | 0.35 | 1.43 |
| TiO ₂ | 1.36 | 1.18 | 0.59 | 0.17 | 1.31 | 0.92 | 0.61 |
| MnO | 0.16 | 0.15 | 0.19 | 0.05 | 0.12 | 0.11 | 0.12 |
| P ₂ O ₅ | 0.20 | 0.18 | 0.06 | 0.02 | 0.16 | 0.12 | 0.06 |
| S | 3842 | 1228 | 20333 | 191049 | 1386 | 963.0 | 69869 |
| Ni | 81.40 | 41.10 | 774.7 | 3853 | <LD | 11.90 | 1598 |
| Cu | 75.10 | 31.30 | 477.5 | 2774 | 19.10 | 24.40 | 1480 |
| Cr | 66.00 | 49.00 | 123.0 | 485.0 | 30.00 | 106.0 | 169.0 |
| Zn | 58.30 | 38.50 | 111.9 | 277.2 | 42.10 | 21.30 | 133.2 |
| Pb | 8.50 | <LD | 17.20 | 32.20 | <LD | <LD | 17.40 |
| Ba | 263.8 | 204.2 | 253.9 | 133.0 | 122.1 | 136.9 | 338.0 |
| Sc | 23.00 | 25.00 | 15.00 | <LD | 24.00 | 26.00 | 13.00 |
| Ga | 23.60 | 24.10 | 20.40 | 17.20 | 21.80 | 21.60 | 14.80 |
| As | <LD | <LD | <LD | 26.00 | <LD | <LD | <LD |
| Rb | 10.20 | 6.13 | 39.72 | 35.42 | 4.42 | 6.54 | 52.25 |
| Sr | 320.3 | 347.3 | 236.3 | 55.60 | 397.8 | 375.6 | 143.2 |
| Y | 21.50 | 21.70 | 9.40 | 12.70 | 22.20 | 16.80 | 13.60 |
| Zr | 87.40 | 78.10 | 43.60 | 103.9 | 85.40 | 51.60 | 105.8 |
| Nb | 4.60 | 3.10 | 2.50 | 4.00 | 4.10 | <LD | 4.70 |
| V | 138.0 | 134.0 | 120.0 | 183.0 | 119.0 | 147.0 | 172.0 |
| Ce | <LD | <LD | <LD | <LD | <LD | <LD | 67.70 |
| Cl | 92.00 | 82.00 | 1096 | 466.0 | 162.0 | 342.0 | 708.0 |
| Th | <LD | <LD | <LD | 5.20 | <LD | <LD | 16.40 |
| U | <LD | <LD | <LD | <LD | <LD | <LD | <LD |
| Total | 95.63% | 93.59% | 98.61% | 126.9% | 93.67% | 93.67% | 102.2% |

Table B.1. Continued

| Sample Name Subdivision, Subunit, etc. | 96-007-065 Transition Gabbro | 96-077-066 Gabbro Hybrid | 96-020-067 Upper Gabbro | 96-020-068 Transition Gabbro | 96-020-069 Gabbro Hybrid | 96-020-070 Semi-mass Sulphide | 97-068-072 Mafic Dike |
|--|------------------------------------|--------------------------------|-------------------------------|------------------------------------|--------------------------------|-------------------------------------|--------------------------|
| SiO ₂ | 41.90 | 44.00 | 44.74 | 44.09 | 42.05 | 64.15 | 46.05 |
| Al ₂ O ₃ | 19.00 | 18.82 | 20.79 | 18.38 | 19.18 | 11.08 | 11.29 |
| Fe ₂ O ₃ T | 13.59 | 12.66 | 8.72 | 11.62 | 13.11 | 8.96 | 16.15 |
| MgO | 5.40 | 5.69 | 5.05 | 6.50 | 5.03 | 4.68 | 6.90 |
| CaO | 9.87 | 9.44 | 10.32 | 9.54 | 9.53 | 1.57 | 7.88 |
| Na ₂ O | 2.40 | 2.88 | 2.82 | 2.75 | 2.54 | 1.40 | 1.97 |
| K ₂ O | 0.37 | 0.36 | 0.30 | 0.40 | 0.39 | 2.21 | 0.80 |
| TiO ₂ | 0.88 | 1.12 | 0.63 | 1.00 | 1.06 | 0.46 | 2.25 |
| MnO | 0.13 | 0.14 | 0.12 | 0.15 | 0.14 | 0.07 | 0.22 |
| P ₂ O ₅ | 0.12 | 0.14 | 0.08 | 0.15 | 0.16 | 0.06 | 0.28 |
| S | 20360 | 8147 | 830.0 | 1753 | 14621 | 12292 | 4716 |
| Ni | 1098 | 377.5 | 26.80 | 78.50 | 992.4 | 252.4 | <LD |
| Cu | 898.6 | 309.3 | 26.10 | 73.30 | 777.2 | 142.3 | 28.90 |
| Cr | 92.00 | 77.00 | 39.00 | 49.00 | 121.0 | 180.0 | 61.00 |
| Zn | 39.30 | 47.60 | 19.00 | 45.30 | 53.40 | 84.80 | 172.9 |
| Pb | 8.90 | <LD | <LD | <LD | 6.20 | 38.40 | 20.30 |
| Ba | 167.1 | 161.5 | 149.0 | 160.0 | 194.1 | 358.8 | 348.1 |
| Sc | 12.00 | 19.00 | 19.00 | 19.00 | <LD | <LD | 31.00 |
| Ga | 23.80 | 23.30 | 19.10 | 22.50 | 28.60 | 15.50 | 22.80 |
| As | <LD | <LD | <LD | <LD | <LD | <LD | <LD |
| Rb | 7.12 | 4.53 | 3.50 | 6.61 | 9.08 | 58.43 | 31.40 |
| Sr | 331.9 | 329.9 | 374.5 | 334.5 | 327.1 | 101.9 | 293.3 |
| Y | 14.40 | 18.20 | 12.40 | 19.20 | 19.40 | 17.40 | 30.80 |
| Zr | 47.30 | 64.70 | 34.60 | 66.20 | 75.10 | 107.6 | 152.9 |
| Nb | 2.20 | 1.80 | 1.70 | 2.20 | 3.50 | 8.40 | 5.80 |
| V | 117.0 | 135.0 | 78.00 | 114.00 | 144.0 | 130.0 | 215.0 |
| Ce | <LD | <LD | <LD | <LD | <LD | 102.7 | <LD |
| Cl | 73.00 | 76.00 | 65.00 | 73.00 | 99.00 | 796.0 | 1835 |
| Th | <LD | <LD | <LD | <LD | <LD | 7.60 | <LD |
| U | <LD | <LD | <LD | <LD | <LD | <LD | <LD |
| Total | 99.11% | 97.49% | 93.89% | 95.18% | 97.20% | 97.99% | 95.33% |

Table B.1. Continued

| Sample Name Subdivision, Subunit, etc. | 97-069-137 Olivine Gabbro | 97-069-138 Mafic Dike | 96-002-002 Transition Gabbro | 96-002-004 Leopard Gabbro | 96-002-007 Mafic Dike | sv96-02-01 Leopard Gabbro | 96-027-008 Upper Gabbro |
|--|---------------------------------|--------------------------|------------------------------------|---------------------------------|--------------------------|---------------------------------|-------------------------------|
| SiO ₂ | 38.11 | 50.34 | 42.17 | 35.90 | 48.80 | 33.66 | 44.75 |
| Al ₂ O ₃ | 11.14 | 13.96 | 16.37 | 13.45 | 13.71 | 12.65 | 21.43 |
| Fe ₂ O ₃ T | 19.36 | 10.09 | 12.97 | 23.21 | 14.4 | 26.58 | 8.68 |
| MgO | 11.40 | 7.51 | 6.42 | 5.29 | 4.88 | 5.81 | 4.90 |
| CaO | 6.07 | 7.28 | 8.31 | 7.36 | 7.64 | 6.83 | 10.63 |
| Na ₂ O | 1.32 | 1.39 | 2.53 | 2.07 | 2.55 | 1.84 | 2.85 |
| K ₂ O | 0.38 | 1.68 | 0.57 | 0.32 | 0.99 | 0.29 | 0.27 |
| TiO ₂ | 0.60 | 0.78 | 1.45 | 0.75 | 2.09 | 0.69 | 0.65 |
| MnO | 0.14 | 0.15 | 0.15 | 0.14 | 0.18 | 0.14 | 0.11 |
| P ₂ O ₅ | 0.09 | 0.18 | 0.20 | 0.10 | 0.31 | 0.08 | 0.09 |
| S | 42370 | 10585 | 9227 | 69654 | 1540 | 95907 | 849.0 |
| Ni | 1855 | <LD | 438.6 | 3472 | <LD | 5118 | 30.20 |
| Cu | 2378 | 40.90 | 300.8 | 2949 | 11.00 | 2885 | 20.60 |
| Cr | 89.00 | 165.0 | 73.00 | 59.00 | 49.00 | 70.00 | 52.00 |
| Zn | 103.8 | 512.4 | 52.60 | 84.50 | 81.40 | 59.00 | 19.90 |
| Pb | 25.20 | 15.50 | <LD | 9.80 | 6.20 | 10.00 | <LD |
| Ba | 138.8 | 385.2 | 265.4 | 120.1 | 568.7 | 95.00 | 170.2 |
| Sc | 15.00 | 30.00 | 15.00 | 18.00 | 33.00 | 21.00 | 22.00 |
| Ga | 20.00 | 18.20 | 23.20 | 14.90 | 23.80 | 15.00 | 21.30 |
| As | <LD | <LD | <LD | <LD | <LD | <LD | <LD |
| Rb | 11.58 | 79.66 | 11.68 | 4.59 | 20.31 | 4.30 | 3.12 |
| Sr | 263.0 | 283.7 | 324.8 | 274.3 | 312.8 | 259.7 | 386.1 |
| Y | 13.50 | 15.30 | 24.00 | 13.80 | 31.00 | 11.50 | 11.20 |
| Zr | 52.50 | 80.20 | 99.80 | 50.00 | 161.8 | 39.40 | 33.10 |
| Nb | <LD | 6.60 | 5.20 | <LD | 10.50 | 1.50 | 2.20 |
| V | 86.00 | 242.0 | 157.0 | 105.0 | 181.0 | 94.00 | 100.0 |
| Ce | <LD | <LD | <LD | <LD | <LD | <LD | <LD |
| Cl | 666.0 | 226.0 | 76.00 | 158.0 | 167.0 | 110.0 | 53.00 |
| Th | <LD | <LD | <LD | 6.00 | 7.90 | <LD | <LD |
| U | <LD | <LD | <LD | <LD | <LD | <LD | <LD |
| Total | 99.90% | 96.27% | 93.69% | 106.9% | 96.24% | 94.69% | 94.69% |

Table B.1. Continued

| Sample Name Subdivision, Subunit, etc. | 96-027-010 Transition Gabbro | 96-027-012 Gabbro Hybrid | 96-009-013 Upper Gabbro | 96-009-014 Upper Gabbro | 96-009-015 Gabbro Hybrid | 96-009-016 Gabbro Hybrid | 96-009-017 Olivine Gabbro |
|--|------------------------------------|--------------------------------|-------------------------------|-------------------------------|--------------------------------|--------------------------------|---------------------------------|
| SiO ₂ | 45.14 | 40.01 | 45.01 | 44.60 | 44.12 | 44.20 | 38.62 |
| Al ₂ O ₃ | 18.67 | 15.29 | 20.57 | 19.30 | 18.40 | 22.31 | 16.01 |
| Fe ₂ O ₃ T | 12.14 | 16.24 | 11.19 | 10.56 | 11.89 | 9.75 | 16.29 |
| MgO | 5.61 | 6.93 | 3.96 | 4.84 | 5.82 | 4.94 | 6.85 |
| CaO | 9.34 | 7.92 | 10.33 | 9.81 | 9.40 | 10.29 | 8.10 |
| Na ₂ O | 3.11 | 2.13 | 2.90 | 2.93 | 2.91 | 2.76 | 2.19 |
| K ₂ O | 0.48 | 0.43 | 0.38 | 0.44 | 0.42 | 0.45 | 0.37 |
| TiO ₂ | 1.31 | 0.97 | 1.23 | 1.14 | 1.28 | 1.14 | 0.79 |
| MnO | 0.16 | 0.15 | 0.15 | 0.14 | 0.16 | 0.12 | 0.14 |
| P ₂ O ₅ | 0.19 | 0.16 | 0.12 | 0.17 | 0.19 | 0.18 | 0.12 |
| S | 1486 | 27516 | 1468 | 1180 | 1300 | 4808 | 32017 |
| Ni | 46.00 | 1631 | 15.90 | 21.80 | 49.80 | 338.9 | 2398 |
| Cu | 30.00 | 1386 | 42.70 | 34.40 | 32.90 | 282.9 | 1868 |
| Cr | 27.00 | 82.00 | 30.00 | 37.00 | 52.00 | 81.00 | 78.00 |
| Zn | 51.80 | 69.50 | 41.80 | 36.00 | 46.30 | 38.70 | 49.60 |
| Pb | <LD | 11.10 | <LD | <LD | <LD | <LD | 6.60 |
| Ba | 281.6 | 201.9 | 170.7 | 208.7 | 216.5 | 200.4 | 185.6 |
| Sc | 20.00 | 12.00 | 15.00 | 18.00 | 16.00 | <LD | 11.00 |
| Ga | 26.60 | 25.50 | 24.50 | 25.10 | 20.90 | 29.00 | 24.10 |
| As | <LD | <LD | <LD | 20.50 | <LD | <LD | <LD |
| Rb | 7.15 | 6.72 | 4.27 | 6.97 | 5.77 | 10.21 | 7.16 |
| Sr | 328.1 | 316.3 | 370.8 | 362.7 | 336.2 | 383.4 | 316.3 |
| Y | 23.90 | 16.70 | 18.00 | 20.40 | 23.40 | 19.30 | 11.60 |
| Zr | 86.00 | 65.20 | 56.80 | 78.90 | 79.80 | 70.20 | 48.40 |
| Nb | 2.40 | 3.10 | 2.90 | 2.50 | 5.40 | 3.10 | 2.60 |
| V | 135.0 | 129.0 | 100.0 | 114.0 | 138.0 | 104.0 | 101.0 |
| Ce | <LD | <LD | <LD | <LD | <LD | <LD | <LD |
| Cl | 72.0 | 59.00 | 126.0 | 83.00 | 65.00 | 128.0 | 81.00 |
| Th | <LD | <LD | <LD | <LD | <LD | <LD | <LD |
| U | <LD | <LD | <LD | <LD | <LD | <LD | <LD |
| Total | 96.65% | 97.61% | 96.33% | 94.38% | 95.04% | 97.57% | 98.11% |

Table B.1. Continued

| Sample Name Subdivision, Subunit, etc. | 96-009-018 Leopard Gabbro | 96-044-043 Gabbro Hybrid | 96-029-073 Upper Gabbro | 96-029-074 Upper Gabbro | 96-029-075 Transition Gabbro | 96-015-084 Upper Gabbro | 96-015-085 Transition Gabbro |
|--|---------------------------------|--------------------------------|-------------------------------|-------------------------------|------------------------------------|-------------------------------|------------------------------------|
| SiO ₂ | 37.54 | 45.91 | 43.23 | 42.23 | 44.14 | 40.55 | 43.03 |
| Al ₂ O ₃ | 14.42 | 17.10 | 16.84 | 18.00 | 18.31 | 10.79 | 17.35 |
| Fe ₂ O ₃ T | 20.76 | 13.45 | 13.93 | 11.65 | 11.77 | 21.42 | 14.82 |
| MgO | 4.72 | 7.34 | 8.25 | 6.81 | 6.41 | 15.27 | 6.36 |
| CaO | 7.74 | 8.76 | 8.44 | 9.14 | 9.34 | 5.67 | 9.01 |
| Na ₂ O | 2.30 | 2.87 | 2.64 | 2.57 | 2.83 | 2.03 | 2.60 |
| K ₂ O | 0.37 | 0.53 | 0.36 | 0.35 | 0.44 | 0.42 | 0.52 |
| TiO ₂ | 0.86 | 1.20 | 0.94 | 0.84 | 1.08 | 0.95 | 1.21 |
| MnO | 0.14 | 0.16 | 0.17 | 0.15 | 0.15 | 0.27 | 0.16 |
| P ₂ O ₅ | 0.12 | 0.18 | 0.15 | 0.11 | 0.14 | 0.16 | 0.14 |
| S | 56848 | 5645 | 1198 | 1046 | 1987 | 1319 | 14527 |
| Ni | 2872 | 90.60 | 59.90 | 61.70 | 139.0 | 179.6 | 717.6 |
| Cu | 2070 | 136.2 | 33.80 | 27.70 | 111.9 | 39.30 | 624.2 |
| Cr | 49.00 | 72.00 | 39.00 | 43.00 | 39.00 | 39.00 | 61.00 |
| Zn | 63.30 | 58.00 | 44.90 | 37.90 | 40.40 | 89.60 | 56.60 |
| Pb | 8.10 | <LD | 5.50 | <LD | <LD | <LD | 7.50 |
| Ba | 182.1 | 252.1 | 179.3 | 140.9 | 197.3 | 159.5 | 203.9 |
| Sc | 14.00 | 20.00 | 19.00 | 14.00 | 20.00 | 26.00 | 26.00 |
| Ga | 21.60 | 20.90 | 24.40 | 25.20 | 23.90 | 15.80 | 18.90 |
| As | <LD | <LD | <LD | <LD | <LD | <LD | <LD |
| Rb | 5.03 | 7.96 | 6.06 | 4.21 | 7.85 | 8.52 | 10.32 |
| Sr | 293.1 | 315.8 | 322.3 | 343.9 | 337.4 | 200.4 | 315.3 |
| Y | 14.80 | 21.20 | 17.70 | 14.90 | 19.00 | 16.80 | 18.80 |
| Zr | 52.30 | 79.50 | 58.10 | 45.90 | 64.80 | 62.50 | 70.00 |
| Nb | 2.50 | 5.00 | 3.20 | <LD | <LD | 3.80 | <LD |
| V | 127.0 | 143.0 | 89.00 | 99.00 | 124.0 | 105.0 | 125.0 |
| Ce | <LD | <LD | <LD | <LD | <LD | <LD | <LD |
| Cl | 107.0 | 117.0 | 76.00 | 93.00 | 118.0 | 200.0 | 48.00 |
| Th | <LD | <LD | <LD | <LD | <LD | <LD | <LD |
| U | <LD | <LD | <LD | <LD | <LD | <LD | <LD |
| Total | 103.9% | 99.08% | 95.37% | 92.24% | 95.26% | 97.99% | 99.11% |

Table B.1. Continued

| Sample Name Subdivision, Subunit, etc. | 96-010-089 Transition Gabbro | 96-010-090 Gabbro Hybrid | 96-010-091 Olivine Gabbro | 96-010-092 Churchill Gneiss | 96-053-177 Mafic Dike | 96-048-093 Upper Gabbro | 96-048-094 Olivine Gabbro |
|--|------------------------------------|--------------------------------|---------------------------------|-----------------------------------|--------------------------|-------------------------------|---------------------------------|
| SiO ₂ | 40.82 | 37.43 | 41.92 | 52.02 | 46.23 | 45.24 | 32.68 |
| Al ₂ O ₃ | 21.04 | 14.95 | 16.20 | 16.50 | 16.05 | 21.09 | 11.24 |
| Fe ₂ O ₃ T | 12.01 | 13.61 | 14.67 | 11.37 | 13.29 | 9.38 | 25.46 |
| MgO | 5.50 | 5.27 | 6.51 | 6.73 | 5.80 | 4.06 | 7.11 |
| CaO | 10.46 | 7.59 | 8.40 | 0.40 | 8.43 | 10.37 | 6.65 |
| Na ₂ O | 2.17 | 2.16 | 2.58 | 1.20 | 2.85 | 3.06 | 1.58 |
| K ₂ O | 0.30 | 0.33 | 0.49 | 3.06 | 0.66 | 0.33 | 0.28 |
| TiO ₂ | 0.61 | 0.91 | 1.17 | 0.50 | 1.55 | 1.05 | 0.68 |
| MnO | 0.13 | 0.13 | 0.16 | 0.05 | 0.18 | 0.12 | 0.14 |
| P ₂ O ₅ | 0.08 | 0.12 | 0.17 | 0.03 | 0.23 | 0.14 | 0.10 |
| S | 12647 | 19140 | 13510 | 17341 | 1846 | 1232 | 73161 |
| Ni | 745.1 | 8.95 | 411.7 | 214.5 | <LD | 22.40 | 1246 |
| Cu | 702.7 | 909.1 | 451.2 | 202.6 | 29.20 | 29.10 | 1095 |
| Cr | 138.0 | 69.00 | 69.00 | 232.0 | 62.00 | 28.00 | 70.00 |
| Zn | 42.00 | 51.00 | 54.00 | 164.7 | 63.90 | 30.00 | 86.00 |
| Pb | 8.40 | 9.20 | 11.50 | 28.10 | <LD | <LD | 19.60 |
| Ba | 138.5 | 150.9 | 236.0 | 657.4 | 384.1 | <LD | 135.6 |
| Sc | <LD | 19.00 | 22.00 | 17.00 | 34.00 | 24.00 | 11.00 |
| Ga | 22.20 | 24.20 | 23.40 | 20.20 | 23.90 | <LD | 14.00 |
| As | <LD | <LD | <LD | <LD | <LD | 4.62 | <LD |
| Rb | 4.55 | 5.84 | 9.69 | 115.5 | 11.43 | 384.7 | 5.80 |
| Sr | 351.0 | 300.2 | 314.4 | 92.70 | 340.4 | 18.70 | 265.1 |
| Y | 9.70 | 16.40 | 21.60 | 17.90 | 26.30 | 61.70 | 12.20 |
| Zr | 33.50 | 56.20 | 80.00 | 175.6 | 108.0 | 4.40 | 44.00 |
| Nb | <LD | 2.30 | 2.70 | 10.90 | 3.90 | 198.2 | <LD |
| V | 110.0 | 1.22 | 145.0 | 161.0 | 164.0 | 109.0 | 101.0 |
| Ce | <LD | <LD | <LD | <LD | <LD | <LD | <LD |
| Cl | 109.0 | 47.00 | 102.0 | 125.0 | 127.0 | 92.00 | 183.0 |
| Th | <LD | <LD | 5.30 | 10.30 | <LD | <LD | <LD |
| U | <LD | <LD | <LD | <LD | <LD | <LD | <LD |
| Total | 96.58% | 87.62% | 95.90% | 96.48% | 95.91% | 95.26% | 104.6% |

Table B.1. Continued

| Sample Name Subdivision, Subunit, etc. | 96-048-095 Olivine Gabbro | 96-034-097 Olivine gabbro | 97-034-098 Gabbro Hybrid | 96-034-099 Olivine Gabbro | 96-034-100 Olivine gabbro | 97-036-109 Upper Gabbro | 96-036-110 Upper Gabbro |
|--|---------------------------------|---------------------------------|--------------------------------|---------------------------------|---------------------------------|-------------------------------|-------------------------------|
| SiO ₂ | 44.55 | 45.23 | 41.21 | 42.94 | 40.88 | 39.71 | 41.65 |
| Al ₂ O ₃ | 15.30 | 19.83 | 19.95 | 15.90 | 13.72 | 15.11 | 17.22 |
| Fe ₂ O ₃ T | 13.59 | 10.03 | 13.86 | 12.86 | 20.17 | 10.81 | 12.41 |
| MgO | 7.65 | 3.78 | 4.68 | 6.45 | 5.69 | 10.35 | 7.95 |
| CaO | 8.24 | 10.31 | 9.70 | 8.36 | 7.57 | 8.44 | 8.88 |
| Na ₂ O | 2.59 | 3.01 | 2.38 | 2.63 | 2.48 | 1.91 | 2.43 |
| K ₂ O | 0.53 | 0.38 | 0.49 | 0.49 | 0.65 | 0.62 | 0.27 |
| TiO ₂ | 1.33 | 1.13 | 0.87 | 1.23 | 1.34 | 0.77 | 0.81 |
| MnO | 0.18 | 0.14 | 0.13 | 0.16 | 0.17 | 0.13 | 0.17 |
| P ₂ O ₅ | 0.21 | 0.16 | 0.12 | 0.19 | 0.24 | 0.08 | 0.10 |
| S | 1864 | 1329 | 22083 | 2816 | 39728 | 1420 | 1063 |
| Ni | 26.90 | 13.50 | 1367 | 73.30 | 244.8 | 24.00 | 40.20 |
| Cu | 31.20 | 33.40 | 1204 | 65.60 | 428.3 | 15.90 | 27.80 |
| Cr | 70.00 | 63.00 | 117.0 | 71.00 | 68.00 | 58.00 | 76.00 |
| Zn | 59.00 | 36.30 | 55.00 | 50.60 | 74.40 | 23.90 | 40.20 |
| Pb | <LD | <LD | <LD | <LD | 13.60 | <LD | <LD |
| Ba | 358.9 | 147.3 | 134.0 | 283.2 | 287.7 | 195.0 | 145.3 |
| Sc | 21.00 | 34.00 | <LD | 19.00 | 21.00 | 17.00 | 22.00 |
| Ga | 21.40 | 23.70 | 21.70 | 18.60 | 20.80 | 17.00 | 22.00 |
| As | <LD | <LD | <LD | <LD | <LD | <LD | <LD |
| Rb | 9.88 | 4.38 | 10.52 | 7.68 | 12.70 | 21.05 | 2.77 |
| Sr | 306.8 | 365.3 | 351.0 | 320.5 | 287.4 | 371.2 | 323.6 |
| Y | 23.30 | 21.80 | 15.30 | 22.40 | 24.60 | 11.20 | 14.40 |
| Zr | 91.60 | 75.40 | 50.90 | 81.10 | 94.90 | 42.40 | 48.20 |
| Nb | 3.50 | 4.20 | 2.50 | 3.60 | 3.70 | <LD | <LD |
| V | 149.0 | 139.0 | 120.0 | 141.0 | 150.0 | 96.00 | 101.0 |
| Ce | <LD | <LD | <LD | <LD | <LD | <LD | <LD |
| Cl | 150.0 | 114.0 | 87.00 | 83.00 | 91.00 | 313.0 | 84.00 |
| Th | <LD | <LD | <LD | <LD | <LD | <LD | <LD |
| U | <LD | <LD | <LD | <LD | <LD | <LD | <LD |
| Total | 94.80% | 94.46% | 99.35% | 92.08% | 103.1% | 88.44% | 92.29% |

Table B.1. Continued

| Sample Name Subdivision, Subunit, etc. | 96-036-111 Gabbro Hybrid | 96-036-112 Gabbro Hybrid | 96-036-113 Olivine Gabbro | sv96-36-01 Leopard Gabbro | sv96-36-02 Upper Gabbro | 97-091-116 Upper Gabbro | 97-091-118 Upper Gabbro |
|--|--------------------------------|--------------------------------|---------------------------------|---------------------------------|-------------------------------|-------------------------------|-------------------------------|
| SiO ₂ | 43.74 | 34.55 | 42.97 | 42.29 | 36.00 | 46.41 | 45.92 |
| Al ₂ O ₃ | 17.77 | 13.38 | 15.60 | 15.69 | 14.61 | 17.89 | 18.55 |
| Fe ₂ O ₃ T | 12.50 | 23.15 | 13.33 | 11.65 | 20.18 | 11.89 | 11.36 |
| MgO | 9.15 | 5.42 | 5.90 | 8.95 | 7.34 | 4.17 | 4.18 |
| CaO | 8.85 | 7.26 | 8.24 | 8.66 | 7.97 | 9.10 | 9.46 |
| Na ₂ O | 2.52 | 1.92 | 2.63 | 2.08 | 1.95 | 2.82 | 3.00 |
| K ₂ O | 0.32 | 0.30 | 0.59 | 0.44 | 0.21 | 0.80 | 0.58 |
| TiO ₂ | 1.02 | 0.68 | 1.25 | 1.07 | 0.58 | 1.79 | 1.59 |
| MnO | 0.16 | 0.14 | 0.16 | 0.14 | 0.14 | 0.15 | 0.15 |
| P ₂ O ₅ | 0.14 | 0.08 | 0.19 | 0.13 | 0.07 | 0.30 | 0.25 |
| S | 1430 | 60618 | 5093 | 547.0 | 47064 | 1606 | 1530 |
| Ni | 90.90 | 525.8 | 60.90 | 31.00 | 667.0 | <LD | <LD |
| Cu | 34.50 | 653.4 | 94.20 | 30.00 | 746.0 | 25.40 | 23.30 |
| Cr | 102.0 | 71.00 | 75.00 | 56.00 | 79.00 | 67.00 | 64.00 |
| Zn | 58.20 | 74.60 | 58.10 | 65.00 | 64.00 | 56.00 | 50.80 |
| Pb | <LD | 9.40 | <LD | <LD | 12.00 | <LD | <LD |
| Ba | 190.3 | 118.8 | 298.4 | 176.0 | 108.0 | 389.9 | 288.1 |
| Sc | 15.00 | <LD | 21.00 | 25.00 | 25.00 | 22.00 | 20.00 |
| Ga | 24.00 | 18.20 | 22.20 | 18.00 | 20.00 | 25.30 | 23.40 |
| As | <LD | <LD | <LD | <LD | <LD | <LD | <LD |
| Rb | 2.96 | 6.38 | 12.41 | 13.60 | 4.60 | 15.61 | 11.16 |
| Sr | 301.4 | 288.7 | 327.4 | 341.2 | 293.3 | 382.6 | 406.0 |
| Y | 17.50 | 11.90 | 22.30 | 18.10 | 8.60 | 26.30 | 22.20 |
| Zr | 66.60 | 39.90 | 86.40 | 64.00 | 30.70 | 123.9 | 100.3 |
| Nb | 2.90 | 2.50 | 3.60 | <LD | <LD | 7.50 | 5.50 |
| V | 145.0 | 103.0 | 144.0 | 115.0 | 111.0 | 143.0 | 138.0 |
| Ce | <LD | <LD | <LD | <LD | <LD | <LD | 74.10 |
| Cl | 70.00 | 95.00 | 106.0 | 278.0 | 141.0 | 145.0 | 164.0 |
| Th | <LD | <LD | <LD | <LD | <LD | <LD | <LD |
| U | <LD | <LD | <LD | <LD | <LD | <LD | <LD |
| Total | 96.67% | 102.3% | 92.31% | 91.58% | 101.1% | 95.90% | 95.58% |

Table B.1. Continued

| Sample Name Subdivision, Subunit, etc. | 97-091-119 Olivine gabbro | 97-091-120 Gabbro Hybrid | 97-091-121 Gabbro Hybrid | 97-091-122 Olivine Gabbro | 97-091-122 Olivine Gabbro (dup) | 97-091-123 Churchill Gneiss | 97-091-128 Mafic Dike |
|--|---------------------------------|--------------------------------|--------------------------------|---------------------------------|---------------------------------------|-----------------------------------|--------------------------|
| SiO ₂ | 40.80 | 43.16 | 39.91 | 46.80 | 45.58 | 57.98 | 45.48 |
| Al ₂ O ₃ | 12.92 | 15.81 | 14.13 | 16.27 | 16.18 | 15.02 | 13.03 |
| Fe ₂ O ₃ T | 18.29 | 13.31 | 15.97 | 14.30 | 13.26 | 10.60 | 14.94 |
| MgO | 10.20 | 6.29 | 6.05 | 5.06 | 4.59 | 0.39 | 6.17 |
| CaO | 7.15 | 8.00 | 7.85 | 8.33 | 8.21 | 5.15 | 8.33 |
| Na ₂ O | 2.24 | 2.43 | 2.13 | 2.91 | 2.85 | 3.02 | 2.35 |
| K ₂ O | 0.47 | 0.66 | 0.56 | 0.90 | 0.90 | 3.67 | 0.47 |
| TiO ₂ | 1.44 | 1.59 | 1.16 | 2.03 | 2.02 | 1.21 | 1.94 |
| MnO | 0.23 | 0.15 | 0.14 | 0.18 | 0.17 | 0.12 | 0.21 |
| P ₂ O ₅ | 0.23 | 0.29 | 0.22 | 0.35 | 0.36 | 0.44 | 0.25 |
| S | 1495 | 2438 | 19080 | 2108 | 1577 | 944.0 | 1370 |
| Ni | 90.40 | 18.40 | 191.4 | 11.30 | <LD | <LD | 7.00 |
| Cu | 39.20 | 45.50 | 346.0 | 26.40 | 24.50 | 10.00 | 17.80 |
| Cr | 91.00 | 83.00 | 72.00 | 67.00 | 59.00 | 11.00 | 94.00 |
| Zn | 86.50 | 72.20 | 74.30 | 75.60 | 70.70 | 126.1 | 58.60 |
| Pb | <LD | <LD | 7.30 | <LD | <LD | 20.30 | <LD |
| Ba | 295.8 | 433.9 | 309.4 | 441.8 | 490.6 | 1862 | 319.2 |
| Sc | 22.00 | 26.00 | 13.00 | 31.00 | 21.00 | 25.00 | 36.00 |
| Ga | 21.20 | 26.00 | 23.60 | 23.00 | 27.30 | 29.50 | 25.00 |
| As | <LD | <LD | <LD | <LD | <LD | <LD | <LD |
| Rb | 7.24 | 11.60 | 12.72 | 17.21 | 16.47 | 81.83 | 8.70 |
| Sr | 266.0 | 355.5 | 373.0 | 325.1 | 341.5 | 294.5 | 322.7 |
| Y | 20.10 | 23.90 | 19.70 | 29.40 | 30.20 | 64.20 | 31.50 |
| Zr | 81.40 | 117.1 | 85.80 | 142.4 | 135.1 | 505.4 | 156.1 |
| Nb | 6.00 | 7.30 | 4.70 | 8.30 | 6.90 | 24.20 | 8.20 |
| V | 144.0 | 144.0 | 104.0 | 178.0 | 173.0 | 28.00 | 209.0 |
| Ce | <LD | <LD | <LD | 71.10 | <LD | 170.3 | <LD |
| Cl | 83.00 | 136.0 | 123.0 | 110.0 | 96.00 | 367.0 | 859.0 |
| Th | <LD | <LD | <LD | <LD | <LD | 5.60 | <LD |
| U | <LD | <LD | <LD | <LD | <LD | <LD | <LD |
| Total | 94.50% | 92.49% | 93.10% | 97.85% | 94.73% | 98.27% | 93.78% |

Table B.1. Continued

| Sample Name Subdivision, Subunit, etc. | w98-022 Anorthosite | sv97-91-04 Anorthosite | 97-079-141 MG Gabbro | 97-079-142 Gabbro Hybrid | 97-079-143 Peridotite | 97-091-144 MG Gabbro | 97-079-145 MG Gabbro |
|--|------------------------|---------------------------|-------------------------|--------------------------------|--------------------------|-------------------------|-------------------------|
| SiO ₂ | 32.83 | 38.11 | 42.20 | 42.79 | 44.90 | 37.24 | 35.43 |
| Al ₂ O ₃ | 5.97 | 13.24 | 15.68 | 16.29 | 15.60 | 7.50 | 6.12 |
| Fe ₂ O ₃ T | 40.72 | 23.30 | 13.95 | 14.40 | 14.05 | 17.27 | 18.49 |
| MgO | 4.05 | 3.41 | 6.42 | 6.96 | 6.08 | 23.80 | 21.07 |
| CaO | 8.33 | 7.96 | 8.38 | 7.88 | 8.50 | 4.57 | 4.50 |
| Na ₂ O | 1.29 | 2.43 | 2.45 | 2.54 | 2.72 | 1.26 | 1.33 |
| K ₂ O | 0.54 | 0.80 | 0.59 | 0.67 | 0.72 | 0.33 | 0.58 |
| TiO ₂ | 5.90 | 2.84 | 1.17 | 1.36 | 1.61 | 1.00 | 1.61 |
| MnO | 0.45 | 0.24 | 0.14 | 0.16 | 0.18 | 0.17 | 0.18 |
| P ₂ O ₅ | 4.18 | 1.83 | 0.16 | 0.22 | 0.23 | 0.32 | 0.56 |
| S | 6615 | 13555 | 12242 | 7852 | 1345 | 6236 | 7591 |
| Ni | <LD | 18.00 | 212.5 | 126.6 | <LD | 1543 | 761.4 |
| Cu | 55.00 | 118.0 | 335.9 | 202.1 | 18.30 | 268.4 | 288.1 |
| Cr | <LD | 64.00 | 78.00 | 87.00 | 74.00 | 151.0 | 164.0 |
| Zn | 316.0 | 138.0 | 70.10 | 69.80 | 61.20 | 61.00 | 126.0 |
| Pb | 8.00 | <LD | 6.20 | <LD | <LD | <LD | 15.30 |
| Ba | 324.0 | 559.0 | 280.6 | 363.8 | 388.4 | 125.4 | 329.6 |
| Sc | 49.00 | 35.00 | 16.00 | 18.00 | 21.00 | <LD | <LD |
| Ga | 12.00 | 25.00 | 22.80 | 23.60 | 23.70 | 9.50 | 12.20 |
| As | <LD | <LD | <LD | <LD | <LD | <LD | <LD |
| Rb | 10.00 | 11.80 | 8.33 | 10.84 | 8.96 | 2.52 | 6.83 |
| Sr | 157.7 | 336.0 | 353.1 | 346.0 | 333.5 | 241.3 | 248.4 |
| Y | 79.70 | 33.90 | 21.60 | 18.90 | 24.10 | 9.40 | 17.80 |
| Zr | 241.8 | 126.7 | 79.30 | 86.60 | 91.00 | 51.90 | 91.10 |
| Nb | 32.50 | 14.30 | 3.50 | 4.80 | 3.80 | 2.30 | 6.90 |
| V | 275.0 | 202.0 | 122.0 | 127.0 | 188.0 | 54.00 | 100.0 |
| Ce | 185.0 | 81.00 | <LD | <LD | <LD | <LD | <LD |
| Cl | 312.0 | 144.0 | 747.0 | 435.0 | 387.0 | 879.0 | 1773 |
| Th | <LD | <LD | <LD | <LD | <LD | <LD | <LD |
| U | <LD | <LD | <LD | <LD | <LD | <LD | <LD |
| Total | 106.2% | 97.77% | 94.48% | 95.46% | 95.13% | 95.42% | 92.20% |

Table B.1. Continued

| Sample Name | 97-079-146 | 97-079-147 | 97-079-148 | sv96-47-03 |
|----------------------------------|------------|------------|------------|------------|
| Subdivision, Subunit, etc. | MG Gabbro | MG Gabbro | MG Gabbro | Peridotite |
| SiO ₂ | 38.01 | 34.47 | 42.62 | 36.89 |
| Al ₂ O ₃ | 10.08 | 13.79 | 15.44 | 6.12 |
| Fe ₂ O ₃ T | 16.77 | 22.32 | 13.26 | 22.20 |
| MgO | 15.68 | 5.74 | 6.13 | 25.80 |
| CaO | 5.89 | 6.85 | 7.87 | 4.00 |
| Na ₂ O | 2.10 | 2.42 | 3.43 | 0.78 |
| K ₂ O | 0.62 | 0.64 | 1.10 | 0.12 |
| TiO ₂ | 1.78 | 1.76 | 3.84 | 0.56 |
| MnO | 0.17 | 0.12 | 0.15 | 0.24 |
| P ₂ O ₅ | 0.62 | 0.51 | 1.29 | 0.07 |
| S | 7082 | 59451 | 1630 | 11847 |
| Ni | 726.3 | 2869 | 44.80 | 460.0 |
| Cu | 269.7 | 2158 | 37.40 | 295.0 |
| Cr | 156.0 | 95.00 | 69.00 | 101.0 |
| Zn | 75.30 | 98.10 | 64.40 | 92.00 |
| Pb | 12.70 | 27.40 | <LD | 7.00 |
| Ba | 305.3 | 269.7 | 622.7 | 51.00 |
| Sc | <LD | <LD | 10.00 | 25.00 |
| Ga | 17.00 | 15.60 | 22.20 | 9.00 |
| As | <LD | <LD | <LD | <LD |
| Rb | 5.72 | 6.27 | 8.62 | 2.80 |
| Sr | 314.3 | 458.0 | 519.2 | 115.9 |
| Y | 17.80 | 17.20 | 28.00 | 9.60 |
| Zr | 102.6 | 114.10 | 195.8 | 33.30 |
| Nb | 6.80 | 9.70 | 13.70 | 1.50 |
| V | 105.0 | 89.00 | 142.0 | 100.0 |
| Ce | <LD | <LD | <LD | <LD |
| Cl | 1060 | 367.0 | 105.0 | 1389 |
| Th | <LD | <LD | <LD | <LD |
| U | <LD | <LD | <LD | <LD |
| Total | 93.85% | 104.3% | 95.77% | 100.0% |

B.1.2 XRF (pressed pellet) – Precision and Accuracy

Thirty-six replicate XRF analyses were performed on the standards BHVO-1, SY-2, PACS-1, and DTS-1, over the period of August 1998 to March 1999. The known values are from Govindaraju (1989). Precision is generally good (3-7 % RSD) to excellent (0-3 % RSD), based on the criteria of Jenner *et al.*, 1990, with the exceptions of Sc and V (Table B.1.1). Accuracy of the thirty-six replicate analysis is good (\pm 3-7% RD) to excellent (\pm 0-3 % RD) with the exception of Y and Nb (Table B.1.1).

Table B.1.1 Precision and accuracy for standards BHVO-1, SY-2, PACS-1, and DTS-1 calculated from 36 determinations over the period of August 1998 to March 1999.

| Element ¹ (the standard used is within brackets) | Average Value (n = 36) | RSD (%) or Precision ² (excellent, good) | Known value (Govindaraju, 1989) | % RD ³ or Accuracy ³ (excellent, good) |
|---|---------------------------|--|---------------------------------------|---|
| SiO ₂ (BHVO-1) | 49.15 | 3.50 (good) | 49.94 | -1.58 (excellent) |
| Al ₂ O ₃ (SY-2) | 12.78 | 3.10 (good) | 12.04 | 6.15 (good) |
| TiO ₂ (BHVO-1) | 2.79 | 6.40 (good) | 2.71 | 2.95 (excellent) |
| Fe ₂ O _{3T} (SY-2) | 6.31 | 3.00 (excellent) | 6.31 | 0.00 (excellent) |
| MgO (BHVO-1) | 7.03 | 3.80 (good) | 7.23 | -2.77 (excellent) |
| MnO (SY-2) | 0.31 | 3.40 (good) | 0.32 | -3.13 (good) |
| CaO (SY-2) | 7.99 | 4.80 (good) | 7.96 | 0.38 (excellent) |
| Na ₂ O (SY-2) | 4.22 | 3.30 (good) | 4.31 | -2.09 (excellent) |
| K ₂ O (SY-2) | 4.34 | 4.50 (good) | 4.44 | -2.25 (excellent) |
| P ₂ O ₅ (SY-2) | 0.42 | 5.10 (good) | 0.43 | -2.33 (excellent) |
| S (PACS-1) | 13200 | 0.82 (excellent) | 32000 | 0.00 (excellent) |
| Sc (BHVO-1) | 33.00 | 9.00 | 32.00 | 3.13 (good) |
| V (BHVO-1) | 317.0 | 7.70 | 317.0 | 0.00 (excellent) |
| Cr (DTS-1) | 3988 | 3.90 (good) | 3990 | -0.05 (excellent) |
| Ni (DTS-1) | 2360 | 0.30 (excellent) | 2360 | 0.00 (excellent) |
| Cu (BHVO-1) | 137.0 | 1.00 (excellent) | 136.0 | 0.74 (excellent) |
| Zn (BHVO-1) | 101.0 | 1.30 (excellent) | 105.0 | -3.81 (good) |
| Sr (SY-2) | 271.0 | 0.40 (excellent) | 271.0 | 0.00 (excellent) |
| Rb (SY-2) | 220.0 | 0.10 (excellent) | 217.0 | 1.38 (excellent) |
| Ba (SY-2) | 450.0 | 3.50 (good) | 460.0 | -2.17 (excellent) |
| Y (SY-2) | 118.0 | 0.30 (excellent) | 128.0 | -7.81 |
| Nb (SY-2) | 34.90 | 1.20 (excellent) | 29.00 | 20.34 |
| Zr (SY-2) | 296.0 | 0.60 (excellent) | 280.0 | 5.71 (good) |

¹All major element oxides reported as weight percent (%) and trace elements reported as parts per million (ppm). ²The RSD % (relative standard deviation) is the standard deviation divided by the average of 36 runs. ³The % RD is the relative difference relative to the known value calculated by: [(average determination - known value) / (known value)] x 100%.

B.2.1 ICP-MS – Analytical Technique

All samples selected for Inductively Coupled Plasma-Mass Spectrometry (ICP-MS) analysis (see Table A.2), were initially reduced to small chips ($<1 \text{ cm}^2$) using a jaw-crusher and then further reduced to powders ($<0.5 \text{ mm}^2$) using a tungsten-carbide puck mill. The jaw crusher and puck mill were repeatedly cleaned between samples. The ICP-MS analytical technique described by Jenner *et al.* (1990) was followed for this study and is summarized below. The ICP-MS analytical data is compiled in Table B.2.

The ICP-MS analytical procedure was as follows: (1) a HF/HNO₃ digestion of a 0.1 g sample aliquot, (2) analysis of the solution by ICP-MS using the method of standard addition to correct for matrix effects. Any sample material that did not dissolve fully was added to HCL/HNO₃. For quality control, the geological reference sample MRG-1 was prepared and analyzed with the samples for this study. The trace elements (Y, Zr, Nb, Hf, Ta, Th, U, Mo, Pb, Bi, Li, Rb, Sr, Cs, Ba, Tl) and the rare earth elements (La, Ce, Pr, Nd, Sm, Eu, Gd, Tb, Dy, Ho, Er, Tm, Yb, Lu) were reported for this technique. The detection limits of the aforementioned elements are described by Longerich *et al.* (1990).

Collection of data was done by an automated computer system and raw data was reduced to readable format using in-house software and spreadsheets. The ICP-MS analytical data is compiled in Table B.2 whereas the precision and accuracy of the results is reported in Section B.2.2.

Table B.2. MUN ICP-MS analytical data. All results are reported in ppm.

| Sample Name Subdivision, Subunit, etc. | 97-069-138 Mafic Dike | 96-048-093 Upper Gabbro | 96-029-073 Upper Gabbro | 97-073-041 Mafic Dike | 97-079-147 MG Gabbro | 97-057-037 Olivine Gabbro | 96-002-004 Leopard Gabbro |
|--|--------------------------|-------------------------------|-------------------------------|--------------------------|-------------------------|---------------------------------|---------------------------------|
| Li | 12.96 | 4.91 | 5.72 | 17.20 | 5.00 | 7.97 | 4.71 |
| Rb | 85.52 | 5.58 | 6.98 | 57.64 | 7.60 | 11.23 | 7.02 |
| Sr | 276.5 | 366.9 | 280.0 | 350.8 | 403.7 | 303.4 | 251.7 |
| Y | 15.39 | 17.63 | 15.99 | 13.78 | 15.42 | 18.25 | 13.10 |
| Zr | 63.66 | 66.17 | 50.20 | 55.26 | 109.1 | 53.05 | 51.11 |
| Nb | 5.75 | 2.72 | 2.53 | 4.47 | 8.76 | 4.55 | 2.16 |
| Mo | 0.80 | 0.64 | 0.48 | 0.88 | 2.00 | 0.37 | 1.34 |
| Cs | 0.71 | 0.03 | 0.04 | 0.26 | 0.05 | 0.16 | 0.05 |
| Ba | 373.8 | 177.8 | 141.1 | 278.9 | 269.6 | 278.5 | 145.0 |
| La | 16.23 | 6.06 | 5.84 | 12.05 | 13.71 | 10.04 | 5.36 |
| Ce | 35.04 | 14.19 | 13.56 | 26.46 | 33.09 | 22.67 | 12.17 |
| Pr | 4.34 | 2.01 | 1.92 | 3.44 | 4.49 | 2.95 | 1.65 |
| Nd | 17.91 | 9.47 | 8.95 | 14.75 | 19.91 | 13.27 | 7.59 |
| Sm | 3.75 | 2.63 | 2.43 | 3.27 | 4.25 | 3.22 | 1.96 |
| Eu | 1.22 | 1.15 | 1.07 | 1.05 | 1.50 | 1.37 | 0.94 |
| Gd | 3.50 | 3.16 | 2.91 | 3.11 | 3.96 | 3.50 | 2.31 |
| Tb | 0.51 | 0.52 | 0.48 | 0.45 | 0.57 | 0.57 | 0.39 |
| Dy | 3.02 | 3.36 | 3.06 | 2.70 | 3.26 | 3.60 | 2.45 |
| Ho | 0.60 | 0.69 | 0.64 | 0.55 | 0.61 | 0.73 | 0.51 |
| Er | 1.72 | 2.01 | 1.83 | 1.56 | 1.64 | 2.07 | 1.50 |
| Tm | 0.25 | 0.28 | 0.26 | 0.22 | 0.22 | 0.29 | 0.22 |
| Yb | 1.63 | 1.80 | 1.66 | 1.42 | 1.38 | 1.88 | 1.39 |
| Lu | 0.25 | 0.27 | 0.25 | 0.21 | 0.20 | 0.28 | 0.21 |
| Hf | 2.13 | 2.01 | 1.83 | 1.66 | 2.97 | 1.71 | 1.72 |
| Ta | 1.51 | 1.97 | 1.42 | 1.07 | 2.07 | 1.14 | 0.92 |
| Tl | 0.51 | 0.04 | 0.06 | 0.34 | 0.08 | 0.06 | 0.09 |
| Pb | 14.62 | 1.69 | 1.53 | 71.27 | 19.45 | 6.98 | 13.62 |
| Bi | 0.03 | 0.02 | 0.01 | 0.05 | 0.28 | 0.03 | 0.37 |
| Th | 2.80 | 0.53 | 0.47 | 2.05 | 0.85 | 1.05 | 0.50 |
| U | 0.55 | 0.08 | 0.07 | 0.42 | 0.16 | 0.12 | 0.07 |

Table B.2. Continued

| Sample Name | 96-015-085 | 96-036-112 | 98-102-149 | 98-102-151 | 98-102-152 | 98-102-153 | 98-102-155 |
|------------------------------|-------------------|---------------|--------------|--------------|-------------------|---------------|----------------|
| Subdivision or Subunit, etc. | Transition Gabbro | Gabbro Hybrid | Upper Gabbro | Upper Gabbro | Transition Gabbro | Gabbro Hybrid | Olivine Gabbro |
| Li | 7.96 | 5.42 | 5.33 | 6.17 | 6.39 | 6.69 | 10.15 |
| Rb | 9.97 | 5.96 | 7.24 | 5.75 | 6.71 | 7.27 | 20.78 |
| Sr | 288.1 | 250.5 | 407.4 | 287.7 | 289.3 | 302.2 | 225.3 |
| Y | 18.10 | 10.53 | 15.72 | 20.07 | 23.43 | 14.25 | 16.10 |
| Zr | 64.36 | 38.76 | 25.37 | 27.10 | 24.63 | 19.52 | 35.62 |
| Nb | 2.85 | 1.71 | 2.89 | 3.03 | 3.56 | 3.39 | 3.32 |
| Mo | 0.85 | 6.69 | 0.68 | 0.46 | 0.68 | 0.94 | 0.73 |
| Cs | 0.14 | 0.09 | 0.03 | 0.03 | 0.05 | 0.07 | 0.30 |
| Ba | 163.1 | 118.1 | 147.7 | 164.4 | 192.8 | 115.1 | 179.3 |
| La | 6.08 | 4.08 | 6.01 | 6.46 | 8.16 | 5.96 | 9.51 |
| Ce | 14.58 | 9.44 | 14.27 | 15.64 | 19.34 | 13.77 | 20.84 |
| Pr | 2.04 | 1.28 | 1.96 | 2.23 | 2.72 | 1.87 | 2.59 |
| Nd | 9.72 | 5.98 | 9.11 | 10.52 | 12.77 | 8.54 | 11.05 |
| Sm | 2.73 | 1.56 | 2.42 | 2.93 | 3.47 | 2.25 | 2.65 |
| Eu | 1.15 | 0.84 | 1.16 | 1.22 | 1.39 | 0.95 | 1.00 |
| Gd | 3.30 | 1.82 | 2.81 | 3.58 | 4.15 | 2.60 | 2.85 |
| Tb | 0.54 | 0.31 | 0.47 | 0.58 | 0.70 | 0.43 | 0.47 |
| Dy | 3.42 | 2.00 | 3.07 | 3.87 | 4.50 | 2.73 | 2.99 |
| Ho | 0.72 | 0.41 | 0.62 | 0.80 | 0.92 | 0.57 | 0.63 |
| Er | 2.09 | 1.19 | 1.75 | 2.28 | 2.64 | 1.63 | 1.87 |
| Tm | 0.30 | 0.17 | 0.25 | 0.33 | 0.38 | 0.24 | 0.27 |
| Yb | 1.92 | 1.13 | 1.58 | 2.08 | 2.38 | 1.56 | 1.79 |
| Lu | 0.28 | 0.17 | 0.23 | 0.30 | 0.35 | 0.23 | 0.27 |
| Hf | 1.99 | 1.19 | 0.93 | 0.94 | 0.99 | 0.89 | 1.12 |
| Ta | 1.59 | 0.72 | 2.07 | 1.56 | 1.58 | 1.90 | 1.63 |
| Tl | 0.12 | 0.06 | 0.03 | 0.04 | 0.04 | 0.04 | 0.15 |
| Pb | 5.19 | 9.35 | 2.13 | 2.57 | 2.77 | 6.21 | 8.78 |
| Bi | 0.08 | 0.15 | 0.12 | 0.02 | 0.02 | 0.10 | 0.05 |
| Th | 0.48 | 0.34 | 0.49 | 0.56 | 0.72 | 0.83 | 2.00 |
| U | 0.08 | 0.05 | 0.07 | 0.07 | 0.10 | 0.10 | 0.26 |

Table B.2. Continued

| Sample Name | 98-102-156 | 98-102-157 | 96-002-006 | 96-034-101 |
|-------------------------------|-----------------------|---------------------|---------------------|---------------------|
| Subdivision, Subunit, etc. | Semi-mass Sulphide | Churchill Gneiss | Churchill Gneiss | Churchill Gneiss |
| Li | 2.58 | 24.10 | 18.36 | 15.72 |
| Rb | 5.97 | 116.2 | 79.42 | 115.2 |
| Sr | 22.72 | 252.6 | 186.2 | 145.8 |
| Y | 1.33 | 11.75 | 14.48 | 8.36 |
| Zr | 12.14 | 116.1 | 123.2 | 215.0 |
| Nb | 0.96 | 8.68 | 12.56 | 5.40 |
| Mo | 9.49 | 1.10 | 3.63 | 3.16 |
| Cs | 0.11 | 2.15 | 0.43 | 0.45 |
| Ba | 47.33 | 661.3 | 611.5 | 609.6 |
| La | 3.01 | 42.17 | 49.42 | 31.17 |
| Ce | 5.62 | 84.29 | 98.62 | 60.25 |
| Pr | 0.60 | 9.65 | 10.65 | 6.54 |
| Nd | 2.05 | 35.29 | 37.69 | 23.84 |
| Sm | 0.30 | 6.14 | 6.07 | 4.12 |
| Eu | 0.10 | 1.48 | 1.12 | 1.18 |
| Gd | 0.26 | 4.39 | 4.26 | 3.40 |
| Tb | 0.04 | 0.53 | 0.54 | 0.46 |
| Dy | 0.24 | 2.70 | 3.06 | 2.16 |
| Ho | 0.05 | 0.47 | 0.56 | 0.32 |
| Er | 0.16 | 1.27 | 1.54 | 0.78 |
| Tm | 0.03 | 0.20 | 0.21 | 0.10 |
| Yb | 0.19 | 1.44 | 1.41 | 0.58 |
| Lu | 0.03 | 0.23 | 0.22 | 0.09 |
| Hf | 0.43 | 3.55 | 3.96 | 6.30 |
| Ta | 0.43 | 1.91 | 1.72 | 1.94 |
| Tl | 0.14 | 0.74 | 0.51 | 0.86 |
| Pb | 2.69 | 27.29 | 55.13 | 19.18 |
| Bi | 0.19 | 0.09 | 0.07 | 0.03 |
| Th | 0.70 | 14.27 | 14.38 | 8.06 |
| U | 0.07 | 1.50 | 1.46 | 0.95 |

B.2.2 ICP-MS – Precision and Accuracy

Five replicate ICP-MS analyses were performed on the standard MRG-1 over the period of May 1999 to November 2000. The known value comes from Govindaraju (1989). Precision is generally good (3-7 % RSD) to excellent (0-3 % RSD) according to the criteria established by Jenner *et al.* (1990), with the exceptions of Li, Y, Zr, Mo, Ba, Lu, Hf, Tl, Pb, and Bi (Table B.1.1). Accuracy of the five replicate analysis is good (\pm 3-7 % RD) to excellent (\pm 0-3 % RD) with the exceptions of Mo, Gd, Lu, Hf, Tl, and Bi (Table B.2.1).

Table B.2.1 Precision and accuracy for the standard MRG-1 calculated from 5 determinations over the period of May 1999 to November 2000 (runs 495 to 633).

| Element ¹ (ppm) | Average Value for MRG-1 (n=5) | Standard Deviation | RSD (%) or Precision ² (excellent, good) | Known value (Govindaraju, 1989) | % RD or Accuracy ³ (excellent, good) |
|-------------------------------|----------------------------------|-----------------------|--|---------------------------------------|--|
| Li | 3.70 | 0.30 | 8.00 | 3.71 | -0.38 (excellent) |
| Rb | 7.63 | 0.50 | 6.50 (good) | 7.65 | -0.24 (excellent) |
| Sr | 269.1 | 1.82 | 0.67 (excellent) | 274.0 | -1.80 (excellent) |
| Y | 12.16 | 1.03 | 8.46 | 11.60 | 4.83 (good) |
| Zr | 95.62 | 6.92 | 7.24 | 93.70 | 2.05(excellent) |
| Nb | 20.88 | 0.98 | 4.71 (good) | 22.30 | -6.35 (good) |
| Mo | 1.15 | 0.18 | 15.37 | 1.26 | -9.05 |
| Cs | 0.59 | 0.01 | 2.26 (excellent) | 0.60 | -1.00 (excellent) |
| Ba | 49.05 | 6.68 | 13.63 | 47.50 | 3.26 (good) |
| La | 9.06 | 0.41 | 4.57 (good) | 9.07 | -0.11 (excellent) |
| Ce | 25.46 | 0.30 | 1.19 (excellent) | 26.20 | -2.81(excellent) |
| Pr | 3.64 | 0.14 | 3.77 (good) | 3.79 | -3.85 (good) |
| Nd | 18.12 | 0.61 | 3.35 (good) | 18.83 | -3.79 (good) |
| Sm | 4.44 | 0.03 | 0.76 (excellent) | 4.51 | -1.55 (excellent) |
| Eu | 1.41 | 0.02 | 1.33 (excellent) | 1.46 | -3.42 (good) |
| Gd | 4.07 | 0.04 | 1.10 (excellent) | 4.41 | -7.66 |
| Tb | 0.55 | 0.02 | 4.07 (good) | 0.55 | 0.00 (excellent) |
| Dy | 2.91 | 0.06 | 1.99 (excellent) | 3.01 | -3.32 (good) |
| Ho | 0.50 | 0.01 | 1.80 (excellent) | 0.51 | -2.75 (excellent) |
| Er | 1.19 | 0.02 | 1.75 (excellent) | 1.21 | -1.98 (excellent) |
| Tm | 0.15 | 0.00 | 2.94 (excellent) | 0.15 | 1.33 (excellent) |
| Yb | 0.81 | 0.02 | 2.76 (excellent) | 0.81 | 0.00(excellent) |
| Lu | 0.10 | 0.01 | 10.00 | 0.11 | -9.09 |
| Hf | 4.09 | 0.43 | 10.45 | 3.76 | 8.67 |
| Ta | 0.82 | 0.04 | 4.97 (good) | 0.83 | -0.96 (excellent) |
| Tl | 0.05 | 0.01 | 16.56 | 0.50 | -89.20 |
| Pb | 4.94 | 0.60 | 12.07 | 5.20 | -5.04 (good) |
| Bi | 0.16 | 0.08 | 47.66 | 0.13 | 21.54 |
| Th | 0.75 | 0.03 | 4.47 (good) | 0.78 | -4.10 (good) |
| U | 0.25 | 0.01 | 4.42 (good) | 0.25 | -0.80 (excellent) |

¹All element data reported as parts per million (ppm). ²The RSD % (relative standard deviation) is the standard deviation divided by the average of 5 runs. ³The % RD is the relative difference relative to the known value calculated by: [(average determination - known value) / (known value)] x 100%.

B.3.1 LAM-ICP-MS – Analytical Technique

All olivine samples analyzed by the LAM-ICP-MS technique were selected from representative petrographic thin sections (100 μm thick). Individual olivine grains were marked and photographed to facilitate the laser ablation process. Prior to the LAM-ICP-MS technique, several olivine grains used for this study were imaged (by secondary electrons) and analyzed using the Cameca SX-50 electron microprobe at the Earth Sciences Department, Memorial University. Major-element electron microprobe analyses were used as internal standards to adjust for differences in ablation yield between samples and the calibration standard.

One hundred and twenty-four euhedral olivine grains from 20 samples were ablated and analyzed using the LAM-ICP-MS method (Table 4.11) described by Taylor *et al.*, 1997. Initially, the olivine grain was viewed on a computer monitor and ablation sites were selected. Data was acquired in peak jumping mode which resulted in singular intensity data per mass peak (time resolved analysis). The ablation process for the entire data acquisition lasted approximately 120 seconds (measurement of argon carrier gas plus ablation time). Ablation pit sizes averaged 30 to 60 μm wide depending on the target size. For quality control, the standard BCR-2 was routinely analyzed under similar operating conditions as olivine to estimate the precision and accuracy of the data. The long term average BCR-2 values from the MUN LAM-ICP-MS are reported by Sylvester *et al.*, (2003) and shown in Table B.3.1. The major oxides MgO and FeO, and trace elements Ni, Cu, and Co were measured using this technique. Routine detection limits for this technique are reported by Taylor *et al.* (1997). The raw counts were converted to data using Convert and Lamtrace software (Lamtrace).

Table B.3. LAM-ICP-MS data of olivine grains from diamond drill holes SVB-97-91, SVB-96-04, SVB-98-102, and SVB-96-09. Major element data reported in wt%, trace element data reported in ppm. < indicates below detection limits.

| Sample | MgO | FeO | Ni | Cu | Co |
|---------|-------|-------|-------|-------|-------|
| 9791116 | 13.60 | 47.96 | 37.64 | <8.51 | 156.7 |
| 9791116 | 13.80 | 48.82 | 56.10 | <2.81 | 172.1 |
| 9791116 | 12.75 | 47.47 | 63.36 | <2.90 | 180.6 |
| 9791116 | 14.27 | 56.04 | 85.76 | <5.74 | 214.7 |
| 9791116 | 12.29 | 48.74 | 72.21 | 3.68 | 183.8 |
| 9791116 | 13.37 | 50.33 | 67.63 | <4.34 | 169.7 |
| 9791116 | 11.65 | 46.64 | 76.23 | <3.06 | 181.7 |
| 9791116 | 13.89 | 53.57 | 60.22 | <5.34 | 157.6 |
| 9791116 | 14.31 | 52.07 | 55.58 | <4.96 | 156.5 |
| 9791118 | 15.91 | 48.25 | 107.9 | 6.41 | 166.6 |
| 9791118 | 16.76 | 51.10 | 114.1 | <7.82 | 171.2 |
| 9791118 | 17.19 | 49.02 | 112.9 | <7.83 | 163.8 |
| 9791118 | 15.68 | 46.65 | 131.3 | <7.84 | 165.6 |
| 9791119 | 27.07 | 37.74 | 258.3 | <5.96 | 170.0 |
| 9791119 | 26.65 | 38.83 | 287.6 | 19.39 | 180.0 |
| 9791119 | 25.52 | 38.29 | 274.7 | 6.65 | 193.1 |
| 9791119 | 27.85 | 39.79 | 290.5 | <6.37 | 182.5 |
| 9791119 | 26.06 | 39.98 | 274.0 | 7.26 | 185.3 |
| 9791119 | 24.48 | 36.87 | 198.4 | <6.57 | 168.6 |
| 9791119 | 24.00 | 37.06 | 203.6 | <5.95 | 171.4 |
| 9791121 | 24.71 | 38.66 | 73.71 | 5.49 | 167.1 |
| 9791121 | 24.14 | 37.94 | 83.53 | <3.13 | 181.4 |
| 9791121 | 23.42 | 38.49 | 73.48 | 6.53 | 165.8 |
| 9791121 | 22.22 | 39.47 | 83.91 | <4.99 | 165.1 |
| 9791121 | 21.46 | 38.95 | 94.46 | 4.88 | 186.2 |
| 9791121 | 20.42 | 32.95 | 67.33 | 4.02 | 160.0 |
| 9791122 | 15.51 | 55.99 | 72.39 | <5.42 | 185.0 |
| 9791122 | 16.74 | 58.97 | 71.71 | <6.59 | 188.9 |
| 9791122 | 17.20 | 60.74 | 82.87 | <3.48 | 211.3 |
| 9791122 | 18.15 | 62.45 | 93.27 | 3.88 | 203.9 |
| 9791122 | 18.53 | 61.44 | 80.22 | <4.98 | 206.4 |
| 9791122 | 13.83 | 42.17 | 59.76 | <3.50 | 137.4 |

| Sample | MgO | FeO | Ni | Cu | Co |
|--------|-------|-------|-------|--------|-------|
| 960419 | 30.78 | 35.27 | 232.4 | <11.88 | 216.9 |
| 960419 | 28.52 | 35.47 | 219.5 | <15.39 | 241.2 |
| 960419 | 25.95 | 33.95 | 229.1 | <18.72 | 173.6 |
| 960419 | 26.46 | 33.95 | 295.1 | <17.11 | 181.0 |
| 960419 | 25.86 | 33.95 | 378.2 | <11.67 | 199.3 |
| 960419 | 29.41 | 35.92 | 487.7 | <16.87 | 225.6 |
| 960419 | 25.84 | 35.93 | 433.1 | <13.92 | 189.1 |
| 960421 | 26.37 | 37.27 | 503.6 | <11.83 | 187.1 |
| 960421 | 21.52 | 35.29 | 463.9 | <13.18 | 176.1 |
| 960421 | 19.86 | 30.46 | 603.6 | 12.29 | 163.3 |
| 960421 | 19.26 | 35.27 | 737.4 | <24.06 | 168.0 |
| 960421 | 16.96 | 35.27 | 657.4 | <21.71 | 155.0 |
| 960421 | 23.12 | 35.27 | 902.0 | <35.32 | 154.4 |
| 960422 | 22.94 | 38.88 | 441.0 | <8.63 | 253.7 |
| 960422 | 23.83 | 41.41 | 481.1 | 9.00 | 293.8 |
| 960422 | 22.83 | 41.05 | 375.1 | 7.06 | 263.4 |
| 960422 | 21.41 | 48.25 | 476.8 | 8.92 | 277.2 |
| 960422 | 22.98 | 48.41 | 444.0 | <9.53 | 269.1 |
| 960422 | 24.32 | 46.95 | 384.6 | 11.18 | 269.1 |
| 960422 | 21.73 | 44.86 | 389.7 | 9.84 | 262.6 |
| 960422 | 22.13 | 44.27 | 337.2 | 8.51 | 259.3 |
| 960423 | 19.30 | 47.97 | 463.0 | 8.09 | 248.7 |
| 960423 | 20.65 | 51.09 | 513.1 | 6.58 | 252.3 |
| 960423 | 20.44 | 49.66 | 485.6 | 8.77 | 250.8 |
| 960423 | 21.52 | 55.62 | 672.6 | 8.05 | 251.6 |
| 960423 | 21.06 | 53.03 | 617.1 | 8.01 | 248.8 |
| 960423 | 20.69 | 50.18 | 571.5 | 7.00 | 248.2 |
| 960423 | 21.54 | 50.06 | 576.9 | 7.61 | 220.4 |
| 960423 | 21.25 | 48.74 | 581.2 | 6.20 | 243.2 |
| 960425 | 23.53 | 48.35 | 490.6 | 9.75 | 289.7 |
| 960425 | 26.95 | 43.80 | 370.9 | 39.49 | 292.7 |
| 960425 | 22.65 | 53.58 | 594.2 | 7.48 | 315.3 |
| 960425 | 25.21 | 45.99 | 401.3 | 8.28 | 295.6 |
| 960425 | 24.44 | 45.28 | 412.3 | 7.60 | 289.8 |
| 960426 | 28.11 | 36.86 | 207.4 | 13.60 | 222.7 |
| 960426 | 27.92 | 40.08 | 236.5 | 9.90 | 248.6 |
| 960426 | 28.57 | 38.39 | 227.3 | 10.83 | 218.3 |
| 960426 | 28.75 | 39.76 | 154.5 | 11.62 | 235.4 |
| 960426 | 20.90 | 27.84 | 121.9 | <7.74 | 164.7 |
| 960426 | 28.33 | 39.55 | 185.5 | 10.19 | 235.1 |

Table B.3. Continued

| <i>Sample</i> | <i>MgO</i> | <i>FeO</i> | <i>Ni</i> | <i>Cu</i> | <i>Co</i> |
|---------------|------------|------------|-----------|-----------|-----------|
| 98102149 | 22.25 | 47.05 | 125.3 | 8.34 | 202.2 |
| 98102149 | 14.53 | 58.38 | 90.75 | 5.37 | 179.0 |
| 98102149 | 15.90 | 59.85 | 95.92 | 12.74 | 198.8 |
| 98102149 | 17.61 | 56.95 | 97.87 | 6.56 | 198.6 |
| 98102149 | 19.09 | 55.90 | 117.2 | 7.43 | 190.9 |
| 98102150 | 30.14 | 39.54 | 204.3 | 13.00 | 215.9 |
| 98102150 | 24.39 | 47.64 | 158.4 | 12.03 | 216.8 |
| 98102150 | 18.81 | 54.21 | 110.0 | 6.91 | 186.5 |
| 98102150 | 16.16 | 58.76 | 101.6 | 6.12 | 172.3 |
| 98102150 | 20.38 | 53.62 | 106.2 | 8.22 | 200.6 |
| 98102150 | 31.46 | 41.26 | 194.0 | 25.80 | 224.0 |
| 98102150 | 27.51 | 38.81 | 189.8 | 13.11 | 202.5 |
| 98102150 | 30.64 | 42.20 | 204.4 | 15.13 | 236.0 |
| 98102151 | 20.32 | 39.40 | 94.82 | <13.81 | 183.7 |
| 98102151 | 20.25 | 42.05 | 129.2 | <16.31 | 183.8 |
| 98102151 | 20.92 | 42.60 | 131.4 | <20.10 | 192.8 |
| 98102151 | 20.41 | 40.86 | 130.0 | <10.97 | 192.3 |
| 98102151 | 19.90 | 45.95 | 171.4 | <9.76 | 204.5 |
| 98102152 | 21.83 | 47.25 | 178.3 | <16.87 | 216.4 |
| 98102152 | 19.86 | 47.25 | 191.5 | <14.42 | 222.2 |
| 98102152 | 17.43 | 41.02 | 193.2 | <8.65 | 198.4 |
| 98102152 | 18.79 | 42.80 | 207.9 | <10.02 | 220.2 |
| 98102152 | 18.02 | 46.68 | 339.7 | <32.48 | 232.5 |
| 98102152 | 18.55 | 44.16 | 356.3 | <13.94 | 211.8 |

| <i>Sample</i> | <i>MgO</i> | <i>FeO</i> | <i>Ni</i> | <i>Cu</i> | <i>Co</i> |
|---------------|------------|------------|-----------|-----------|-----------|
| 960914 | 18.66 | 41.14 | 156.9 | 6.70 | 176.2 |
| 960914 | 19.14 | 45.58 | 163.3 | 6.89 | 185.9 |
| 960914 | 19.40 | 46.59 | 182.0 | 6.85 | 197.4 |
| 960914 | 22.05 | 55.18 | 175.0 | 7.67 | 217.9 |
| 960914 | 18.11 | 42.77 | 144.9 | 7.14 | 175.6 |
| 960914 | 19.43 | 49.23 | 143.7 | 6.97 | 193.3 |
| 960915 | 27.38 | 59.90 | 275.6 | 10.91 | 276.9 |
| 960915 | 19.17 | 41.25 | 187.1 | 6.89 | 187.0 |
| 960915 | 21.34 | 43.27 | 200.7 | 7.60 | 186.2 |
| 960915 | 20.90 | 45.95 | 199.0 | 7.65 | 199.5 |
| 960913 | 17.50 | 50.36 | 111.2 | 6.00 | 190.1 |
| 960913 | 15.37 | 49.71 | 85.38 | 6.03 | 166.4 |
| 960913 | 16.26 | 47.80 | 90.15 | 5.94 | 170.0 |
| 960917 | 28.12 | 34.83 | 469.8 | 10.55 | 257.5 |
| 960917 | 27.09 | 35.92 | 491.7 | 10.47 | 263.3 |
| 960917 | 28.47 | 36.93 | 457.2 | 11.43 | 281.6 |
| 960917 | 28.74 | 38.64 | 456.7 | 10.78 | 279.6 |
| 960917 | 30.75 | 42.46 | 448.9 | 11.60 | 306.6 |
| 960917 | 27.74 | 38.91 | 386.5 | 10.12 | 275.7 |
| 960917 | 27.26 | 38.98 | 406.9 | 10.61 | 284.8 |
| 960917 | 26.26 | 38.29 | 368.9 | 13.74 | 285.6 |
| 960918 | 22.03 | 51.67 | 624.8 | 7.87 | 286.0 |
| 960918 | 19.75 | 50.30 | 551.5 | 8.89 | 266.8 |
| 960918 | 20.80 | 47.61 | 538.4 | 7.80 | 274.4 |
| 960918 | 19.88 | 46.93 | 514.7 | 6.43 | 254.7 |
| 960918 | 20.88 | 49.32 | 516.7 | 6.92 | 260.7 |
| 960918 | 20.45 | 49.39 | 527.1 | 10.08 | 263.5 |

B.3.2 LAM-ICP-MS – Precision and Accuracy

Twenty replicate LAM-ICP-MS analyses were performed on the standard BCR-2 over the period of April to November 1999. The long term Memorial University average value for standard BCR-2 (1996-2002, n = 235) was compiled by Sylvester *et al.* (2003). The precision and accuracy for the chalcophile elements Ni and Cu are elevated as illustrated in Table B.3.1. However, Longerich *et al.* (1996) stated that the chalcophile elements Ni and Cu often show poor precision and accuracy due to fractionation effects during sample ablation and transportation.

Table B.3.1. Precision and accuracy for the standard BCR-2 calculated from 20 determinations over the period April to November, 1999.

| Element ¹ | Average Value (n = 20) | RSD (%) or Precision ² | MUN long term average 1996-2002 (n=235) | % RD ³ or Accuracy ³ |
|----------------------|---------------------------|--------------------------------------|--|--|
| MgO | 3.56 | 32.69 | Not quoted | - |
| FeO | 12.05 | 14.69 | Not quoted | - |
| Co | 35.29 | 7.13 | 37.27 | -5.31 |
| Ni | 12.98 | 47.38 | 10.17 | 27.63 |
| Cu | 21.58 | 15.16 | 17.54 | 22.93 |

¹All major element oxides reported as weight percent (%) and trace elements reported as parts per million (ppm). ²The RSD % (relative standard deviation) is the standard deviation divided by the average of 20 measurements. ³The % RD is the relative difference relative to the known value calculated by: [(average determination - known value) / (known value)] x 100%.

B.4.1 Sulphur Isotope Analysis – Analytical Technique

Core samples containing sulphides (*eg.* pyrrhotite and chalcopyrite) and silicate minerals (*eg.* plagioclase, olivine, *etc.*) were initially reduced to small fragments (0.5 cm^2) using a claw hammer, and then further reduced in size (0.05 to 0.2 cm^2) by gently grinding in a ceramic bowl. The fine particles were placed in a shallow, transparent plastic dish, placed under a binocular microscope, and individual sulphide grains were removed using needle-nose tweezers. Extreme care was taken to avoid removing silicate minerals and only the sulphide grain was retrieved for analysis. Sulphide grains were also separated by mineralogy, that is, pyrrhotite versus chalcopyrite. The sulphide separates were ground to a fine powder, placed in a small glass vial, and labeled using the correct sample identification and sulphide mineral separate.

Each sulphide separate was then placed into a small tin capsule and weighed on a microbalance according to predetermined weights (chalcopyrite = 0.095 mg , pyrrhotite = 0.090 mg ; Pye, 1998). A 0.1 mg quantity of vanadium pentoxide was added to the capsule with the sulphide sample. The capsule was reduced in size by repeated folding and added to an elemental analyzer whereby the sample was combusted. SO_2 gas was separated from other combustion gases by gas chromatography, and the gases entered the ion source of the Finnigan MAT 252 isotope-ratio mass spectrometer through a split interface. The integrated peak areas for $^{32}\text{SO}_2 +$ and $^{34}\text{SO}_2 +$ are compared to the response for a standard gas sample to determine the $\delta^{34}\text{S}$ value of the sample (Glesemann *et al.*, 1994). Sulphide standards, NBS-123 and MUN-PY, were routinely run to calibrate the isotope analyzer, and to determine precision and accuracy of the results.

Table B.4. Sulphur isotope character of magmatic sulphides from the Basal Gabbro Subdivision of the Pants Lake Intrusion, Churchill Province gneiss, and footwall anorthosite (unknown affinity). The $\delta^{34}\text{S}$ values are reported with respect to the Canyon Diablo Troilite internal standard. The mean and standard deviation of each sample population is reported in Section 5.4 (Analytical Results). (* Indicates duplicate sample taken).

| Sulphide Texture | Mineral separate | $\delta^{34}\text{S}$ value (‰) | Reference Location / DDH # | Host, grain size (sample) |
|-----------------------------------|------------------|---------------------------------|----------------------------|-----------------------------|
| Massive sulphide | Chalcopyrite | -3.21 | N Gabbro / 97-75 | BG, cg (NAI-1) |
| Massive sulphide | Pyrrhotite | -2.79 | N Gabbro / 97-75 | BG, cg (NAI-2) |
| Massive sulphide | Chalcopyrite | -2.81/-2.38* | N Gabbro / 97-75 | BG, cg (75-C1) |
| Massive sulphide | Pyrrhotite | -3.12 | N Gabbro / 97-75 | BG, cg (75-C2) |
| Sulphide blotch | Pyrrhotite | -3.26 | N Gabbro / 98-116 | BG, cg (116-174) |
| Sulphide fragment (?) | Pyrrhotite | -2.51 | N Gabbro / 97-96 | BG, cg (96-B) |
| Massive sulphides | Pyrrhotite | -3.33 | N Gabbro / 97-96 | BG, cg (96-A) |
| Massive sulphide | Pyrrhotite | -2.95 | N Gabbro / 98-131 | BG, cg (98-131) |
| Massive sulphide | Pyrrhotite | -2.41/-2.41* | N Gabbro / 98-113 | BG, cg (113-169) |
| Semi-mass sulphide | Pyrrhotite | -2.07 | N Gabbro / 96-20 | BG, cg (20-71) |
| Sulphide blotch | Pyrrhotite | -2.37 | C Gabbro / 96-15 | BG, cg (15-86B) |
| Sulphide blotch | Pyrrhotite | -2.60 | N Gabbro / 97-57 | BG, cg (57-36) |
| Sulphide blotch | Pyrrhotite | -2.16 | N Gabbro / 96-20 | BG, cg (20-69) |
| Massive sulphide | Pyrrhotite | -2.48 | N Gabbro / 97-58 | BG, cg (58-54) |
| Sulphide blotch | Pyrrhotite | -1.93 | N Gabbro / 96-04 | BG, cg (04-24) |
| Sulphide blotch | Pyrrhotite | -2.24 | N Gabbro / 97-73 | BG, cg (73-40) |
| North & Central Gabbro | | Range | -3.33 to -1.93 | Ave (n = 18) = -2.61 |
| Diss. Sulphide | Pyrrhotite | -5.25 | S Gabbro / 96-36 | BG, mg (36-112) |
| Diss. Sulphide | Pyrrhotite | -1.99 | S Gabbro / 96-36 | BG, mg (36-113) |
| Sulphide band | Pyrrhotite | -2.51 | S Gabbro / 96-34 | BG, cg (34-100) |
| Diss/blotch sulphide | Pyrrhotite | -3.54/-3.92* | S Gabbro / 97-79 | BG, mg (79-141) |
| Sulphide blotch | Pyrrhotite | -2.56 | S Gabbro / 97-79 | BG, cg (79-147) |
| Diss. Sulphide | Pyrrhotite | -2.12 | S Gabbro / 97-79 | BG, cg (79-146) |
| South Gabbro | | Range | -5.25 to -1.99 | Ave (n = 7) = -3.13 |
| Diss. Sulphide | Pyrrhotite | -1.33/-1.32* | N Gabbro / 98-136 | CP gneiss, mg (98-136) |
| Diss. Sulphide | Pyrrhotite | -4.78 | N Gabbro / 97-96 | CP gneiss, mg (97-96) |
| Diss. Sulphide | Pyrrhotite | -2.85 | N Gabbro / 97-58 | CP gneiss, mg (58-55) |
| Diss. Sulphide | Pyrrhotite | -4.91 | S Gabbro / 96-47 | CP gneiss, fg (47-106) |
| Churchill Province gneiss | | Range | -4.91 to -1.32 | Ave (n = 5) = -3.04 |
| Diss. Sulphide | Pyrrhotite | -0.99 | N Gabbro / 97-92 | Anorthosite, cg (92-12) |
| Diss. Sulphide | Pyrrhotite | -2.51 | N Gabbro / 97-92 | Anorthosite, cg (92-12) |
| Diss. Sulphide | Pyrrhotite | -6.43 | N Gabbro / 97-92 | Anorthosite, cg (92-8) |
| Diss. Sulphide | Pyrrhotite | -5.95 | N Gabbro / 97-92 | Anorthosite, fg (92-8) |
| Diss. Sulphide | Pyrrhotite | -4.29 | N Gabbro / 97-92 | Anorthosite, cg (92-11) |
| Anorthosite | | Range | -6.43 to -0.99 | Ave (n = 5) = -4.03 |

B.4.2 Sulphur Isotope Analysis – Precision and Accuracy

Ten replicate analyses were performed on the standards NBS-123 (ZnS) and MUN-PY (FeS₂) over the period of January to March 1999. The known value for the standard, NBS-123 is reported by the National Institute of Standards and Technology, whereas MUN-PY is a Memorial University internal standard. Precision and accuracy of the two standards over this period is reported in Table B.4.1.

Table B.4.1 Precision and accuracy for standards NBS-123 and MUN-PY calculated from 10 measurements over the period of January to March 1999.

| Sulphur Isotope Standard | Average Value (‰) (n = 10) | RSD (%) or Precision ¹ | Known value (‰) (NIST, MUN) | % RD ³ or Accuracy ² |
|---------------------------------|----------------------------|-----------------------------------|-----------------------------|--|
| $\delta^{34}\text{S}$ (NBS-123) | +17.17 | 0.030 | +17.09 | 0.47 |
| $\delta^{34}\text{S}$ (MUN-PY) | +1.27 | 0.34 | +1.26 | 0.79 |

¹The RSD % (relative standard deviation) is the standard deviation divided by the average of 10 measurements. ²The % RD is the relative difference relative to the known value calculated by: [(average determination - known value) / (known value)] x 100%.

Appendix C: Logs of Diamond Drill holes used in Study

Diamond Drill Log
Hole No. SVB-96-02

| Interval (meters) | Description |
|-------------------|--|
| 0.0-2.6 | Overburden |
| 2.6-13.7 | Fine-grained olivine gabbro: Light greenish-grey, olivine concentration variable (10-15 %), locally 20-25 % olivine. Transition Gabbro appearance near top of interval as small, 20-40 cm isolated intervals. Pyroxene and sulphide concentration increases down hole. Sulphides occur as rounded to sub-rounded blotches with minor disseminations. Blotchy sulphides appear to be concentrated with the medium-grained bands. |
| 13.7-25.9 | Fine-grained olivine gabbro (weak leopard texture): Dark grey with a faint olivine green color, distinct leopard texture with rounded (0.7-1.0 cm) pyroxenes in a matrix of interstitial sulphides and fine-grained olivine. Gneiss fragments are common where olivine content increases and the leopard texture weakens. Net texture develops with concentrated gneiss fragments. Small isolated zone of fine-grained olivine and pyroxene (width ~7 cm) intermixed with leopard texture. Sulphides blotches present as well, dissipates towards the lower contact. |
| 25.9-54.3 | Fine-grained olivine gabbro: Dark olive-grey, similar to interval 2.6-13.7. Abundant gneiss inclusions (partially digested), 4-5 %, locally 10 % inclusions. Sulphides have a blotchy texture. |
| 54.3-60.7 | Paragneiss: Typical medium-grained gneiss, minor garnet concentrations, garnet altered to green color and rimmed with feldspar. |
| 60.7-86.9 | Fine-grained olivine gabbro: Typical fine-grained olivine gabbro, possible large anhealed fault zone, with carbonate and pyrrhotite in fracture. |
| 86.9-91.0 | Paragneiss: Leucocratic, medium to coarse-grained, moderately foliated, graphite and pyrrhotite in narrow bands. Upper contact is gradational (over 40 cm). Chalcopyrite blotches present. |
| 91.0-94.5 | Fine-grained mafic dike (olivine gabbro?): Chilled margin, sharp contact, coarsens in center. Minor gneiss inclusions present in center of dike. |

Diamond Drill Log
Hole No. SVB-96-04

| Interval (meters) | Description |
|-------------------|--|
| 0.0-1.5 | Overburden |
| 1.5-24.1 | Coarse to medium-grained olivine gabbro: Melanocratic, olivine rich (10-15%), cumulate texture. Plagioclase grains (seriate/bladed) define cumulate texture, granular to fine-grained olivine grains. Pyroxene present where plagioclase grains appear very coarse-grained (1 cm). Narrow intervals (~4-6 cm) of olivine-rich core. Towards lower contact, the olivine content increases substantially, such that the plagioclase grains are isolated. This transition is over an interval of 1.5 m. Grain size decreases as well. Magnetite is present in trace amounts. |
| 24.1-34.2 | Fine-grained olivine gabbro: Melanocratic (greenish tint), fine grained. Consist of olivine and pyroxene with larger plagioclase lathes (>0.5cm) although not abundant. Fine-grained olivine abundance increases to 15-20 %, pyroxene may be slightly poikilotic, olivine increase locally, plagioclase also increases locally. |
| 34.2-54.4 | Transition gabbro: Forest green color, high concentrations of olivine with partially digested gneiss fragments. Sulphide content variable. 1-2% po and exsolved chalcopyrite. Generally occurs as large blotches (clots) with intergrowths of plagioclase (associated with medium-grained bands). Disseminated sulphide associated with fine-grained olivine gabbro without the transition gabbro texture. Sulphides are rounded where magnetite is present. Overall, core has a fragmental appearance defined by medium-grained bands of plagioclase and pyroxene and fine-grained olivine. Transition gabbro texture is not consistent. Ilmenite/magnetite may be present. |
| 54.4-64.2 | Fine-grained olivine gabbro: Fine-grained, purple-green, pyroxene content increases locally, poikilotic texture, small olivine rich intervals (1-2 cm), few well-digested gneiss fragments present, large blotches of sulphide (1-2%), generally pyrrhotite rich with exsolutions of chalcopyrite. Contact with upper interval relatively sharp. Lower contact is also well defined. |
| 64.2-103.6 (EOH) | Graphitic/garnetiferous paragneiss: Dark grey, medium grained, local pyrrhotite and graphite, moderately foliated. |

Diamond Drill Log
Hole No. SVB-96-07

| Interval (meters) | Description |
|-------------------|--|
| 0.0-2.3 | Overburden |
| 2.3-29.7 | Coarse-grained gabbro: Grey-green, granular olivines, seriate textured plagioclase, weak porphyritic texture. Small local intervals of pegmatite (4-10 cm). Lower contact is sharp. |
| 29.7-35.5 | Transition gabbro: 30-40% leucocratic bands, 2-3% sulphides, sulphides are blotchy with intergrowths of plagioclase, minor chalcopyrite, possibly magnetite. Texture dissipates towards lower contact. |
| 35.5-39.5 | Gabbro hybrid: Purple to dark green, fine-grained, poikilitic texture, small intervals that are more leucocratic, sulphides are blotchy. Lower contact was not observed (lost core). Well digested inclusions present. |
| 39.5-54.9 | Paragneiss |
| 54.9-70.6 (EOH) | Orthogneiss |

Diamond Drill Log
Hole No. SVB-96-08

| Interval (meters) | Description |
|-------------------|--|
| 0.0-2.3 | Overburden |
| 2.3-11.9 | Coarse-grained gabbro: Megacrystic, coarse-grained gabbro with cumulate, seriate plagioclase, and intercumulate pyroxene and olivines. Pyroxenes exhibit a poikilolitic/granular habit within small (20-30 cm), local intervals whereby the plagioclase grain size increases. Bottom contact is probably fault bounded. |
| 11.9-19.2 | Gneiss breccia: Typically melanocratic with injections of thin (4-5 cm) medium-grained felsic dikes. Fragmental appearance. Composition, color, and texture is heterogeneous. Small blotches of pyrrhotite located throughout core. One gneiss inclusion has a thin veinlet of pyrrhotite. Lower contact is sharp, possible fault (altered gabbro adjacent to contact). |
| 19.2-25.0 | Altered coarse-grained gabbro: Melanocratic, green to grey-green, coarse-grained plagioclase cumulate with intercumulate pyroxene. Unable to determine olivine percentage (serpentinization). Plagioclase grains have a light green color. Lower contact is relatively sharp. |
| 25.0-27.5 | Transition gabbro: Melanocratic, fine-grained olivine gabbro with 5-10 % leucocratic bands. Minor (> 1%) small blotches of pyrrhotite. Sharp lower contact. |
| 27.5-33.4 | Gneiss breccia: Leucocratic to melanocratic, injections of felsic dikes intermittent, host large clast (max 5 cm). Other local intervals with fine-grained greenish matrix with numerous fragments. Minor sulphide (fragments) >0.5 %. 2-3% quartz veins ~ 10 cm wide. At lower interval (31.9-33.4 m) sulphide content increases dramatically, 25-25% locally, intermixed with either felsic dikes or leucocratic medium-grained gneiss. Semi-massive sulphide intervals locally. Sulphides appear fragmental even though they are unseparated. Minor graphite. Lower contact is quite diffuse. |
| 33.4-44.0 (EOH) | Paragneiss: Leucocratic, coarse-grained paragneiss with large (1-2 cm) retrograde garnets (rounded, with dark green rims). Weakly to moderately foliated. Minor quartz veins present. |

Diamond Drill Log
Hole No. SVB-96-09

| Interval (meters) | Description |
|-------------------|--|
| 0.0-3.5 | Overburden |
| 3.5-51.2 | Coarse-grained olivine gabbro: Typical coarse-grained gabbro with plagioclase grains up to 1 cm. Cumulate textured, pyroxene and olivine are intercumulate. 2-3 % olivine, 10-15 % pyroxene. Local sections of core are pegmatite with very coarse-grained pyroxenes (2-5 cm). |
| 51.2-62.9 | Transition gabbro: Typical transition gabbro texture adjacent to the upper contact. The texture that defines this unit dissipates towards the bottom contact. Gneiss inclusions are rare, but present. Minor disseminated and blotchy sulphides present (>5%). |
| 62.9-66.7 | Fine-grained olivine gabbro: Dark greyish-green, typically fine grained. 20-25 % fine-grained granular olivines. Minor disseminated sulphides. |
| 66.7-68.4 | Fine-grained olivine gabbro (with leopard textured): Small interval of fine-grained olivine gabbro defined by a faint to well-pronounced leopard texture. 15-20 % disseminated sulphides. |
| 68.4-85.2 | Fine-grained olivine gabbro: Dark greyish-green, fine-grained, olivine gabbro. Minor to trace disseminated sulphides. Minor small partially digested gneiss inclusions. Lower contact is gradational (over 20-30 cm). |
| 85.2-143.1 (EOH) | Paragneiss: Typical basement paragneiss. Small intervals of mafic dikes present. |

Diamond Drill Log
Hole No. SVB-96-10

| Interval (meters) | Description |
|-------------------|--|
| 0.0-1.5 | Overburden |
| 1.5-9.8 | <p>Coarse-grained gabbro: Coarse-grained plagioclase, cumulate grains are cloudy white displaying a seriate texture. Intercumulate olivines and pyroxenes. At 7.7 to 8.2 m the core has a transition gabbro texture with 20-30 % thin leucocratic bands. Diffuse contact between transition gabbro interval. The lower contact is sharp.</p> |
| 9.8-28.8 | <p>Transition gabbro: Typically melanocratic and very fine-grained. Abundance of fragments/inclusions near the upper contact, dissipates gradually towards lower contact. Inclusion rich zone, closely packed, small, rounded to angular, black interior, thin white rims (30-40 % inclusions). Matrix consist of fine-grained olivine gabbro. This closely packed network of inclusions decrease and inclusions are spatially separated, fragments have irregular boundaries (subrounded to rounded). These inclusions decrease in abundance towards lower interval to 3-5 %. Sulphides occur as irregular, intergrown clots of pyrrhotite. Sulphide clots are up to 2 cm (1 cm average). Minor disseminated sulphides present as well. Matrix increases towards bottom consisting of melanocratic, dark green, fine-grained olivine gabbro. Fragments are weakly orientated perpendicular to the core axis.</p> |
| 28.8-35.6 | <p>Fine-grained olivine gabbro: Dark greenish-grey, fine-grained to aphanitic, fairly homogeneous (texturally and compositionally) with exception to the presence of sulphides and inclusions. Gradual upper contact (both units blend into each other). Lower contact is gradual over 10-15 cm. Gneissic fragments are partially digested with melanocratic core, leucocratic rim, between 1-3 cm, isolated and constitute 3-5 % of interval. These inclusions are slightly aligned to the core axis. Sulphides are also sparse, consisting of pyrrhotite rich blotches (typically >1 cm), some clots are subrounded. Minor disseminated sulphides are also present. Sulphide content is less than 1 %.</p> |
| 35.6-51.2 (EOH) | <p>Paragneiss: Top two meters are altered, although not beyond recognition of the original texture. Generally leucocratic, coarse-grained. Garnets are retrogressed. Sulphides are frequent, occurs as small (1-2 cm), semi-massive bands or between/surrounding grains. Core is weakly foliated. Small (60-70 cm) interval of melanocratic gneiss with 2 cm massive sulphide band.</p> |

Diamond Drill Log
Hole No. SVB-96-15

| Interval (meters) | Description |
|-------------------|--|
| 0.0-1.5 | Overburden |
| 1.5-57.8 | Medium to coarse-grained gabbro: Melanocratic, cumulate textured with interstitial olivines and pyroxenes, slightly poikilitic. Top 18 meters (approximately), the core has a lighter color defined by coarse-grained plagioclase (seriate textured). The remainder of the interval has a darker appearance, medium grain size. Core is moderately fractured with alteration around the fracture margins (chlorite/serpentine and quartz veins). |
| 57.8-75.1 | Transition gabbro: Typical texture, leucocratic, medium to coarse-grained bands constitute 20-25 % of interval. Bands are not perpendicular to core axis. A few small (>1 cm) sulphide blotches are present. Gradational lower contact. |
| 75.1-81.4 | Gabbro hybrid (with leopard texture): Melanocratic (dark violet, black, grey-green), fine-grained to aphanitic. Minor leucocratic inclusions, concentrated near the top of the interval (first 50 cm's). This blends into a darker green, fine-grained composition. Faint leopard texture within center (50-60 cm). Shows oikocryst of pyroxene with interstitial sulphides and granular olivines. Sulphide content increases 10-15 %, one large clot and net-textured in leopard texture interval. This texture dissipates into a poikilitic texture. Slight increase in plagioclase content, however the interval remains the same color. The majority of sulphides occurs within the center of the upper interval. 2-3 % large clots. Lower interval contains ~ 1% disseminated sulphides. Lower contact is gradational. |
| 81.1-91.9 | Gneissic breccia: Upper interval (81.4-84.4 m); melanocratic, fine to medium-grained, greenish-black, prismatic plagioclase grains intergrown with sulphide clots. Patchy appearance in places, 1-2 % sulphides. Minor quartz veining. Sulphides have a range of textures containing intergrowths. The lower portion of this interval is melanocratic (possible fault zone?). Appears similar to a cement with a fine-grained greenish matrix, numerous heterogeneous fragments. Most fragments are less than 1 cm. Sulphides occur as small, irregular clots within the matrix. Sharp lower contact. Lower interval (84.4-91.9 m); The upper meter has a breccia appearance, not as well defined. Intrusions of leucocratic injections (10-15 %). Within lower interval, fragments are large (between 2-30 cm), angular to slightly "melted" edges, black, fine-grained, moderately foliated, increase in graphite and pyrrhotite. These fragments constitute 85-90 % of the interval. Matrix appears to be silicious (gneissic derivative ?), coarse to medium-grained, white to slightly-pinkish tan. Lacks clots of pyrrhotite or any substantial amount of sulphides. The lower meter of this interval, the breccia texture dissipates. |

Diamond Drill Log
Hole No. SVB-96-15 (continued)

| Interval (meters) | Description |
|--------------------------|---|
| 91.9-96.8 | Graphitic gneiss: Melanocratic, aphanitic, totally engulfed with graphite and pyrrhotite (hardly recognizes the upper or lower contact). Interval is extensively crenulated, original metamorphic texture is non-existent. Graphite content dissipates towards lower contact. |
| 96.8-118.9 (EOH) | Paragneiss: Typical paragneiss, minor graphitic content, minor retrograde garnets, typically melanocratic and coarse-grained. Texture begins to increase near end of hole. Minor pyrrhotite present. |

Diamond Drill Log
Hole No. SVB-96-16

| Interval (meters) | Description |
|-------------------|---|
| 0.0-1.2 | Overburden |
| 1.2-28.9 | Coarse-grained gabbro: Coarse-grained cumulate gabbro with seriate textured plagioclase and intercumulate pyroxenes. Random small (20-40 cm) intervals of megacrystic gabbro and medium-grained gabbro. Lower contact is quite diffuse, gradual decrease in grain size. |
| 28.9-72.2 (EOH) | Medium-grained gabbro: Homogeneous texture and appearance, generally melnoacratic, cumulate texture, olivine content increases locally by 5 %. Pyroxene and olivine have a granular texture where present. Local megacrystic intervals present, similar to megacryst in above unit. No visible sulphides. |

Diamond Drill Log
Hole No. SVB-96-17

| Interval (meters) | Description |
|-------------------|--|
| 0.0-1.5 | Overburden |
| 1.5-22.6 | <p>Coarse-grained gabbro: Coarse-grained gabbro (appears to be an equal amount of leucocratic and melanocratic grains). Seriate textured cloudy white plagioclase, poikilitic to cumulate textured. Intercumulate olivines and pyroxenes (green to deep purple), spotted appearance defined by poikilitic texture. Numerous small (10-15 cm) intervals of megacryst consisting of large, bladed grains of plagioclase with large interstitial pyroxenes. Minor magnetite present. Lower contact is gradational.</p> |
| 22.6-23.8 | <p>Fine-grained olivine gabbro: Typical melanocratic fine-grained olivine gabbro. Olivine content is ~ 15-20 %, other mineral abundances include 50-60 % plagioclase, the remainder being pyroxene. Interval has a cumulate texture, equigranular grains. Barren of visible sulphides. Lower contact is gradational.</p> |
| 23.8-25.9 | <p>Transition gabbro: Typical texture defined by thin, leucocratic bands (50 % of interval). Bands range in thickness, generally 1-3 cm. Larger bands have are very coarse grained. Sulphide content is quite low (trace), lower contact is gradational over 20 cm.</p> |
| 25.9-33.0 | <p>Gabbro hybrid: This interval is quite heterogeneous. In many aspects, this interval represent the typical transition gabbro, in other cases, the interval represents a breccia of some sort. The top portion of this interval (25.9-32.1 m) has an overall melanocratic appearance (dark green to black) and generally fine grained (aphanitic). The top 50 cm is cumulate, coarse-grained plagioclase and intercumulate pyroxene that grades into a medium-grained gabbro. This gives way to the aphanatic, melanocratic appearance which is consistent to the lower contact. Between 27.3-27.8 m the interval appears to host two differing gneissic inclusions. Towards the lower contact, the interval has a fragmental appearance containing quartz-feldspar and small clots of pyrrhotite. Graphite is also present as small isolated specks or as small, rounded clusters. The remainder of the interval is fairly homogeneous, consistent matrix color and composition. Sulphide content ranges from 2-5 cm, consist of pyrrhotite with minor chalcopyrite. The sulphides have a different appearance, that is, the sulphides are rounded or fragmental. Minor disseminated sulphides. The lower contact is quite diffuse.</p> |
| 33.0-37.5 | Core interval missing |
| 37.5-50.3 | <p>Graphitic paragneiss (altered): Melanocratic to leucocratic, coarse to fine grained, relict metamorphic textures and composition preserved. Abundant graphite along foliation planes constituting 10-15 %. Thin veinlets of quartz is present. Minor pyrrhotite. Diffuse upper and lower contacts.</p> |
| 50.3-63.1 (EOH) | <p>Garnetiferous paragneiss: Medium to coarse-grained, leucocratic, moderately foliated, greenish retrograde rounded garnets are quite common (10%). Trace graphite and pyrrhotite present.</p> |

Diamond Drill Log
Hole No. SVB-96-20

| Interval (meters) | Description |
|-------------------|---|
| 0.0-3.0 | Overburden |
| 3.0-29.3 | Coarse-grained gabbro: Dark greenish-grey with cumulate seriate, subhedral plagioclase grains and intercumulate pyroxene and olivine. Small pegmatite intervals common as well as small local intervals with a poikilitic texture. Lower portion of core has a darker appearance near the lower contact. Decrease in grain size noted as well. The lower contact is sharp. |
| 29.3-36.1 | Transition gabbro: Typical texture with 15-20 % medium-grained, leucocratic bands. Sulphide blotches constitute > 1 % of interval. Sulphide blotches contain pyrrhotite with minor chalcopyrite. Blotches are associated with the leucocratic bands. Lower contact is quite diffuse, over an interval of 30-40 cm. |
| 36.1-37.8 | Gabbro hybrid: Greenish-purple (melanocratic), 5 % recognizable inclusions, interval has a weak poikilitic texture. 2-3 % sulphide blotches occurring as small irregular blotches and minor disseminated sulphide, lower contact appears fractured (?). |
| 37.8-39.4 | Orthogneiss with semi-massive sulphide: Upper contact appears sharp, fragmented appearance. This interval has a brecciated appearance, weak gneiss texture. Abundance of brecciated and cemented appearance. Semi-massive intervals (very short, 2-3 cm) throughout interval. 15 % sulphide, mostly pyrrhotite. Minor sulphide clasts (?). Sulphide fragments are typically small, well defined boundaries. Bottom contact is quite diffuse since most of the sulphide is associated with the gneissic breccia. |
| 39.4-46.3 (EOH) | Orthogneiss: Leucocratic, coarse-grained, contains quartz-feldspar, minor concentration of sulphides near upper contact. |

Diamond Drill Log
Hole No. SVB-96-27

| Interval (meters) | Description |
|-------------------|---|
| 0.0-1.1 | Overburden |
| 1.1-6.5 | Coarse-grained gabbro: Coarse-grained (partially leucocratic) gabbro with plagioclase content as high as 60 %. Local 5 cm wide pegmatites intervals defined by coarse-grained pyroxene and 1-2 cm plagioclase grains. Lower contact is gradational to non-distinct. The invasion of fine-grained olivine throughout the lower contact zone gives the core an olivine gabbro appearance (late phase?). |
| 6.5-13.3 | Medium-grained gabbro: Greenish color, olivine and pyroxene content variable. Olivine as high as 15-20 % locally. |
| 13.3-24.1 | Transition gabbro: Fine to medium-grained gabbro defined by thin medium grained bands injected in a fine-grained olivine gabbro matrix. 3-5 % partially digested gneiss inclusions. 1-2 % disseminated and blotchy sulphides, generally associated with inclusions. |
| 24.1-25.2 | Fine-grained olivine gabbro (leopard texture): Typical fine-grained olivine gabbro with a faint leopard textured sulphide (>5% sulphide). |
| 25.2-39.1 | Melanocratic fine-grained olivine gabbro: Dark, fine-grained olivine gabbro with partially digested gneiss inclusions and 1 % blotchy sulphides. Olivine concentration variable and patchy (not as abundant as in the upper intervals). The lower contact is very fine-grained (possible chill margin). |
| 39.1-82.3 (EOH) | Garnetiferous paragneiss: Typical paragneiss. Medium-grained, moderately to well foliated. Small, isolated occurrences of mafic dikes. Trace pyrrhotite, often associated with graphite. |

Diamond Drill Log
Hole No. SVB-96-29

| Interval (meters) | Description |
|-------------------|--|
| 0.0-0.6 | Overburden |
| 0.6-29.0 | <p>Coarse-grained gabbro: Typical coarse-grained gabbro with cumulate, euhedral to subhedral, seriate textured plagioclase with interstitial pyroxenes and olivines. Olivines have a local granular texture. Throughout the core interval there are local variations in grain size (ie. megacrystic defined by very coarse-grained, euhedral plagioclase and intercumulate pyroxene to a medium-grained gabbro). Towards the lower contact, beginning at 25.0 m, the core becomes darker due to decrease in grain size and abundance of plagioclase. The section of the interval becomes very coarse-grained and has a local "patchy" appearance. The lower contact is sharp.</p> |
| 29.0-33.6 | <p>Medium-grained olivine gabbro: Medium-grained, melanocratic with white cumulate plagioclase and interstitial/granular olivines and pyroxenes. (salt-n-pepper appearance). Completely homogeneous, with little change in grain size or modal abundance.</p> |
| 33.6-34.4 | <p>Transition gabbro: Typical texture with 30-50 % leucocratic bands. The leucocratic bands appear similar to the medium-grained gabbro above. Distinct, sharp upper contact, diffuse lower contact (over 20-30 cm).</p> |
| 34.4-37.5 | <p>Gabbro hybrid: Dark green to purple, fine-grained (aphanitic), heterogeneous, numerous partially, small leucocratic fragments (inclusions), rounded to angular. Inclusions do not appear to be the same composition. Small local interval (inclusion?) (20-30 cm) defined as a leucocratic, coarse-grained, serpentized, white, medium to coarse-grained plagioclase, minor graphite associated with it. Sulphides occur as medium-grained disseminations and as small to large blotches (>1 to 3 cm). Sulphide content over interval ~ 3%. Both the upper and lower contact are diffuse.</p> |
| 37.5-40.9 | <p>Gabbro hybrid (non-typical): Blotchy appearance, dramatic increase in leucocratic minerals (plagioclase?), granular olivines/pyroxenes, appear to have been reworked (original texture obsolete), sections of interval are light to dark-green, slightly purple (serpentinization and chloritization common). Minor small blotches with minor disseminated sulphide dispersed throughout interval. Sulphides consist of pyrrhotite (1-2%). Gradational upper contact (over 10-15 cm), diffuse lower contact. Local fragmental intervals.</p> |
| 40.9-45.6 | <p>Gabbro hybrid: Upper meter is a fine-grained, greenish-purple (aphanitic), blotchy to poikilitic texture. Contains 2-4 % pyrrhotite blotches with trace chalcopyrite. Minor disseminated sulphides. Small interval (2 cm) of pyrrhotite with sharp contacts. From 41.8-42.8, sulphide content increases, transition gabbro appears faint to non-existent. Quite altered, large fragments of sulphide, wispy sulphides, disseminated (associated with graphite), small leucocratic medium-grained interval (10 cm), sulphides may get as high as semi-massive.</p> |

Diamond Drill Log
Hole No. SVB-96-29 (continued)

| Interval (meters) | Description |
|-------------------|---|
| 40.9-45.6 | <p>Gabbro hybrid (continued): At 42.8-43.5, greyish interval of brecciated gneiss (?), blitzed with cloudy white quartz (possible fault zone?), fine-grained greyish green matrix, small phenocryst of quartz or feldspar. Below this interval, towards the lower contact, the sulphide content decreases. Unit has a darker appearance, sulphides occur as wisps (thin veinlets) although not common, small (>1 cm) irregular blotches and disseminations. The lower contact is very diffuse, unable to determine the precise contact.</p> |
| 45.6-49.7 | <p>Paragneiss (altered): Greyish-green appearance, alteration quite pervasive, numerous thin discordant quartz veins, minor sericite alteration. Minor biotite present. Faint metamorphic texture preserved. Pyrite and pyrrhotite present in fractures. Diffuse upper and lower contacts. Whole interval could possibly be a fault zone (?).</p> |
| 49.7-76.2 (EOH) | <p>Leucocratic garnetiferous paragneiss: Coarse-grained paragneiss with 5 % retrograde greenish garnets. Core appears blitzed with quartz, local melanocratic intervals. Minor pyrrhotite and graphite present.</p> |

Diamond Drill Log
Hole No. SVB-96-34

| Interval (meters) | Description |
|-------------------|--|
| 0.0–2.1 | Overburden |
| 2.1–26.3 | <p>Coarse-grained leucocratic gabbro: Interval has a variety of plagioclase textures and grain sizes. Plagioclase grains range from 0.5 to 3 cm (seriate textured) and sometimes forms a cumulate or poikilitic texture. Near the top portion of this interval, bladed plagioclase grains are more prominent with interstitial pyroxenes and olivines. The general texture is poikilitic whereby poikilitic plagioclase contains interstitial, very fine-grained pyroxene or olivine. There are a few minor intervals of megacryst ranging from 5 to 15 cm in thickness composed of very large plagioclase and pyroxene, +/- ilmenite or magnetite. The lower contact is gradational.</p> |
| 26.3–27.5 | <p>Transition gabbro: Upper 50 cm, not as well defined. Interval is melanocratic, fine-grained olivine gabbro which grades into the typical texture. Sulphide content increases to 2-3 % in this interval. Sulphides are large clots with irregular boundaries marked by intergrowths of plagioclase.</p> |
| 27.5–41.1 | <p>Melanocratic fine-grained olivine gabbro: Dark, fine-grained to aphanitic with coarse, blotchy grains of pyrrhotite and minor gneissic inclusions. Inclusions are sparse, randomly orientated, typically melanocratic with thin, white rims. Inclusions range in size (>1 cm to 4 cm). The degree of digestion is also variable. Sulphides generally occur as large clots with sharp well-defined boundaries as well as blotches with irregular boundaries. Both range in size (>1 to 3 cm, lengthwise). Minor disseminated sulphides also occur randomly throughout interval. Lower contact appears abrupt. Graphite content is noticeable at the contact (up to 5 %).</p> |
| 41.1–48.8 (EOH) | <p>Quartzofeldspathic paragneiss: Typically leucocratic, coarse-grained, weakly to moderately foliated. Appears altered throughout interval. Quite graphitic (up to 10 % locally). Pyrrhotite is also present (up to 5 % locally).</p> |

Diamond Drill Log
Hole No. SVB-96-36

| Interval (meters) | Description |
|-------------------|--|
| 0.0-1.2 | Overburden |
| 1.2-87.1 | <p>Coarse-grained gabbro: Typically light greyish-green, coarse-grained, cumulate to poikilolitic textures and apparently altered. From 1.2 to 19.6 m, interval is light greyish white defined by seriate white subhedral plagioclase matrix supporting altered greenish (pyroxene?) rimmed phenocryst. Phenocryst are slightly rounded, typically with a light green center and darker green rim which grades into a plagioclase groundmass. Very large grained isolated plagioclase phenocryst are present as well. This texture dissipates into a darker green unit (from 19.6 to 36.6m) which appears altered (chloritized/serpentinized). The rock texture and composition is difficult to determine. Interval has a blotchy appearance locally. Between 36.6 to 45.0 m, the interval has a sub-ophitic texture defined by cloudy white plagioclase grains with interstitial fine to medium-grained pyroxene and/or olivine. The lower contact is gradational. From 45.0 to 48.0 the interval is similar to the interval between 19.6 to 36.6 m. From 48.0 to 78.2, the interval has a light grey to dark green, coarse to medium-grained cumulate to sub-ophitic texture defined by cloudy white seriate textured plagioclase and intercumulate pyroxene. This interval varies locally from coarse to medium-grained. Small (10-15 cm) intervals of megacryst are frequent. The lower contact of this interval is relatively sharp. This portion of the interval gives way to an interval similar to 1.2 to 19.6 m. The bottom of this interval (83.8 to 87.1 m) the interval is medium to fine-grained gabbro.</p> |
| 87.1-100.9 | <p>Medium-grained gabbro (olivine gabbro): Melanocratic, medium grained, possibly slightly chloritized, equigranular, trace pyrrhotite is present, minor partially digested leucocratic inclusions present as well (~5%).</p> |
| 100.9-149.2 (EOH) | <p>Melanocratic fine-grained olivine gabbro: This interval is noted by the increase in inclusions as well as the increase in the sulphide content. At the top of the interval, inclusions are more prominent (10 to 15 %), although generally isolated. Sulphide content increase locally. Within the center of the unit, sulphide content is predominant (113 to 127 meter interval), generally disseminated, minor net-textured gabbro observed. Sulphide content decreases past the 127 meters. After 127 m, the interval remains very fine-grained, equigranular with minor clots of sulphide present. Towards the EOH, grain size appears to increase slightly, a few minor fragments are present.</p> |

Diamond Drill Log
Hole No. SVB-96-44

| Interval (meters) | Description |
|-------------------|---|
| 0.0-3.0 | Overburden |
| 3.0-25.2 | Coarse-grained gabbro: Seriately textured, cloudy-white, euhedral to subhedral plagioclase grains. Fine-grained intercumulate pyroxene with minor olivine (2-5%). Local small (5-8 cm) intervals of pegmatite defined by very coarse-grained (1-1.5 cm) plagioclase grains, granular (?) pyroxenes and minor magnetite grains. ~ 3 m above lower contact, the core is medium to fine-grained with an increased olivine content (10-15 %). Lower contact is fairly abrupt, noted by decrease in grain size and olivine content increase. |
| 25.2-27.6 | Transition gabbro: Melanocratic, fine-grained olivine gabbro displaying the typical texture. 20-25 % thin, medium-grained gabbroic bands. 2-3 % sulphides, blotches and disseminations distributed throughout the core interval. Sulphide blotches are associated with the medium-grained bands. |
| 27.6-39.9 | Melanocratic fine-grained olivine gabbro: Dark grey, very fine-grained, > 5% digested gneissic inclusions ranging in size (> 1-2 cm). 2-3 % disseminated sulphides, with 2-3 % larger (0.5-1 cm) sulphide blotches. The upper contact is diffuse and non-distinct. The lower contact is relatively abrupt, however, near the last 20-30 cm of interval, the dark color dissipates due to an overall increase in plagioclase. |
| 39.9-47.5 (EOH) | Quartz-feldspathic orthogneiss: Leucocratic, coarse-grained, granular texture of anhedral plagioclase and altered pyroxene grains. Weakly to moderately foliated. Small blebs of chalcopyrite near contact. Mafic dike located at 40.5-41.1 m. Dike has chilled margins, medium-grained in center. Large digested gneiss inclusions present in dike. |

Diamond Drill Log
Hole No. SVB-96-47

| Interval (meters) | Description |
|-------------------|---|
| 0.00 – 4.6 | Overburden |
| 4.6-7.6 | Olivine gabbro (olivine gabbro): Melanocratic (dark green), contains variable amounts of leucocratic inclusions (approximately 20 – 25 %). Inclusions appear coarse-grained with dark interior minerals and white rims (transition gabbro). Inclusions are not well-defined because of the blotchy appearance. Matrix is fine-grained, dark green, olivine gabbro. Sulphides are not common, few clots of pyrrhotite are present. The lower contact is gradational. |
| 7.6-14.3 | Medium to coarse-grained gabbro: Typically melanocratic with variable amounts of sulphide. Upper contact is fine-grained and contains numerous, small (0.5 to 1 cm) amygdules of carbonate (?) confined to a zone over 40 – 50 cm. Below 8.3 m, the grain size increases to medium or coarse-grained with a cumulate textured plagioclase and interstitial olivine and pyroxenes. Slight greenish color (alteration; slight quartz/carbonate veining throughout interval. Sulphides occur as small irregular clots of pyrrhotite with small amounts of chalcopyrite. Sulphides occur in upper 2/3 of interval and dissipates towards the lower contact. The lower contact is noted by the gradational decrease in grain size. |
| 14.3-54.0 | Melanocratic fine-grained olivine gabbro: Dark green to dark grey, fine-grained to aphanatic. Generally barren of sulphides except in small, local (60–80 cm) intervals. Sulphides are generally disseminated with a few small clots present as well. Towards the lower contact, sulphide content increases to approximately 1-2%, unit is consistently aphanatic over 3-4 m with a few sulphide clots present. Lower contact is slightly altered, few veins are present (quartz?), graphite is present. The lower contact is quite sharp. |
| 54.0-57.0 | Graphitic gneiss: Melanocratic, generally fine-grained, well foliated. Graphite content as high as 15 % locally. Pyrrhotite present as well. Graphite and pyrrhotite present along foliation planes. Graphite content decreases towards lower contact. |
| 57.0-67.1 (EOH) | Paragneiss: Leucocratic to melanocratic, well foliated. Melanocratic layers contain graphite. Small interval of semi-massive sulphide (30 cm) presents at ~58.5 m. Semi-massive sulphide interval has a melted appearance. |

Diamond Drill Log
Hole No. SVB-96-48

| Interval (meters) | Description |
|-------------------|---|
| 0.00 – 3.0 | Overburden |
| 3.0 – 24.5 | Coarse-grained leucocratic gabbro: Cumulate textured with seriate textured plagioclase and interstitial olivine and pyroxene. Plagioclase grains are cloudy white, bladed and randomly orientated (range in size ~ 0.5 to 1 cm lengthwise). Olivine and pyroxenes grains are of equal abundance ~ 15 % total. 1 to 2 small intervals (20 cm) of megacrystic gabbro are present. |
| 24.5 – 29.1 | Transition gabbro: Typical texture consisting of 60 to 70 % mg bands in a finer-grained olivine gabbro matrix. Numerous sulphide clots are common ranging in size (>1 cm to 3 cm) and abundance (1 to 3 %). Sulphide clots have an irregular boundary with plagioclase intergrowths along the sulphide clot boundary. Chalcopyrite commonly located along the periphery of the sulphide clot. Minor, fine grained disseminated sulphide present as well. The upper contact is gradational over 20 cm while the lower contact is abrupt. |
| 29.1 – 30.1 | Aphanitic dike / fragment (?): Black to very dark green, very fine-grained with 3 to 4 small (3-4 cm) leucocratic inclusions (gneissic?). Small sulphide clots are dispersed throughout the interval. Sharp lower and upper contacts. |
| 30.1 – 40.2 | Gabbro hybrid: Melanocratic, fine-grained, possibly olivine gabbro. Abundance of inclusions (20 % +). Upper contact is sharp, lower contact is marked by an alter gabbro. Gneissic fragments are generally more digested, scarce (randomly orientated). Small local zones consisting of 20 to 30 % inclusions over a 50 to 60 cm interval are common in the center. Sulphide content increases locally, appears to be spatially associated with areas of increased inclusions. Sulphides consist of pyrrhotite clots. Lower contact (3 to 4 meters) is altered (chloritized, serpentinized) along with several thin quartz veins. |
| 40.2 – 47.2 | Leopard textured gabbro: Melanocratic, fine-grained olivine gabbro with 10 – 15 % sulphides. Sulphides increase and decrease intermittently. The upper contact is somewhat altered. About a meter below the upper contact, sulphide content increases, poikiocryst of pyroxenes forms within “net textured” sulphide. This texture dissipates slightly down the interval. Small intervals are present whereby sulphide content decreases to 1%. The lower contact is generally barren of sulphides. |
| 47.2 – 63.7 | Melanocratic fine-grained olivine gabbro: Dark, grey-green, fine-grained to aphanitic, gneissic inclusions are present but are not common. Sulphide clots are present as well and appear to increase towards the lower contact. The lower contact is marked by a chilled margin. |
| 63.7 – 76.2 (EOH) | Garnetiferous paragneiss: Generally leucocratic, coarse-grained with numerous pseudomorphs of garnets, moderately foliated, minor pyrrhotite present. Moderately altered below upper contact. |

Diamond Drill Log
Hole No. SVB-96-52

| Interval (meters) | Description |
|-------------------|---|
| 0.0-10.5 | Overburden |
| 10.5-26.2 | <p>Fine-grained gabbro: Dark, greyish-green color, typically fine-grained with local sections of medium-grained gabbro. Upper sections of core interval, beginning at 10.5 to 15.3 m, is intruded by a coarse-grained, 10-50 cm wide granite/monzonite. The lower contact is sharp, however inclusions of the upper gabbro are contained within the fine-grained gabbro over 80 cm above the contact. Small intervals (1-5 cm) of coarse-grained plagioclase and pyroxene are frequent, yet isolated. Core is slightly to moderately magnetic in places. Trace disseminated to small clots of pyrrhotite are located near the lower contact associated with the inclusions of upper gabbro.</p> |
| 26.2-41.0 | <p>Coarse-grained gabbro: Coarse-grained gabbro with mottled appearance. Entire interval is coarse-grained containing variable amounts of plagioclase and pyroxene (+/- olivine). Between 26.2 to 34.0 m, interval contains numerous green, rounded grains which have a pale green center with thin dark, green rims. These altered grains range between 0.5-2.0 cm and are supported by a leucocratic matrix of cumulate, seriate textured pale white grains with interstitial medium to fine-grained purplish pyroxene and minor (>5 %) greenish-yellow olivine. These altered grains dissipate towards 34.0 m. Between 34.0-41.0 m, this section is typically coarse-grained with seriate, cumulate pale white plagioclase and interstitial pyroxenes and olivines. Towards the lower contact the pyroxenes and olivines displays a granular texture, defined by dark-green mineral accumulation encompassed by medium grained plagioclase. The lower contact is noted by a 40 cm fine-grained gabbro followed by a 5 cm pegmatite composed of large plagioclase grains and large pyroxene grains.</p> |
| 41.0-66.2 | <p>Medium-grained gabbro: Grey-green color, medium-grained, homogeneous composition and texture. Appears to have a consistent granular texture defined by somewhat rounded olivine/pyroxene grains with discontinuous, linked, cloudy white plagioclase grains dispersed evenly within the olivine and pyroxene grains. Between 47.9-48.5 m, megacrystic gabbro with very coarse-grained, bladed white and purple intercumulate pyroxenes. Lower contact of interval is gradational over 10 cm.</p> |
| 66.2-86.2 | <p>Transition gabbro: Defined by a fine-grained, forest-green, olivine gabbro with small (0.5-1 cm) leucocratic, medium-grained, seriate textured plagioclase rimming medium-grained purplish pyroxene. These bands are both randomly orientated and orientated perpendicular to the core axis. Sulphides and inclusions are dispersed intermittently throughout the interval with the greatest concentration near the lower contact. Sulphides occur as small, irregular blotches of pyrrhotite (+/- chalcopyrite). Sulphide content ~ 1 %. Inclusions range in shape and size (1-5 cm). Between 84.2-85.5 m, inclusion dominate interval. Inclusions are gneissic and gabbroic(?). A few aphanitic mafic dikes located near the lower contact. Lower contact is diffuse.</p> |

Diamond Drill Log
Hole No. SVB-96-52 (continued)

| Interval (meters) | Description |
|-------------------|---|
| 86.2-92.6 | <p>Fine-grained gabbro: Typically dark green color, fine-grained with dispersed disseminated and blotchy sulphides. Upper contact is quite diffuse. Between 86.2-87.1 m, interval includes medium to fine-grained pyroxenes which gives the core a purplish-grey appearance and lacks any significant sulphides. This gives way to a fine-grained phase with 1-2 % disseminated and blotchy sulphides. Sulphides consist of pyrrhotite (minor chalcopyrite). Small digested inclusions (> 1 %) are recognizable cloudy white plagioclase lathes. Disseminated sulphides are dispersed evenly throughout section. The lower contact includes an angular gneissic inclusion within a possible chilled-margin. At 92.0 m, a small (2 cm) band of semi-massive pyrrhotite is present,</p> |
| 92.6-131.4 (EOH) | <p>Paragneiss: Light to dark grey, coarse to medium grained gneiss with numerous, rounded retrogressed green garnets. Between 92.6-94.0 m, gneiss appears brecciated with angular gneiss fragments supported by a leucocratic quartz-feldspar medium-grained groundmass (although not consistent throughout interval). Core is moderately foliated. Between 99.2-101.1, grey, fine-grained mafic dike with chilled-margins, medium-grained center. Minor pyrrhotite content.</p> |

Diamond Drill Log
Hole No. SVB-96-53

| Interval (meters) | Description |
|-------------------|---|
| 0.0-3.1 | Overburden |
| 3.1-11.4 | <p>Paragneiss: Grey to light-grey, medium to coarse-grained. Weakly foliated, garnets are extensively retrogressed. Between 9.4 to 11.4, the gneiss has a brecciated appearance and is intensely altered. Fragments within the breccia are angular, supported by a grey, fine-grained matrix. Lower contact is diffuse.</p> |
| 11.4-23.4 | <p>Coarse-grained gabbro: Greyish-green color, typically coarse-grained with local medium-grained intervals. Local intervals contain numerous large rounded grains (pale green center with darker green rims) as well as large pale, cloudy white subhedral, plagioclase phenocryst. Altered minerals supported by a coarse to medium-grained plagioclase/pyroxene +/- olivine cumulate matrix. Lower contact is sharp.</p> |
| 23.4-29.1 | <p>Fine-grained olivine gabbro: Interval is fairly homogeneous throughout the interval with respect to the color, texture and grain size. Beginning at 26 m, the plagioclase becomes visible as well as the presence of sulphides. Sulphides are typically fine-grained and disseminated (few minor small blotches). Gneissic inclusions are small and have a dark interior with a white exterior. Towards the bottom of the interval, the sulphide and inclusions dissipate considerably and the grain-size decreases. The last 20 cm of the interval, it is medium-grained with minor sulphide blotches present. Lower contact is sharp.</p> |
| 29.1-64.6 | <p>Paragneiss: Grey to light grey, coarse to medium-grained, garnetiferous paragneiss, weakly foliated, moderately foliated. Upper portion of interval (first 1.5 m), slightly altered.</p> |
| 64.6-77.9 | <p>Mafic diabase dike: Melanocratic, fine-grained, dark greenish-grey color, contains numerous rounded amygdules (quartz, calcite) ranging from 0.1 to 1 cm and plagioclase phenocryst. Concentration of plagioclase phenocryst and amygdules are within the center of the dike. Sharp upper and lower contacts.</p> |
| 77.9-85.0 (EOH) | <p>Paragneiss: Same as above. No alteration noted.</p> |

Diamond Drill Log
Hole No. SVB-97-57

| Interval (meters) | Description |
|-------------------|---|
| 0.0-150.7 | Coarse to medium-grained olivine gabbro: Typically melanocratic, cumulate textured, plagioclase lathes are euhedral to subhedral, interstitial olivine and pyroxene. Upper portion of core has a spotted appearance whereby coarse-grained plagioclase cumulate clusters while pyroxene and olivine are concentrated around the clusters. Local intervals of plagioclase and pyroxene megacryst. Trace magnetite present. |
| 150.7-155.2 | Fine to medium-grained olivine gabbro: Olivine content ~ 15-20%, pyroxene 5-8%, remainder is plagioclase. Plagioclase grains are subhedral (4-5 mm). Olivine and pyroxene grains are cumulate. Plagioclase content increases locally. Interval is slightly magnetic. |
| 155.2-159.6 | Transition gabbro: Typical texture defined by fine-grained olivine gabbro interrupted by thin bands of medium-grained pyroxene and plagioclase grains. Small intervals of coarse-grained plagioclase present (bladed-random appearance). Minor sulphide concentration (>1%). Sulphide blotches with intergrowths of plagioclase grains. Consist of pyrrhotite with exsolved chalcopyrite. |
| 159.6-167.6 | Gabbro hybrid: Dark color, fine-grained, pyroxene cumulate(?). Olivine rich locally. Partially digested gneiss fragments near upper contact and scattered throughout interval (~5%). Sulphide blotches are present. Sulphide content ~ 5-10%. Small interval of semi-massive sulphide located @ 166.2-166.4 with minor gneissic fragments. Below semi-massive sulphide interval, gneiss fragments increase in abundance. |
| 167.6-169.9 | Fine-grained olivine gabbro: May represent part of a chilled-margin sequence. Overall, is greenish-grey, and fine-grained. Relatively barren of sulphides and gneissic fragments. Lower contact is relatively sharp, upper contact is gradational. |
| 169.9-190.5 (EOH) | Paragneiss: Dark color, moderately to strongly foliated, contains clots of sulphide (~2%) consisting of pyrrhotite and chalcopyrite. Minor garnets present. |

Diamond Drill Log
Hole No. SVB-97-58

| Interval (meters) | Description |
|-------------------|--|
| 0.0-0.3 | Overburden |
| 0.3-59.1 | <p>Medium to coarse-grained gabbro: Patchy appearance (defined by clusters of cloudy white plagioclase and oikocryst of dark green pyroxenes), plagioclase grains are cumulate, euhedral to subhedral. Occurrence of anhedral plagioclase grains (slightly oval, > 2 cm) randomly scattered throughout the core. Minor intercumulate olivine (> 5%). Lower contact is quite discrete over 20 cm, noted by change in color (ie. greenish to greyish) and change in texture.</p> |
| 59.1-166.6 | <p>Medium to coarse-grained olivine gabbro: Typical medium to coarse-grained gabbro, leucocratic. Variations in texture and color. Pegmatitic intervals defined by large, elongate, subhedral plagioclase and intercumulate pyroxene and magnetite. Lower interval has a poikilitic near contact. Lower contact is quite sharp, noted by color change, ie. leucocratic to melanocratic.</p> |
| 166.6-171.7 | <p>Melanocratic coarse-grained gabbro: Dark green with seriate textured plagioclase cumulate and interstitial pyroxenes. 2-3% olivine, trace pyrrhotite and magnetite. Lower contact is sharp.</p> |
| 171.7-178.8 | <p>Transition gabbro: Melanocratic, fine-grained adjacent to the top, medium-grained towards the bottom. At 175.4-176.6, distinct "breccia" texture. 10-15% medium-grained, leucocratic appearance. The "breccia" texture dissipates to a coarse-grained, leucocratic, plagioclase cumulate with oikocryst of pyroxene and olivine. This former texture continues to medium-grained, equal granular texture. Lower contact is not distinct, noted by a color and grain size change (ie. medium/fine to medium grained).</p> |
| 178.8-182.8 | <p>Medium to coarse-grained olivine gabbro: Leucocratic, cumulate textured gabbro. Seriate, cloudy white plagioclase with interstitial pyroxene and fine-grained olivine. Lower contact is diffuse.</p> |
| 182.8-189.0 | <p>Medium to coarse-grained olivine gabbro: Same as above interval except for a darker appearance. Definite granular texture with seriated plagioclase. The lower contact is diffuse, grades into a fine-grained olivine gabbro.</p> |
| 189.0-192.0 | <p>Fine-grained olivine gabbro: Melanocratic, dark green/dark purple (mixture). 1-2 % partially digested gneiss inclusions. Faint "breccia" appearance. Minor disseminated and blotchy sulphides. Blotchy sulphides are ~ 1 cm. 1% sulphides near lower contact. Lower contact is diffuse.</p> |

Diamond Drill Log
Hole No. SVB-97-58 (continued)

| Interval (meters) | Description |
|-------------------|--|
| 192.0-201.5 | Transition gabbro: Typical "breccia" texture defined by fine-grained olivine gabbro (greenish) separated by leucocratic thin layers perpendicular to the core axis. Medium-grained bands contain dark pyroxene grains, rimmed with plagioclase (1-2 mm). Rare fragmental appearance, especially near bottom where texture is not as well defined. Throughout the sequence, 2-4% large blotches of sulphide, mainly pyrrhotite, with minor chalcopyrite and magnetite. Some of the blotches are rounded, other blotches have an irregular shape. Sulphide content increases near the lower contact. |
| 201.5-204.2 | Melanocratic fine-grained olivine gabbro: Dark green-purple, 5-10 % digested gneiss inclusions. Slightly aphanitic locally. Gneiss inclusions do not have a well defined boundary. Sulphides are generally blotchy (0.5-0.7 cm; max 1.5 cm diameter), 5-6% sulphides, minor disseminated sulphides locally. Sharp lower contact. |
| 204.2-204.9 | Semi-massive sulphides: Consisting mostly of pyrrhotite with minor chalcopyrite (>1%). Sulphides appear to have been "melted" into the basement paragneiss. Rounded fragments of chloritized (?) garnets and quartz-feldspar are surrounded by a sulphide matrix. Relatively sharp lower and upper contacts. 1.4 m below this interval, sulphides are found (not as abundant) with similar textures as in this interval. |
| 204.9-210.3 (EOH) | Paragneiss: Leucocratic, coarse-grained, weakly foliated, 8-10% pseudomorphs of garnets within a quartz-feldspar matrix. Minor bands of pyrrhotite. Pyrite located in fractures. |

Diamond Drill Log
Hole No. SVB-97-59

| Interval (meters) | Description |
|-------------------|--|
| 0-3.7 | Overburden |
| 3.7-25.4 | Coarse-grained gabbro: Greyish-green color, overall coarse-grained defined by plagioclase grains. Local medium grain sections. Plagioclase grains are euhedral to subhedral, and displays a seriated texture locally. Pyroxene is the next dominant mineral (~10%). Minor concentrations of olivine. Both olivine and pyroxene are interstitial and fine-grained. |
| 25.4-40.4 | Coarse-grained gabbro (fault zone?): Moderately altered and fractured, vuggy in places filled with quartz. Alteration is intense in places (serpentine/chlorite), and in other places not existent. Plagioclase has a cloudy white color with interstitial fine-grained, dark green minerals (olivine/pyroxene ?). |
| 40.4-50.45 | Coarse-grained olivine gabbro: Melanocratic to leucocratic (marble appearance), coarse-grained oikocryst of olivine with interstitial plagioclase (euhedral, >1 cm) and fine-grained pyroxene, 5-10%. Small intervals of fine-grained olivine gabbro (troctolite?) over 3-4 cm with diffuse contacts. Entire interval is slightly magnetic. |
| 50.45-62.7 | Coarse-grained olivine gabbro: Melanocratic, cumulate textured, locally megacrystic, plagioclase displays seriate texture and is randomly orientated. Plagioclase grains sometimes cluster. Interstitial material consist of olivine and pyroxene, both minerals are coarse-grained. Magnetite and trace amounts of pyrrhotite present. Upper contact is sharp, lower contact is diffuse over 1-2 m and the grain size of the plagioclase begins to decrease. |
| 62.7-285.9 | Fine-grained olivine gabbro: Melanocratic, fine-grained olivine gabbro. Cumulate, cloudy white plagioclase with interstitial pyroxene and olivine. Olivine content variable, ~8-10%, locally as high as 20%. Small intervals of core are medium-grained with an increased plagioclase content. Medium-grained intervals interrupted by small zones of dark bands (very magnetic). Plagioclase abundance increases, as well as grain size increase towards lower contact. |
| 285.9-289.4 | Fine-grained olivine gabbro (mafic dike?): Fine to very fine-grained, green to black, olivine to pyroxene rich interval. Weakly foliated. Olivine and pyroxene are interstitial to cumulate cloudy white plagioclase grains. Both the upper contact and lower contact are gradual. Minor medium to coarse-grained plagioclase phenocryst grains present. Small interval (5-7 cm) of this interval located in following interval near the upper contact. |
| 289.4-369.3 | Medium to coarse-grained gabbro: Similar to gabbro in upper interval, cumulate texture, olivine content variable (5-15%). Olivine abundance increases towards lower contact, 20-25% locally with diffuse contacts. Lower contact towards interval is quite variable, there are intervals of coarse-grained pyroxene with plagioclase, fine-grained olivine gabbro and medium-grained olivine gabbro. Contacts are sharp. Trace disseminated sulphides present. |

Diamond Drill Log
Hole No. SVB-97-59 (continued)

| Interval (meters) | Description |
|--------------------------|--|
| 369.3-384.1 | Transition gabbro: Generally fine-grained, composed of 20-30% olivine with medium-grained bands of plagioclase and pyroxene. Texture becomes well defined towards lower contact and then dissipates. Sulphide blotches are associated with the medium-grained bands. |
| 384.1-388.1 | Gabbro hybrid: Fine-grained, greenish color, presence of digested gneiss inclusions. Sulphide blotches are associated with the gneiss inclusions. |
| 388.1-407.5 (EOH) | Orthogneiss: Leucocratic, moderately to strongly foliated, contains quartz and plagioclase + other mafic minerals, graphite and biotite. Minor blotches of pyrrhotite and chalcopyrite distributed throughout core interval (concentrated near upper contact). |

Diamond Drill Log
Hole No. SVB-97-60

| Interval (meters) | Description |
|-------------------|--|
| 0.0-2.7 | Overburden |
| 2.7-144.5 | Coarse-grained gabbro: Coarse-grained gabbro with cloudy white subhedral, seriate and cumulate textured plagioclase with intercumulate (locally, granular) coarse to medium-grained pyroxene. Minor interstitial olivine (locally up to 5%). Small intervals of megacrysts with plagioclase and pyroxene grains up to 1-2 cm. Minor magnetite present. The upper portion of this interval has a poikilitic texture with patches of medium-grained plagioclase and pyroxene within a matrix of fine-grained olivine gabbro. Lower contact is sharp. |
| 144.5-160.3 | Medium to coarse-grained olivine gabbro: This interval is noted by the overall decrease in grain size and increase in ol content. Interval appears to be darker than above interval. Plagioclase grains are smaller (>0.5 cm). Pyroxenes have a granular habit. Interval is slightly magnetic. Local patchy textured (as noted above). Few megacrystic intervals (small ~20-25 cm). Lower contact is quite diffuse over 30-40 cm, olivine content increase as well. |
| 160.3-168.0 | Transition gabbro: Typical texture with leucocratic, thin bands of medium-grained gabbro within a fine-grained olivine gabbro. However @ 163.2 m, the typical "breccia" texture decreases to give way to an extremely "brecciated" texture. Sulphide content appears consistent throughout core interval (1-2%), of blotchy sulphides containing pyrrhotite with exsolved chalcopyrite. Blotches vary in size and shape. Minor disseminated sulphide. Lower contact is sharp. |
| 168.0-181.7 | Gabbro hybrid: Dark color, fairly homogeneous composition, minor partially digested gneiss inclusions (sparse, 1-3 cm). Blotchy sulphides occur in places where gneiss fragments are concentrated. Sulphides blotches have an irregular boundary. Disseminated sulphide concentrated near upper portion of interval. Lower contact is quite sharp. |
| 181.7-189.0 (EOH) | Quartz-feldspathic paragneiss: Melanocratic, coarse to medium grained, moderately to strongly foliated. Minor graphite, pyrrhotite and chalcopyrite. |

Diamond Drill Log
Hole No. SVB-97-61

| Interval (meters) | Description |
|-------------------|--|
| 0.0-1.7 | Overburden |
| 1.7-40.4 | Medium to coarse-grained gabbro: Light green, medium to coarse-grained gabbro with cumulate texture defined by seriate textured plagioclase. Minor, small (1-2 cm) anhedral (rounded) plag grains. Mottled appearance near lower contact (over 4-5 m). Minor olivine concentration (>5%), interstitial fine-grained pyroxene appears altered near lower contact. Trace amounts of biotite present. Small intervals (10-20 cm) of granular texture present locally. |
| 40.4-116.1 | Coarse-grained olivine gabbro: Cumulate textured, plagioclase displays a seriate texture with interstitial olivine and pyroxene. Generally homogeneous except for small local intervals of medium grained olivine gabbro. Lower contact is quite diffuse over 10-20 cm. Towards bottom of hole, plagioclase content appears to increase while olivine and pyroxene has a granular texture. |
| 116.1-117.5 | Transition gabbro: Typical texture with 20-40% medium-grained bands perpendicular to core axis. Minor disseminated sulphide and small blotches (~3%). Diffuse lower contact, "breccia" texture dissipates. |
| 117.5-120.2 | Gabbro hybrid: Fine-grained olivine gabbro with a greenish color, multiple digested gneiss fragments (hardly recognizable). Contains blotchy sulphides with irregular boundaries. Minor disseminated sulphides. Lower contact is quite diffuse, determined on the basis of color change. Semi-massive sulphide near lower contact (>10 cm). |
| 120.2-123.5 | Graphitic gneiss: Melanocratic, sulphide rich (semi-massive) interval over 40-50 cm. |
| 123.5-134.4 (EOH) | Quartz-feldspathic paragneiss: Melanocratic, moderately to strongly foliated, small interval of felsic dike (?) with a graphitic texture. |

Diamond Drill Log
Hole No. SVB-97-68

| Interval (meters) | Description |
|--------------------------|---|
| 0.0-11.3 | Overburden |
| 11.3-69.3 | Medium-grained paragneiss: Fine to medium-grained, dark grey to medium greenish grey; composed of quartz and biotite with garnets and feldspar. |
| 69.3-72.8 | Fine-grained diabase dike: Dark green, fine-grained, massive with minor plagioclase phenocryst. Upper and lower contact are gradational. Minor sulphide blotches and disseminated sulphide. |
| 72.8-76.4 | Medium-grained paragneiss: Same as above |
| 76.4-89.0 (EOH) | Medium to coarse-grained garnetiferous paragneiss: Medium to coarse-grained, light greenish grey, dominantly quartz, plagioclase and feldspar rich with narrow biotite layers. Minor sulphides present (disseminated, associated with biotite), graphite present as well. |

Diamond Drill Log
Hole No. SVB-97-69

| Interval (meters) | Description |
|-------------------|---|
| 0.0-1.9 | Overburden |
| 1.9-13.1 | <p>Coarse-grained gabbro: Greyish-green, generally coarse-grained with local medium-grained intervals. Cumulate texture defined by cloudy, pale white, seriate, subhedral plagioclase with associated interstitial pyroxene. Olivine content > 5%. As well, small intervals of very coarse-grained pegmatites dispersed throughout interval. Towards the lower contact, cumulate texture gives way to sub-ophitic texture. At 8.2-9.1, transition gabbro texture, separated by coarse to medium-grained gabbro from this interval (rare).</p> |
| 13.1-20.2 | <p>Gabbro hybrid: Dark green to greenish-purple, fine-grained, chlorite/serpentine alteration, original mineralogy hard to recognize. Contains numerous blotches of pyrrhotite scattered throughout interval with the greatest concentration near the center. Sulphide blotches have an irregular shape with plagioclase intergrowths. Chalcopyrite occurs as thin internal wisps or are located around the pyrrhotite rims. Sulphides constitute ~ 2 %. At 20.1-20.2, semi-massive pyrrhotite with gneiss inclusions, trace chalcopyrite. Lower contact is quite diffuse, graphite content is ~ 5-10 %.</p> |
| 20.2-107.0 (EOH) | <p>Paragneiss: Typically coarse-grained, leucocratic, moderately foliated. Graphite is sporadic, greatest concentration of graphite located near top of interval (first 4-5m). Pyrrhotite is unevenly distributed, generally associated with graphite bands. Numerous mafic dikes are located throughout interval. Felsic intrusions are also common.</p> |

Diamond Drill Log
Hole No. SVB-97-73

| Interval (meters) | Description |
|-------------------|--|
| 0.0-3.0 | Overburden |
| 3.0-23.4 | Coarse-grained gabbro: |
| 23.4-52.4 | Coarse-grained to pegmatitic gabbro: |
| 52.4-110.8 | Fine-grained gabbro: |
| 110.8-202.9 | Medium-grained gabbro: |
| 202.9-271.9 | <p>Fine-grained gabbro: Cumulate plagioclase with interstitial olivine (10-15%) and pyroxene (10-15%). Olivine content based on color (lime-green). Homogeneous throughout interval regarding the grain size and modal abundance. Lower contact is gradational, over a length of 1-2 m whereby grain size increases to medium or coarse-grained. Core also appears chloritized/serpentinized near lower contact.</p> |
| 271.9-331.6 | <p>Medium-grained olivine gabbro: Light grey, cumulate plagioclase with intercumulate olivine and pyroxene. Locally enriched in narrow intervals of fine-grained olivine gabbro. Lower contact is quite heterogeneous. Ranges to fine-grained olivine gabbro (small intervals of 10-20 cm), medium-grained gabbro, pegmatitic gabbro. The last 4-5 m of interval the core is fine-grained with 10-15% olivine. The lower contact is diffuse, plagioclase abundance increases locally.</p> |
| 331.6-342.7 | <p>Fine-grained olivine gabbro: Interval has a fairly homogeneous texture and composition. Consist of oikiocryst of fine-grained olivine within seriated plagioclase grains and coarse-grained pyroxene. Minor disseminated sulphides present. Lower contact is diffuse, over 1-1.5 m.</p> |
| 342.7-353.8 | <p>Transition gabbro: Typical texture with coarse-grained to medium-grained bands intruded into fine-grained olivine gabbro. Sulphide blotches, with pyrrhotite and minor exsolved chalcopyrite, intergrown with the plagioclase lathes. Lower contact is diffuse, "breccia" texture not as well defined. Biotite and graphite become apparent. Sulphides begin to dissipate.</p> |
| 353.8-450.0 (EOH) | <p>Graphitic paragneiss: Leucocratic, medium to coarse-grained. Upper 4 m has an abundance of graphite (~30%), crenulated and contains clots of pyrrhotite. Graphite and sulphide content dissipates away from contact. Interval contains small diabase dike with chilled margins and trace disseminated sulphides.</p> |

Diamond Drill Log
Hole No. SVB-97-79

| Interval (meters) | Description |
|-------------------|--|
| 0.0-9.29 | Overburden |
| 9.29-68.4 | Quartzo-feldspathic, garnetiferous paragneiss: Leucocratic, medium to coarse-grained. Moderately to strongly foliated (ie. first half of interval). Small melanocratic interval in center (@ 34-44 m) with 4-5 % pyrrhotite paralleling foliation. Mafic dikes present with chilled margins. Lower interval of gneiss (44-68.5 m) is quartz-feldspar rich, but lacks strong foliation. Lower contact is diffuse. |
| 68.4-221.5 | Medium-grained gabbro: |
| 221.5-246.0 | Coarse-grained gabbro: Coarse-grained with small local medium-grained intervals. White, seriate textured plagioclase. Cumulate textured, locally granular. Olivine content low, > 5%. Gradational upper contact. Lower contact marked by intense alteration. 1-2 cm white subhedral plagioclase grains common. |
| 246.0-249.3 | Medium-grained gabbro: Dark grey, medium-grained gabbro. Significant decrease in plagioclase. Lower contact is intrusive with quartz-feldspar intrusion (10 cm wide). |
| 249.3-255.0 | Fine-grained olivine gabbro: Melanocratic (dark greenish-grey), fine-grained, homogeneous textured and composition throughout interval. Olivine content ~ 20-30%, pyroxene ~ 20-30%, plagioclase ~ 40 %. Olivine is the cumulate phase. Quartz-feldspar-biotite intrusions present in center of interval. The lower contact is quite sharp, as is the upper contact. The upper contact appears to be marked by a 20 cm altered interval of greenish-beige appearance (sericitized plagioclase). This interval lacks any visible sulphides. |
| 255.0-257.0 | Fine-grained olivine gabbro matrix: This interval contains numerous inclusions concentrated near the top (first 30-40 cm) of interval (possibly gneissic derivative?). This gives way to a coarse-grained pyroxene-plagioclase rich zone of variable textures. The fine-grained olivine gabbro appears as blotches surrounded by plagioclase and plagioclase, as well as interval of massive pyroxene-plagioclase. Sulphide blotches are present, but rare. |
| 257.0-257.6 | Semi-massive sulphide: Small interval of semi-massive sulphide consisting of mainly pyrrhotite with minor chalcopyrite. Appears to have melted into host rock. Massive at top of interval, sulphide content decreases downwards. Rounded, sharp contacts are quite evident. Gangue material has a purplish-green appearance and is fine to medium-grained. |
| 257.6-258.5 | Fine-grained olivine gabbro: Contains numerous blotches of sulphides and inclusions. Within the center of interval, possible relict gneiss fragment with weak foliation. 2-3 cm sulphide blotch with abundant chalcopyrite. Sulphides dispersed and concentrated towards lower contact. |

Diamond Drill Log
Hole No. SVB-97-79 (continued)

| Interval (meters) | Description |
|-------------------|--|
| 258.5-266.1 | Melanocratic, fine-grained olivine gabbro: Dark, greyish-green, fine-grained olivine gabbro. Lacks sulphides or inclusions. Chilled lower contact. |
| 266.1-362.5 | Medium-grained gabbro: |
| 362.5-617.9 | Medium to fine-grained olivine gabbro: |
| 617.9-640.1 | Medium-grained gabbro: Greyish-green, medium-grained (locally fine-grained) gabbro. Numerous fractures altered to sericite and carbonate. First inclusion appears @ 617.9 m. Inclusions are typically leucocratic, medium to coarse-grained, consisting of plagioclase and pyroxene (?). Percentage of inclusions ~ 2%. Inclusions are widely spaced. Lower contact is marked by darker colour. Sulphides occur with inclusions. |
| 640.1-668.1 | Dark green, medium-grained gabbro (peridotite?): Highly fractured, possibly fault zone? Typically medium-grained, includes numerous inclusions (medium-grained, plagioclase abundant, pyrrhotite association, leucocratic, large, partially digested, 1-2% of interval) Disseminated sulphide, ~ 1% of interval. Interval is more competent towards bottom of interval. |
| 668.1-681.4 | Medium-grained gabbro: Similar to interval above (617.9-640.1 m), but with less inclusions and less sulphides. |
| 681.4-711.5 | Medium-grained gabbro: Inclusion content increases (3-4 %), as does sulphide content (1-3 %) with small blotches. Overall, interval is medium grained (sm. Local intervals of fine-grained gabbro noted near the bottom of interval). Inclusion content increases near lower contact. Inclusions are typically white rimmed with a dark core. Appears that the interval contains granular olivines-pyroxenes with white medium-grained plagioclase lathes. |
| 711.5-723.6 | Coarse-grained gabbro: Greyish-green, very coarse-grained, cumulate textured with cumulate texture and interstitial olivine and pyroxene and sulphide. 1-3 % sulphides, generally pyrrhotite with minor chalcopyrite and magnetite. Lower contact is subtle. |
| 723.6-742.5 | Medium-grained gabbro: Medium-grained, granular textured, 5-10 % blotchy to trace disseminated sulphide. Sulphide blotches intergrown with plagioclase. Sulphide content dissipates towards lower contact. Sulphide blotches have small blebs of pentlandite (not common). |
| 742.5-757.9 | Medium-grained gabbro: Granular texture, lacks sulphides and inclusions, chilled lower contact |
| 757.9-999.7 (EOH) | Gneiss (not logged) |

Diamond Drill Log
Hole No. SVB-97-81

| Interval (meters) | Description |
|-------------------|---|
| 0.0-4.1 | Overburden |
| 4.1-145.5 | Coarse-grained gabbro: Leucocratic, very coarse-grained, cumulate plagioclase (cloudy white, euhedral, ~ 1 cm) with intercumulate pyroxene and fine-grained olivine (?). Plagioclase grains are randomly orientated. The lower portion of this interval, below 51.8 m, is a melanocratic, cumulate plagioclase with intercumulate olivine. Locally leucocratic whereby plagioclase size increases. Small interval (0.5 m) of olivine gabbro near the lower contact. |
| 145.5-149.6 | Transition gabbro: Dark green color, fine-grained olivine gabbro near the top of this interval. Grades into a typical "breccia" texture at 148 m. Sulphides (1-2%) occur as irregular blotches (>1 cm) of pyrrhotite and chalcopyrite. |
| 149.6-151.0 | Gabbro hybrid: Greenish-purple with partially digested gneiss inclusions and trace, disseminated sulphides. At the top of this interval, small (>1cm) sulphide blotches increase in concentration. Small (10 cm), medium-grained, leucocratic interval located at 150.1 m. Sulphide concentration increase below this, disseminated and sulphide blotches. Plagioclase content may be increasing as well. The upper contact is relatively sharp, the lower contact is moderately diffuse noted by an increase in sulphides. |
| 151.0-151.9 | Semi-massive sulphide: Semi-massive pyrrhotite hosted in paragneiss. Sulphide and gangue contacts are rounded. Appears that sulphide liquid melted into the basement. Minor chalcopyrite. The lower contact is relatively sharp. |
| 151.9-198.1(EOH) | Garnetiferous paragneiss: Coarse-grained, quartz-feldspar, paragneiss with 10% retrograde garnets near the bottom and top of interval. Rose colored garnets near the center. Minor pyrrhotite and chalcopyrite in the first 5-6 m of interval. |

Diamond Drill Log
Hole No. SVB-97-91

| Interval (meters) | Description |
|--------------------|---|
| 0.0-19.5 | Overburden |
| 19.5-126.8 | Coarse to medium-grained gabbro: |
| 126.8-158.1 | Fine-grained olivine gabbro: Melanocratic, fine-grained olivine gabbro with occasional digested inclusions towards the lower contact, disseminated sulphide as well as sulphide clots present (>1%). Diffuse upper and lower contacts. |
| 158.1-160.2 | Gabbro hybrid: Olivine gabbro host, inclusions concentrated near the top part of the interval and dissipate towards the lower contact. Sulphide clots are dispersed evenly over interval (5-10 % sulphides). Gradational lower contact. |
| 160.2-167.7 | Melanocratic olivine gabbro: Typically fine-grained, chilled lower contact. Lacks any significant amount of sulphides. Small, isolated inclusions are present but are rare. |
| 167.7-229.3 | Coarse to medium-grained gabbro: |
| 229.3-1098.8 (EOH) | Coarse-grained leucogabbro/anorthosite: |

Diamond Drill Log
Hole No. SVB-97-92

| Interval (meters) | Description |
|-------------------|---|
| 0.00-7.6 | Overburden |
| 7.6-18.4 | Monzonite-gneiss: Fragmental, broken core of medium to coarse-grained melanocratic gneiss with retrogressed green garnets, moderately foliated. Monzonite occurs at top of interval (boulder?), lower contact is abrupt. |
| 18.4-195.1 | Coarse-grained black gabbro: Dark grey color (defined by plagioclase) with minor concentrations of forest green intervals (olivine increased?). Cumulate, seriated textured plagioclase lathes with interstitial pyroxenes and olivines. The first 60-70 meters of the interval appears altered, possibly representing the upper contact. As well, near the upper contact there are large phenocryst of plagioclase. |
| 195.1-240.6 | Coarse to medium-grained black gabbro: Dark grey color, dominantly coarse-grained but becomes medium-grained towards the lower contact. Typically plagioclase cumulate with interstitial pyroxenes and olivines. However, towards the lower contact (10-15 m), the appearance of a finer grained phase (granular olivines) with a medium-grained gabbro to give the interval a blotchy appearance. |
| 240.6-245.0 | Fine-grained olivine gabbro: Dominantly, greenish-grey, fine-grained olivine gabbro. Near upper contact, medium-grained sections appear although not consistent (240-242 m). At 242 m, olivine concentration increases while plagioclase and pyroxenes occur as irregular blotches (weak transition gabbro appearance). Small blotches of sulphide occurs near 242.7 m but are not very abundant. At 243.5-245.0 m, sulphides increase, although less than 1%. Dark, rounded inclusions are present in this interval as well. |
| 245.0-249.9 | Melanocratic fine-grained gabbro: Dark, fine-grained gabbro with 3-5% sulphides, weakly leopard textured, dark purple blotches surrounded by disseminated sulphides and fine-grained olivine, blotches of sulphide are common. Upper contact is diffuse, spread over 10 cm. Lower contact is noted by the decrease in sulphides. Inclusions are rare. |
| 249.9-257.0 | Melanocratic fine-grained gabbro: Dark grey and fine-grained. Sulphide content is quite low, except near the upper contact (first 1.5 m) where blotches and disseminated sulphides are more pronounced. Lower contact is marked by the presence of monzonite intrusions. |
| 257.0-260.8 | Quartz monzonite: Medium grained, leucocratic, quartz-bearing, sharp irregular contacts. |
| 260.8-265.9 | Melanocratic fine-grained gabbro: Dark grey appearance, similar to above interval. Contains trace disseminated and blotchy sulphides. Lower contact is diffuse (uncertain) and may be part of another rock group (Harp Lake?). |
| EOH at 1097.3 m | Re-logging finishes at 265.9 m |

Diamond Drill Log
Hole No. SVB-98-102

| Interval (meters) | Description |
|-------------------|--|
| 0.00-0.60 | Overburden |
| 0.60-154.7 | Coarse-grained black gabbro: Dark greyish appearance, typically coarse-grained throughout interval, plagioclase grains are greyish which gives the core a grey appearance. Plagioclase has a seriated texture and are the cumulate phase while pyroxene and minor olivine is interstitial. At the first 30 to 40 meters, very coarse grained (1-2 cm) plagioclase lathes, randomly and sparsely distributed throughout the core. This feature dissipates going down throughout the core. As well, within the cg interval there are other smaller intervals which are medium grained, typically 8-9 m in thickness and closer to the lower contact. Narrow megacrystic intervals of about 10-20 cm also exist and are common throughout the entire interval. Megacryst are typically plagioclase and pyroxene bearing. The bottom contact is diffuse and is noted by the change in texture as well as the appearance of granular olivine. |
| 154.7-169.1 | Medium-grained black gabbro: This interval has a dark greyish-green appearance defined by granular fg greenish olivine gabbro(?) surrounded by a medium-grained gabbro consisting of plagioclase and pyroxene. It has the appearance of transition gabbro texture, but is difficult to determine due to the color of the plagioclase (dark grey). Some of the plagioclase grains have a white rim, possibly alteration? There is however, more of a blotchy texture. Narrow megacrystic intervals of plagioclase and pyroxene are rarer than the above interval but do exist. Lower contact is defined by a narrow megacryst (20-30 cm). |
| 169.1-172.7 | Fine-grained black gabbro: Overall, dark-greyish green appearance, including numerous variations including transition gabbro and gabbro hybrid. Top portion of interval is fine grained with little else except for minor medium-grained bands to give interval a weak transition gabbro appearance. These medium-grained bands dissipate at 172.1 m. Sulphide blotches occur as well as white rimmed digested gneiss inclusions but as not as abundant as the following interval. The first significant inclusion occurs at 171.0 m as does the first visible sulphide blotch. Inclusions and sulphides begin to gradually increase as does the sulphide blotches. Inclusions have a white center and a dark green rim, sulphide blotches are intergrown with plagioclase, minor disseminated sulphides are present as well. |
| 172.7-175.6 | Gabbro hybrid (Inclusion rich): Numerous inclusions of various degrees of digestion supported by a fine-grained greenish matrix (olivine gabbro?). Inclusions are closely packed and range in size (>1-4 cm). The larger inclusions have a white center with a dark green rim while the smaller inclusion are the opposite. Sulphide blotches and minor disseminated sulphides are distributed evenly throughout the interval (~ 1% of total interval). 20-30% inclusions. Both upper and lower contacts are diffuse. |

Diamond Drill Log
Hole No. SVB-98-102 (continued)

| Interval (meters) | Description |
|-------------------|---|
| 175.6-177.6 | Fine-grained gabbro: Greyish appearance, does not appear to have as much olivine as above intervals. Appears to have increased amounts of plagioclase grains, top portion includes inclusions similar to previous interval. Sulphide blotches remain the same composition and abundance. At 176.7 m, sulphide content increases dramatically to near semi-massive. Sulphides have appearance of percolating or melting into the rock. Biotite may be present with host lithology, as well as extremely digested inclusions. (176.7-177.6 ~ 20% sulphide). |
| 177.6-185.2 | Paragneiss with semi-massive sulphide: Paragneiss has dark greenish color, sulphides are distributed unevenly. Two semi-massive sulphide interval exist (largest intervals) @ 179.8-181.1m and 181.6-181.7m. Several smaller sulphide intervals exist as well. One small sulphide interval appears to hosting black fragments (?). Some gneissic intervals appear to have injections of fine-grained greenish material (gabbroic?). Disseminated sulphide present along foliation planes. |
| 185.2-220.0 | Melacratic gneiss: Dark color, medium-grained, moderately foliated, high concentration of graphite and pyrrhotite (blotchy texture), retrogressed garnets present. |
| 220.0-274.6 (EOH) | Leucocratic paragneiss: Lighter color than the above interval, moderately to strongly foliated, garnets are more recognizable, minor pyrrhotite and graphite present along foliation planes. |

Diamond Drill Log
Hole No. SVB-98-113

| Interval (meters) | Description |
|-------------------|---|
| 0.0-2.6 | Overburden |
| 2.6-79.2 | <p>Coarse-grained black gabbro: Overall grey to dark grey color, coarse-grained with small intermediate medium-grained intervals. The initial 50+ meters, the rock has an altered (?) appearance, possible "upper sequence" gabbro defined by lighter grey interval with darker grey blebs that are surrounded by leucocratic white masses. As well, phenocryst of large (1-2 cm) plagioclase grains, white to pale white also frequent interval. Below 50 meters, rock loses altered appearance, typically coarse-grained appearance with seriate, cumulate dark grey plagioclase and interstitial pyroxene (purplish-pink) and olivine. There are also megacrystic intervals, although not very thick (ie, 10-15 cm), consisting of large dark plagioclase grains with intercumulate dark purple pyroxene. Towards the lower contact, the grain size dissipates to medium-grained, though the texture and color remains the same.</p> |
| 79.2-87.6 | <p>Medium to fine-grained black olivine gabbro: Dark greyish-green color, medium grained to fine-grained olivine gabbro, cumulate plagioclase at the top of interval, near the middle of interval, granular olivines become more pronounced. Lower contact is quite diffuse, over 30-40 cm. Lower portion of core is relatively fine to medium-grained and has a greenish/purple appearance.</p> |
| 87.6-99.8 | <p>Fine-grained olivine gabbro: Interval has an overall greenish-purple blotchy to mottled appearance (comparable to the gabbro hybrid). The first appearance of visible sulphides occurs at 87.7 m as small, disseminations, but increases downhole. Blotchy sulphides are the most common sulphide texture and increases downhole although less 1% overall. Sulphide blotches are typically irregular shaped, with small plagioclase intergrowths and are typically 1-3 cm. Disseminated sulphide increases towards the lower contact. From 99.3-99.8, the interval is barren of sulphides except for trace disseminated sulphides. Blotchy sulphides consist of pyrrhotite with minor chalcopyrite within the center. Small inclusions of pentlandite are sometimes observed. The majority of inclusions occur between 87.9-95.5 m. Inclusions are typically leucocratic, partially digested with thin, dark green rims (inclusions make up 1% of the total interval). Inclusions range in size, from 1-4 cm, larger inclusions occur at 89.0 m. Some inclusions have a dark color.</p> |
| 99.8-100.4 | <p>Massive sulphide: Massive sulphide consisting of pyrrhotite, minor chalcopyrite, rarer pentlandite and small dark colored inclusions of gabbroic or gneissic gangue. At the top of the interval, 15 cm of semi-massive sulphide with thin, wispy zones of fine-grained greenish material (olivine gabbro?), below this interval sulphides become more concentrated, inclusions of gneiss are present towards the lower contact.</p> |

Diamond Drill Log
Hole No. SVB-98-113 (continued)

| Interval (meters) | Description |
|--------------------------|--|
| 100.4-108.2 | Melanocratic gneiss: Dark, medium to coarse-grained and biotite rich. Contains disseminated sulphides (pyrrhotite mostly), as well as small blotches of chalcopyrite and pyrrhotite, fine-grained greenish blotches are common (possibly related to the olivine gabbro), rock is moderately to well foliated, quartz rich veins are present as well. |
| 108.2-213.1 (EOH) | Garnetiferous paragneiss: Typically coarse-grained with leucocratic, garnetiferous banding, moderately foliated with 1-2 occurrences of diabase mafic dikes (> 1m). Biotite rich zones locally. |

Diamond Drill Log
Hole No. SVB-98-116

| Interval (meters) | Description |
|--------------------|--|
| 0.00-52.8 | Overburden |
| 52.8-104.1 | Coarse-grained black gabbro: Dark greyish-purple appearance, typically coarse-grained with short intervals (10-20 cm) of megacryst. Plagioclase is typically greyish with a cumulate texture. Plagioclase is also seriated. Pale purplish-pink pyroxenes and forest green olivines are intercumulate. Lower contact noted by a decrease in grain size and an increase in olivine content. |
| 104.1-107.1 | Medium-grained black gabbro: Dark greyish-purple appearance, overall interval is medium grained with minor fine-grained small intervals. Olivines have a granular texture in places where plagioclase cumulate is not as pronounced, giving the core interval a local blotchy appearance. |
| 107.1-111.5 | Transition gabbro: Dark forest-green color with small bands of coarser grained melanocratic minerals perpendicular to the core axis, as well as orientated in places. Typical appearance of fine-grained olivine gabbro with intermittent medium-grained pyroxene and plagioclase. Texture is quite pronounced, medium-grained minerals constitute 30-35% of interval. Sulphide blotches are not common, although blotches are associated with the medium-grained bands. First visible sulphide occurs at 107.4 m, and increases towards the lower contact, blotches increase in size as well. Lower contact is diffuse. |
| 111.5-123.0 | Gabbro hybrid: This interval is considered a gabbro hybrid based on the texture and color of the host rock. Overall, the interval is fine-grained with a forest green to purplish-pink color, giving the interval a blotchy/mixed appearance. At the top of the interval, first 1.5 meters, the core has a faint transition gabbro texture, although the medium-grained bands are not as common as the above interval. Digested inclusions are dispersed throughout the interval, although the bulk of the inclusions are concentrated near the top of the interval. Inclusions are well digested and range in size (between 1-4 cm). Cores are typically white with dark rims. Inclusions make up ~ 1% of interval. Sulphides are scattered throughout interval, blotches are most common texture with plagioclase intergrowths, possibly related to medium-grained pyroxene and plagioclase bands. Sulphide blotches constitute 1-2 % of the interval and are typically 1 cm. Towards the bottom contact, disseminated sulphide is dominant over an interval of 30-40 cm, followed by a barren interval of 40-60 cm. |
| 123.0-123.15 | Semi-massive sulphide: Semi-massive sulphide located between gneiss and gabbro. 50-60% pyrrhotite, while the remainder is gangue material, appearance of a melted, well-defined contact between the sulphides and the gangue. |
| 123.15-208.2 (EOH) | Quartz-feldspar paragneiss: Melanocratic to leucocratic, coarse to medium-grained paragneiss. Upper portion, first 10-12 m, core is darker containing dark green blotches (retrogressed garnets?) and abundant biotite. Pyrrhotite and chalcopyrite blotches are frequent. |

Appendix D: Geochronological Reports

**REPORT ON THE U/Pb ZIRCON + BADELEYITE AGE OF
CRYSTALLIZATION
OF SAMPLE SVB97-67, 150M FROM SOUTH VOISEY'S BAY**

by

GREG DUNNING
DEPARTMENT OF EARTH SCIENCES
MEMORIAL UNIVERSITY
ST. JOHN'S, NEWFOUNDLAND

RESULTS SO FAR ON SOUTH VOISEY'S BAY GEOCHRONOLOGY

Sample SVB97-67, 150M

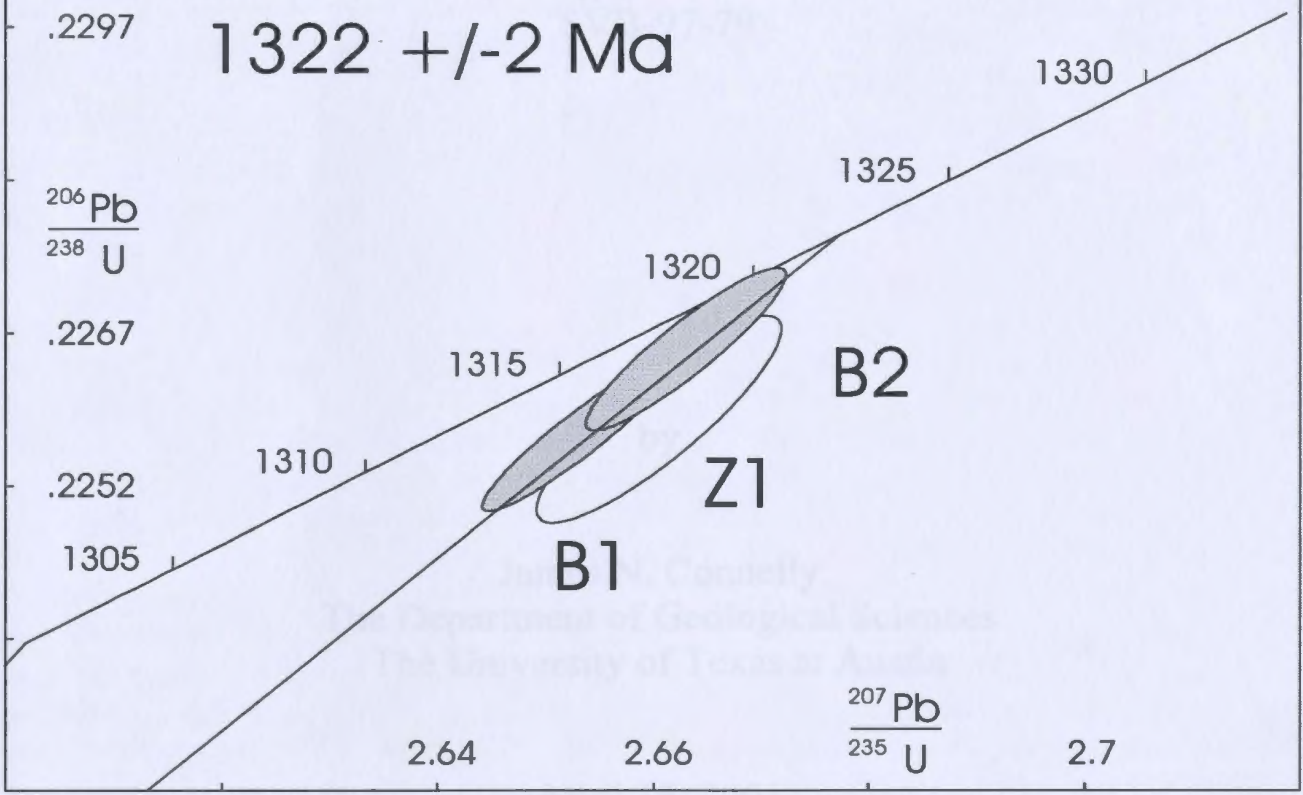
This sample yielded angular fragments of clear zircon and tiny plates and equant prisms of baddeleyite (ZrO₂). Two fractions of baddeleyite and one of zircon were selected and abraded prior to analysis and all three analyses overlap with one baddeleyite (shaded) touching the concordia curve. The baddeleyite analyses yield ²⁰⁷Pb/²⁰⁶Pb ages of 1321.3 and 1321.4 Ma. The line shown was fitted to all three points and a point at 50 +/-50 Ma, to constrain the lower intercept to pass close to the origin. This has the effect of calculating an upper intercept age based on the average of the three analyses and an uncertainty controlled by the precision of the three measurements. In this case the calculated age is 1322.2 +/-2 Ma - a reliable age of igneous crystallization.

TABLE: U/Pb DATA FOR SAMPLE SVB97-67 FROM SOUTH VOISEY'S BAY

| Fraction | Weight [mg] | Concentration | | Measured | | Corrected Atomic Ratios | | | | | Age [Ma] | | | | |
|-----------------------|----------------|---------------|--------------------|-------------------------------|-------------------------|-------------------------|------------------------|------------------------|-------------------------|------------------------|------------------------|-------------------------|------|------|------|
| | | U | Pb rad [ppm] | total common Pb [pg] | 206Pb ----- 204Pb | 208Pb ----- 206Pb | 206Pb ----- 238U | 207Pb ----- 235U | 207Pb ----- 206Pb | 206Pb ----- 238U | 207Pb ----- 235U | 207Pb ----- 206Pb | | | |
| SVB150M | | | | | | | | | | | | | | | |
| Z1 frags abr | 0.007 | 232 | 71.4 | 10 | 2252 | 0.4962 | 0.22599 | 84 | 2.6621 | 94 | 0.08544 | 16 | 1313 | 1318 | 1325 |
| B1 tiny prms weak abr | 0.016 | 221 | 49.0 | 9 | 5419 | 0.0557 | 0.22584 | 62 | 2.6547 | 74 | 0.08525 | 8 | 1313 | 1316 | 1321 |
| B2 tiny prms weak abr | 0.012 | 183 | 40.8 | 9 | 3444 | 0.0547 | 0.22667 | 66 | 2.6646 | 76 | 0.08526 | 10 | 1317 | 1319 | 1321 |

SVB97-67 150M

1322 +/- 2 Ma



**REPORT ON U-PB GEOCHRONOLOGY FOR SAMPLE
SVB-97-79**

by

**James N. Connelly
The Department of Geological Sciences
The University of Texas at Austin**

April 15, 2001

INTRODUCTION

Drill core from the Nain Plutonic Suite from Labrador was submitted to the Geochronology Laboratory at The University of Texas at Austin for U-Pb baddeleyite dating. The samples yielded sufficient quantity and quality of baddeleyite to be treated with standard analytical techniques.

METHODS

Rock samples were crushed to mineral size under clean conditions using a jaw crusher and disc pulverizer, and minerals were separated using a Wilfley table, disposable sieves, heavy liquids and a Frantz magnetic separator at The University of Texas at Austin. Baddeleyite crystals were characterised using a binocular reflected-light microscope and transmitted light petrographic microscope (with condenser lens inserted to minimize edge refraction).

Multiple grains were selected for analysis on the basis of optical properties to ensure that only the highest quality grains were analysed. Minerals selected were too small to be abraded (Krogh 1982). After final selection they were washed successively in distilled 4N nitric acid, water and acetone. They were loaded dry into Teflon™ capsules with a mixed $^{205}\text{Pb}/^{235}\text{U}$ isotopic tracer solution and dissolved with HF and HNO_3 . Chemical separation of U and Pb from dissolved baddeleyite solution using minicolumns (0.055 ml resin volume; after Krogh 1973) resulted in total procedural blanks of approximately 1 and .25 pg for Pb and U, respectively. Pb and U were loaded together with silica gel and phosphoric acid onto an outgassed filament of zone-refined rhenium ribbon and analysed on a multi-collector Finnigan-MAT 261 thermal ionization mass spectrometer operating in dynamic mode with all masses measured sequentially on a single axial Secondary Electron Multiplier (SEM) - ion counting system. Initial common Pb was corrected for using appropriate Stacey and Kramers (1975) and ages were calculated using decay constants of Jaffey et al. (1971). Errors on isotopic ratios were calculated by propagating uncertainties in measurement of isotopic ratios, fractionation and amount of blank with a program written by J.N. Connelly. Results are reported in Table 1 with 2σ errors. Linear regressions were performed using the procedure of Davis (1982). Ages listed in the text, table and figures are quoted with 2σ errors.

References

- Davis, D.W., 1982, Optimum linear regression and error estimation applied to U-Pb data: Canadian Journal of Earth Sciences, v. 23, p. 2141-2149.
- Jaffey, A.H., Flynn, K.F., Glendenin, L.E. Bentley, W.C., and Essling, A.M., 1971, Precision measurements of half-lives and specific activities of ^{238}U and ^{235}U : Physical Reviews, v. 4, p. 1889-1906.
- Krogh, T.E., 1973, A low-contamination method for hydrothermal decomposition of baddeleyite and extraction of U and Pb for isotopic age determination: Geochimica Cosmochimica Acta, v. 37, p. 485-494.
- Krogh, T.E., 1982, Improved accuracy of U-Pb baddeleyite ages by the creation of more concordant systems using an abrasion technique: Geochimica Cosmochimica Acta, v. 46, p. 637-649.
- Stacey, J.C. and Kramers, J.D., 1975, Approximation of terrestrial lead isotope evolution by a two-stage model: Earth and Planetary Science Letters, v. 26, p. 207-221.

Sample Number SVB-97-79

An approximately 4 kg sample of drill core yielded very small (35-75 μm), clear, brown striated euhedral baddeleyite fragments. Analysis of four fractions, comprising between 3 and 5 micrograms (see Table 1), cluster between 1.4-1.7% discordant along $\text{Pb}^{207}/\text{Pb}^{206}$ lines (Fig. 1). Attempts with various fractions to cause spread along a discordia line (and thus enable a statistical regression of four points) were unsuccessful. To obtain a meaningful statistically-defined upper intercept age from these near concordant points, the lower intercept of the line was pinned at 100 ± 100 Ma. This constraint is justified by the lack of a known regional metamorphic or thermal event after the emplacement of the Nain Plutonic Suite. The upper intercept error therefore reflects a very conservative lower intercept range between 0-200 Ma. Regressing the three points with this lower intercept range yields an upper intercept age of 1338 ± 2 Ma, which is interpreted to represent the crystallization age of this igneous body.

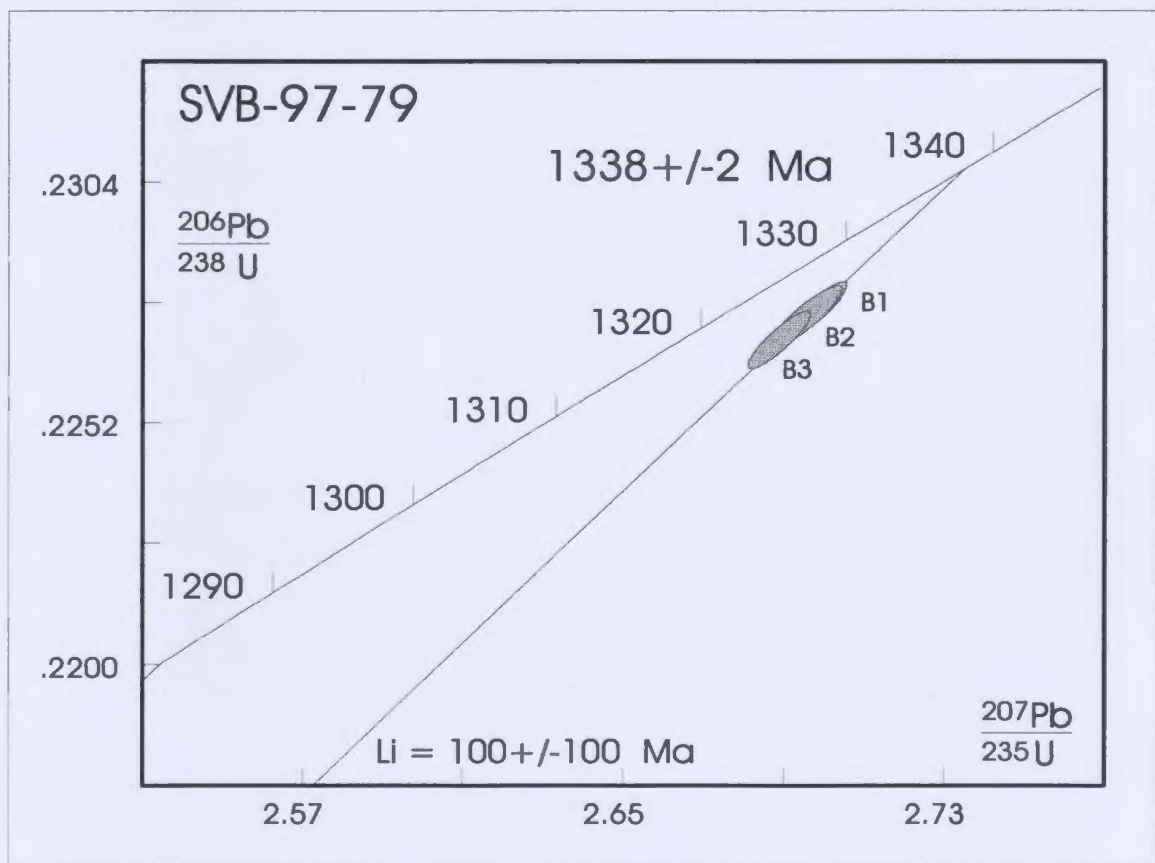


Figure 1: U-Pb concordia diagram for sample SVB-97-79 (B = baddeleyite).

Table 1. U-Pb geochronology data.

| Fraction | Weight [mg] | Concentration | | Measured | | *Corrected Atomic Ratios | | | | | | Ages [Ma] | | | |
|----------------------|----------------|---------------|-----------------|--------------------------------|---|---|--|--|---|---|--|--|---|------|------|
| | | U [ppm] | Pb ^R | Common Pb ^T [pg] | $\frac{^{206}\text{Pb}}{^{204}\text{Pb}}$ | $\frac{^{208}\text{Pb}}{^{206}\text{Pb}}$ | $\frac{^{206}\text{Pb}}{^{238}\text{U}}$ | $\frac{^{207}\text{Pb}}{^{235}\text{U}}$ | $\frac{^{207}\text{Pb}}{^{206}\text{Pb}}$ | $\frac{^{207}\text{Pb}}{^{206}\text{Pb}}$ | $\frac{^{206}\text{Pb}}{^{238}\text{U}}$ | $\frac{^{207}\text{Pb}}{^{235}\text{U}}$ | $\frac{^{207}\text{Pb}}{^{206}\text{Pb}}$ | | |
| SVB-97-79 | | | | | | | | | | | | | | | |
| B1 m sm euh clr brn | 0.005 | 138 | 29.7 | 3 | 3820 | 0.0110 | 0.22767 | 48 | 2.6985 | 58 | 0.08597 | 10 | 1322 | 1328 | 1337 |
| B2 m vsm euh clr brn | 0.003 | 153 | 32.7 | 3 | 2498 | 0.0078 | 0.22750 | 54 | 2.6956 | 72 | 0.08594 | 10 | 1321 | 1327 | 1337 |
| B3 m vsm euh clr brn | 0.004 | 139 | 29.9 | 3 | 3276 | 0.0208 | 0.22699 | 50 | 2.6888 | 64 | 0.08591 | 10 | 1319 | 1325 | 1336 |

Abbreviations are: brn-brown; clr-clear; euh-euhedral; m-multiple grain fractions; sm-small (50-75 μm); vsm-very small (<50 μm).

*Ratios corrected for fractionation, 1 pg and .25 pg laboratory Pb and U blanks respectively and initial common Pb calculated using Pb isotopic compositions of Stacey and Kramers (1975). All fractions extensively abraded. Two-sigma uncertainties on isotopic ratios are reported after the ratios and refer to the final digits.

Canada, UTM Zone 20

- Contour interval 20 meters
- Elevations in meters above mean sea level

trusion

p

Project

td.

te:

10, 2001

5

